On particles, fibers and suspension flows

Partikel, Fäden und Suspensionsströmungen

Dem Fachbereich IV
der Universität Trier zur
Erlangung des Doktorgrades Dr. rer. nat.

vorgelegt von

Alexander Vibe
aus Temirtau

Als Dissertation genehmigt vom Fachbereich IV
der Universität Trier

Tag der mündlichen Prüfung: 11. August 2020

Berichterstatter: Prof. Dr. Nicole Marheineke (Betreuerin)
                                            Prof. Dr. Eberhard Bänsch
                                            Prof. Dr. Leonhard Frerick

Acknowledgment

I express my deep gratitude to Prof. Dr. Nicole Marheineke for the suggestion of the fascinating and challenging research topics considered in this work. I am especially very grateful for her patience, for her encouragement of my independent research and for always taking care to provide helpful professional advice whenever I asked for it. Prof. Dr. Marheineke's engagement and dedication to show up opportunities for personal and professional development in combination with wide-ranging and precise mathematical knowledge and experience made it possible for me to develop a firm grasp of different topics from applied mathematics and mathematics in general.

I also want to thank Prof. Dr. Bänsch, Dr. Raimund Wegener and Stefanie Reuter for the much appreciated critical input and suggestions in our discussions during my time at the FAU Erlangen-Nürnberg. Additionally, I'd want to express my gratitude to the colleagues at the Fraunhofer ITWM, Department Transport Processes for the hospitality during my visits there, especially to Dr. Raimund Wegener, Dr. Dietmar Hietel, Dr. Simone Gramsch and Dr. Walter Arne. A big thank you goes also to Prof. Dr. Felix Lindner and Dr. Holger Stroot with whom I had the pleasure to publish a very interesting joint research paper. Furthermore, I am very thankful for my great colleagues in the working groups at the FAU Erlangen-Nürnberg and at the Trier University, who supported me with helpful discussions and suggestions, namely Sarah Hauschild, Dr. Björn Liljegren-Sailer, Dr. Yi Lu, Dr. Stefan Schießl, Nadine Stahl, Kevin Tolle, Dr. Manuel Wieland and Marc Harmening.

Additionally, I also want to express my special thanks to all my former colleagues at the chair of Applied Mathematics I at FAU Erlangen-Nürnberg. In particular, I thank Prof. Dr. Peter Knabner as the head of the department, Dr. Alexander Prechtel and Balthasar Reuter for the administration and help with all concerns connected to the IT infrastructure and especially Prof. Dr. Florian Frank for the introduction to the department. I also want to express my gratitude for the friendly welcome and nice working atmosphere to the colleagues at the department of mathematics of the Trier University. A great thank you goes also to Cornelia Weber and Astrid Bigott at the FAU Erlangen-Nürnberg as well as to Doris Karpa and Monika Thieme-Trapp at the Trier University, who took care of all organizational issues.

This work was largely made possible by the funding of the Federal Ministry of Education and Research (BMBF) of the OPAL project (Optimization of air-lay-processes, 05M13), which was a collaboration of FAU Erlangen-Nürnberg, TU Kaiserslautern, Fraunhofer ITWM, and our partners from industry, Autefa Solutions Germany GmbH and IDEAL Automotive GmbH. I want to thank all my colleagues of this joint research project, namely Prof. Dr. Bänsch, Prof. Dr. Klar, Prof. Dr. Leugering, Prof. Dr. Marheineke, Dr. Raimund Wegener, Dr. Simone Gramsch, Dr. Dieter Hietel, Dr. Christian Neßler, Stefanie Reuter, and Dr. Christoph Strohmeyer.

I also thank Prof. Dr. Eberhard Bänsch and Prof. Dr. Leonhard Frerick for reviewing the present work, as well as Prof. Dr. Martin Schmidt for accepting the role of the chairman of my doctoral exam.

Finally, my deepest gratitude goes to my friends and my family, who supported me during this enriching albeit challenging time. It wouldn't have been possible without you!

Zusammenfassung der Arbeit

Diese Arbeit beschäftigt sich mit typischen mathematischen Herausforderungen, welche im Bereich der Modellierung und Simulation von Fertigungsprozessen der Papierproduktion oder technischer Textilien auftauchen. Im Besonderen widmet sich der vorliegende Text einerseits approximativen Modellen für die Bewegung kleiner trägheitsbehafteter Partikel in einem inkompressiblen Newtonschen Fluid. Des Weiteren werden effektive makroskopische Approximationen verdünnter Partikelsuspensionen in einem beschränkten Gebiet betrachtet, die sowohl allgemeine Verteilungen als auch Partikelträgheit berücksichtigen. Außerdem werden Methoden zur Reduzierung der Rechenzeit bei Simulationen dünner elastischer Fäden in einer turbulenten Strömung betrachtet.

Wir untersuchen das über die Partikeloberfläche gekoppelte Partikel-Fluid Problem, welches durch die Navier-Stokes Gleichungen in Kombination mit den Impulsbilanzgleichungen eines starren Körpers beschrieben wird. Durch die Wahl einer bestimmten asymptotischen Skalierung für das Verhältnis der Partikel- und Fluiddichte sowie der Anwendung der asymptotischen Entwicklung der Lösungskomponenten, leiten wir Näherungen des Ausgangsproblems her. Die resultierenden approximierenden Systeme unterscheiden sich je nach gewählter Dichteskalierung im physikalischen Verhalten, was uns die Charakterisierung der jeweiligen Trägheitsregime erlaubt.

Des Weiteren wenden wir das asymptotische Vorgehen auch auf den Fall vieler Partikel an, welche von einem Newtonschen Fluid umgeben sind. Unter einer Reihe von Annahmen an die Kombination von Partikelgröße und -anzahl, leiten wir asymptotische Approximationen des Gesamtsystems her. Diese Näherungssysteme beschreiben auch die Partikelbewegung, wodurch wir mit Hilfe eines Mean-Field Ansatzes imstande sind, die Kontinuitätsgleichung für die Wahrscheinlichkeitsdichte der Partikel herzuleiten. Die Kopplung der Letzteren an die Approximation der Impulsbilanz des Fluids ergibt die makroskopische Suspensionsbeschreibung, welche sowohl nicht-gleichmäßige Partikelverteilungen als auch kleine Trägheitseffekte der Partikel berücksichtigt.

Ein dünner Faden, welcher einer turbulenten Luftströmung ausgesetzt ist, kann als stochastischer, nicht dehnbarer, eindimensional parametrisierter Kirchhoff-Balken modelliert werden. Das heißt, er wird durch eine stochastische, partielle differentialalgebraische Gleichung beschrieben. Die Simulation solcher Modelle erfordert das Lösen großer, nicht linearer Gleichungssysteme durch das Newton-Verfahren. Um die benötigte Rechenzeit solcher Simulationen zu verringern, untersuchen wir unterschiedliche Lösungsschätzer für das Newton-Verfahren. Zusätzlich erforschen wir die Auswirkungen unterschiedlicher Glättungsmethoden des Wiener Prozesses, welche die treibende stochastische Kraft regularisieren, auf die Lösung und die Performanz der Fadensimulation. Des Weiteren untersuchen wir die Anwendbarkeit der "Wiener chaos expansion" zur Simulation stochastischer Fadendynamik.

Abstract

This work studies typical mathematical challenges occurring in the modeling and simulation of manufacturing processes of paper or industrial textiles. In particular, we consider three topics: approximate models for the motion of small inertial particles in an incompressible Newtonian fluid, effective macroscopic approximations for a dilute particle suspension contained in a bounded domain accounting for a non-uniform particle distribution and particle inertia, and possibilities for a reduction of computational cost in the simulations of slender elastic fibers moving in a turbulent fluid flow.

We consider the full particle-fluid interface problem given in terms of the Navier-Stokes equations coupled to momentum equations of a small rigid body. By choosing an appropriate asymptotic scaling for the particle-fluid density ratio and using an asymptotic expansion for the solution components, we derive approximations of the original interface problem. The approximate systems differ according to the chosen scaling of the density ratio in their physical behavior allowing the characterization of different inertial regimes.

We extend the asymptotic approach to the case of many particles suspended in a Newtonian fluid. Under specific assumptions for the combination of particle size and particle number, we derive asymptotic approximations of this system. The approximate systems describe the particle motion which allows to use a mean field approach in order to formulate the continuity equation for the particle probability density function. The coupling of the latter with the approximation for the fluid momentum equation then reveals a macroscopic suspension description which accounts for non-uniform particle distributions in space and for small particle inertia.

A slender fiber in a turbulent air flow can be modeled as a stochastic inextensible one-dimensionally parametrized Kirchhoff beam, i.e., by a stochastic partial differential algebraic equation. Its simulations involve the solution of large non-linear systems of equations by Newton's method. In order to decrease the computational time, we explore different methods for the estimation of the solution. Additionally, we apply smoothing techniques to the Wiener Process in order to regularize the stochastic force driving the fiber, exploring their respective impact on the solution and performance. We also explore the applicability of the Wiener chaos expansion as a solution technique for the simulation of the fiber dynamics.

Contents

1 Introduction

1.1 Motivation

An important key for sustainable prosperity of modern societies is the resource effi-
cient manufacturing of goods. A major element here is the usage of materials with
properties tailored to the specific application. Carbon fiber reinforced plastics, as an
example, play a substantial role in weight reduction for aircraft fuselage or for the body
of automobiles, while at the same time possessing the stability of classical metal alloys
preserving the necessary safety requirements in these fields of mobility [3, 22, 43, 123].
Such architectured materials range from exactly engineered metamaterials with struc-
tures designed on nanoscale [76, 94] over hybrid materials built of layers of different base
materials with an optimized distribution with respect to desired properties [6, 74] to
virtually infinitely long mats of non-woven fabrics with stochastic micro-structure [54].
Due to the availability and computational power of modern computers, it is possible
to design and adjust such materials in a very cost and resource efficient way by using
numerical simulations. However, in order to achieve meaningful and realistic predic-
tions and allow the precise control of material properties, the corresponding simulation
tools must combine different mathematical models which depict the production steps
of the complete manufacturing process [54, 122]. Such models are in general valid on
different length and time scales which makes it difficult to combine them directly. A
non-woven fabric for example consists of around 10^5 fibers per m^2 of final material [54].
The formation of this mat is achieved by the deposition of fibers by a turbulent air
flow onto a conveyor belt. While being subjected to the stochastic fluid flow, the fibers
move with velocities of around $30m/s$. Being elastic, they possess inner dynamics and
interact with the carrier fluid, possibly disturbing it. As soon as they reach the con-
veyor belt, they are transported with merely $0.03m/s$ with no relevant changes to the
local structure of the fabric. Hence, during the interaction with the air flow, the prob-
lem description consists of instationary coupled stochastic partial differential equations,
where the large number of degrees of freedom poses a severe numerical challenge. After
the deposition the product is characterized by the stochastic topology of the resulting
graph. The relevant material properties on the other hand are determined by tensile
strength tests whose exact description consists of stationary solutions of a large system
of partial differential equations with prescribed shifts of the material at the boundaries
of the stochastic graph. Thus, although only the net force is relevant for the behavior
of the final product, the full mathematical description determines every individual fiber
load, making a full scale simulation impracticable. These challenges motivate advances
in mathematical modeling, analysis and algorithmic development. Just to name a few
examples in the field of industrial textiles from recent years, such developments involve
advances in modeling and simulation in melt-blowing processes [67], spinning processes

and viscoelastic jets [87], numerical schemes for growing viscoelastic jets [5], analysis and numerics for partial differential algebraic equations of elastic fibers [56], process simulation of aerodynamic manufacturing of textiles [54], versatile numerical strategies for viscous jets subject to high elongations [109], simulation of industrial melt-blowing processes under turbulence [124].

1.2 Objectives

This work is related to different aspects of particle- and fiber-laden fluid flows which occur in the manufacturing of paper or industrial textiles. In particular, we pursue three major objectives. The first is an extension of asymptotic results for the system describing the motion of an isolated particle suspended in a Newtonian incompressible fluid with regard to finite particle inertia. The second objective is the derivation of an effective macroscopic suspension model which approximates a dilute particle suspension within an incompressible Newtonian carrier fluid, accounting for particle inertia effects and for non-uniform particle distributions. Finally, we also seek to increase the efficiency of numerical fiber simulations in the case of elastic inextensible Kirchhoff beams subjected to stochastic forces by presenting algorithmic extensions to modern numerical schemes.

1.3 Structure

Since this three topics address different mathematical areas and differ in their scope and methodology, this work is divided into three chapters, corresponding to the objectives laid out above. Each chapter has its own introduction with the classification of the topic, an overview of the literature and a detailed explanation of its structure. Similarly, each chapter also has its own conclusion stating and discussing the relevant results. Here we give only a brief overview of each section.

In the first part, Sec. 2, we start with the discussion of the dynamics of a small rigid particle of arbitrary shape suspended in an incompressible Newtonian fluid. The mathematical model describing this problem is given by the Navier-Stokes equations coupled with the linear and angular momentum balances of the particle. We use asymptotic expansions of the solution components in powers of the particle size parameter in order to derive a hierarchy of equations, which approximate the original problem. Different inertial effects are realized by an appropriate asymptotic scaling of the density ratio between the particle and the fluid. The resulting approximate systems then reveal different models depending on the chosen inertial regime in accordance with the expected physical behavior.

In Sec. 3 we extend the results derived in Sec. 2 to the case of a large but finite number of isolated particles whose linear and angular momenta are coupled to the Navier-Stokes equations describing the surrounding fluid. The model accounts for hydrodynamic particle interaction and for particle inertia, neglecting direct particle-particle interactions, i.e., impacts or particle clusters connected by friction or adhesive forces. We again derive an asymptotic approximation which accounts for small particle inertia, exploring the boundaries of this approach. Then we formulate a mean field model which approximates the suspension as the number of particles goes to infinity while the particle size decreases to zero. The resulting model consists of a Navier-

Stokes-like momentum equation for the fluid coupled to a continuity equation for the probability density function of particle position and orientation. The resulting model simplifies to classical models for prolate ellipsoids or spheres, given the corresponding assumptions on the particle shape and distribution in space.

In Sec. 4, we consider the dynamics of a slender elastic fiber modeled as a one-dimensionally parametrized inextensible Kirchhoff beam. The fiber dynamics is governed by a partial differential algebraic equation of hyperbolic type with a small elliptic regularization term. The system becomes stochastic if the aerodynamic force is assumed turbulent. We use a spatial semi-discretization by finite volumes combined with finite differences on a staggered grid in order to discretize the problem. The time-integration is performed by the implicit Euler scheme due to stability reasons. In order to reduce the computation time, we study estimation methods for the associated Newton iteration, which are motivated by semi-explicit integration schemes. In addition, we explore the effects of different regularization methods for the white noise as well as the applicability of the Wiener chaos expansion as a direct solution technique.

The appendix App. A is dedicated to collect properties of (skew-)symmetric matrices and rotation matrices often used in the arguments of this work, it additionally contains the essential definitions and statements connected with manifolds and matrix Lie-groups which play an important role in the mean field description of the suspension. Appendix B collects statements concerning the stationary Stokes problem; in particular, the analytical solutions for the Stokes problem in the exterior domain of an ellipsoid. Finally, App. C encapsulates additional numerical simulation data of the stochastic fiber simulations in order to increase readability of Sec. 4. Accordingly, the appendices App. A and App. B are mainly used in Sec. 2 and Sec. 3, while App. C is associated with Sec. 4.

1.4 Main results

The main result of the first part of this work is the extension of asymptotic approximations for the coupled system of a small rigid particle moving in an incompressible Newtonian fluid with regard to small particle inertia. By introducing an asymptotic scaling of the density ratio, we deduce different asymptotic models which show physically meaningful behavior while preserving the mathematical structure of the approximation.

In the second part we derive an asymptotic mean field description of a suspension of small rigid particles suspended in an incompressible Newtonian fluid. Instead of using classical techniques of statistical modeling, we rely only on asymptotic analysis and rigorous restriction on particle size and their minimal distance of separation. This way we are able to derive an effective description which consists of a Navier-Stokes like momentum equation for the fluid coupled with a continuity equation for the particle phase space. The latter is composed of the particle position and its orientation in the special orthogonal group. The macroscopic description simplifies to classical models in case of a uniform particle distribution in space and under neglect of hydrodynamic interaction, yet it is also able to depict non-uniform particle distributions and hydrodynamic particle interaction.

In the third part we explore different strategies for the reduction of computational costs in numerical fiber simulations of elastic inextensible Kirchhoff beams subjected to

stochastic forces. In particular, we present two novel predictor methods for the Newton iteration which solves the non-linear equations associated with the discretized partial differential algebraic equations describing the fiber motion. Both methods yield an estimation for the first Newton iteration and lead to a moderate reduction of the overall computational time. We also investigate the effect of various correlation techniques for the white noise driving the fiber. We observe that the correlated stochastic fields reduce the computational cost by a smaller amount than the usage of the already mentioned predictor techniques. Finally, we also successfully apply the Wiener chaos expansion to the stochastic, inextensible fiber model with a linear air-drag force term.

The publications which provide the basis of this work are listed in the following.

Publications preceding this thesis

Journal articles

- A. Vibe, N. Marheineke. "Impact of weak particle inertia on a dilute suspension of ellipsoids". In: *Journal of Computational and Theoretical Transport* 45(5) (2016), pp. 396–409. [117]

- F. Lindner, N. Marheineke, H. Stroot, A. Vibe, R. Wegener. "Stochastic dynamics for inextensible fibers in a spatially semi-discrete setting". In: *Stochastics and Dynamics* 17(2) (2017). [84]

- A. Vibe, N. Marheineke. "Modeling of macroscopic stresses in a dilute suspension of small weakly inertial particles". In: *Kinetic & Related Models* 11(6) (2018), pp. 1443–1474. [119]

Proceedings and book contributions

- A. Vibe, N. Marheineke. "Wiener chaos expansion for an inextensible Kirchhoff beam driven by stochastic forces". In: *Progress in Industrial Mathematics at ECMI 2016*. Ed. by P. Quintela et al. Springer, 2017, pp. 761–768. [120]

- A. Vibe, N. Marheineke. "Mean field surrogate model of a dilute and chaotic particle suspension". In: *PAMM – Proceedings in Applied Mathematics and Mechanics*. Ed. by J. Eberhardsteiner and M. Schöberl. Vol. 19. Wiley-VCH, 2019. [118]

The articles [117] and [119] are connected with the first two parts of the present work, Sec. 2 and Sec. 3. In [117] we study the asymptotic one-particle models in detail by using numerical simulations of the resulting particle equations of motion. In [119] we present the asymptotic approximation of a particle suspension, where we rely strongly on the hypothesis of ergodicity, finding similar macroscopic models to the ones presented in Sec. 3 in the present thesis. The proceeding [118], which accompanies a presentation at the 90th Annual Meeting of the International Association of Applied Mathematics and Mechanics (GAMM 2019), presents the fully coupled macroscopic mean field models derived in Sec. 3.4.2.

The article [84] deals with the analysis and numerics of the semi-discretized system describing the motion of the stochastic, inextensible Kirchhoff beam discussed throughout the last part of the present work, Sec. 4. It is a collaboration with Prof. Dr. Felix

Lindner, Prof. Dr. Nicole Marheineke, Dr. Raimund Wegener, and Dr. Holger Stroot. The proof of existence and uniqueness of a global strong solution presented in [84] is based largely on the ideas of Dr. Stroot who used this topic in his dissertation [113]. The numerical experiments which are examined in [84] and which are similarly used in Sec. 4.5.4 of the present work, on the other hand, were largely provided by myself.

Finally, the proceeding [120] connected with a presentation at the 19th European Conference on Mathematics for Industry focuses on the Wiener chaos expansion for the stochastic partial differential algebraic equation of the stochastic Kirchhoff fiber; it is utilized in Sec. 4.4.2 and Sec. 4.5.6 in the final part of this work.

2 Asymptotics for inertial particles

2.1 Introduction

The analysis of the motion of a single particle in a Newtonian fluid and its influence on the solvent plays a crucial role in the understanding of the behavior of a particle suspension. In the field of rigid particles, Stokes [112] found an analytical solution for the disturbance flow generated by a rigid sphere which moves with a constant translational velocity in a linear ambient velocity field in an unbounded domain. Oberbeck extended this work in [96] by considering an ellipsoidal particle. His results were generalized by Edwardes, who added constant rotational motion of the particle in [40]. Jeffery found in [70] the description of the evolution of the principal axis of a prolate ellipsoid of revolution in a linear surrounding flow. He derived his famous equation (Jeffery's equation) by using analytical solutions of the stationary Stokes problem in the unbounded exterior of the ellipsoidal particle with linear boundary conditions on the particle boundary.

All this classical results hold for the case of a stationary ambient velocity field and an inertia-free particle in an unbounded domain. The general case of an inertial, arbitrarily shaped particle moving through a Newtonian fluid of finite Reynolds number (ratio between fluid inertia and viscosity) in a bounded domain does neither admit analytical solutions for the disturbance velocity field, nor for the particle motion. Junk & Illner [71] proposed in this case an asymptotic approach for inertia-free particles. By using asymptotic expansions in the small size ratio (ratio between the characteristic particle length scale and the one associated to the fluid) they derived lower order corrections to an undisturbed incompressible Navier-Stokes flow in a bounded domain which approximate the effect of the particle presence. At the same time this approach yields approximations for the particle motion, revealing Jeffery's equation as a special case.

Our aim in this chapter is to extend the asymptotic approach of [71] with regard to particle inertia. In particular, we desire to derive lower order asymptotic approximations to an undisturbed flow, which are still valid if the particle and the fluid have different densities. Similarly to the original approach, our resulting approximating model should also provide an approximate description of the particle motion which accounts for particle inertia. We achieve this goal by introducing an appropriate asymptotic scaling for the density ratio (density of the rigid body with respect to the one of the fluid), which does not affect the validity of the asymptotic approach. The resulting model describes the particles as tracer particles in leading approximation order, i.e., they follow the streamlines of the undisturbed fluid flow. The first order corrections of particle velocity then consist of contributions which depend on the chosen scaling of the density. This allows the characterization of different inertial regimes for which
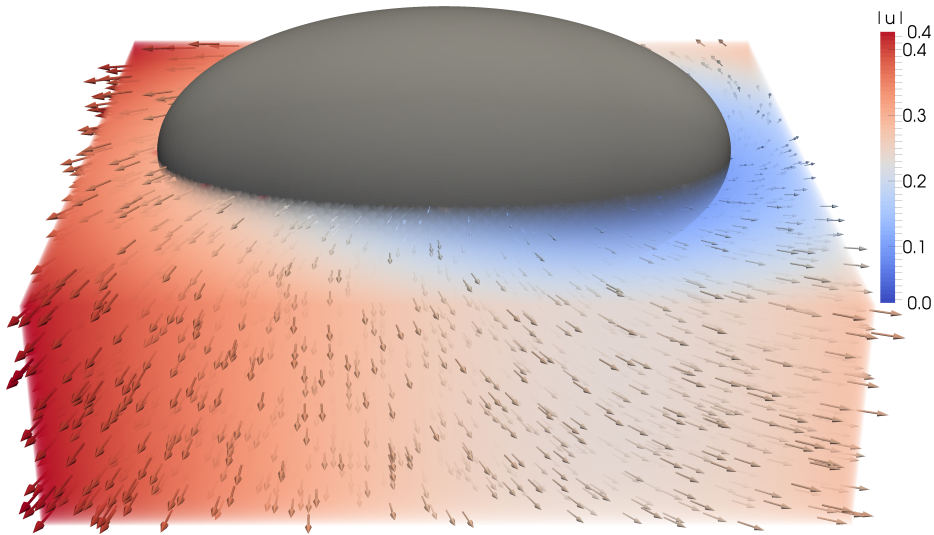
Figure 2.1.: Cutout of the velocity in the vicinity of an ellipsoidal particle moving with
the fluid.

the asymptotic approach is valid. The velocity corrections to the undisturbed flow also
depend on the chosen inertial regime, while still preserving the structure of the orig-
inal approximation by [71]. In particular, the disturbance velocity fields are given as
solutions of stationary Stokes equations in the exterior of the particle domain embed-
ded into the bounded fluid domain (see Fig. 2.1 for the velocity approximation in the
vicinity of an ellipsoid). Furthermore, any approximation order depends only on the
lower orders allowing a hierarchical computation of the approximation. The novelty of
this work consists in the extension of asymptotic models for the particle motion in a
surrounding incompressible Newtonian fluid to the case of different particle and fluid
density, exploring the boundaries of this asymptotic method.

This chapter is based on the preliminary works [116, 117, 119] and is structured
as follows: we introduce the physical system of the coupled interface problem in Sec-
tion 2.2, where we also discuss an extension of the Newtonian stresses onto the particle
domain, which is redundant in this chapter, but is necessary later for the suspension
model. After stating the dimensionless formulation in Sec. 2.2.5, we propose an asymp-
totic model for different types of inertial regimes in Section 2.3, where we also discuss
the asymptotic approach according to [71] with the necessary modifications in our case.
We formulate the general asymptotic result in Sec. 2.3.3 and discuss a slightly different
asymptotic approach which is based on [41] in Sec. 2.3.4. In Section 2.4 we apply
our results to the well-known example of ellipsoidal particles and study the proposed
asymptotic models for the particle motion focusing on the different inertia regimes. In
Section 2.5 we briefly discuss our results and observations.

2.2 Particle-fluid model

We first introduce the particle-fluid model by identifying the physical quantities which
describe the motion of the particle, adapting the well-known Navier-Stokes equations
as the description of a Newtonian fluid and coupling the particle and fluid motion
via Newton's second law. Additionally, also introduce a redundant description of the

particle motion at the end of this section which we need later in Section 3.4.

2.2.1 Particle Kinematics

We model a particle as a rigid body, i.e., forces acting on the particle do not introduce deformations which also implies that the spacing between particle points does not change in time, [55]. We also assume that the particle has a uniform mass distribution and therefore a uniform particle density $\rho_p > 0$. We choose the particle reference state [39] as a bounded open domain $\mathcal{E} \subset \mathbb{R}^3$ with a smooth boundary $\partial \mathcal{E}$ and the center of mass lying in the origin, i.e.,

$$\int_{\mathcal{E}} \boldsymbol{y} \, \mathrm{d}\boldsymbol{y} = \boldsymbol{0} \,.$$

Furthermore, we assume that the position of any material point is determined by a time-dependent translation $\boldsymbol{c} : \mathbb{R}_0^+ \to \mathbb{R}^3$ and an orthonormal right-handed director triad $\boldsymbol{d}_i : \mathbb{R}_0^+ \to \mathbb{S}^2$, $i = 1, 2, 3$. Denoting by $\boldsymbol{e}_i$, $i = 1, 2, 3$ the Cartesian unit vectors, we introduce the rotation matrix $(\mathbf{R}(t))_{ij} = \boldsymbol{e}_i \cdot \boldsymbol{d}_j(t)$, $i, j = 1, 2, 3$ and a time-dependent rigid body motion $\boldsymbol{x} : \mathbb{R}^3 \times \mathbb{R}_0^+ \to \mathbb{R}^3$ given by

$$\boldsymbol{x}(\boldsymbol{y}, t) = \mathbf{R}(t) \cdot \boldsymbol{y} + \boldsymbol{c}(t) \,. \tag{2.1}$$

Then, the time-dependent particle domain is given as the image of the reference state under the rigid motion (2.1), $\mathcal{E}(t) = \boldsymbol{x}(\mathcal{E}, t)$ for any $t \geq 0$. This way, the dynamical behavior of the particle can be fully described by the dynamics of the center of mass and the director triad.

Under the assumption that the particle moves smoothly in time, we find for a fixed $\overline{\boldsymbol{y}} \in \mathcal{E}$ the velocity of the corresponding material point $\overline{\boldsymbol{x}} = \boldsymbol{x}(\overline{\boldsymbol{y}}, t)$ given by

$$\hat{\boldsymbol{v}}(t; \overline{\boldsymbol{x}}) = \frac{\mathrm{d}}{\mathrm{d}t} \boldsymbol{x}(\overline{\boldsymbol{y}}, t) = \partial_t \boldsymbol{x}(\overline{\boldsymbol{y}}, t) \,.$$

Denoting by $\boldsymbol{y}(., t)$ the inverse mapping of $\boldsymbol{x}(., t)$ for any $t \geq 0$, we therefore introduce the Eulerian velocity field

$$\widetilde{\boldsymbol{v}}(\boldsymbol{x}, t) = \partial_t \boldsymbol{x}(\boldsymbol{y}(\boldsymbol{x}, t), t) = \frac{\mathrm{d}}{\mathrm{d}t} \mathbf{R}(t) \cdot \mathbf{R}^T(t) \cdot (\boldsymbol{x} - \boldsymbol{c}(t)) + \frac{\mathrm{d}}{\mathrm{d}t} \boldsymbol{c}(t) \tag{2.2}$$

for any $\boldsymbol{x} \in \mathcal{E}(t)$, $t \geq 0$. As shown in the appendix, the matrix appearing in (2.2) is skew-symmetric and can be identified with a unique angular velocity vector $\boldsymbol{\omega} : \mathbb{R}_0^+ \to \mathbb{R}^3$ according to Lemma A.55 by using the identity

$$B(\boldsymbol{\omega}(t)) = \frac{\mathrm{d}}{\mathrm{d}t} \mathbf{R}(t) \cdot \mathbf{R}^T(t) \,,$$

where $B : \mathbb{R}^3 \to \mathbb{R}^{3 \times 3}$ is a parametrization of the skew-symmetric matrices in $\mathbb{R}^3$ as defined in appendix A.2. Furthermore, we denote the time derivative of the center of mass as $\boldsymbol{v} = \mathrm{d}\boldsymbol{c}/\mathrm{d}t$. This allows the definition of the linear and angular momenta of the particle:

$$\boldsymbol{i}(t) = \int_{\mathcal{E}(t)} \rho_p \widetilde{\boldsymbol{v}}(\boldsymbol{x}, t) \, \mathrm{d}\boldsymbol{x} = \rho_p |\mathcal{E}| \frac{\mathrm{d}}{\mathrm{d}t} \boldsymbol{c}(t) = \rho_p |\mathcal{E}| \boldsymbol{v}(t) \,, \tag{2.3}$$

$$\boldsymbol{\ell}(t) = \int_{\mathcal{E}(t)} (\boldsymbol{x} - \boldsymbol{c}(t)) \times \rho_p \widetilde{\boldsymbol{v}}(\boldsymbol{x}, t) \, \mathrm{d}\boldsymbol{x} = -\int_{\mathcal{E}(t)} B(\boldsymbol{x} - \boldsymbol{c}(t))^2 \, \mathrm{d}\boldsymbol{x} \cdot \rho_p \boldsymbol{\omega}(t)$$

$$= \mathbf{R}(t) \cdot \int_{\mathcal{E}} \|\boldsymbol{y}\|^2 \mathbf{I} - \boldsymbol{y} \otimes \boldsymbol{y} \, \mathrm{d}\boldsymbol{y} \cdot \mathbf{R}^T(t) \cdot \rho_p \boldsymbol{\omega}(t) \tag{2.4}$$

$$= \rho_p |\mathcal{E}| \mathbf{R}(t) \cdot \hat{\mathbf{J}} \cdot \mathbf{R}(t)^T \cdot \boldsymbol{\omega}(t) = \rho_p |\mathcal{E}| \mathbf{J}(t) \cdot \boldsymbol{\omega}(t) \,,$$

where we used (A.10d) and abbreviated the inertia tensor by $\mathbf{J}(t) = \mathbf{R}(t) \cdot \hat{\mathbf{J}} \cdot \mathbf{R}(t)^T$ with the time-independent part

$$\hat{\mathbf{J}} = |\mathcal{E}|^{-1} \int_{\mathcal{E}} \|\boldsymbol{y}\|^2 \mathbf{I} - \boldsymbol{y} \otimes \boldsymbol{y} \, \mathrm{d}\boldsymbol{y} \,. \tag{2.5}$$

2.2.2 Fluid model

We model the fluid which contains the particle as incompressible with the density $\rho_f > 0$ and Newtonian with dynamic viscosity $\mu_f > 0$. Both, the particle and the fluid are located in a regular open domain Ω with the fluid domain denoted by $\Omega(t) = \Omega \backslash \overline{\mathcal{E}}(t)$. The fluid behavior is completely described by the dynamics of its solenoidal velocity $\boldsymbol{u} : \Omega(t) \times \mathbb{R}_0^+ \to \mathbb{R}^3$. Assuming no outer forces except gravity, the fluid dynamics is described by the Navier-Stokes equations [47] given by

$$\rho_f \mathrm{D}_t \boldsymbol{u}(\boldsymbol{x}, t) = \nabla \cdot \mathbf{S}[\boldsymbol{u}](\boldsymbol{x}, t)^T + g \rho_f \boldsymbol{e}_g \,, \quad \nabla \cdot \boldsymbol{u}(\boldsymbol{x}, t) = 0 \quad \text{for } \boldsymbol{x} \in \Omega(t) \,. \tag{2.6a}$$

We denote by $\mathrm{D}_t \boldsymbol{u} = \partial_t \boldsymbol{u} + [\boldsymbol{u} \cdot \nabla] \boldsymbol{u}$ the material derivative, by $\mathbf{S}[\boldsymbol{u}] = -p\mathbf{I} + \mu_f(\nabla \boldsymbol{u} + \nabla \boldsymbol{u}^T)$ the Newtonian stress tensor with the pressure $p : \Omega(t) \times \mathbb{R}_0^+ \to \mathbb{R}$ denoting the Lagrangian multiplier to the incompressibility, and the direction of gravity as well as the gravitational acceleration by $\boldsymbol{e}_g$, resp. g. The symmetric deformation gradient of $\boldsymbol{u}$ is often abbreviated as $\mathbf{E}[\boldsymbol{u}] = 0.5(\nabla \boldsymbol{u} + \nabla \boldsymbol{u}^T)$ throughout this work. The system is completed by an initial condition on $\Omega(0)$, boundary conditions on $\partial\Omega$ and the no-slip boundary condition on $\partial\mathcal{E}(t)$. The latter is given for $t \geq 0$ as

$$\boldsymbol{u}(\boldsymbol{x}, t) = \boldsymbol{\omega}(t) \times (\boldsymbol{x} - \boldsymbol{c}(t)) + \boldsymbol{v}(t) \,. \tag{2.6b}$$

2.2.3 Particle dynamics

The particle is accelerated by gravity and hydrodynamic forces. Thus, the particle dynamics are given by

$$\frac{\mathrm{d}}{\mathrm{d}t} \boldsymbol{i}(t) = \int_{\partial\mathcal{E}(t)} \mathbf{S}[\boldsymbol{u}](\boldsymbol{x}, t) \cdot \boldsymbol{n} \, \mathrm{d}s + g \rho_p |\mathcal{E}| \boldsymbol{e}_g \,, \tag{2.6c}$$

$$\frac{\mathrm{d}}{\mathrm{d}t} \boldsymbol{\ell}(t) = \int_{\partial\mathcal{E}(t)} (\boldsymbol{x} - \boldsymbol{c}(t)) \times \mathbf{S}[\boldsymbol{u}](\boldsymbol{x}, t) \cdot \boldsymbol{n} \, \mathrm{d}s \,. \tag{2.6d}$$

The vector $\boldsymbol{n}$ denotes the outer normal vector to the particle surface pointing into the fluid domain. The complete system is then given by (2.6) together with boundary conditions of the fluid on $\partial\Omega$ and initial conditions for the fluid velocity, particle velocity, its position and orientation.

2.2.4 Extension of the Stokes system to the particle domain

In Section 3.4 we derive a macroscopic suspension model which requires the definition of velocities and stresses on the whole domain Ω, including the interior of the particle. Thus, we consider here also the Eulerian description of the velocity in the particle domain. Following the approach of [99], we treat the particle as a fluid with a rigidity constraint. Its velocity $\widetilde{\boldsymbol{v}} : \mathcal{E}(t) \times \mathbb{R}_0^+ \to \mathbb{R}^3$ as given in (2.2) obeys

$$\rho_p \mathrm{D}_t \widetilde{\boldsymbol{v}} = \nabla \cdot \mathbf{T}^T + \rho_p g \boldsymbol{e}_g \,, \qquad \nabla \widetilde{\boldsymbol{v}} + \nabla \widetilde{\boldsymbol{v}}^T = \mathbf{0} \,, \qquad \boldsymbol{x} \in \mathcal{E}(t) \,, \qquad (2.7\text{a})$$

$$\widetilde{\boldsymbol{v}} = \boldsymbol{u} \,, \qquad \mathbf{T} \cdot \boldsymbol{n} = \mathbf{S}[\boldsymbol{u}] \cdot \boldsymbol{n} \,, \qquad \boldsymbol{x} \in \partial\mathcal{E}(t) \,. \qquad (2.7\text{b})$$

Here, $\mathbf{T} : \mathcal{E}(t) \times \mathbb{R}_0^+ \to \mathbb{R}^{3\times3}$ denotes the non-Newtonian stress which acts as Lagrange multiplier to the rigidity constraint in (2.7a). It can be expressed as symmetric gradient field of the three-dimensional unknown $\boldsymbol{\lambda} : \mathcal{E}(t)\times\mathbb{R}_0^+ \to \mathbb{R}^3$, i.e., $\mathbf{T} = \mathbf{T}[\boldsymbol{\lambda}] = \nabla\boldsymbol{\lambda}+\nabla\boldsymbol{\lambda}^T$ [99]. Given the solution $\boldsymbol{c}, \mathbf{R}$ and $\boldsymbol{u}$ of (2.6), we use (2.2) as well as Lemma A.55 which simplifies (2.7) to a boundary value problem for $\mathbf{T}$, resp. $\boldsymbol{\lambda}$:

$$\rho_p \left(\left(\frac{\mathrm{d}^2}{\mathrm{d}t^2}\mathbf{R} \right) \cdot \mathbf{R}^T \cdot (\boldsymbol{x} - \boldsymbol{c}) + \frac{\mathrm{d}}{\mathrm{d}t}\boldsymbol{v} \right) = \nabla \cdot \mathbf{T}[\boldsymbol{\lambda}]^T + \rho_p g \boldsymbol{e}_g \,, \qquad \boldsymbol{x} \in \mathcal{E}(t) \,, \qquad (2.8\text{a})$$

$$\mathbf{T}[\boldsymbol{\lambda}] \cdot \boldsymbol{n} = \mathbf{S}[\boldsymbol{u}] \cdot \boldsymbol{n} \,, \qquad \boldsymbol{x} \in \partial\mathcal{E}(t) \,. \qquad (2.8\text{b})$$

Remark 1. *There are other possibilities of an extension of stresses and velocities to the particle domain. One is to consider $\mathcal{E}$ as a part of the fluid domain and use singularity solutions which express the Stokes solutions by means of the Oseen-Burgers tensor (Green's dyadic) [72]. Solutions of this kind have the disadvantage of not being bounded in the neighborhood of the origin, which is an important requirement in our modeling as we will see in Section 3. Alternatively, one could also think of a continuous extension of the Dirichlet conditions (2.6b) to $\mathcal{E}$ and model the stresses as Newtonian. This leads to a discontinuity in the stresses at the particle boundary which contradicts the desire for at least a continuous macroscopic stress on Ω.*

2.2.5 Dimensionless formulation

In order to analyze the problem we introduce characteristic scales of the system and derive the dimensionless formulation of the problem. In order to keep a simple notation we do not distinguish between the physical quantities equipped with units and non-dimensionalized functions which will be used from here on. We model a small freely moving particle in an ambient fluid. Therefore, we assume that the particle and fluid motion take place on the same time and space scale, whereas the size of the particle domain is much smaller than that of the fluid domain. Hence, we set $\overline{x}, \overline{y}$ as the characteristic lengths of the fluid and the particle assuming that their ratio fulfills $\epsilon = \overline{y}/\overline{x} \ll 1$. This way, the rigid body motion (2.1) and its inverse become

$$\boldsymbol{x}(\boldsymbol{y}, t; \epsilon) = \epsilon \mathbf{R}(t) \cdot \boldsymbol{y} + \boldsymbol{c}(t) \,, \qquad (2.9\text{a})$$

$$\boldsymbol{y}(\boldsymbol{x}, t; \epsilon) = \epsilon^{-1} \mathbf{R}^T(t) \cdot (\boldsymbol{x} - \boldsymbol{c}(t)) \,. \qquad (2.9\text{b})$$

This also implies that the time-dependent particle domain is ϵ-dependent, which we emphasize by the corresponding subscript, i.e., $\mathcal{E}_\epsilon(t) = \boldsymbol{x}(\mathcal{E}, t; \epsilon)$ with the reference

particle domain $\mathcal{E}$ being independent of ϵ. In particular, the volume fulfills $|\mathcal{E}_\epsilon(t)| = \epsilon^3|\mathcal{E}|$. Consistently also the fluid domain containing the small particle is denoted by $\Omega_\epsilon(t) = \Omega \setminus \overline{\mathcal{E}}_\epsilon(t)$ with ϵ-independent domain Ω.

Using $\overline{u}$ as the characteristic velocity of both, particle and fluid motion and $\overline{t} = \overline{x}/\overline{u}$ as characteristic time, we introduce the dimensionless quantities which characterize the system. The Reynolds number which describes the ratio of inertial and viscous forces of the fluid is given as $\mathrm{Re} = \rho_f \overline{u}\overline{x}/\mu_f$. The Froude number describing the ratio of inertial and gravitational effects is set as $\mathrm{Fr} = \overline{u}/\sqrt{\overline{x}g}$. Finally, we scale the pressure by $\overline{p} = \overline{u}\mu_f/\overline{x}$ and arrive at the dimensionless system

$$\mathrm{Re}\, \mathrm{D}_t \boldsymbol{u} = \nabla \cdot \mathbf{S}[\boldsymbol{u}]^T + \mathrm{Re}\, \mathrm{Fr}^{-2}\, \boldsymbol{e}_g \,, \quad \nabla \cdot \boldsymbol{u} = 0 \,, \quad \boldsymbol{x} \in \Omega_\epsilon \,, \qquad (2.10\mathrm{a})$$

$$\boldsymbol{u} = \boldsymbol{\omega} \times (\boldsymbol{x} - \boldsymbol{c}) + \boldsymbol{v} \,, \qquad\qquad\qquad \boldsymbol{x} \in \partial\mathcal{E}_\epsilon \,, \qquad (2.10\mathrm{b})$$

$$\frac{\mathrm{d}}{\mathrm{d}t}\boldsymbol{c} = \boldsymbol{v} \,, \qquad \frac{\mathrm{d}}{\mathrm{d}t}\mathbf{R} = B(\boldsymbol{\omega}) \cdot \mathbf{R} \,, \qquad\qquad (2.10\mathrm{c})$$

$$\rho\epsilon\, \mathrm{Re}\, |\mathcal{E}|\frac{\mathrm{d}}{\mathrm{d}t}\boldsymbol{v} = \int_{\partial\mathcal{E}} \mathbf{S}[\boldsymbol{u}] \cdot \mathbf{R} \cdot \boldsymbol{n}\, \mathrm{d}s + \rho\epsilon\, \mathrm{Re}\, \mathrm{Fr}^{-2}\, |\mathcal{E}|\boldsymbol{e}_g \,, \qquad (2.10\mathrm{d})$$

$$\rho\epsilon^2\, \mathrm{Re}\, |\mathcal{E}|\frac{\mathrm{d}}{\mathrm{d}t}\left(\mathbf{J} \cdot \boldsymbol{\omega}\right) = \mathbf{R} \cdot \int_{\partial\mathcal{E}} \boldsymbol{y} \times \left(\mathbf{R}^T \cdot \mathbf{S}[\boldsymbol{u}] \cdot \mathbf{R} \cdot \boldsymbol{n}\right)\, \mathrm{d}s \,. \qquad (2.10\mathrm{e})$$

The density ratio of particle and fluid is given by $\rho = \rho_p/\rho_f$. In contrast to Section 2.2.2 and 2.2.3, the Newtonian stress tensor is given here and in the following by $\mathbf{S}[\boldsymbol{u}] = -p\mathbf{I} + \nabla\boldsymbol{u} + \nabla\boldsymbol{u}^T$. The inertia tensor is given analogously to (2.5). The functions appearing in model (2.10) are assumed being smooth on their respective domains of definition, which allows to use Taylor expansions in order to construct approximations to the complete system. We note that the integrals in (2.10d) and (2.10e) are transformed to the reference domain $\mathcal{E}$, this implies that the Newtonian stress tensor is evaluated at $\boldsymbol{x} = \boldsymbol{x}(\boldsymbol{y}, t; \epsilon)$ with $\boldsymbol{y} \in \mathcal{E}$.

In order to formulate also the boundary value problem for the stress in the particle domain (2.8) in dimensionless form, we scale the non-Newtonian stress tensor analogously to the pressure by $\overline{T} = \mu_f \overline{u}/\overline{x}$. Setting $\mathbf{T}(\boldsymbol{x}, t) = \mathbf{R}(t) \cdot \tilde{\mathbf{T}}(\boldsymbol{y}(\boldsymbol{x}, t; \epsilon), t) \cdot \mathbf{R}^T(t)$ and transforming the equations onto the reference domain $\mathcal{E}$ the system (2.8) becomes

$$\rho\, \mathrm{Re}\left(\frac{\mathrm{d}^2}{\mathrm{d}t^2}\left(\epsilon\mathbf{R}(t) \cdot \boldsymbol{y} + \boldsymbol{c}(t)\right) - \mathrm{Fr}^{-2}\, \boldsymbol{e}_g\right) = \epsilon^{-1}\mathbf{R}(t) \cdot \nabla \cdot \tilde{\mathbf{T}}^T(\boldsymbol{y}, t) \,, \quad \boldsymbol{y} \in \mathcal{E} \,, \qquad (2.11\mathrm{a})$$

$$\mathbf{R}^T(t) \cdot \mathbf{S}[\boldsymbol{u}](\boldsymbol{x}(\boldsymbol{y}, t; \epsilon), t) \cdot \mathbf{R}(t) \cdot \boldsymbol{n} = \tilde{\mathbf{T}}(\boldsymbol{y}, t) \cdot \boldsymbol{n} \,, \qquad\qquad \boldsymbol{y} \in \partial\mathcal{E} \,. \quad (2.11\mathrm{b})$$

2.3 Asymptotic approaches

In this section we use formal asymptotic expansions to derive an approximation of the solution to the system (2.10). We generalize the asymptotic approach of [71] by taking into account particle inertia. In order to do this, we first introduce a classification of inertial regimes considered in this work.

2.3.1 Tracer particles of different inertial type

As we will state in Lemma 4, our asymptotic approach results in particles which mainly follow the streamlines of the surrounding fluid. Hence, we refer to them as "tracer

$\alpha_\rho(\epsilon) = \epsilon^r$	Name of type	Behavior of density ratio
$r \geq 1$	light weighted tracer particles	$\rho_\epsilon \to 0$
$r = 0$	normal tracer particles	$\rho_\epsilon \equiv \mathrm{const}$
$r = -1$	heavy tracer particles	$\rho_\epsilon \to \infty$

Table 2.1.: Classification of inertial types by means of the density scaling function for $\epsilon \to 0$, cf. (2.12).

particles" (TP). To distinguish between different types of inertial regimes, we introduce an ϵ-dependent density scaling function $\alpha_\rho(\epsilon)$ and consider an ϵ-dependent density ratio ρ_ϵ given by

$$\rho_\epsilon = \alpha_\rho(\epsilon)\rho\,. \tag{2.12}$$

The freely selectable density scaling function has no physical meaning, but allows to balance the inertial terms in the particle momentum balance in different ways by replacing the actual density ratio in (2.10) and (2.11) with ρ_ϵ. This yields several models of inertial particles. In particular, we set $\alpha_\rho(\epsilon) = \epsilon^r$, $r \in \mathbb{Z}$, and define three inertial regimes with respect to the behavior of the density ratio in the limit $\epsilon \to 0$, i.e., heavy ($r = -1$), normal ($r = 0$) and light weighted ($r \geq 1$) tracer particles, see Table 2.1. For $r = 0$ the density ratio satisfies $\rho_\epsilon \equiv \mathrm{const}$ leading to the inertia-free particle model that was investigated in [71]. The cases $r \leq -2$ are not covered by the asymptotic simplification as we will comment on in Remark 7.

2.3.2 Asymptotic expansion

We assume that under the considered inertia types the particle influences the carrier flow locally but not globally. This way we follow [71] and make the following assumptions.

Assumption 2 (Particle-fluid interaction).

1) *The fluid is essentially undisturbed by the particle.*

2) *The fluid motion induces a rotation of the particle of $\mathcal{O}(1)$.*

3) *The particle is far away from the boundary of the fluid domain $\partial\Omega$.*

In particular, Assumption 2 implies that the fluid velocity, pressure, and the particle motion described by (2.10) raise from an undisturbed Navier-Stokes problem on the complete domain Ω whose velocity and pressure, $(\boldsymbol{u}_0, p_0) : \Omega \times \mathbb{R}_0^+ \to \mathbb{R}^3 \times \mathbb{R}$ are given by

$$\mathrm{Re}\,\mathrm{D}_t \boldsymbol{u}_0 = \nabla \cdot \mathbf{S}[\boldsymbol{u}_0]^T + \mathrm{Re}\,\mathrm{Fr}^{-2}\,\boldsymbol{e}_g\,, \qquad \nabla \cdot \boldsymbol{u}_0 = 0 \tag{2.13}$$

for $(\boldsymbol{x}, t) \in \Omega \times \mathbb{R}^+$ with prescribed initial and boundary conditions. The initial as well as the boundary conditions on $\partial\mathcal{E}_\epsilon(t)$ of $\boldsymbol{u}$ are then derived from $\boldsymbol{u}_0$ and it holds $\boldsymbol{u} = \boldsymbol{u}_0$ on $\partial\Omega$. The relation of the disturbed to the undisturbed problem is investigated in the following asymptotic analysis.

For the quantities of the particle we take a regular expansion in powers of ϵ, while the fields of the fluid flow are separated in a global and a local part:

$$\boldsymbol{a} = \sum_{i=0}^{\infty} \epsilon^i \boldsymbol{a}_i \quad \text{for } \boldsymbol{a} \in \{\boldsymbol{c}, \boldsymbol{v}, \boldsymbol{\omega}, \mathbf{R}\}, \quad \boldsymbol{u} = \boldsymbol{u}_0 + \mathbf{R} \cdot \boldsymbol{u}_{\mathrm{loc}}, \quad p = p_0 + p_{\mathrm{loc}}.$$

The local fields of the fluid quantities are expressed in the local coordinates of the particle reference state

$$\boldsymbol{u}_{\mathrm{loc}}(\boldsymbol{x}, t; \epsilon) = \sum_{i=1}^{\infty} \epsilon^i \boldsymbol{u}_{\mathrm{loc},i}(\boldsymbol{y}(\boldsymbol{x}, t; \epsilon), t), \quad p_{\mathrm{loc}}(\boldsymbol{x}, t; \epsilon) = \sum_{i=1}^{\infty} \epsilon^{i-1} p_{\mathrm{loc},i}(\boldsymbol{y}(\boldsymbol{x}, t; \epsilon), t).$$

The scaling is chosen in such a way that the gradient of the pressure balances the Laplacian of the velocity. It is a consequence of the fact that the bijective mapping between the reference and time-dependent state is ϵ-dependent, see (2.9b). (This way the chain rule generates a factor of ϵ^{-1} every time $\boldsymbol{u}_{\mathrm{loc}}$ is being differentiated with respect to $\boldsymbol{x}$ or t.)

In order to derive an asymptotic system for the description of the non-Newtonian stresses in the particle domain described by (2.11), we set $\tilde{\mathbf{T}}$ similar to the fluid quantities as a composition of the Newtonian stress of $\boldsymbol{u}_0$ and some disturbance,

$$\tilde{\mathbf{T}}(\boldsymbol{y}, t; \epsilon) = \mathbf{R}^T(t) \cdot \mathbf{S}[\boldsymbol{u}_0](\boldsymbol{x}(\boldsymbol{y}, t; \epsilon), t) \cdot \mathbf{R}(t) + \mathbf{T}_{\mathrm{loc}}(\boldsymbol{y}, t; \epsilon). \tag{2.14}$$

The asymptotic expansion of $\mathbf{T}_{\mathrm{loc}}$ is then chosen analogously to the local pressure p_{loc}.

2.3.3 Asymptotic analysis

Our goal is to formulate a solution of the complete system (2.10) up to an error of $\mathcal{O}(\epsilon)$. Therefore, we consider only a finite number of asymptotic coefficients in the expansions. To address them we set

$$\boldsymbol{a}^e = \sum_{i=0}^{2} \epsilon^i \boldsymbol{a}_i \quad \text{for } \boldsymbol{a} \in \{\boldsymbol{c}, \boldsymbol{v}\}, \qquad \boldsymbol{a}^e = \sum_{i=0}^{1} \epsilon^i \boldsymbol{a}_i \quad \text{for } \boldsymbol{a} \in \{\boldsymbol{\omega}, \mathbf{R}\}, \tag{2.15a}$$

$$\boldsymbol{u}^e = \boldsymbol{u}_0 + \mathbf{R}^e \sum_{i=1}^{2} \epsilon^i \boldsymbol{u}_{\mathrm{loc},i}, \qquad p^e = p_0 + \sum_{i=1}^{2} \epsilon^{i-1} p_{\mathrm{loc},i}. \tag{2.15b}$$

Inserting the truncated expansion into (2.9) yields the following form of the bijective mapping between the reference and the time-dependent state:

$$\boldsymbol{x}^e(\boldsymbol{y}, t; \epsilon) = \epsilon \mathbf{R}^e(t; \epsilon) \cdot \boldsymbol{y} + \boldsymbol{c}^e(t; \epsilon), \quad \boldsymbol{y}^e(\boldsymbol{x}, t; \epsilon) = \epsilon^{-1} (\mathbf{R}^e(t; \epsilon))^{-1} \cdot (\boldsymbol{x} - \boldsymbol{c}^e(t; \epsilon)).$$

It is shown in ([71], Lemma 5) that $(\mathbf{R}^e)^{-1} = (\mathbf{R}^e)^T + \mathcal{O}(\epsilon^2)$ and $\| (\mathbf{R}^e)^{-1} \| = \mathcal{O}(1)$, thus $\boldsymbol{y}^e$ is well-defined. The asymptotic coefficients of the mapping $\boldsymbol{x}^e$ are particularly given by

$$\boldsymbol{x}^e(\boldsymbol{y}, t; \epsilon) = \sum_{i=0}^{2} \epsilon^i \boldsymbol{x}_i(\boldsymbol{y}, t),$$

$$\text{with } \boldsymbol{x}_0(\boldsymbol{y}, t) \equiv \boldsymbol{c}_0(t), \quad \boldsymbol{x}_i(\boldsymbol{y}, t) = \mathbf{R}_{i-1}(t) \cdot \boldsymbol{y} + \boldsymbol{c}_i(t), \quad i = 1, 2.$$

Moreover, in the following we use Taylor expansions for smooth functions of the form $f(\boldsymbol{x}(\boldsymbol{y}, t; \epsilon))$ in $\boldsymbol{c}_0$, i.e.,

$$
\begin{aligned}
f(\boldsymbol{x}) &= f(\boldsymbol{c}_0) + \left[\left(\epsilon \boldsymbol{x}_1 + \epsilon^2 \boldsymbol{x}_2 \right) \cdot \nabla \right] f(\boldsymbol{c}_0) \\
&\quad + 0.5 \left[\left(\epsilon \boldsymbol{x}_1 + \epsilon^2 \boldsymbol{x}_2 \right) \otimes \left(\epsilon \boldsymbol{x}_1 + \epsilon^2 \boldsymbol{x}_2 \right) : \nabla^2 \right] f(\boldsymbol{c}_0) + \mathcal{O}(\epsilon^3) \\
&= \sum_{i=0}^{2} \epsilon^i \mathrm{D}_i f(\boldsymbol{c}_0) + \mathcal{O}(\epsilon^3),
\end{aligned}
$$

with the differential operators $\mathrm{D}_i = \mathrm{D}_i(\boldsymbol{y}, t)$ determined as

$$\mathrm{D}_0 \equiv 1, \qquad \mathrm{D}_1 = \boldsymbol{x}_1 \cdot \nabla, \qquad \mathrm{D}_2 = \boldsymbol{x}_2 \cdot \nabla + 0.5 \boldsymbol{x}_1 \otimes \boldsymbol{x}_1 : \nabla^2.$$

To emphasize the general structure of the asymptotic result in the subsequent lemma and to stress the relevance of certain terms which appear in a similar way in the context of suspension modeling in Section 3.3.2 we introduce abbreviations for some expressions.

Abbreviation 3. *Throughout this chapter we consider the following model-relevant functions for $\alpha_\rho(\epsilon) = \epsilon^r$, $r \geq -1$, they describe Dirichlet conditions $\boldsymbol{h}_i$, force contributions $\boldsymbol{f}_i$ and torque contributions $\boldsymbol{g}_i$:*

$$\boldsymbol{h}_1 = \mathbf{R}_0^T \cdot \left(\boldsymbol{v}_1 + B(\boldsymbol{\omega}_0) \cdot \mathbf{R}_0 \cdot \boldsymbol{y} - \mathrm{D}_1 \boldsymbol{u}_0 \right),$$

$$\boldsymbol{h}_2 = \mathbf{R}_0^T \cdot \left(\boldsymbol{v}_2 + (B(\boldsymbol{\omega}_0) \cdot \mathbf{R}_1 + B(\boldsymbol{\omega}_1) \cdot \mathbf{R}_0) \cdot \boldsymbol{y} - \mathrm{D}_2 \boldsymbol{u}_0 - \mathbf{R}_1 \cdot \boldsymbol{u}_{\mathrm{loc},1} \right),$$

$$\boldsymbol{f}_1 = \begin{cases} \boldsymbol{0}, & r \geq 0 \\ \boldsymbol{k}_0, & r = -1 \end{cases},$$

$$\boldsymbol{f}_2 = -\mathbf{R}_0^T \cdot \mathbf{R}_1 \cdot \boldsymbol{f}_1 - |\mathcal{E}| \mathbf{R}_0^T \cdot \nabla \cdot \mathbf{S}[\boldsymbol{u}_0]^T + \begin{cases} \boldsymbol{0}, & r \geq 1 \\ \boldsymbol{k}_0, & r = 0 \\ \boldsymbol{k}_1, & r = -1 \end{cases},$$

$$\boldsymbol{g}_1 = \boldsymbol{0}, \quad r \geq -1,$$

$$\boldsymbol{g}_2 = -\mathbf{R}_0^T \cdot \mathbf{R}_1 \cdot \boldsymbol{g}_1 - \int_{\partial\mathcal{E}} \boldsymbol{y} \times \left(\mathbf{R}_0^T \cdot \mathrm{D}_1 \mathbf{S}[\boldsymbol{u}_0] \cdot \mathbf{R}_0 \cdot \boldsymbol{n} \right) \mathrm{d}s + \begin{cases} \boldsymbol{0}, & r \geq 0 \\ \boldsymbol{\ell}_0, & r = -1 \end{cases},$$

where the linear and angular accelerations, $\boldsymbol{k}_i$ resp. $\boldsymbol{\ell}_0$ are abbreviated by

$$\boldsymbol{k}_0 = \rho |\mathcal{E}| \mathbf{R}_0^T \cdot \nabla \cdot \mathbf{S}[\boldsymbol{u}_0], \quad \boldsymbol{k}_1 = \rho \operatorname{Re} |\mathcal{E}| \mathbf{R}_0^T \cdot \frac{\mathrm{d}}{\mathrm{d}t} \boldsymbol{v}_1,$$

$$\boldsymbol{\ell}_0 = \rho \operatorname{Re} |\mathcal{E}| \mathbf{R}_0^T \cdot \frac{\mathrm{d}}{\mathrm{d}t} \left(\mathbf{R}_0 \cdot \hat{\mathbf{J}} \cdot \mathbf{R}_0^T \cdot \boldsymbol{\omega}_0 \right).$$

The derivatives of the global flow $\boldsymbol{u}_0$ and the Newtonian stresses are evaluated in $\boldsymbol{c}_0$.

Lemma 4 (Asymptotic one-particle model). *Assume that the following four requirements (R1)-(R4) hold, then $\boldsymbol{u}^e$, p^e, $\boldsymbol{c}^e$, $\boldsymbol{v}^e$, $\boldsymbol{\omega}^e$, and $\mathbf{R}^e$ defined in (2.15) are a solution of the complete system (2.10) up to an order of $\mathcal{O}(\epsilon)$ for $\epsilon \downarrow 0$.*

(R1) *The global flow velocity $\boldsymbol{u}_0$ and pressure p_0 are smooth solutions of the incompressible Navier-Stokes equations (2.13) with prescribed boundary conditions on $\partial\Omega$ and a sufficiently smooth initial condition $\boldsymbol{u}_0(.,0)$.*

(R2) *The particle related coefficients satisfy the following set of conditions: The center of mass obeys*

$$\frac{\mathrm{d}}{\mathrm{d}t}\boldsymbol{c}_i(t) = \boldsymbol{v}_i(t)\,, \quad i = 0,1,2 \tag{2.16a}$$

with the initial conditions $\boldsymbol{c}_0(0) = \boldsymbol{c}(0)$, $\boldsymbol{c}_i(0) = \boldsymbol{0}$, $i = 1,2$ and with the zero-order velocity fulfilling the so-called "tracer condition"

$$\boldsymbol{v}_0(t) = \boldsymbol{u}_0(\boldsymbol{c}_0(t),t)\,. \tag{2.16b}$$

Additionally, the matrices $\mathbf{R}_0$, $\mathbf{R}_1$ solve the differential equations

$$\frac{\mathrm{d}}{\mathrm{d}t}\mathbf{R}_0 = B(\boldsymbol{\omega}_0)\cdot\mathbf{R}_0\,, \qquad \frac{\mathrm{d}}{\mathrm{d}t}\mathbf{R}_1 = B(\boldsymbol{\omega}_1)\cdot\mathbf{R}_0 + B(\boldsymbol{\omega}_0)\cdot\mathbf{R}_1 \tag{2.16c}$$

with the initial conditions $\mathbf{R}_0(0) = \mathbf{R}(0)$ and $\mathbf{R}_1(0) = \boldsymbol{0}$.

(R3) *For every $t > 0$ the local fields indicated by $i = 1,2$ solve the stationary Stokes equations on the unbounded exterior of $\mathcal{E}$*

$$\nabla p_{\mathrm{loc},i} = \Delta\boldsymbol{u}_{\mathrm{loc},i}\,, \qquad \nabla\cdot\boldsymbol{u}_{\mathrm{loc},i} = 0 \tag{2.17a}$$

with the following Dirichlet, integral and decay conditions

$$\boldsymbol{u}_{\mathrm{loc},i}(\boldsymbol{y},t) = \boldsymbol{h}_i(\boldsymbol{y},t)\,, \quad \boldsymbol{y}\in\partial\mathcal{E}\,, \tag{2.17b}$$

$$\int_{\partial\mathcal{E}}\mathbf{S}[\boldsymbol{u}_{\mathrm{loc},i}]\cdot\boldsymbol{n}\,\mathrm{d}s = \boldsymbol{f}_i\,, \tag{2.17c}$$

$$\int_{\partial\mathcal{E}}\boldsymbol{y}\times(\mathbf{S}[\boldsymbol{u}_{\mathrm{loc},i}]\cdot\boldsymbol{n})\,\mathrm{d}s = \boldsymbol{g}_i\,, \tag{2.17d}$$

$$\|\boldsymbol{u}_{\mathrm{loc},i}\| \in \mathcal{O}(\|\boldsymbol{y}\|^{-1})\,, \qquad \|\nabla\boldsymbol{u}_{\mathrm{loc},i}\|, |p_{\mathrm{loc},i}| \in \mathcal{O}(\|\boldsymbol{y}\|^{-2}) \quad as\ \|\boldsymbol{y}\|\to\infty\,. \tag{2.17e}$$

The functions $\boldsymbol{h}_i$, $\boldsymbol{f}_i$, and $\boldsymbol{g}_i$ are given in Abbreviation 3.

(R4) *The density scaling function (2.12) is given as $\alpha_\rho(\epsilon) = \epsilon^r$ with $r \geq -1$.*

Proof. The proof results from a straight forward computation where the asymptotic coefficients are inserted into the full system (2.10) and Taylor expansions are applied for the global flow fields, whenever they are evaluated at the particle boundary as carried out in [71] for normal tracer particles. The introduction of the different inertial types does not change the general mathematical structure of the problem but only affects the linear and angular momentum balances of the particle, i.e., the functions $\boldsymbol{f}_i$, $\boldsymbol{g}_i$ in (R3). We sketch the steps of the proof for the sake of completeness.

Inserting the asymptotic expansions for $\boldsymbol{c}$, $\boldsymbol{v}$, $\boldsymbol{\omega}$ and $\mathbf{R}$ in (2.10c) and applying (2.16a), (2.16c) shows that the particle kinematics (2.10c) is fulfilled up to an order of $\mathcal{O}(\epsilon^2)$.

The conservation of mass in (2.10a) is fulfilled exactly since each local velocity field is assumed to be divergence-free.

Considering the no-slip equation (2.10b), the use of the asymptotic expansions and the Taylor series of $\boldsymbol{u}_0$ in $\boldsymbol{c}_0$ results in the following conditions that are exactly the Dirichlet conditions of $\boldsymbol{u}_{\mathrm{loc},i}$ (2.17b) and the tracer condition (2.16b),

$$\boldsymbol{u}_0(\boldsymbol{c}_0(t),t) = \boldsymbol{v}_0\,,$$
$$\mathbf{R}_0 \cdot \boldsymbol{u}_{\mathrm{loc},1}(\boldsymbol{y},t) = \boldsymbol{v}_1 + B(\boldsymbol{\omega}_0) \cdot \mathbf{R}_0 \cdot \boldsymbol{y} - \mathrm{D}_1 \boldsymbol{u}_0(\boldsymbol{c}_0(t),t)\,,$$
$$\mathbf{R}_0 \cdot \boldsymbol{u}_{\mathrm{loc},2}(\boldsymbol{y},t) = \boldsymbol{v}_2 + (B(\boldsymbol{\omega}_0) \cdot \mathbf{R}_1 + B(\boldsymbol{\omega}_1) \cdot \mathbf{R}_0) \cdot \boldsymbol{y} - \mathrm{D}_2 \boldsymbol{u}_0(\boldsymbol{c}_0(t),t) - \mathbf{R}_1 \cdot \boldsymbol{u}_{\mathrm{loc},1}(\boldsymbol{y},t)\,.$$

Inserting the asymptotic expansion in the momentum equation of the fluid and applying the chain rule for the local fields yields

$$\mathrm{Re}(\partial_t \boldsymbol{u}_0 + (\boldsymbol{u}_0 \cdot \nabla)\boldsymbol{u}_0) - \nabla \cdot \mathbf{S}[\boldsymbol{u}_0]^T - \mathrm{Re}\,\mathrm{Fr}^{-2}\,\boldsymbol{e}_g$$
$$= \mathbf{R}^e \cdot \nabla \cdot \left(\epsilon^{-1}\mathbf{S}[\boldsymbol{u}_{\mathrm{loc},1}]^T + \mathbf{S}[\boldsymbol{u}_{\mathrm{loc},2}]^T\right) + \mathcal{O}(\epsilon)\,.$$

Since $\boldsymbol{u}_0$ satisfies the Navier-Stokes equations and the local fields satisfy the stationary Stokes equations according to (R1) and (R3), the momentum balance holds up to an error of $\mathcal{O}(\epsilon)$.

As for the momentum balances of the particle, we insert the asymptotic expansion on both sides of the equations. On the right-hand side we use a Taylor series for the term $\mathbf{S}[\boldsymbol{u}_0]$ in $\boldsymbol{c}_0$ and keep the integrals for the local fields, this leads to

$$\rho\,\mathrm{Re}\,|\mathcal{E}|\epsilon^{r+1}\mathbf{R}_0^T \cdot \left(\frac{\mathrm{d}}{\mathrm{d}t}\boldsymbol{v}_0 - \frac{1}{\mathrm{Fr}^2}\boldsymbol{e}_g + \epsilon\frac{\mathrm{d}}{\mathrm{d}t}\boldsymbol{v}_1\right) \qquad (2.18a)$$
$$= \int_{\partial\mathcal{E}} \mathbf{S}[\boldsymbol{u}_{\mathrm{loc},1}] \cdot \boldsymbol{n}\,\mathrm{d}s + \epsilon \int_{\partial\mathcal{E}} \left(\mathbf{R}_0^T \cdot \mathrm{D}_1\mathbf{S}[\boldsymbol{u}_0] \cdot \mathbf{R}_0 + \mathbf{R}_0^T \cdot \mathbf{R}_1 \cdot \mathbf{S}[\boldsymbol{u}_{\mathrm{loc},1}] + \mathbf{S}[\boldsymbol{u}_{\mathrm{loc},2}]\right) \cdot \boldsymbol{n}\,\mathrm{d}s$$

for the linear momentum and

$$\rho\,\mathrm{Re}\,|\mathcal{E}|\epsilon^{r+2}\mathbf{R}_0^T \cdot \left(\frac{\mathrm{d}}{\mathrm{d}t}\left(\mathbf{R}_0 \cdot \hat{\mathbf{J}} \cdot \mathbf{R}_0^T \cdot \boldsymbol{\omega}_0\right)\right.$$
$$\left. + \epsilon\frac{\mathrm{d}}{\mathrm{d}t}\left(\mathbf{R}_0 \cdot \hat{\mathbf{J}} \cdot \mathbf{R}_0^T \cdot \boldsymbol{\omega}_1 + \left(\mathbf{R}_0 \cdot \hat{\mathbf{J}} \cdot \mathbf{R}_1^T + \mathbf{R}_1 \cdot \hat{\mathbf{J}} \cdot \mathbf{R}_0^T\right) \cdot \boldsymbol{\omega}_0\right)\right)$$
$$= \int_{\partial\mathcal{E}} \boldsymbol{y} \times \mathbf{S}[\boldsymbol{u}_{\mathrm{loc},1}] \cdot \boldsymbol{n}\,\mathrm{d}s + \epsilon\left(\int_{\partial\mathcal{E}} \boldsymbol{y} \times \left(\mathbf{R}_0^T \cdot \mathrm{D}_1\mathbf{S}[\boldsymbol{u}_0] \cdot \mathbf{R}_0 + \mathbf{S}[\boldsymbol{u}_{\mathrm{loc},2}]\right) \cdot \boldsymbol{n}\,\mathrm{d}s\right.$$
$$\left. + \mathbf{R}_0^T \cdot \mathbf{R}_1 \cdot \int_{\partial\mathcal{E}} \boldsymbol{y} \times \left(\mathbf{S}[\boldsymbol{u}_{\mathrm{loc},1}] \cdot \boldsymbol{n}\right)\mathrm{d}s\right) \qquad (2.18b)$$

for the angular momentum. In combination with the tracer condition (2.16b) and the Navier-Stokes equations (2.13), these form exactly the integral conditions (2.17c) and (2.17d).

The requirement (R4) is needed to avoid contradictory conditions as we explain in Remark 7. $\qquad\square$

In Lemma 4 we assume that (R3) is fulfilled despite the fact that the problem seems to be overdetermined at first glance by the presence of Dirichlet as well as integral conditions on $\partial\mathcal{E}$. In fact, Remark B.9 in Appendix B.2 shows that there is a one-to-one relation between the forces and torques $\boldsymbol{f}_i, \boldsymbol{g}_i$ and the velocity at the particle boundary $\boldsymbol{h}_i$. This relationship yields a system of ordinary differential equations for the asymptotic coefficients of the particle position and orientation as we will comment on in Remark 6. The coupling is given by the following Lemma.

Lemma 5 (Solvability conditions of Stokes problem). *Let $\boldsymbol{w}_q$, p_q, $q = 1, \ldots, 6$, be the solutions of the following six stationary Stokes problems related to the boundary conditions of the three elementary translations and rotations:*

$$\nabla \cdot \mathbf{S}[\boldsymbol{w}_q]^T = \mathbf{0}\,, \qquad \nabla \cdot \boldsymbol{w}_q = 0\,, \qquad q = 1, \ldots, 6\,, \quad \boldsymbol{y} \in \mathbb{R}^3 \setminus \overline{\mathcal{E}}\,,$$

$$\boldsymbol{w}_q = \boldsymbol{e}_q\,, \qquad \boldsymbol{w}_{q+3} = \mathbf{B}_q \cdot \boldsymbol{y}\,, \quad q = 1, 2, 3\,, \qquad \boldsymbol{y} \in \partial\mathcal{E}\,,$$

$$\|\boldsymbol{w}_q\| \in \mathcal{O}(\|\boldsymbol{y}\|^{-1})\,, \quad \|\nabla \boldsymbol{w}_q\|, |p_q| \in \mathcal{O}(\|\boldsymbol{y}\|^{-2})\,, \quad \|\boldsymbol{y}\| \to \infty\,, \qquad (2.19)$$

with $\{\mathbf{B}_q\}_q$ denoting the basis of skew-symmetric matrices in $\mathbb{R}^{3\times 3}$ given in (A.8b) in App. A.2. Set the following surface moments associated with $\boldsymbol{w}_q$, $q = 1, \ldots, 6$ to be

$$\boldsymbol{s}_q = \int_{\partial\mathcal{E}} \boldsymbol{y} \times (\mathbf{S}[\boldsymbol{w}_q] \cdot \boldsymbol{n})\, \mathrm{d}s\,, \qquad \boldsymbol{t}_q = \int_{\partial\mathcal{E}} (\mathbf{S}[\boldsymbol{w}_q] \cdot \boldsymbol{n})\, \mathrm{d}s\,,$$

$$\mathbf{V}_q = \int_{\partial\mathcal{E}} \boldsymbol{y} \otimes (\mathbf{S}[\boldsymbol{w}_q] \cdot \boldsymbol{n})\, \mathrm{d}s\,, \qquad W_q = \int_{\partial\mathcal{E}} \boldsymbol{y} \otimes \boldsymbol{y} \otimes (\mathbf{S}[\boldsymbol{w}_q] \cdot \boldsymbol{n})\, \mathrm{d}s\,.$$

1) *Let (R3) of Lemma 4 be fulfilled, then the following solvability conditions hold:*

$$\begin{pmatrix} \boldsymbol{s}_q \\ \boldsymbol{t}_q \end{pmatrix} \cdot \begin{pmatrix} \mathbf{R}_0^T \cdot \boldsymbol{\omega}_0 \\ \mathbf{R}_0^T \cdot \boldsymbol{v}_1 \end{pmatrix} \qquad\qquad\qquad\qquad (2.20\mathrm{a})$$

$$= \left(\mathbf{R}_0^T \cdot \partial_{\boldsymbol{x}} \boldsymbol{u}_0^T \cdot \mathbf{R}_0\right) : \mathbf{V}_q + \left(\mathbf{R}_0^T \cdot \partial_{\boldsymbol{x}} \boldsymbol{u}_0 \cdot \boldsymbol{c}_1\right) \cdot \boldsymbol{t}_q + \begin{cases} \boldsymbol{e}_q \cdot \boldsymbol{f}_1 & q = 1, 2, 3 \\ \boldsymbol{e}_{q-3} \cdot \boldsymbol{g}_1/\sqrt{2} & q = 4, 5, 6 \end{cases},$$

$$\begin{pmatrix} \boldsymbol{s}_q \\ \boldsymbol{t}_q \end{pmatrix} \cdot \begin{pmatrix} \mathbf{R}_0^T \cdot \boldsymbol{\omega}_1 \\ \mathbf{R}_0^T \cdot \boldsymbol{v}_2 \end{pmatrix} \qquad\qquad\qquad\qquad (2.20\mathrm{b})$$

$$= \left(\mathbf{R}_1^T \cdot \left(B(\boldsymbol{\omega}_0) + \partial_{\boldsymbol{x}} \boldsymbol{u}_0^T\right) \cdot \mathbf{R}_0 - \mathbf{R}_0^T \cdot \left(B(\boldsymbol{\omega}_0) + \partial_{\boldsymbol{x}} \boldsymbol{u}_0^T\right) \cdot \mathbf{R}_0 \cdot \mathbf{R}_1^T \cdot \mathbf{R}_0 + \mathbf{L}\right) : \mathbf{V}_q$$

$$+ \left(\mathbf{R}_0^T \cdot \left(\mathbf{R}_1 \cdot \mathbf{R}_0^T \cdot \left(\boldsymbol{v}_1 - \partial_{\boldsymbol{x}} \boldsymbol{u}_0 \cdot \boldsymbol{c}_1\right) + 0.5[\boldsymbol{c}_1 \otimes \boldsymbol{c}_1 : \nabla^2]\boldsymbol{u}_0 + \partial_{\boldsymbol{x}} \boldsymbol{u}_0 \cdot \boldsymbol{c}_2\right)\right) \cdot \boldsymbol{t}_q$$

$$+ \sum_{k,\ell,m} K_{k\ell m}(W_q)_{k\ell m} + \begin{cases} \boldsymbol{e}_q \cdot \boldsymbol{f}_2 & q = 1, 2, 3 \\ \boldsymbol{e}_{q-3} \cdot \boldsymbol{g}_2/\sqrt{2} & q = 4, 5, 6 \end{cases}$$

with $(\mathbf{R}_0)_{ij} = \boldsymbol{e}_i \cdot \boldsymbol{p}_j$, $(\mathbf{L})_{ij} = [\boldsymbol{p}_i \otimes \boldsymbol{c}_1 : \nabla^2](\boldsymbol{u}_0 \cdot \boldsymbol{p}_j)$ and with the third order tensor $K_{k\ell m} = 0.5[\boldsymbol{p}_k \otimes \boldsymbol{p}_\ell : \nabla^2](\boldsymbol{u}_0 \cdot \boldsymbol{p}_m)$.

2) *Let (2.20) hold. Let $(\boldsymbol{u}_{\mathrm{loc},i}, p_{\mathrm{loc},i})$ be the solution of the stationary Stokes problem (2.17a) with the Dirichlet condition (2.17b) and with the decay property (2.17e), then the integral conditions (2.17c) and (2.17d) are fulfilled.*

3) *Let (2.20) hold. Let $(\boldsymbol{u}_{\mathrm{loc},i}, p_{\mathrm{loc},i})$ be the solution of the stationary Stokes problem (2.17a) with the integral conditions (2.17c) and (2.17d) and with the decay property (2.17e), then the Dirichlet condition (2.17b) is fulfilled.*

4) *The linear systems (2.20) are invertible.*

Proof. The key ingredient for this proof is the existence of the Green formula for solutions of the Stokes problem, Lemma B.1, Appendix B.1 which connects the stresses and boundary conditions of two Stokes solutions and needs the decay properties (2.17e) as well as those in (2.19).

For 1): The equations (2.17c) and (2.17d) are equivalent to

$$\boldsymbol{e}_q \cdot \boldsymbol{f}_i = \boldsymbol{e}_q \cdot \int_{\partial \mathcal{E}} \mathsf{S}[\boldsymbol{u}_{\mathrm{loc},i}] \cdot \boldsymbol{n} \, \mathrm{d}s = \int_{\partial \mathcal{E}} \boldsymbol{w}_q \cdot (\mathsf{S}[\boldsymbol{u}_{\mathrm{loc},i}] \cdot \boldsymbol{n}) \, \mathrm{d}s \,, \tag{2.21a}$$

$$\boldsymbol{e}_q \cdot \boldsymbol{g}_i = \boldsymbol{e}_q \cdot \int_{\partial \mathcal{E}} B(\boldsymbol{y}) \cdot \mathsf{S}[\boldsymbol{u}_{\mathrm{loc},i}] \cdot \boldsymbol{n} \, \mathrm{d}s = \int_{\partial \mathcal{E}} \left(B(\boldsymbol{y})^T \cdot \boldsymbol{e}_q \right) \cdot (\mathsf{S}[\boldsymbol{u}_{\mathrm{loc},i}] \cdot \boldsymbol{n}) \, \mathrm{d}s$$

$$= \int_{\partial \mathcal{E}} (\boldsymbol{e}_q \times \boldsymbol{y}) \cdot (\mathsf{S}[\boldsymbol{u}_{\mathrm{loc},i}] \cdot \boldsymbol{n}) \, \mathrm{d}s = \sqrt{2} \int_{\partial \mathcal{E}} \boldsymbol{w}_{q+3} \cdot (\mathsf{S}[\boldsymbol{u}_{\mathrm{loc},i}] \cdot \boldsymbol{n}) \, \mathrm{d}s \tag{2.21b}$$

for $q = 1, 2, 3$. With the help of the Green formula the roles of $\boldsymbol{w}_q$ and $\boldsymbol{u}_{\mathrm{loc},i}$ in the right-hand sides of (2.21) can be interchanged. Thus, relations (2.21) are equivalent to

$$\boldsymbol{e}_q \cdot \boldsymbol{f}_i = \int_{\partial \mathcal{E}} \boldsymbol{h}_i \cdot \mathsf{S}[\boldsymbol{w}_q] \cdot \boldsymbol{n} \, \mathrm{d}s \,, \quad \frac{1}{\sqrt{2}} \boldsymbol{e}_q \cdot \boldsymbol{g}_i = \int_{\partial \mathcal{E}} \boldsymbol{h}_i \cdot \mathsf{S}[\boldsymbol{w}_{q+3}] \cdot \boldsymbol{n} \, \mathrm{d}s \tag{2.22}$$

for $q = 1, 2, 3$. We note that for $i = 1, 2$ the terms $\boldsymbol{h}_i$ of Abbreviation 3 have the form

$$\boldsymbol{h}_i = \mathbf{R}_0^T \cdot \boldsymbol{v}_i + \mathbf{R}_0^T \cdot B(\boldsymbol{\omega}_{i-1}) \cdot \mathbf{R}_0 \cdot \boldsymbol{y} - \boldsymbol{r}_i = \mathbf{R}_0^T \cdot \boldsymbol{v}_i + B(\mathbf{R}_0^T \cdot \boldsymbol{\omega}_{i-1}) \cdot \boldsymbol{y} - \boldsymbol{r}_i \,,$$

where we used (A.10c), and abbreviated $\boldsymbol{r}_1 = \mathbf{R}_0^T \cdot \mathrm{D}_1 \boldsymbol{u}_0$ as well as $\boldsymbol{r}_2 = \mathbf{R}_0^T \cdot \Big(\mathbf{R}_1 \cdot \boldsymbol{u}_{\mathrm{loc},1} + \mathrm{D}_2 \boldsymbol{u}_0 - B(\boldsymbol{\omega}_0) \cdot \mathbf{R}_1 \cdot \boldsymbol{y} \Big)$. Inserting $\boldsymbol{h}_i$ and sorting the resultant terms with respect to $\boldsymbol{\omega}_{i-1}$ and $\boldsymbol{v}_i$ leads to

$$\left(\mathbf{R}_0^T \cdot \boldsymbol{\omega}_{i-1} \right) \cdot \boldsymbol{s}_q + \left(\mathbf{R}_0^T \cdot \boldsymbol{v}_i \right) \cdot \boldsymbol{t}_q = \int_{\partial \mathcal{E}} \boldsymbol{r}_i \cdot \mathsf{S}[\boldsymbol{w}_q] \cdot \boldsymbol{n} \, \mathrm{d}s + \begin{cases} \boldsymbol{e}_q \cdot \boldsymbol{f}_i & q = 1, 2, 3 \\ \boldsymbol{e}_{q-3} \cdot \boldsymbol{g}_i / \sqrt{2} & q = 4, 5, 6 \end{cases}, \tag{2.23}$$

which directly results in (2.20).

For 2): We consider the relation (2.20) which is equivalent to (2.23) and thus to (2.22) since $\boldsymbol{h}_i$ is the Dirichlet condition of $\boldsymbol{u}_{\mathrm{loc},i}$ by assumption. Applying the Green formula we then get (2.21), which are exactly the integral conditions.

For 3): As already shown (2.20) is equivalent to (2.22). The assumption that the integral conditions are fulfilled is equivalent to (2.21). Combining both results gives the equalities

$$\int_{\partial \mathcal{E}} \boldsymbol{w}_q \cdot (\mathsf{S}[\boldsymbol{u}_{\mathrm{loc},i}] \cdot \boldsymbol{n}) \, \mathrm{d}s = \int_{\partial \mathcal{E}} \boldsymbol{h}_i \cdot \mathsf{S}[\boldsymbol{w}_q] \cdot \boldsymbol{n} \, \mathrm{d}s \,,$$

$$\int_{\partial \mathcal{E}} \boldsymbol{w}_{q+3} \cdot (\mathsf{S}[\boldsymbol{u}_{\mathrm{loc},i}] \cdot \boldsymbol{n}) \, \mathrm{d}s = \int_{\partial \mathcal{E}} \boldsymbol{h}_i \cdot \mathsf{S}[\boldsymbol{w}_{q+3}] \cdot \boldsymbol{n} \, \mathrm{d}s \,.$$

Since $\boldsymbol{u}_{\mathrm{loc},i}$ and $\boldsymbol{w}_q$ fulfill the decay property the above equations imply $\boldsymbol{u}_{\mathrm{loc},i} = \boldsymbol{h}_i$ on $\partial \mathcal{E}$ by means of the Green formula.

For 4): Considering the matrix given as $M_{ij} = (\boldsymbol{t}_i, \boldsymbol{s}_i)_j$, $i, j = 1, \ldots, 6$ we immediately find

$$M = \hat{\tilde{A}} \cdot \begin{bmatrix} \mathbf{I} & \\ & \sqrt{2}\mathbf{I} \end{bmatrix}$$

with $\hat{\tilde{A}}$ being a negative definite matrix as shown in Remark B.9 in Appendix B.2. This implies linear independence of the six vectors $(\boldsymbol{t}_q, \boldsymbol{s}_q)$, $q = 1, \ldots, 6$, thus the system (2.20) is invertible for all right-hand sides. $\qquad \square$

$\ell \backslash r$	-3	-2	-1	0	1
-2	$\boldsymbol{k}_0 = \boldsymbol{0}$				
-1	$\boldsymbol{k}_1 = \boldsymbol{0}$	$\boldsymbol{k}_0 = \boldsymbol{0}$			
0	$\boldsymbol{k}_2 = \boldsymbol{m}_1^v$	$\boldsymbol{k}_1 = \boldsymbol{m}_1^v$	$\boldsymbol{k}_0 = \boldsymbol{m}_1^v$	$\boldsymbol{0} = \boldsymbol{m}_1^v$	$\boldsymbol{0} = \boldsymbol{m}_1^v$
1	$\boldsymbol{k}_3 = \boldsymbol{m}_2^v$	$\boldsymbol{k}_2 = \boldsymbol{m}_2^v$	$\boldsymbol{k}_1 = \boldsymbol{m}_2^v$	$\boldsymbol{k}_0 = \boldsymbol{m}_2^v$	$\boldsymbol{0} = \boldsymbol{m}_2^v$

$\ell \backslash r$	-3	-2	-1	0	1
-1	$\boldsymbol{\ell}_0 = \boldsymbol{0}$				
0	$\boldsymbol{\ell}_1 = \boldsymbol{m}_1^\omega$	$\boldsymbol{\ell}_0 = \boldsymbol{m}_1^\omega$	$\boldsymbol{0} = \boldsymbol{m}_1^\omega$	$\boldsymbol{0} = \boldsymbol{m}_1^\omega$	$\boldsymbol{0} = \boldsymbol{m}_1^\omega$
1	$\boldsymbol{\ell}_2 = \boldsymbol{m}_2^\omega$	$\boldsymbol{\ell}_1 = \boldsymbol{m}_2^\omega$	$\boldsymbol{\ell}_0 = \boldsymbol{m}_2^\omega$	$\boldsymbol{0} = \boldsymbol{m}_2^\omega$	$\boldsymbol{0} = \boldsymbol{m}_2^\omega$

Table 2.2.: Balances of the accelerations with the integral terms (given in Remark 7) in (2.24) for the different inertial regimes. Each row shows the $\mathcal{O}(\epsilon^\ell)$-correction of the momentum equations and each column corresponds to the choice of the density scaling function $\alpha_\rho(\epsilon) = \epsilon^r$.

Remark 6.

1) *The solvability conditions (2.20) together with the particle related equations (2.16) build a system of nonlinear ordinary differential equations (ODEs) for $\boldsymbol{c}_i$ and $\mathbf{R}_{i-1}$, $i = 1, 2$, where the ODE for the ith asymptotic coefficient depends on lower order coefficients, while the surface moments depend only on the geometry of the particle. The order of the corresponding ODEs depends on the choice of the density scaling function α_ρ. In the case $\alpha_\rho(\epsilon) = \epsilon^{-2}$, for example, $\boldsymbol{f}_1$ depends on $\mathrm{d}\boldsymbol{v}_1/\mathrm{d}t$ and thus the ODE (2.16a) together with (2.20a) becomes second order for $\boldsymbol{c}_1$ with an additional initial condition $\boldsymbol{v}_1(0) = \boldsymbol{0}$. However, under suitable regularity assumptions on $\boldsymbol{u}_0$, the corresponding right-hand sides of the ODE systems are at least continuous and thus at least local solutions exist by Theorem of Peano.*

2) *Solving the solvability conditions of the Stokes problems (2.20) determines the Dirichlet conditions (2.17b). However, it is not our aim to examine the existence, uniqueness and regularity of the Stokes solutions given by (2.17b), (2.17e) in general. Instead, we discuss a very important special case in Section 2.4 where analytical solutions are available.*

3) *Just like in [71], Lemma 4 and 5 imply a procedure for constructing a $\mathcal{O}(\epsilon)$-approximation to the solution of (2.10): First, the Navier-Stokes equations (2.13) are solved to get $\boldsymbol{u}_0$ and p_0, then the path $\boldsymbol{c}_0$ of the particle is obtained from the tracer condition (2.16b). The solution of the solvability conditions (2.20a) together with the corresponding differential equations (2.16) for $i = 1$ provides the coefficients $\boldsymbol{c}_1$, $\boldsymbol{v}_1$ and $\boldsymbol{\omega}_0$, $\mathbf{R}_0$ that define the Dirichlet condition (2.17b). The stationary Stokes problem (2.17) for $i = 1$ is solved. Finally, the last two steps are repeated to get $\boldsymbol{u}_{\mathrm{loc},2}$ which completes the procedure.*

Remark 7 (Density ratio scaling). *We want to point out the effect of the density ratio scaling introduced in (2.12). The momentum balances of the particle (2.18) can be written as*

$$\epsilon^{r+1}\sum_{i=0}^{\infty}\epsilon^i\boldsymbol{k}_i = \sum_{i=0}^{\infty}\epsilon^i\boldsymbol{m}_{i+1}^v\,, \qquad \epsilon^{r+2}\sum_{i=0}^{\infty}\epsilon^i\boldsymbol{\ell}_i = \sum_{i=0}^{\infty}\epsilon^i\boldsymbol{m}_{i+1}^\omega\,, \qquad (2.24)$$

where $\boldsymbol{k}_i$ and $\boldsymbol{\ell}_i$ denote the linear and angular accelerations of the particle (see Abbreviation 3) and $\boldsymbol{m}_{i+1}^v, \boldsymbol{m}_{i+1}^\omega$ describe the corresponding integral terms appearing on the right-hand sides of (2.18a) and (2.18b). The integral terms connect the accelerations to the Dirichlet conditions of the corresponding local flow fields via the solvability conditions (2.20); see Table 2.2 for the effect of the density ratio scaling. Since the tracer condition (2.16b) arises from the Dirichlet condition on the particle boundary, it is independent of the density scaling function α_ρ. This implies that for $r \leq -2$ the particle momentum balance yields the condition $\nabla \cdot \mathbf{S}[\boldsymbol{u}_0] = \mathbf{0}$ (see Table 2.2) in contradiction to the claim, $\boldsymbol{u}_0$ solving the Navier-Stokes equations in Ω, corresponding to (R1) of Lemma 4. This fact indicates that in this regime Assumption 2, 1) does not hold anymore, since the inertial effects of the particle are too strong and the perturbation of the surrounding fluid is of the same order as $\boldsymbol{u}_0$. Thus, consistent with the asymptotic, we restrict our classification of inertial types in Table 2.1 and throughout this work to $r \geq -1$.

Finally, we also formulate a result for the non-Newtonian stresses in the particle domain given in (2.11). Analogously to the case of the fluid quantities we use a Taylor series in $\boldsymbol{c}_0$ for the Newtonian part in (2.14), i.e., for $\mathbf{S}[\boldsymbol{u}_0](\boldsymbol{x}(\boldsymbol{y},t;\epsilon),t)$. The truncated expansion then reads as

$$\tilde{\mathbf{T}}^e = \mathbf{T}_{\text{loc},1} + \mathbf{R}_0^T \cdot \mathbf{S}[\boldsymbol{u}_0] \cdot \mathbf{R}_0$$
$$+ \epsilon\left(\mathbf{T}_{\text{loc},2} + \mathbf{R}_0^T \cdot D_1\mathbf{S}[\boldsymbol{u}_0] \cdot \mathbf{R}_0 + \mathbf{R}_1^T \cdot \mathbf{S}[\boldsymbol{u}_0] \cdot \mathbf{R}_0 + \mathbf{R}_0^T \cdot \mathbf{S}[\boldsymbol{u}_0] \cdot \mathbf{R}_1\right)$$

and we formulate the asymptotic model for the stresses in the following Lemma 8.

Lemma 8 (Asymptotic model of stresses in particle domain). *Let the requirements of Lemma 4 be fulfilled. Let $\mathbf{T}_{\text{loc},i} = \nabla\boldsymbol{\lambda}_{\text{loc},i} + \nabla\boldsymbol{\lambda}_{\text{loc},i}^T$, $i = 1,2$ be the solutions of the following boundary value problems for $t > 0$*

$$\nabla \cdot \mathbf{T}_{\text{loc},i}^T = \hat{\boldsymbol{f}}_i\,, \qquad\qquad \boldsymbol{y} \in \mathcal{E}\,, \qquad (2.25\text{a})$$

$$\mathbf{T}_{\text{loc},i} \cdot \boldsymbol{n} = \mathbf{S}[\boldsymbol{u}_{\text{loc},i}] \cdot \boldsymbol{n}\,, \qquad\qquad \boldsymbol{y} \in \partial\mathcal{E}\,, \qquad (2.25\text{b})$$

where the force terms are given by

$$\hat{\boldsymbol{f}}_1 = \begin{cases} \mathbf{0}\,, & r \geq 0 \\ |\mathcal{E}|^{-1}\boldsymbol{k}_0\,, & r = -1 \end{cases}\,,$$

$$\hat{\boldsymbol{f}}_2 = -\mathbf{R}_0^T \cdot \nabla \cdot \mathbf{S}[\boldsymbol{u}_0]^T - \mathbf{R}_0^T \cdot \mathbf{R}_1 \cdot \hat{\boldsymbol{f}}_1 + \begin{cases} \mathbf{0}\,, & r \geq 1 \\ |\mathcal{E}|^{-1}\boldsymbol{k}_0\,, & r = 0 \\ \rho\,\text{Re}\,\mathbf{R}_0^T \cdot \left(\frac{\text{d}}{\text{d}t}\boldsymbol{v}_1 + \frac{\text{d}^2}{\text{d}t^2}\mathbf{R}_0 \cdot \boldsymbol{y}\right), & r = -1 \end{cases}\,.$$

Then $\tilde{\mathbf{T}}^e$, $\mathbf{R}^e$, $\boldsymbol{c}^e$ solve the system (2.11) at least up to an error of $\mathcal{O}(\epsilon)$.

Proof. Similarly to the proof of Lemma 4, the approximation order follows from a straight forward computation.

Inserting $\tilde{\mathbf{T}}^e$ on the left side of (2.11b), using the expansion described in the proof of Lemma 4 for $\mathbf{S}[\boldsymbol{u}]$ on the right-hand side and taking (2.25b) into account yields that (2.11b) holds up to $\mathcal{O}(\epsilon^2)$.

When taking the divergence of $\tilde{\mathbf{T}}^e$ with respect to $\boldsymbol{y}$, the terms of the form $\mathbf{R}_i \cdot \mathbf{S}[\boldsymbol{u}_0] \cdot \mathbf{R}_j$ vanish, since the Newtonian stresses are evaluated at $\boldsymbol{c}_0$. With the asymptotic expansions of $\mathbf{R}$ and $\boldsymbol{c}$ (2.11a) is fulfilled up to $\mathcal{O}(\epsilon)$ provided that (2.25a) holds. $\qquad\square$

Remark 9 (Local velocity fields and forces in particle domain)**.**

1) *By construction, the stress* $\mathbf{T}$ *induces a rigid body velocity* $\widetilde{\boldsymbol{v}} = \epsilon(\mathrm{d}\mathbf{R}/\mathrm{d}t) \cdot \boldsymbol{y} + \boldsymbol{v}$ *in* $\mathcal{E}$, *while its approximation* $\mathbf{T}^e = \mathbf{R}^e \cdot \tilde{\mathbf{T}}^e \cdot \mathbf{R}^{eT}$ *results in the approximation of* $\widetilde{\boldsymbol{v}}$, *namely*

$$\widetilde{\boldsymbol{v}}^e = \boldsymbol{v}_0 + \epsilon \left(\frac{\mathrm{d}}{\mathrm{d}t}\mathbf{R}_0 \cdot \boldsymbol{y} + \boldsymbol{v}_1 \right) + \epsilon^2 \left(\frac{\mathrm{d}}{\mathrm{d}t}\mathbf{R}_1 \cdot \boldsymbol{y} + \boldsymbol{v}_2 \right), \qquad \boldsymbol{y} \in \mathcal{E}.$$

Since the functions $\boldsymbol{v}_i$ *and* $\mathbf{R}_i$ *do not depend on* $\boldsymbol{y}$, *we can rewrite* $\widetilde{\boldsymbol{v}}^e$ *as*

$$\widetilde{\boldsymbol{v}}^e = \boldsymbol{u}_0(\boldsymbol{x}(\boldsymbol{y},t,\epsilon),t) + \epsilon\mathbf{R}^e(\boldsymbol{h}_1(\boldsymbol{y},t) + \epsilon\boldsymbol{h}_2(\boldsymbol{y},t)) + \mathcal{O}(\epsilon^3)$$

using Abbreviation 3, where $\boldsymbol{h}_i(\boldsymbol{y},t)$ *is the continuous extension of the Dirichlet conditions of* $\boldsymbol{u}_{\mathrm{loc},i}$ *from Lemma 4 to* $\mathcal{E}$. *This way we can extend the local disturbance velocity fields to* $\mathcal{E}$ *by setting* $\boldsymbol{u}_{\mathrm{loc},i} = \boldsymbol{h}_i$. *The so defined velocity is bounded by the assumptions of Lemma 4.*

2) *The force terms* $\hat{\boldsymbol{f}}_i$ *are not equal to* $\boldsymbol{f}_i$ *of Abbreviation 3, but* $\int_{\mathcal{E}} \hat{\boldsymbol{f}}_i \mathrm{d}\boldsymbol{y} = \boldsymbol{f}_i$ *holds true consistent with* (2.25b).

2.3.4 Alternative asymptotic expansion

There exist also other asymptotic reductions of the coupled particle-fluid problem (2.10). In [41] steady ambient flows are considered, for which analytical results for the overall torque on the particle exist, see, e.g., [70, 72]. Einarsson et al. [41] apply an asymptotic expansion in the Stokes number St on the angular particle velocity and insert the corresponding expressions into (2.10e). The Stokes number denotes the ratio of the particle relaxation time (which is proportional to the particle mass divided by its typical length and the fluid dynamic viscosity, in case of small particles) with respect to the fluid relaxation time (proportional to the typical fluid velocity gradient rate, $\|\nabla \boldsymbol{u}\|$). This results in an evolution equation for the particle orientation with Jeffery's angular velocity in leading order and a correction term of $\mathcal{O}(\mathrm{St})$. The linear particle motion is neglected since stationary linear ambient flows are treated. Although this is a rather different approach, we can easily adapt the idea to our framework by expanding the linear and angular velocities according to (2.15a), without using an ϵ-expansion for the center of mass $\boldsymbol{c}$ and the rotation $\mathbf{R}$. Performing the asymptotic analysis analogously to Section 2.3.3 we arrive at the ϵ-dependent equations for the particle motion

$$\frac{\mathrm{d}}{\mathrm{d}t}\boldsymbol{c} = \boldsymbol{v}_0 + \epsilon\boldsymbol{v}_1 + \epsilon^2\boldsymbol{v}_2, \qquad \frac{\mathrm{d}}{\mathrm{d}t}\mathbf{R} = B(\boldsymbol{\omega}_0) \cdot \mathbf{R} + \epsilon B(\boldsymbol{\omega}_1) \cdot \mathbf{R}, \qquad (2.26)$$

which replace the equations for the particle center of mass (2.16a) and rotation (2.16c). The leading order velocity, $\boldsymbol{v}_0$ is still given by the tracer condition $\boldsymbol{v}_0(t) = \boldsymbol{u}_0(\boldsymbol{c}(t), t)$. The terms for Dirichlet and integral conditions of the local fields read similarly to Abbreviation 3 as

$$\boldsymbol{h}_1 = \mathbf{R}^T \cdot \boldsymbol{v}_1 + B(\mathbf{R}^T \cdot \boldsymbol{\omega}_0) \cdot \boldsymbol{y} - \mathbf{R}^T \cdot \partial_{\boldsymbol{x}} \boldsymbol{u}_0 \cdot \mathbf{R} \cdot \boldsymbol{y},$$

$$\boldsymbol{h}_2 = \mathbf{R}^T \cdot \boldsymbol{v}_2 + B(\mathbf{R}^T \cdot \boldsymbol{\omega}_1) \cdot \boldsymbol{y} - 0.5[\mathbf{R} \cdot \boldsymbol{y} \otimes \mathbf{R} \cdot \boldsymbol{y} : \nabla^2] \boldsymbol{u}_0,$$

$$\boldsymbol{f}_1 = \begin{cases} \boldsymbol{0}, & r \geq 0 \\ \boldsymbol{k}_0, & r = -1 \end{cases}, \qquad \boldsymbol{f}_2 = -|\mathcal{E}| \mathbf{R}^T \cdot \nabla \cdot \mathbf{S}[\boldsymbol{u}_0]^T + \begin{cases} \boldsymbol{0}, & r \geq 1 \\ \boldsymbol{k}_0, & r = 0 \\ \boldsymbol{k}_1, & r = -1 \end{cases},$$

$$\boldsymbol{g}_1 = \boldsymbol{0}, \qquad \boldsymbol{g}_2 = \begin{cases} \boldsymbol{0}, & r \geq 0 \\ \boldsymbol{\ell}_0, & r = -1 \end{cases},$$

with the linear and angular accelerations

$$\boldsymbol{k}_0 = \rho \operatorname{Re} |\mathcal{E}| \mathbf{R}^T \cdot \left(\frac{\mathrm{d}}{\mathrm{d}t} \boldsymbol{v}_0 - \operatorname{Fr}^{-2} \boldsymbol{e}_g \right), \quad \boldsymbol{k}_1 = \rho \operatorname{Re} |\mathcal{E}| \mathbf{R}^T \cdot \frac{\mathrm{d}}{\mathrm{d}t} \boldsymbol{v}_1,$$

$$\boldsymbol{\ell}_0 = \rho \operatorname{Re} |\mathcal{E}| \mathbf{R}^T \cdot \frac{\mathrm{d}}{\mathrm{d}t} \left(\mathbf{R} \cdot \hat{\mathbf{J}} \cdot \mathbf{R}^T \cdot \boldsymbol{\omega}_0 \right).$$

The compatibility conditions of Lemma 5 also formally simplify to

$$\begin{pmatrix} \boldsymbol{s}_q \\ \boldsymbol{t}_q \end{pmatrix} \cdot \begin{pmatrix} \mathbf{R}^T \cdot \boldsymbol{\omega}_{i-1} \\ \mathbf{R}^T \cdot \boldsymbol{v}_i \end{pmatrix} = \begin{cases} (\mathbf{R}^T \cdot \partial_{\boldsymbol{x}} \boldsymbol{u}_0^T \cdot \mathbf{R}) : \mathbf{V}_q, & i = 1 \\ \sum_{k,\ell,m} K_{k\ell m} (W_q)_{k\ell m}, & i = 2 \end{cases} + \begin{cases} \boldsymbol{e}_q \cdot \boldsymbol{f}_i, & q = 1, 2, 3 \\ \boldsymbol{e}_{q-3} \cdot \boldsymbol{g}_i / \sqrt{2}, & q = 4, 5, 6 \end{cases}$$

for $i = 1, 2$.

There are, however, two major differences to the systems in Lemma 4. In the latter, the differential equations are hierarchical, i.e., $\boldsymbol{c}_0$ is obtained from the tracer condition, which determines the needed values of the carrier flow and its derivatives in the other equations. Then $\mathbf{R}_0$ is obtained from the $\mathcal{SO}(3)$-equation and so on. In contrast to this, the system (2.26) is fully coupled in general. This is due to the fact that $\boldsymbol{u}_0$ is evaluated at $\boldsymbol{c}$ which enters the equation for the rotation. Additionally, in the heavy tracer particles regime the derivative of $\boldsymbol{v}_1$ enters the system, which behaves like $\mathrm{d}\boldsymbol{k}_0/\mathrm{d}t$ due to the linear dependence in the compatibility conditions. Thus, the equation for the center of mass in (2.26) becomes second order. Additionally, since the second derivative is scaled with ϵ^2, the ODE for $\boldsymbol{c}$ changes its nature to a singularly perturbed problem. This behavior can be avoided by using the initial expansion $\boldsymbol{v} = \boldsymbol{v}_0 + \epsilon \boldsymbol{v}_1 + \epsilon^2 \boldsymbol{v}_2 + \mathcal{O}(\epsilon^3)$ and neglecting terms of higher order, since

$$\epsilon^2 \frac{\mathrm{d}^2}{\mathrm{d}t^2} \boldsymbol{c} = \epsilon^2 \mathrm{D}_t \boldsymbol{u}_0 + \mathcal{O}(\epsilon^3). \tag{2.27}$$

2.4 Numerical study of asymptotic particle model for ellipsoidal geometry

In this section we apply the asymptotic model for inertial particles given in Lemma 4 to the case of ellipsoidal particles. This shape has the property that it is simple

enough, such that analytical solutions for the local velocity fields are available while the geometry is sufficiently complex such that orientation plays an important role. Moreover, it is often used as a supplemental model for more complicated objects such as blood cells [37], rigid rods [30], or fibers [85]. Thus, various macroscopic models for particle and fiber suspensions are based on the behavior of ellipsoids. Therefore, we want to examine, how our asymptotic particle model behaves in this important case.

As explained in Remark 6 3), the particle behavior according to Lemma 4 is determined by solving the compatibility conditions of Lemma 5. In order to achieve this, we have to calculate the surface moments appearing in (2.20); Appendix B.3 covers this task. Here, we only present the relevant results.

2.4.1 General properties

An ellipsoid is given as $\mathcal{E} = \mathbf{D}\mathcal{B}_1$, where $\mathcal{B}_1$ denotes the unit ball in $\mathbb{R}^3$ and $\mathbf{D}$ is the diagonal matrix carrying the lengths of the semi axes $d_i > 0$, $i = 1, 2, 3$, given as $\mathbf{D} = \mathrm{diag}(d_1, d_2, d_3)$. The surface moments of Lemma 5 are given as

$$
\boldsymbol{s}_q = \mathbf{0}\,, \quad \boldsymbol{s}_{q+3} = \zeta_{q+3}|\mathcal{E}|(\mathbf{D}^2 - \mathrm{tr}(\mathbf{D}^2)\mathbf{I}) \cdot \boldsymbol{e}_q\,, \quad \boldsymbol{t}_q = 3\zeta_q|\mathcal{E}|\boldsymbol{e}_q\,, \qquad \boldsymbol{t}_{q+3} = \mathbf{0}\,,
$$
$$
\mathbf{V}_q = \mathbf{0}\,, \quad \mathbf{V}_{q+3} = \zeta_{q+3}|\mathcal{E}|\mathbf{D}^2 \cdot B(\boldsymbol{e}_q)\,, \qquad W_q = \zeta_q|\mathcal{E}|\mathbf{D}^2 \otimes \boldsymbol{e}_q\,, \quad W_{q+3} = 0\,,
$$

with the geometry dependent constants ζ_q, $q = 1, 2, 3$. The explicit expressions for ζ_q in the general case are stated in Appendix B.3. From (2.20) we see that the structure of the surface moments implies a decoupling of the conditions for the linear and angular velocities. We are particularly interested in the case of prolate ellipsoids.

2.4.2 Prolate ellipsoids

For a prolate ellipsoid the lengths of the semi axes satisfy $d_1 > d_2 = d_3 > 0$. It is convenient to introduce the aspect ratio $a_r = d_1/d_2 > 1$ and the parameter $\nu = (a_r^2 - 1)(a_r^2 + 1)^{-1}$. The time-invariant inertia tensor reads as

$$
\hat{\mathbf{J}} = \frac{d_2^2}{5} \mathrm{diag}(2\,,\ a_r^2 + 1\,,\ a_r^2 + 1)\,.
$$

Furthermore, we set the vectors $\boldsymbol{p}_i = \mathbf{R}_0 \cdot \boldsymbol{e}_i$ and $\boldsymbol{q}_i = \mathbf{R}_1 \cdot \boldsymbol{e}_i$ associated with the rotation and introduce the quantities

$$
\theta = \frac{1}{2a_r(a_r^2 - 1)^{1/2}} \ln \frac{a_r + (a_r^2 - 1)^{1/2}}{a_r - (a_r^2 - 1)^{1/2}}\,, \qquad \chi^o = \frac{2a_r\theta}{d_2}\,,
$$
$$
\alpha_1^o = \frac{1}{d_1 d_2^2} \frac{2}{a_r^2 - 1} \left(a_r^2\theta - 1\right)\,, \qquad\qquad \alpha_2^o = \frac{1}{d_1 d_2^2} \frac{a_r^2}{a_r^2 - 1} \left(-\theta + 1\right)\,,
$$
$$
\mathbf{Z} = -12|\mathcal{E}|(d_1 d_2^2)^{-1} \mathrm{diag}(\chi^o + d_1^2\alpha_1^o\,,\ \chi^o + d_2^2\alpha_2^o\,,\ \chi^o + d_2^2\alpha_2^o)^{-1}\,, \tag{2.28a}
$$
$$
\mathbf{H} = -4|\mathcal{E}|(d_1 d_2^2)^{-1} \mathrm{diag}(2d_2^2\alpha_2^o\,,\ d_1^2\alpha_1^o + d_2^2\alpha_2^o\,,\ d_1^2\alpha_1^o + d_2^2\alpha_2^o)^{-1}\,. \tag{2.28b}
$$

This way, we can express the velocities $\boldsymbol{v}_i$, $i = 1, 2$ of Lemma 5 as

$$
\boldsymbol{v}_1 = \partial_{\boldsymbol{x}}\boldsymbol{u}_0 \cdot \boldsymbol{c}_1 + \mathbf{R}_0 \cdot \mathbf{Z}^{-1} \cdot \boldsymbol{f}_1\,, \tag{2.29a}
$$

$$\boldsymbol{v}_2 = \partial_{\boldsymbol{x}}\boldsymbol{u}_0 \cdot \boldsymbol{c}_2 + \mathbf{R}_1 \cdot \mathbf{Z}^{-1} \cdot \boldsymbol{f}_1 + 0.5[\boldsymbol{c}_1 \otimes \boldsymbol{c}_1 : \nabla^2]\boldsymbol{u}_0 + \frac{1}{6}[\mathbf{R}_0 \cdot \mathbf{D}^2 \cdot \mathbf{R}_0^T : \nabla^2]\boldsymbol{u}_0$$
$$+ \mathbf{R}_0 \cdot \mathbf{Z}^{-1} \cdot \boldsymbol{f}_2 \,, \tag{2.29b}$$

and the angular velocities $\boldsymbol{\omega}_0, \boldsymbol{\omega}_1$ as

$$\boldsymbol{\omega}_0 = 0.5\nabla \times \boldsymbol{u}_0 + \nu \boldsymbol{p}_1 \times \mathbf{E}[\boldsymbol{u}_0] \cdot \boldsymbol{p}_1 \,, \tag{2.29c}$$
$$\boldsymbol{\omega}_1 = \nu \left(\boldsymbol{p}_1 \times (\mathbf{E}[\boldsymbol{u}_0] \cdot \boldsymbol{q}_1) - (\mathbf{E}[\boldsymbol{u}_0] \cdot \boldsymbol{p}_1) \times \boldsymbol{q}_1\right) + \widetilde{\boldsymbol{\omega}}_1 \,, \tag{2.29d}$$
$$\widetilde{\boldsymbol{\omega}}_1 = 0.2\mathbf{R}_0 \cdot \hat{\mathbf{J}}^{-1} \cdot \mathbf{H}^{-1} \cdot \boldsymbol{g}_2 - 0.5[\boldsymbol{c}_1 \cdot \nabla](\boldsymbol{p}_2 \cdot (\partial_{\boldsymbol{x}}\boldsymbol{u}_0 - \partial_{\boldsymbol{x}}\boldsymbol{u}_0^T) \cdot \boldsymbol{p}_3)\boldsymbol{p}_1$$
$$+ (a_r^2 + 1)^{-1}\boldsymbol{p}_1 \times (a_r^2[\boldsymbol{p}_1 \otimes \boldsymbol{c}_1 : \nabla^2]\boldsymbol{u}_0 - [\boldsymbol{c}_1 \cdot \nabla^2](\boldsymbol{u}_0 \cdot \boldsymbol{p}_1)) \,.$$

Remark 10 (Jeffery equation). *The expression for $\boldsymbol{\omega}_0$ in (2.29c) together with the differential equation for the first director,*

$$\frac{\mathrm{d}}{\mathrm{d}t}\boldsymbol{p}_1 = \boldsymbol{\omega}_0 \times \boldsymbol{p}_1 \,,$$

is often called Jeffery's equation in remembrance of [70]. In the asymptotic context the equation was derived for normal tracer ellipsoids in the work of Junk & Illner [71].

Remark 11 (Velocities of the alternative asymptotic approach). *In the case of the asymptotic expansion discussed in Section 2.3.4, $\boldsymbol{\omega}_0$ is formally still the Jeffery angular velocity while the other velocities are given as*

$$\boldsymbol{v}_1 = \mathbf{R} \cdot \mathbf{Z}^{-1} \cdot \boldsymbol{f}_1 \,, \qquad \boldsymbol{v}_2 = \frac{1}{6}[(\mathbf{R} \cdot \mathbf{D}^2 \cdot \mathbf{R}^T) : \nabla^2]\boldsymbol{u}_0 + \mathbf{R} \cdot \mathbf{Z}^{-1} \cdot \boldsymbol{f}_2 \,,$$
$$\boldsymbol{\omega}_1 = 0.2\mathbf{R} \cdot \hat{\mathbf{J}}^{-1} \cdot \mathbf{H}^{-1} \cdot \boldsymbol{g}_2 \,,$$

with $\boldsymbol{u}_0$ evaluated at $\boldsymbol{c}$ as pointed out in Section 2.3.4.

2.4.3 Numerics

To study the performance of the asymptotic micro-scale models and the impact of weak inertia, we perform numerical simulations for rotational and translational particle motions. We particularly focus on linear stationary carrier flows in an unbounded domain $\Omega = \mathbb{R}^3$, already revealing some important properties of the asymptotic models. In general, $\boldsymbol{u}_0(\boldsymbol{x}) = \mathbf{A} \cdot \boldsymbol{x} + \boldsymbol{b}$ solves the Navier-Stokes equations (2.13), if $\mathrm{tr}(\mathbf{A}) = 0$ and $\mathbf{A}^2$ is symmetric. The pressure is then given as $p_0 = -0.5\,\mathrm{Re}\,\boldsymbol{x} \cdot \mathbf{A}^2 \cdot \boldsymbol{x} + \mathrm{Re}\,\mathrm{Fr}^{-2}\,\boldsymbol{h} \cdot \boldsymbol{x}$, where $\boldsymbol{h} = \boldsymbol{e}_g - \mathrm{Fr}^2\,\mathbf{A} \cdot \boldsymbol{b}$.

For the numerical treatment we introduce a convenient parametrization for the particle-associated directors in (2.16c). Since $\mathbf{R}_0$ is an orthogonal matrix, we parametrize the $\mathcal{SO}(3)$-group via the three Euler angles $\boldsymbol{\psi} : \mathbb{R}_0^+ \to \mathbb{R}^3$, see, e.g., [27, 51], yielding

$$\mathbf{M}_1 \cdot \frac{\mathrm{d}}{\mathrm{d}t}\boldsymbol{\psi} = \boldsymbol{\omega}(\boldsymbol{\psi}) \,, \qquad \mathbf{M}_1 = \begin{bmatrix} 0 & -\sin(\psi_1)\sin(\psi_3) & -\cos(\psi_1) \\ 0 & -\cos(\psi_1)\sin(\psi_3) & \sin(\psi_1) \\ -1 & -\cos(\psi_3) & 0 \end{bmatrix} \,. \tag{2.30}$$

As for the equation for $\mathbf{R}_1$ we use the fact that $\mathbf{R}_1 \cdot \mathbf{R}_0^T$ is skew-symmetric [71]. Thus, we apply (A.9) and consider $\boldsymbol{\tau} : \mathbb{R}_0^+ \to \mathbb{R}^3$ given as $\boldsymbol{\tau} = B^{-1}(\mathbf{R}_1 \cdot \mathbf{R}_0^T)$. By using

$$\frac{\mathrm{d}}{\mathrm{d}t}B(\boldsymbol{\tau}) = B(\boldsymbol{\omega}_0) \cdot B(\boldsymbol{\tau}) + B(\boldsymbol{\omega}_1) - B(\boldsymbol{\tau}) \cdot B(\boldsymbol{\omega}_0) = B(\boldsymbol{\omega}_0 \times \boldsymbol{\tau} + \boldsymbol{\omega}_1)$$

we arrive at the evolution equation for $\boldsymbol{\tau}$, i.e.,

$$\frac{\mathrm{d}}{\mathrm{d}t}\boldsymbol{\tau} = \Big(B(\boldsymbol{\omega}_0) + \nu\,(B(\mathbf{E}[\boldsymbol{u}_0]\cdot\boldsymbol{p}_1)\cdot B(\boldsymbol{p}_1) - B(\boldsymbol{p}_1)\cdot\mathbf{E}[\boldsymbol{u}_0]\cdot B(\boldsymbol{p}_1))\Big)\cdot\boldsymbol{\tau} + \widetilde{\boldsymbol{\omega}}_1\,, \quad (2.31)$$

with $\boldsymbol{\tau}(0) = \mathbf{0}$.

Remark 12 (Equations associated with the alternative asymptotic expansion for steady linear flows). *A big disadvantage of the asymptotic approach introduced in Section 2.3.4 is the coupling between the equations for the linear motion and the rotation. In the special case of linear stationary flows, the derivatives of $\boldsymbol{u}_0$ do not depend on the position. This implies that the rotation equation (2.26) becomes independent of the evolution of $\boldsymbol{c}$. In particular, the asymptotic angular velocities read as*

$$\boldsymbol{\omega}_0 = 0.5\nabla\times\boldsymbol{u}_0 + \nu\boldsymbol{p}_1\times\mathbf{E}[\boldsymbol{u}_0]\cdot\boldsymbol{p}_1\,, \quad \boldsymbol{\omega}_1 = 0.2\rho|\mathcal{E}|\operatorname{Re}\mathbf{R}\cdot\hat{\mathbf{J}}^{-1}\mathbf{H}^{-1}\cdot\mathbf{R}^T\cdot\mathbf{M}_2\cdot\frac{\mathrm{d}}{\mathrm{d}t}\boldsymbol{p}_1\,,$$

$$\mathbf{M}_2 = \left[\frac{d_2^2(1-a_r^2)}{5}((\boldsymbol{p}_1\cdot\boldsymbol{\omega}_0)\mathbf{I} + \boldsymbol{p}_1\otimes\boldsymbol{\omega}_0) + \nu\mathbf{R}_0\cdot\hat{\mathbf{J}}\cdot\mathbf{R}_0^T\cdot(B(\boldsymbol{p}_1)\cdot\mathbf{E} - B(\mathbf{E}\cdot\boldsymbol{p}_1))\right]\,,$$

where $\boldsymbol{p}_1 = \mathbf{R}\cdot\boldsymbol{e}_1$. Using the $\mathcal{SO}(3)$-group parametrization (2.30), we obtain

$$\mathbf{M}\frac{\mathrm{d}}{\mathrm{d}t}\boldsymbol{\psi} = \boldsymbol{\omega}_0\,, \qquad \mathbf{M} = \mathbf{M}_1 - 0.2\epsilon\rho|\mathcal{E}|\operatorname{Re}\mathbf{R}\cdot(\hat{\mathbf{J}}\cdot\mathbf{H})^{-1}\cdot\mathbf{R}^T\cdot\mathbf{M}_2\cdot\mathbf{M}_3\,, \qquad (2.32)$$

where $\mathbf{M}_3\cdot\mathrm{d}\boldsymbol{\psi}/\mathrm{d}t = \mathrm{d}\boldsymbol{p}_1/\mathrm{d}t$. For the linear motion, we introduce the following quantities

$$\mathbf{N}_1 = \mathbf{R}\cdot\mathbf{Z}^{-1}\cdot\mathbf{R}^T\,, \quad \mathbf{N}_2 = B(\boldsymbol{\omega})\cdot\mathbf{N}_1 - \mathbf{N}_1\cdot B(\boldsymbol{\omega})$$

with $\boldsymbol{\omega} = \boldsymbol{\omega}_0 + \epsilon\boldsymbol{\omega}_1$, yielding the inertia-associated equations for the particle center of mass $\boldsymbol{c}$ for the light-weighted (lTP), normal (nTP) and heavy (hTP) tracer particles

$$\frac{\mathrm{d}}{\mathrm{d}t}\boldsymbol{c} = \boldsymbol{u}_0 + \epsilon^2|\mathcal{E}|\mathbf{N}_1\cdot\nabla p_0\,, \qquad\qquad\qquad lTP, \qquad (2.33\mathrm{a})$$

$$\frac{\mathrm{d}}{\mathrm{d}t}\boldsymbol{c} = \boldsymbol{u}_0 + \epsilon^2|\mathcal{E}|(1-\rho)\mathbf{N}_1\cdot\nabla p_0 \qquad\qquad\qquad (2.33\mathrm{b})$$

$$+ \epsilon^2\rho\operatorname{Re}|\mathcal{E}|\mathbf{N}_1\cdot\mathbf{A}\cdot\left(\frac{\mathrm{d}}{\mathrm{d}t}\boldsymbol{c} - \boldsymbol{u}_0\right)\,, \qquad nTP,$$

$$\frac{\mathrm{d}}{\mathrm{d}t}\boldsymbol{c} = \boldsymbol{u}_0 + \epsilon^2|\mathcal{E}|\mathbf{N}_1\cdot\nabla p_0 \qquad\qquad\qquad\qquad (2.33\mathrm{c})$$

$$- \epsilon\rho\operatorname{Re}|\mathcal{E}|\mathbf{N}_1\cdot(\mathbf{I} + \epsilon\rho\operatorname{Re}|\mathcal{E}|\mathbf{N}_2)\cdot\operatorname{Fr}^{-2}\boldsymbol{e}_g\,, \quad hTP,\ if\ \epsilon\rho\operatorname{Re}\mathbf{A} = \mathbf{0}\,.$$

Finally, for $\epsilon\rho\operatorname{Re}\mathbf{A} \neq \mathbf{0}$ in the heavy TP regime, the linear motion is given by the singularly disturbed system

$$\frac{\mathrm{d}}{\mathrm{d}t}\boldsymbol{c} = \boldsymbol{v}\,, \qquad\qquad\qquad\qquad (2.33\mathrm{d})$$

$$\mathbf{A}\cdot\frac{\mathrm{d}}{\mathrm{d}t}\boldsymbol{v} = -(\epsilon\rho\operatorname{Re}|\mathcal{E}|\mathbf{N}_1)^{-2}\cdot\Big(\boldsymbol{u}_0 - \boldsymbol{v} + \epsilon|\mathcal{E}|(\epsilon-\rho)\mathbf{N}_1\cdot\nabla p_0$$

$$- (\epsilon\rho|\mathcal{E}|)^2\operatorname{Re}\mathbf{N}_1\cdot\mathbf{N}_2\cdot\nabla p_0 - \epsilon\rho\operatorname{Re}|\mathcal{E}|\mathbf{N}_1\cdot\mathbf{A}\cdot(\boldsymbol{u}_0 - \boldsymbol{v})$$

$$- (\epsilon\rho\operatorname{Re}|\mathcal{E}|)^2\mathbf{N}_1\cdot\mathbf{N}_2\cdot\mathbf{A}\cdot(\boldsymbol{u}_0 - \boldsymbol{v})\Big)\,.$$

Using the expression (2.26) and dropping terms of order $\mathcal{O}(\epsilon^3)$, we get the approximative equations

$$\frac{\mathrm{d}}{\mathrm{d}t}\boldsymbol{c} = \boldsymbol{u}_0 + \epsilon^2|\mathcal{E}|\mathbf{N}_1 \cdot \nabla p_0\,, \qquad\qquad lTP, \qquad\qquad (2.34\text{a})$$

$$\frac{\mathrm{d}}{\mathrm{d}t}\boldsymbol{c} = \boldsymbol{u}_0 + \epsilon^2|\mathcal{E}|(1-\rho)\mathbf{N}_1 \cdot \nabla p_0\,, \qquad\qquad nTP, \qquad\qquad (2.34\text{b})$$

$$\frac{\mathrm{d}}{\mathrm{d}t}\boldsymbol{c} = \boldsymbol{u}_0 + \epsilon|\mathcal{E}|(\epsilon-\rho)\mathbf{N}_1 \cdot \nabla p_0 - (\epsilon\rho|\mathcal{E}|)^2 \operatorname{Re}\mathbf{N}_1 \cdot (\mathbf{A} \cdot \mathbf{N}_1 + \mathbf{N}_2) \cdot \nabla p_0 \qquad (2.34\text{c})$$
$$+ \, (\epsilon\rho \operatorname{Re}|\mathcal{E}|\mathbf{N}_1)^2 \cdot \mathbf{A}^2 \cdot \boldsymbol{u}_0\,, \qquad\qquad hTP$$

We integrate the resulting systems (2.16), (2.30), (2.31), respectively (2.32) and (2.33) by the application of different quadrature rules: By using a trapezoidal rule for the equations of the center of mass in the case of light-weighted and normal TP model we preserve periodical trajectories in the case of a rotational ambient fluid flow studied in the following. The equations associated with the rotation and the heavy TP model are solved via the implicit Euler method. The solution of the corresponding nonlinear equations is done by a Newton iteration. Since the ODEs related to the orthogonal group (2.30) and (2.32) may involve a singular Jacobian, we apply the singular value decomposition to solve a least-squares problem for the Newton update.

Rotational behavior We investigate the impact of the different inertia regimes on the orientational behavior of the ellipsoid. Since for normal and light-weighted tracer ellipsoids the source term in (2.31), $\tilde{\boldsymbol{\omega}}_1$, vanishes, we have $\boldsymbol{\tau}(t) \equiv \boldsymbol{0}$ for all $t \geq 0$. Thus, the rotatory behavior is completely given by $\mathbf{R}_0$, which is characterized by the well-known Jeffery's angular velocity $\boldsymbol{\omega}_0$, see [70]. For the case of heavy TP, we discuss our asymptotic results with respect to the work [41]. For a comparable scaling, we note that the Stokes number St and particle Reynolds number Re_p used in [41] become*

$$\operatorname{St} = \rho_\epsilon \epsilon^2|\mathcal{E}|\operatorname{Re} = \epsilon\rho|\mathcal{E}|\operatorname{Re}, \qquad \operatorname{Re}_p = a_r \rho_\epsilon^{-1}\operatorname{St} = a_r \epsilon^2|\mathcal{E}|\operatorname{Re}\,.$$

For the simulations we choose a shear flow $\boldsymbol{u}_0 = x_2\boldsymbol{e}_1$ and neglect gravity (Fr $\to \infty$). Additionally, we set $\boldsymbol{c}(0) = \boldsymbol{0}$, which implies $\boldsymbol{v}_0(t) \equiv \boldsymbol{v}_1(t) \equiv \boldsymbol{v}_2(t) \equiv \boldsymbol{0}$. The other parameters are exemplarily taken as $\operatorname{Re} = 10^{-2}$, $d_1 = 5$, $\epsilon = 0.1$, $\rho = 0.25\alpha^Y/(\operatorname{Re}\epsilon|\mathcal{E}|)$, where $\alpha^Y = 40\pi d_1 a_r^2 Y^C/(a_r^2 + 1)$ with the "resistance function" Y^C according to [72, p. 64]. Figure 2.2 shows that the first director of the ellipsoid moves to an orbit near to the equator owing to the inertial particle effects – independent of the chosen asymptotic approach. However, since in our framework $\mathbf{R}_0 + \epsilon\mathbf{R}_1$ is not an orthogonal matrix, the impact of $\mathbf{R}_1$ grows tremendously with time as clearly seen in the error $\|\boldsymbol{d}^e\| - 1$ in Fig. 2.2, revealing its role as a "secular term" [65]. Hence, the approximation $\mathbf{R} \approx \mathbf{R}_0 + \epsilon\mathbf{R}_1$ is not valid for t of order $t \gg \epsilon^{-1}$. The alternative asymptotic expansion discussed in Section 2.3.4 and Remark 12 overcomes this limitation and yields very promising results in comparison to [41], see Fig. 2.3.

---

*To link the parameters considered in this Section with those in [41], we scale the particle volume by the length of the small semi-axis (thus $d_2 = 1$), choose the typical flow-gradient rate as the ratio of characteristic velocity with respect to the characteristic length $\bar{x}$, and use the density scaling (2.12).

†The Lambert azimuthal projection is defined as $(X_1, X_2)(\boldsymbol{p}) = (p_1, p_2)\sqrt{2/(1+p_3)}$, [41].
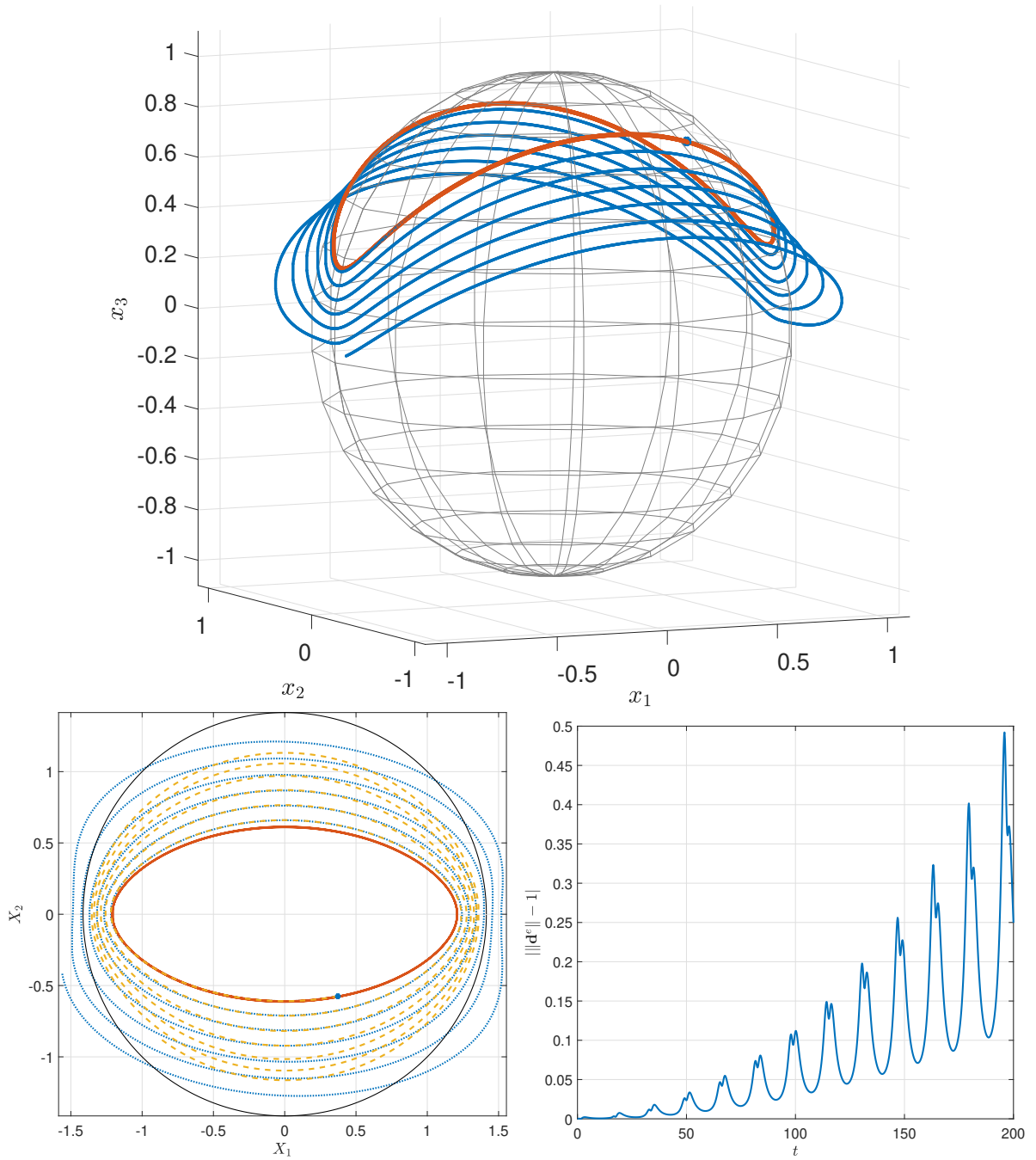
Figure 2.2.: Orientation of an ellipsoid in a shear flow. Top: 3d trajectory of $\boldsymbol{d}^e = \boldsymbol{p}_1 + \epsilon \boldsymbol{q}_1$ (blue) and Jeffery orbit (red, bold). Bottom, left: Lambert azimuthal projection[†] of the orientation trajectory to the 2d plane. Orientation $\boldsymbol{d}^e$ according to (2.16c) (blue, dotted), Jeffery orbit projection (red, solid), orientation according to [41] (yellow, dashed), initial configuration (blue dot), and the equator (black, thin). Bottom, right: Deviation of $\boldsymbol{d}^e$ from the unit sphere w.r.t. time.
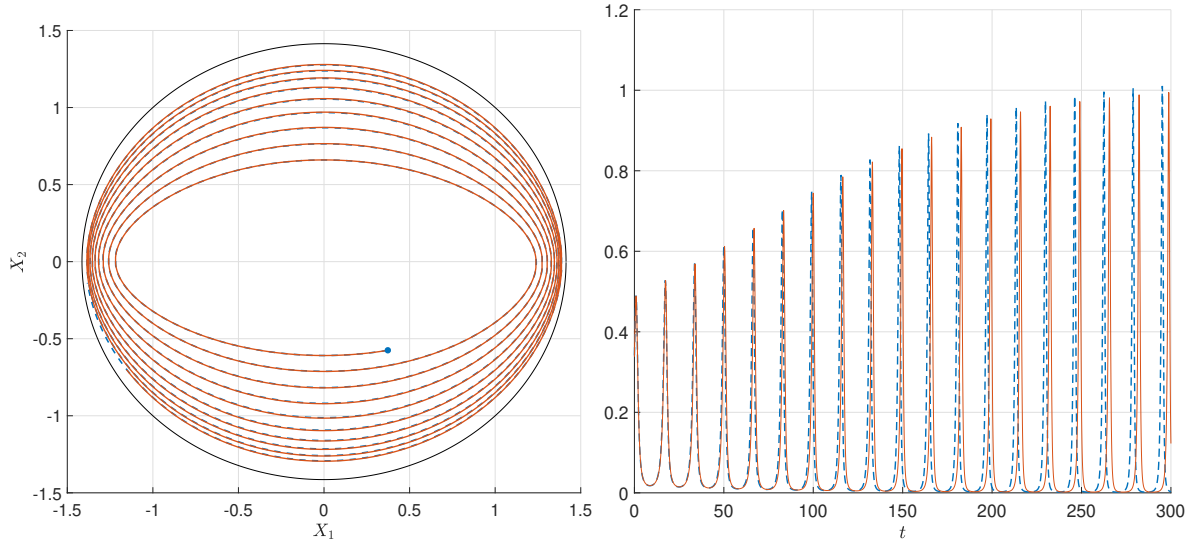
Figure 2.3.: Left: Projected† trajectory of $\boldsymbol{p}_1$ according to (2.32) (blue, dashed) and to [41] (red, solid) as well as the norm of the resulting angular velocities (right).

Translational behavior To understand what happens for the translational particle motion, we take gravity into account. We set $\boldsymbol{e}_g = -\boldsymbol{e}_3$ and consider a rotational flow $\boldsymbol{u}_0 = -x_2\boldsymbol{e}_1 + x_1\boldsymbol{e}_2$. For the other parameters we exemplarily take Fr $= 1$, Re $= 5$, $\epsilon = 0.1$, $d_1 = 2$, $d_2 = 1$. We note that the light-weighted inertia regime is independent of the density ratio ρ. Furthermore, since for $\rho = 0$ the accelerations $\boldsymbol{k}_0, \boldsymbol{k}_1$ vanish, the normal and heavy TP behave the same way as the light-weighted ones. In this case, the particle initially moves upwards and additionally to the center of the $\boldsymbol{e}_1$-$\boldsymbol{e}_2$-plane, since it is subject to a buoyancy force and thus follows the negative pressure gradient (Fig. 2.4). This behavior can be also observed for normal TP in the case $\rho < 1$. For $\rho \equiv 1$, the particle moves at a periodical path according to $\boldsymbol{u}_0$. For $\rho > 1$, the gravity and inertial drift being oriented to the outward in the $\boldsymbol{e}_1$-$\boldsymbol{e}_2$-plane dominate. For heavy TP and $\rho > 1$, this effect strongly dominates over pressure and buoyancy. Therefore, the overall behavior is qualitatively in agreement with the physical expectations. However, also here the limitations on the time scale where the asymptotics is reasonable become obvious. In the light-weighted TP-regime, the particle does not stay at the origin of the $\boldsymbol{e}_1$-$\boldsymbol{e}_2$-plane, instead after some time the drift starts to dominate. This is a consequence of the fact that the equation for the second order velocity is only dependent on $\boldsymbol{c}_0$, thus the approximation $\boldsymbol{v}^e \approx \boldsymbol{v}_0 + \epsilon\boldsymbol{v}_1 + \epsilon^2\boldsymbol{v}_2$ is dominated by the contribution of the secular term for $t \gg \epsilon^{-1}$ (Fig. 2.5). Analogously to the rotational case, this shortcoming does not appear in the particle motion corresponding to the alternative asymptotic approach (Remark 12, Fig. 2.6).
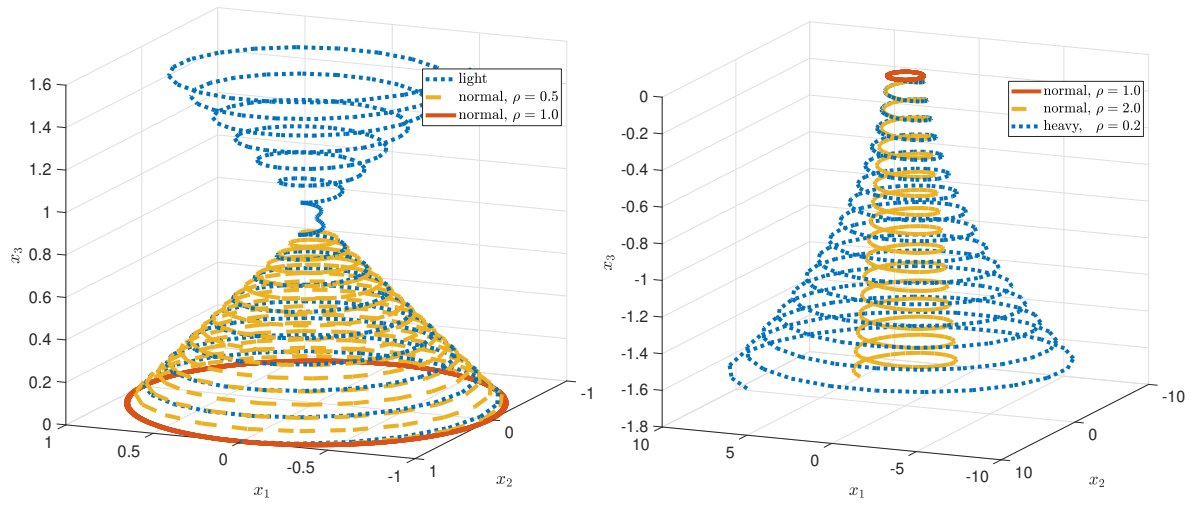
Figure 2.4.: Motion of center of mass according to Lemma 4. Left: light-weighted TP (ρ is not a parameter) and normal TP for $\rho = 0.5$, $\rho = 1$. Right: Normal TP for $\rho = 1$, $\rho = 2$ and heavy TP, $\rho = 0.2$.
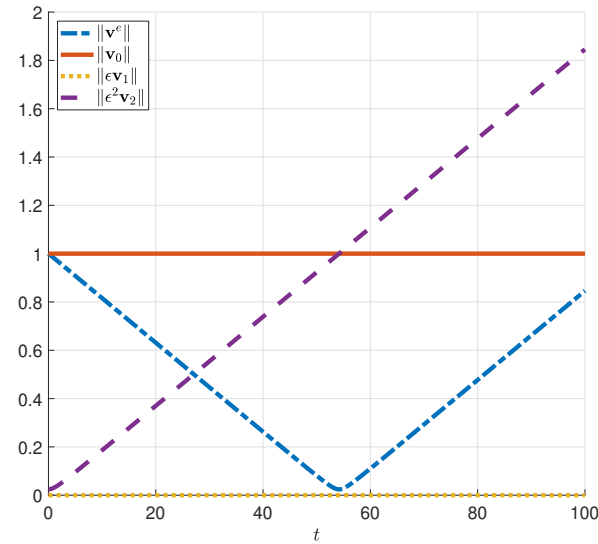

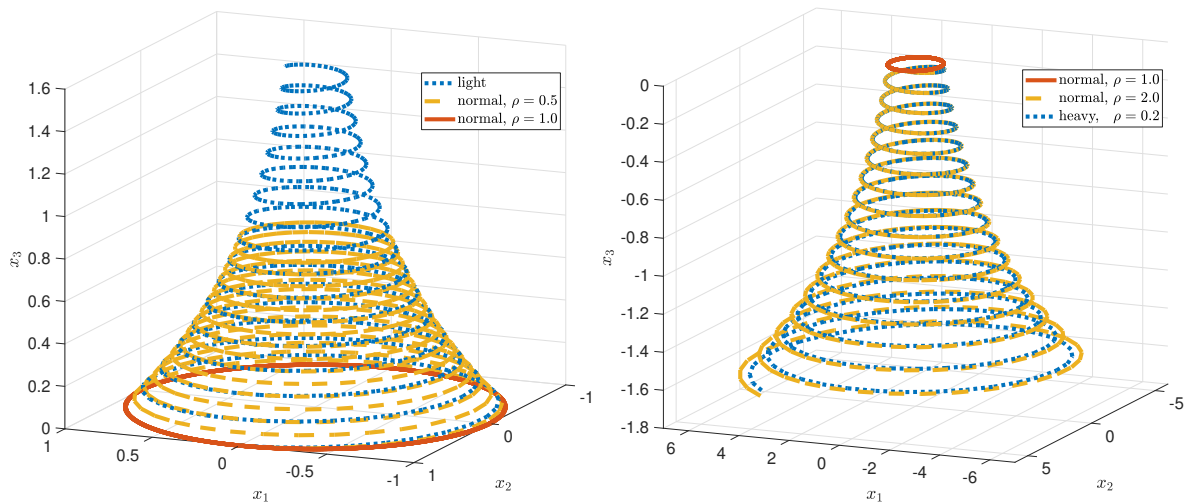Figure 2.5.: Light-weighted TP regime. Norm of the different velocities.

Figure 2.6.: Motion of center of mass according to (2.33). Left: light-weighted TP (ρ is not a parameter) and normal TP for $\rho = 0.5$, $\rho = 1$. Right: Normal TP for $\rho = 1$, $\rho = 2$ and heavy TP, $\rho = 0.2$.

2.5 Conculsion

We dedicated the studies in this chapter to the extension of an asymptotic description of the particle-fluid problem to the case of inertial particles. The underlying problem is given by the incompressible Navier-Stokes equations in a bounded domain coupled to the second order ordinary differential equations describing the momentum balances of an arbitrarily shaped rigid body moving in the fluid. The characteristic length scale of the particle is much smaller than that of the surrounding fluid flow, which motivates the asymptotic expansion of the solution components in the size ratio ϵ (ratio of particle size with respect to the characteristic length scale of the flow). The underlying asymptotic analysis was presented in [71] for inertialess particles. In order to take inertia into account, we introduced an appropriate asymptotic scaling of the density ratio as summarized in Tab. 2.1 and derived an asymptotic approximation of the full problem (Lemma 4, Lemma 5, Lemma 8) for $\epsilon \to 0$ which retains the structure of the original approximation given in [71] but accounts for small inertial effects.

The problem under consideration describes an incompressible Newtonian fluid contained in a bounded domain with a small immersed rigid particle interacting with the flow. Particle and fluid interact by hydrodynamic forces. As outer forces only gravity is considered. In order to extend the asymptotic results for a macroscopic suspension model in Sec. 3.4, we also consider a model which extends the viscous stresses onto the particle domain in Sec. 2.2.4 as proposed by [99]. We reformulate both systems, the particle-fluid system and the one describing the stresses on the particle domain, in dimensionless form in Sec. 2.2.5 using the Reynolds number (defined with respect to the fluid quantities), the Froude number, the density and size ratios ρ, ϵ. While the size ratio is assumed small $\epsilon \ll 1$, the density ratio is rescaled artificially in Sec. 2.3.1 by powers of ϵ in order to allow different asymptotic models. To be exact, we characterize three inertial regimes (light-weighted, normal and heavy tracer particle regime). Despite this modification, we keep the basic assumptions of [71] regarding the system behavior. In particular, we still assume that due to the vanishing particle volume the

fluid is essentially undisturbed by the particle. We also do not take boundary effects into account. These assumptions allow the usage of the same asymptotic ansatz for the solution components as in [71], namely a regular expansion in powers of ϵ for the particle quantities and a splitting of the fluid quantities into a global and a local part. The global part is assumed independent of ϵ, while the local one as being of $\mathcal{O}(\epsilon)$-magnitude. Furthermore, the local contributions are expressed in terms of the local particle coordinates and expanded in powers of ϵ.

The asymptotic approximation then follows by plugging the truncated expansions into the full problems and deducing the needed balance laws for the expansion coefficients. As for the particle-fluid problem (2.10), the resulting approximation is summarized in Lemma 4 and Lemma 5. Here, the first order approximation consists of stationary Stokes problems on the exterior of the particle domain which define the local velocity and pressure contributions for the fluid, and which are coupled to an undisturbed incompressible Navier-Stokes problem on the bounded domain. The particle motion is approximated by a tracer condition in the lowest order corrected by small velocity contributions which strongly depend on the chosen density scaling. This influence is discussed in detail in Rem. 7. The corresponding asymptotic approximation for the stresses in the particle domain (2.11) is stated in Lemma 8 and consists of a stationary boundary value problem depending on the approximation of (2.10) described by Lemma 4.

As seen later in the numerical studies in Sec. 2.4, the investigated asymptotic expansion can lead to secular terms which dominate the dynamic particle behavior, despite being assumed as higher order corrections. Hence, we also investigate a modified asymptotic expansion in Sec. 2.3.4, where the particle center of mass and orientation are not expanded. This leads to a coupling in the approximation of the particle equations. Nonetheless, the central results formulated in Lemma 4, Lemma 5 and Lemma 8 hold with accordingly modified equations.

In Sec. 2.4 we examine both asymptotic approaches by applying them to the well-studied case of ellipsoidal particles. In particular, we consider prolate ellipsoidal geometry and investigate the influence of the prescribed inertial scaling on the translational particle motion as well as on the dynamic orientation behavior. We recover the famous Jeffery's equation for the dynamical behavior of the principal axis of a prolate ellipsoid for normal and light-weighted particles. In the case of heavy tracer ellipsoids, Jeffery's angular velocity is still present in the equations but is disturbed by the correction terms. We observe meaningful physical behavior for both asymptotical approaches. In particular, the translational particle motion behaves according to the prescribed inertial regime, i.e., heavy particles are dominated by inertial drift, light-weighted particles show buoyant behavior and normal tracer particles with $\rho \equiv 1$ follow the fluid streamlines. Considering the orientation behavior, the observations are consistent with results from literature.

Despite the validity of the asymptotic results for the heavy particles regime as introduced in Sec. 2.3.1, the particles are still tracer particles in leading order approximation in both asymptotic expansion variants. Therefore, the asymptotic description is unable to depict true inertial behavior and recover particle equations of motion driven by a drag force. If the corresponding assumption on the particle influence is dropped (Assumption 2, 1)), the effect of particle presence on the surrounding fluid strongly depends on the relative velocity and fluid viscosity, i.e., on the Reynolds number defined

with respect to the relative velocity and the particle length scale. This not only implies that the dimensionless formulation in Sec. 2.2.5 is no longer valid, but it also leads to instationary local velocities already at moderate Reynolds numbers (e.g., Kármán vortex streets at Re $\gtrsim$ 80 for cylindrical objects [110]). This completely changes the structure of the approximation compared to Lemma 4 and needs approaches tailored to the chosen Reynolds number. The derived asymptotic model presented here therefore lies between the inertialess motion of tracer particles and fully inertial movement of particles driven by a Stokes drag. Another major drawback of the presented approaches in this chapter is that the asymptotic scaling of the density ratio is artificial, thus, we can not decide on the basis of a given set of physical parameters, which inertial regime is suitable for the approximation of the corresponding scenario. Instead, the resulting simulations must be compared to observations from experiments in order to decide, which inertial regime is applicable. The already mentioned problem in the long-time behavior of the asymptotic approximation which stems from the expansion of the particle center of mass and its rotation can be eliminated by the alternative asymptotic expansion of Sec. 2.3.4 at the cost of more sophisticated coupling in the approximation.

The novelty of the presented work lies in the addition of small inertial effects in asymptotic approaches for the coupled particle-fluid problem describing an immersed rigid body in a surrounding incompressible Newtonian fluid. We introduced a concept of asymptotic particle inertia which admits meaningful solutions in the framework of [71]. We found that the asymptotic procedure proposed by [71], which is based on asymptotic expansions in the size ratio ϵ and does neither demand the surrounding fluid to be inertialess, nor to be located in an infinite domain, is indeed also applicable to the case of particles with a density different to that of the surrounding fluid. Moreover, we also showed that this procedure admits more complex models, inspired by [41], which are capable of portraying the physical behavior of the particle on a larger time scale by avoiding secular terms due to approximations in the particle center-of-mass and rotation. This way we provide the foundation of a consistent asymptotic suspension model in Section 3.

3 Modeling of suspension flows

3.1 Introduction

Fluids with small suspended particles or fibers play an important role in various fields of natural sciences and engineering. Fiber-loaden flows, for example, are used to produce nonwoven materials or paper [54, 86, 88], red blood cells, plankton or ash are transported in the corresponding media and domains [37, 57, 106]. Such problems connect aspects of fluid mechanics, statistical physics and, depending on the particular application, further scientific fields as, e.g., electrodynamics or acoustics [1, 107]. One very important task associated with the analysis of suspensions is the modeling of the particle influence on the surrounding carrier flow. This influence is dependent on the particle size and mass, the inter-particle spacing and on the characteristics of the flow. Considering a physical model, also the scale of interest is of crucial importance. In general, the particles are initially distributed stochastically in the space domain, they then interact with the fluid and each other being perturbed by fluctuations in a turbulent flow. On smaller scales also thermodynamic effects introduce probabilistic particle motions. On microscale where every particle has a significant size and thus an important impact on the streamlines, a cut-out of the suspension domain is strongly dominated by stochastic effects. On macroscale on the other hand, where the size of the particles is small compared to the dimensions of the flow, the suspension may be described as a homogeneous, non-Newtonian fluid. The model for the particle influence is then given by an expression for the stresses, resp. forces which balance the momentum equation for the homogeneous suspension velocity. The derivation of such models range from imposing an ad hoc material model [18] to coupling a Fokker-Planck equation deduced from microscale properties with a fluid momentum balance equation [8]. The

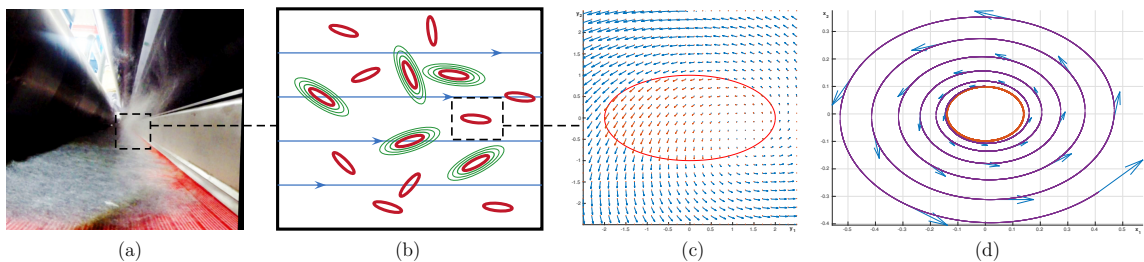(a)   (b)   (c)   (d)

Figure 3.1.: (a) Fiber suspension flow in an air-lay process for nonwoven production. (b) Sketch of meso-scale suspension model: small particles induce local perturbations of the surrounding fluid. (c) Fluid and particle velocity according to asymptotic micro-scale model. (d) Particle trajectory due to inertia.

latter methods account for the fluid micro-structure and try to derive the macroscopic properties directly from the microscopic particle behavior as exemplarily sketched in Fig. 3.1.

Einstein [42] formulated the macroscopic description of a dilute suspension of small rigid spheres in a stationary Newtonian fluid as a change in viscosity of the carrier fluid. He derived his results by first considering the motion of a single particle in a sufficiently small region of the suspension domain, where the flow of the carrier fluid may be treated as linear, and then solving the stationary Stokes equations for the disturbance flow. The contribution of many particles then followed by a superposition of every single disturbance velocity field. A mathematical proof of the increase in viscosity for the case of a finite domain was presented in [58]. Jeffery used an analogous approach for ellipsoidal inertia-free particles in [70]. These results were generalized by Batchelor in [12]. Using ensemble averages, the latter presented a general framework for modeling of stresses in a suspension of rigid particles in an incompressible Navier-Stokes flow. He applied his theory to a dilute suspension of ellipsoidal inertia-free particles and derived an analytical term for the particle-stresses in the macroscopic description by using results of Jeffery. The study of non-dilute suspensions involves the modeling of the interactions between particles as, e.g., in [11, 35, 46, 80]. Another general approach for suspension modeling was presented in [126], where Cauchy's stress principle was applied to the suspension, reproducing classical results as well as showing additional effects induced by spatial non-uniformities of the dispersed phase. The influence of particle concentration was also considered in [103, 104]. Rigorous asymptotical homogenization strategies for suspensions were used, for example, in [15, 17, 49].

We aim for the derivation of a model that approximates a suspension of small rigid particles in a Newtonian incompressible fluid flow which interact only by hydrodynamic forces and where no outer forces except of gravity are present. The model should be able to take small inertial effects into account and describe both, the particle motion due to the fluid and the effect of the particle presence onto the fluid dynamics. The derivation is based on the asymptotic approach of [71] and on the procedure for the derivation of mean field models due to [20, 53]. The final model then consists of the momentum equation for the fluid coupled with a transport equation for the particle probability on the respective phase space. The novelty of this work is the consideration of small particle inertia in the macroscopic suspension description as well as the derivation of the corresponding macroscopic model from a fully coupled deterministic particles-fluid problem using an asymptotic expansion in the small size ratio parameter ϵ without applying the ergodicity assumption for the particle dynamics in space.

This chapter is based mainly on [118, 119] and the preliminary master's thesis [116]. It is structured as follows: we extend the mathematical model of a single particle in an incompressible Newtonian fluid presented in Section 2.2 to the case of many particles which interact only by hydrodynamic forces in Section 3.2 also discussing the topic of concentration regimes in Section 3.2.2, subsequently in Section 3.3 we introduce the asymptotic expansion which forms the foundation of the asymptotic and kinetic models in this chapter. The asymptotic ansatz is given as an extension of the one in Section 2.3 and leads to the Theorem 21 describing the suspension behavior in Section 3.3.2 which is similar to the result (Lemma 4) of the one particle case of Section 2.3.3. By analyzing the resulting asymptotic approximation we derive a characterization of the particle phase which consists of a system of equations of motion

for the particles whose velocities are algebraic functions of the leading order fluid velocity. This observation gives raise to the derivation of a transport equation for the particle probability on the corresponding phase space in Section 3.4.1, where also the needed notation for the kinetic model is introduced. Then in Section 3.4.2, we finally derive the kinetic model which encompasses the model due to Batchelor [12] as well as the one derived in [119]. The main results are summarized in Theorems 36, 38, 40 and the connection to [119] is found in Corollary 42. Finally, we illustrate the results by applying the models to special geometries in Section 3.5 and discuss the results in Section 3.6.

3.2 Full-scale suspension model

In this section we extend the particle-fluid model presented in Sec. 2.2.5 to the case of N particles suspended in the fluid stating the system of equations we aim to approximate. We also discuss the topic of concentration regimes associated with suspensions in the context of the asymptotic framework.

3.2.1 Model equations

Following the particle-fluid model (2.10) of Section 2.2.5, we consider a suspension as a system of N_ϵ particles of the same shape and density in a Newtonian fluid. The particle number is modeled as being dependent on the size ratio ϵ, its precise definition is discussed in Section 3.2.2. The joint bounded domain of particles and fluid is denoted by $\Omega \subset \mathbb{R}^3$. By $\Omega_\epsilon = \Omega \setminus \cup_i \overline{\mathcal{E}}_\epsilon^i$ we abbreviate the domain of the Newtonian fluid, where $\mathcal{E}_\epsilon^i$ is the domain of ith particle. Similarly to (2.9), we introduce the scaled rigid body motion of each particle by means of the following mappings:

$$\boldsymbol{x} : \mathbb{R}^3 \times \mathbb{R}^3 \times \mathcal{SO}(3) \times \mathbb{R}^+ \to \mathbb{R}^3, \quad (\boldsymbol{y}, \boldsymbol{z}, \mathbf{R}, \epsilon) \mapsto \epsilon \mathbf{R} \cdot \boldsymbol{y} + \boldsymbol{z},$$

$$\boldsymbol{y} : \mathbb{R}^3 \times \mathbb{R}^3 \times \mathcal{SO}(3) \times \mathbb{R}^+ \to \mathbb{R}^3, \quad (\boldsymbol{x}, \boldsymbol{z}, \mathbf{R}, \epsilon) \mapsto \epsilon^{-1} \mathbf{R}^T \cdot (\boldsymbol{x} - \boldsymbol{z}).$$

Denoting by $\boldsymbol{c}^i, \mathbf{R}^i$ the center of mass and orientation of ith particle and presupposing an ϵ-independent particle shape domain $\mathcal{E} \subset \mathbb{R}^3$, it holds $\mathcal{E}_\epsilon^i(t) = \boldsymbol{x}(\mathcal{E}, \boldsymbol{c}^i(t), \mathbf{R}^i(t), \epsilon)$ and $\mathcal{E} = \boldsymbol{y}(\mathcal{E}_\epsilon^i(t), \boldsymbol{c}^i, \mathbf{R}^i(t), \epsilon)$. To shorten notation, we often use the abbreviation $\boldsymbol{x}^i(\boldsymbol{y}) \equiv \boldsymbol{x}(\boldsymbol{y}, \boldsymbol{c}^i(t), \mathbf{R}^i(t), \epsilon)$ and analogously $\boldsymbol{y}^i(\boldsymbol{x})$, with the dependencies on t and ϵ being understood. Especially the dependence of functions on the time parameter is often suppressed throughout this chapter. As outer forces we consider only gravity, and we assume that particles influence each other only by hydrodynamic interaction, thus, the distance between particles is always sufficiently high, such that surface tension and direct impacts of particles may be ignored. We keep the characteristic values defined with respect to the fluid quantities. Therefore, the Reynolds and Froude number describe the inertial effects in relation to viscosity resp. gravity and ρ_ϵ denotes the scaled density according to (2.12). The complete suspension dynamics is then given by the Navier-Stokes equations in Ω_ϵ, the no-slip conditions on each particle boundary, suitable boundary conditions for the fluid velocity on $\partial \Omega$ and the equations of motion for each particle, i.e., for $i = 1, \ldots, N_\epsilon$ and $t \in (0, T)$ for some $T > 0$:

$$\mathrm{Re}\, \mathrm{D}_t \boldsymbol{u} = \nabla \cdot \mathbf{S}[\boldsymbol{u}]^T + \mathrm{Re}\, \mathrm{Fr}^{-2} \boldsymbol{e}_g, \ \nabla \cdot \boldsymbol{u} = 0, \quad \boldsymbol{x} \in \Omega_\epsilon, \qquad (3.1\mathrm{a})$$

$$\boldsymbol{u} = \boldsymbol{\omega}^i \times \left(\boldsymbol{x} - \boldsymbol{c}^i\right) + \boldsymbol{v}^i\,, \qquad\qquad \boldsymbol{x} \in \partial \mathcal{E}^i_\epsilon\,, \qquad \text{(3.1b)}$$

$$\frac{\mathrm{d}}{\mathrm{d}t}\boldsymbol{c}^i = \boldsymbol{v}^i\,, \qquad \frac{\mathrm{d}}{\mathrm{d}t}\mathbf{R}^i = B(\boldsymbol{\omega}^i)\cdot\mathbf{R}^i\,, \qquad\qquad \text{(3.1c)}$$

$$\rho_\epsilon \epsilon \operatorname{Re}|\mathcal{E}|\frac{\mathrm{d}}{\mathrm{d}t}\boldsymbol{v}^i = \int_{\partial\mathcal{E}} \mathbf{S}[\boldsymbol{u}]\cdot\mathbf{R}^i\cdot\boldsymbol{n}\,\mathrm{d}s + \rho_\epsilon\epsilon\operatorname{Re}\operatorname{Fr}^{-2}|\mathcal{E}|\boldsymbol{e}_g\,, \qquad \text{(3.1d)}$$

$$\rho_\epsilon \epsilon^2 \operatorname{Re}|\mathcal{E}|\frac{\mathrm{d}}{\mathrm{d}t}\left(\mathbf{J}^i\cdot\boldsymbol{\omega}^i\right) = \mathbf{R}^i\cdot\int_{\partial\mathcal{E}} \boldsymbol{y}\times\left(\mathbf{R}^{iT}\cdot\mathbf{S}[\boldsymbol{u}]\cdot\mathbf{R}^i\cdot\boldsymbol{n}\right)\,\mathrm{d}s\,, \qquad \text{(3.1e)}$$

with the Newtonian stresses of $\boldsymbol{u}$ in (3.1d), (3.1e) evaluated at $\boldsymbol{x}^i(\boldsymbol{y})$. The boundary condition at $\partial\Omega$ is given by $\boldsymbol{u} = \boldsymbol{u}_{\partial\Omega}$ and the initial conditions are prescribed as $(\boldsymbol{c}^i, \mathbf{R}^i, \boldsymbol{v}^i, \boldsymbol{\omega}^i)(0)$ and $\boldsymbol{u}(.,0)$ consistent to the boundary conditions at $\partial\Omega_\epsilon(0)$. We define also the inner-particle stresses analogously to (2.11) for $i = 1, \dots, N_\epsilon$ as the solution of

$$\rho_\epsilon \operatorname{Re}\left(\frac{\mathrm{d}^2}{\mathrm{d}t^2}\boldsymbol{x}^i(\boldsymbol{y}) - \operatorname{Fr}^{-2}\boldsymbol{e}_g\right) = \epsilon^{-1}\mathbf{R}^i(t)\cdot\nabla_{\boldsymbol{y}}\cdot\tilde{\mathbf{T}}^{iT}(\boldsymbol{y},t)\,, \qquad \boldsymbol{y}\in\mathcal{E}\,, \qquad \text{(3.2a)}$$

$$\mathbf{R}^{iT}(t)\cdot\mathbf{S}[\boldsymbol{u}](\boldsymbol{x}^i(\boldsymbol{y}),t)\cdot\mathbf{R}^i(t)\cdot\boldsymbol{n} = \tilde{\mathbf{T}}^i(\boldsymbol{y},t)\cdot\boldsymbol{n}\,, \qquad \boldsymbol{y}\in\partial\mathcal{E}\,. \qquad \text{(3.2b)}$$

Remark 13. *Unlike in Section 2, in this chapter we deal with functions which simultaneously depend explicitly on the global variable $\boldsymbol{x}\in\Omega$ and on the local variable $\boldsymbol{y}\in\mathbb{R}^3\supset\mathcal{E}$, say $f\in\mathcal{C}^1(\Omega\times\mathbb{R}^3;\mathbb{R})$. The term "global" here refers to the role of the variable referencing the position of f in the system domain Ω aiming to parametrize the macroscopic behavior of f. While the "local" variable addresses microscopic variations of f on the scale of the particle size ϵ which generally decay far away from the particle center of mass. In order to distinguish the respective differential operators, we use the subscript $._{\boldsymbol{y}}$ for the differentiation with respect to the local variable. The differential operators without this subscript are associated with the global variable $\boldsymbol{x}$, i.e.,*

$$\nabla f = \sum_i \boldsymbol{e}_i\partial_{x_i}f\,, \quad \nabla_{\boldsymbol{y}}f = \sum_i \boldsymbol{e}_i\partial_{y_i}f\,.$$

This notation for the gradient is transferred in a natural way to the divergence and Laplace operators, and to the symmetric deformation gradient, i.e., for $\boldsymbol{f}\in\mathcal{C}^2(\Omega\times\mathbb{R}^3;\mathbb{R}^3)$

$$\nabla_{\boldsymbol{y}}\cdot\boldsymbol{f} = \sum_i \partial_{y_i}f_i\,, \quad \Delta_{\boldsymbol{y}}\boldsymbol{f} = \nabla_{\boldsymbol{y}}\cdot\nabla_{\boldsymbol{y}}\boldsymbol{f}\,, \quad \mathbf{E}_{\boldsymbol{y}}[\boldsymbol{f}] = \frac{1}{2}\left(\nabla_{\boldsymbol{y}}\boldsymbol{f} + \nabla_{\boldsymbol{y}}\boldsymbol{f}^T\right)\,.$$

In particular, this motivates also the notation of the Newtonian stress tensor with respect to the local variable, i.e., for a solenoidal velocity $\boldsymbol{u}\in\mathcal{C}^1(\Omega\times\mathbb{R}^3;\mathbb{R}^3)$ and an associated pressure p

$$\mathbf{S}_{\boldsymbol{y}}[\boldsymbol{u}] = 2\mathbf{E}_{\boldsymbol{y}}[\boldsymbol{u}] - p\mathbf{I}\,.$$

Although this distinction is needed only in Section 3.4, we use it throughout this chapter and apply this notation also for functions which depend solely on the local coordinates, as done in (3.2a).

3.2.2 Concentration regimes

Before deriving an asymptotical model for (3.1), we have to introduce further quantities which characterize a suspension. In particular, we have to make assumptions on the distance between particles which is closely related to the topic of the solid concentration in the suspension. Usually, one characterizes the suspension behavior roughly by three different regimes: the concentrated, semi-dilute and dilute concentration regime [35]. In "concentrated" suspensions the volume fraction $\phi_\epsilon \in [0, 1]$, given by

$$\phi_\epsilon = \frac{N_\epsilon \epsilon^3 |\mathcal{E}|}{|\Omega|} \,, \tag{3.3}$$

may approach $\phi_\epsilon = 1$. In this case, direct particle interactions dominate the overall behavior and the suspension exhibits solid-like behavior. In the "semi-dilute" case, particles cannot move freely in the solvent but direct inertial particle interactions are rare, while hydrodynamic interactions must be taken into account, in this case the suspension behaves visco-elastic. Finally, one calls a suspension in which the particles move freely and do not interact with each other "dilute". In general circumstances, such a characterisation cannot be applied, since the particle distribution may be inhomogeneous with areas highly populated with solids as well as regions filled completely with the solvent. Additionally, even under the assumption of a homogeneous suspension, exact boundaries on ϕ_ϵ depend on the particle geometry. For cylinders or prolate ellipsoidal particles the concentration regimes can be characterized by means of the aspect ratio of the corresponding semi-axes by considering the mean interparticle distance, or analogously the mean free space occupied by only one particle. Such characterisations yield finite bounds on the volume fraction, the particle number concentration, or the mean particle distance [35, 36].

As already pointed out, the suspension model (3.1) only accounts for hydrodynamic particle interactions, which implies that we only consider dilute or semi-dilute suspensions. In particular, we call a suspension described by (3.1) dilute if hydrodynamic interaction between particles can be neglected and semi-dilute otherwise. To make this distinction precise in the asymptotic context, we first consider the mean particle distance ι_ϵ which is subject to the condition $\iota_\epsilon^3 N_\epsilon + |\cup_i \mathcal{E}_\epsilon^i| \leq |\Omega|$, this yields

$$\iota_\epsilon \leq \left(\frac{|\Omega|}{N_\epsilon} - \epsilon^3 |\mathcal{E}| \right)^{1/3} \,.$$

Thus, for ϵ small enough the mean particle distance is bounded by $N_\epsilon^{-1/3}$. Since we are only interested in the behavior of ι_ϵ as $\epsilon \to 0$, we may set geometry dependent constants to unity and

$$\iota_\epsilon = N_\epsilon^{-1/3} \,. \tag{3.4}$$

Additionally, we use ι_ϵ not as a statistical quantity of the average particle distance but instead as a minimal distance between particle centers, i.e., we demand that the particle configuration for all $\epsilon > 0$ and all $t \geq 0$ fulfills

$$\|\boldsymbol{c}^i - \boldsymbol{c}^j\| > \iota_\epsilon \,, \quad i \neq j \,, \quad i, j = 1, \ldots, N_\epsilon \,. \tag{3.5}$$

Furthermore, we set $N_\epsilon = \epsilon^{-\beta}$ with $\beta \in [0, 3)$ which not only implies that the volume fraction fulfills $\phi_\epsilon < 1$, but even $\phi_\epsilon \to 0$ for $\epsilon \to 0$ as seen in (3.3). This choice also implies

$$\epsilon \in o(\iota_\epsilon) \quad \text{as } \epsilon \to 0. \tag{3.6}$$

As we see in the following, the vanishing of ϕ_ϵ still allows for hydrodynamic particle interactions, it therefore covers also the semi-dilute case to some extent.

Remark 14 (Particle distance)**.** *The condition on the particle distance as given in* (3.5) *only accounts for the particle centers of mass and not for the actual particle distance* $d(\mathcal{E}_\epsilon^i, \mathcal{E}_\epsilon^j)$ *with d given by*

$$d(\mathcal{A}, \mathcal{B}) = \inf_{\boldsymbol{x} \in \mathcal{A}, \boldsymbol{y} \in \mathcal{B}} \|\boldsymbol{x} - \boldsymbol{y}\|$$

for $\mathcal{A}, \mathcal{B} \subset \mathbb{R}^3$. Because of (3.6) *and the boundedness of $\mathcal{E}$ there exists an $\epsilon > 0$ such that $\iota_\epsilon / \epsilon > 2 \sup_{\boldsymbol{y} \in \mathcal{E}} \|(\mathbf{R}^i - \mathbf{R}^j) \cdot \boldsymbol{y}\|$ and due to* (3.5) *it follows*

$$\epsilon^{-1} \|\boldsymbol{c}^i - \boldsymbol{c}^j\| > \iota_\epsilon / \epsilon > 2 \sup_{\boldsymbol{y} \in \mathcal{E}} \|(\mathbf{R}^i - \mathbf{R}^j) \cdot \boldsymbol{y}\|.$$

This way, we find for $\boldsymbol{x} \in \mathcal{E}_\epsilon^i$ and $\boldsymbol{z} \in \mathcal{E}_\epsilon^j$

$$\begin{aligned}
\|\boldsymbol{x} - \boldsymbol{z}\| &= \|\epsilon(\mathbf{R}^i - \mathbf{R}^j) \cdot \boldsymbol{y} + \boldsymbol{c}^i - \boldsymbol{c}^j\| \geq \epsilon |\epsilon^{-1} \|\boldsymbol{c}^i - \boldsymbol{c}^j\| - \|(\mathbf{R}^i - \mathbf{R}^j) \cdot \boldsymbol{y}\|| \\
&> 0.5 \|\boldsymbol{c}^i - \boldsymbol{c}^j\|.
\end{aligned}$$

Thus, $d(\mathcal{E}_\epsilon^i, \mathcal{E}_\epsilon^j) \geq 0.5 \|\boldsymbol{c}^i - \boldsymbol{c}^j\|$ for ϵ small enough, i.e., conditions on the particle distance and on the separation of the centers of mass differ only in a constant factor, yielding the same behavior as $\epsilon \to 0$.

3.3 Leading order asymptotic approximation

In this section we adapt our asymptotic approach of Section 2.3 to a multi-particle system. Under an appropriate set of assumptions on the particle configuration, we formulate an asymptotic approximation to the solution of the fully coupled fluid-N_ϵ-particle system.

3.3.1 Assumptions and asymptotic expansion

The underlying assumptions for the asymptotic approximation of (3.1) are given in Assumption 15.

Assumption 15 (Particle fluid interaction in suspension)**.**

1) *The fluid is essentially undisturbed by the particles.*

2) *The fluid motion induces a rotation of each particle of order $\mathcal{O}(1)$.*

3) *The minimal distance between particles and between each particle and the boundary is given by $\iota_\epsilon > 0$.*

4) The suspension is dilute or semi-dilute.

The points 1), 2) of Assumption 15 are identical to the one particle case and allow the asymptotic approximation of the suspension model by an undisturbed Navier-Stokes flow as well as postulating the rotational particle behavior as $\epsilon \to 0$. The demand of a minimal particle distance ensures that particles are sufficiently far from each other. In particular, we use relation (3.4) for ι_ϵ. The last point allows the construction of the asymptotic solution to (3.1) as a superposition of the single particle contributions of Section 2.3. This implies especially that the solution of (3.1) is a small perturbation of $(\boldsymbol{u}_0, p_0) : \Omega \times [0, T] \to \mathbb{R}^3 \times \mathbb{R}$ which solve the Navier-Stokes system (2.13) in $\Omega \times [0, T]$ with prescribed boundary and initial data. Under these assumptions, it is again our task to relate the asymptotic quantities of the multi particle system to the undisturbed velocity $\boldsymbol{u}_0$ and pressure p_0.

In order to shorten notation, we take the asymptotic expansion of Section 2.3.4 not expanding the center of mass and the rotation of each particle. However, the following considerations can be analogously carried out in the case of the full expansion used in Section 2.3.2 for a single particle. Additionally, we also use a regular expansion for the particle accelerations. In total, we have

$$\boldsymbol{v}^i = \sum_{j=0}^{\infty} \epsilon^j \boldsymbol{v}^i_j , \qquad\qquad \boldsymbol{\omega}^i = \sum_{j=0}^{\infty} \epsilon^j \boldsymbol{\omega}^i_j ,$$

$$\frac{\mathrm{d}}{\mathrm{d}t} \boldsymbol{v}^i = \sum_{j=0}^{\infty} \epsilon^j \boldsymbol{a}^i_j , \qquad\qquad \frac{\mathrm{d}}{\mathrm{d}t} (\mathbf{J}^i \cdot \boldsymbol{\omega}^i) = \sum_{j=0}^{\infty} \epsilon^j \boldsymbol{\psi}^i_j$$

for $i = 1, \ldots, N_\epsilon$. The fluid velocity and pressure are split in a global, undisturbed part and a local contribution due to the particle presence,

$$\boldsymbol{u} = \boldsymbol{u}_0 + \boldsymbol{u}_{\mathrm{loc}} , \quad p = p_0 + p_{\mathrm{loc}} .$$

The local fields are set as a superposition of each particle contribution, $\boldsymbol{u}^i_{\mathrm{loc}}$, which possess a regular expansion in ϵ, i.e.,

$$\boldsymbol{u}_{\mathrm{loc}}(\boldsymbol{x}, t, \epsilon) = \sum_{i=1}^{N_\epsilon} \sum_{j=1}^{\infty} \epsilon^j \mathbf{R}^i \cdot \boldsymbol{u}^i_{\mathrm{loc},j}(\boldsymbol{y}^i(\boldsymbol{x}), t) ,$$

$$p_{\mathrm{loc}}(\boldsymbol{x}, t, \epsilon) = \sum_{i=1}^{N_\epsilon} \sum_{j=1}^{\infty} \epsilon^{j-1} p^i_{\mathrm{loc},j}(\boldsymbol{y}^i(\boldsymbol{x}), t) .$$

3.3.2 Asymptotic suspension approximation

Before we formulate the asymptotic solution to (3.1), we first state two auxiliary results. The first one is related to the well-definition of the superposition of the local velocity fields.

Lemma 16 (Estimations on the local fields)**.** *Let $\boldsymbol{u}^i$, $i = 1, \ldots, N_\epsilon$, be $\mathcal{C}^K(\mathbb{R}^3 \setminus \overline{\mathcal{E}}; \mathbb{R}^3)$-functions continuous at $\partial\mathcal{E}$ with uniformly bounded boundary values $\boldsymbol{u}^i_{|\partial\mathcal{E}}$. Furthermore, we assume that the following decay property holds: For all $\boldsymbol{y} \in \mathbb{R}^3$ with $\|\boldsymbol{y}\| > 2R$ for an $R > 1/2$ such that $\mathcal{E} \subset \mathcal{B}_R(\mathbf{0})$, the velocity fields $\boldsymbol{u}^i$ fulfill*

$$\|\nabla^k_{\boldsymbol{y}} \boldsymbol{u}^i(\boldsymbol{y})\| \le c(\mathcal{E}, k) \|\boldsymbol{u}^i\|_{1,\partial\mathcal{E}} \|\boldsymbol{y}\|^{-(\ell+k)} \tag{3.7}$$

for some $\ell \geq 1$ and all $0 \leq k \leq K$. The particle number is given by $N_\epsilon = \epsilon^{-\beta}$, $\beta \in [0,3)$ and the minimal particle distance fulfills (3.5) with ι_ϵ given by (3.4). Then there exists an $\bar\epsilon > 0$ such that for all $0 < \epsilon < \bar\epsilon$ the following estimations for $\boldsymbol{x} \in \Omega_\epsilon$ hold.

C1) *Assume the following conditions on β for all $k \leq K$: $\beta \leq \ell - 1$ for $\ell + k \in [1,3)$, $\beta < \ell - 1$ for $\ell + k = 3$ ($\beta = 0$ for $\ell = 1, k = 2$), $\beta \leq 3(\ell - 1)/(\ell + k)$ for $\ell + k > 3$. Then*

$$\epsilon^{-1-k} \sum_{j \in \mathcal{I}} \left\| \nabla_{\boldsymbol{y}}^k \boldsymbol{u}^j(\boldsymbol{y}^j(\boldsymbol{x})) \right\| \leq c \sup_i \|\boldsymbol{u}^i\|_{1,\partial\mathcal{E}}, \tag{3.8}$$

where $\mathcal{I} = \{1, \ldots, N_\epsilon\}$ if $\|\boldsymbol{x} - \boldsymbol{c}^i\| \geq \iota_\epsilon$ for all i and $\mathcal{I} = \{1, \ldots, N_\epsilon\} \setminus \{i\}$ if $\|\boldsymbol{x} - \boldsymbol{c}^i\| < \iota_\epsilon$ for an $1 \leq i \leq N_\epsilon$.

C2) *Assume the following conditions on β for all $k \leq K$: $\beta \leq \ell$ for $\ell + k \in [1,3)$, $\beta < \ell$ for $\ell + k = 3$, $\beta \leq 3\ell/(\ell + k)$ for $\ell + k > 3$. Then*

$$\epsilon^{-k} \sum_{j \in \mathcal{I}} \left\| \nabla_{\boldsymbol{y}}^k \boldsymbol{u}^j(\boldsymbol{y}^j(\boldsymbol{x})) \right\| \leq c \sup_i \|\boldsymbol{u}^i\|_{1,\partial\mathcal{E}}, \tag{3.9}$$

where $\mathcal{I} = \{1, \ldots, N_\epsilon\}$ if $\|\boldsymbol{x} - \boldsymbol{c}^i\| \geq \iota_\epsilon$ for all i and $\mathcal{I} = \{1, \ldots, N_\epsilon\} \setminus \{i\}$ if $\|\boldsymbol{x} - \boldsymbol{c}^i\| < \iota_\epsilon$ for an $1 \leq i \leq N_\epsilon$.

The constants c in (3.8)-(3.9) do not depend on ϵ and $\boldsymbol{u}^i$.

Proof. We group particles by considering the following cover of Ω by spherical shells around any $\boldsymbol{x} \in \Omega$

$$\mathcal{U}_{\boldsymbol{x}}^k = \{\boldsymbol{z} \in \Omega \mid (k-1)\iota_\epsilon \leq \|\boldsymbol{z} - \boldsymbol{x}\| < k\iota_\epsilon\}, \quad k = 1, \ldots, N_U.$$

Since Ω is a bounded domain, the number of shells needed to cover Ω is bounded by $N_U = \text{diam}(\Omega)\iota_\epsilon^{-1}$. The volume of kth shell can be bounded by

$$|\mathcal{U}_{\boldsymbol{x}}^k| \leq \frac{28}{3}\pi\iota_\epsilon^3 k^2. \tag{3.10}$$

Since the suspension is assumed to possess property (3.5), the number of particles in each shell, N_k, must fulfill $\iota_\epsilon^3 N_k + \epsilon^3 N_k |\mathcal{E}| \leq |\mathcal{U}_{\boldsymbol{x}}^k|$. In combination with (3.10) and (3.5) we thus find for ϵ small enough

$$N_k \leq \frac{28}{3}\pi k^2.$$

Finally, we introduce the index sets $\mathcal{I}_{\boldsymbol{x}}^k = \{i \in \{1, \ldots, N_\epsilon\} \mid \boldsymbol{c}^i \in \mathcal{U}_{\boldsymbol{x}}^k\}$. Now, we fix $i \in \{1, \ldots, N_\epsilon\}$ and let $\boldsymbol{x} \in \partial\mathcal{E}_\epsilon^i$, then $\boldsymbol{x} = \boldsymbol{x}^i(\boldsymbol{y})$ for $\boldsymbol{y} \in \partial\mathcal{E}$ and applying (3.5), (3.6) we find for $i \neq j$

$$\|\boldsymbol{y}^j(\boldsymbol{x}^i(\boldsymbol{y}))\| = \|\epsilon^{-1}\mathbf{R}^{jT} \cdot (\boldsymbol{c}^i - \boldsymbol{c}^j) + \mathbf{R}^{jT} \cdot \mathbf{R}^i \cdot \boldsymbol{y}\| \geq |\epsilon^{-1}\|\boldsymbol{c}^i - \boldsymbol{c}^j\| - \|\boldsymbol{y}\||$$
$$> 0.5\epsilon^{-1}\|\boldsymbol{c}^i - \boldsymbol{c}^j\| \tag{3.11}$$

for ϵ small enough. Then, noting that $\mathcal{I}_{\boldsymbol{c}^i}^1 = \{i\}$ and using the decay property of $\boldsymbol{u}^j$ given by (3.7), we find

$$\epsilon^{-k} \sum_{j \neq i} \left\| \nabla_{\boldsymbol{y}}^k \boldsymbol{u}^j(\boldsymbol{y}^j(\boldsymbol{x})) \right\| \leq \epsilon^{-k} \sum_{m=2}^{N_U} \sum_{j \in \mathcal{I}_{\boldsymbol{c}^i}^m} \left\| \nabla_{\boldsymbol{y}}^k \boldsymbol{u}^j(\boldsymbol{y}^j(\boldsymbol{x}^i(\boldsymbol{y}))) \right\|$$

$$\leq c \sup_i \|\boldsymbol{u}^i\|_{1,\partial\mathcal{E}} \epsilon^\ell \sum_{m=2}^{N_U} \sum_{j\in\mathcal{I}_{\boldsymbol{c}^i}^m} \|\boldsymbol{c}^i - \boldsymbol{c}^j\|^{-(\ell+k)}$$

$$\leq c \sup_i \|\boldsymbol{u}^i\|_{1,\partial\mathcal{E}} \epsilon^\ell \iota_\epsilon^{-(\ell+k)} \sum_{m=2}^{N_U} \frac{m^2}{(m-1)^{\ell+k}}$$

$$\leq c \sup_i \|\boldsymbol{u}^i\|_{1,\partial\mathcal{E}} \epsilon^\ell \iota_\epsilon^{-(\ell+k)} \sum_{m=1}^{N_U-1} m^{2-(\ell+k)} \qquad (3.12)$$

with c independent of ϵ. For an arbitrary $\boldsymbol{x} \in \Omega_\epsilon$, if $\|\boldsymbol{x} - \boldsymbol{c}^i\| < \iota_\epsilon$ for some $i \in \{1,\ldots,N_\epsilon\}$, $\mathcal{I}_{\boldsymbol{x}}^1 = \{i\}$ and (3.12) holds. Otherwise

$$\|\boldsymbol{y}^j(\boldsymbol{x})\| = \epsilon^{-1}\|\boldsymbol{x} - \boldsymbol{c}^j\| \geq \epsilon^{-1}\iota_\epsilon$$

for all $j = 1,\ldots,N_\epsilon$, thus $\mathcal{I}_{\boldsymbol{x}}^1 = \emptyset$ and

$$\epsilon^{-k} \sum_{j=1}^{N_\epsilon} \|\nabla_{\boldsymbol{y}}^k \boldsymbol{u}^j(\boldsymbol{y}^j(\boldsymbol{x}))\| \leq c \sup_i \|\boldsymbol{u}^i\|_{1,\partial\mathcal{E}} \epsilon^\ell \iota_\epsilon^{-(\ell+k)} \sum_{m=1}^{N_U-1} m^{2-(\ell+k)}.$$

For $\ell + k \in [1,2]$, $m^{2-(\ell+k)} \leq N_U^{2-(\ell+k)}$, therefore we find in combination with (3.4)

$$\epsilon^\ell \iota_\epsilon^{-(\ell+k)} \sum_{m=1}^{N_U-1} m^{2-(\ell+k)} \leq c\epsilon^\ell \iota_\epsilon^{-(\ell+k)} N_U^{3-(\ell+k)} \leq c\epsilon^\ell \iota_\epsilon^{-3} = c\epsilon^{\ell-\beta} \in \begin{cases} \mathcal{O}(\epsilon) & \text{for C1} \\ \mathcal{O}(1) & \text{for C2} \end{cases}$$

with c independent of ϵ. For $\ell + k \in (2,3)$ and $\ell + k = 3$ we find by means of the Euler-Maclaurin formula, see, e.g., [2]

$$\sum_{m=1}^{N_U-1} m^{2-(\ell+k)} \leq c N_U^{3-(\ell+k)}, \quad \text{for } \ell+k \in (2,3), \qquad \text{and} \quad \sum_{m=1}^{N_U-1} m^{-1} \leq c\ln(N_U),$$

with $c = c(\ell)$ but independent of ϵ. Thus, for $\ell + k \in (2,3)$ again

$$\epsilon^\ell \iota_\epsilon^{-(\ell+k)} \sum_{m=1}^{N_U-1} m^{2-(\ell+k)} \leq \epsilon^{\ell-\beta} \in \begin{cases} \mathcal{O}(\epsilon) & \text{for C1} \\ \mathcal{O}(1) & \text{for C2} \end{cases}$$

and for $\ell + k = 3$

$$\epsilon^\ell \iota_\epsilon^{-3} \sum_{m=1}^{N_U-1} m^{-1} \leq c\epsilon^\ell \iota_\epsilon^{-3} \ln(N_U) \leq c\epsilon^{\ell-\beta}\ln(\epsilon^{-\beta/3}) \in \begin{cases} o(\epsilon) & \text{for C1} \\ o(1) & \text{for C2} \end{cases}.$$

For $\ell + k > 3$, the series $\sum_{m=1}^\infty m^{2-(\ell+k)} < \infty$, thus

$$\epsilon^\ell \iota_\epsilon^{-(\ell+k)} \sum_{m=1}^{N_U-1} m^{2-\ell} \leq c\epsilon^{\ell-(\ell+k)\beta/3} \in \begin{cases} \mathcal{O}(\epsilon) & \text{for C1} \\ \mathcal{O}(1) & \text{for C2} \end{cases}.$$

Hence, we showed (3.8) and (3.9). $\qquad\square$

Next, we state a second auxiliary statement, which is connected to the well-posedness of the particle related local stationary Stokes problems. In the following lemma we often deal with functions which depend on variables in $(\Omega \times \mathcal{SO}(3))^{N_\epsilon}$ that are sufficiently regular for any $\epsilon > 0$, say $f \in \mathcal{C}^K((\Omega \times \mathcal{SO}(3))^{N_\epsilon}; \mathbb{R})$. In this case $\|f\|_{\mathcal{C}^K} < c$ with a constant c which in general depends on N_ϵ and might be unbounded as ϵ approaches zero. The asymptotic approximations are meaningful only if the corresponding constants are bounded uniformly in ϵ. Hence, we define the following function space in order to shorten notation.

Definition 17 ($\mathcal{C}_N^K$-functions)**.** *For $K \geq 0$ and $n, N \geq 1$, consider a function $f \in \mathcal{C}^K((\Omega \times \mathcal{SO}(3))^N \times \mathbb{R}; \mathbb{R}^n)$. Then $f \in \mathcal{C}_N^K$ if for all $(\boldsymbol{z}^i, \mathbf{V}^i) \in \mathcal{C}^\infty(\mathbb{R}; \Omega \times \mathcal{SO}(3))$ with $\max_i \|\boldsymbol{z}^i\|_{\mathcal{C}^K} < c_1$, $\max_i \|\mathbf{V}^i\|_{\mathcal{C}^K} < c_1$ for some $c_1 > 0$ independent of N, there exists a constant $c_2 < \infty$ independent of N, such that*

$$\left\| t \mapsto f(\boldsymbol{z}^1(t), \mathbf{V}^1(t), \ldots, \boldsymbol{z}^N(t), \mathbf{V}^N(t), t) \right\|_{\mathcal{C}^K(\mathbb{R}; \mathbb{R}^n)} < c_2.$$

Additionally, we also introduce the following abbreviations for the forces and torques on each particle, which are related to the expansion of the particle accelerations and are similar to those in Abbreviation 3.

Abbreviation 18. *We set for $i = 1, \ldots, N_\epsilon$*

$$\begin{aligned}
\boldsymbol{k}_k^i &= \boldsymbol{0} & &\text{for } k < 0\,, \\
\boldsymbol{k}_0^i &= \rho \operatorname{Re} |\mathcal{E}| \mathbf{R}^{iT} \cdot (\boldsymbol{a}_0^i - \operatorname{Fr}^{-2} \boldsymbol{e}_g)\,, & & \\
\boldsymbol{k}_k^i &= \rho \operatorname{Re} |\mathcal{E}| \mathbf{R}^{iT} \cdot \boldsymbol{a}_k^i & &\text{for } k \geq 1\,, \\
\boldsymbol{\ell}_k^i &= \boldsymbol{0} & &\text{for } k < 0\,, \\
\boldsymbol{\ell}_k^i &= \rho \operatorname{Re} |\mathcal{E}| \mathbf{R}^{iT} \cdot \boldsymbol{\psi}_k^i & &\text{for } k \geq 0\,.
\end{aligned}$$

Then, the forces and torques depend on the density scaling function $\alpha_\rho(\epsilon) = \epsilon^r$ and are given as $\boldsymbol{f}_1^i = \boldsymbol{k}_{-1-r}^i$, $\boldsymbol{g}_1^i = \boldsymbol{\ell}_{-2-r}^i$ and for $k \geq 2$

$$\boldsymbol{f}_k^i = -\frac{1}{(k-2)!} \mathbf{R}^{iT} \cdot \int_{\mathcal{E}} [\mathbf{R}^i \cdot \boldsymbol{y} \cdot \nabla]^{k-2} \nabla \cdot \mathbf{S}[\boldsymbol{u}_0]\, \mathrm{d}\boldsymbol{y} + \boldsymbol{k}_{k-2-r}^i\,, \tag{3.13a}$$

$$\boldsymbol{g}_k^i = -\frac{1}{(k-2)!} \int_{\mathcal{E}} \boldsymbol{y} \times \mathbf{R}^{iT} \cdot [\mathbf{R}^i \cdot \boldsymbol{y} \cdot \nabla]^{k-2} \nabla \cdot \mathbf{S}[\boldsymbol{u}_0]\, \mathrm{d}\boldsymbol{y} + \boldsymbol{\ell}_{k-3-r}^i\,, \tag{3.13b}$$

where the derivatives of $\boldsymbol{u}_0$ are evaluated at $(\boldsymbol{c}^i(t), t)$.

Lemma 19 (Asymptotic solution to particle related equations up to order n)**.** *We make the following set of assumptions.*

R1) *The functions $\boldsymbol{u}_0 \in \mathcal{C}^\infty(\Omega \times (0, T); \mathbb{R}^3)$ and $p_0 \in \mathcal{C}^\infty(\Omega \times (0, T); \mathbb{R})$ denote a given solenoidal velocity in Ω and a corresponding pressure.*

R2) *The minimal particle distance fulfills (3.5) with ι_ϵ given by (3.4). The density scaling function (2.12) is given as $\alpha_\rho(\epsilon) = \epsilon^r$ with $r \geq -1$.*

R3) *For $i = 1, \ldots, N_\epsilon$ and $k = 1, \ldots, n$, $\boldsymbol{u}_{\mathrm{loc}, k}^i(., t) \in \mathcal{C}^\infty(\mathbb{R}^3 \setminus \overline{\mathcal{E}}; \mathbb{R}^3)$, continuous at $\partial \mathcal{E}$, $p_{\mathrm{loc}, k}^i(., t) \in \mathcal{C}^\infty(\mathbb{R}^3 \setminus \overline{\mathcal{E}}; \mathbb{R})$ are for each $t \in [0, T]$ solutions of the stationary Stokes equations,*

$$\Delta_{\boldsymbol{y}} \boldsymbol{u}_{\mathrm{loc}, k}^i = \nabla_{\boldsymbol{y}} p_{\mathrm{loc}, k}^i\,, \quad \nabla_{\boldsymbol{y}} \cdot \boldsymbol{u}_{\mathrm{loc}, k}^i = 0\,. \tag{3.14}$$

The boundary conditions for $\boldsymbol{y} \in \partial \mathcal{E}$ are given as

$$\boldsymbol{u}^i_{\mathrm{loc},k}(\boldsymbol{y}) = \mathbf{R}^{iT} \cdot \left(\boldsymbol{v}^i_k + B(\boldsymbol{\omega}^i_{k-1}) \cdot \mathbf{R}^i \cdot \boldsymbol{y} - \frac{1}{k!}[\mathbf{R}^i \cdot \boldsymbol{y} \cdot \nabla]^k \boldsymbol{u}_0 - \boldsymbol{r}^i_k(\boldsymbol{y}) \right), \quad (3.15\mathrm{a})$$

where the derivatives of $\boldsymbol{u}_0$ are evaluated at $(\boldsymbol{c}^i(t), t)$ and with the velocity vectors $\boldsymbol{r}^i_k$ set as

$$\boldsymbol{r}^i_1 \equiv \mathbf{0}\,,$$
$$\boldsymbol{r}^i_k(\boldsymbol{y}) = \epsilon^{-1} \sum_{j \neq i} \mathbf{R}^j \cdot \boldsymbol{u}^j_{\mathrm{loc},k-1}(\boldsymbol{y}^j(\boldsymbol{x}^i(\boldsymbol{y}))) \quad \textit{for } k \geq 2\,. \qquad (3.15\mathrm{b})$$

The decay properties for $\|\boldsymbol{y}\| \to \infty$ as well as the integral conditions read as

$$\nabla^m_{\boldsymbol{y}} \boldsymbol{u}^i_{\mathrm{loc},k} \in \mathcal{O}(\|\boldsymbol{y}\|^{-(1+m)})\,, \quad m = 0,1\,, \quad p^i_{\mathrm{loc},k} \in \mathcal{O}(\|\boldsymbol{y}\|^{-2})\,, \qquad (3.15\mathrm{c})$$

$$\int_{\partial \mathcal{E}} \mathbf{S}_{\boldsymbol{y}}[\boldsymbol{u}^i_{\mathrm{loc},k}] \cdot \boldsymbol{n}\,\mathrm{d}s = \boldsymbol{f}^i_k\,, \quad \int_{\partial \mathcal{E}} \boldsymbol{y} \times \mathbf{S}_{\boldsymbol{y}}[\boldsymbol{u}^i_{\mathrm{loc},k}] \cdot \boldsymbol{n}\,\mathrm{d}s = \boldsymbol{g}^i_k\,, \qquad (3.15\mathrm{d})$$

with $\boldsymbol{f}^i_k, \boldsymbol{g}^i_k$ given in Abbreviation 18.

R4) *The particle centers of mass and their orientations behave according to*

$$\frac{\mathrm{d}}{\mathrm{d}t} \boldsymbol{c}^i = \sum_{k=0}^{n} \epsilon^k \boldsymbol{v}^i_k\,, \quad \frac{\mathrm{d}}{\mathrm{d}t} \mathbf{R}^i = \sum_{k=0}^{n-1} \epsilon^k B(\boldsymbol{\omega}^i_k) \cdot \mathbf{R}^i \qquad (3.16)$$

for $t > 0$ with initial data $\boldsymbol{c}^i(0), \mathbf{R}^i(0)$ for $i \in \{1, \ldots, N_\epsilon\}$ and where the velocities $\boldsymbol{v}^i_k, \boldsymbol{\omega}^i_{k-1} \in \mathcal{C}^{\min(K+3+r-k,K)}((0,T); \mathbb{R}^3)$ are uniformly bounded for each $t \geq 0$.

R5) *The particle number fulfills one of the following assumptions: The particle number N_ϵ is constant independent of ϵ. Alternatively, if the condition for the quadratic decay of the local velocity fields (B.3) of Corollary B.4, Appendix B.2 holds for all $\boldsymbol{u}^i_{\mathrm{loc},k}$, $k \in \{1, \ldots, n-1\}$ and $i = 1, \ldots, N_\epsilon$, then the particle number is given by $N_\epsilon = \epsilon^{-\beta}$ with β subject to the conditions C1) of Lemma 16 for $K = \max(n-2-r, 1)$, $\ell = 2$.*

Then, the truncated expansions

$$\boldsymbol{v}^{ie} = \sum_{j=0}^{n} \epsilon^j \boldsymbol{v}^i_j\,, \qquad\qquad \boldsymbol{\omega}^{ie} = \sum_{j=0}^{n-1} \epsilon^j \boldsymbol{\omega}^i_j\,, \qquad (3.17\mathrm{a})$$

$$\left(\frac{\mathrm{d}}{\mathrm{d}t} \boldsymbol{v}^i \right)^e = \sum_{j=0}^{n-1} \epsilon^j \boldsymbol{a}^i_j\,, \qquad\qquad \left(\frac{\mathrm{d}}{\mathrm{d}t}(\mathbf{J}^i \cdot \boldsymbol{\omega}^i) \right)^e = \sum_{j=0}^{n-2} \epsilon^j \boldsymbol{\psi}^i_j\,, \qquad (3.17\mathrm{b})$$

$$\boldsymbol{u}^e = \boldsymbol{u}_0 + \boldsymbol{u}^e_{\mathrm{loc}}\,, \qquad\qquad p = p_0 + p^e_{\mathrm{loc}}\,, \qquad (3.17\mathrm{c})$$

$$\boldsymbol{u}^e_{\mathrm{loc}} = \sum_{i=1}^{N_\epsilon} \sum_{j=1}^{n} \epsilon^j \mathbf{R}^i \cdot \boldsymbol{u}^i_{\mathrm{loc},j}\,, \qquad\qquad p^e_{\mathrm{loc}} = \sum_{i=1}^{N_\epsilon} \sum_{j=1}^{n} \epsilon^{j-1} p^i_{\mathrm{loc},j} \qquad (3.17\mathrm{d})$$

yield the following approximation orders for the particle related equations (3.1b)-(3.1e)

$$\boldsymbol{u}^e = \boldsymbol{\omega}^{ie} \times \left(\boldsymbol{x} - \boldsymbol{c}^i \right) + \boldsymbol{v}^{ie} + \mathcal{O}(\epsilon^{n+1})\,, \quad \boldsymbol{x} \in \partial \mathcal{E}^i_\epsilon\,, \qquad (3.18\mathrm{a})$$

$$\frac{\mathrm{d}}{\mathrm{d}t}\boldsymbol{c}^i = \boldsymbol{v}^{ie} + \mathcal{O}(\epsilon^{n+1})\,, \qquad \frac{\mathrm{d}}{\mathrm{d}t}\mathbf{R}^i = B(\boldsymbol{\omega}^{ie})\cdot\mathbf{R}^i + \mathcal{O}(\epsilon^n)\,, \tag{3.18b}$$

$$\rho_\epsilon\epsilon\operatorname{Re}|\mathcal{E}|\left(\frac{\mathrm{d}}{\mathrm{d}t}\boldsymbol{v}^i\right)^e = \int_{\partial\mathcal{E}}\mathbf{S}[\boldsymbol{u}^e]\cdot\mathbf{R}^i\cdot\boldsymbol{n}\,\mathrm{d}s + \rho_\epsilon\epsilon\operatorname{Re}\operatorname{Fr}^{-2}|\mathcal{E}|\boldsymbol{e}_g + \mathcal{O}(\epsilon^n)\,, \tag{3.18c}$$

$$\rho_\epsilon\epsilon^2\operatorname{Re}|\mathcal{E}|\left(\frac{\mathrm{d}}{\mathrm{d}t}(\mathbf{J}^i\cdot\boldsymbol{\omega}^i)\right)^e = \mathbf{R}^i\cdot\int_{\partial\mathcal{E}}\boldsymbol{y}\times\left(\mathbf{R}^{iT}\cdot\mathbf{S}[\boldsymbol{u}^{ie}]\cdot\mathbf{R}^i\cdot\boldsymbol{n}\right)\,\mathrm{d}s + \mathcal{O}(\epsilon^n) \tag{3.18d}$$

with the linear and angular velocities for any $t \geq 0$ given as

$$\boldsymbol{v}_0^i(t) = \boldsymbol{u}_0(\boldsymbol{c}^i(t), t)\,, \tag{3.19a}$$

$$(\boldsymbol{v}_k^i(t), \boldsymbol{\omega}_{k-1}^i(t)) = F_k^i(\boldsymbol{c}^1(t), \mathbf{R}^1(t), \ldots, \boldsymbol{c}^{N_\epsilon}(t), \mathbf{R}^{N_\epsilon}(t), t) \tag{3.19b}$$

with functions $F_k^i \in \mathcal{C}_{N_\epsilon}^{\min(K+3+r-k,K)}$, $k = 1, \ldots, n$ and $i = 1, \ldots, N_\epsilon$.

Proof. First of all, we note that due to $\boldsymbol{r}_1^i \equiv \boldsymbol{0}$ and R1), $\boldsymbol{u}_{\mathrm{loc},1}^i|_{\partial\mathcal{E}} \in \mathcal{C}(\partial\mathcal{E})$ and Lemma B.3 in Appendix B.2 is applicable for each $t \geq 0$. Thus, Corollary B.4 holds, i.e.,

$$\|\nabla_{\boldsymbol{y}}^m \boldsymbol{u}_{\mathrm{loc},1}^i(\boldsymbol{y})\| \leq c\|\boldsymbol{u}_{\mathrm{loc},1}^i\|_{1,\partial\mathcal{E}}\|\boldsymbol{y}\|^{-(\ell+m)} \tag{3.20}$$

with $c = c(\mathcal{E}, m)$ for all $m \geq 0$ and $\ell \in \{1, 2\}$ according to R5). Due to (3.15a) we find

$$\|\boldsymbol{u}_{\mathrm{loc},1}^i\|_{1,\partial\mathcal{E}} \leq c\left(\|\boldsymbol{v}_1^i\| + \|\boldsymbol{\omega}_0^i\| + \|\nabla\boldsymbol{u}_0(\boldsymbol{c}^i, t)\|\right)$$

with $c = c(\mathcal{E})$. Applying R1) and R4) then yields a uniform bound on $\boldsymbol{u}_{\mathrm{loc},1}^i|_{\partial\mathcal{E}}$, which implies that Lemma 16 holds. This ensures that $\boldsymbol{r}_2^i$ given by (3.15b) is well-defined, continuous at $\partial\mathcal{E}$ and bounded. Therefore, we can repeat each of the above arguments and deduce a uniform bound on $\boldsymbol{u}_{\mathrm{loc},2}^i|_{\partial\mathcal{E}}$ in terms of the bound in R4) and $\max_{m=1,2}\sup_{\boldsymbol{x}\in\Omega}\|\nabla^m\boldsymbol{u}_0(\boldsymbol{x}, t)\|$. Iteration of this chain shows: For each $t \geq 0$, the velocity fields $\boldsymbol{u}_{\mathrm{loc},k}^i|_{\partial\mathcal{E}}$, $k = 1, \ldots, n$ are uniformly bounded and Lemma 16 holds, which implies that $\boldsymbol{r}_k^i$ is well-defined for all $k \leq n$ and all $\epsilon > 0$.

Analyzing the system of particle related equations, we start with the no-slip condition (3.1b). Inserting the expansions of the velocities and using a Taylor expansion for $\boldsymbol{u}_0$ at $\boldsymbol{c}^i$ for $\boldsymbol{x} = \boldsymbol{x}^i(\boldsymbol{y}) = \boldsymbol{c}^i + \epsilon\mathbf{R}^i\cdot\boldsymbol{y}$ with $\boldsymbol{y} \in \partial\mathcal{E}$ yields

$$\sum_{k=0}^n \epsilon^k\frac{1}{k!}[\mathbf{R}^i\cdot\boldsymbol{y}\cdot\nabla]^k\boldsymbol{u}_0(\boldsymbol{c}^i, t) + \sum_{j\neq i}\sum_{k=1}^n \epsilon^k\mathbf{R}^j\cdot\boldsymbol{u}_{\mathrm{loc},k}^j + \sum_{k=1}^n \epsilon^k\mathbf{R}^i\cdot\boldsymbol{u}_{\mathrm{loc},k}^i$$

$$= \sum_{k=1}^n \epsilon^k B(\boldsymbol{\omega}_{k-1}^i)\cdot\mathbf{R}^i\cdot\boldsymbol{y} + \sum_{k=0}^n \epsilon^k\boldsymbol{v}_k^i + \mathcal{O}(\epsilon^{n+1})\,.$$

Using the relations (3.19a) and (3.15a) the approximation order (3.18a) follows. Next, we insert the velocity expansions into (3.1c) finding

$$\frac{\mathrm{d}}{\mathrm{d}t}\boldsymbol{c}^i = \sum_{j=0}^n \epsilon^j\boldsymbol{v}_j^i + \mathcal{O}(\epsilon^{n+1})\,, \qquad \frac{\mathrm{d}}{\mathrm{d}t}\mathbf{R}^i = B\left(\sum_{j=0}^{n-1}\epsilon^j\boldsymbol{\omega}_j^i\right)\cdot\mathbf{R}^i + \mathcal{O}(\epsilon^n)\,,$$

which in combination with (3.16) shows (3.18b).

Considering the balance of momenta for each particle, we insert the expansions for the particle acceleration on the left-hand sides and for the fluid velocity on the right-hand sides. This yields

$$
\rho_\epsilon \epsilon \operatorname{Re} |\mathcal{E}| \left(\sum_{j=0}^{n-1} \epsilon^j \boldsymbol{a}_j^i - \operatorname{Fr}^{-2} \boldsymbol{e}_g \right)
$$

$$
= \epsilon^{-2} \int_{\partial \mathcal{E}_\epsilon^i} \mathbf{S}[\boldsymbol{u}_0] \cdot \boldsymbol{n} \, \mathrm{d}s + \sum_{k=1}^{n} \epsilon^{k-1} \mathbf{R}^i \cdot \int_{\partial \mathcal{E}} \mathbf{S}_{\boldsymbol{y}}[\boldsymbol{u}_{\mathrm{loc},k}^i] \cdot \boldsymbol{n} \, \mathrm{d}s
$$

$$
+ \sum_{j \neq i} \sum_{k=1}^{n} \epsilon^{k-3} \mathbf{R}^j \cdot \int_{\partial \mathcal{E}_\epsilon^i} \mathbf{S}_{\boldsymbol{y}}[\boldsymbol{u}_{\mathrm{loc},k}^j] \cdot \mathbf{R}^{jT} \cdot \boldsymbol{n} \, \mathrm{d}s + \mathcal{O}(\epsilon^n)
$$

$$
= \epsilon^{-2} \int_{\mathcal{E}_\epsilon^i} \nabla \cdot \mathbf{S}[\boldsymbol{u}_0] \, \mathrm{d}\boldsymbol{x} + \sum_{k=1}^{n} \epsilon^{k-1} \mathbf{R}^i \cdot \int_{\partial \mathcal{E}} \mathbf{S}_{\boldsymbol{y}}[\boldsymbol{u}_{\mathrm{loc},k}^i] \cdot \boldsymbol{n} \, \mathrm{d}s
$$

$$
+ \sum_{j \neq i} \sum_{k=1}^{n} \epsilon^{k-4} \mathbf{R}^j \cdot \int_{\mathcal{E}_\epsilon^i} \nabla_{\boldsymbol{y}} \cdot \mathbf{S}_{\boldsymbol{y}}[\boldsymbol{u}_{\mathrm{loc},k}^j] \, \mathrm{d}\boldsymbol{x} + \mathcal{O}(\epsilon^n) \tag{3.21}
$$

in case of (3.1d) and

$$
\rho_\epsilon \epsilon^2 \operatorname{Re} |\mathcal{E}| \sum_{j=0}^{n-2} \epsilon^j \boldsymbol{\psi}_j^i
$$

$$
= \epsilon^{-3} \int_{\partial \mathcal{E}_\epsilon^i} (\boldsymbol{x} - \boldsymbol{c}^i) \times \mathbf{S}[\boldsymbol{u}_0] \cdot \boldsymbol{n} \, \mathrm{d}s + \sum_{k=1}^{n} \epsilon^{k-1} \mathbf{R}^i \cdot \int_{\partial \mathcal{E}} \boldsymbol{y} \times \mathbf{S}_{\boldsymbol{y}}[\boldsymbol{u}_{\mathrm{loc},k}^i] \cdot \boldsymbol{n} \, \mathrm{d}s
$$

$$
+ \sum_{j \neq i} \sum_{k=1}^{n} \epsilon^{k-4} \int_{\partial \mathcal{E}_\epsilon^i} (\boldsymbol{x} - \boldsymbol{c}^i) \times \mathbf{R}^j \cdot \mathbf{S}_{\boldsymbol{y}}[\boldsymbol{u}_{\mathrm{loc},k}^j] \cdot \mathbf{R}^{jT} \cdot \boldsymbol{n} \, \mathrm{d}s + \mathcal{O}(\epsilon^n)
$$

$$
= \epsilon^{-3} \int_{\mathcal{E}_\epsilon^i} (\boldsymbol{x} - \boldsymbol{c}^i) \times \nabla \cdot \mathbf{S}[\boldsymbol{u}_0] \, \mathrm{d}\boldsymbol{x} + \sum_{k=1}^{n} \epsilon^{k-1} \mathbf{R}^i \cdot \int_{\partial \mathcal{E}} \boldsymbol{y} \times \mathbf{S}_{\boldsymbol{y}}[\boldsymbol{u}_{\mathrm{loc},k}^i] \cdot \boldsymbol{n} \, \mathrm{d}s
$$

$$
+ \sum_{j \neq i} \sum_{k=1}^{n} \epsilon^{k-5} \int_{\mathcal{E}_\epsilon^i} (\boldsymbol{x} - \boldsymbol{c}^i) \times \mathbf{R}^j \cdot \nabla_{\boldsymbol{y}} \cdot \mathbf{S}_{\boldsymbol{y}}[\boldsymbol{u}_{\mathrm{loc},k}^j] \, \mathrm{d}\boldsymbol{x} + \mathcal{O}(\epsilon^n) \tag{3.22}
$$

for (3.1e). We used here the following property of functions with values in the space of symmetric matrices $\mathbf{S} \in \mathcal{C}^1(\mathcal{E}; \mathcal{M}_{\mathrm{sym}})$ (see Appendix A.2):

$$
\int_{\partial \mathcal{E}} \boldsymbol{y} \times \mathbf{S} \cdot \boldsymbol{n} \, \mathrm{d}s = \int_{\mathcal{E}} \nabla_{\boldsymbol{y}} \cdot (B(\boldsymbol{y}) \cdot \mathbf{S})^T \, \mathrm{d}\boldsymbol{y}
$$

$$
= \int_{\mathcal{E}} B(\boldsymbol{y}) \cdot \nabla_{\boldsymbol{y}} \cdot \mathbf{S} \, \mathrm{d}\boldsymbol{y} + \sum_{i=1}^{3} \int_{\mathcal{E}} \sqrt{2} \boldsymbol{e}_i (\mathbf{B}_i : \mathbf{S}) \, \mathrm{d}\boldsymbol{y} \,,
$$

where $\{\mathbf{B}_i\}_{i=1,2,3}$ is a basis of skew-symmetric matrices and the last term vanishes due to orthogonality (see (A.8b) and (A.8c) in the appendix). Since $\boldsymbol{u}_{\mathrm{loc},k}^i, p_{\mathrm{loc},k}^i$ solve the stationary Stokes equations, the summation terms over $j \neq i$ in (3.21) and (3.22) are identical to zero and applying a Taylor expansion of $\nabla \cdot \mathbf{S}[\boldsymbol{u}_0]$ in $\boldsymbol{c}^i$ yields the relations

$$\sum_{k=0}^{n-1} \epsilon^k \int_{\partial\mathcal{E}} \mathbf{S}_{\boldsymbol{y}}[\boldsymbol{u}_{\mathrm{loc},k+1}^i] \cdot \boldsymbol{n} \, \mathrm{d}s$$

$$= -\sum_{k=1}^{n-1} \frac{\epsilon^k}{(k-1)!} \mathbf{R}^{iT} \cdot \int_{\mathcal{E}} [\mathbf{R}^i \cdot \boldsymbol{y} \cdot \nabla]^{k-1} \nabla \cdot \mathbf{S}[\boldsymbol{u}_0] \, \mathrm{d}\boldsymbol{y}$$

$$+ \rho_\epsilon \epsilon \operatorname{Re} |\mathcal{E}| \mathbf{R}^{iT} \cdot \left(\sum_{k=0}^{n-1} \epsilon^k \boldsymbol{a}_k^i - \operatorname{Fr}^{-2} \boldsymbol{e}_g \right) + \mathcal{O}(\epsilon^n) \tag{3.23}$$

$$\sum_{k=0}^{n-1} \epsilon^k \int_{\partial\mathcal{E}} \boldsymbol{y} \times \mathbf{S}_{\boldsymbol{y}}[\boldsymbol{u}_{\mathrm{loc},k+1}^i] \cdot \boldsymbol{n} \, \mathrm{d}s$$

$$= -\sum_{k=1}^{n-1} \frac{\epsilon^k}{(k-1)!} \int_{\mathcal{E}} \boldsymbol{y} \times \mathbf{R}^{iT} \cdot [\mathbf{R}^i \cdot \boldsymbol{y} \cdot \nabla]^{k-1} \nabla \cdot \mathbf{S}[\boldsymbol{u}_0] \, \mathrm{d}\boldsymbol{y}$$

$$+ \rho_\epsilon \epsilon \operatorname{Re} |\mathcal{E}| \mathbf{R}^{iT} \cdot \sum_{k=1}^{n-1} \epsilon^k \boldsymbol{\psi}_{k-1}^i + \mathcal{O}(\epsilon^n) \,. \tag{3.24}$$

This shows in combination with (3.15d) the approximation orders of (3.18c) and (3.18d). In order to show the well-definition of the velocities $\boldsymbol{v}_k^i, \boldsymbol{\omega}_{k-1}^i$, i.e., the relation (3.19b) we first note that the tracer condition $\boldsymbol{v}_0^i = \boldsymbol{u}_0(\boldsymbol{c}^i, t)$ generates an ϵ-dependence of $\mathrm{d}\boldsymbol{v}_0^i/\mathrm{d}t$. Therefore, we introduce an additional expansion for $\mathrm{d}\boldsymbol{v}_k^i/\mathrm{d}t$ of the following form

$$\frac{\mathrm{d}}{\mathrm{d}t} \boldsymbol{v}_k^i = \sum_{\ell=0}^{n} \epsilon^\ell \dot{\boldsymbol{v}}_{k,\ell}^i + \mathcal{O}(\epsilon^{n+1})$$

with $\dot{\boldsymbol{v}}_{k,\ell}^i$ being not explicitly dependent on ϵ. Therefore, the acceleration reads as

$$\frac{\mathrm{d}}{\mathrm{d}t} \boldsymbol{v}^i = \sum_{k=0}^{n-1} \epsilon^k \sum_{\ell=0}^{k} \dot{\boldsymbol{v}}_{\ell,k-\ell}^i + \mathcal{O}(\epsilon^n) = \sum_{k=0}^{n-1} \epsilon^k \boldsymbol{a}_k^i + \mathcal{O}(\epsilon^n) \,. \tag{3.25}$$

In case of angular velocity, we use an analogous approach setting

$$\frac{\mathrm{d}}{\mathrm{d}t} \boldsymbol{\omega}_k^i = \sum_{\ell=0}^{n-1} \epsilon^\ell \dot{\boldsymbol{\omega}}_{k,\ell}^i + \mathcal{O}(\epsilon^n) \,,$$

we also note that

$$\frac{\mathrm{d}}{\mathrm{d}t} (\mathbf{J}^i \cdot \boldsymbol{\omega}^i) = \mathbf{J}^i \cdot \frac{\mathrm{d}}{\mathrm{d}t} \boldsymbol{\omega}^i + B(\boldsymbol{\omega}^i) \cdot \mathbf{J}^i \cdot \boldsymbol{\omega}^i \,.$$

Thus, the relation for the angular acceleration reads as

$$\frac{\mathrm{d}}{\mathrm{d}t} (\mathbf{J}^i \cdot \boldsymbol{\omega}^i) = \sum_{k=0}^{n-2} \epsilon^k \sum_{\ell=0}^{k} \mathbf{J}^i \cdot \dot{\boldsymbol{\omega}}_{\ell,k-\ell}^i + B(\boldsymbol{\omega}_\ell^i) \cdot \mathbf{J}^i \cdot \boldsymbol{\omega}_{k-\ell}^i + \mathcal{O}(\epsilon^{n-1})$$

$$= \sum_{k=0}^{n-2} \epsilon^k \boldsymbol{\psi}_k^i + \mathcal{O}(\epsilon^{n-1}) \,. \tag{3.26}$$

Using the relation between the integral and boundary conditions for $\boldsymbol{u}_{\mathrm{loc},k}^i$ stated in Lem. 5, we find

$$
\begin{pmatrix} \boldsymbol{v}_k^i \\ \boldsymbol{\omega}_{k-1}^i \end{pmatrix} = \begin{bmatrix} \mathbf{R}^i & \\ & \mathbf{R}^i \end{bmatrix} \cdot \mathbf{A}^{-1} \cdot \left(\begin{bmatrix} \mathbf{I} & \\ & \frac{1}{\sqrt{2}}\mathbf{I} \end{bmatrix} \cdot \begin{pmatrix} \boldsymbol{f}_k^i \\ \boldsymbol{g}_k^i \end{pmatrix} + D_k^i \boldsymbol{u}_0 + u_k^i \right), \quad \text{with} \qquad (3.27)
$$

$$
D_k^i \boldsymbol{u}_0 = \frac{1}{k!} \left(\int_{\partial\mathcal{E}} \mathbf{R}^{iT} \cdot [\mathbf{R}^i \cdot \boldsymbol{y} \cdot \nabla]^k \boldsymbol{u}_0 \cdot \mathbf{S}_{\boldsymbol{y}}[\boldsymbol{w}_q] \cdot \boldsymbol{n}\, \mathrm{d}s \right)_{q=1,\dots,6},
$$

$$
u_k^i = \left(\int_{\partial\mathcal{E}} \mathbf{R}^{iT} \cdot \boldsymbol{r}_k^i(\boldsymbol{y}) \cdot \mathbf{S}_{\boldsymbol{y}}[\boldsymbol{w}_q] \cdot \boldsymbol{n}\, \mathrm{d}s \right)_{q=1,\dots,6},
$$

$$
\mathbf{A} = (\boldsymbol{t}_q, \boldsymbol{s}_q)_{q=1,\dots,6},
$$

where $\boldsymbol{w}_q, \boldsymbol{t}_q, \boldsymbol{s}_q$ are given in Lemma 5. Now we have to show that the right-hand side of the equation for $\boldsymbol{v}_k^i, \boldsymbol{\omega}_{k-1}^i$ is indeed independent of $\boldsymbol{v}_\ell^j, \boldsymbol{\omega}_{\ell-1}^j$ for $\ell \geq k$ and all $j \in \{1, \dots, N_\epsilon\}$. Thus, we show that $(\boldsymbol{v}_k^i, \boldsymbol{\omega}_{k-1}^i) = F_k^i(\boldsymbol{c}^1, \dots, \mathbf{R}^{N_\epsilon}, t)$, F_k^i being a sufficiently smooth function for each $k = 1, \dots, n$ and $i \leq N_\epsilon$. In the following we use the partition $F_k^i = (F_{k,v}^i, F_{k,\omega}^i)$ to address the components belonging to the linear and angular velocities.

We make the following considerations only for the heavy particle case, i.e., $r = -1$. For $r \geq 0$, the following arguments can be applied analogously. We start with $k = 1$: In this case, $\boldsymbol{g}_1^i = \boldsymbol{0}$ and $u_1^i = 0$, while $\boldsymbol{f}_1^i = \boldsymbol{k}_0^i$ which depends on $\boldsymbol{a}_0^i$. Since

$$
\frac{\mathrm{d}}{\mathrm{d}t}\boldsymbol{v}_0^i = \mathrm{D}_t \boldsymbol{u}_0 + \sum_{k=1}^n \epsilon^k \partial_{\boldsymbol{x}} \boldsymbol{u}_0 \cdot \boldsymbol{v}_k^i + \mathcal{O}(\epsilon^{n+1}),
$$

we identify $\boldsymbol{a}_0^i = \dot{\boldsymbol{v}}_{0,0}^i = \mathrm{D}_t \boldsymbol{u}_0$ and $\dot{\boldsymbol{v}}_{0,k}^i = \partial_{\boldsymbol{x}} \boldsymbol{u}_0 \cdot \boldsymbol{v}_k^i$ for $k \geq 1$. Therefore, $(\boldsymbol{v}_1^i, \boldsymbol{\omega}_0^i) = F_1(\boldsymbol{c}^i, \mathbf{R}^i, t) = F_1^i(\boldsymbol{c}^1, \dots, \mathbf{R}^{N_\epsilon}, t)$, which is a smooth mapping since $\boldsymbol{u}_0$ is smooth. In order to move on to the general case, we first show that the interaction term u_2^i is indeed expressible as a sufficiently smooth function $(\mathbb{R}^3 \times \mathcal{SO}(3))^{N_\epsilon} \times \mathbb{R}^+ \to \mathbb{R}^6$. Therefore, we analyze the term $\boldsymbol{r}_2^i$. Taking the time dependence into account, we have

$$
\boldsymbol{r}_2^i(\boldsymbol{y}, t) = \epsilon^{-1} \sum_{j \neq i} \mathbf{R}^j(t) \cdot \boldsymbol{u}_{\mathrm{loc},1}^j(\boldsymbol{y}(\boldsymbol{x}(\boldsymbol{y}, \boldsymbol{c}^i(t), \mathbf{R}^i(t), \epsilon), \boldsymbol{c}^j(t), \mathbf{R}^j(t), \epsilon), t)
$$

where the time dependence of the local fields is due to the boundary conditions. For the multi-index $\kappa \in \{1, 2, 3\}^m$ and $m \geq 2$, we set $\boldsymbol{w}_\kappa, p_\kappa$ as the solution to

$$
\Delta_{\boldsymbol{y}} \boldsymbol{w}_\kappa - \nabla_{\boldsymbol{y}} p_\kappa = \boldsymbol{0}, \quad \nabla_{\boldsymbol{y}} \cdot \boldsymbol{w}_\kappa = 0, \quad \boldsymbol{y} \in \mathbb{R}^3 \setminus \overline{\mathcal{E}}, \qquad (3.28)
$$

$$
\boldsymbol{w}_\kappa(\boldsymbol{y}) = \boldsymbol{e}_{\kappa_1} \prod_{i=2}^m y_{\kappa_i}, \quad \boldsymbol{y} \in \partial\mathcal{E}
$$

with decay properties (3.15c) and $\boldsymbol{w}_\kappa, p_\kappa$ for $\kappa \in \{1, 2, 3\}$ given in (2.19). Then, the boundary condition for $\boldsymbol{u}_{\mathrm{loc},1}^i$ can be expressed as

$$
\boldsymbol{u}_{\mathrm{loc},1}^i\big|_{\partial\mathcal{E}} = \sum_{\ell=1}^3 (\mathbf{R}^{iT} \cdot \boldsymbol{v}_1^i)_\ell \boldsymbol{e}_\ell + \sum_{\ell,m=1}^3 \left(B(\mathbf{R}^{iT} \cdot \boldsymbol{\omega}_0^i) - \mathbf{R}^{iT} \cdot \partial_{\boldsymbol{x}} \boldsymbol{u}_0 \cdot \mathbf{R}^i \right)_{\ell m} \boldsymbol{e}_\ell y_m.
$$

By the linearity of the homogeneous stationary Stokes equations, we therefore can express the local field as

$$
\begin{aligned}
\boldsymbol{u}_{\mathrm{loc},1}^i(\boldsymbol{y}, t) &= \sum_{\ell=1}^3 \left(\mathbf{R}^{iT}(t) \cdot F_{1,v}(\boldsymbol{c}^i(t), \mathbf{R}^i(t), t) \right)_\ell \boldsymbol{w}_\ell(\boldsymbol{y}) \\
&\quad + \sum_{\ell,m=1}^3 \Big(B(\mathbf{R}^{iT}(t) \cdot F_{1,\omega}(\boldsymbol{c}^i(t), \mathbf{R}^i(t), t)) \\
&\qquad - \mathbf{R}^{iT}(t) \cdot \partial_{\boldsymbol{x}} \boldsymbol{u}_0(\boldsymbol{c}^i(t), t) \cdot \mathbf{R}^i(t) \Big)_{\ell m} \boldsymbol{w}_{\ell m}(\boldsymbol{y}) \\
&= \boldsymbol{U}_{\mathrm{loc},1}(\boldsymbol{y}, \boldsymbol{c}^i(t), \mathbf{R}^i(t), t)
\end{aligned}
\tag{3.29}
$$

with $\boldsymbol{U}_{\mathrm{loc},1} \in \mathcal{C}^\infty(\mathbb{R}^3 \backslash \mathcal{E} \times \Omega \times \mathbb{R}^{3\times3} \times \mathbb{R}^+; \mathbb{R}^3)$ since $\boldsymbol{u}_0$ is assumed smooth and Lemma B.3 applies to every $\boldsymbol{w}_\kappa$. Therefore, we have

$$
\begin{aligned}
\boldsymbol{r}_2^i(\boldsymbol{y}, t) &= \epsilon^{-1} \sum_{j \neq i} \mathbf{R}^j(t) \cdot \boldsymbol{U}_{\mathrm{loc},1}(\boldsymbol{y}(\boldsymbol{x}(\boldsymbol{y}, \boldsymbol{c}^i(t), \mathbf{R}^i(t), \epsilon), \boldsymbol{c}^j(t), \mathbf{R}^j(t), \epsilon), \boldsymbol{c}^j(t), \mathbf{R}^j(t), t) \\
&= \boldsymbol{R}_2^i(\boldsymbol{y}, \boldsymbol{c}^1, \ldots, \mathbf{R}^{N_\epsilon}, t)
\end{aligned}
$$

where $\boldsymbol{R}_2^i : \mathcal{B}_{0.5\iota_\epsilon/\epsilon} \times (\Omega \times \mathbb{R}^{3\times3})^{N_\epsilon} \times \mathbb{R}^+ \to \mathbb{R}^3$. As $\boldsymbol{U}_{\mathrm{loc},1}$ is smooth in every variable, so is $\boldsymbol{R}_2^i$ for every $\epsilon > 0$. We have to check, whether $\boldsymbol{R}_2^i \in \mathcal{C}_{N_\epsilon}^K$. The kth time derivative of $\boldsymbol{r}_2^i$ involves terms of the form

$$
\epsilon^{-1-\ell} \sum_{j \neq i} \nabla_{\boldsymbol{y}}^\ell \boldsymbol{u}_{\mathrm{loc},1}^j(\boldsymbol{y}^j(\boldsymbol{x}^i(\boldsymbol{y})))
\tag{3.30}
$$

for $0 \leq \ell \leq k$, these are bounded independent of ϵ due to R5) and Lemma 16 whenever $k \leq K = \max(n - 2 - r, 1)$. As already mentioned, we consider only the case $r = -1$ here, $r \geq 0$ resulting in similar results with accordingly weaker constraints on the particle number. Therefore, we have $K = \max(n - 1, 1)$ with the cases of $n \in \{0, 1\}$ already considered. Thus, $K = n - 1 \geq 1$ is assumed from here on. As shown above, $\boldsymbol{R}_2^i$ is smooth in all variables and thus $\boldsymbol{R}_2^i \in \mathcal{C}^K(\mathcal{B}_{0.5\iota_\epsilon/\epsilon} \times (\Omega \times \mathbb{R}^{3\times3})^{N_\epsilon} \times \mathbb{R}^+; \mathbb{R}^3)$. Moreover, $\boldsymbol{R}_2^i(\boldsymbol{y}, .) \in \mathcal{C}_{N_\epsilon}^K$, as (3.30) is finite for $0 \leq \ell \leq K$. This implies that u_2^i is expressible as a $\mathcal{C}_{N_\epsilon}^K$-function. The vectors $(\boldsymbol{f}_2^i, \boldsymbol{g}_2^i)$ are given in terms of $\mathbf{R}^i, \boldsymbol{u}_0(\boldsymbol{c}^i, t)$, and $\boldsymbol{k}_1^i, \boldsymbol{\ell}_0^i$. The latter fulfill

$$
\begin{aligned}
\boldsymbol{k}_1^i &= \rho \operatorname{Re} |\mathcal{E}| \mathbf{R}^{iT} \cdot \boldsymbol{a}_1^i = \rho \operatorname{Re} |\mathcal{E}| \mathbf{R}^{iT} \cdot (\dot{\boldsymbol{v}}_{0,1}^i + \dot{\boldsymbol{v}}_{1,0}^i), \\
\boldsymbol{\ell}_0^i &= \rho \operatorname{Re} |\mathcal{E}| \mathbf{R}^{iT} \cdot \boldsymbol{\psi}_0^i = \rho \operatorname{Re} |\mathcal{E}| \mathbf{R}^{iT} \cdot (\mathbf{J}^i \cdot \dot{\boldsymbol{\omega}}_{0,0}^i + B(\boldsymbol{\omega}_0) \cdot \mathbf{J}^i \cdot \boldsymbol{\omega}_0^i)
\end{aligned}
$$

with $\dot{\boldsymbol{v}}_{0,1}^i = \partial_{\boldsymbol{x}} \boldsymbol{u}_0(\boldsymbol{c}^i, t) \cdot \boldsymbol{v}_1^i$, and where $(\dot{\boldsymbol{v}}_{1,0}^i, \dot{\boldsymbol{\omega}}_{0,0}^i)$ are the leading order terms of

$$
\frac{\mathrm{d}}{\mathrm{d}t}(\boldsymbol{v}_1^i, \boldsymbol{\omega}_0^i) = \partial_{\boldsymbol{c}} F_1^i \cdot \sum_{k=0}^n \epsilon^k \boldsymbol{v}_k^i + \sum_{k=0}^{n-1} \epsilon^k \sum_{\ell,m=1}^3 \partial_{R_{\ell m}} F_1^i (B(\boldsymbol{\omega}_k^i) \cdot \mathbf{R}^i)_{\ell m} + \partial_t F_1^i + \mathcal{O}(\epsilon^n).
$$

Thus, the velocities $(\boldsymbol{v}_2^i, \boldsymbol{\omega}_1^i)$ are given as

$$
(\boldsymbol{v}_2^i, \boldsymbol{\omega}_1^i) = F_2^i(\boldsymbol{c}^1, \ldots, \mathbf{R}^{N_\epsilon}, t) = F_2(\boldsymbol{c}^i, \mathbf{R}^i, t) + \begin{bmatrix} \mathbf{R}^i & \\ & \mathbf{R}^i \end{bmatrix} \cdot \mathbf{A}^{-1} \cdot u_2^i(\boldsymbol{c}^1, \ldots, \mathbf{R}^{N_\epsilon}, t)
$$

with a smooth function F_2. Therefore, $F_2^i \in \mathcal{C}_{N_\epsilon}^K$ holds. Next, we assume the following regularities:

$$\boldsymbol{R}_k^i \in \mathcal{C}^{K+2-k}(\mathcal{B}_{0.5\iota_\epsilon/\epsilon} \times (\Omega \times \mathbb{R}^{3\times3})^{N_\epsilon} \times \mathbb{R}^+; \mathbb{R}^3),$$
$$\boldsymbol{R}_k^i(\boldsymbol{y}, .) \in \mathcal{C}_{N_\epsilon}^{K+2-k},$$

and $(\boldsymbol{v}_k^i, \boldsymbol{\omega}_{k-1}^i) = F_k^i(\boldsymbol{c}^1, \ldots, \mathbf{R}^{N_\epsilon}, t)$ with $F_k^i \in \mathcal{C}_{N_\epsilon}^{K+2-k}$ for all $2 \leq k \leq m$ for an $m \leq n - 1$. Then we find for all $k \leq m$

$$\frac{\mathrm{d}}{\mathrm{d}t}(\boldsymbol{v}_k^i, \boldsymbol{\omega}_{k-1}^i) = \sum_{j=1}^{N_\epsilon} \partial_{\boldsymbol{c}^j} F_k^i \cdot \boldsymbol{v}^j + \partial_{\mathbf{R}^j} F_k^i : B(\boldsymbol{\omega}^j) \cdot \mathbf{R}^j + \partial_t F_k^i$$

$$= \partial_t F_k^i + \sum_{\ell=0}^{m-1} \epsilon^\ell \sum_{j=1}^{N_\epsilon} \partial_{\boldsymbol{c}^j} F_k^i \cdot \boldsymbol{v}_\ell^j + \partial_{\mathbf{R}^j} F_k^i : B(\boldsymbol{\omega}_\ell^j) \cdot \mathbf{R}^j + \mathcal{O}(\epsilon^m).$$

We therefore identify

$$(\dot{\boldsymbol{v}}_{k,\ell}^i, \dot{\boldsymbol{\omega}}_{k-1,\ell}^i) = \delta_{\ell,0}\partial_t F_k^i + \sum_{j=1}^{N_\epsilon} \partial_{\boldsymbol{c}^j} F_k^i \cdot \boldsymbol{v}_\ell^j + \partial_{\mathbf{R}^j} F_k^i : B(\boldsymbol{\omega}_\ell^j) \cdot \mathbf{R}^j \tag{3.31}$$

$$= \delta_{\ell,0}\partial_t F_k^i + \sum_{j=1}^{N_\epsilon} \partial_{\boldsymbol{c}^j} F_k^i \cdot F_{\ell,v}^j + \partial_{\mathbf{R}^j} F_k^i : B(F_{\ell+1,\omega}^j) \cdot \mathbf{R}^j = G_{k,\ell}^i$$

for $k \leq m$ and $\ell \leq m-1$. The function $G_{k,\ell}^i = G_{k,\ell}^i(\boldsymbol{c}^1, \ldots, \mathbf{R}^{N_\epsilon}, t)$ is in $\mathcal{C}_{N_\epsilon}^{\min(K+1-\ell, K+1-k)}$. Now we consider $k = m + 1$, then $(\boldsymbol{v}_{m+1}^i, \boldsymbol{\omega}_m^i)$ are given by (3.27), thus they depend on u_{m+1}^i which is determined by $\boldsymbol{r}_{m+1}^i$, and on $\boldsymbol{f}_{m+1}^i$ as well as $\boldsymbol{g}_{m+1}^i$. The latter two are expressed in terms of $\boldsymbol{a}_m^i$ and $\boldsymbol{\psi}_{m-1}^i$ which depend on

$$\dot{\boldsymbol{v}}_{0,m}^i, (\dot{\boldsymbol{v}}_{1,m-1}^i, \dot{\boldsymbol{\omega}}_{0,m-1}^i), \ldots, (\dot{\boldsymbol{v}}_{m,0}^i, \dot{\boldsymbol{\omega}}_{m-1,0}^i),$$
$$\boldsymbol{\omega}_0^i, \boldsymbol{\omega}_1^i, \ldots, \boldsymbol{\omega}_{m-1}^i.$$

As shown above, $\dot{\boldsymbol{v}}_{0,m}^i = \partial_{\boldsymbol{x}}\boldsymbol{u}_0 \cdot \boldsymbol{v}_m^i = \partial_{\boldsymbol{x}}\boldsymbol{u}_0 \cdot F_{m,v}^i$ and for $k = 1, \ldots, m$ the relation $(\dot{\boldsymbol{v}}_{k,m-k}^i, \dot{\boldsymbol{\omega}}_{k-1,m-k}^i) = G_{k,m-k}^i(\boldsymbol{c}^1, \ldots, \mathbf{R}^{N_\epsilon}, t)$ holds. Since $K + 1 - k \geq K + 1 - m$ as well as $K + 1 - (m - k) > K + 1 - m$ for $k = 1, \ldots, m$ and $K + 2 - m > K + 1 - m$, the terms $\boldsymbol{f}_{m+1}^i, \boldsymbol{g}_{m+1}^i$ therefore can be expressed as functions in $\mathcal{C}_{N_\epsilon}^{K+1-m}$. The interaction term, on the other hand, can be expressed as

$$\boldsymbol{r}_{m+1}^i(\boldsymbol{y}, t) = \epsilon^{-1} \sum_{j \neq i} \mathbf{R}^j(t) \cdot \boldsymbol{U}_{\mathrm{loc},m}^j(\boldsymbol{y}(\boldsymbol{x}(\boldsymbol{y}, \boldsymbol{c}^i(t), \mathbf{R}^i(t), \epsilon), \boldsymbol{c}^j(t), \mathbf{R}^j(t), \epsilon), \boldsymbol{c}^j(t), \mathbf{R}^j(t), t)$$

$$= \boldsymbol{R}_{m+1}^i(\boldsymbol{y}, \boldsymbol{c}^1, \ldots, \mathbf{R}^{N_\epsilon}, t)$$

with $\boldsymbol{U}_{\mathrm{loc},m}^i : \mathbb{R}^3 \setminus \mathcal{E} \times (\Omega \times \mathbb{R}^{3\times3})^{N_\epsilon} \times \mathbb{R}^+ \to \mathbb{R}^3$ given as

$$\boldsymbol{U}_{\mathrm{loc},m}^i = \sum_{a=1}^{3} (\mathbf{R}^{iT} \cdot F_{m,v}^i)_a \boldsymbol{w}_a + \sum_{a,b=1}^{3} (B(\mathbf{R}^{iT} \cdot F_{m,\omega}^i))_{ab} \boldsymbol{w}_{ab}$$

$$- \frac{1}{m!} \sum_{a,b=1}^{3} \sum_{\substack{q_1,\ldots,q_m=1 \\ r_1,\ldots,r_m=1}}^{3} R_{ba}^i \prod_{c=1}^{m} R_{q_c r_c}^i \partial_{x_{q_1},\ldots,x_{q_m}}(\boldsymbol{u}_0)_b \boldsymbol{w}_{a,r_1,\ldots,r_m} - \mathbf{R}^{iT} \cdot \boldsymbol{h}_m^i.$$

Here, $\boldsymbol{h}_m^i : \mathbb{R}^3 \setminus \mathcal{E} \times (\Omega \times \mathbb{R}^{3\times3})^{N_\epsilon} \times \mathbb{R}^+ \to \mathbb{R}^3$ is the velocity field which solves the homogeneous stationary Stokes equations with decay properties (3.15c) and with the boundary condition $\boldsymbol{h}_m^i = \boldsymbol{R}_m^i$ on $\partial\mathcal{E}$. Since $\boldsymbol{R}_m^i$ is not a polynomial function on $\partial\mathcal{E}$, we use a more general argument in order to show the regularity of $\boldsymbol{h}_m^i$ which involves the fundamental solution of the stationary Stokes equations on the exterior of a compact domain. The underlying theorems are found in Appendix B.2. Since $\boldsymbol{R}_m^i(\boldsymbol{y},.) \in \mathcal{C}_{N_\epsilon}^{K+2-m}$ and continuous in $\boldsymbol{y}$, Lemma B.2 yields a surface density $\boldsymbol{\psi}[\boldsymbol{R}_m^i](\boldsymbol{y},.) \in \mathcal{C}_{N_\epsilon}^{K+2-m}$, continuous in $\boldsymbol{y}$. Then Lemma B.3 shows that $\boldsymbol{h}_m^i(.,\boldsymbol{c}^1,\dots,\mathbf{R}^{N_\epsilon},t) \in \mathcal{C}^\infty(\mathbb{R}^3 \setminus \mathcal{E}; \mathbb{R}^3)$, inheriting the regularity on $(\Omega \times \mathbb{R}^{3\times3})^{N_\epsilon} \times \mathbb{R}^+$ from the surface density on $\partial\mathcal{E}$. Thus, $\boldsymbol{U}_{\text{loc},m}^i \in \mathcal{C}^{K+2-m}(\mathbb{R}^3 \setminus \mathcal{E} \times (\Omega \times \mathbb{R}^{3\times3})^{N_\epsilon} \times \mathbb{R}^+; \mathbb{R}^3)$ follows. In particular, this implies $\boldsymbol{R}_{m+1}^i \in \mathcal{C}^{K+1-m}(\mathcal{B}_{0.5\ell_\epsilon/\epsilon} \times (\Omega \times \mathbb{R}^{3\times3})^{N_\epsilon} \times \mathbb{R}^+; \mathbb{R}^3)$ and $\boldsymbol{R}_{m+1}^i(\boldsymbol{y},.) \in \mathcal{C}_{N_\epsilon}^{K+1-m}$.

Therefore, $(\boldsymbol{v}_{m+1}^i, \boldsymbol{\omega}_m^i) = F_{m+1}^i(\boldsymbol{c}^1,\dots,\mathbf{R}^{N_\epsilon},t)$ with a function $F_{m+1}^i \in \mathcal{C}_{N_\epsilon}^{K+1-m}$ independent of $\boldsymbol{v}_\ell^j, \boldsymbol{\omega}_{\ell-1}^j$ for $\ell \geq m+1$ and $j \leq N_\epsilon$ by induction. This shows (3.19b) and the well-posedness of the stationary Stokes equations for the local fields in case of heavy particles. Considering the cases for $r \geq 0$ we note that the regularity of F_k^i for $k \geq 2$ can never exceed the regularity of the interaction term given by K, hence $F_k^i \in \mathcal{C}_{N_\epsilon}^{\min(K+3+r-k,K)}$. $\qquad\square$

Remark 20. *We note that the statements of Lemma 19 do not necessarily need $\mathcal{C}^\infty$ in space and time. In fact, we see from (3.27) and (3.13) that*

$$\boldsymbol{u}_0 \in \mathcal{C}^{\max(\lfloor \frac{n}{2+r} \rfloor, 1)}((0,T); \mathcal{C}^{n+1}(\Omega; \mathbb{R}^3))$$
$$p_0 \in \mathcal{C}^{\max(\lfloor \frac{n-2-r}{2+r} \rfloor, 0)}((0,T); \mathcal{C}^n(\Omega; \mathbb{R}))$$

is sufficient for R1) of Lemma 19, where $\lfloor \alpha \rfloor = \max_{k \in \mathbb{N}}\{k \leq \alpha\}$ for any $\alpha \in \mathbb{R}$ is the floor function.

Now, we are able to formulate a first order approximation for the complete suspension problem (3.1).

Theorem 21 (Asymptotic solution of a dilute particle suspension). *Let the assumptions of Lemma 19 hold for $n = 2$ with $\boldsymbol{u}_0, p_0$ be smooth solutions of the Navier-Stokes problem in Ω for $t > 0$:*

$$\text{Re}\, D_t \boldsymbol{u}_0 = \nabla \cdot \mathbf{S}[\boldsymbol{u}_0] + \text{Re}\, \text{Fr}^{-2}\, \boldsymbol{e}_g, \quad \nabla \cdot \boldsymbol{u}_0 = 0 \qquad (3.32)$$

with boundary conditions at $\partial\Omega$ and an initial condition for $t = 0$. Then the system (3.1) is approximated up to an order of $\mathcal{O}(\epsilon)$ by the expansions given in (3.17).

Proof. Since Lemma 19 already states an approximation of at least order $\mathcal{O}(\epsilon)$ for the relations (3.1b)-(3.1e) in case $n = 2$, we only have to examine the approximation order for the momentum balance and mass conservation (3.1a). Mass conservation follows immediately, since $\boldsymbol{u}_0$ as well as $\boldsymbol{u}_{\text{loc},k}^i$ are assumed divergence free, thus

$$\nabla \cdot \boldsymbol{u}^e = \mathcal{O}(\epsilon^2).$$

For the left-hand side of the momentum balance in Ω_ϵ in (3.1a) we find

$$\operatorname{Re} \mathrm{D}_t \boldsymbol{u}_0 + \operatorname{Re} \sum_{k=0}^{n-1} \sum_{i=1}^{N_\epsilon} \epsilon^k \mathbf{R}^i \cdot \partial_{\boldsymbol{y}} \boldsymbol{u}_{\mathrm{loc},k+1}^i \cdot \mathbf{R}^{iT} \cdot \boldsymbol{u}_0 \tag{3.33}$$

$$- \operatorname{Re} \sum_{k=0}^{n-1} \sum_{i=1}^{N_\epsilon} \epsilon^k \mathbf{R}^i \cdot \partial_{\boldsymbol{y}} \boldsymbol{u}_{\mathrm{loc},k+1}^i \cdot \mathbf{R}^{iT} \cdot (B(\boldsymbol{\omega}^i) \cdot (\boldsymbol{x} - \boldsymbol{c}^i) + \boldsymbol{v}^i)$$

$$+ \operatorname{Re} \sum_{k=1}^{n-1} \sum_{i=1}^{N_\epsilon} \epsilon^k (B(\boldsymbol{\omega}^i) \cdot \mathbf{R}^i \cdot \boldsymbol{u}_{\mathrm{loc},k}^i + \mathbf{R}^i \cdot \partial_t \boldsymbol{u}_{\mathrm{loc},k}^i + \partial_{\boldsymbol{x}} \boldsymbol{u}_0 \cdot \mathbf{R}^i \cdot \boldsymbol{u}_{\mathrm{loc},k}^i)$$

$$+ \operatorname{Re} \sum_{k=1}^{n-1} \sum_{i,j=1}^{N_\epsilon} \epsilon^k \sum_{\ell=0}^{k-1} \mathbf{R}^i \cdot \partial_{\boldsymbol{y}} \boldsymbol{u}_{\mathrm{loc},k-\ell}^i \cdot \mathbf{R}^{iT} \cdot \mathbf{R}^j \cdot \boldsymbol{u}_{\mathrm{loc},\ell+1}^j + \mathcal{O}(\epsilon^n)$$

$$= \operatorname{Re} \mathrm{D}_t \boldsymbol{u}_0 + \operatorname{Re} \sum_{i=1}^{N_\epsilon} \mathbf{R}^i \cdot \partial_{\boldsymbol{y}} \boldsymbol{u}_{\mathrm{loc},1}^i \cdot \mathbf{R}^{iT} \cdot (\boldsymbol{u}_0 - B(\boldsymbol{\omega}^i) \cdot (\boldsymbol{x} - \boldsymbol{c}^i) - \boldsymbol{v}^i) + \mathcal{O}(\epsilon)$$

since all terms are bounded due to Lemma 16. Assuming $\|\boldsymbol{x} - \boldsymbol{c}^i\| < \iota_\epsilon$ for some $i \in \{1, \dots, N_\epsilon\}$, it holds

$$\sum_{j=1}^{N_\epsilon} \mathbf{R}^j \cdot \partial_{\boldsymbol{y}} \boldsymbol{u}_{\mathrm{loc},1}^j \cdot \mathbf{R}^{jT} \cdot \left(\boldsymbol{u}_0 - B(\boldsymbol{\omega}^j) \cdot (\boldsymbol{x} - \boldsymbol{c}^j) - \boldsymbol{v}^j \right)$$

$$= \mathbf{R}^i \cdot \partial_{\boldsymbol{y}} \boldsymbol{u}_{\mathrm{loc},1}^i \cdot \mathbf{R}^{iT} \cdot \left(\boldsymbol{u}_0 - B(\boldsymbol{\omega}^i) \cdot (\boldsymbol{x} - \boldsymbol{c}^i) - \boldsymbol{v}^i \right) + \mathcal{O}(\epsilon) \tag{3.34}$$

due to (3.8), the fact that $\|\boldsymbol{v}^j\| \le \max_{\boldsymbol{x} \in \Omega} \|\boldsymbol{u}_0\| + \mathcal{O}(\epsilon) < \infty$, and $\|\boldsymbol{\omega}_0^j\| \in \mathcal{O}(1)$ by assumption. Now we fix an arbitrary $R > 0$ and assume $\|\boldsymbol{x} - \boldsymbol{c}^i\| < \epsilon R$, then $\boldsymbol{u}_0(\boldsymbol{x}, t) = \boldsymbol{u}_0(\boldsymbol{c}^i(t), t) + \mathcal{O}(\epsilon R)$ and the remaining term in (3.34) is of order $\mathcal{O}(\epsilon R)$. Otherwise, $\iota_\epsilon > \|\boldsymbol{x} - \boldsymbol{c}^i\| > \epsilon R$ and we can again use the property $\epsilon \in o(\iota_\epsilon)$ in combination with the decay properties of the local fields (3.7)

$$\left\| \mathbf{R}^i \cdot \partial_{\boldsymbol{y}} \boldsymbol{u}_{\mathrm{loc},1}^i \cdot \mathbf{R}^{iT} \cdot \left(\boldsymbol{u}_0 - B(\boldsymbol{\omega}^i) \cdot (\boldsymbol{x} - \boldsymbol{c}^i) - \boldsymbol{v}^i \right) \right\| \le c \|\partial_{\boldsymbol{y}} \boldsymbol{u}_{\mathrm{loc},1}^i\| \|\boldsymbol{x} - \boldsymbol{c}^i\|$$

$$\le c \epsilon^{\ell+1} \|\boldsymbol{x} - \boldsymbol{c}^i\|^{-(\ell+1)} \|\boldsymbol{x} - \boldsymbol{c}^i\| < c \epsilon R^{-\ell}$$

with c depending on R but independent of ϵ. The remaining case of $\|\boldsymbol{x} - \boldsymbol{c}^i\| > \iota_\epsilon$ for all $i = 1, \dots, N_\epsilon$ implies that the left-hand side in (3.34) is $\mathcal{O}(\epsilon)$ due to (3.8). Thus, the momentum balance in (3.1a) is given by

$$\operatorname{Re} \mathrm{D}_t \boldsymbol{u}_0 = \nabla \cdot \mathbf{S}[\boldsymbol{u}_0] + \operatorname{Re} \mathrm{Fr}^{-2} \boldsymbol{e}_g + \sum_{k=1}^{2} \epsilon^{k-2} \sum_{i=1}^{N_\epsilon} \mathbf{R}^i \cdot \nabla_{\boldsymbol{y}} \cdot \mathbf{S}_{\boldsymbol{y}}[\boldsymbol{u}_{\mathrm{loc},k}^i] + \mathcal{O}(\epsilon). \tag{3.35}$$

Applying the assumption on $\boldsymbol{u}_0$ and (3.14), we immediately conclude that the momentum balance is fulfilled up to $\mathcal{O}(\epsilon)$. $\qquad\square$

Remark 22 (Coupling of the asymptotic system)**.**

1) *The coupling of boundary conditions and forces on the particle boundary implies that the velocities $\boldsymbol{v}_2^i, \boldsymbol{\omega}_1^i$ depend on $N_\epsilon - 1$ local velocity fields $\boldsymbol{u}_{\mathrm{loc},1}^j$. Since the*

latter depend on $\boldsymbol{v}_1^j, \boldsymbol{\omega}_0^j$ and thus on $\boldsymbol{u}_0(\boldsymbol{c}^j(t), t)$, the evolution of $\boldsymbol{c}^i$ depends on the behavior of all other particles in the system due to (3.27). This forms a hydrodynamic interaction of particles, but since the interaction takes place in the second order system, the particle rotation is not affected in leading order. Thus, there is no particle interaction up to $\mathcal{O}(\epsilon)$. Therefore, we call this concentration regime dilute.

2) *An application of the asymptotic expansion of Section 2.3.3 used in Lemma 4 leads again to a complete decoupling of the equations belonging to the approximation order $k = 0, 1, 2$. Thus, in this case we recover the hierarchical structure explained in Remark 6 3).*

Remark 23 (Extension of the asymptotical model to the semi-dilute regime)**.** *Analyzing the formal proof of Lemma 19, we see that we can mitigate the restrictions on N_ϵ in (R2) by imposing condition C2) of Lemma 16 on β. In this case, the velocity term $\boldsymbol{r}_k^i$, previously given by (3.15b), becomes dependent on the local velocity contributions of order k instead of order $k - 1$,*

$$\boldsymbol{r}_k^i(\boldsymbol{y}) = \sum_{j \neq i} \mathbf{R}^j \cdot \boldsymbol{u}_{\mathrm{loc},k}^j(\boldsymbol{y}^j(\boldsymbol{x}^i(\boldsymbol{y})))$$

due to (3.9) and introduces a coupling between all particle velocities within kth approximation order. This implies that u_k^i in (3.27), the term which contains $\boldsymbol{r}_k^i$, becomes dependent on $\boldsymbol{v}_k^i, \boldsymbol{\omega}_{k-1}^i$, precisely the quantities which are defined by (3.27). Hence, (3.27) becomes a coupled nonlinear equation for $\boldsymbol{v}_k^i, \boldsymbol{\omega}_{k-1}^i$, $i = 1, \ldots, N_\epsilon$. The solvability of this system depends on the configuration of the particle system. Under the assumption, that a solution $\overline{v}_k = (\boldsymbol{v}_k^1, \boldsymbol{\omega}_{k-1}^1, \ldots, \boldsymbol{v}_k^{N_\epsilon}, \boldsymbol{\omega}_{k-1}^{N_\epsilon})$ exists for every k and the corresponding nonlinear function $F_k : (\Omega \times \mathcal{SO}(3))^{N_\epsilon} \times (\mathbb{R}^3 \times \mathbb{R}^3)^{N_\epsilon} \to (\mathbb{R}^3 \times \mathbb{R}^3)^{N_\epsilon}$ has the property that $\partial_{\boldsymbol{v}^1, \boldsymbol{\omega}^1, \ldots, \boldsymbol{v}^{N_\epsilon}, \boldsymbol{\omega}^{N_\epsilon}} F_k$ is regular at $\overline{v}_k$, one can still show that the right-hand side of the equation is independent of higher order velocities $\boldsymbol{v}_\ell^i, \boldsymbol{\omega}_{\ell-1}^i$ for $\ell > k$.

Remark 24 (Chaos assumption)**.** *The requirement R5) of Lemma 19 in general restricts the particle number N_ϵ to a constant number. As we see later (see Remark 37), this prevents us from deriving a connection between mean field models and the original system (3.1). We point out, that R5) is needed in order to ensure that the hydrodynamic interaction (3.15b) is always well-defined, i.e., $\boldsymbol{r}_k^i$ is bounded despite the fact, that the superposition is scaled by ϵ^{-1}. On the other hand, the only possibility in order to avoid the factor ϵ^{-1} leads to the problem discussed in Remark 23, i.e., to a large, coupled, nonlinear system of equations for all particle velocities of kth order. Thus, the only way to mitigate the condition R5), is to set an assumption on the particle configuration itself. In particular, we say that the suspension fulfills the chaos assumption, if the following estimations hold with a constant $c < \infty$ independent of ϵ:*

$$\max_i \left\{ \|\boldsymbol{r}_2^i\|_{\mathcal{C}^1}, \ \ldots, \ \|\boldsymbol{r}_n^i\|_{\mathcal{C}^1} \right\} \le c. \tag{3.36a}$$

Additionally, in case of heavy particles

$$\max_i \left\{ \|\boldsymbol{r}_2^i\|_{\mathcal{C}^{n-1}}, \ \|\boldsymbol{r}_3^i\|_{\mathcal{C}^{n-2}}, \ \ldots, \ \|\boldsymbol{r}_n^i\|_{\mathcal{C}^1} \right\} \le c \tag{3.36b}$$

or, in case of normal particles and $n = 2m$, $m \in \mathbb{N}$

$$\max_i \left\{ \|\boldsymbol{r}_2^i\|_{\mathcal{C}^m}, \ \|\boldsymbol{r}_3^i\|_{\mathcal{C}^{m-1}}, \ \|\boldsymbol{r}_4^i\|_{\mathcal{C}^{m-1}}, \ \ldots, \ \|\boldsymbol{r}_{n-1}^i\|_{\mathcal{C}^1}, \ \|\boldsymbol{r}_n^i\|_{\mathcal{C}^1} \right\} \leq c \qquad (3.36c)$$

or, in case of normal particles and $n = 2m + 1$, $m \in \mathbb{N}$

$$\max_i \left\{ \|\boldsymbol{r}_2^i\|_{\mathcal{C}^m}, \ \|\boldsymbol{r}_3^i\|_{\mathcal{C}^m}, \ \ldots, \ \|\boldsymbol{r}_{n-1}^i\|_{\mathcal{C}^1}, \ \|\boldsymbol{r}_n^i\|_{\mathcal{C}^1} \right\} \leq c. \qquad (3.36d)$$

The set $\mathcal{C}^k$ denotes here $\mathcal{C}^k = \mathcal{C}^k(\mathbb{R}^3 \setminus \overline{\mathcal{E}} \times (0,T); \mathbb{R}^3)$. The light-weighted particles regime also needs assumptions on higher order derivatives of the interaction term if $n \geq 4 + r$ but since we do not consider such approximation orders in what follows, we omit these conditions.

Due to (3.36a), the interaction (3.15b) is well-defined for all $k \leq n$, hence the first part of the proof of Lemma 19 dedicated to the well-definition of the boundary conditions of $\boldsymbol{u}_{\mathrm{loc},k}^i$ works without Lemma 16. The last part of the proof uses (3.8) again in order to show that $\boldsymbol{R}_k^i \in \mathcal{C}_{N_\epsilon}^{K+2-k}$ by using the definition of $\boldsymbol{R}_k^i$ in terms of $\boldsymbol{U}_{\mathrm{loc},k-1}^j$. By replacing requirement R5) with (3.36), this approach is out of reach, since we can not guarantee that $\|\boldsymbol{R}_k^i\|$ is small for particle configurations essentially different to $(\boldsymbol{c}^1, \ldots, \mathbf{R}^{N_\epsilon})$. Instead, we consider the following argument: Fix $\epsilon > 0$ and take $(\boldsymbol{z}^1, \ldots, \mathbf{V}^{N_\epsilon})$ in a small neighborhood $\mathcal{U} \subset (\Omega \times \mathbb{R}^{3 \times 3})^{N_\epsilon}$ of $(\boldsymbol{c}^1, \ldots, \mathbf{R}^{N_\epsilon})$, such that $\sum_{i=1}^{N_\epsilon} \|\boldsymbol{c}^i - \boldsymbol{z}^i\|^2 + \|\mathbf{R}^i - \mathbf{V}^i\|^2 < \epsilon^2/N_\epsilon^2$. Since $\boldsymbol{U}_{\mathrm{loc},1}(\boldsymbol{y}, \boldsymbol{z}, \mathbf{R}, t)$ as given in (3.29) is a smooth function, we have

$$\|\boldsymbol{R}_2^i(\boldsymbol{y}, \boldsymbol{z}^1, \ldots, \mathbf{V}^{N_\epsilon}, t)\| \leq \|\boldsymbol{R}_2^i(\boldsymbol{y}, \boldsymbol{c}^1, \ldots, \mathbf{R}^{N_\epsilon}, t)\| + c\epsilon^{-1} \sum_{j \neq i} \frac{\epsilon}{N_\epsilon} = \|\boldsymbol{r}_2^i(\boldsymbol{y}, t)\| + c$$

with c independent of N_ϵ. Similarly, by imposing (3.36b) we can show that

$$\|t \mapsto \boldsymbol{R}_2^i(\boldsymbol{y}, \boldsymbol{z}^1(t), \ldots, \mathbf{V}^{N_\epsilon}(t), t)\|_{\mathcal{C}^K(\mathbb{R}; \mathbb{R}^3)} < c$$

with c independent of N_ϵ for all smooth curves $t \mapsto (\boldsymbol{z}^1(t), \ldots, \mathbf{V}^{N_\epsilon}(t)) \in \mathcal{U}$. This then leads to the conclusion that although $F_2^i \notin \mathcal{C}_{N_\epsilon}^K$, we still have $F_2^i \in \mathcal{C}^K((\Omega \times \mathbb{R}^{3 \times 3})^{N_\epsilon} \times (0,T); \mathbb{R}^6)$ and the expression $\|t \mapsto F_2^i(\boldsymbol{z}^1(t), \ldots, \mathbf{V}^{N_\epsilon}(t), t)\|_{\mathcal{C}^K(\mathbb{R}; \mathbb{R}^3)}$ is bounded independent of N_ϵ for all test functions with values in $\mathcal{U}$. Hence, we can repeat the final induction steps in the proof of Lemma 19 by using this generalization of $\mathcal{C}_{N_\epsilon}^K$ to test functions in a small neighborhood of the chaotic particle configuration. Thus, by replacing R5) with the chaos assumption, Lemma 19 holds in an accordingly weaker sense, i.e., the functions F_k^i are only well-defined in a small neighborhood of $(\boldsymbol{c}^1, \ldots, \mathbf{R}^{N_\epsilon})$.

Since we directly assume that the interaction terms are small instead of using Lem. 16, we do not have natural restrictions on the particle number and thus $\beta \to 3$ becomes a viable option in this case. Nevertheless, we use the restriction $N_\epsilon = \epsilon^{-\beta}$ with $\beta < 1$. This is the natural choice in case of Lemma 16 for $\ell = 2, K = 1$. Moreover, in [68] the analysis of sedimentation of rigid spherical particles in a viscous fluid yields the characterization of a dilute suspension regime by the condition

$$N_\epsilon \ll \left(\frac{\iota_\epsilon}{\epsilon} \right)^{3/2}. \qquad (3.37)$$

By using (3.4) condition (3.37) yields $N_\epsilon \ll \epsilon^{-1}$, which is fulfilled if $\beta < 1$ is chosen. Additionally, in this case (3.9) is fulfilled for $\ell = 1$ and $K = 1$ which means that we do

not need additional assumptions in order to estimate the sums in (3.33) (Theorem 21). This implies that Theorem 21 holds without modification even if we replace R5) of Lemma 19 with the chaos assumption.

We emphasize that the combination of the chaos assumption and the equations of motion for the particles can very well lead to a contradicting model in general situations as conditions (3.36) are a priori neither easy to prove nor to falsify.

The stresses in the particle domain (3.2) can be handled analogously to Lemma 8. We set the expansion of the stress terms as

$$\tilde{\mathbf{T}}^{ie} = \sum_{k=0}^{n-1} \epsilon^k \mathbf{T}^i_{\mathrm{loc},k+1} + \epsilon^k \mathbf{R}^{iT} \cdot \left(\frac{1}{k!} [\mathbf{R}^i \cdot \boldsymbol{y} \cdot \nabla]^k \mathbf{S}[\boldsymbol{u}_0] + \sum_{j \neq i} \mathbf{S}[\epsilon \mathbf{R}^j \cdot \boldsymbol{u}^j_{\mathrm{loc},k+1}] \right) \cdot \mathbf{R}^i \quad (3.38)$$

and formulate the following result:

Lemma 25 (Asymptotic model of stresses in particle domain of a suspension). *Let the requirements of Lemma 19 be fulfilled. Let* $\mathbf{T}^i_{\mathrm{loc},k} = \nabla_{\boldsymbol{y}} \boldsymbol{\lambda}^i_{\mathrm{loc},k} + \nabla_{\boldsymbol{y}} \boldsymbol{\lambda}^{iT}_{\mathrm{loc},k}$, $k = 1, \ldots, n$, $i = 1, \ldots, N_\epsilon$ *be the solutions of the following boundary value problems for* $t > 0$

$$\nabla_{\boldsymbol{y}} \cdot \mathbf{T}^{iT}_{\mathrm{loc},k} = \hat{\boldsymbol{f}}^i_k, \qquad\qquad \boldsymbol{y} \in \mathcal{E}, \qquad\qquad (3.39a)$$

$$\mathbf{T}^i_{\mathrm{loc},k} \cdot \boldsymbol{n} = \mathbf{S}_{\boldsymbol{y}}[\boldsymbol{u}^i_{\mathrm{loc},k}] \cdot \boldsymbol{n}, \qquad\qquad \boldsymbol{y} \in \partial\mathcal{E}, \qquad\qquad (3.39b)$$

where the force terms $\hat{\boldsymbol{f}}^i_k$ *are given as*

$$\hat{\boldsymbol{f}}^i_1 = \hat{\boldsymbol{k}}^i_{-1-r}\,,$$

$$\hat{\boldsymbol{f}}^i_k = -\frac{1}{(k-2)!} \mathbf{R}^{iT} \cdot [\mathbf{R}^i \cdot \boldsymbol{y} \cdot \nabla]^{k-2} \nabla \cdot \mathbf{S}[\boldsymbol{u}_0] + \hat{\boldsymbol{k}}^i_{k-2-r} \quad \textit{for } k \geq 2\,,$$

and where $\hat{\boldsymbol{k}}^i_k$ *are set as*

$$\hat{\boldsymbol{k}}^i_k = \mathbf{0} \qquad\qquad\qquad\qquad\qquad\qquad\qquad \textit{for } k < 0\,,$$

$$\hat{\boldsymbol{k}}^i_0 = \rho \operatorname{Re} \mathbf{R}^{iT} \cdot \left(\mathrm{D}_t \boldsymbol{u}_0(\boldsymbol{c}^i, t) - \mathrm{Fr}^{-2} \boldsymbol{e}_g \right),$$

$$\hat{\boldsymbol{k}}^i_k = \rho \operatorname{Re} \mathbf{R}^{iT} \cdot \sum_{m=0}^{k} \dot{\boldsymbol{v}}^i_{m,k-m}$$

$$+ \rho \operatorname{Re} \mathbf{R}^{iT} \cdot \sum_{m=0}^{k-1} \left(B(\dot{\boldsymbol{\omega}}^i_{m,k-m-1}) + B(\boldsymbol{\omega}^i_m) \cdot B(\boldsymbol{\omega}^i_{k-m-1}) \right) \cdot \mathbf{R}^i \cdot \boldsymbol{y} \qquad \textit{for } k \geq 1$$

with the terms $\dot{\boldsymbol{v}}^i_{m,k-m}, \dot{\boldsymbol{\omega}}^i_{m,k-m-1}$ *given in (3.31).*

Then $\tilde{\mathbf{T}}^{ie}$ *solve the system (3.2) at least up to an error of* $\mathcal{O}(\epsilon^{n-1})$.

Proof. The proof is analogous to Lemma 8. Using the expansion of the fluid velocity (3.17) on the left-hand side of the boundary condition (3.2b) and applying a Taylor expansion of $\mathbf{S}[\boldsymbol{u}_0]$ in $\boldsymbol{c}^i$, we get

$$\sum_{k=0}^{n-1} \frac{\epsilon^k}{k!} \mathbf{R}^{iT} \cdot [\mathbf{R}^i \cdot \boldsymbol{y} \cdot \nabla]^k \mathbf{S}[\boldsymbol{u}_0] \cdot \mathbf{R}^i \cdot \boldsymbol{n}$$

$$+ \sum_{k=1}^{n} \mathbf{R}^{iT} \cdot \sum_{j \neq i} \mathbf{S}[\epsilon^k \mathbf{R}^j \cdot \boldsymbol{u}^j_{\mathrm{loc},k}] \cdot \mathbf{R}^i \cdot \boldsymbol{n} + \sum_{k=1}^{n} \epsilon^{k-1} \mathbf{S_y}[\boldsymbol{u}^i_{\mathrm{loc},k}] \cdot \boldsymbol{n} + \mathcal{O}(\epsilon^n)$$

$$= \tilde{\mathbf{T}}^{ie} \cdot \boldsymbol{n} + \mathcal{O}(\epsilon^n) \,.$$

Application of (3.38) and (3.39b) then shows that the boundary condition is fulfilled up to $\mathcal{O}(\epsilon^n)$. For the accelerations, we use an analogous expansion as in the proof of Lemma 19:

$$\frac{\mathrm{d}^2}{\mathrm{d}t^2} \boldsymbol{x}^i(\boldsymbol{y}) = \sum_{m=1}^{n-1} \epsilon^m \sum_{k=0}^{m-1} B(\dot{\boldsymbol{\omega}}^i_{k,m-k-1}) \cdot \mathbf{R}^i \cdot \boldsymbol{y} + B(\boldsymbol{\omega}^i_k) \cdot B(\boldsymbol{\omega}^i_{m-k-1}) \cdot \mathbf{R}^i \cdot \boldsymbol{y}$$

$$+ \sum_{m=0}^{n-1} \epsilon^m \sum_{k=0}^{m} \dot{\boldsymbol{v}}^i_{k,m-k} + \mathcal{O}(\epsilon^n) = \sum_{m=0}^{n-1} \epsilon^m \hat{\boldsymbol{a}}^i_m + \mathcal{O}(\epsilon^n) \,.$$

Applying this expansion in (3.2a) and using (3.38) we get

$$\rho_\epsilon \, \mathrm{Re} \left(\sum_{k=0}^{n-1} \epsilon^k \hat{\boldsymbol{a}}^i_k - \mathrm{Fr}^{-2} \boldsymbol{e}_g \right) + \mathcal{O}(\epsilon^{n-1})$$

$$= \sum_{k=0}^{n-1} \epsilon^{k-1} \mathbf{R}^i \cdot \nabla_{\boldsymbol{y}} \cdot \mathbf{T}^{iT}_{\mathrm{loc},k+1} + \sum_{k=1}^{n-1} \frac{\epsilon^{k-1}}{(k-1)!} [\mathbf{R}^i \cdot \boldsymbol{y} \cdot \nabla]^{k-1} \nabla \cdot \mathbf{S}[\boldsymbol{u}_0]$$

$$+ \sum_{j \neq i} \sum_{k=0}^{n-1} \epsilon^{k-1} \mathbf{R}^{iT} \cdot \mathbf{R}^j \cdot \nabla_{\boldsymbol{y}} \cdot \mathbf{S_y}[\boldsymbol{u}^j_{\mathrm{loc},k+1}]^T \,.$$

With (3.14) and (3.39a), the momentum equation for the particle domain is then fulfilled up to an error of $\mathcal{O}(\epsilon^{n-1})$. $\qquad \square$

Remark 26. *Just as in Remark 9, the force terms $\hat{\boldsymbol{f}}^i_k$ in Lemma 25 are related to the forces and torques (3.13) of Lemma 19 by*

$$\int_{\mathcal{E}} \hat{\boldsymbol{f}}^i_k \, \mathrm{d}\boldsymbol{y} = \boldsymbol{f}^i_k \,, \quad \int_{\mathcal{E}} \boldsymbol{y} \times \hat{\boldsymbol{f}}^i_k \, \mathrm{d}\boldsymbol{y} = \boldsymbol{g}^i_k \tag{3.40}$$

as can be seen by integrating. We show here only the relation for the $\boldsymbol{g}^i_k$ terms. We note that the claim is identical to $\boldsymbol{\ell}^i_k = \int_{\mathcal{E}} \boldsymbol{y} \times \hat{\boldsymbol{k}}^i_{k+1} \, \mathrm{d}\boldsymbol{y}$ for $k \geq 0$. Therefore,

$$\int_{\mathcal{E}} \boldsymbol{y} \times \hat{\boldsymbol{k}}^i_{k+1} \, \mathrm{d}\boldsymbol{y} - \boldsymbol{\ell}^i_k$$

$$= \rho \, \mathrm{Re} \int_{\mathcal{E}} B(\boldsymbol{y}) \cdot \mathbf{R}^{iT} \cdot \sum_{m=0}^{k} \left(B(\dot{\boldsymbol{\omega}}^i_{m,k-m}) + B(\boldsymbol{\omega}^i_m) \cdot B(\boldsymbol{\omega}^i_{k-m}) \right) \cdot \mathbf{R}^i \cdot \boldsymbol{y} \, \mathrm{d}\boldsymbol{y}$$

$$- \rho \, \mathrm{Re} \, |\mathcal{E}| \mathbf{R}^{iT} \cdot \sum_{m=0}^{k} \mathbf{J}^i \cdot \dot{\boldsymbol{\omega}}^i_{m,k-m} + B(\boldsymbol{\omega}^i_m) \cdot \mathbf{J}^i \cdot \boldsymbol{\omega}^i_{k-m}$$

$$= \rho \operatorname{Re} |\mathcal{E}| \mathbf{R}^{iT} \cdot \sum_{m=0}^{k} \Big(\frac{1}{|\mathcal{E}|} \int_{\mathcal{E}} B(\mathbf{R}^i \cdot \boldsymbol{y}) \cdot B(\dot{\boldsymbol{\omega}}_{m,k-m}^i) \cdot \mathbf{R}^i \cdot \boldsymbol{y} \, \mathrm{d}\boldsymbol{y} - \mathbf{J}^i \cdot \dot{\boldsymbol{\omega}}_{m,k-m}^i$$

$$+ \frac{1}{|\mathcal{E}|} \int_{\mathcal{E}} B(\mathbf{R}^i \cdot \boldsymbol{y}) \cdot B(\boldsymbol{\omega}_m^i) \cdot B(\boldsymbol{\omega}_{k-m}^i) \cdot \mathbf{R}^i \cdot \boldsymbol{y} \, \mathrm{d}\boldsymbol{y} - B(\boldsymbol{\omega}_m^i) \cdot \mathbf{J}^i \cdot \boldsymbol{\omega}_{k-m}^i \Big)$$

$$= \rho \operatorname{Re} |\mathcal{E}| \mathbf{R}^{iT} \cdot \sum_{m=0}^{k} \Big(\frac{-1}{|\mathcal{E}|} \int_{\mathcal{E}} B(\mathbf{R}^i \cdot \boldsymbol{y})^2 \, \mathrm{d}\boldsymbol{y} \cdot \dot{\boldsymbol{\omega}}_{m,k-m}^i - \mathbf{J}^i \cdot \dot{\boldsymbol{\omega}}_{m,k-m}^i$$

$$+ B(\boldsymbol{\omega}_m^i) \cdot \frac{-1}{|\mathcal{E}|} \int_{\mathcal{E}} B(\mathbf{R}^i \cdot \boldsymbol{y})^2 \, \mathrm{d}\boldsymbol{y} \cdot \boldsymbol{\omega}_{k-m}^i - B(\boldsymbol{\omega}_m^i) \cdot \mathbf{J}^i \cdot \boldsymbol{\omega}_{k-m}^i$$

$$- \frac{1}{|\mathcal{E}|} \int_{\mathcal{E}} \mathbf{R}^i \cdot \boldsymbol{y} \otimes \mathbf{R}^i \cdot \boldsymbol{y} \, \mathrm{d}\boldsymbol{y} \cdot (\boldsymbol{\omega}_m^i \times \boldsymbol{\omega}_{k-m}^i) \Big)$$

where we used (A.10d). *Since* $|\mathcal{E}|^{-1} \int_{\mathcal{E}} B(\mathbf{R}^i \cdot \boldsymbol{y})^2 \, \mathrm{d}\boldsymbol{y} = -\mathbf{J}^i$, *see* (2.5) *and* (A.10d), *it follows*

$$\int_{\mathcal{E}} \boldsymbol{y} \times \hat{\boldsymbol{k}}_{k+1}^i \, \mathrm{d}\boldsymbol{y} - \boldsymbol{\ell}_k^i = -\rho \operatorname{Re} \mathbf{R}^{iT} \cdot \int_{\mathcal{E}} \mathbf{R}^i \cdot \boldsymbol{y} \otimes \mathbf{R}^i \cdot \boldsymbol{y} \, \mathrm{d}\boldsymbol{y} \cdot \sum_{m=0}^{k} \boldsymbol{\omega}_m^i \times \boldsymbol{\omega}_{k-m}^i .$$

Finally, since $\boldsymbol{v} \times \boldsymbol{v} = \mathbf{0}$ *for all* $\boldsymbol{v} \in \mathbb{R}^3$,

$$\sum_{m=0}^{k} \boldsymbol{\omega}_m^i \times \boldsymbol{\omega}_{k-m}^i = \sum_{0 \leq m < k/2} \boldsymbol{\omega}_m^i \times \boldsymbol{\omega}_{k-m}^i - \sum_{k/2 < m \leq k} \boldsymbol{\omega}_{k-m}^i \times \boldsymbol{\omega}_m^i$$

$$= \sum_{0 \leq m < k/2} \boldsymbol{\omega}_m^i \times \boldsymbol{\omega}_{k-m}^i - \sum_{0 \leq \ell < k/2} \boldsymbol{\omega}_\ell^i \times \boldsymbol{\omega}_{k-\ell}^i = \mathbf{0} .$$

3.4 Kinetic suspension model

In Theorem 21 and Remark 23 we found that given the solution of a Navier-Stokes problem $\boldsymbol{u}_0, p_0$ in Ω, we can approximate a dilute or semi-dilute suspension given by (3.1) up to an error of $\mathcal{O}(\epsilon)$ by a superposition of stationary Stokes fields and expressing the velocity of the particle in terms of $\boldsymbol{u}_0$. In order to construct higher order corrections, we could introduce higher order local velocity fields which then incorporate the time derivatives of the superposition of the lower order local velocity fields and the corresponding convective terms as source terms. Instead, we want to propose a different approach which uses a mean field description for the particle behavior but preserves the structure of Theorem 21.

3.4.1 Mean field approximation for particle dynamics

As a preliminary step, we introduce the empirical measure μ_{N_ϵ} on $\Omega \times \mathcal{SO}(3)$ for N_ϵ given positions $\boldsymbol{c}^i \in \Omega$ and rotations $\mathbf{R}^i \in \mathcal{SO}(3)$ given as

$$\mu_{N_\epsilon}(A \times B) = \frac{1}{N_\epsilon} \sum_{j=1}^{N_\epsilon} \delta_{\boldsymbol{c}^j}(A) \delta_{\mathbf{R}^j}(B) \tag{3.41}$$

for any $A \times B \in \mathcal{A}$, $\mathcal{A}$ denoting the Borel σ-Algebra on $\Omega \times \mathcal{SO}(3)$ and $\delta_{\boldsymbol{c}^i}, \delta_{\mathbf{R}^i}$ the respective Dirac-measures. We note that the centers of mass as well as the rotations

in the context of the present work are time-dependent in general, thus, so is μ_{N_ϵ}. Parameter-dependencies of measures are indicated by appropriate indices, hence, $\mu_{N_\epsilon} = \mu_{N_\epsilon,t}$. However, as stated at the beginning of this chapter we often suppress the time-dependency of quantities if it is obvious from context or if a detailed discussion of the regularity of the dependency is not needed. The proof of Lemma 19 shows that $(\boldsymbol{v}_1^i, \boldsymbol{\omega}_0^i) = F_1(\boldsymbol{c}^i, \mathbf{R}^i, t)$ with F_1 being a smooth function not depending on the particle index. The explicit dependence of the functions F_k^i on i for $k \geq 2$ is a consequence of the particle interaction (3.15b). Using the empirical measure and the expression for $\boldsymbol{u}_{\mathrm{loc},1}^i$ given in (3.29) we can set

$$\boldsymbol{r}_2[\mu_{N_\epsilon}](\boldsymbol{x}, t) = \epsilon^{-1} N_\epsilon \int_{\Omega \times \mathcal{SO}(3)} \mathbf{R} \cdot \boldsymbol{U}_{\mathrm{loc},1}(\boldsymbol{y}(\boldsymbol{x}, \boldsymbol{z}, \mathbf{R}, \epsilon), \boldsymbol{z}, \mathbf{R}, t) \chi(\iota_\epsilon^{-1} \mathbf{R}^T \cdot (\boldsymbol{x} - \boldsymbol{z})) \, \mathrm{d}\mu_{N_\epsilon}(\boldsymbol{z}, \mathbf{R}) \,,$$

where the mapping χ denotes a smooth cutoff function with $\chi = 1$ on $\mathbb{R}^3 \setminus \mathcal{B}_{1/2}$ and $\chi = 0$ on $\mathcal{B}_{1/4}$. Then due to (3.6), ϵ/ι_ϵ becomes arbitrarily small as $\epsilon \to 0$. In particular, for any $\boldsymbol{y} \in \mathcal{E}$ it holds for all sufficiently small ϵ

$$\|\iota_\epsilon^{-1} \mathbf{R}^{iT} \cdot (\boldsymbol{x}^i(\boldsymbol{y}) - \boldsymbol{c}^i)\| \leq \frac{\epsilon}{\iota_\epsilon} \sup_{\boldsymbol{y} \in \mathcal{E}} \|\boldsymbol{y}\| < \frac{1}{4} \,.$$

Using this relation and (3.5), we also have for any $\boldsymbol{y} \in \mathcal{E}$ and $i \neq j$

$$\frac{1}{2} \|\boldsymbol{c}^i - \boldsymbol{c}^j\| - \epsilon \|\boldsymbol{y}\| > \iota_\epsilon \left(\frac{1}{2} - \frac{\epsilon}{\iota_\epsilon} \sup_{\boldsymbol{y} \in \mathcal{E}} \|\boldsymbol{y}\| \right) > \frac{\iota_\epsilon}{4} > 0 \,.$$

This immediately implies for any $\boldsymbol{y} \in \mathcal{E}$ and $i \neq j$ the following relation

$$\|\iota_\epsilon^{-1} \mathbf{R}^{jT} \cdot (\boldsymbol{x}^i(\boldsymbol{y}) - \boldsymbol{c}^j)\| \geq \iota_\epsilon^{-1} |\|\boldsymbol{c}^i - \boldsymbol{c}^j\| - \epsilon \|\boldsymbol{y}\|| > \frac{\|\boldsymbol{c}^i - \boldsymbol{c}^j\|}{2\iota_\epsilon} > \frac{1}{2} \,.$$

These estimations imply for $\boldsymbol{x} = \boldsymbol{x}^i(\boldsymbol{y})$ the identity $\boldsymbol{r}_2[\mu_{N_\epsilon}](\boldsymbol{x}^i(\boldsymbol{y}), t) \equiv \boldsymbol{r}_2^i(\boldsymbol{y}, t)$, the latter stated in (3.15b). This also shows

$$F_2^i(\boldsymbol{c}^1, \mathbf{R}^1, \ldots, \boldsymbol{c}^{N_\epsilon}, \mathbf{R}^{N_\epsilon}, t) = F_2[\mu_{N_\epsilon}](\boldsymbol{c}^i, \mathbf{R}^i, t) \,,$$

where F_2 is given analogously to the discussion in proof of Lemma 19 as

$$F_2[\mu_{N_\epsilon}](\boldsymbol{c}, \mathbf{R}, t) = \begin{bmatrix} \mathbf{R} & \\ & \mathbf{R} \end{bmatrix} \cdot \mathbf{A}^{-1} \cdot \left(\begin{bmatrix} \mathbf{I} & \\ & \frac{1}{\sqrt{2}}\mathbf{I} \end{bmatrix} \cdot \begin{pmatrix} \boldsymbol{f}_2 \\ \boldsymbol{g}_2 \end{pmatrix} + D_2 \boldsymbol{u}_0 + u_2[\mu_{N_\epsilon}] \right)(\boldsymbol{c}, \mathbf{R}, t) \,,$$

with the terms

$$u_2[\mu_{N_\epsilon}](\boldsymbol{c}, \mathbf{R}, t) = \left(\int_{\partial \mathcal{E}} \mathbf{R}^T \cdot \boldsymbol{r}_2[\mu_{N_\epsilon}](\boldsymbol{x}(\boldsymbol{y}, \boldsymbol{c}, \mathbf{R}, \epsilon), t) \cdot \mathbf{S}_{\boldsymbol{y}}[\boldsymbol{w}_q](\boldsymbol{y}) \cdot \boldsymbol{n} \, \mathrm{d}s_y \right)_{q=1,\ldots,6} \,,$$

$$D_k \boldsymbol{u}_0(\boldsymbol{c}, \mathbf{R}, t) = \frac{1}{k!} \left(\int_{\partial \mathcal{E}} \mathbf{R}^T \cdot [\mathbf{R} \cdot \boldsymbol{y} \cdot \nabla]^k \boldsymbol{u}_0(\boldsymbol{c}, t) \cdot \mathbf{S}_{\boldsymbol{y}}[\boldsymbol{w}_q](\boldsymbol{y}) \cdot \boldsymbol{n} \, \mathrm{d}s_y \right)_{q=1,\ldots,6} \,,$$

$$\boldsymbol{f}_2(\boldsymbol{c}, \mathbf{R}, t) = -|\mathcal{E}|\mathbf{R}^T \cdot \nabla \cdot \mathbf{S}[\boldsymbol{u}_0](\boldsymbol{c}, t)$$
$$+ \rho \operatorname{Re} |\mathcal{E}|\mathbf{R}^T \cdot (\partial_{\boldsymbol{x}} \boldsymbol{u}_0(\boldsymbol{c}, t) \cdot F_{1,v}(\boldsymbol{c}, \mathbf{R}, t) + G_{1,0,v}(\boldsymbol{c}, \mathbf{R}, t)) \,,$$

$$\boldsymbol{g}_2(\boldsymbol{c}, \mathbf{R}, t) = - \int_{\mathcal{E}} \boldsymbol{y} \times \mathbf{R}^T \cdot \nabla \cdot \mathbf{S}[\boldsymbol{u}_0](\boldsymbol{c}, t) \, \mathrm{d}\boldsymbol{y} + \rho \operatorname{Re} |\mathcal{E}| \mathbf{R}^T \cdot \Big(\mathbf{J}(\mathbf{R}) \cdot G_{1,0,\omega}(\boldsymbol{c}, \mathbf{R}, t)$$

$$+ B(F_{1,\omega}(\boldsymbol{c}, \mathbf{R}, t)) \cdot \mathbf{J}(\mathbf{R}) \cdot F_{1,\omega}(\boldsymbol{c}, \mathbf{R}, t) \Big),$$

where $\mathbf{J}(\mathbf{R}) = \mathbf{R} \cdot \hat{\mathbf{J}} \cdot \mathbf{R}^T$ with $\hat{\mathbf{J}}$ given in (2.5) and where $G_{1,0}$ is set as

$$G_{1,0}(\boldsymbol{c}, \mathbf{R}, t) = (G_{1,0,v}, G_{1,0,\omega})(\boldsymbol{c}, \mathbf{R}, t) = \partial_t F_1(\boldsymbol{c}, \mathbf{R}, t) + \partial_{\boldsymbol{c}} F_1(\boldsymbol{c}, \mathbf{R}, t) \cdot \boldsymbol{u}_0(\boldsymbol{c}, t)$$

$$+ \sum_{m,n=1}^{3} \partial_{R_{mn}} F_1(\boldsymbol{c}, \mathbf{R}, t)(B(F_{1,\omega}(\boldsymbol{c}, \mathbf{R}, t)) \cdot \mathbf{R})_{mn} \, .$$

For $k > 2$, F_k^i can be expressed in a similar way as

$$F_k^i(\boldsymbol{c}^1, \dots, \mathbf{R}^{N_\epsilon}, t) = F_k[\mu_{N_\epsilon}](\boldsymbol{c}^i, \mathbf{R}^i, t).$$

In these cases $\boldsymbol{u}_{\mathrm{loc},k-1}^i(\boldsymbol{y}, t) = \boldsymbol{U}_{\mathrm{loc},k-1}[\mu_{N_\epsilon}](\boldsymbol{y}, \boldsymbol{c}^i, \mathbf{R}^i, t)$, thus $\boldsymbol{r}_k[\mu_{N_\epsilon}]$ is an iterated integral operator with respect to the measure μ_{N_ϵ}. Additionally, also the force terms $(\boldsymbol{f}_k^i, \boldsymbol{g}_k^i) = (\boldsymbol{f}_k, \boldsymbol{g}_k)[\mu_{N_\epsilon}](\boldsymbol{c}^i, \mathbf{R}^i, t)$ are integral operators acting on the empirical measure, as they incorporate the expressions of the type (3.30). Using these expressions, we formulate the following lemma.

Lemma 27 (Mean field pde of the particle description)**.** *Let the assumptions of Lemma 19 be fulfilled. Then the system*

$$\frac{\mathrm{d}}{\mathrm{d}t} \boldsymbol{c}^i(t) = \boldsymbol{u}_0(\boldsymbol{c}^i(t), t) + \sum_{k=1}^{n} \epsilon^k F_{k,v}^i(\boldsymbol{c}^1(t), \dots, \mathbf{R}^{N_\epsilon}(t), t) \tag{3.42a}$$

$$\frac{\mathrm{d}}{\mathrm{d}t} \mathbf{R}^i(t) = \sum_{k=0}^{n-1} \epsilon^k B \left(F_{k+1,\omega}^i(\boldsymbol{c}^1(t), \dots, \mathbf{R}^{N_\epsilon}(t), t) \right) \cdot \mathbf{R}^i(t) \tag{3.42b}$$

with initial data $(\boldsymbol{c}^1(0), \dots, \mathbf{R}^{N_\epsilon}(0)) \in (\Omega \times \mathcal{SO}(3))^{N_\epsilon}$ *has a unique solution* $(\boldsymbol{c}^1, \dots, \mathbf{R}^{N_\epsilon})$ *with* $(\boldsymbol{c}^1, \dots, \mathbf{R}^{N_\epsilon}) \in \mathcal{C}^1(\mathbb{R}^+; (\Omega \times \mathcal{SO}(3))^{N_\epsilon})$. *Moreover, the empirical measure*

$$\mu_{N_\epsilon, t} = \frac{1}{N_\epsilon} \sum_{j=1}^{N_\epsilon} \delta_{\boldsymbol{c}^j(t)} \delta_{\mathbf{R}^j(t)}$$

is a weak solution in the sense of distributions to the mean field equation (see Remark A.38 in Appendix A.1)

$$\partial_t \psi_\epsilon + \nabla_{\boldsymbol{x}} \cdot (\boldsymbol{u}_0 \psi_\epsilon) + \sum_{k=1}^{n} \epsilon^k \nabla_{\boldsymbol{x}} \cdot (F_{k,v}[\psi_\epsilon] \psi_\epsilon) - \sum_{k=0}^{n-1} \epsilon^k \mathcal{L}[B(F_{k+1,\omega}[\psi_\epsilon])](\psi_\epsilon)$$

$$- \sum_{k=0}^{n-1} \epsilon^k \mathrm{div}_{\mathcal{G}} (\mathcal{L}[B(F_{k+1,\omega}[\psi_\epsilon])]) \psi_\epsilon = 0 \, . \tag{3.43}$$

The terms $\mathcal{L}[\mathbf{M}](\boldsymbol{x}, ., t) \in \mathcal{TSO}(3)$ *for a skew-symmetric matrix* $\mathbf{M}$ *denote the vector fields associated to the left Lie derivative on* $\mathcal{SO}(3)$ *and* $\mathrm{div}_{\mathcal{G}}(\mathcal{L})$ *the corresponding divergence on* $\mathcal{SO}(3)$ *discussed in Remark A.32.*

Proof. Since Lemma 19 holds, the right-hand side of the system (3.42) is at least in $\mathcal{C}^1_{N_\epsilon}$ and as Ω and $\mathcal{SO}(3)$ are bounded, the right-hand side of (3.42) is Lipschitz-continuous in $(\Omega \times \mathcal{SO}(3))^{N_\epsilon}$ and continuous in t. Thus, the first claim follows by Picard-Lindelöf.

For the second part, we consider the weak form of (3.43) (see (A.6) in Remark A.38). Let a test function $\sigma \in \mathcal{C}^1(\Omega \times \mathcal{SO}(3); \mathbb{R})$ be given, then the empirical measure fulfills

$$\frac{\mathrm{d}}{\mathrm{d}t} \int_{\Omega \times \mathcal{SO}(3)} \sigma \, \mathrm{d}\mu_{N_\epsilon,t} = \frac{1}{N_\epsilon} \sum_{i=1}^{N_\epsilon} \frac{\mathrm{d}}{\mathrm{d}t} \sigma(\boldsymbol{c}^i(t), \mathbf{R}^i(t)) \,.$$

By Remark A.37 and (3.42b), the right-hand side can be expressed as

$$\frac{\mathrm{d}}{\mathrm{d}t} \int_{\Omega \times \mathcal{SO}(3)} \sigma \, \mathrm{d}\mu_{N_\epsilon,t} = \frac{1}{N_\epsilon} \sum_{i=1}^{N_\epsilon} \left(\partial_{\boldsymbol{x}}\sigma \cdot \frac{\mathrm{d}}{\mathrm{d}t}\boldsymbol{c}^i(t) - \mathcal{L}\left[\sum_{k=0}^{n-1} \epsilon^k B\left(F_{k+1,\omega}^i\right) \right]\bigg|_{\mathbf{R}^i(t)} (\sigma(\boldsymbol{c}^i(t), .)) \right) \,.$$

Since $F_k^i(\boldsymbol{c}^1, \dots, \mathbf{R}^{N_\epsilon}, t) = F_k[\mu_{N_\epsilon,t}](\boldsymbol{c}^i, \mathbf{R}^i, t)$ and due to (3.42a) as well as Lemma A.28, we then find

$$\frac{\mathrm{d}}{\mathrm{d}t} \int_{\Omega \times \mathcal{SO}(3)} \sigma(\boldsymbol{x}, \mathbf{R}) \, \mathrm{d}\mu_{N_\epsilon,t}(\boldsymbol{x}, \mathbf{R}) = \int_{\Omega \times \mathcal{SO}(3)} \partial_{\boldsymbol{x}}\sigma \cdot \left(\boldsymbol{u}_0 + \sum_{k=1}^{n} \epsilon^k F_{k,v}[\mu_{N_\epsilon,t}] \right) (\boldsymbol{x}, \mathbf{R}) \, \mathrm{d}\mu_{N_\epsilon,t}(\boldsymbol{x}, \mathbf{R})$$

$$- \sum_{k=0}^{n-1} \epsilon^k \int_{\Omega \times \mathcal{SO}(3)} \mathcal{L}[B(F_{k+1,\omega}[\mu_{N_\epsilon,t}])](\sigma(\boldsymbol{x}, .))(\boldsymbol{x}, \mathbf{R}) \, \mathrm{d}\mu_{N_\epsilon,t}(\boldsymbol{x}, \mathbf{R}) \,,$$

which is exactly the weak form of (3.43). □

Next, we expand the operators F_k onto a larger class of measures. By $\mathcal{P}(\Omega)$ we denote the set of all Borel probability measures over Ω, analogously $\mathcal{P}(\mathcal{SO}(3))$ is the set of Borel probability measures over $\mathcal{SO}(3)$. In order to proceed, we first note that the Dirichlet boundary conditions (3.15a) can be expressed as

$$\boldsymbol{u}_{\mathrm{loc},k}^i(\boldsymbol{y}) = \boldsymbol{U}_{\mathrm{loc},k,\partial\mathcal{E}}[\mu_{N_\epsilon}](\boldsymbol{y}, \boldsymbol{c}^i, \mathbf{R}^i, t)$$

with $\boldsymbol{U}_{\mathrm{loc},k,\partial\mathcal{E}}[\mu_{N_\epsilon}]$ given in terms of $F_k[\mu_{N_\epsilon}], \boldsymbol{r}_k[\mu_{N_\epsilon}]$, and $\boldsymbol{u}_0$. Then we find the following result for the operators F_k, $k \geq 0$ in case of general Borel probability measures in $\mathcal{P}(\Omega) \times \mathcal{P}(\mathcal{SO}(3))$.

Lemma 28. *Let the assumptions of Lemma 19 hold under the sharper condition on β given as*

$$\beta \leq 3\frac{\ell - 1}{\ell + K + 3}$$

then the operators F_k fulfill $\|F_k[\psi]\|_{\mathcal{C}^{m_k}(\Omega \times \mathcal{SO}(3) \times (0,T); \mathbb{R}^6)} < c$ independent of ϵ with $m_k = \min(K + 3 + r - k, K)$, $k = 0, \dots, n$ for any $\psi \in \mathcal{P}(\Omega) \times \mathcal{P}(\mathcal{SO}(3))$.

Proof. Following the discussion from the beginning of Section 3.4.1, we start with F_0. Since $F_0 = (\boldsymbol{u}_0, \boldsymbol{0}) = (\boldsymbol{u}_0, \boldsymbol{0})(\boldsymbol{x}, t)$ and $F_1 = F_1(\boldsymbol{x}, \mathbf{R}, t)$, with $F_0 \in \mathcal{C}^\infty(\Omega \times (0,T); \mathbb{R}^6)$ as well as $F_1 \in \mathcal{C}^\infty(\Omega \times \mathcal{SO}(3) \times (0,T); \mathbb{R}^6)$ and F_0, F_1 not depending on the interaction terms, there is nothing to show in these cases. As for F_2, it depends on $\boldsymbol{r}_2[\psi]$, the latter being a smooth function for any finite $\epsilon > 0$. We have to check, under which

conditions $\|\boldsymbol{r}_2[\psi]\|_{\mathcal{C}^K}$ is bounded independent of ϵ for $\psi \in \mathcal{P}(\Omega) \times \mathcal{P}(\mathcal{SO}(3))$, which then immediately shows the corresponding bound for $F_2[\psi] \in \mathcal{C}^K(\Omega \times \mathcal{SO}(3) \times \mathbb{R}^+; \mathbb{R}^6)$. For $\boldsymbol{x} \in \Omega$ and $t > 0$ we find for $0 \leq k \leq K$

$$\|\partial_t^k \boldsymbol{r}_2[\psi](\boldsymbol{x},t)\| \leq \epsilon^{-1} N_\epsilon \int_{\Omega \setminus \mathcal{B}_{\iota_\epsilon/4}(\boldsymbol{x}) \times \mathcal{SO}(3)} \|\partial_t^k \boldsymbol{U}_{\mathrm{loc},1}(\boldsymbol{y}(\boldsymbol{x},\boldsymbol{z},\mathbf{R},\epsilon),\boldsymbol{z},\mathbf{R},t)\chi(\iota_\epsilon^{-1}\mathbf{R}^T \cdot (\boldsymbol{x}-\boldsymbol{z}))\| \, \mathrm{d}\psi$$

since $\chi(\iota_\epsilon^{-1}\mathbf{R}^T \cdot (\boldsymbol{x}-\boldsymbol{z})) = 0$ if $\|\boldsymbol{x}-\boldsymbol{z}\| \leq \iota_\epsilon/4$. Next, since χ is a smooth cut-off function and due to $\|\boldsymbol{y}(\boldsymbol{x},\boldsymbol{z},\mathbf{R},\epsilon)\| \geq \iota_\epsilon \epsilon^{-1}/4$ in combination with the decay properties of $\boldsymbol{U}_{\mathrm{loc},1}$ given in Corollary B.4,

$$\|\partial_t^k \boldsymbol{r}_2[\psi](\boldsymbol{x},t)\| \leq c\epsilon^{-1} N_\epsilon \left(\frac{\epsilon}{\iota_\epsilon}\right)^\ell \int_{\Omega \setminus \mathcal{B}_{\iota_\epsilon/4}(\boldsymbol{x}) \times \mathcal{SO}(3)} \|\partial_t^k \boldsymbol{U}_{\mathrm{loc},1,\partial\mathcal{E}}(.,\boldsymbol{z},\mathbf{R},t)\|_{1,\partial\mathcal{E}} \, \mathrm{d}\psi$$

$$\leq c\epsilon^{-1} N_\epsilon \left(\frac{\epsilon}{\iota_\epsilon}\right)^\ell \int_{\Omega \times \mathcal{SO}(3)} \|\partial_t^k \boldsymbol{U}_{\mathrm{loc},1,\partial\mathcal{E}}(.,\boldsymbol{z},\mathbf{R},t)\|_{1,\partial\mathcal{E}} \, \mathrm{d}\psi$$

for some $\ell \geq 1$ and $c = c(\mathcal{E},\chi)$. Since $\boldsymbol{U}_{\mathrm{loc},1,\partial\mathcal{E}}$ is given in terms of F_1 and $\boldsymbol{u}_0$ which are smooth, we have a well-defined

$$C = \max_{0 \leq k \leq K} \sup_{(\boldsymbol{z},\mathbf{R},t) \in \Omega \times \mathcal{SO}(3) \times (0,T)} \|\partial_t^k \boldsymbol{U}_{\mathrm{loc},1,\partial\mathcal{E}}(.,\boldsymbol{z},\mathbf{R},t)\|_{1,\partial\mathcal{E}} < \infty$$

which is independent of ϵ. Thus,

$$\|\partial_t^k \boldsymbol{r}_2[\psi](\boldsymbol{x},t)\| \leq c\epsilon^{-1} N_\epsilon \left(\frac{\epsilon}{\iota_\epsilon}\right)^\ell C \int_{\Omega \times \mathcal{SO}(3)} \mathrm{d}\psi = cC\epsilon^{-1+\ell} N_\epsilon^{1+\ell/3} = cC\epsilon^{\ell-1-\beta(1+\ell/3)}$$

by applying (3.4) and $N_\epsilon = \epsilon^{-\beta}$. This way we find that $\|\partial_t^k \boldsymbol{r}_2[\psi](\boldsymbol{x},t)\| < c$ independent of ϵ for any $k \geq 0$ and $(\boldsymbol{x},t) \in \Omega \times (0,T)$ if $\beta \leq 3(\ell-1)/(\ell+3)$, which is true as $K \geq 1$. Similarly, we find

$$\|\nabla^k \boldsymbol{r}_2[\psi](\boldsymbol{x},t)\| \leq c\epsilon^{-1-k} N_\epsilon \int_{\Omega \setminus \mathcal{B}_{\iota_\epsilon/2}(\boldsymbol{x}) \times \mathcal{SO}(3)} \|\nabla_{\boldsymbol{y}}^k \boldsymbol{U}_{\mathrm{loc},1}(\boldsymbol{y}(\boldsymbol{x},\boldsymbol{z},\mathbf{R},\epsilon),\boldsymbol{z},\mathbf{R},t)\| \, \mathrm{d}\psi$$

$$+ c\epsilon^{-1} N_\epsilon \sum_{m=0}^k \int_{\mathcal{B}_{\iota_\epsilon/2}(\boldsymbol{x}) \setminus \mathcal{B}_{\iota_\epsilon/4}(\boldsymbol{x}) \times \mathcal{SO}(3)}^{-k+m} \iota_\epsilon^{-m} \|\nabla_{\boldsymbol{y}}^{k-m} \boldsymbol{U}_{\mathrm{loc},1}(\boldsymbol{y}(\boldsymbol{x},\boldsymbol{z},\mathbf{R},\epsilon),\boldsymbol{z},\mathbf{R},t)\| \, \mathrm{d}\psi$$

with c depending on $\nabla_{\boldsymbol{y}}^m \chi$ for $m = 0,\ldots,k$. Using once again the decay properties of $\boldsymbol{U}_{\mathrm{loc},1}$, we find

$$\|\nabla^k \boldsymbol{r}_2[\psi](\boldsymbol{x},t)\| \leq c\epsilon^{-1-k} N_\epsilon \left(\frac{\epsilon}{\iota_\epsilon}\right)^{\ell+k} \int_{\Omega \setminus \mathcal{B}_{\iota_\epsilon/2}(\boldsymbol{x}) \times \mathcal{SO}(3)} \|\boldsymbol{U}_{\mathrm{loc},1,\partial\mathcal{E}}(.,\boldsymbol{z},\mathbf{R},t)\|_{1,\partial\mathcal{E}} \, \mathrm{d}\psi$$

$$+ c\epsilon^{-1} N_\epsilon \sum_{m=0}^k \epsilon^{-k+m} \iota_\epsilon^{-m} \left(\frac{\epsilon}{\iota_\epsilon}\right)^{\ell+k-m} \int_{\mathcal{B}_{\iota_\epsilon/2}(\boldsymbol{x}) \setminus \mathcal{B}_{\iota_\epsilon/4}(\boldsymbol{x}) \times \mathcal{SO}(3)} \|\boldsymbol{U}_{\mathrm{loc},1,\partial\mathcal{E}}(.,\boldsymbol{z},\mathbf{R},t)\|_{1,\partial\mathcal{E}} \, \mathrm{d}\psi$$

$$\leq cC\epsilon^{-1+\ell} N_\epsilon \iota_\epsilon^{-\ell-k} = cC\epsilon^{-1+\ell} \epsilon^{-\beta(3+\ell+k)/3} \, .$$

Hence, $\|\nabla^k \boldsymbol{r}_2[\psi](\boldsymbol{x},t)\| < \infty$ if $\beta \leq 3(\ell-1)/(\ell+k+3)$. In total, the $\mathcal{C}^K(\Omega \times (0,T);\mathbb{R}^3)$-norm of $\boldsymbol{r}_2[\psi]$ is bounded independent of ϵ, given $\beta \leq 3(\ell-1)/(\ell+K+3)$.

Then also $F_2[\psi] \in \mathcal{C}^K(\Omega \times \mathcal{SO}(3) \times (0,T); \mathbb{R}^6)$ as well as $\boldsymbol{U}_{\mathrm{loc},2,\partial\mathcal{E}}[\psi] \in \mathcal{C}^K(\partial\mathcal{E} \times \Omega \times \mathcal{SO}(3) \times (0,T); \mathbb{R}^3)$ with norms bounded independent of ϵ. Applying Lemma B.3 for any $(\boldsymbol{z}, \mathbf{R}, t) \in \Omega \times \mathcal{SO}(3) \times (0,T)$, $\boldsymbol{U}_{\mathrm{loc},2}[\psi](., \boldsymbol{z}, \mathbf{R}, t) \in \mathcal{C}^\infty(\mathbb{R}^3 \setminus \mathcal{E}; \mathbb{R}^3)$ and $\boldsymbol{U}_{\mathrm{loc},2}[\psi] \in \mathcal{C}^K(\mathbb{R}^3 \setminus \mathcal{E} \times \Omega \times \mathcal{SO}(3) \times (0,T); \mathbb{R}^3)$. Since

$$C = \max_{0 \le k \le K} \sup_{(\boldsymbol{z}, \mathbf{R}, t) \in \Omega \times \mathcal{SO}(3) \times (0,T)} \|\partial_t^k \boldsymbol{U}_{\mathrm{loc},2,\partial\mathcal{E}}(., \boldsymbol{z}, \mathbf{R}, t)\|_{1,\partial\mathcal{E}} < \infty$$

we can repeat each step in the analysis of $\boldsymbol{r}_2[\psi]$ and arrive analogously at $\boldsymbol{r}_3[\psi] \in \mathcal{C}^K(\Omega \times (0,T))$. However, in case of heavy particles we lose regularity in $F_3[\psi]$ due to the fact that F_3 incorporates the terms $(\boldsymbol{f}_3, \boldsymbol{g}_3)[\psi]$ which depend on partial derivatives of $F_2[\psi]$ in the heavy particles regime. Hence, we find only $\|F_3[\psi]\|_{\mathcal{C}^{K-1}} < c$. By iterating this procedure, we find $F_k[\psi] \in \mathcal{C}^{K+2-k}(\Omega \times \mathcal{SO}(3) \times (0,T); \mathbb{R}^6)$ is uniformly bounded for $0 \le k \le n$ in case of heavy particles. In case of the remaining inertial regimes, we again have the property that the interaction terms restrict the maximal regularity and hence $F_k[\psi] \in \mathcal{C}^{\min(K+3+r-k,K)}(\Omega \times \mathcal{SO}(3) \times (0,T); \mathbb{R}^6)$ as proposed. $\qquad\square$

Remark 29 (Transport operators in case of chaos assumption). *In Remark 24 we discussed that Lemma 19 still holds if we replace the condition on the particle number by the chaos assumption for the hydrodynamic interaction terms $\boldsymbol{r}_k^i$. Similarly, it is desirable to replace the condition on β in Lemma 28 by an appropriate condition on $\boldsymbol{r}_k[\psi]$. In fact, the conditions (3.36) are not sufficient to derive uniform bounds for $\boldsymbol{r}_k[\psi]$, since (3.36) only imply that $\|\boldsymbol{r}_k(\boldsymbol{x},t)\|$ is bounded independent of ϵ if $\psi = \mu_{N_\epsilon}$ and for $\boldsymbol{x} \in \mathcal{E}_\epsilon^i$ for each $i \in \{1, \ldots, N_\epsilon\}$. Hence, in order to have well-defined F_k, we have to expand (3.36) by the assumption*

$$\|\boldsymbol{r}_k[\psi]\|_{\mathcal{C}^{\min(K+3+r-k,K)}} < c \tag{3.44}$$

for $k = 2, \ldots, n$ with c independent of ϵ.

3.4.2 Mean field approximation for the complete system

Now that we have formulated a mean field approximation for (3.1b)-(3.1e), we aim for an analogous result incorporating the momentum equation for the fluid (3.1a) which is based on Lemma 19. Since we are deriving an expression for an equation which will govern the dynamics of $\boldsymbol{u}_0$, we emphasize the dependence of various participating terms on $\boldsymbol{u}_0$ by expanding the notation accordingly, i.e., we write for example $F_k = F_k[\psi, \boldsymbol{u}_0]$ in this section. In order to derive the governing macroscopic equations, we note that (3.33) in the proof of Theorem 21 contains the relevant terms which must be incorporated into the dynamic equation for $\boldsymbol{u}_0$ for a corresponding error behavior in Ω_ϵ. In every $\mathcal{E}_\epsilon^i$, on the other hand, the velocity is given as a continuation of the boundary condition to the particle domain. Thus, we denote the continuation of the local velocity fields onto $\mathbb{R}^3$ by

$$\widetilde{\boldsymbol{U}}_{\mathrm{loc},k}[\mu_{N_\epsilon}, \boldsymbol{u}_0](\boldsymbol{y}, \boldsymbol{c}, \mathbf{R}, t) = \boldsymbol{U}_{\mathrm{loc},k}[\mu_{N_\epsilon}, \boldsymbol{u}_0](\boldsymbol{y}, \boldsymbol{c}, \mathbf{R}, t)\mathbb{1}_{\mathbb{R}^3 \setminus \mathcal{E}}(\boldsymbol{y})$$
$$+ \boldsymbol{U}_{\mathrm{loc},k,\partial\mathcal{E}}[\mu_{N_\epsilon}, \boldsymbol{u}_0](\boldsymbol{y}, \boldsymbol{c}, \mathbf{R}, t)\mathbb{1}_{\mathcal{E}}(\boldsymbol{y}).$$

This way, $\widetilde{\boldsymbol{U}}_{\mathrm{loc},k}[\mu_{N_\epsilon}, \boldsymbol{u}_0](., \boldsymbol{c}, \mathbf{R}, t) \in \mathcal{W}_{\mathrm{loc}}^{1,p}(\mathbb{R}^3; \mathbb{R}^3)$ for any $p \ge 1$ and we can express the left-hand side of (3.1a) for any $\boldsymbol{x} \in \Omega$ analogously to (3.33) as

$$\operatorname{Re} D_t \boldsymbol{u}_0 + \operatorname{Re} \sum_{k=0}^{n-1} \epsilon^k N_\epsilon \int_{\Omega \times \mathcal{SO}(3)} \mathbf{R} \cdot \partial_{\boldsymbol{y}} \widetilde{\boldsymbol{U}}_{\mathrm{loc},k+1}[\mu_{N_\epsilon,t}, \boldsymbol{u}_0] \cdot \mathbf{R}^T \, \mathrm{d}\mu_{N_\epsilon,t} \cdot \boldsymbol{u}_0$$

$$- \operatorname{Re} \sum_{k=0}^{n-1} \epsilon^k N_\epsilon \sum_{\ell=0}^{k} \int_{\Omega \times \mathcal{SO}(3)} \mathbf{R} \cdot \partial_{\boldsymbol{y}} \widetilde{\boldsymbol{U}}_{\mathrm{loc},k+1-\ell}[\mu_{N_\epsilon,t}, \boldsymbol{u}_0] \cdot \mathbf{R}^T$$

$$\cdot \left(B(F_{\ell+1,\omega}[\mu_{N_\epsilon,t}, \boldsymbol{u}_0]) \cdot (\boldsymbol{x} - \boldsymbol{z}) + F_{\ell,v}[\mu_{N_\epsilon,t}, \boldsymbol{u}_0] \right) \mathrm{d}\mu_{N_\epsilon,t}$$

$$+ \operatorname{Re} \sum_{k=1}^{n-1} \epsilon^k N_\epsilon \sum_{\ell=0}^{k-1} \int_{\Omega \times \mathcal{SO}(3)} B(F_{\ell+1,\omega}[\mu_{N_\epsilon,t}, \boldsymbol{u}_0]) \cdot \mathbf{R} \cdot \widetilde{\boldsymbol{U}}_{\mathrm{loc},k}[\mu_{N_\epsilon}, \boldsymbol{u}_0] \, \mathrm{d}\mu_{N_\epsilon,t}$$

$$+ \operatorname{Re} \sum_{k=1}^{n-1} \epsilon^k N_\epsilon \int_{\Omega \times \mathcal{SO}(3)} \mathbf{R} \cdot \partial_t \widetilde{\boldsymbol{U}}_{\mathrm{loc},k}[\mu_{N_\epsilon,t}, \boldsymbol{u}_0] \, \mathrm{d}\mu_{N_\epsilon,t}$$

$$+ \operatorname{Re} \sum_{k=1}^{n-1} \epsilon^k N_\epsilon \partial_{\boldsymbol{x}} \boldsymbol{u}_0 \cdot \int_{\Omega \times \mathcal{SO}(3)} \mathbf{R} \cdot \widetilde{\boldsymbol{U}}_{\mathrm{loc},k}[\mu_{N_\epsilon,t}, \boldsymbol{u}_0] \, \mathrm{d}\mu_{N_\epsilon,t}$$

$$+ \operatorname{Re} \sum_{k=1}^{n-1} \epsilon^k N_\epsilon^2 \sum_{\ell=0}^{k-1} \int_{\Omega \times \mathcal{SO}(3)} \mathbf{R} \cdot \partial_{\boldsymbol{y}} \widetilde{\boldsymbol{U}}_{\mathrm{loc},k-\ell}[\mu_{N_\epsilon,t}, \boldsymbol{u}_0] \cdot \mathbf{R}^T \, \mathrm{d}\mu_{N_\epsilon,t}$$

$$\cdot \int_{\Omega \times \mathcal{SO}(3)} \mathbf{R} \cdot \widetilde{\boldsymbol{U}}_{\mathrm{loc},\ell+1}[\mu_{N_\epsilon,t}, \boldsymbol{u}_0] \, \mathrm{d}\mu_{N_\epsilon,t}$$

$$= \operatorname{Re} D_t \boldsymbol{u}_0 + \operatorname{Re} \sum_{k=0}^{n-1} \epsilon^k H_k[\mu_{N_\epsilon}, \boldsymbol{u}_0].$$

Considering the right-hand side of (3.1a) the stresses in Ω_ϵ are given naturally as Newtonian. For $\boldsymbol{x} \in \mathcal{E}_\epsilon^i$ we apply the model for stresses in the particle domain, and use the results of Lemma 25. Thus, the complete stress tensor reads as

$$\boldsymbol{\Sigma} = \left(\mathbf{S}[\boldsymbol{u}_0] + \sum_{i=1}^{N_\epsilon} \sum_{k=0}^{n-1} \epsilon^k \mathbf{R}^i \cdot \mathbf{S}_{\boldsymbol{y}}[\boldsymbol{u}_{\mathrm{loc},k+1}^i] \cdot \mathbf{R}^{iT} \right) \mathbb{1}_{\Omega_\epsilon}$$

$$+ \sum_{i=1}^{N_\epsilon} \left(\mathbf{S}[\boldsymbol{u}_0] + \sum_{k=0}^{n-1} \left(\epsilon^k \mathbf{R}^i \cdot \mathbf{T}_{\mathrm{loc},k+1}^i \cdot \mathbf{R}^{iT} + \sum_{j \neq i} \epsilon^k \mathbf{R}^j \cdot \mathbf{S}_{\boldsymbol{y}}[\boldsymbol{u}_{\mathrm{loc},k+1}^j] \cdot \mathbf{R}^{jT} \right) \right) \mathbb{1}_{\mathcal{E}_\epsilon^i}$$

$$\tag{3.45}$$

$$= \mathbf{S}[\boldsymbol{u}_0] + \sum_{i=1}^{N_\epsilon} \sum_{k=0}^{n-1} \epsilon^k \mathbf{R}^i \cdot \mathbf{S}_{\boldsymbol{y}}[\boldsymbol{u}_{\mathrm{loc},k+1}^i] \cdot \mathbf{R}^{iT} \mathbb{1}_{\Omega \setminus \mathcal{E}_\epsilon^i} + \sum_{i=1}^{N_\epsilon} \sum_{k=0}^{n-1} \epsilon^k \mathbf{R}^i \cdot \mathbf{T}_{\mathrm{loc},k+1}^i \cdot \mathbf{R}^{iT} \mathbb{1}_{\mathcal{E}_\epsilon^i}.$$

This way, the stresses in the domain are continuous in the normal direction across the boundary of each particle and, although $\boldsymbol{\Sigma}(.,t) \notin \mathcal{W}^{1,p}(\Omega)$ for any $p \geq 1$ due to the jump in the stresses, we still have for any $\phi \in \mathcal{C}^1(\Omega; \mathbb{R})$ vanishing on $\partial\Omega$

$$\sum_\ell \int_\Omega \partial_{x_\ell} \phi \left(\Sigma_{j\ell} - S[\boldsymbol{u}_0]_{j\ell} \right) \mathrm{d}\boldsymbol{x} = -\boldsymbol{e}_j \cdot \sum_{i=1}^{N_\epsilon} \sum_{k=0}^{n-1} \epsilon^{k-1} \mathbf{R}^i \cdot \int_{\mathcal{E}_\epsilon^i} \phi \nabla_{\boldsymbol{y}} \cdot \mathbf{T}_{\mathrm{loc},k+1}^i \mathrm{d}\boldsymbol{x}$$

and hence a meaningful notion of divergence. Thus, the forces in Ω are given as

$$\nabla \cdot \boldsymbol{\Sigma} = \nabla \cdot \mathbf{S}[\boldsymbol{u}_0] + \sum_{i=1}^{N_\epsilon} \sum_{k=0}^{n-1} \epsilon^{k-1} \mathbf{R}^i \cdot \nabla_{\boldsymbol{y}} \cdot \mathbf{T}_{\mathrm{loc},k+1}^i \mathbb{1}_{\mathcal{E}_\epsilon^i}. \tag{3.46}$$

Analogously to the local velocity fields also the pressures $p_{\text{loc},k}^i$ can be understood as functionals of $\boldsymbol{u}_0$ and the empirical measure, evaluated at a given position $\boldsymbol{c} \in \Omega$ and rotation $\mathbf{R} \in \mathcal{SO}(3)$, i.e., $p_{\text{loc},k}^i(\boldsymbol{y}, t) = P_{\text{loc},k}[\mu_{N_\epsilon}, \boldsymbol{u}_0](\boldsymbol{y}, \boldsymbol{c}^i, \mathbf{R}^i, t)$. Hence, the Newtonian stress of the local fields becomes a functional acting on $\boldsymbol{U}_{\text{loc},k}, P_{\text{loc},k}$. Since the terms $\hat{\boldsymbol{f}}_k^i$ in Lemma 25 can also be expressed by functionals $\hat{\boldsymbol{f}}_k[\mu_{N_\epsilon}, \boldsymbol{u}_0](\boldsymbol{y}, \boldsymbol{c}^i, \mathbf{R}^i, t)$ similar to $\boldsymbol{f}_k, \boldsymbol{g}_k$ in Section 3.4.1, we can set $\mathbf{T}_{\text{loc},k}^i(\boldsymbol{y}, t) = \mathbf{T}_{\text{loc},k}[\mu_{N_\epsilon}, \boldsymbol{u}_0](\boldsymbol{y}, \boldsymbol{c}^i, \mathbf{R}^i, t)$. Now we can express $\boldsymbol{\Sigma}$ with the help of the empirical measure as

$$\boldsymbol{\Sigma}[\mu_{N_\epsilon}, \boldsymbol{u}_0] = \mathbf{S}[\boldsymbol{u}_0]$$

$$- N_\epsilon \sum_{k=0}^{n-1} \epsilon^k \int_{\Omega \times \mathcal{SO}(3)} P_{\text{loc},k+1}[\mu_{N_\epsilon}, \boldsymbol{u}_0] \mathbb{I}\mathbb{1}_{\mathbb{R}^3 \setminus \mathcal{E}}(\boldsymbol{y}(\boldsymbol{x}, \boldsymbol{z}, \mathbf{R}, \epsilon)) \, \mathrm{d}\mu_{N_\epsilon} \qquad (3.47\text{a})$$

$$+ \sum_{k=0}^{n-1} \epsilon^k 2\mathbf{E}\left[N_\epsilon \epsilon \int_{\Omega \times \mathcal{SO}(3)} \mathbf{R} \cdot \widetilde{\boldsymbol{U}}_{\text{loc},k+1}[\mu_{N_\epsilon}, \boldsymbol{u}_0] \, \mathrm{d}\mu_{N_\epsilon} \right] \qquad (3.47\text{b})$$

$$+ N_\epsilon \sum_{k=0}^{n-1} \epsilon^k \int_{\Omega \times \mathcal{SO}(3)} \mathbf{R} \cdot \left(\mathbf{T}_{\text{loc},k+1}[\mu_{N_\epsilon}, \boldsymbol{u}_0] \right. \qquad (3.47\text{c})$$

$$\left. - 2\mathbf{E}_{\boldsymbol{y}}[\boldsymbol{U}_{\text{loc},k+1,\partial\mathcal{E}}[\mu_{N_\epsilon}, \boldsymbol{u}_0]] \right) \cdot \mathbf{R}^T \mathbb{1}_{\mathcal{E}}(\boldsymbol{y}(\boldsymbol{x}, \boldsymbol{z}, \mathbf{R}, \epsilon)) \, \mathrm{d}\mu_{N_\epsilon}$$

$$= \mathbf{S}[\boldsymbol{u}_0] + \sum_{k=0}^{n-1} \epsilon^k \boldsymbol{\Sigma}_k[\mu_{N_\epsilon}, \boldsymbol{u}_0]$$

since $\widetilde{\boldsymbol{U}}_{\text{loc},k}[\mu_{N_\epsilon}, \boldsymbol{u}_0](., \boldsymbol{c}, \mathbf{R}, t) \in \mathcal{W}^{1,p}(\mathbb{R}^3; \mathbb{R}^3)$. Similarly, the forces due to $\boldsymbol{\Sigma}$ in Ω, (3.46) are given as

$$\nabla \cdot \boldsymbol{\Sigma}[\mu_{N_\epsilon}, \boldsymbol{u}_0] = \nabla \cdot \mathbf{S}[\boldsymbol{u}_0] \qquad (3.48)$$

$$+ \sum_{k=0}^{n-1} \epsilon^{k-1} N_\epsilon \int_{\Omega \times \mathcal{SO}(3)} \mathbf{R} \cdot \nabla_{\boldsymbol{y}} \cdot \mathbf{T}_{\text{loc},k+1}[\mu_{N_\epsilon}, \boldsymbol{u}_0] \mathbb{1}_{\mathcal{E}}(\boldsymbol{y}(\boldsymbol{x}, \boldsymbol{z}, \mathbf{R}, \epsilon)) \, \mathrm{d}\mu_{N_\epsilon} .$$

We stress that $\nabla \cdot \boldsymbol{\Sigma}[\mu_{N_\epsilon}, \boldsymbol{u}_0]$ given in (3.48) is indeed the weak divergence of $\boldsymbol{\Sigma}[\mu_{N_\epsilon}, \boldsymbol{u}_0]$ given in (3.47): Testing $\boldsymbol{e}_j \cdot \boldsymbol{\Sigma}[\mu_{N_\epsilon}, \boldsymbol{u}_0]$ for any $j = 1, 2, 3$ with the gradient of a test function ϕ over Ω, we get an expression which depends on the empirical measure μ_{N_ϵ}. Inserting the definition of the latter yields (3.45) tested by $\nabla\phi$ over Ω, which is exactly the expression of the weak divergence of $\boldsymbol{\Sigma}$, which in turn is stated in (3.46). In total we have

$$\sum_{\ell} \int_{\Omega} \partial_{x_\ell} \phi \Sigma_{j\ell}[\mu_{N_\epsilon}, \boldsymbol{u}_0] \mathrm{d}\boldsymbol{x} = -\boldsymbol{e}_j \cdot \int_{\Omega} \phi \nabla \cdot \mathbf{S}[\boldsymbol{u}_0] + \sum_{k=0}^{n-1} \sum_{i=1}^{N_\epsilon} \epsilon^{k-1} \phi \mathbf{R}^i \cdot \nabla_{\boldsymbol{y}} \cdot \mathbf{T}_{loc,k+1}^i \mathbb{1}_{\mathcal{E}_\epsilon^i} \mathrm{d}\boldsymbol{x}$$

$$= -\boldsymbol{e}_j \cdot \int_{\Omega} \phi \nabla \cdot \mathbf{S}[\boldsymbol{u}_0] \mathrm{d}\boldsymbol{x}$$

$$- \boldsymbol{e}_j \cdot \int_{\Omega} \phi \sum_{k=0}^{n-1} \epsilon^{k-1} N_\epsilon \int_{\Omega \times \mathcal{SO}(3)} \mathbf{R} \cdot \nabla_{\boldsymbol{y}} \cdot \mathbf{T}_{loc,k+1}[\mu_{N_\epsilon}, \boldsymbol{u}_0] \mathbb{1}_{\mathcal{E}}(\boldsymbol{y}(\boldsymbol{x}, \boldsymbol{z}, \mathbf{R}, \epsilon)) \mathrm{d}\mu_{N_\epsilon} \mathrm{d}\boldsymbol{x}$$

which is the jth component of (3.48) tested by ϕ over Ω.

Remark 30 (Limitations of the model)**.** *Having formulated an expression for the stresses in the domain as well as for the convective terms of (3.1a), it is desirable to expand the operators H_k and $\boldsymbol{\Sigma}_k$ onto a larger class of measures and consider the coupled mean field problem of the form*

$$\operatorname{Re} \operatorname{D}_t \boldsymbol{u}_0 + \operatorname{Re} \sum_{k=0}^{n-1} \epsilon^k H_k[\psi_\epsilon, \boldsymbol{u}_0] - \nabla \cdot \mathbf{S}[\boldsymbol{u}_0] - \sum_{k=0}^{n-1} \epsilon^k \nabla \cdot \boldsymbol{\Sigma}_k[\psi_\epsilon, \boldsymbol{u}_0] = \mathbf{0}, \quad \boldsymbol{x} \in \Omega,$$

$$\nabla \cdot \boldsymbol{u}_0 = 0, \quad \boldsymbol{x} \in \Omega,$$

with the partial differential equation for ψ_ϵ given as

$$\partial_t \psi_\epsilon + \nabla_{\boldsymbol{x}} \cdot (\boldsymbol{u}_0 \psi_\epsilon) + \sum_{k=1}^{n} \epsilon^k \nabla_{\boldsymbol{x}} \cdot (F_{k,v}[\psi_\epsilon, \boldsymbol{u}_0]\psi_\epsilon) + \sum_{k=0}^{n-1} \epsilon^k \mathcal{L}[-B(F_{k+1,\omega}[\psi_\epsilon, \boldsymbol{u}_0])](\psi_\epsilon)$$

$$+ \sum_{k=0}^{n-1} \epsilon^k \operatorname{div}_{\mathcal{G}}(\mathcal{L}[-B(F_{k+1,\omega}[\psi_\epsilon, \boldsymbol{u}_0])])\psi_\epsilon = 0, \quad (\boldsymbol{x}, \mathbf{R}) \in \Omega \times \mathcal{SO}(3),$$

for $t \in (0, T)$ with an initial condition for $\boldsymbol{u}_0, \psi_\epsilon$ as well as boundary conditions on $\partial\Omega$ for $\boldsymbol{u}_0$ and ψ_ϵ. But since we used Taylor expansions of $\boldsymbol{u}_0$ in our approach, the operators $H_k, \boldsymbol{\Sigma}_k, F_k$ carry higher order time and space derivatives of $\boldsymbol{u}_0$ for higher values of k. To be precise, in case of heavy particles, F_2 (and as a consequence $H_1, \boldsymbol{\Sigma}_1$) incorporates second order time and space derivatives of $\boldsymbol{u}_0$ and in any case, F_3 (as well as $H_2, \boldsymbol{\Sigma}_2$) carries at least the third order space derivatives of $\boldsymbol{u}_0$ as can be seen from proof of Lemma 19. Since those higher order derivatives appear multiplied with powers of ϵ, we have to consider singular perturbation problems in the corresponding cases which require additional initial and boundary conditions. The latter are not naturally occurring in the suspension problem (3.1), which is the reason, why we use the restriction $n \leq 1$ for heavy particles and $n \leq 2$ for normal and light-weighted ones from here on.

Next, we expand the operators $H_k, \boldsymbol{\Sigma}_k$ to a larger class of measures analogously to the procedure for F_k in Lemma 28. In this case, however, we do not use general Borel probability measures. Instead, we consider a particular subset of Borel measures over Ω, $\mathcal{P}^C(\Omega) \subset \mathcal{P}(\Omega)$, namely the set of Borel probability measures which are absolutely continuous with respect to the Lebesgue measure and whose Radon derivatives ϱ are at least continuously differentiable and fulfill $\|\varrho\|_{\mathcal{C}(\Omega)} < C$. Thus, any $\psi \in \mathcal{P}^C(\Omega) \times \mathcal{P}(\mathcal{SO}(3))$ fulfills for Borel sets $A \in \mathcal{B}(\Omega), B \in \mathcal{B}(\mathcal{SO}(3))$

$$\psi(A \times B) = \int_A \psi_{\boldsymbol{z}}(B) \, \mathrm{d}\boldsymbol{z}, \tag{3.49}$$

with $\boldsymbol{z} \mapsto \psi_{\boldsymbol{z}}(\mathcal{SO}(3))$ being at least continuously differentiable and fulfilling the property $\psi_{\boldsymbol{z}}(\mathcal{SO}(3)) < C$ for all $\boldsymbol{z} \in \Omega$. We point out that the Radon derivative of ψ with respect to the Lebesgue measure over Ω, $\psi_{\boldsymbol{z}}$, is in itself a measure over $\mathcal{SO}(3)$. Hence, its spatial dependency is denoted as a parametric dependency for measures as stated at the beginning of Section 3.4.1. As usual, $\psi_{\boldsymbol{z}}$ is additionally time-dependent, i.e. $\psi_{\boldsymbol{z}} = \psi_{\boldsymbol{z},t}$. However, this notation is suppressed whenever this dependency is clear from context and if the regularity of the mapping is not important.

Lemma 31. *Let the assumptions of Lemma 28 hold for $K \geq 1$, then*

$$H_k[\psi, \boldsymbol{u}_0] \in \mathcal{L}^p(\Omega \times (0,T); \mathbb{R}^3),$$
$$\boldsymbol{\Sigma}_k[\psi, \boldsymbol{u}_0] \in \mathcal{L}^p(\Omega \times (0,T); \mathbb{R}^{3 \times 3})$$

for $k = 0$ in case of heavy particles and $k \in \{0,1\}$ for normal or light-weighted particles for any $\psi \in \mathcal{P}^C(\Omega) \times \mathcal{P}(\mathcal{SO}(3))$ and any $p \in [1, \infty]$.

Proof. We start with H_0. Since $\boldsymbol{u}_0, F_1$ are smooth, we have

$$\|H_0[\psi, \boldsymbol{u}_0](\boldsymbol{x}, t)\| \leq cN_\epsilon \int_{\Omega \times \mathcal{SO}(3)} \|\partial_{\boldsymbol{y}} \widetilde{\boldsymbol{U}}_{\mathrm{loc},1}\|(\|\boldsymbol{u}_0\| + \|F_{1,\omega}[\boldsymbol{u}_0]\|)\, \mathrm{d}\psi \leq cN_\epsilon \int_{\Omega \times \mathcal{SO}(3)} \|\partial_{\boldsymbol{y}} \widetilde{\boldsymbol{U}}_{\mathrm{loc},1}\|\, \mathrm{d}\psi$$

The constant c depends on $\boldsymbol{u}_0$ and $\mathcal{E}$ but is independent of ϵ. As $\iota_\epsilon = N_\epsilon^{-1/3} > N_\epsilon^{-1}$ for all $N_\epsilon > 1$ we can decompose Ω into the direct sum $\Omega = (\Omega \setminus \mathcal{B}_{\iota_\epsilon}) \cup (\mathcal{B}_{\iota_\epsilon} \setminus \mathcal{B}_{1/N_\epsilon}) \cup \mathcal{B}_{1/N_\epsilon}$ with balls around $\boldsymbol{x}$. On the first two sets we use the decay properties of $\partial_{\boldsymbol{y}} \boldsymbol{U}_{\mathrm{loc},1}$ (Corollary B.4) and on the last one, we estimate $\partial_{\boldsymbol{y}} \widetilde{\boldsymbol{U}}_{\mathrm{loc},1}$ by the $\mathcal{L}^1$-norm of $\boldsymbol{U}_{\mathrm{loc},1}$ on $\partial \mathcal{E}$ for $\boldsymbol{z} \in \mathcal{B}_{1/N_\epsilon} \setminus \mathcal{E}_\epsilon$ and by the maximum of $\partial_{\boldsymbol{y}} \boldsymbol{U}_{\mathrm{loc},1,\partial\mathcal{E}}$ for $\boldsymbol{z} \in \mathcal{E}_\epsilon$. Then, by setting

$$D = \max_{k \in \{0,1\}} \sup_{(\boldsymbol{y}, \boldsymbol{z}, \mathbf{R}, t) \in \mathcal{E} \times \Omega \times \mathcal{SO}(3) \times (0,T)} \|\nabla^k \boldsymbol{U}_{\mathrm{loc},1,\partial\mathcal{E}}(\boldsymbol{y}, \boldsymbol{z}, \mathbf{R}, t)\|,$$

with D independent of ϵ and $D < \infty$, we get

$$\|H_0[\psi, \boldsymbol{u}_0](\boldsymbol{x}, t)\| \leq cDN_\epsilon \left(\int_{\Omega \setminus \mathcal{B}_{\iota_\epsilon}} (\epsilon \iota_\epsilon^{-1})^{\ell+1} \psi_{\boldsymbol{z}}\, \mathrm{d}\boldsymbol{z} + \int_{\mathcal{B}_{\iota_\epsilon} \setminus \mathcal{B}_{1/N_\epsilon}} (\epsilon N_\epsilon)^{\ell+1} \psi_{\boldsymbol{z}}\, \mathrm{d}\boldsymbol{z} + \int_{\mathcal{B}_{1/N_\epsilon}} \psi_{\boldsymbol{z}}\, \mathrm{d}\boldsymbol{z} \right).$$

Finally, applying the estimation $\psi_{\boldsymbol{z}} \leq C$ and using the definitions of $N_\epsilon, \iota_\epsilon$, we get

$$\|H_0[\psi, \boldsymbol{u}_0](\boldsymbol{x}, t)\| \leq cCD \left(\epsilon^{\ell+1-\beta/3(\ell+4)} + \epsilon^{(\ell+1)(1-\beta)} + \epsilon^{2\beta} \right)$$

which is bounded, given

$$\beta \leq 3 \frac{\ell+1}{\ell+4}. \tag{3.50}$$

The relation (3.50) is true as due to Lemma 28

$$\beta \leq 3 \frac{\ell-1}{\ell+K+3} \leq 3 \frac{\ell-1}{\ell+4} < 3 \frac{\ell+1}{\ell+4} < 1.$$

Hence, the term $\|H_0[\psi, \boldsymbol{u}_0]\|$ is bounded independent of ϵ for all $(\boldsymbol{x}, t) \in \Omega \times (0,T)$. In case of normal or light-weighted particles, we first note that Lemma 28 shows $\|\boldsymbol{U}_{\mathrm{loc},2,\partial\mathcal{E}}[\psi, \boldsymbol{u}_0]\|_{\mathcal{C}^1} < \infty$ independent of ϵ, thus

$$D = \max_{i \in \{1,2\}} \max_{\substack{0 \leq j+k \leq 1 \\ j,k \geq 0}} \sup_{(\boldsymbol{y}, \boldsymbol{z}, \mathbf{R}, t) \in \mathcal{E} \times \Omega \times \mathcal{SO}(3) \times (0,T)} \|\partial_t^j \nabla_{\boldsymbol{y}}^k \boldsymbol{U}_{\mathrm{loc},i,\partial\mathcal{E}}(\boldsymbol{y}, \boldsymbol{z}, \mathbf{R}, t)\| < \infty$$

and $\|F_2\|_{\mathcal{C}^1} < c$ holds independent of ϵ. Thus, we find analogously to H_0

$$\|H_1[\psi, \boldsymbol{u}_0]\| \leq cCD(\epsilon^{(1-\beta)\ell} + \epsilon^{\ell+1-\beta(\ell+4)/3} + \epsilon^{\ell-\beta(\ell+3)/3} + \epsilon^{2\beta}),$$

65

which is uniformly bounded for any $\epsilon > 0$, if

$$\beta \leq 3\frac{\ell}{\ell + 3} < 3\frac{\ell + 1}{\ell + 4} \,. \tag{3.51}$$

The relation (3.51) is true since β fulfills

$$\beta \leq 3\frac{\ell - 1}{\ell + 4} < 3\frac{\ell}{\ell + 3} \,.$$

As for the stresses, we find similarly for $i \in \{0, 1\}$

$$\|\boldsymbol{\Sigma}_i[\psi, \boldsymbol{u}_0]\| \leq cCD(\epsilon^{\ell + 1 - \beta(\ell + 4)/3} + \epsilon^{(\ell + 1)(1 - \beta)} + \epsilon^{2\beta} + \epsilon^{3 - \beta}) \,,$$

which is finite since (3.50) is true. $\qquad\square$

Next, we approximate the terms (3.47c) of $\boldsymbol{\Sigma}_k$ in $\mathcal{L}^p(\Omega)$. To be precise, given a function $f \in \mathcal{L}^p(\Omega; \mathbb{R}^n)$ we are looking for some $\widetilde{f} \in \mathcal{L}^p(\Omega; \mathbb{R}^n)$, such that

$$\left\| \int_\Omega (\widetilde{f} - f)\theta \mathrm{d}\boldsymbol{x} \right\| \leq c\epsilon^r$$

for all $\theta \in \mathcal{C}_0^\infty(\Omega; \mathbb{R})$. In order to keep the notation short, we write in this case

$$f \overset{\star}{=} \widetilde{f} + \mathcal{O}(\epsilon^r) \,.$$

Lemma 32. *Let the assumptions of Lemma 31 hold and let $\psi \in \mathcal{P}^C(\Omega) \times \mathcal{P}(\mathcal{SO}(3))$. Then the following relations hold on $\mathcal{L}^p(\Omega)$ for $p \in (1, \infty)$:*

$$N_\epsilon \int_{\Omega \times \mathcal{SO}(3)} \boldsymbol{R} \cdot \left(\mathbf{T}_{\mathrm{loc},k}[\psi, \boldsymbol{u}_0] - 2\mathbf{E}_{\boldsymbol{y}}[\boldsymbol{U}_{\mathrm{loc},k,\partial\mathcal{E}}[\psi, \boldsymbol{u}_0]] \right) \cdot \boldsymbol{R}^T \mathbb{1}_\mathcal{E}(\boldsymbol{y}(\boldsymbol{x}, \boldsymbol{z}, \boldsymbol{R}, t)) \, \mathrm{d}\psi$$

$$\overset{\star}{=} \epsilon^3 N_\epsilon \int_{\mathcal{SO}(3)} \boldsymbol{R} \cdot \int_\mathcal{E} \mathbf{T}_{\mathrm{loc},k}[\psi, \boldsymbol{u}_0] - 2\mathbf{E}_{\boldsymbol{y}}[\boldsymbol{U}_{\mathrm{loc},k,\partial\mathcal{E}}[\psi, \boldsymbol{u}_0]] \, \mathrm{d}\boldsymbol{y} \cdot \boldsymbol{R}^T \, \mathrm{d}\psi_{\boldsymbol{x}} + \mathcal{O}(\epsilon^4 N_\epsilon)$$

for $k = 1$ in case of heavy particles and $1 \leq k \leq 2$ for normal or light-weighted ones. In case of normal or light-weighted particles we additionally have

$$N_\epsilon \int_{\Omega \times \mathcal{SO}(3)} \boldsymbol{R} \cdot \left(\mathbf{T}_{\mathrm{loc},1}[\psi, \boldsymbol{u}_0] - 2\mathbf{E}_{\boldsymbol{y}}[\boldsymbol{U}_{\mathrm{loc},1,\partial\mathcal{E}}[\psi, \boldsymbol{u}_0]] \right) \cdot \boldsymbol{R}^T \mathbb{1}_\mathcal{E}(\boldsymbol{y}(\boldsymbol{x}, \boldsymbol{z}, \boldsymbol{R}, t)) \, \mathrm{d}\psi$$

$$\overset{\star}{=} \epsilon^3 N_\epsilon \int_{\mathcal{SO}(3)} \boldsymbol{R} \cdot \int_\mathcal{E} \mathbf{T}_{\mathrm{loc},1}[\psi, \boldsymbol{u}_0] - 2\mathbf{E}_{\boldsymbol{y}}[\boldsymbol{U}_{\mathrm{loc},1,\partial\mathcal{E}}[\psi, \boldsymbol{u}_0]] \, \mathrm{d}\boldsymbol{y} \cdot \boldsymbol{R}^T \, \mathrm{d}\psi_{\boldsymbol{x}}$$

$$- \epsilon^4 N_\epsilon \sum_{\ell m} \partial_{x_\ell} \int_{\mathcal{SO}(3)} \boldsymbol{R} \cdot \int_\mathcal{E} (\mathbf{T}_{\mathrm{loc},1}[\psi, \boldsymbol{u}_0] - 2\mathbf{E}_{\boldsymbol{y}}[\boldsymbol{U}_{\mathrm{loc},1,\partial\mathcal{E}}[\psi, \boldsymbol{u}_0]]) \, y_m \, \mathrm{d}\boldsymbol{y} \cdot \boldsymbol{R}^T R_{m\ell}^T \, \mathrm{d}\psi_{\boldsymbol{x}}$$

$$+ \mathcal{O}(\epsilon^5 N_\epsilon) \,.$$

Proof. Before showing the claims, we note that for fixed $\boldsymbol{z} \in \Omega$ and all $\boldsymbol{x} \in \Omega$ the following identity hold

$$\mathbb{1}_\mathcal{E}(\boldsymbol{y}(\boldsymbol{x}, \boldsymbol{z}, \boldsymbol{R}, \epsilon)) = \mathbb{1}_{\mathcal{E}_\epsilon(\boldsymbol{z})}(\boldsymbol{x}) \,.$$

For any $\theta \in \mathcal{C}_0^\infty(\Omega; \mathbb{R})$ we find in case of (3.47c)

$$\int_\Omega \theta N_\epsilon \int_{\Omega \times \mathcal{SO}(3)} \mathbf{R} \cdot \left(\mathbf{T}_{\mathrm{loc},k}[\psi, \boldsymbol{u}_0] - 2\mathbf{E}_{\boldsymbol{y}}[\boldsymbol{U}_{\mathrm{loc},k,\partial \mathcal{E}}[\psi, \boldsymbol{u}_0]] \right) \cdot \mathbf{R}^T \mathbb{1}_{\mathcal{E}}(\boldsymbol{y}(\boldsymbol{x}, \boldsymbol{z}, \mathbf{R}, \epsilon)) \, \mathrm{d}\psi \, \mathrm{d}\boldsymbol{x}$$

$$= N_\epsilon \int_{\Omega \times \mathcal{SO}(3)} \mathbf{R} \cdot \int_\Omega \theta \left(\mathbf{T}_{\mathrm{loc},k}[\psi, \boldsymbol{u}_0] - 2\mathbf{E}_{\boldsymbol{y}}[\boldsymbol{U}_{\mathrm{loc},k,\partial \mathcal{E}}[\psi, \boldsymbol{u}_0]] \right) \cdot \mathbf{R}^T \mathbb{1}_{\mathcal{E}_\epsilon(\boldsymbol{z})}(\boldsymbol{x}) \, \mathrm{d}\boldsymbol{x} \, \mathrm{d}\psi$$

$$= N_\epsilon \int_{\Omega \times \mathcal{SO}(3)} \mathbf{R} \cdot \int_{\mathcal{E}_\epsilon(\boldsymbol{z})} \theta \left(\mathbf{T}_{\mathrm{loc},k}[\psi, \boldsymbol{u}_0] - 2\mathbf{E}_{\boldsymbol{y}}[\boldsymbol{U}_{\mathrm{loc},k,\partial \mathcal{E}}[\psi, \boldsymbol{u}_0]] \right) \, \mathrm{d}\boldsymbol{x} \cdot \mathbf{R}^T \, \mathrm{d}\psi \, .$$

In this relation θ is evaluated at $\boldsymbol{x}$. Since $\boldsymbol{x} \in \mathcal{E}_\epsilon(\boldsymbol{z})$, $\boldsymbol{x} = \boldsymbol{z} + \epsilon \mathbf{R} \cdot \boldsymbol{y}$ with $\boldsymbol{y} \in \mathcal{E}$ and as θ is smooth, $\theta(\boldsymbol{x}) = \theta(\boldsymbol{z}) + \mathcal{O}(\epsilon)$. Moreover, the matrices are evaluated at $(\boldsymbol{y}(\boldsymbol{x}, \boldsymbol{z}, \mathbf{R}, \epsilon), \boldsymbol{z}, \mathbf{R}, t) = (\boldsymbol{y}, \boldsymbol{z}, \mathbf{R}, t)$. Thus, we get the following overall relation

$$\int_\Omega \theta N_\epsilon \int_{\Omega \times \mathcal{SO}(3)} \mathbf{R} \cdot \left(\mathbf{T}_{\mathrm{loc},k}[\psi, \boldsymbol{u}_0] - 2\mathbf{E}_{\boldsymbol{y}}[\boldsymbol{U}_{\mathrm{loc},k,\partial \mathcal{E}}[\psi, \boldsymbol{u}_0]] \right) \cdot \mathbf{R}^T \mathbb{1}_{\mathcal{E}}(\boldsymbol{y}(\boldsymbol{x}, \boldsymbol{z}, \mathbf{R}, \epsilon)) \, \mathrm{d}\psi \, \mathrm{d}\boldsymbol{x}$$

$$= \int_{\Omega \times \mathcal{SO}(3)} \theta(\boldsymbol{z}) \epsilon^3 N_\epsilon \mathbf{R} \cdot \int_{\mathcal{E}} \mathbf{T}_{\mathrm{loc},k}[\psi, \boldsymbol{u}_0] - 2\mathbf{E}_{\boldsymbol{y}}[\boldsymbol{U}_{\mathrm{loc},k,\partial \mathcal{E}}[\psi, \boldsymbol{u}_0]] \, \mathrm{d}\boldsymbol{y} \cdot \mathbf{R}^T \, \mathrm{d}\psi + \mathcal{O}(\epsilon^4 N_\epsilon)$$

$$= \int_\Omega \theta \epsilon^3 N_\epsilon \int_{\mathcal{SO}(3)} \mathbf{R} \cdot \int_{\mathcal{E}} \mathbf{T}_{\mathrm{loc},k}[\psi, \boldsymbol{u}_0] - 2\mathbf{E}_{\boldsymbol{y}}[\boldsymbol{U}_{\mathrm{loc},k,\partial \mathcal{E}}[\psi, \boldsymbol{u}_0]] \, \mathrm{d}\boldsymbol{y} \cdot \mathbf{R}^T \, \mathrm{d}\psi_{\boldsymbol{x}} \, \mathrm{d}\boldsymbol{x} + \mathcal{O}(\epsilon^4 N_\epsilon)$$

for $k = 1$ in case of heavy particles and $1 \leq k \leq 2$ for normal or light-weighted ones. In the latter case, we have to add another approximation order to the expression associated with $k = 1$. In this case we have

$$\int_\Omega \theta N_\epsilon \int_{\Omega \times \mathcal{SO}(3)} \mathbf{R} \cdot \left(\mathbf{T}_{\mathrm{loc},1}[\psi, \boldsymbol{u}_0] - 2\mathbf{E}_{\boldsymbol{y}}[\boldsymbol{U}_{\mathrm{loc},1,\partial \mathcal{E}}[\psi, \boldsymbol{u}_0]] \right) \cdot \mathbf{R}^T \mathbb{1}_{\mathcal{E}}(\boldsymbol{y}(\boldsymbol{x}, \boldsymbol{z}, \mathbf{R}, t)) \, \mathrm{d}\psi \, \mathrm{d}\boldsymbol{x}$$

$$- \int_\Omega \theta \epsilon^3 N_\epsilon \int_{\mathcal{SO}(3)} \mathbf{R} \cdot \int_{\mathcal{E}} \mathbf{T}_{\mathrm{loc},1}[\psi, \boldsymbol{u}_0] - 2\mathbf{E}_{\boldsymbol{y}}[\boldsymbol{U}_{\mathrm{loc},1,\partial \mathcal{E}}[\psi, \boldsymbol{u}_0]] \, \mathrm{d}\boldsymbol{y} \cdot \mathbf{R}^T \, \mathrm{d}\psi_{\boldsymbol{x}} \, \mathrm{d}\boldsymbol{x}$$

$$= \int_\Omega \partial_{x_\ell} \theta \epsilon^4 N_\epsilon \int_{\mathcal{SO}(3)} \mathbf{R} \cdot \int_{\mathcal{E}} \left(\mathbf{T}_{\mathrm{loc},1}[\psi, \boldsymbol{u}_0] - 2\mathbf{E}_{\boldsymbol{y}}[\boldsymbol{U}_{\mathrm{loc},1,\partial \mathcal{E}}[\psi, \boldsymbol{u}_0]] \right) y_m \, \mathrm{d}\boldsymbol{y} \cdot \mathbf{R}^T R_{m\ell}^T \, \mathrm{d}\psi_{\boldsymbol{z}} \, \mathrm{d}\boldsymbol{z}$$

$$+ \mathcal{O}(\epsilon^5 N_\epsilon) \, .$$

Since $\boldsymbol{z} \mapsto \psi_{\boldsymbol{z}}(\mathcal{SO}(3)) \in \mathcal{C}^1(\Omega; \mathbb{R})$, $\mathbf{T}_{\mathrm{loc},1} \in \mathcal{C}^1(\mathcal{E} \times \Omega \times \mathcal{SO}(3) \times (0, T); \mathbb{R}^{3 \times 3})$ and $\boldsymbol{U}_{\mathrm{loc},1,\partial \mathcal{E}} \in \mathcal{C}^\infty(\mathcal{E} \times \Omega \times \mathcal{SO}(3) \times (0, T); \mathbb{R}^3)$ we finally have

$$\int_\Omega \partial_{x_\ell} \theta \epsilon^4 N_\epsilon \int_{\mathcal{SO}(3)} \mathbf{R} \cdot \int_{\mathcal{E}} \left(\mathbf{T}_{\mathrm{loc},1}[\psi, \boldsymbol{u}_0] - 2\mathbf{E}_{\boldsymbol{y}}[\boldsymbol{U}_{\mathrm{loc},1,\partial \mathcal{E}}[\psi, \boldsymbol{u}_0]] \right) y_m \, \mathrm{d}\boldsymbol{y} \cdot \mathbf{R}^T R_{m\ell}^T \, \mathrm{d}\psi_{\boldsymbol{z}} \, \mathrm{d}\boldsymbol{z}$$

$$= -\int_\Omega \theta \epsilon^4 N_\epsilon \partial_{x_\ell} \int_{\mathcal{SO}(3)} \mathbf{R} \cdot \int_{\mathcal{E}} \left(\mathbf{T}_{\mathrm{loc},1}[\psi, \boldsymbol{u}_0] - 2\mathbf{E}_{\boldsymbol{y}}[\boldsymbol{U}_{\mathrm{loc},1,\partial \mathcal{E}}[\psi, \boldsymbol{u}_0]] \right) y_m \, \mathrm{d}\boldsymbol{y} \cdot \mathbf{R}^T R_{m\ell}^T \mathrm{d}\psi_{\boldsymbol{x}} \mathrm{d}\boldsymbol{x} \, .$$

$$\square$$

Lemma 32 shows that the terms associated with the particle stresses in $\boldsymbol{\Sigma}_k$ can be approximated by integral values of $\mathbf{T}_{\mathrm{loc},k}$. Since $\mathbf{T}_{\mathrm{loc},k}$ as well as $\boldsymbol{u}_{\mathrm{loc},k,\partial \mathcal{E}}$ are at least continuously differentiable in $\mathcal{E}$, we can apply the following relations analogously to [12]

$$\sum_j \int_{\mathcal{E}} \nabla_{\boldsymbol{y}} \cdot (T_{ij} y_k \boldsymbol{e}_j) \mathrm{d}\boldsymbol{y} = \int_{\mathcal{E}} (\nabla_{\boldsymbol{y}} \cdot \mathbf{T}^T)_i y_k \mathrm{d}\boldsymbol{y} + \int_{\mathcal{E}} T_{ik} \mathrm{d}\boldsymbol{y} \, ,$$

$$\int_{\mathcal{E}} \partial_{y_j} u_i \,\mathrm{d}\boldsymbol{y} = \int_{\mathcal{E}} \nabla_{\boldsymbol{y}} \cdot (u_i \boldsymbol{e}_j) \,\mathrm{d}\boldsymbol{y} = \int_{\partial\mathcal{E}} u_i n_j \,\mathrm{d}s$$

which hold for a matrix $\mathbf{T} \in \mathcal{C}^1(\mathcal{E}; \mathbb{R}^{3\times3})$ and a velocity $\boldsymbol{u} \in \mathcal{C}^1(\mathcal{E}; \mathbb{R}^3)$. This yields together with the boundary condition for the particle stresses (3.39b)

$$\int_{\mathcal{E}} \mathbf{T}_{\mathrm{loc},k}[\psi, \boldsymbol{u}_0] - 2\mathbf{E}_{\boldsymbol{y}}[\boldsymbol{U}_{\mathrm{loc},k,\partial\mathcal{E}}[\psi, \boldsymbol{u}_0]] \,\mathrm{d}\boldsymbol{y} \tag{3.52}$$
$$= \int_{\partial\mathcal{E}} \mathbf{S}_{\boldsymbol{y}}[\boldsymbol{U}_{\mathrm{loc},k}] \cdot \boldsymbol{n} \otimes \boldsymbol{y} - \boldsymbol{U}_{\mathrm{loc},k,\partial\mathcal{E}}[\psi, \boldsymbol{u}_0] \otimes \boldsymbol{n} - \boldsymbol{n} \otimes \boldsymbol{U}_{\mathrm{loc},k,\partial\mathcal{E}}[\psi, \boldsymbol{u}_0] \,\mathrm{d}s(\boldsymbol{y})$$
$$- \int_{\mathcal{E}} \nabla_{\boldsymbol{y}} \cdot \mathbf{T}_{\mathrm{loc},k}[\psi, \boldsymbol{u}_0] \otimes \boldsymbol{y} \,\mathrm{d}\boldsymbol{y} \,.$$

Remark 33 (Pressure terms in $\boldsymbol{\Sigma}_k$). *The expressions for $\boldsymbol{\Sigma}_k$ contain the pressures $P_{\mathrm{loc},k}$ in (3.47a). In Lemma 31 we showed that the corresponding expressions are in $\mathcal{L}^p(\Omega)$. Analogously to Lemma 32 it holds that the weak derivative of (3.47a) is given by*

$$\nabla\widetilde{p}_k = N_\epsilon \nabla \int_{\Omega\times\mathcal{SO}(3)} P_{\mathrm{loc},k}[\psi, \boldsymbol{u}_0](\boldsymbol{y}(\boldsymbol{x}, \boldsymbol{z}, \mathbf{R}, \epsilon), \boldsymbol{z}, \mathbf{R}, t) \mathbb{1}_{\mathbb{R}^3\setminus\mathcal{E}}(\boldsymbol{y}(\boldsymbol{x}, \boldsymbol{z}, \mathbf{R}, \epsilon)) \,\mathrm{d}\psi$$
$$\stackrel{\star}{=} \epsilon^2 N_\epsilon \int_{\mathcal{SO}(3)} \mathbf{R} \cdot \int_{\partial\mathcal{E}} P_{\mathrm{loc},k}[\psi, \boldsymbol{u}_0](\boldsymbol{y}, \boldsymbol{x}, \mathbf{R}, t) \boldsymbol{n} \,\mathrm{d}s(\boldsymbol{y}) \,\mathrm{d}\psi_{\boldsymbol{x}}(\mathbf{R})$$
$$- \epsilon^3 N_\epsilon \nabla \cdot \left(\int_{\mathcal{SO}(3)} \mathbf{R} \cdot \int_{\partial\mathcal{E}} P_{\mathrm{loc},k}[\psi, \boldsymbol{u}_0](\boldsymbol{y}, \boldsymbol{x}, \mathbf{R}, t) \boldsymbol{n} \otimes \boldsymbol{y} \,\mathrm{d}s(\boldsymbol{y}) \cdot \mathbf{R}^T \,\mathrm{d}\psi_{\boldsymbol{x}}(\mathbf{R}) \right)^T$$
$$+ \epsilon^{-1} N_\epsilon \int_{\Omega\times\mathcal{SO}(3)} \mathbf{R} \cdot \nabla_{\boldsymbol{y}} P_{\mathrm{loc},k}[\psi, \boldsymbol{u}_0](\boldsymbol{y}(\boldsymbol{x}, \boldsymbol{z}, \mathbf{R}, \epsilon), \boldsymbol{z}, \mathbf{R}, t) \mathbb{1}_{\mathbb{R}^3\setminus\mathcal{E}}(\boldsymbol{y}(\boldsymbol{x}, \boldsymbol{z}, \mathbf{R}, \epsilon)) \,\mathrm{d}\psi$$
$$+ \mathcal{O}(\epsilon^4 N_\epsilon) \,.$$

Analogously to Lemma 31, it holds

$$\left\| \epsilon^{-1} N_\epsilon \int_{\Omega\times\mathcal{SO}(3)} \mathbf{R} \cdot \nabla_{\boldsymbol{y}} P_{\mathrm{loc},k}[\psi, \boldsymbol{u}_0](\boldsymbol{y}(\boldsymbol{x}, \boldsymbol{z}, \mathbf{R}, \epsilon), \boldsymbol{z}, \mathbf{R}, t) \mathbb{1}_{\mathbb{R}^3\setminus\mathcal{E}}(\boldsymbol{y}(\boldsymbol{x}, \boldsymbol{z}, \mathbf{R}, \epsilon)) \,\mathrm{d}\psi \right\|$$
$$\leq cCD(\epsilon^{\ell+1-\beta(\ell+5)/3} + \epsilon^{\ell+1-\beta(\ell+2)} + \epsilon^{2\beta-1}) \,.$$

Hence, for $\beta \geq 0.5$ and $\beta \leq (\ell+1)/(\ell+2)$, we get a uniform bound on $\nabla\widetilde{p}_k$ and thus $\widetilde{p}_k \in \mathcal{W}^{1,p}(\Omega; \mathbb{R})$ is a well-defined force term. However, since any force given as the gradient of a scalar field in Ω is canceled out by the pressure generated by the condition of solenoidity, we do not consider the terms $\widetilde{p}_k$ explicitly in the final model analogously to [12]. Therefore, we also don't impose further conditions on β which would ensure that $\nabla\widetilde{p}_k$ is well-defined.

Remark 34 (Velocity fluctuations, additional force terms). *The expression (3.47b) contains the term*

$$\epsilon^2 N_\epsilon \widetilde{\boldsymbol{U}}_k = N_\epsilon \epsilon \int_{\Omega\times\mathcal{SO}(3)} \mathbf{R} \cdot \widetilde{\boldsymbol{U}}_{\mathrm{loc},k+1}[\psi, \boldsymbol{u}_0] \,\mathrm{d}\psi$$

originating in the superposition of local particle velocities. Usually in suspension modeling, the analogous terms associated with the superposition are modeled as a velocity

fluctuation with zero mean, cf. [12, 119]. In the present case we don't apply ensemble averaging and keep the corresponding terms in the model. Analogously to the approach in the proof of Lemma 31, we find

$$\|\epsilon^2 N_\epsilon \widetilde{\boldsymbol{U}}_k\| \le c(\epsilon^{\ell+1-\beta(\ell+3)/3} + \epsilon^{\ell+1-\beta\ell} + \epsilon^{2\beta+1}),$$

$$\|\nabla \epsilon^2 N_\epsilon \widetilde{\boldsymbol{U}}_k\| \le c(\epsilon^{\ell+1-\beta(\ell+4)/3} + \epsilon^{(\ell+1)(1-\beta)} + \epsilon^{2\beta}),$$

$$\|\nabla^2 \epsilon^2 N_\epsilon \widetilde{\boldsymbol{U}}_k\| \le c(\epsilon^{\ell+1-\beta(\ell+2)/3} + \epsilon^{(\ell+1)(1-\beta)} + \epsilon^{3\beta-1}).$$

The expressions are bounded independent of ϵ if $\beta \ge 1/3$ and due to Lemma 28.

It should be noted, that the interplay of the pressure contributions (3.47a), the velocities $\widetilde{\boldsymbol{U}}_k$ (3.47b) and the particle stresses (3.47c) together generate the force (3.48). By combining the pressure terms with the global pressure (see Remark 33) and using the approximation of the terms carrying the particle stresses due to Lemma 32, we have a valid approximation of the stress $\boldsymbol{\Sigma}_k$ but we lose the property (3.48). In fact, it holds for any $\theta \in \mathcal{C}_0^1(\Omega; \mathbb{R})$ and $k \ge 0$

$$\int_\Omega \theta \epsilon^{k-1} N_\epsilon \int_{\Omega \times \mathcal{SO}(3)} \mathbf{R} \cdot \nabla_{\boldsymbol{y}} \cdot \mathbf{T}_{\mathrm{loc},k+1}[\psi, \boldsymbol{u}_0] \mathbb{1}_\mathcal{E}(\boldsymbol{y}(\boldsymbol{x}, \boldsymbol{z}, \mathbf{R}, \epsilon)) \,\mathrm{d}\psi \,\mathrm{d}\boldsymbol{x}$$

$$= \epsilon^{k-1} N_\epsilon \int_{\Omega \times \mathcal{SO}(3)} \mathbf{R} \cdot \int_{\mathcal{E}_\epsilon(\boldsymbol{z})} \theta \nabla_{\boldsymbol{y}} \cdot \mathbf{T}_{\mathrm{loc},k+1}[\psi, \boldsymbol{u}_0] \,\mathrm{d}\boldsymbol{x} \,\mathrm{d}\psi$$

$$= \epsilon^{k+2} N_\epsilon \int_\Omega \theta \int_{\mathcal{SO}(3)} \mathbf{R} \cdot \boldsymbol{f}_{k+1}[\psi, \boldsymbol{u}_0] \,\mathrm{d}\psi_{\boldsymbol{x}} \,\mathrm{d}\boldsymbol{x}$$

$$- \epsilon^{k+3} N_\epsilon \int_\Omega \theta \nabla \cdot \left(\int_{\mathcal{SO}(3)} \mathbf{R} \cdot \int_\mathcal{E} \hat{\boldsymbol{f}}_{k+1}[\psi, \boldsymbol{u}_0] \otimes \boldsymbol{y} \,\mathrm{d}\boldsymbol{y} \cdot \mathbf{R}^T \,\mathrm{d}\psi_{\boldsymbol{x}} \right)^T \,\mathrm{d}\boldsymbol{x}$$

$$+ \mathcal{O}(\epsilon^4 N_\epsilon)$$

where we used Remark 26 and (3.39a). The second term of the above expression can be found as the divergence of the stress terms in Lemma 32 by applying (3.52). The term

$$\boldsymbol{b}_{k+1}[\psi, \boldsymbol{u}_0] = \epsilon^{k+2} N_\epsilon \int_{\mathcal{SO}(3)} \mathbf{R} \cdot \boldsymbol{f}_{k+1}[\psi, \boldsymbol{u}_0] \,\mathrm{d}\psi_{\boldsymbol{x}}, \tag{3.53}$$

however is not recovered. It is also not part of $\nabla \cdot 2 N_\epsilon \epsilon^2 \mathbf{E}[\widetilde{\boldsymbol{U}}_k]$, as, e.g.,

$$\nabla \cdot 2 N_\epsilon \epsilon^2 \mathbf{E}[\widetilde{\boldsymbol{U}}_0] = c \int_{\Omega \times \mathcal{SO}(3)} \mathbf{R} \cdot \Delta_{\boldsymbol{y}} \boldsymbol{U}_{\mathrm{loc},1}(\boldsymbol{y}(\boldsymbol{x}, \boldsymbol{z}, \mathbf{R}, \epsilon), \boldsymbol{z}, \mathbf{R}, t) \mathbb{1}_{\mathbb{R}^3 \setminus \mathcal{E}}(\boldsymbol{y}(\boldsymbol{x}, \boldsymbol{z}, \mathbf{R}, \epsilon)) \,\mathrm{d}\psi$$

which does not admit an approximation of the form (3.53). Hence, we incorporate $\boldsymbol{b}_{k+1}$ as an additional force besides the approximation of $\nabla \cdot \boldsymbol{\Sigma}_k^T$ in the momentum equation of the fluid.

For normal or light-weighted particles, we also might consider an additional term in the residual for $k = 0$, but since $\nabla_{\boldsymbol{y}} \cdot \mathbf{T}_{\mathrm{loc},1} \equiv \boldsymbol{0}$ in this case, we find $\boldsymbol{b}_1 \equiv \boldsymbol{0}$.

For the following theorem we introduce the following additional abbreviations.

Abbreviation 35. *For $\psi \in \mathcal{P}^C(\Omega) \times \mathcal{P}(\mathcal{SO}(3))$ and $\boldsymbol{u} \in \mathcal{C}^1(\Omega \times (0, T); \mathbb{R}^3)$*

$$\widetilde{\boldsymbol{U}}_k[\psi, \boldsymbol{u}](\boldsymbol{x}, t) = \epsilon^{-1} \int_{\Omega \times \mathcal{SO}(3)} \mathbf{R} \cdot \widetilde{\boldsymbol{U}}_{\mathrm{loc},k+1}[\psi, \boldsymbol{u}](\boldsymbol{y}(\boldsymbol{x}, \boldsymbol{z}, \mathbf{R}, \epsilon), \boldsymbol{z}, \mathbf{R}, t) \,\mathrm{d}\psi(\boldsymbol{z}, \mathbf{R}),$$

$$\widetilde{\mathbf{H}}_0[\psi, \boldsymbol{u}](\boldsymbol{x}, t) = \epsilon^{-1} \int_{\Omega \times \mathcal{SO}(3)} (\boldsymbol{u}(\boldsymbol{x}, t) - \boldsymbol{u}(\boldsymbol{z}, t) - B(F_{1,\omega}[\boldsymbol{u}](\boldsymbol{z}, \mathbf{R}, t)))$$
$$\otimes \mathbf{R} \cdot \widetilde{U}_{\mathrm{loc},1}[\boldsymbol{u}](\boldsymbol{y}(\boldsymbol{x}, \boldsymbol{z}, \mathbf{R}, \epsilon), \boldsymbol{z}, \mathbf{R}, t) \, \mathrm{d}\psi(\boldsymbol{z}, \mathbf{R}) \,,$$
$$\boldsymbol{\Sigma}_k^p[\psi, \boldsymbol{u}](\boldsymbol{x}, t) = \frac{|\Omega|}{|\mathcal{E}|} \int_{\mathcal{SO}(3)} \mathbf{R} \cdot \int_{\partial \mathcal{E}} \mathbf{S}_{\boldsymbol{y}}[U_{\mathrm{loc},k}[\psi, \boldsymbol{u}]](\boldsymbol{y}, \boldsymbol{x}, \mathbf{R}, t) \cdot \boldsymbol{n} \otimes \boldsymbol{y}$$
$$- \, \boldsymbol{U}_{\mathrm{loc},k,\partial\mathcal{E}}[\psi, \boldsymbol{u}](\boldsymbol{y}, \boldsymbol{x}, \mathbf{R}, t) \otimes \boldsymbol{n}$$
$$- \, \boldsymbol{n} \otimes \boldsymbol{U}_{\mathrm{loc},k,\partial\mathcal{E}}[\psi, \boldsymbol{u}](\boldsymbol{y}, \boldsymbol{x}, \mathbf{R}, t) \, \mathrm{d}s(\boldsymbol{y}) \cdot \mathbf{R}^T \, \mathrm{d}\psi_{\boldsymbol{x}}(\mathbf{R})$$

with $\widetilde{\boldsymbol{U}}_{\mathrm{loc},1}[\psi, \boldsymbol{u}] = \widetilde{\boldsymbol{U}}_{\mathrm{loc},1}[\boldsymbol{u}]$.

In order to forumlate our central Theorems for the particle approximation, we have to introduce a metric for measures. We apply here the Wasserstein (or Monge-Kantorovich) metric [52, 53] which is given as

$$d(\psi_1, \psi_2) = \sup_{\substack{\theta \in \mathcal{L}ip(\Omega \times \mathcal{SO}(3)) \\ \mathrm{Lip}(\theta) \leq 1}} \left| \int_{\Omega \times \mathcal{SO}(3)} \theta(\boldsymbol{z}, \mathbf{R}) \, \mathrm{d}\psi_1(\boldsymbol{z}, \mathbf{R}) - \int_{\Omega \times \mathcal{SO}(3)} \theta(\boldsymbol{z}, \mathbf{R}) \, \mathrm{d}\psi_2(\boldsymbol{z}, \mathbf{R}) \right| \quad (3.54)$$

with $\mathcal{L}ip(\mathcal{A})$ denoting the set of Lipschitz continuous functions θ over a set $\mathcal{A}$ with Lipschitz constant $\mathrm{Lip}(\theta)$.

Theorem 36 (Mean field approximation of a particle suspension up to $\mathcal{O}(\epsilon)$ for normal or light-weighted particles). *Let the density scaling function (2.12) be given as $\alpha_\rho(\epsilon) = \epsilon^r$ with $r \geq 0$, the particle number as $N_\epsilon = \epsilon^{-\beta}$ with $\beta \geq 1/3$ subject to the condition of Lemma 28 for $K = 1$ as well as ϕ_ϵ given by (3.3). Assume that $\boldsymbol{u}_0 \in \mathcal{C}^1((0, T); \mathcal{C}^3(\Omega; \mathbb{R}^3))$, $p_0 \in \mathcal{C}^0((0, T); \mathcal{C}^2(\Omega; \mathbb{R}))$, and the time-parametrized measure $\psi_t \in \mathcal{P}^C(\Omega) \times \mathcal{P}(\mathcal{SO}(3))$, with its spatial Radon derivative (see (3.49)) fulfilling $(\boldsymbol{x}, t) \mapsto \psi_{\boldsymbol{x},t}(\mathcal{SO}(3)) \in \mathcal{C}^1(\Omega \times (0, T); \mathbb{R}_0^+)$, solve*

$$\mathrm{Re}\,\mathrm{D}_t\boldsymbol{u}_0 = \nabla \cdot \mathbf{S}[\boldsymbol{u}_0] + \phi_\epsilon \nabla \cdot \boldsymbol{\Sigma}_0^p[\psi_t, \boldsymbol{u}_0] + 2N_\epsilon \epsilon^2 \nabla \cdot \mathbf{E}[\widetilde{U}_0[\psi_t, \boldsymbol{u}_0]] \quad (3.55a)$$
$$+ \mathrm{Re}\,\mathrm{Fr}^{-2}\,\boldsymbol{e}_g$$
$$+ \phi_\epsilon |\Omega| \psi_{\boldsymbol{x},t}(\mathcal{SO}(3)) \Big(\rho_\epsilon \, \mathrm{Re}(\mathrm{D}_t\boldsymbol{u}_0 - \mathrm{Fr}^{-2}\,\boldsymbol{e}_g) - \nabla \cdot \mathbf{S}[\boldsymbol{u}_0] \Big)$$
$$- N_\epsilon \epsilon^2 \, \mathrm{Re}\,\nabla \cdot \widetilde{\mathbf{H}}_0[\psi_t, \boldsymbol{u}_0] \,,$$
$$\nabla \cdot \boldsymbol{u}_0 = 0 \,, \quad (3.55b)$$

in $\Omega \times (0, T)$ coupled with the weak formulation (A.6) of

$$\partial_t \psi_t + \nabla_{\boldsymbol{x}} \cdot (\boldsymbol{u}_0 \psi_t) + \epsilon \nabla_{\boldsymbol{x}} \cdot (F_{1,v}[\boldsymbol{u}_0] \psi_t) = \mathcal{L}[B(F_{1,\omega}[\boldsymbol{u}_0])](\psi_t) \quad (3.55c)$$
$$+ \mathrm{div}_{\mathcal{G}}(\mathcal{L}[B(F_{1,\omega}[\boldsymbol{u}_0])])\psi_t$$

in $\Omega \times \mathcal{SO}(3)$ with boundary data for $\boldsymbol{u}_0, \psi_t$ at $\partial\Omega$ as well as initial conditions $\boldsymbol{u}_0(., 0), \psi_0$. Additionally, let $(\boldsymbol{c}^i, \mathbf{R}^i) \in \mathcal{C}^2((0, T); \Omega \times \mathcal{SO}(3))$, $i = 1, \ldots, N_\epsilon$ be given subject to the condition (3.5) and whose empirical measure fulfills

$$d(\mu_{N_\epsilon, t}, \psi_t) < c\epsilon^4 N_\epsilon \quad (3.56)$$

with $c = c(T)$ but independent of ϵ. Then (3.55) is an approximation of the suspension problem (3.1) up to an error of $\mathcal{O}(\epsilon)$.

Proof. First, by using $(\boldsymbol{c}^i(t), \mathbf{R}^i(t))$ we set the particle domains as $\mathcal{E}^i_\epsilon = \boldsymbol{x}(\mathcal{E}, \boldsymbol{c}^i, \mathbf{R}^i, \epsilon)$. Then since $\lfloor \frac{2}{2+r} \rfloor \leq 1$ for $r \geq 0$ and $\lfloor \frac{-r}{2+r} \rfloor \leq 0$ we can apply Remark 20 for $n = 2$ and hence construct an asymptotic solution to the particle related equations (3.1b)-(3.1e) by means of Lemma 19 up to an error of $\mathcal{O}(\epsilon^2)$. Since the empirical measure, $\mu_{N_\epsilon,t}$, of $(\boldsymbol{c}^i, \mathbf{R}^i)$ fulfills (3.56) and $\boldsymbol{u}_0, F_1$ are at least $\mathcal{C}^1$, we have for any $\theta \in \mathcal{C}^2(\Omega \times \mathcal{SO}(3))$

$$
\begin{aligned}
&\frac{\mathrm{d}}{\mathrm{d}t} \int_{\Omega \times \mathcal{SO}(3)} \theta \, \mathrm{d}\psi_t - \int_{\Omega \times \mathcal{SO}(3)} \nabla_{\boldsymbol{x}} \theta \cdot (\boldsymbol{u}_0 + \epsilon F_{1,v}[\boldsymbol{u}_0]) + \mathcal{L}[B(-F_{1,\omega}[\boldsymbol{u}_0])](\theta) \, \mathrm{d}\psi_t \\
&= \frac{\mathrm{d}}{\mathrm{d}t} \int_{\Omega \times \mathcal{SO}(3)} \theta \, \mathrm{d}\mu_{N_\epsilon,t} - \int_{\Omega \times \mathcal{SO}(3)} \nabla_{\boldsymbol{x}} \theta \cdot (\boldsymbol{u}_0 + \epsilon F_{1,v}[\boldsymbol{u}_0]) + \mathcal{L}[B(-F_{1,\omega}[\boldsymbol{u}_0])](\theta) \, \mathrm{d}\mu_{N_\epsilon,t} \\
&\quad + \mathcal{O}(\epsilon^4 N_\epsilon) \, .
\end{aligned}
$$

The terms $\mathrm{d}\theta(\boldsymbol{c}^i, \mathbf{R}^i)/\mathrm{d}t$ can be related to the directional derivatives of θ in $\Omega \times \mathcal{SO}(3)$ by using the fact that ∂/∂_{x_i} and the Lie derivatives span the tangent space $\mathcal{T}_{(\boldsymbol{x},\mathbf{R})} \Omega \times \mathcal{SO}(3)$, see Rem. A.37. In particular, we have

$$
\frac{\mathrm{d}}{\mathrm{d}t} \theta(\boldsymbol{c}^i, \mathbf{R}^i) = \left[\frac{\mathrm{d}}{\mathrm{d}t} \boldsymbol{c}^i \cdot \nabla_{\boldsymbol{x}} \right] \theta(\boldsymbol{c}^i, \mathbf{R}^i) - \mathcal{L} \left[\frac{\mathrm{d}}{\mathrm{d}t} \mathbf{R}^i \cdot \mathbf{R}^{iT} \right] \bigg|_{\mathbf{R}^i} (\theta(\boldsymbol{c}^i, .)) \, .
$$

Due to the linearity of the differential operators appearing here (see Lemma A.28), it follows up to an error of $c\epsilon^4 N_\epsilon$

$$
\begin{aligned}
\frac{1}{N_\epsilon} \sum_{i=1}^{N_\epsilon} &\left[\left(\frac{\mathrm{d}}{\mathrm{d}t} \boldsymbol{c}^i - (\boldsymbol{u}_0(\boldsymbol{c}^i, t) + \epsilon F_{1,v}[\boldsymbol{u}_0](\boldsymbol{c}^i, \mathbf{R}^i, t)) \right) \cdot \nabla_{\boldsymbol{x}} \right] \theta(\boldsymbol{c}^i, \mathbf{R}^i) \\
&- \mathcal{L} \left[\frac{\mathrm{d}}{\mathrm{d}t} \mathbf{R}^i \cdot \mathbf{R}^{iT} - B(F_{1,\omega}[\boldsymbol{u}_0](\boldsymbol{c}^i, \mathbf{R}^i, t)) \right] \bigg|_{\mathbf{R}^i} (\theta(\boldsymbol{c}^i, .)) = 0 \, . \quad (3.57)
\end{aligned}
$$

The relation (3.57) holds for any $\theta \in \mathcal{C}^2(\Omega \times \mathcal{SO}(3))$ and therefore specifically for any $\theta \in \mathcal{C}^2(\Omega \times \mathbb{R}^{3 \times 3})$. This way the Lie derivatives can be directly related to partial derivatives on $\mathbb{R}^{3 \times 3}$ by applying the definition of the Lie derivative and the chain rule. Thus, the relation (3.57) becomes a scalar product for vectors in $\mathbb{R}^{12 N_\epsilon}$. Since $\|\boldsymbol{c}^i - \boldsymbol{c}^j\| > \iota_\epsilon$, for any $Z \in \mathbb{R}^{12 N_\epsilon}$ we can construct a $\theta \in \mathcal{C}^2(\Omega \times \mathbb{R}^{3 \times 3})$ such that

$$
(\partial_{\boldsymbol{x},\mathbf{R}} \theta(\boldsymbol{c}^1, \mathbf{R}^1), \dots, \partial_{\boldsymbol{x},\mathbf{R}} \theta(\boldsymbol{c}^{N_\epsilon}, \mathbf{R}^{N_\epsilon})) = Z \, ,
$$

thus (3.57) is true if and only if

$$
\frac{\mathrm{d}}{\mathrm{d}t} \boldsymbol{c}^i = \boldsymbol{u}_0 + \epsilon F_{1,v}[\boldsymbol{u}_0](\boldsymbol{c}^i, \mathbf{R}^i, t) \, , \quad \frac{\mathrm{d}}{\mathrm{d}t} \mathbf{R}^i = B(F_{1,\omega}[\boldsymbol{u}_0])(\boldsymbol{c}^i, \mathbf{R}^i, t) \cdot \mathbf{R}^i \quad (3.58)
$$

with initial conditions $(\boldsymbol{c}^i(0), \mathbf{R}^i(0))$ for all $i = 1, \dots, N_\epsilon$. In fact, the relation (3.58) equals (3.16) with the velocity expressions (3.19) up to an error of $\mathcal{O}(\epsilon)$.

As for the fluid momentum equation, we note that (3.55a) implies for any divergence-free $\boldsymbol{\theta} \in \mathcal{C}_0^2(\Omega)$

71

$$\int_\Omega \left(\operatorname{Re} \mathrm{D}_t \boldsymbol{u}_0 - \nabla \cdot \mathbf{S}[\boldsymbol{u}_0] - \operatorname{Re} \operatorname{Fr}^{-2} \boldsymbol{e}_g \right) \cdot \boldsymbol{\theta} \, \mathrm{d}\boldsymbol{x}$$

$$= - \int_\Omega \epsilon^3 N_\epsilon \frac{|\mathcal{E}|}{|\Omega|} \boldsymbol{\Sigma}_0^p[\psi_t, \boldsymbol{u}_0] : \nabla \boldsymbol{\theta} \, \mathrm{d}\boldsymbol{x} + \int_\Omega \epsilon \widetilde{\boldsymbol{U}}_0[\psi_t, \boldsymbol{u}_0] \cdot \Delta \boldsymbol{\theta} \, \mathrm{d}\boldsymbol{x}$$

$$+ \int_\Omega \boldsymbol{\theta} \cdot \int_{\mathcal{SO}(3)} \epsilon^3 N_\epsilon |\mathcal{E}| \left(\rho_\epsilon \operatorname{Re}(\mathrm{D}_t \boldsymbol{u}_0 - \operatorname{Fr}^{-2} \boldsymbol{e}_g) - \nabla \cdot \mathbf{S}[\boldsymbol{u}_0] \right) \mathrm{d}\psi_{\boldsymbol{x},t}(\mathbf{R}) \, \mathrm{d}\boldsymbol{x}$$

$$+ \int_\Omega N_\epsilon \epsilon^2 \operatorname{Re} \widetilde{\mathbf{H}}_0[\psi_t, \boldsymbol{u}_0] : \nabla \boldsymbol{\theta}^T \, \mathrm{d}\boldsymbol{x} \,.$$

Since $\widetilde{\boldsymbol{U}}_{\mathrm{loc},1}[\mu_{N_\epsilon}, \boldsymbol{u}_0](., \boldsymbol{c}, \mathbf{R}, t) \in \mathcal{W}^{1,\infty}(\mathbb{R}^3; \mathbb{R}^3)$ and smooth in the arguments $\boldsymbol{c}, \mathbf{R}$, the mapping $(\boldsymbol{c}, \mathbf{R}) \mapsto \widetilde{\boldsymbol{U}}_{\mathrm{loc},k}[\mu_{N_\epsilon}, \boldsymbol{u}_0](\boldsymbol{y}(\boldsymbol{x}, \boldsymbol{c}, \mathbf{R}, \epsilon), \boldsymbol{c}, \mathbf{R}, t) \in \mathcal{W}^{1,\infty}(\Omega \times \mathcal{SO}(3); \mathbb{R}^3)$ for any $\boldsymbol{x} \in \Omega$. By Sobolev inequality [45], the latter mapping has a Lipschitz continuous version and therefore $\widetilde{\mathbf{H}}_0[\psi_t, \boldsymbol{u}_0] = \widetilde{\mathbf{H}}_0[\mu_{N_\epsilon,t}, \boldsymbol{u}_0] + \mathcal{O}(\epsilon^4 N_\epsilon)$ and analogously $\widetilde{\boldsymbol{U}}_0[\psi_t, \boldsymbol{u}_0] = \widetilde{\boldsymbol{U}}_0[\mu_{N_\epsilon,t}, \boldsymbol{u}_0] + \mathcal{O}(\epsilon^4 N_\epsilon)$. Additionally, we have

$$\int_\Omega \boldsymbol{\theta} \cdot \int_{\mathcal{SO}(3)} \epsilon^3 N_\epsilon |\mathcal{E}| \left(\rho_\epsilon \operatorname{Re}(\mathrm{D}_t \boldsymbol{u}_0 - \operatorname{Fr}^{-2} \boldsymbol{e}_g) - \nabla \cdot \mathbf{S}[\boldsymbol{u}_0] \right) \mathrm{d}\psi_{\boldsymbol{x},t}(\mathbf{R}) \, \mathrm{d}\boldsymbol{x}$$

$$= \int_{\Omega \times \mathcal{SO}(3)} \boldsymbol{\theta} \cdot \epsilon^3 N_\epsilon |\mathcal{E}| \left(\rho_\epsilon \operatorname{Re}(\mathrm{D}_t \boldsymbol{u}_0 - \operatorname{Fr}^{-2} \boldsymbol{e}_g) - \nabla \cdot \mathbf{S}[\boldsymbol{u}_0] \right) \mathrm{d}\psi_t(\boldsymbol{x}, \mathbf{R})$$

$$= \int_{\Omega \times \mathcal{SO}(3)} \boldsymbol{\theta} \cdot \epsilon^3 N_\epsilon |\mathcal{E}| \left(\rho_\epsilon \operatorname{Re}(\mathrm{D}_t \boldsymbol{u}_0 - \operatorname{Fr}^{-2} \boldsymbol{e}_g) - \nabla \cdot \mathbf{S}[\boldsymbol{u}_0] \right) \mathrm{d}\mu_{N_\epsilon,t}(\boldsymbol{x}, \mathbf{R}) + \mathcal{O}(\epsilon^4 N_\epsilon)$$

since the integrands are at least $\mathcal{C}^1$. Analogously we find

$$\int_\Omega \epsilon^3 N_\epsilon \frac{|\mathcal{E}|}{|\Omega|} \boldsymbol{\Sigma}_0^p[\psi_t, \boldsymbol{u}_0] : \nabla \boldsymbol{\theta} \, \mathrm{d}\boldsymbol{x}$$

$$= \int_{\Omega \times \mathcal{SO}(3)} \epsilon^3 N_\epsilon \mathbf{R} \cdot \int_{\partial \mathcal{E}} \mathbf{S}_{\boldsymbol{y}}[\boldsymbol{U}_{\mathrm{loc},1}[\psi, \boldsymbol{u}]](\boldsymbol{y}, \boldsymbol{x}, \mathbf{R}, t) \cdot \boldsymbol{n} \otimes \boldsymbol{y} - \boldsymbol{U}_{\mathrm{loc},1,\partial\mathcal{E}}[\psi, \boldsymbol{u}](\boldsymbol{y}, \boldsymbol{x}, \mathbf{R}, t) \otimes \boldsymbol{n}$$

$$- \boldsymbol{n} \otimes \boldsymbol{U}_{\mathrm{loc},1,\partial\mathcal{E}}[\psi, \boldsymbol{u}](\boldsymbol{y}, \boldsymbol{x}, \mathbf{R}, t) \, \mathrm{d}s(\boldsymbol{y}) \cdot \mathbf{R}^T : \nabla \boldsymbol{\theta} \, \mathrm{d}\mu_{N_\epsilon,t}(\boldsymbol{x}, \mathbf{R}) + \mathcal{O}(\epsilon^4 N_\epsilon) \,.$$

Using the transformation (3.52) and the property $\int_\mathcal{E} \nabla_{\boldsymbol{y}} \cdot \mathbf{T}_{\mathrm{loc},1} \otimes \boldsymbol{y} \, \mathrm{d}\boldsymbol{y} = \mathbf{0}$ we get

$$\int_\Omega \epsilon^3 N_\epsilon \frac{|\mathcal{E}|}{|\Omega|} \boldsymbol{\Sigma}_0^p[\psi_t, \boldsymbol{u}_0] : \nabla \boldsymbol{\theta} \, \mathrm{d}\boldsymbol{x}$$

$$= \int_{\Omega \times \mathcal{SO}(3)} \epsilon^3 N_\epsilon \mathbf{R} \cdot \int_\mathcal{E} \mathbf{T}_{\mathrm{loc},1}[\boldsymbol{u}_0] - 2\mathbf{E}_{\boldsymbol{y}}[\boldsymbol{U}_{\mathrm{loc},1,\partial\mathcal{E}}[\boldsymbol{u}_0]] \, \mathrm{d}\boldsymbol{y} \cdot \mathbf{R}^T : \nabla \boldsymbol{\theta} \, \mathrm{d}\mu_{N_\epsilon,t}(\boldsymbol{x}, \mathbf{R}) + \mathcal{O}(\epsilon^4 N_\epsilon) \,.$$

Using the definition of the empirical measure, we continue by repeating the steps in the proof of Lemma 32 in reversed order

$$\int_{\Omega \times \mathcal{SO}(3)} \epsilon^3 N_\epsilon \mathbf{R} \cdot \int_\mathcal{E} \mathbf{T}_{\mathrm{loc},1}[\boldsymbol{u}_0] - 2\mathbf{E}_{\boldsymbol{y}}[\boldsymbol{U}_{\mathrm{loc},1,\partial\mathcal{E}}[\boldsymbol{u}_0]] \, \mathrm{d}\boldsymbol{y} \cdot \mathbf{R}^T : \nabla \boldsymbol{\theta} \, \mathrm{d}\mu_{N_\epsilon,t}(\boldsymbol{x}, \mathbf{R})$$

$$= \sum_{i=1}^{N_\epsilon} \epsilon^3 \mathbf{R}^i \cdot \int_\mathcal{E} \left(\mathbf{T}_{\mathrm{loc},1}[\boldsymbol{u}_0] - 2\mathbf{E}_{\boldsymbol{y}}[\boldsymbol{U}_{\mathrm{loc},1,\partial\mathcal{E}}[\boldsymbol{u}_0]] \right)(\boldsymbol{y}, \boldsymbol{c}^i, \mathbf{R}^i, t) \, \mathrm{d}\boldsymbol{y} \cdot \mathbf{R}^{iT} : \nabla \boldsymbol{\theta}(\boldsymbol{c}^i)$$

$$= \sum_{i=1}^{N_\epsilon} \mathbf{R}^i \cdot \int_{\mathcal{E}_\epsilon^i} \left(\mathbf{T}_{\mathrm{loc},1}[\boldsymbol{u}_0] - 2\mathbf{E}_{\boldsymbol{y}}[\boldsymbol{U}_{\mathrm{loc},1,\partial\mathcal{E}}[\boldsymbol{u}_0]] \right) (\boldsymbol{y}(\boldsymbol{x}, \boldsymbol{c}^i, \mathbf{R}^i, \epsilon), \boldsymbol{c}^i, \mathbf{R}^i, t) : \nabla\boldsymbol{\theta}(\boldsymbol{x}) \, \mathrm{d}\boldsymbol{x} \cdot \mathbf{R}^{iT}$$
$$+ \, \mathcal{O}(\epsilon^4 N_\epsilon)$$
$$= \int_\Omega \int_{\Omega \times \mathcal{SO}(3)} N_\epsilon \mathbf{R} \cdot \left(\mathbf{T}_{\mathrm{loc},1}[\boldsymbol{u}_0] - 2\mathbf{E}_{\boldsymbol{y}}[\boldsymbol{U}_{\mathrm{loc},1,\partial\mathcal{E}}[\boldsymbol{u}_0]] \right) (\boldsymbol{y}(\boldsymbol{x}, \boldsymbol{c}, \mathbf{R}, \epsilon), \boldsymbol{c}, \mathbf{R}, t) \cdot \mathbf{R}^T$$
$$\cdot \, \mathbb{1}_{\mathcal{E}}(\boldsymbol{y}(\boldsymbol{x}, \boldsymbol{c}, \mathbf{R}, \epsilon)) \, \mathrm{d}\mu_{N_\epsilon, t} : \nabla\boldsymbol{\theta}(\boldsymbol{x}) \, \mathrm{d}\boldsymbol{x} + \mathcal{O}(\epsilon^4 N_\epsilon) \,.$$

Therefore, in total we have up to an error of $\mathcal{O}(\epsilon^4 N_\epsilon)$

$$\int_\Omega \left(\mathrm{Re}\, \mathrm{D}_t \boldsymbol{u}_0 - \nabla \cdot \mathbf{S}[\boldsymbol{u}_0] - \mathrm{Re}\, \mathrm{Fr}^{-2} \, \boldsymbol{e}_g \right) \cdot \boldsymbol{\theta} \, \mathrm{d}\boldsymbol{x}$$
$$= -\int_\Omega \int_{\Omega \times \mathcal{SO}(3)} N_\epsilon \mathbf{R} \cdot \left(\mathbf{T}_{\mathrm{loc},1}[\boldsymbol{u}_0] - 2\mathbf{E}_{\boldsymbol{y}}[\boldsymbol{U}_{\mathrm{loc},1,\partial\mathcal{E}}[\boldsymbol{u}_0]] \right) \cdot \mathbf{R}^T \cdot \mathbb{1}_{\mathcal{E}}(\boldsymbol{y}(\boldsymbol{x}, \boldsymbol{c}, \mathbf{R}, \epsilon)) \, \mathrm{d}\mu_{N_\epsilon, t} : \nabla\boldsymbol{\theta} \, \mathrm{d}\boldsymbol{x}$$
$$- \int_\Omega 2\mathbf{E} \left[N_\epsilon \epsilon \int_{\Omega \times \mathcal{SO}(3)} \mathbf{R} \cdot \widetilde{\boldsymbol{U}}_{\mathrm{loc},1}[\boldsymbol{u}_0] \, \mathrm{d}\mu_{N_\epsilon, t} \right] : \nabla\boldsymbol{\theta} \, \mathrm{d}\boldsymbol{x}$$
$$+ \int_{\Omega \times \mathcal{SO}(3)} \boldsymbol{\theta} \cdot \epsilon^3 N_\epsilon |\mathcal{E}| \left(\rho_\epsilon \, \mathrm{Re}(\mathrm{D}_t \boldsymbol{u}_0 - \mathrm{Fr}^{-2} \, \boldsymbol{e}_g) - \nabla \cdot \mathbf{S}[\boldsymbol{u}_0] \right) \mathrm{d}\mu_{N_\epsilon, t}(\boldsymbol{x}, \mathbf{R})$$
$$- \int_\Omega N_\epsilon \epsilon^2 \, \mathrm{Re}\, \nabla \cdot \widetilde{\mathbf{H}}_0[\mu_{N_\epsilon, t}, \boldsymbol{u}_0] \cdot \boldsymbol{\theta} \, \mathrm{d}\boldsymbol{x} \,.$$

The next step is now to recover the pressure, but first we note that the expression

$$\int_{\Omega \times \mathcal{SO}(3)} \boldsymbol{\theta} \cdot \epsilon^3 N_\epsilon |\mathcal{E}| \left(\rho_\epsilon \, \mathrm{Re}(\mathrm{D}_t \boldsymbol{u}_0 - \mathrm{Fr}^{-2} \, \boldsymbol{e}_g) - \nabla \cdot \mathbf{S}[\boldsymbol{u}_0] \right) \mathrm{d}\mu_{N_\epsilon, t}(\boldsymbol{x}, \mathbf{R})$$

stems from the observation in Remark 34 that by approximating the stresses in the suspension, we neglected a force which was generated by fluctuations on the small particle domains, i.e.,

$$\int_\Omega \boldsymbol{\theta} \cdot \int_{\Omega \times \mathcal{SO}(3)} \epsilon^{-1} N_\epsilon \mathbf{R} \cdot \left(\nabla_{\boldsymbol{y}} \cdot \mathbf{T}_{\mathrm{loc},1}[\boldsymbol{u}_0] + \epsilon \nabla_{\boldsymbol{y}} \cdot \mathbf{T}_{\mathrm{loc},2} \right) \mathbb{1}_{\mathcal{E}}(\boldsymbol{y}(\boldsymbol{x}, \boldsymbol{z}, \mathbf{R}, t)) \, \mathrm{d}\mu_{N_\epsilon, t}(\boldsymbol{z}, \mathbf{R}) \, \mathrm{d}\boldsymbol{x}$$

By recovering the original expression for the stresses, we drop this correction term. Finally, by adding the pressure term (3.47a) tested with $\nabla\boldsymbol{\theta}$, we recover the complete $\boldsymbol{\Sigma}_0[\mu_{N_\epsilon, t}, \boldsymbol{u}_0]$ from (3.47), i.e.,

$$\int_\Omega \left(\mathrm{Re}\, \mathrm{D}_t \boldsymbol{u}_0 - \nabla \cdot \mathbf{S}[\boldsymbol{u}_0] - \mathrm{Re}\, \mathrm{Fr}^{-2} \, \boldsymbol{e}_g \right) \cdot \boldsymbol{\theta} \, \mathrm{d}\boldsymbol{x}$$
$$= - \int_\Omega \boldsymbol{\Sigma}_0[\mu_{N_\epsilon, t}, \boldsymbol{u}_0] : \nabla\boldsymbol{\theta} \, \mathrm{d}\boldsymbol{x} - \int_\Omega N_\epsilon \epsilon^2 \, \mathrm{Re}\, \nabla \cdot \widetilde{\mathbf{H}}_0[\mu_{N_\epsilon, t}, \boldsymbol{u}_0] \cdot \boldsymbol{\theta} \, \mathrm{d}\boldsymbol{x} \,.$$

Considering the last term, we have due to the solenoidity of $\boldsymbol{u}_0$

$$N_\epsilon \epsilon^2 \nabla \cdot \widetilde{\mathbf{H}}_0[\mu_{N_\epsilon, t}, \boldsymbol{u}_0](\boldsymbol{x}, t)$$
$$= N_\epsilon \int_{\Omega \times \mathcal{SO}(3)} \mathbf{R} \cdot \partial_{\boldsymbol{y}} \widetilde{\boldsymbol{U}}_{\mathrm{loc},1}[\boldsymbol{u}_0] \cdot \mathbf{R}^T \cdot \left(\boldsymbol{u}(\boldsymbol{x}, t) - \boldsymbol{u}(\boldsymbol{z}, t) - B(F_{1,\omega}[\boldsymbol{u}](\boldsymbol{z}, \mathbf{R}, t)) \right) \mathrm{d}\mu_{N_\epsilon, t}$$
$$= H_0[\mu_{N_\epsilon, t}, \boldsymbol{u}_0] \,.$$

Since $\boldsymbol{\theta}$ was arbitrary, $\boldsymbol{u}_0$ solves up to an error of $\mathcal{O}(\epsilon^4 N_\epsilon)$

$$\operatorname{Re} \mathrm{D}_t \boldsymbol{u}_0 + \operatorname{Re} H_0[\mu_{N_\epsilon, t}, \boldsymbol{u}_0] = \nabla \cdot \boldsymbol{\Sigma}_0[\mu_{N_\epsilon, t}, \boldsymbol{u}_0] + \nabla \cdot \mathsf{S}[\boldsymbol{u}_0] + \operatorname{Re} \operatorname{Fr}^{-2} \boldsymbol{e}_g$$

in Ω. Hence, it holds in Ω_ϵ

$$\begin{aligned}
\mathbf{0} &= \operatorname{Re} \mathrm{D}_t \boldsymbol{u}_0 + \operatorname{Re} H_0[\mu_{N_\epsilon, t}, \boldsymbol{u}_0] - \nabla \cdot \boldsymbol{\Sigma}_0[\mu_{N_\epsilon, t}, \boldsymbol{u}_0] - \nabla \cdot \mathsf{S}[\boldsymbol{u}_0] - \operatorname{Re} \operatorname{Fr}^{-2} \boldsymbol{e}_g \\
&= \operatorname{Re} \mathrm{D}_t \boldsymbol{u}^e - \nabla \cdot \mathsf{S}[\boldsymbol{u}^e] - \operatorname{Re} \operatorname{Fr}^{-2} \boldsymbol{e}_g + \mathcal{O}(\epsilon)
\end{aligned}$$

and therefore, $\boldsymbol{u}^e$ is an approximation up to $\mathcal{O}(\epsilon)$ of (3.1a). $\qquad \square$

Remark 37 (Comparison between mean field and asymptotic approximation). *We note that Theorem 36 and Theorem 21 yield the same approximation order. Moreover, the latter holds also for heavy particles, is determined by a less complicated momentum equation for the fluid and has only a three-dimensional problem domain in comparison with the six-dimensional $\Omega \times \mathcal{SO}(3)$ of (3.55). However, Theorem 21 also needs the construction of N_ϵ local velocity fields by Lemma 19 together with corresponding particle paths and rotations unlike the mean field model of Theorem 36. We also note that for $\epsilon \to 0$, the system (3.55) approaches the undisturbed Navier-Stokes equations (3.32), as all terms depending on the transport equation (3.55c) drop out and the latter then depends on the former but not vice versa. Therefore, (3.55) can be seen as a continuous model for the large system of equations of Theorem 21.*

Considering the heavy particles regime, we know from Lemma 19 that it is characterized by $\boldsymbol{f}_1 \sim \operatorname{Re} \mathrm{D}_t \boldsymbol{u}_0 - \operatorname{Re} \operatorname{Fr}^{-2} \boldsymbol{e}_g$ which is not zero unless $\operatorname{Re} = 0$, the case of no inertia. Due to (3.27) this implies that $\boldsymbol{v}_1 \neq \mathbf{0}$ which leads to a non-vanishing $\mathcal{O}(\|\boldsymbol{y}\|^{-1})$ term in the local velocity $\boldsymbol{u}_{\mathrm{loc},1}$. Thus, the decay constant in Lemma 16 is $\ell = 1$ and the only admissible condition on β in the definition of the particle number is $\beta = 0$ (condition C1) of Lemma 16). This of course implies a constant particle number which is completely fine in case of the asymptotic approximation of Theorem 21. In combination with condition (3.56) on the other hand, this results in a contradiction since we can not approximate the integral of every Lipschitz continuous function by a finite number of fixed points: If we assume that the empirical measure $\mu_{N,t}$ for $N \equiv \mathrm{const}$ fulfills (3.56) with $\psi_t \in \mathcal{P}^C(\Omega) \times \mathcal{P}(\mathcal{SO}(3))$, we can take $\theta(\boldsymbol{z}, \mathbf{R}) \equiv \tilde{\theta}_1(\boldsymbol{z})$ as a test function with $\tilde{\theta}_1 \geq 0$ being a Lipschitz continuous function in Ω with $\operatorname{supp}(\tilde{\theta}_1) = \mathcal{B}_\delta(\boldsymbol{c}^1)$ and $\tilde{\theta}_1(\boldsymbol{c}^1) = 0.5\delta = \|\tilde{\theta}_1\|_{\mathcal{C}(\Omega)}$ for any $\delta < \iota_\epsilon = N^{-1/3} \equiv \mathrm{const}$. Then, we have

$$\begin{aligned}
\left| \int_{\Omega \times \mathcal{SO}(3)} \theta \, \mathrm{d}\psi_t \right| &= \left| \int_{\mathcal{B}_\delta(\boldsymbol{c}^1)} \tilde{\theta}_1 \psi_{\boldsymbol{x},t}(\mathcal{SO}(3)) \, \mathrm{d}\boldsymbol{x} \right| \leq 0.5\delta^4 |\mathcal{B}_1| \max_{\boldsymbol{x} \in \mathcal{B}_\delta(\boldsymbol{c}^1)} |\psi_{\boldsymbol{x},t}(\mathcal{SO}(3))| \\
&\leq 0.5\delta^4 |\mathcal{B}_1| \| \boldsymbol{x} \mapsto \psi_{\boldsymbol{x},t}(\mathcal{SO}(3)) \|_{\mathcal{C}(\Omega)} = 0.5\delta^4 |\mathcal{B}_1| C
\end{aligned}$$

with C independent of ϵ and δ. Since $\int_{\Omega \times \mathcal{SO}(3)} \theta \, \mathrm{d}\mu_{N,t} = 0.5\delta/N$ it holds

$$d(\mu_{N,t}, \psi_t) \geq \left| \frac{1}{2N} \delta - \frac{1}{2} \delta^4 |\mathcal{B}_1| C \right|$$

and thus for a fixed $\delta < (2N|\mathcal{B}_1|C)^{-1/3}$, $d(\mu_{N,t}, \psi_t) \geq 0.25\delta/N$ which is a contradiction to (3.56) for ϵ small enough.

In order to derive an analogous result for the heavy particle regime or to get a higher order approximation in case of normal or light-weighted particles, we have to drop the strict condition $N \equiv$ const as discussed in Remark 37. From the relations (3.50) and (3.51) in Lemma 31 we find that $H_0, \boldsymbol{\Sigma}_0$ have uniform $\mathcal{L}^p$-bounds for all $\beta < 1$, given that the chaos assumption (3.44) of Remark 29 holds. The same is true for $H_1, \boldsymbol{\Sigma}_1$ if $\beta < 3/4$. Thus Lemma 32 holds, i.e., $\boldsymbol{\Sigma}_k^p$ is well-defined. Moreover, the estimations in Remark 34 show that $\|\nabla^\ell \epsilon^2 N_\epsilon \widetilde{\boldsymbol{U}}_k\| < c$ independent of ϵ without additional assumptions for $\ell \in 0, 1, 2$. Thus, we have the following two Theorems with proofs completely analogous to Theorem 36.

Theorem 38 (Mean field approximation of a particle suspension up to $\mathcal{O}(\epsilon)$ for heavy particles). *Let the density scaling function (2.12) be given as $\alpha_\rho(\epsilon) = \epsilon^{-1}$, the particle number as $N_\epsilon = \epsilon^{-\beta}$ with $1/3 \leq \beta < 1$ and ϕ_ϵ given by (3.3). Let also (3.44) hold for $K = 1, n = 2$. Assume that $\boldsymbol{u}_0 \in \mathcal{C}^2((0,T); \mathcal{C}^3(\Omega; \mathbb{R}^3))$ and $p_0 \in \mathcal{C}^1((0,T); \mathcal{C}^2(\Omega; \mathbb{R}))$, $\psi_t \in \mathcal{P}^C(\Omega) \times \mathcal{P}(\mathcal{SO}(3))$ with $(\boldsymbol{x}, t) \mapsto \psi_{\boldsymbol{x},t}(\mathcal{SO}(3)) \in \mathcal{C}^1(\Omega \times (0,T); \mathbb{R}_0^+)$ solve (3.55). Additionally, let $(\boldsymbol{c}^i, \mathbf{R}^i) \in \mathcal{C}^2((0,T); \Omega \times \mathcal{SO}(3))$, $i = 1, \dots, N_\epsilon$ be given subject to the condition (3.5) and whose empirical measure fulfills (3.56). Then (3.55) is an approximation of the suspension problem (3.1) up to an error of $\mathcal{O}(\epsilon)$.*

For the second theorem we need additional Abbreviations:

Abbreviation 39. *For $\psi \in \mathcal{P}^C(\Omega) \times \mathcal{P}(\mathcal{SO}(3))$ and $\boldsymbol{u} \in \mathcal{C}^1(\Omega \times (0,T); \mathbb{R}^3)$*

$$\widetilde{\mathbf{H}}_1[\psi, \boldsymbol{u}](\boldsymbol{x}, t)$$
$$= \epsilon^{-1} \int_{\Omega \times \mathcal{SO}(3)} (\boldsymbol{u}(\boldsymbol{x}, t) - \boldsymbol{u}(\boldsymbol{z}, t) - B(F_{1,\omega}[\boldsymbol{u}](\boldsymbol{z}, \mathbf{R}, t))) \otimes \mathbf{R} \cdot \widetilde{\boldsymbol{U}}_{\mathrm{loc},2}[\psi, \boldsymbol{u}](\boldsymbol{y}(\boldsymbol{x}), \boldsymbol{z}, \mathbf{R}, t)$$
$$- (F_{1,v}[\boldsymbol{u}](\boldsymbol{z}, \mathbf{R}, t) + B(F_{2,\omega}[\psi, \boldsymbol{u}](\boldsymbol{z}, \mathbf{R}, t)) \cdot (\boldsymbol{x} - \boldsymbol{z})) \otimes \mathbf{R} \cdot \widetilde{\boldsymbol{U}}_{\mathrm{loc},1}[\boldsymbol{u}](\boldsymbol{z}, \mathbf{R}, t) \, \mathrm{d}\psi(\boldsymbol{z}, \mathbf{R}) \,,$$

$$\widetilde{\boldsymbol{\Sigma}}_1^p[\psi, \boldsymbol{u}](\boldsymbol{x}, t) = \frac{|\Omega|}{|\mathcal{E}|} \sum_{\ell m} \partial_{x_\ell} \int_{\mathcal{SO}(3)} \mathbf{R} \cdot \int_{\mathcal{E}} \left(\mathbf{T}_{\mathrm{loc},1}[\boldsymbol{u}](\boldsymbol{y}, \boldsymbol{x}, \mathbf{R}, t) \right.$$
$$\left. - 2 \mathbf{E}_{\boldsymbol{y}}[\boldsymbol{U}_{\mathrm{loc},1,\partial\mathcal{E}}[\boldsymbol{u}]](\boldsymbol{y}, \boldsymbol{x}, \mathbf{R}, t) \right) y_m \, \mathrm{d}s(\boldsymbol{y}) \cdot \mathbf{R}^T R_{m\ell}^T \, \mathrm{d}\psi_{\boldsymbol{x}} \,,$$

$$\widetilde{\mathbf{G}}_1[\psi, \boldsymbol{u}](\boldsymbol{x}, t) = \epsilon^{-1} \int_{\Omega \times \mathcal{SO}(3)} (\partial_{\boldsymbol{x}} \boldsymbol{u}(\boldsymbol{x}, t) + B(F_{1,\omega}[\boldsymbol{u}](\boldsymbol{z}, \mathbf{R}, t))) \cdot \mathbf{R} \cdot \widetilde{\boldsymbol{U}}_{\mathrm{loc},1}[\boldsymbol{u}](\boldsymbol{y}(\boldsymbol{x}), \boldsymbol{z}, \mathbf{R}, t)$$
$$+ \mathbf{R} \cdot \partial_t \widetilde{\boldsymbol{U}}_{\mathrm{loc},1}[\boldsymbol{u}](\boldsymbol{y}(\boldsymbol{x}), \boldsymbol{z}, \mathbf{R}, t) \, \mathrm{d}\mu(\boldsymbol{z}, \mathbf{R})$$

with the $(\boldsymbol{z}, \mathbf{R})$-dependent abbreviation $\boldsymbol{y}(\boldsymbol{x}) \equiv \boldsymbol{y}(\boldsymbol{x}, \boldsymbol{z}, \mathbf{R}, \epsilon)$.

Theorem 40 (Mean field approximation of a particle suspension up to $\mathcal{O}(\epsilon^2)$ for normal or light-weighted particles). *Let the density scaling function (2.12) be given as $\alpha_\rho(\epsilon) = \epsilon^r$, $r \geq 0$, the particle number as $N_\epsilon = \epsilon^{-\beta}$ with $1/3 \leq \beta < 1$ and ϕ_ϵ given by (3.3). Let also (3.44) hold for $K = 1, n = 3$. Assume that $\boldsymbol{u}_0 \in \mathcal{C}^1((0,T); \mathcal{C}^4(\Omega; \mathbb{R}^3))$ and $p_0 \in \mathcal{C}^0((0,T); \mathcal{C}^3(\Omega; \mathbb{R}))$, $\psi_t \in \mathcal{P}^C(\Omega) \times \mathcal{P}(\mathcal{SO}(3))$ with $(\boldsymbol{x}, t) \mapsto \psi_{\boldsymbol{x},t}(\mathcal{SO}(3)) \in \mathcal{C}^1(\Omega \times (0,T); \mathbb{R}_0^+)$ solve*

$$\mathrm{Re}\,\mathrm{D}_t \boldsymbol{u}_0 = \nabla \cdot \mathbf{S}[\boldsymbol{u}_0] + \phi_\epsilon \nabla \cdot \boldsymbol{\Sigma}_0^p[\psi_t, \boldsymbol{u}_0] + \epsilon \phi_\epsilon \nabla \cdot (\boldsymbol{\Sigma}_1^p - \widetilde{\boldsymbol{\Sigma}}_1^p)[\psi_t, \boldsymbol{u}_0] \qquad (3.59\mathrm{a})$$

$$+ 2N_\epsilon \epsilon^2 \nabla \cdot \mathbf{E}[\widetilde{\boldsymbol{U}}_0[\psi_t, \boldsymbol{u}_0]] + 2N_\epsilon \epsilon^3 \nabla \cdot \mathbf{E}[\widetilde{\boldsymbol{U}}_1[\psi_t, \boldsymbol{u}_0]]$$

$$+ \mathrm{Re}\,\mathrm{Fr}^{-2}\, \boldsymbol{e}_g$$

$$+ \phi_\epsilon |\Omega| \psi_{\boldsymbol{x},t}(\mathcal{SO}(3))\Big(\rho_\epsilon \,\mathrm{Re}(\mathrm{D}_t \boldsymbol{u}_0 - \mathrm{Fr}^{-2}\, \boldsymbol{e}_g) - \nabla \cdot \mathbf{S}[\boldsymbol{u}_0]\Big)$$

$$- N_\epsilon \epsilon^2 \,\mathrm{Re}\, \nabla \cdot (\widetilde{\mathbf{H}}_0[\psi_t, \boldsymbol{u}_0] + \epsilon \widetilde{\mathbf{H}}_1[\psi_t, \boldsymbol{u}_0])\,,$$

$$- N_\epsilon^2 \epsilon^4 \,\mathrm{Re}\, \widetilde{\boldsymbol{U}}_0[\psi, \boldsymbol{u}] \cdot \nabla \widetilde{\boldsymbol{U}}_0[\psi, \boldsymbol{u}]$$

$$- N_\epsilon \epsilon^2 \,\mathrm{Re}\, \widetilde{\mathbf{G}}_1[\psi, \boldsymbol{u}]$$

$$\nabla \cdot \boldsymbol{u}_0 = 0\,, \qquad (3.59\mathrm{b})$$

in $\Omega \times (0,T)$ *coupled with the weak formulation* (A.6) *of*

$$\partial_t \psi_t + \nabla_{\boldsymbol{x}} \cdot (\boldsymbol{u}_0 \psi_t) + \sum_{k=1}^2 \epsilon^k \nabla_{\boldsymbol{x}} \cdot (F_{k,v}[\boldsymbol{u}_0]\psi_t) = \sum_{k=1}^2 \epsilon^{k-1}(\mathcal{L}[B(F_{k,\omega}[\boldsymbol{u}_0]](\psi_t) \qquad (3.59\mathrm{c})$$

$$+ \mathrm{div}_{\mathcal{G}}(\mathcal{L}[B(F_{k,\omega}[\boldsymbol{u}_0])])\psi_t$$

in $\Omega \times \mathcal{SO}(3)$ *with boundary data for* $\boldsymbol{u}_0, \psi_t$ *at* $\partial\Omega$ *as well as initial conditions* $\boldsymbol{u}_0(.,0), \psi_0$.
Additionally, let $(\boldsymbol{c}^i, \mathbf{R}^i) \in \mathcal{C}^3((0,T); \Omega \times \mathcal{SO}(3))$, $i = 1,\dots,N_\epsilon$ *be given subject to the condition* (3.5) *and whose empirical measure fulfills*

$$\mathrm{d}(\mu_{N_\epsilon,t}, \psi_t) < c\epsilon^5 N_\epsilon \qquad (3.60)$$

with $c = c(T)$ *but independent of* ϵ. *Then* (3.59) *is an approximation of the suspension problem* (3.1) *up to an error of* $\mathcal{O}(\epsilon^2)$.

Remark 41 (Estimation of interaction terms in momentum equation)**.** *We can improve the estimations for* $\widetilde{\boldsymbol{U}}_0$ *(Remark 34) and* $\widetilde{\mathbf{H}}_0$ *(Lemma 31). In fact, we find*

$$\|\widetilde{\boldsymbol{U}}_0\| \le c(\epsilon^{\ell-1-\beta\ell/3} + \epsilon^{(\ell-1)(1-\beta)} + \epsilon^{3\beta-1})\,.$$

Hence, for $\beta \in [1/3,1)$ *with* $\beta \le 3(\ell-1)/\ell$, $\|\widetilde{\boldsymbol{U}}_0\|$ *is bounded independent of* ϵ. *The same holds for* $\widetilde{\mathbf{H}}_0$. *If the decay constant of the Stokes fields is* $\ell = 1$, *this bound is not useful. In this case we can use the chaos assumption. It holds for* $k \ge 1$

$$\left\| N_\epsilon^{-1} \boldsymbol{r}_{k+1}[\psi, \boldsymbol{u}] - \widetilde{\boldsymbol{U}}_{k-1}[\psi, \boldsymbol{u}] \right\| = \left\| \epsilon^{-1} \int_{\Omega \times \mathcal{SO}(3)} \mathbf{R} \cdot \Big(\boldsymbol{U}_{\mathrm{loc},k}[\psi, \boldsymbol{u}]\chi - \widetilde{\boldsymbol{U}}_{\mathrm{loc},k}[\psi, \boldsymbol{u}]\Big)\,\mathrm{d}\psi \right\|$$

$$= \epsilon^{-1} \left\| \int_{\mathcal{B}_{0.5\iota_\epsilon} \backslash \mathcal{B}_{0.25\iota_\epsilon} \times \mathcal{SO}(3)} (\chi - 1)\mathbf{R} \cdot \boldsymbol{U}_{\mathrm{loc},k}[\psi, \boldsymbol{u}]\,\mathrm{d}\psi - \int_{\mathcal{B}_{0.25\iota_\epsilon} \backslash \mathcal{B}_{1/N_\epsilon} \times \mathcal{SO}(3)} \mathbf{R} \cdot \boldsymbol{U}_{\mathrm{loc},k}[\psi, \boldsymbol{u}]\,\mathrm{d}\psi \right.$$

$$\left. - \int_{\mathcal{B}_{1/N_\epsilon} \times \mathcal{SO}(3)} \mathbf{R} \cdot \widetilde{\boldsymbol{U}}_{\mathrm{loc},k}[\psi, \boldsymbol{u}]\,\mathrm{d}\psi \right\|$$

$$\le cC\epsilon^{-1}\left(\int_{\mathcal{B}_{0.5\iota_\epsilon} \backslash \mathcal{B}_{0.25\iota_\epsilon}} \epsilon \|\boldsymbol{x} - \boldsymbol{z}\|^{-1}\,\mathrm{d}\boldsymbol{z} + \int_{\mathcal{B}_{0.25\iota_\epsilon} \backslash \mathcal{B}_{1/N_\epsilon}} \epsilon \|\boldsymbol{x} - \boldsymbol{z}\|^{-1}\,\mathrm{d}\boldsymbol{z} + \frac{1}{N_\epsilon^3}\right) \le c\iota_\epsilon^2 + cN_\epsilon\iota_\epsilon^3 + c\frac{1}{\epsilon N_\epsilon^3}\,.$$

By choosing $N_\epsilon = \epsilon^{-\beta}$ with $\beta \geq 1/3$, we thus find a uniform bound for $\|N_\epsilon^{-1} \boldsymbol{r}_{k+1}[\psi, \boldsymbol{u}] - \widetilde{\boldsymbol{U}}_{k-1}[\psi, \boldsymbol{u}]\|$. Then by imposing condition (3.44) of Remark 29, we find

$$\|\widetilde{\boldsymbol{U}}_{k-1}[\psi, \boldsymbol{u}]\| \leq \|N_\epsilon^{-1} \boldsymbol{r}_{k+1}[\psi, \boldsymbol{u}]\| + \left\|\widetilde{\boldsymbol{U}}_{k-1}[\psi, \boldsymbol{u}] - N_\epsilon^{-1} \boldsymbol{r}_{k+1}[\psi, \boldsymbol{u}]\right\| \leq c$$

independent of ϵ. The same procedure for $\widetilde{\mathbf{H}}_0$ is not applicable without further assumptions. Instead, we construct a bound for a particular case. We choose $\beta = 0.5$, then $\epsilon^2 N_\epsilon = \epsilon^{4/3} \epsilon^{1/6}$ and $\epsilon^{1/6} \widetilde{\mathbf{H}}_0$ fulfills

$$\|\epsilon^{1/6} \widetilde{\mathbf{H}}_0\| \leq c(\epsilon^0 + \epsilon^{1/6} + \epsilon^{2/3}) < 3c.$$

Therefore (3.55a) reads formally as

$$\begin{aligned}
\mathrm{Re}\, \mathrm{D}_t \boldsymbol{u}_0 - \mathrm{Re}\, \mathrm{Fr}^{-2}\, \boldsymbol{e}_g &= \nabla \cdot \mathbf{S}[\boldsymbol{u}_0] + \phi_\epsilon \nabla \cdot \boldsymbol{\Sigma}_0^p[\psi_t, \boldsymbol{u}_0] + 2\epsilon^{3/2} \nabla \cdot \mathbf{E}[\widetilde{\boldsymbol{U}}_0[\psi_t, \boldsymbol{u}_0]] \\
&\quad + \phi_\epsilon |\Omega| \psi_{\boldsymbol{x},t}(\mathcal{SO}(3))\Big(\rho_\epsilon \mathrm{Re}(\mathrm{D}_t \boldsymbol{u}_0 - \mathrm{Fr}^{-2}\, \boldsymbol{e}_g) - \nabla \cdot \mathbf{S}[\boldsymbol{u}_0]\Big) \\
&\quad - \epsilon^{4/3} \mathrm{Re}\, \nabla \cdot \widetilde{\mathbf{H}}_0[\psi_t, \boldsymbol{u}_0].
\end{aligned}$$

Since $\phi_\epsilon = N_\epsilon \epsilon^3 = \epsilon^{5/2}$ and $\rho_\epsilon = \epsilon^{-r} \rho = \mathcal{O}(\epsilon^{-1})$ in case of heavy particles,

$$\begin{aligned}
\phi_\epsilon \rho_\epsilon (\mathrm{Re}\, \mathrm{D}_t \boldsymbol{u}_0 - \mathrm{Re}\, \mathrm{Fr}^{-2}\, \boldsymbol{e}_g) &= \phi_\epsilon \rho_\epsilon \nabla \cdot \mathbf{S}[\boldsymbol{u}_0] + \mathcal{O}(\epsilon^4) + \mathcal{O}(\epsilon^3) + \mathcal{O}(\epsilon^{2+5/6}) \\
&= \phi_\epsilon \rho_\epsilon \nabla \cdot \mathbf{S}[\boldsymbol{u}_0] + o(\phi_\epsilon).
\end{aligned}$$

Thus, we can further approximate the momentum equation as

$$\begin{aligned}
\mathrm{Re}\, \mathrm{D}_t \boldsymbol{u}_0 - \mathrm{Re}\, \mathrm{Fr}^{-2}\, \boldsymbol{e}_g &= \nabla \cdot \mathbf{S}[\boldsymbol{u}_0] + \phi_\epsilon \nabla \cdot \boldsymbol{\Sigma}_0^p[\psi_t, \boldsymbol{u}_0] + 2\epsilon^{3/2} \nabla \cdot \mathbf{E}[\widetilde{\boldsymbol{U}}_0[\psi_t, \boldsymbol{u}_0]] \quad (3.61) \\
&\quad + \phi_\epsilon(\rho_\epsilon - 1)|\Omega| \psi_{\boldsymbol{x},t}(\mathcal{SO}(3)) \nabla \cdot \mathbf{S}[\boldsymbol{u}_0] \\
&\quad - \epsilon^{4/3} \mathrm{Re}\, \nabla \cdot \widetilde{\mathbf{H}}_0[\psi_t, \boldsymbol{u}_0] + o(\phi_\epsilon).
\end{aligned}$$

Applying the estimations of Remark 41, we formulate the following corollary to Theorem 36 and Theorem 38.

Corollary 42. *Let the assumptions of Theorem 36 or Theorem 38 hold with the sharper condition $\beta = 1/2$. Furthermore, assume that the spatial particle distribution is uniform, $\psi(\boldsymbol{x}, \mathbf{R}, t) \equiv |\Omega|^{-1} \widetilde{\psi}(\mathbf{R}, t)$. Then the momentum equation for the fluid (3.55a) reads as*

$$\begin{aligned}
\mathrm{Re}\, \mathrm{D}_t \boldsymbol{u}_0 &= (1 + \phi_\epsilon(\rho_\epsilon - 1))\nabla \cdot \mathbf{S}[\boldsymbol{u}_0] + \mathrm{Re}\, \mathrm{Fr}^{-2}\, \boldsymbol{e}_g + \phi_\epsilon \nabla \cdot \boldsymbol{\Sigma}_0^p[\psi_t, \boldsymbol{u}_0] \\
&\quad + 2\epsilon^{3/2} \nabla \cdot \mathbf{E}[\widetilde{\boldsymbol{U}}_0[\psi_t, \boldsymbol{u}_0]] - \epsilon^{4/3} \mathrm{Re}\, \nabla \cdot \widetilde{\mathbf{H}}_0[\psi_t, \boldsymbol{u}_0]
\end{aligned}$$

with $\widetilde{\boldsymbol{U}}_0, \widetilde{\mathbf{H}}_0$ given in Abbreviation 35 and $\boldsymbol{\Sigma}_0^p$ given as the mean value with respect to the measure on $\mathcal{SO}(3)$, $\widetilde{\psi}$:

$$\begin{aligned}
\boldsymbol{\Sigma}_0^p[\psi, \boldsymbol{u}_0](\boldsymbol{x}, t) = \frac{1}{|\mathcal{E}|} \mathbb{E}\Big[&\mathbf{R} \mapsto \mathbf{R} \cdot \int_{\partial \mathcal{E}} \mathbf{S}_{\boldsymbol{y}}[\boldsymbol{U}_{\mathrm{loc},1}[\boldsymbol{u}_0]](\boldsymbol{y}, \boldsymbol{x}, \mathbf{R}, t) \cdot \boldsymbol{n} \otimes \boldsymbol{y} \\
&- \boldsymbol{U}_{\mathrm{loc},1,\partial\mathcal{E}}[\boldsymbol{u}_0](\boldsymbol{y}, \boldsymbol{x}, \mathbf{R}, t) \otimes \boldsymbol{n} \\
&- \boldsymbol{n} \otimes \boldsymbol{U}_{\mathrm{loc},1,\partial\mathcal{E}}[\boldsymbol{u}_0](\boldsymbol{y}, \boldsymbol{x}, \mathbf{R}, t)\, \mathrm{d}s(\boldsymbol{y}) \cdot \mathbf{R}^T\Big].
\end{aligned}$$

Remark 43 (Differences to [119])**.** *We point out, that the particle extra stress tensor $\boldsymbol{\Sigma}_0^p$ in Corollary 42 corresponds to the one derived by Batchelor [12] in case of an inertia-free suspension in an unbounded domain. It was also recovered in our previous work [119] in the case of a homogeneous uniform distribution of inertial particles and under the assumption of ergodicity. In this case, there exists for any $\boldsymbol{x} \in \Omega$ a representative averaging volume, $\mathcal{V}(\boldsymbol{x}, t)$ containing $N_\epsilon(\boldsymbol{x}, t)$ particles, such that*

$$\mathbb{E}[\mathbf{R} \mapsto f(\boldsymbol{x}, \mathbf{R}, t)] = \frac{1}{|\mathcal{V}(\boldsymbol{x}, t)|} \sum_{k=1}^{N_\epsilon(\boldsymbol{x}, t)} f(\boldsymbol{x}, \mathbf{R}^k, t).$$

Using this assumption, we also derived additional force terms due to particle inertia. In Corollary 42 we recover only one part of the latter found in [119], namely the term belonging to the fluid viscosity,

$$\phi_\epsilon(\rho_\epsilon - 1)\nabla \cdot \mathbf{S}[\boldsymbol{u}_0].$$

The missing term compared to [119] belongs to $\boldsymbol{b}_2[\psi, \boldsymbol{u}_0]$ (as does $\phi_\epsilon(\rho_\epsilon - 1)\nabla \cdot \mathbf{S}[\boldsymbol{u}_0]$) given in (3.53) in the case of heavy particles. To be precise, it is the term associated to $G_{1,0,v}(\boldsymbol{c}, \mathbf{R}, t)$ (see discussion at the beginning of Section 3.4.1) which carries the time derivative of F_1 and thus the second time derivative of $\boldsymbol{u}_0$. Due to the limitations of the model discussed in Remark 30, we can't account for this additional force although it is of order $\mathcal{O}(\epsilon^{3/2})$, as this would change the type of the equations significantly.

Another difference is the presence of the terms due to interaction, $\widetilde{\boldsymbol{U}}_0, \widetilde{\mathbf{H}}_0$. In [119] they are omitted as the local velocity fields are modeled as small velocity fluctuations, whose superposition equals to the vanishing mean value. Thus, we can reconstruct this behavior in Corollary 42 by intensifying the chaos assumption (3.44) to $\|\boldsymbol{r}_k[\psi]\|_{\mathcal{C}^{\min(K+3+r-k, K)}} = 0$.

3.5 Applications to special particle geometries

Suspensions of particles that have the same density as the surrounding viscous carrier fluid and possess a highly symmetrical shape, e.g., spherical or ellipsoidal geometry, are often discussed in literature. The structure of the stresses due to particles is well-known in these cases, see [12] and [81]. They also often serve as proof-of-concept examples for newly derived models, as, e.g., in [34] and [64]. In this section we illustrate our kinetic suspension model based on the asymptotical approach which accounts for small particle inertia by comparing the model with the classical results of [42] and [12].

In order to present closed analytic expressions for the transport operators and stress tensors in the corresponding theorems from Section 3.4.1 and 3.4.2, we first introduce fundamental solutions of the stationary Stokes problems on the considered geometries, calculate the resulting surface moments afterwards, and finally show the resulting expressions for the operators appearing in the macroscopic description of the suspension.

3.5.1 Rigid spheres

Stokes solutions and surface moments A rigid sphere of radius 1 is given as $\mathcal{E} = \mathcal{B}_1$. In this case $\boldsymbol{u}_c, \boldsymbol{u}_\ell : \mathbb{R}^3 \setminus \mathcal{E} \to \mathbb{R}^3$ and $p_c, p_\ell : \mathbb{R}^3 \setminus \mathcal{E} \to \mathbb{R}$ given as

$$\boldsymbol{u}_c(\boldsymbol{y}) = \frac{3}{4}\|\boldsymbol{y}\|^{-1}\left(\boldsymbol{v} + \|\boldsymbol{y}\|^{-2}(\boldsymbol{y} \cdot \boldsymbol{v})\boldsymbol{y} + \frac{1}{3}\|\boldsymbol{y}\|^{-2}\boldsymbol{v} - \|\boldsymbol{y}\|^{-4}(\boldsymbol{y} \cdot \boldsymbol{v})\boldsymbol{y}\right), \tag{3.62a}$$

$$\boldsymbol{u}_\ell(\boldsymbol{y}) = \frac{5}{2}\|\boldsymbol{y}\|^{-5}\left(1 - \|\boldsymbol{y}\|^{-2}\right)(\boldsymbol{y} \cdot \mathbf{C} \cdot \boldsymbol{y})\boldsymbol{y} + \frac{1}{2}\|\boldsymbol{y}\|^{-3}\left(\mathbf{C} - \mathbf{C}^T + \|\boldsymbol{y}\|^{-2}\left(\mathbf{C} + \mathbf{C}^T\right)\right)\cdot\boldsymbol{y}\,,$$
(3.62b)

$$p_c = \frac{3}{2}(\boldsymbol{y}\cdot\boldsymbol{v})\|\boldsymbol{y}\|^{-3}\,,\quad p_\ell = 5(\boldsymbol{y}\cdot\mathbf{C}\cdot\boldsymbol{y})\|\boldsymbol{y}\|^{-5}$$
(3.62c)

for $\boldsymbol{v} \in \mathbb{R}^3$ and $\mathbf{C} \in \mathbb{R}^{3\times3}$ with $\mathrm{tr}(\mathbf{C}) = 0$ are smooth solutions of the homogeneous stationary Stokes equations on the exterior of $\mathcal{E}$ with boundary conditions $\boldsymbol{u}_c(\boldsymbol{y}) = \boldsymbol{v}$ and $\boldsymbol{u}_\ell(\boldsymbol{y}) = \mathbf{C}\cdot\boldsymbol{y}$ on $\partial\mathcal{E}$ (e.g., see [72]). The viscous stresses at the boundary in normal direction are then given as

$$\mathbf{S}_{\boldsymbol{y}}[\boldsymbol{u}_c](\boldsymbol{y}) \cdot \boldsymbol{n} = -\frac{3}{2}\boldsymbol{v}\,,\quad \mathbf{S}_{\boldsymbol{y}}[\boldsymbol{u}_\ell](\boldsymbol{y}) \cdot \boldsymbol{n} = -3\mathbf{C}\cdot\boldsymbol{y}\,,\quad \boldsymbol{y} \in \partial\mathcal{E}\,.$$

The model-relevant surface moments then follow as

$$\int_{\partial\mathcal{E}} \mathbf{S}_{\boldsymbol{y}}[\boldsymbol{u}_c] \cdot \boldsymbol{n}\,\mathrm{d}s = -6\pi\boldsymbol{v}\,,\qquad \int_{\partial\mathcal{E}} \mathbf{S}_{\boldsymbol{y}}[\boldsymbol{u}_\ell] \cdot \boldsymbol{n}\,\mathrm{d}s = \mathbf{0}\,,$$

$$\int_{\partial\mathcal{E}} \boldsymbol{y} \times \mathbf{S}_{\boldsymbol{y}}[\boldsymbol{u}_c] \cdot \boldsymbol{n}\,\mathrm{d}s = \mathbf{0}\,,\qquad \int_{\partial\mathcal{E}} \boldsymbol{y} \times \mathbf{S}_{\boldsymbol{y}}[\boldsymbol{u}_\ell] \cdot \boldsymbol{n}\,\mathrm{d}s = -4\pi B^{-1}(\mathbf{C} - \mathbf{C}^T)\,,$$

$$\int_{\partial\mathcal{E}} \boldsymbol{y} \otimes \mathbf{S}_{\boldsymbol{y}}[\boldsymbol{u}_c] \cdot \boldsymbol{n}\,\mathrm{d}s = \mathbf{0}\,,\qquad \int_{\partial\mathcal{E}} \boldsymbol{y} \otimes \mathbf{S}_{\boldsymbol{y}}[\boldsymbol{u}_\ell] \cdot \boldsymbol{n}\,\mathrm{d}s = -4\pi\mathbf{C}^T\,.$$

Where we used the definition of the reference state, i.e., $\int_{\mathcal{E}} \boldsymbol{y}\,\mathrm{d}\boldsymbol{y} = \mathbf{0}$, the relation $\int_{\partial\mathcal{B}} y_i y_j\,\mathrm{d}s = 4\pi/3\delta_{ij}$ due to the divergence theorem, and

$$\int_{\partial\mathcal{E}} \boldsymbol{y} \times \mathbf{C} \cdot \boldsymbol{y}\,\mathrm{d}s = \sum_{ijk\ell} \boldsymbol{e}_i\epsilon_{ijk}C_{k\ell}\int_{\partial\mathcal{E}} y_j y_\ell\,\mathrm{d}s = \frac{4}{3}\pi\sum_{ijk}\boldsymbol{e}_i\epsilon_{ijk}C_{kj} = \frac{4}{3}\pi\sqrt{2}\sum_i \boldsymbol{e}_i(\mathbf{B}_i : \mathbf{C})$$

$$= \frac{4}{6}\pi\sqrt{2}\sum_i \boldsymbol{e}_i(\mathbf{B}_i : (\mathbf{C} - \mathbf{C}^T)) = \frac{4}{3}\pi B^{-1}(\mathbf{C} - \mathbf{C}^T)$$

with $\{\mathbf{B}_i\}_i$ being an orthonormal basis of the skew-symmetric matrices and B^{-1} being the inverse of B given in (A.9b) (cf. Appendix A.2). This way we can express the vectors $\boldsymbol{t}_q, \boldsymbol{s}_q$ for $q = 1, \dots, 6$ given in Lemma 5 as

$$\boldsymbol{t}_q = -6\pi\boldsymbol{e}_q\,,\quad \boldsymbol{s}_{q+3} = -4\pi\sqrt{2}\boldsymbol{e}_q\,,\quad \boldsymbol{t}_{q+3} = \mathbf{0} = \boldsymbol{s}_q\,,\quad q = 1, 2, 3\,,$$

since $\mathbf{B}_q - \mathbf{B}_q^T = 2\mathbf{B}_q$ and $2B^{-1}(\mathbf{B}_q) = \sqrt{2}\boldsymbol{e}_q$. The matrix $A = (\boldsymbol{t}_q, \boldsymbol{s}_q)_{q=1,\dots,6}$ is then given as

$$A = \begin{bmatrix} -6\pi\mathbb{1}_{3\times3} & \\ & -4\pi\sqrt{2}\mathbb{1}_{3\times3} \end{bmatrix}\,.$$

Transport operators and particle extra stress tensor Similarly to the determination of the surface moments we find for $D_1\boldsymbol{u}_0$ given in (3.27) for $q = 1, 2, 3$ the relations $\boldsymbol{e}_q \cdot D_1\boldsymbol{u}_0 = 0$ and

$$\boldsymbol{e}_{q+3} \cdot D_1\boldsymbol{u}_0 = (\mathbf{R}^T \cdot \partial_{\boldsymbol{x}}\boldsymbol{u}_0^T \cdot \mathbf{R}) : (4\pi\mathbf{B}_q) = -2\pi(\mathbf{R}^T \cdot (\partial_{\boldsymbol{x}}\boldsymbol{u}_0 - \partial_{\boldsymbol{x}}\boldsymbol{u}_0^T) \cdot \mathbf{R}) : \mathbf{B}_q\,.$$

Applying (A.10c), we find for any skew-symmetric matrix $\mathbf{M}$

$$\mathbf{R}^T \cdot \mathbf{M} \cdot \mathbf{R} = \mathbf{R}^T \cdot B \circ B^{-1}(\mathbf{M}) \cdot \mathbf{R} = B(\mathbf{R}^T \cdot B^{-1}(\mathbf{M}))\,.$$

Additionally, since $B(\nabla \times \boldsymbol{u}_0) = \partial_{\boldsymbol{x}} \boldsymbol{u}_0 - \partial_{\boldsymbol{x}} \boldsymbol{u}_0^T$, we have

$$\mathbf{R}^T \cdot (\partial_{\boldsymbol{x}} \boldsymbol{u}_0 - \partial_{\boldsymbol{x}} \boldsymbol{u}_0^T) \cdot \mathbf{R} = B(\mathbf{R}^T \cdot \nabla \times \boldsymbol{u}_0) = \sqrt{2} \sum_i \boldsymbol{e}_i \cdot (\mathbf{R}^T \cdot \nabla \times \boldsymbol{u}_0) \mathbf{B}_i\,.$$

Therefore, it holds $D_1 \boldsymbol{u}_0 = (\mathbf{0}, -2\pi\sqrt{2} \mathbf{R}^T \cdot \nabla \times \boldsymbol{u}_0)$. The term F_1 then follows from (3.27) as

$$F_1(\boldsymbol{c}, \mathbf{R}, t) = \begin{cases} \left(-\frac{2}{9}\rho \operatorname{Re}(\mathrm{D}_t \boldsymbol{u}_0(\boldsymbol{c}, t) - \operatorname{Fr}^{-2}\boldsymbol{e}_g)\,,\ \frac{1}{2}\nabla \times \boldsymbol{u}_0(\boldsymbol{c}, t)\right), & r = -1 \\ \left(\mathbf{0}\,,\ \frac{1}{2}\nabla \times \boldsymbol{u}_0(\boldsymbol{c}, t)\right)\,, & r \geq 0 \end{cases}, \quad (3.63)$$

hence, $F_1(\boldsymbol{c}, \mathbf{R}, t) = F_1(\boldsymbol{c}, t)$. From (3.63) we note that the angular velocity is given as the local vorticity of the fluid, while the first order correction of the linear velocity is zero in normal and light-weighted regimes and is given by the fluid inertia scaled with the density ratio in the case of heavy particles. The boundary condition on the first order disturbance velocity follows due to (3.15a) as

$$\boldsymbol{U}_{\text{loc},1,\partial\mathcal{E}}[\boldsymbol{u}_0](\boldsymbol{y}, \boldsymbol{c}, \mathbf{R}, t) = \mathbf{R}^T \cdot \boldsymbol{v}_1[\boldsymbol{u}_0](\boldsymbol{c}, t) - \mathbf{R}^T \cdot \mathbf{E}[\boldsymbol{u}_0](\boldsymbol{c}, t) \cdot \mathbf{R} \cdot \boldsymbol{y}\,, \quad (3.64)$$

with $\boldsymbol{v}_1 \equiv \mathbf{0}$ for $r \geq 0$ and $\boldsymbol{v}_1 = -2\rho \operatorname{Re}(\mathrm{D}_t \boldsymbol{u}_0 - \operatorname{Fr}^{-2}\boldsymbol{e}_g)/9$ for heavy particles. Thus, $\boldsymbol{U}_{\text{loc},1}$ is completely determined by (3.62) with $\boldsymbol{v}, \mathbf{C}$ given via the velocity terms in (3.64). It holds

$$\mathbf{R} \cdot \int_{\partial\mathcal{E}} \boldsymbol{U}_{\text{loc},1,\partial\mathcal{E}}[\boldsymbol{u}_0] \otimes \boldsymbol{n}\,\mathrm{d}s = \boldsymbol{v}_1(\boldsymbol{c}, t) \otimes \int_{\partial\mathcal{E}} \boldsymbol{n}\,\mathrm{d}s - \mathbf{E}[\boldsymbol{u}_0](\boldsymbol{c}, t) \cdot \mathbf{R} \cdot \int_{\partial\mathcal{E}} \boldsymbol{y} \otimes \boldsymbol{n}\,\mathrm{d}s$$

$$= -\frac{4}{3}\pi \mathbf{E}[\boldsymbol{u}_0](\boldsymbol{c}, t) \cdot \mathbf{R}\,,$$

$$\int_{\partial\mathcal{E}} \mathbf{S}_{\boldsymbol{y}}[\boldsymbol{U}_{\text{loc},1}[\boldsymbol{u}_0]] \cdot \boldsymbol{n} \otimes \boldsymbol{y}\,\mathrm{d}s = 4\pi \mathbf{R}^T \cdot \mathbf{E}[\boldsymbol{u}_0](\boldsymbol{c}, t) \cdot \mathbf{R}\,.$$

Hence, we get an analytical expression for $\boldsymbol{\Sigma}_0^p$, given in Abbreviation 35, as

$$\boldsymbol{\Sigma}_0^p[\psi, \boldsymbol{u}_0](\boldsymbol{x}, t) = \frac{20}{3}\pi \frac{|\Omega|}{|\mathcal{E}|} \int_{\mathcal{SO}(3)} \mathbf{E}[\boldsymbol{u}_0](\boldsymbol{x}, t)\,\mathrm{d}\psi_{\boldsymbol{x},t}(\mathbf{R}) = \frac{5}{2}|\Omega|\psi_{\boldsymbol{x},t}(\mathcal{SO}(3)) 2\mathbf{E}[\boldsymbol{u}_0](\boldsymbol{x}, t)\,.$$

This way we get the following follow-up to Corollary 42.

Corollary 44. *Let the assumptions of Corollary 42 hold and $\mathcal{E} = \mathcal{B}_1$. Then the momentum equation for the fluid (3.55a) reads as*

$$\operatorname{Re}\mathrm{D}_t \boldsymbol{u}_0 = (1 + \phi_\epsilon(\rho_\epsilon - 1))\nabla \cdot \mathbf{S}[\boldsymbol{u}_0] + \frac{5}{2}\phi_\epsilon \Delta \boldsymbol{u}_0 + \operatorname{Re}\operatorname{Fr}^{-2}\boldsymbol{e}_g$$

$$+ 2\epsilon^{3/2}\nabla \cdot \mathbf{E}[\widetilde{\boldsymbol{U}}_0[\psi_t, \boldsymbol{u}_0]] - \epsilon^{4/3}\operatorname{Re}\nabla \cdot \widetilde{\mathbf{H}}_0[\psi_t, \boldsymbol{u}_0]\,.$$

Apart from the inertial terms and the terms due to interaction, the momentum equation in Corollary 44 contains the well-known $2.5\phi_\epsilon$ increase of viscosity found by Einstein [42], which is proven for bounded domains and stationary Stokes equations in [58] and further studied, e.g., in [49].

Remark 45 (Applicability of quadratic decay assumption). *In case of normal or light-weighted particles (3.63) shows that $\boldsymbol{U}_{\text{loc},1,\partial\mathcal{E}}$ has only a linear part, which implies that $\boldsymbol{U}_{\text{loc},1}$ is completely given by (3.62b) with $\mathbf{C} = -\mathbf{R}^T \cdot \mathbf{E}[\boldsymbol{u}_0](\boldsymbol{c}, t) \cdot \mathbf{R}$. This implies that $\|\boldsymbol{U}_{\text{loc},1}\| \in \mathcal{O}(\|\boldsymbol{y}^{-2}\|)$ for large $\|\boldsymbol{y}\|$. Thus, Theorem 36 holds without the chaos assumption.*

Remark 46 (Solution to the continuity equation). *The solvability of the coupled system* (3.55) *is out of scope of this work. Under the assumption, that a sufficiently regular solution exists, we can state an explicit expression for the solution of* (3.55c) *using classical results for the continuity equation in order to illustrate our model. For example, assume that* $\psi_t, \boldsymbol{u}_0, p_0$ *solve the System of Corrollary 44 with periodic boundary conditions on* $\partial\Omega$*. The characteristics of the underlying ordinary differential equations, see, e.g.,* [20]*, are for* $s, t \in [0, T]$ *solutions of the problem*

$$\frac{\mathrm{d}}{\mathrm{d}t}\boldsymbol{c}(t) = \boldsymbol{a}(\boldsymbol{c}(t), t), \quad \frac{\mathrm{d}}{\mathrm{d}t}\mathbf{R}(t) = B\left(\boldsymbol{\omega}(\boldsymbol{c}(t), t)\right) \cdot \mathbf{R}(t), \tag{3.65}$$
$$\boldsymbol{c}(s) = \boldsymbol{x}, \quad \mathbf{R}(s) = \mathbf{P}$$

with $\boldsymbol{a} = \boldsymbol{u}_0 + \epsilon \boldsymbol{v}_1[\boldsymbol{u}_0]$ *and* $\boldsymbol{\omega} = \frac{1}{2}\nabla \times \boldsymbol{u}_0$*. Thus, the characteristic flow in* Ω *is given as* $X(t, s, \boldsymbol{x}) = \boldsymbol{c}(t)$*. Due to the periodicity of the boundary conditions,* $X(t, s, \boldsymbol{x}) \in \Omega$ *for all* $t, s \in [0, T]$ *and* $\boldsymbol{x} \in \Omega$*, moreover* $X(t, s, .)$ *is a* $\mathcal{C}^1$ *diffeomorphism of* Ω *with inverse* $X(s, t, .)$ *that fulfills*

$$X(t_1, t_2, X(t_2, t_3, \boldsymbol{x})) = X(t_1, t_3, \boldsymbol{x}) \tag{3.66}$$

for all $\boldsymbol{x} \in \Omega$ *and* $t_1, t_2, t_3 \in [0, T]$*. Hence, the following relations hold*

$$\partial_t X(t, s, \boldsymbol{x}) = \boldsymbol{a}(X(t, s, \boldsymbol{x}), t), \tag{3.67}$$
$$\partial_s X(t, s, \boldsymbol{x}) = -\partial_{\boldsymbol{x}} X(t, s, \boldsymbol{x}) \cdot \boldsymbol{a}(\boldsymbol{x}, s), \tag{3.68}$$

the first stems from the definition, the second from differentiating (3.66) *with respect to* t_2 *and applying a change of variables. Taking the space derivative of* (3.66) *and applying the determinant yields for* $J(t, s, \boldsymbol{x}) = \det(\nabla_{\boldsymbol{x}} X(t, s, \boldsymbol{x}))$ *the relation*

$$J(t_1, t_2, X(t_2, t_3, \boldsymbol{x}))J(t_2, t_3, \boldsymbol{x}) = J(t_1, t_3, \boldsymbol{x}). \tag{3.69}$$

Similarily to the behavior of X *one can show* [20]

$$\partial_t J(t, s, \boldsymbol{x}) = (\epsilon \nabla_{\boldsymbol{x}} \cdot \boldsymbol{v}_1[\boldsymbol{u}_0])(X(t, s, \boldsymbol{x}), t)J(t, s, \boldsymbol{x}), \tag{3.70}$$
$$\partial_s J(t, s, \boldsymbol{x}) = -\nabla_{\boldsymbol{x}} \cdot (J(t, s, \boldsymbol{x})\boldsymbol{a}(\boldsymbol{x}, s)). \tag{3.71}$$

In the present case, $\boldsymbol{\omega}$ *is independent of* $\mathbf{R}$ *but as the following considerations are rather general, we allow explicitly* $\boldsymbol{\omega} = \boldsymbol{\omega}(\boldsymbol{x}, \mathbf{R}, t)$*. The characteristic flow in* $\mathcal{SO}(3)$ *is denoted by* $Y(t, s, \boldsymbol{x}, \mathbf{P}) = \mathbf{R}(t)$*, which depends on* $X(t, s, \boldsymbol{x})$ *and fulfills*

$$\partial_t Y(t, s, \boldsymbol{x}, \mathbf{P}) = B(\boldsymbol{\omega}(X(t, s, \boldsymbol{x}), Y(t, s, \boldsymbol{x}, \mathbf{P}), t)) \cdot Y(t, s, \boldsymbol{x}, \mathbf{P}), \quad Y(s, s, \boldsymbol{x}, \mathbf{P}) = \mathbf{P}. \tag{3.72}$$

By definition of Y *it holds*

$$Y(t_1, t_2, X(t_2, t_3, \boldsymbol{x}), Y(t_2, t_3, \boldsymbol{x}, \mathbf{R})) = Y(t_1, t_3, \boldsymbol{x}, \mathbf{R}) \tag{3.73}$$

for all $t_1, t_2, t_3 \in [0, T]$*, and* $(\boldsymbol{x}, \mathbf{R}) \in \Omega \times \mathcal{SO}(3)$*. Hence,* $Y(t, s, \boldsymbol{x}, .)$ *is a* $\mathcal{C}^1$ *diffeomorphism on* $\mathcal{SO}(3)$ *with inverse* $Y(s, t, X(t, s, \boldsymbol{x}), .)$*. Differentiating* (3.73) *with respect to* t_2 *yields*

$$0 = \partial_s Y_{ij} + [\partial_t X(t_2, t_3, \boldsymbol{x}) \cdot \nabla_{\boldsymbol{x}}]Y_{ij} + \mathrm{d}Y(., t_3, \boldsymbol{x}, \mathbf{R})_{t_2}\left(\left.\frac{\partial}{\partial t}\right|_{t_2}\right)(Y_{ij}(t_1, t_2, X(t_2, t_3, \boldsymbol{x}), .)),$$

with $dY(., t_3, \boldsymbol{x}, \mathbf{R})_{t_2}$ denoting the differential of the curve $Y(., t_3, \boldsymbol{x}, \mathbf{R})$ as defined in Definition A.14. By using Remark A.37 and the relations (3.67) as well as (3.72) and using the substitutions $\boldsymbol{x} = X(t_3, t_2, \boldsymbol{x}'), \mathbf{R} = Y(t_3, t_2, \boldsymbol{x}', \mathbf{R}'), t = t_1, s = t_2$, we then find

$$\partial_s Y_{ij}(t, s, \boldsymbol{x}', \mathbf{R}') = -[\boldsymbol{a}(\boldsymbol{x}', s) \cdot \nabla_{\boldsymbol{x}}] Y_{ij}(t, s, \boldsymbol{x}', \mathbf{R}') + \mathcal{L}[B(\boldsymbol{\omega}(\boldsymbol{x}', \mathbf{R}', s))]|_{\mathbf{R}'} (Y_{ij}(t, s, \boldsymbol{x}', .)) . \tag{3.74}$$

Next, we consider the function $K(t, s, \boldsymbol{x}, \mathbf{R}) = \det(C[Y(t, s, \boldsymbol{x}, .)](\mathbf{R}))$ with the mapping $C[Y(t, s, \boldsymbol{x}, .)] : \mathcal{SO}(3) \to \mathbb{R}^{3 \times 3}$ defined in Theorem A.50 of Appendix A.1. It fulfills

$$\frac{\partial}{\partial t} (C[Y(t, s, \boldsymbol{x}, .)](\mathbf{R}))_{ji} = \frac{\partial}{\partial t} \sum_{k\ell m} (\mathbf{B}_j)_{m\ell} Y_{km}(t, s, \boldsymbol{x}, \mathbf{R}) \, \mathcal{R}[\mathbf{B}_i]|_{\mathbf{R}} (Y_{k\ell}(t, s, \boldsymbol{x}, .))$$

$$= \sum_{k\ell mn} (\mathbf{B}_j)_{m\ell} B(\boldsymbol{\omega})_{kn} Y_{nm}(t, s, \boldsymbol{x}, \mathbf{R}) \, \mathcal{R}[\mathbf{B}_i]|_{\mathbf{R}} (Y_{k\ell}(t, s, \boldsymbol{x}, .))$$

$$+ \sum_{k\ell m} (\mathbf{B}_j)_{m\ell} Y_{km}(t, s, \boldsymbol{x}, \mathbf{R}) \frac{\partial}{\partial t} \frac{\partial}{\partial \tau} Y_{k\ell}(t, s, \boldsymbol{x}, \mathbf{R} \cdot \exp(\tau \mathbf{B}_i))\Big|_{\tau=0}$$

where we used (3.72) with $\boldsymbol{\omega} = \boldsymbol{\omega}(X(t, s, \boldsymbol{x}), Y(t, s, \boldsymbol{x}, \mathbf{R}), t)$ and the definition of the right Lie derivative. Since $Y_{k\ell}$ is $\mathcal{C}^1$ in each of its variables, it follows with (3.72)

$$\frac{\partial}{\partial t} \frac{\partial}{\partial \tau} Y_{k\ell}(t, s, \boldsymbol{x}, \mathbf{R} \cdot \exp(\tau \mathbf{B}_i))\Big|_{\tau=0}$$

$$= \sum_{n} \frac{\partial}{\partial \tau} B(\boldsymbol{\omega}(X(t, s, \boldsymbol{x}), Y(t, s, \boldsymbol{x}, \mathbf{R} \cdot \exp(\tau \mathbf{B}_i)), t))_{kn} Y_{n\ell}(t, s, \boldsymbol{x}, \mathbf{R} \cdot \exp(\tau \mathbf{B}_i))\Big|_{\tau=0}$$

$$= \sum_{n} B(\boldsymbol{\omega}(X(t, s, \boldsymbol{x}), Y(t, s, \boldsymbol{x}, \mathbf{R}), t))_{kn} \, \mathcal{R}[\mathbf{B}_i]|_{\mathbf{R}} (Y_{n\ell}(t, s, \boldsymbol{x}, .))$$

$$+ \sum_{np} \sqrt{2} (\mathbf{B}_p)_{kn} Y_{n\ell}(t, s, \boldsymbol{x}, \mathbf{R}) \frac{\partial}{\partial \tau} \omega_p(X(t, s, \boldsymbol{x}), Y(t, s, \boldsymbol{x}, \mathbf{R} \cdot \exp(\tau \mathbf{B}_i)), t)\Big|_{\tau=0} ,$$

where we applied the expression (A.9a) of the skew-symmetric mapping $B(.)$ in terms of the orthonormal basis $\{\mathbf{B}_1, \mathbf{B}_2, \mathbf{B}_3\}$ of the Lie algebra of the special orthogonal group, $\mathfrak{so}(3)$. In order to evaluate the derivative of the component ω_p, we use the chain rule stated in Lemma A.51, which reveals

$$\frac{\partial}{\partial \tau} \omega_p(X(t, s, \boldsymbol{x}), Y(t, s, \boldsymbol{x}, \mathbf{R} \cdot \exp(\tau \mathbf{B}_i)), t)\Big|_{\tau=0}$$

$$= \sum_{q} (C[Y(t, s, \boldsymbol{x}, .)](\mathbf{R}))_{qi} \, \mathcal{R}[\mathbf{B}_q]|_{Y(t, s, \boldsymbol{x}, \mathbf{R})} (\omega_p(X(t, s, \boldsymbol{x}), ., t)) .$$

In total, the time derivative of $C_{ji}[Y(t, s, \boldsymbol{x}, .)]$ reads as

$$\frac{\partial}{\partial t} C_{ji}[Y(t, s, \boldsymbol{x}, .)](\mathbf{R}) = \sum_{k\ell} \left(B(\boldsymbol{\omega}) \cdot Y \cdot \mathbf{B}_j + B(\boldsymbol{\omega})^T \cdot Y \cdot \mathbf{B}_j \right)_{k\ell} \mathcal{R}[\mathbf{B}_i]|_{\mathbf{R}} (Y_{k\ell}(t, s, \boldsymbol{x}, .))$$

$$+ \sqrt{2} \sum_{pq} \mathrm{tr} \left(Y \cdot \mathbf{B}_j \cdot Y^T \cdot \mathbf{B}_p^T \right) C_{qi}[Y(t, s, \boldsymbol{x}, .)](\mathbf{R}) \, \mathcal{R}[\mathbf{B}_q]|_{Y(t, s, \boldsymbol{x}, \mathbf{R})} (\omega_p(X(t, s, \boldsymbol{x}), ., t)) .$$

Due to the skew-symmetry of $B(.)$, the first sum in the identity above vanishes. Considering the second sum, we find from (A.9a), $\mathbf{B}_i = B(\boldsymbol{e}_i)/\sqrt{2}$. Applying (A.10b) and the Grassmann identity (A.10d) shows

$$Y \cdot \mathbf{B}_j \cdot Y^T \cdot \mathbf{B}_p^T = -\frac{1}{2} B(Y \cdot \boldsymbol{e}_j) \cdot B(\boldsymbol{e}_p) = -\frac{1}{2} (\boldsymbol{e}_p \otimes Y \cdot \boldsymbol{e}_j - \boldsymbol{e}_p \cdot Y \cdot \boldsymbol{e}_j \mathsf{I}) .$$

The trace of this expression then follows as $\mathrm{tr}(Y \cdot \mathbf{B}_j \cdot Y^T \cdot \mathbf{B}_p^T) = \boldsymbol{e}_p \cdot Y \cdot \boldsymbol{e}_j$. Next, we express the right Lie derivative with the left one using Lemma A.29, which gives

$$\mathcal{R}[\mathbf{B}_q]|_Y (\omega_p(X(t,s,\boldsymbol{x}),.,t)) = -\sum_n (Y \cdot \mathbf{B}_q \cdot Y^T) : \mathbf{B}_n \, \mathcal{L}[\mathbf{B}_n]|_Y (\omega_p(X(t,s,\boldsymbol{x}),.,t))$$

$$= \frac{-1}{\sqrt{2}} \sum_n B(Y \cdot \boldsymbol{e}_q) : \mathbf{B}_n \, \mathcal{L}[\mathbf{B}_n]|_Y (\omega_p(X(t,s,\boldsymbol{x}),.,t))$$

$$= -\sum_{\ell n} \boldsymbol{e}_\ell \cdot Y \cdot \boldsymbol{e}_q (\mathbf{B}_\ell : \mathbf{B}_n) \, \mathcal{L}[\mathbf{B}_n]|_Y (\omega_p(X(t,s,\boldsymbol{x}),.,t))$$

$$= -\sum_n \boldsymbol{e}_n \cdot Y \cdot \boldsymbol{e}_q \, \mathcal{L}[\mathbf{B}_n]|_Y (\omega_p(X(t,s,\boldsymbol{x}),.,t)) ,$$

where we again used (A.9a), (A.10b) and the orthonormality of $\{\mathbf{B}_i\}_i$. Thus, we conclude

$$\frac{\partial}{\partial t} (C[Y(t,s,\boldsymbol{x},.)](\mathbf{R}))_{ji}$$

$$= -\sqrt{2} \sum_{npq} Y_{pj} Y_{nq} (C[Y(t,s,\boldsymbol{x},.)](\mathbf{R}))_{qi} \, \mathcal{L}[\mathbf{B}_n]|_Y (\omega_p(X(t,s,\boldsymbol{x}),.,t)) .$$

Using Jacobi's formula [105], we then find for the time derivative of the determinant

$$\frac{\partial}{\partial t} K(t,s,\boldsymbol{x},\mathbf{R}) = \sum_{ij} (\mathrm{adj}(C[Y(t,s,\boldsymbol{x},.)](\mathbf{R})))_{ij} \cdot \left(\frac{\partial}{\partial t} C[Y(t,s,\boldsymbol{x},.)](\mathbf{R}) \right)_{ji}$$

$$= K(t,s,\boldsymbol{x},\mathbf{R}) \left(-\sqrt{2} \sum_{jnpq} Y_{pj} Y_{nq} \delta_{qj} \, \mathcal{L}[\mathbf{B}_n]|_Y (\omega_p(X(t,s,\boldsymbol{x}),.,t)) \right)$$

$$= -K(t,s,\boldsymbol{x},\mathbf{R}) \left(\sum_n \mathcal{L}[\mathbf{B}_n]|_Y (\sqrt{2}\omega_n(X(t,s,\boldsymbol{x}),.,t)) \right)$$

where adj denotes the transpose of the cofactor matrix, i.e., $\mathrm{adj}(\mathbf{C}) \cdot \mathbf{C} = \mathbf{C} \cdot \mathrm{adj}(\mathbf{C}) = \det(\mathbf{C})\mathsf{I}$ for any invertible matrix $\mathbf{C}$. Using the divergence operator given in Rem. A.32, we find in total

$$\frac{\partial}{\partial t} K(t,s,\boldsymbol{x},\mathbf{R}) = -K(t,s,\boldsymbol{x},\mathbf{R}) \mathrm{div}_{\mathcal{G}}(\mathcal{L}[B(\boldsymbol{\omega}(X(t,s,\boldsymbol{x}),.,t))])(Y(t,s,\boldsymbol{x},\mathbf{R})) . \quad (3.75)$$

Since $Y(s,s,\boldsymbol{x},\mathbf{R}) = \mathbf{R}$, a direct calculation shows $C[Y(s,s,\boldsymbol{x},.)](\mathbf{R}) = \mathsf{I}$. Thus, $K(s,s,\boldsymbol{x},\mathbf{R}) = 1$, which immediately implies $K(t,s,\boldsymbol{x},\mathbf{R}) > 0$. On the other hand, the application of the operator $C[.]$ to (3.73) gives

$$(C[Y(t_1, t_3, \boldsymbol{x}, .)](\mathbf{R}))_{ij}$$
$$= \sum_{k\ell m} (\mathbf{B}_i)_{m\ell} Y_{km}(t_1, t_3, \boldsymbol{x}, \mathbf{R}) \frac{\mathrm{d}}{\mathrm{d}\tau} Y_{k\ell}(t_1, t_2, X(t_2, t_3, \boldsymbol{x}), Y(t_2, t_3, \boldsymbol{x}, \mathbf{R} \cdot \exp(\tau \mathbf{B}_j)))\Big|_{\tau=0},$$

which combined with the chain rule of Lemma A.51 shows

$$C[Y(t_1, t_2, X(t_2, t_3, \boldsymbol{x}), .)](Y(t_2, t_3, \boldsymbol{x}, \mathbf{R})) \cdot C[Y(t_2, t_3, \boldsymbol{x}, .)](\mathbf{R}) = C[Y(t_1, t_3, \boldsymbol{x}, .)](\mathbf{R}).$$

Applying the determinant to this identity implies for K

$$K(t_1, t_2, X(t_2, t_3, \boldsymbol{x}), Y(t_2, t_3, \boldsymbol{x}, \mathbf{R}))K(t_2, t_3, \boldsymbol{x}, \mathbf{R}) = K(t_1, t_3, \boldsymbol{x}, \mathbf{R}). \qquad (3.76)$$

In order to derive the equation for $\partial_s K$, we differentiate (3.76) with respect to t_2, where we again use Definition A.14 and Remark A.37 for the calculation of

$$\frac{\mathrm{d}}{\mathrm{d}\tau}(\tau \mapsto K(t_1, t_2, X(t_2, t_3, \boldsymbol{x}), Y(\tau, t_3, \boldsymbol{x}, \mathbf{R}))).$$

Applying (3.67), (3.72), (3.75), the positivity of K and using the substitutions $\boldsymbol{x} = X(t_3, t_2, \boldsymbol{x}')$, $\mathbf{R} = Y(t_3, t_2, \boldsymbol{x}', \mathbf{R}')$, $t = t_1$, $s = t_2$, then yields

$$\partial_s K(t, s, \boldsymbol{x}', \mathbf{R}') = -[\boldsymbol{a}(\boldsymbol{x}', s) \cdot \nabla_{\boldsymbol{x}}]K(t, s, \boldsymbol{x}', \mathbf{R}') + \mathcal{L}[B(\boldsymbol{\omega}(\boldsymbol{x}', \mathbf{R}', s))](K(t, s, \boldsymbol{x}', .))$$
$$+ K(t, s, \boldsymbol{x}', \mathbf{R}')\mathrm{div}_{\mathcal{G}}(\mathcal{L}[B(\boldsymbol{\omega}(\boldsymbol{x}', ., s))])(\mathbf{R}'). \qquad (3.77)$$

Due to (3.66) and (3.73), the characteristic flow Z in $\Omega \times \mathcal{SO}(3)$, given in terms of X, Y as $Z(t, s, (\boldsymbol{x}, \mathbf{R})) = (X(t, s, \boldsymbol{x}), Y(t, s, \boldsymbol{x}, \mathbf{R}))$, fulfills for all $t_1, t_2, t_3 \in [0, T]$ and $(\boldsymbol{x}, \mathbf{R}) \in \Omega \times \mathcal{SO}(3)$

$$Z(t_1, t_2, Z(t_2, t_3, (\boldsymbol{x}, \mathbf{R}))) = Z(t_1, t_2, (X(t_2, t_3, \boldsymbol{x}), Y(t_2, t_3, \boldsymbol{x}, \mathbf{R})))$$
$$= \Big(X(t_1, t_2, X(t_2, t_3, \boldsymbol{x})), Y(t_1, t_2, X(t_2, t_3, \boldsymbol{x}), Y(t_2, t_3, \boldsymbol{x}, \mathbf{R}))\Big)$$
$$= (\boldsymbol{x}, \mathbf{R}).$$

Thus, Z is one-to-one and the push-forward measure [111], $\psi_t(.) = \psi_0(Z^{-1}(t, 0, .))$, fulfills

$$\psi_t(\Omega \times \mathcal{SO}(3)) = \psi_0(Z^{-1}(t, 0, \Omega \times \mathcal{SO}(3))) = \psi_0(\Omega \times \mathcal{SO}(3)) = 1.$$

Furthermore, ψ_t is a solution to (3.55c) as for all $\phi \in \mathcal{C}_0^1(\Omega) \times \mathcal{C}^1(\mathcal{SO}(3))$ it holds

$$\frac{\mathrm{d}}{\mathrm{d}t} \int_{\Omega \times \mathcal{SO}(3)} \phi(\boldsymbol{x}, \mathbf{R}) \, \mathrm{d}\psi_t = \frac{\mathrm{d}}{\mathrm{d}t} \int_{Z^{-1}(t, 0, \Omega \times \mathcal{SO}(3))} \phi(\boldsymbol{x}, \mathbf{R}) \, \mathrm{d}\psi_t = \frac{\mathrm{d}}{\mathrm{d}t} \int_{\Omega \times \mathcal{SO}(3)} \phi(X(t, 0, \boldsymbol{x}), Y(t, 0, \boldsymbol{x}, \mathbf{R})) \, \mathrm{d}\psi_0$$

$$= \int_{\Omega \times \mathcal{SO}(3)} \boldsymbol{a}(X(t, 0, \boldsymbol{x}), t) \cdot \nabla_{\boldsymbol{x}}\phi(X(t, 0, \boldsymbol{x}), Y(t, 0, \boldsymbol{x}, \mathbf{R}))$$
$$- \mathcal{L}[B(\boldsymbol{\omega}(X(t, 0, \boldsymbol{x}), Y(t, 0, \boldsymbol{x}, \mathbf{R}), t))](\phi)(X(t, 0, \boldsymbol{x}), Y(t, 0, \boldsymbol{x}, \mathbf{R})) \, \mathrm{d}\psi_0$$

$$= \int_{\Omega \times \mathcal{SO}(3)} \boldsymbol{a}(\boldsymbol{x}, t) \cdot \nabla_{\boldsymbol{x}}\phi(\boldsymbol{x}, \mathbf{R}) - \mathcal{L}[B(\boldsymbol{\omega}(\boldsymbol{x}, \mathbf{R}, t))](\phi)(\boldsymbol{x}, \mathbf{R}) \, \mathrm{d}\psi_t$$

due to the change of variables formula [111] and Remark A.37. Let, additionally, ψ_t being absolutely continuous with respect to $\lambda(A)h(B)$ for $A \times B \in \mathcal{B}(\Omega) \times \mathcal{B}(\mathcal{SO}(3))$, λ denoting the Lebesgue measure on Ω and h the Haar measure on $\mathcal{SO}(3)$. Denote the Radon derivative of ψ_t with respect to λh by $\varrho \in \mathcal{C}^1(\Omega \times \mathcal{SO}(3) \times (0,T); \mathbb{R}_0^+)$. Then the transport equation (3.55c) reads as

$$\partial_t \varrho + \nabla_{\boldsymbol{x}} \cdot (\boldsymbol{a}\varrho) = \mathcal{L}\left[B\left(\boldsymbol{\omega}\right)\right](\varrho) + \varrho \operatorname{div}_{\mathcal{G}}(\mathcal{L}[B(\boldsymbol{\omega})]) \tag{3.78}$$

with initial condition ϱ^0. We set

$$\varrho(\boldsymbol{x}, \mathbf{R}, t) = \varrho^0(X(0, t, \boldsymbol{x}), Y(0, t, \boldsymbol{x}, \mathbf{R}))J(0, t, \boldsymbol{x})K(0, t, \boldsymbol{x}, \mathbf{R}).$$

Due to (3.70), $J > 0, K > 0$ for all $(\boldsymbol{x}, \mathbf{R}) \in \Omega \times \mathcal{SO}(3)$ and hence $\varrho(\boldsymbol{x}, \mathbf{R}, t) \geq 0$ for all $(\boldsymbol{x}, \mathbf{R}, t) \in \Omega \times \mathcal{SO}(3) \times [0, T]$. In fact, ϱ is a solution to (3.78): A straightforward calculation shows with application of (3.68), (3.71) and (3.77)

$$\partial_t \varrho = -\nabla_{\boldsymbol{x}} \cdot (\boldsymbol{a}\varrho) + \mathcal{L}\left[B\left(\boldsymbol{\omega}\right)\right](\varrho) + \varrho \operatorname{div}_{\mathcal{G}}(\mathcal{L}[B(\boldsymbol{\omega})]) + JKE,$$

where the residual term E is given by

$$E(0, t, \boldsymbol{x}, \mathbf{R}) = \left(\frac{\mathrm{d}}{\mathrm{d}s}\varrho^0(X(0,t,\boldsymbol{x}), Y(0,s,\boldsymbol{x}, \mathbf{R})) \bigg|_{s=t} \right. \tag{3.79}$$
$$+ \sum_i a_i(\boldsymbol{x}, t)\, \frac{\mathrm{d}}{\mathrm{d}z_i}\varrho^0(X(0,t,\boldsymbol{x}), Y(0,t,\boldsymbol{z}, \mathbf{R})) \bigg|_{\boldsymbol{z}=\boldsymbol{x}}$$
$$\left. - \frac{\mathrm{d}}{\mathrm{d}\tau}\varrho^0(X(0,t,\boldsymbol{x}), Y(0,t,\boldsymbol{x}, \exp(-\tau B(\boldsymbol{\omega})) \cdot \mathbf{R})) \bigg|_{\tau=0} \right).$$

In order to show that $E \equiv 0$, we first note that since $Y \in \mathcal{SO}(3)$, the following relations hold by Lemma A.30

$$Y(0, s, \boldsymbol{x}, \mathbf{R})^T \cdot \partial_s Y(0, s, \boldsymbol{x}, \mathbf{R}) \in \mathfrak{so}(3), \quad Y(0, s, \boldsymbol{x}, \mathbf{R})^T \cdot \partial_{x_i} Y(0, s, \boldsymbol{x}, \mathbf{R}) \in \mathfrak{so}(3).$$

Using Remark A.36 this implies

$$\frac{\mathrm{d}}{\mathrm{d}s}\varrho^0(X(0,t,\boldsymbol{x}), Y(0,s,\boldsymbol{x}, \mathbf{R})) \bigg|_{s=t} = \sum_{jk\ell m}(\mathbf{B}_j)_{km}Y_{k\ell}^T\partial_s Y_{\ell m}\,\mathcal{R}\left[\mathbf{B}_j\right]|_Y(\varrho^0(X(0,t,\boldsymbol{x}), .)),$$

$$\frac{\mathrm{d}}{\mathrm{d}z_i}\varrho^0(X(0,t,\boldsymbol{x}), Y(0,t,\boldsymbol{z}, \mathbf{R})) \bigg|_{\boldsymbol{z}=\boldsymbol{x}} = \sum_{jk\ell m}(\mathbf{B}_j)_{km}Y_{k\ell}^T\partial_{x_i} Y_{\ell m}\,\mathcal{R}[\mathbf{B}_j]|_Y(\varrho^0(X(0,t,\boldsymbol{x}), .))$$

with $Y = Y(0, t, \boldsymbol{x}, \mathbf{R})$. In order to evaluate the last term in (3.79), we note that by Prop. A.20, the relation (A.10c) and the linearity of $B(.)$

$$\exp(-\tau B(\boldsymbol{\omega})) \cdot \mathbf{R} = \mathbf{R} \cdot \exp(\tau B(-\mathbf{R}^T \cdot \boldsymbol{\omega})).$$

Therefore, the chain rule of Lemma A.51 is applicable, and we find

$$\frac{\mathrm{d}}{\mathrm{d}\tau} \varrho^0(X(0,t,\boldsymbol{x}), Y(0,t,\boldsymbol{x}, \exp(-\tau B(\boldsymbol{\omega})) \cdot \mathbf{R}))\Big|_{\tau=0}$$

$$= \sum_{ijk\ell m} \left(B(-\mathbf{R}^T \cdot \boldsymbol{\omega}) : \mathbf{B}_i\right) (\mathbf{B}_j)_{km} Y_{k\ell}^T \, \mathcal{R}[\mathbf{B}_i]|_{\mathbf{R}} \, (Y_{\ell m}(0,t,\boldsymbol{x},.)) \, \mathcal{R}[\mathbf{B}_j]|_Y \, (\varrho^0(X(0,t,\boldsymbol{x}),.)) \,.$$

Using Lemma A.29, the identity $\mathbf{B}_i = B(\boldsymbol{e}_i)/\sqrt{2}$ and (A.10b), we get

$$\sum_i \left(B(-\mathbf{R}^T \cdot \boldsymbol{\omega}) : \mathbf{B}_i\right) \mathcal{R}[\mathbf{B}_i]|_{\mathbf{R}} = \sqrt{2} \sum_{ijk\ell n} R_{\ell i} R_{jk}^T \omega_k \, (\mathbf{B}_j : \mathbf{B}_i) \, (\mathbf{B}_\ell : \mathbf{B}_n) \, \mathcal{L}[\mathbf{B}_n]|_{\mathbf{R}}$$

$$= \sum_n \sqrt{2}\omega_n \, \mathcal{L}[\mathbf{B}_n]|_{\mathbf{R}} = \mathcal{L}[B(\boldsymbol{\omega})]|_{\mathbf{R}} \,.$$

Thus, combining the expressions above, the relation (3.79) is given as

$$E = \sum_{jk\ell m} (\mathbf{B}_j)_{km} Y_{k\ell}^T \, \mathcal{R}\,[\mathbf{B}_j]|_Y \, (\varrho^0(X(0,t,\boldsymbol{x}),.)) \Big(\partial_s Y_{\ell m}$$

$$+ \sum_i a_i \partial_{x_i} Y_{\ell m} - \mathcal{L}[B(\boldsymbol{\omega})]|_{\mathbf{R}} \, (Y_{\ell m}(0,t,\boldsymbol{x},.))\Big)$$

which is zero by (3.74).

In the present case, according to (3.63), $F_{1,\omega} = \boldsymbol{\omega}$ is independent of $\mathbf{R}$, thus it holds $\mathrm{div}_{\mathcal{G}}(\mathcal{L}[B(\boldsymbol{\omega})]) = 0$ and due to (3.75), $K = 1$. Moreover, the characteristic flow X is preserving Lebesgue measure if

$$0 = \nabla_{\boldsymbol{x}} \cdot \epsilon \boldsymbol{v}_1[\boldsymbol{u}_0] = \frac{2}{9}\epsilon\rho \, \mathrm{Re} \begin{cases} 0.5\|\nabla \times \boldsymbol{u}_0\|^2 - \|\mathbf{E}[\boldsymbol{u}_0]\|_F^2, & r = -1 \\ 0, & r \geq 0 \end{cases} . \qquad (3.80)$$

Thus, in case of heavy particles only if the square vorticity magnitude of the fluid is balanced by the square shear rate magnitude for all $(\boldsymbol{x},t) \in \Omega \times [0,T]$. The preservation of Lebesgue measure under $X(t,s,.)$ is a prequisite of ergodicity in space [21], which is an important assumption for the models in [119]. Another important assumption in [119] is that of a uniform distribution in space for all $t \in [0,T]$. If (3.80) holds, and if the initial particle distribution is uniform in Ω, i.e., $\varrho_0(\boldsymbol{x},\mathbf{R}) = |\Omega|^{-1}\hat{\varrho}_0(\mathbf{R})$ with the probability density function $\hat{\varrho}_0$ on $\mathcal{SO}(3)$, it stays uniform: In this case we have

$$\int_{A \times \mathcal{SO}(3)} \varrho(\boldsymbol{x},\mathbf{R},t) \, \mathrm{d}\boldsymbol{x}\mathrm{d}h(\mathbf{R}) = |\Omega|^{-1}\int_{X(t,0,X(0,t,A)) \times \mathcal{SO}(3)} \hat{\varrho}_0(Y(0,t,\boldsymbol{x},\mathbf{R})) \, \mathrm{d}\boldsymbol{x}\mathrm{d}h(\mathbf{R})$$

$$= |\Omega|^{-1}\int_{X(0,t,A) \times \mathcal{SO}(3)} \hat{\varrho}_0(Y(0,t,X(t,0,\boldsymbol{x}),\mathbf{R})) \, \mathrm{d}\boldsymbol{x}\mathrm{d}h(\mathbf{R}) = |\Omega|^{-1}\int_{X(0,t,A) \times Y(t,0,\boldsymbol{x},\mathcal{SO}(3))} \hat{\varrho}_0(Y(0,t,X(t,0,\boldsymbol{x}),\mathbf{R})) \, \mathrm{d}\boldsymbol{x}\mathrm{d}h(\mathbf{R})$$

$$= |\Omega|^{-1}\int_{X(0,t,A) \times \mathcal{SO}(3)} \hat{\varrho}_0(\mathbf{R})K(t,0,\boldsymbol{x},Y(t,0,\boldsymbol{x},\mathbf{R})) \, \mathrm{d}\boldsymbol{x}\mathrm{d}h(\mathbf{R}) = |\Omega|^{-1}\int_{X(0,t,A) \times \mathcal{SO}(3)} \hat{\varrho}_0(\mathbf{R}) \, \mathrm{d}\boldsymbol{x}\mathrm{d}h(\mathbf{R}) = |\Omega|^{-1}\int_A \mathrm{d}\boldsymbol{x}$$

where we used Theorem A.50 and the property of the determinants $J = 1 = K$.

3.5.2 Rigid ellipsoids

Stokes solutions and surface moments The ellipsoidal geometry was already discussed in Section 2.4 with details in the Appendix B.3. Here we only briefly collect the essential results. An ellipsoid is given as $\mathcal{E} = \mathbf{D}\mathcal{B}_1$ with a diagonal matrix $\mathbf{D} = \operatorname{diag}(d_1, d_2, d_3)$ with the lengths of the semi-axes given as $d_i > 0$. By using ellipsoidal coordinates we can define similarly to the case of a rigid sphere (3.62) two velocity fields $\boldsymbol{u}_{Ob}, \boldsymbol{u}_{Je}$ (due to Oberbeck [96] and Jeffery [70]) which form solutions of the homogeneous stationary Stokes equations on the exterior of $\mathcal{E}$ and fulfill boundary conditions $\boldsymbol{u}_{Ob}(\boldsymbol{y}) = \boldsymbol{v}$, $\boldsymbol{u}_{Je}(\boldsymbol{y}) = \mathbf{C} \cdot \boldsymbol{y}$ for given vector $\boldsymbol{v} \in \mathbb{R}^3$ and a trace-free matrix $\mathbf{C} \in \mathbb{R}^{3 \times 3}$ (Lemma B.11). The surface moments $\boldsymbol{t}_q, \boldsymbol{s}_q, \mathbf{V}_q$ (see Lemma 5) are then given as

$$\boldsymbol{t}_q = 3\zeta_q |\mathcal{E}| \boldsymbol{e}_q\,, \quad \boldsymbol{s}_{q+3} = \zeta_{q+3} |\mathcal{E}| (\mathbf{D}^2 - \operatorname{tr}(\mathbf{D}^2)\mathbf{I}) \cdot \boldsymbol{e}_q\,, \quad \boldsymbol{t}_{q+3} = \mathbf{0} = \boldsymbol{s}_q\,, q = 1, 2, 3\,,$$

with constants ζ_q given in Appendix B.3. The matrix A is then again given as a diagonal matrix,

$$A = \begin{bmatrix} 3|\mathcal{E}| \operatorname{diag}(\zeta_q, q = 1, 2, 3) & \\ & |\mathcal{E}| \operatorname{diag}(\zeta_{q+3}(d_q^2 - \operatorname{tr}(\mathbf{D}^2)), q = 1, 2, 3) \end{bmatrix}\,.$$

Transport operators and particle extra stress tensor Additionally, since the surface moment $\mathbf{V}_q$ fulfills

$$\mathbf{V}_q = \mathbf{0}\,, \quad \mathbf{V}_{q+3} = \zeta_{q+3} |\mathcal{E}| \mathbf{D}^2 \cdot B(\boldsymbol{e}_q) = \zeta_{q+3} |\mathcal{E}| \left[d_1^2 \boldsymbol{e}_1 \times \boldsymbol{e}_q\,, \ d_2^2 \boldsymbol{e}_2 \times \boldsymbol{e}_q\,, \ d_3^2 \boldsymbol{e}_3 \times \boldsymbol{e}_q \right]^T\,,$$

for $q = 1, 2, 3$, it holds $\boldsymbol{e}_q \cdot D_1 \boldsymbol{u}_0 = 0$, $q = 1, 2, 3$ and

$$\boldsymbol{e}_{q+3} \cdot D_1 \boldsymbol{u}_0 = (\mathbf{R}^T \cdot \partial_{\boldsymbol{x}} \boldsymbol{u}_0^T \cdot \mathbf{R}) : \mathbf{V}_{q+3} = \zeta_{q+3} |\mathcal{E}| \sum_{i,j} [\boldsymbol{p}_i \cdot \nabla](\boldsymbol{p}_j \cdot \boldsymbol{u}_0) d_i^2 (\boldsymbol{e}_i \times \boldsymbol{e}_q \cdot \boldsymbol{e}_j)$$

$$= -\zeta_{q+3} |\mathcal{E}| \sum_{i,j} d_i^2 [\boldsymbol{p}_i \cdot \nabla](\boldsymbol{p}_j \cdot \boldsymbol{u}_0) \epsilon_{qij} = -\zeta_{q+3} |\mathcal{E}| \sum_{i,j} \epsilon_{qij} d_i^2 \boldsymbol{p}_j \cdot \partial_{\boldsymbol{x}} \boldsymbol{u}_0 \cdot \boldsymbol{p}_i$$

$$= -\zeta_{q+3} |\mathcal{E}| \sum_{i,j} \epsilon_{qij} d_i^2 \boldsymbol{p}_j \cdot B(\frac{1}{2}\nabla \times \boldsymbol{u}_0) \cdot \boldsymbol{p}_i - \zeta_{q+3} |\mathcal{E}| \sum_{i,j} \epsilon_{qij} d_i^2 \boldsymbol{p}_j \cdot \mathbf{E}[\boldsymbol{u}_0] \cdot \boldsymbol{p}_i\,,$$

where we denoted the columns of the rotation matrix as $\boldsymbol{p}_i = \mathbf{R} \cdot \boldsymbol{e}_i$. By expressing the angular velocity in terms of $\boldsymbol{p}_k$, we get

$$\sum_{i,j} \epsilon_{qij} d_i^2 \boldsymbol{p}_j \cdot B\left(\frac{1}{2}\nabla \times \boldsymbol{u}_0\right) \cdot \boldsymbol{p}_i = \sum_{i,j,k} (\frac{1}{2}\nabla \times \boldsymbol{u}_0 \cdot \boldsymbol{p}_k) \epsilon_{qij} \epsilon_{kij} d_i^2$$

$$= \sum_{i,k} (\frac{1}{2}\nabla \times \boldsymbol{u}_0 \cdot \boldsymbol{p}_k)(\delta_{qk}\delta_{ii} - \delta_{qi}\delta_{ik}) d_i^2 = \boldsymbol{e}_q \cdot (\operatorname{tr}(\mathbf{D}^2)\mathbf{I} - \mathbf{D}^2) \cdot \mathbf{R}^T \cdot \frac{1}{2}\nabla \times \boldsymbol{u}_0 =: \boldsymbol{e}_q \cdot \widetilde{\boldsymbol{\omega}}_0\,.$$

On the other hand, it holds

$$\sum_{i,j,q} \boldsymbol{e}_q \epsilon_{qij} d_i^2 \boldsymbol{p}_j \cdot \mathbf{E}[\boldsymbol{u}_0] \cdot \boldsymbol{p}_i = \begin{bmatrix} d_2^2 - d_3^2 & & \\ & d_3^2 - d_1^2 & \\ & & d_1^2 - d_2^2 \end{bmatrix} \cdot \begin{pmatrix} \boldsymbol{p}_3 \cdot \mathbf{E}[\boldsymbol{u}_0] \cdot \boldsymbol{p}_2 \\ \boldsymbol{p}_1 \cdot \mathbf{E}[\boldsymbol{u}_0] \cdot \boldsymbol{p}_3 \\ \boldsymbol{p}_2 \cdot \mathbf{E}[\boldsymbol{u}_0] \cdot \boldsymbol{p}_1 \end{pmatrix} =: \widehat{\boldsymbol{\omega}}_0\,.$$

Finally, $D_1 \boldsymbol{u}_0 = (\boldsymbol{0}, -|\mathcal{E}| \operatorname{diag}(\zeta_{q+3}, q = 1, 2, 3) \cdot (\widetilde{\boldsymbol{\omega}}_0 + \widehat{\boldsymbol{\omega}}_0))$ follows. The term F_1 is then given as

$$F_1 = (\boldsymbol{v}_1, \frac{1}{2}\nabla \times \boldsymbol{u}_0 + \mathbf{R} \cdot (\operatorname{tr}(\mathbf{D}^2)\mathbf{I} - \mathbf{D}^2)^{-1} \cdot \widehat{\boldsymbol{\omega}}_0) \tag{3.81}$$

with $\boldsymbol{v}_1 \equiv \boldsymbol{0}$ for $r \geq 0$ and $\boldsymbol{v}_1 = \rho \operatorname{Re} \mathbf{R} \cdot \operatorname{diag}(\zeta_q^{-1}, q = 1, 2, 3) \cdot \mathbf{R}^T \cdot (\mathrm{D}_t \boldsymbol{u}_0 - \operatorname{Fr}^{-2} \boldsymbol{e}_g)/3$ for heavy particles. It is not hard to see that we recover F_1 for rigid spheres, if $d_1 = d_2 = d_3$. The boundary velocity then follows as

$$\boldsymbol{U}_{\mathrm{loc},1,\partial\mathcal{E}} = \mathbf{R}^T \cdot \boldsymbol{v}_1 + \left(B((\operatorname{tr}(\mathbf{D}^2)\mathbf{I} - \mathbf{D}^2)^{-1} \cdot \widehat{\boldsymbol{\omega}}_0) - \mathbf{R}^T \cdot \mathbf{E}[\boldsymbol{u}_0] \cdot \mathbf{R} \right) \cdot \boldsymbol{y}$$
$$= \mathbf{R}^T \cdot \boldsymbol{v}_1 + \mathbf{A}_1 \cdot \boldsymbol{y},$$

with the matrix $\mathbf{A}_1$ given as

$$\mathbf{A}_1 = \begin{bmatrix} -\boldsymbol{p}_1 \cdot \mathbf{E}[\boldsymbol{u}_0] \cdot \boldsymbol{p}_1 & -\frac{2d_1^2}{d_1^2+d_2^2}\boldsymbol{p}_1 \cdot \mathbf{E}[\boldsymbol{u}_0] \cdot \boldsymbol{p}_2 & -\frac{2d_1^2}{d_3^2+d_1^2}\boldsymbol{p}_1 \cdot \mathbf{E}[\boldsymbol{u}_0] \cdot \boldsymbol{p}_3 \\ -\frac{2d_2^2}{d_1^2+d_2^2}\boldsymbol{p}_2 \cdot \mathbf{E}[\boldsymbol{u}_0] \cdot \boldsymbol{p}_1 & -\boldsymbol{p}_2 \cdot \mathbf{E}[\boldsymbol{u}_0] \cdot \boldsymbol{p}_2 & -\frac{2d_2^2}{d_2^2+d_3^2}\boldsymbol{p}_2 \cdot \mathbf{E}[\boldsymbol{u}_0] \cdot \boldsymbol{p}_3 \\ -\frac{2d_3^2}{d_3^2+d_1^2}\boldsymbol{p}_3 \cdot \mathbf{E}[\boldsymbol{u}_0] \cdot \boldsymbol{p}_1 & -\frac{2d_3^2}{d_2^2+d_3^2}\boldsymbol{p}_3 \cdot \mathbf{E}[\boldsymbol{u}_0] \cdot \boldsymbol{p}_2 & -\boldsymbol{p}_3 \cdot \mathbf{E}[\boldsymbol{u}_0] \cdot \boldsymbol{p}_3 \end{bmatrix}.$$

Analogously to the case of rigid spheres, the boundary velocity is given by a constant (in $\boldsymbol{y}$) and linear velocity. Thus, the local velocity field $\boldsymbol{U}_{\mathrm{loc},1}$ is given by the linear combination of the Oberbeck and Jeffery solutions given in Lemma B.11 in Appendix B.3 with the corresponding velocity components given by $\mathbf{R}^T \cdot \boldsymbol{v}_1 = \mathbf{R}^T \cdot \boldsymbol{v}_1(\boldsymbol{c}, \mathbf{R}, t)$ and $\mathbf{A}_1 = \mathbf{A}_1(\boldsymbol{c}, \mathbf{R}, t)$. This yields the following relation that can be computed by means of the techniques provided in Appendix B.3,

$$\int_{\partial\mathcal{E}} \mathbf{S}_{\boldsymbol{y}}[\boldsymbol{U}_{\mathrm{loc},1}[\boldsymbol{u}_0]] \cdot \boldsymbol{n} \otimes \boldsymbol{y} - \boldsymbol{U}_{\mathrm{loc},1}[\boldsymbol{u}_0] \otimes \boldsymbol{n} - \boldsymbol{n} \otimes \boldsymbol{U}_{\mathrm{loc},1}[\boldsymbol{u}_0]\mathrm{d}s$$
$$= |\mathcal{E}| \left(\frac{8}{\delta}\mathbf{M} - 4(\mathbf{M} : \operatorname{diag}(\alpha_1^o, \alpha_2^o, \alpha_3^o))\mathbf{I} \right), \tag{3.82}$$

where $\delta = d_1 d_2 d_3$. For the definition of the geometry dependent scalars α_i^o and matrix $\mathbf{M}$ we refer to Appendix B.3.

Prolate ellipsoids In the general case (3.82) admits no further simplifications, but for prolate ellipsoids the lengths of the semi axes satisfy $d_1 > d_2 = d_3 > 0$, which leads to a much simpler form of (3.82) and thus, $\boldsymbol{\Sigma}_0^p$. As introduced in Section 2.4.2, we use the aspect ratio $a_r = d_1/d_2 > 1$ and the parameter $\nu = (a_r^2 - 1)(a_r^2 + 1)^{-1}$ in this case. Then F_1 becomes

$$F_1 = (\boldsymbol{v}_1, \frac{1}{2}\nabla \times \boldsymbol{u}_0 + \nu \boldsymbol{p}_1 \times \mathbf{E}[\boldsymbol{u}_0] \cdot \boldsymbol{p}_1),$$

now carrying the Jeffery-velocity term, see Remark 10. As for the term associated with the particle-stresses $\boldsymbol{\Sigma}_0^p$ given (3.82), it can be shown by a technical but straight forward calculation [116] that

$$\frac{4}{\delta}\mathbf{R} \cdot \mathbf{M} \cdot \mathbf{R}^T = a_1 \boldsymbol{p}_1 \otimes \boldsymbol{p}_1 \otimes \boldsymbol{p}_1 \otimes \boldsymbol{p}_1 : \mathbf{E}[\boldsymbol{u}_0] + a_2(\boldsymbol{p}_1 \otimes \boldsymbol{p}_1 \cdot \mathbf{E}[\boldsymbol{u}_0] + \mathbf{E}[\boldsymbol{u}_0] \cdot \boldsymbol{p}_1 \otimes \boldsymbol{p}_1)$$
$$+ a_3 \mathbf{E}[\boldsymbol{u}_0], \tag{3.83}$$

with $\delta = d_1 d_2^2$ and the geometry dependent constants a_i given in Abbreviation 47 (cf. Appendix B.3).

Abbreviation 47 (Geometrical parameters for ellipsoidal geometry). *The geometrical parameters a_1, a_2, a_3 of (3.83) are given as (cf. [50, 101])*

$$a_1 = \frac{4}{d_1 d_2^2}\left(\frac{\gamma_1^o}{4\gamma_2^o \beta_1^o d_2^2} - 2b_1 - b_2\right), \quad a_2 = \frac{4b_1}{d_1 d_2^2}, \quad a_3 = \frac{4b_2}{d_1 d_2^2}$$

in terms of the following quantities

$$b_1 = \frac{a_r^2(2a_r^2\theta - \theta - 1)}{2d_1 d_2^2(a_r^4 - 1)\beta_2^o(d_2^2\alpha_2^o + d_1^2\alpha_1^o)} - b_2, \qquad b_2 = \frac{1}{4\beta_1^o d_2^2},$$

$$\theta = \frac{1}{2a_r(a_r^2 - 1)^{1/2}}\ln\frac{a_r + (a_r^2 - 1)^{1/2}}{a_r - (a_r^2 - 1)^{1/2}},$$

$$\alpha_1^o = \frac{1}{d_1 d_2^2}\frac{2}{a_r^2 - 1}\left(a_r^2\theta - 1\right), \qquad\qquad \alpha_2^o = \frac{1}{d_1 d_2^2}\frac{a_r^2}{a_r^2 - 1}\left(-\theta + 1\right),$$

$$\beta_1^o = \frac{1}{d_1 d_2^4}\frac{a_r^2}{4(a_r^2 - 1)^2}\left(3\theta + 2a_r^2 - 5\right), \qquad \beta_2^o = \frac{1}{d_1 d_2^4}\frac{1}{(a_r^2 - 1)^2}\left(-3a_r^2\theta + a_r^2 + 2\right),$$

$$\gamma_1^o = \frac{1}{d_1 d_2^2}\frac{a_r^2}{4(a_r^2 - 1)^2}\left(-(4a_r^2 - 1)\theta + 2a_r^2 + 1\right), \quad \gamma_2^o = \frac{1}{d_1 d_2^2}\frac{a_r^2}{(a_r^2 - 1)^2}\left((2a_r^2 + 1)\theta - 3\right).$$

The isotropic part in (3.82), ($\mathbf{M} : \text{diag}(\alpha_1^o, \alpha_2^o, \alpha_3^o)$) can be analogously expressed in terms of $\boldsymbol{p}_1$ and $\mathbf{E}[\boldsymbol{u}_0]$. But since it forms a scalar function depending on $\boldsymbol{c}, \mathbf{R}, t$, entering the system by its spatial gradient, we can shift the isotropic part into the pressure of the Newtonian stresses as already done in Remark 33 with the local pressures. Using (3.82) and (3.83) in the expression of the particle extra stresses in Abbreviation 35, we find

$$\begin{aligned}
\boldsymbol{\Sigma}_0^p[\psi, \boldsymbol{u}](\boldsymbol{x}, t) &= 2|\Omega| \int_{\mathcal{SO}(3)} a_1 \boldsymbol{p}_1 \otimes \boldsymbol{p}_1 \otimes \boldsymbol{p}_1 \otimes \boldsymbol{p}_1 : \mathbf{E}[\boldsymbol{u}_0](\boldsymbol{x}, t) \\
&\quad + a_2(\boldsymbol{p}_1 \otimes \boldsymbol{p}_1 \cdot \mathbf{E}[\boldsymbol{u}_0](\boldsymbol{x}, t) + \mathbf{E}[\boldsymbol{u}_0](\boldsymbol{x}, t) \cdot \boldsymbol{p}_1 \otimes \boldsymbol{p}_1) + a_3 \mathbf{E}[\boldsymbol{u}_0](\boldsymbol{x}, t)\, \mathrm{d}\psi_{\boldsymbol{x}} \\
&= 2|\Omega|\Big(a_1 \mathbb{E}[\boldsymbol{p}_1 \otimes \boldsymbol{p}_1 \otimes \boldsymbol{p}_1 \otimes \boldsymbol{p}_1] : \mathbf{E}[\boldsymbol{u}_0] \\
&\quad + a_2(\mathbb{E}[\boldsymbol{p}_1 \otimes \boldsymbol{p}_1] \cdot \mathbf{E}[\boldsymbol{u}_0] + \mathbf{E}[\boldsymbol{u}_0] \cdot \mathbb{E}[\boldsymbol{p}_1 \otimes \boldsymbol{p}_1]) + a_3\mathbf{E}[\boldsymbol{u}_0]\Big)(\boldsymbol{x}, t)
\end{aligned}$$

with $\mathbb{E}$ denoting the expectation with respect to the marginal probability $\psi_{\boldsymbol{x}, t}$ on $\mathcal{SO}(3)$. It should be noted that $\mathbb{E}[.] = \mathbb{E}[.](\boldsymbol{x}, t)$ as $\psi_{\boldsymbol{x}, t}$ is depending on the position and time. In case of a uniform particle distribution in space we get the well-known form of the particle-stresses (e.g., see [81]) as stated in the following corollary.

Corollary 48. *Let the assumptions of Corollary 42 hold and $\mathcal{E} = \mathbf{D}\mathcal{B}_1$ with $\mathbf{D} = \text{diag}(d_1, d_2, d_2)$, $d_i > 0$. Then the momentum equation for the fluid (3.55a) reads as*

$$\begin{aligned}
\text{Re}\,\mathrm{D}_t \boldsymbol{u}_0 &= (1 + \phi_\epsilon(\rho_\epsilon - 1))\nabla \cdot \mathbf{S}[\boldsymbol{u}_0] + 2\phi_\epsilon \nabla \cdot \widetilde{\boldsymbol{\Sigma}} + \text{Re}\,\text{Fr}^{-2}\boldsymbol{e}_g \\
&\quad + 2\epsilon^{3/2}\nabla \cdot \mathbf{E}[\widetilde{U}_0[\psi_t, \boldsymbol{u}_0]] - \epsilon^{4/3}\,\text{Re}\,\nabla \cdot \widetilde{\mathbf{H}}_0[\psi_t, \boldsymbol{u}_0],
\end{aligned}$$

where the stress tensor is given by

$$\begin{aligned}
\widetilde{\boldsymbol{\Sigma}}(\boldsymbol{x}, t) &= a_1 \mathbb{E}[\boldsymbol{p}_1 \otimes \boldsymbol{p}_1 \otimes \boldsymbol{p}_1 \otimes \boldsymbol{p}_1] : \mathbf{E}[\boldsymbol{u}_0](\boldsymbol{x}, t) \\
&\quad + a_2(\mathbb{E}[\boldsymbol{p}_1 \otimes \boldsymbol{p}_1] \cdot \mathbf{E}[\boldsymbol{u}_0](\boldsymbol{x}, t) + \mathbf{E}[\boldsymbol{u}_0](\boldsymbol{x}, t) \cdot \mathbb{E}[\boldsymbol{p}_1 \otimes \boldsymbol{p}_1]) + a_3\mathbf{E}[\boldsymbol{u}_0](\boldsymbol{x}, t),
\end{aligned}$$

with constants a_i given in Abbreviation 47.

Remark 49 (Quadratic decay and transport equation).

1) *Similarly to Remark 45 we find from (3.81) and Lemma B.11 that for normal and light-weighted particles the local velocity $\boldsymbol{U}_{\text{loc},1}$ decays as $\|\boldsymbol{y}\|^{-2}$. Hence the chaos assumption is not needed for Theorem 36 to hold.*

2) *In order to illustrate the transport equation (3.55c) in case of normal or light-weighted particles, we use an analogous problem to the one in Remark 46. Thus, we consider for the system (3.65) with $\boldsymbol{a}(\boldsymbol{x},t) = \boldsymbol{u}_0(\boldsymbol{x},t)$ and $\boldsymbol{\omega}(\boldsymbol{x},\mathbf{R},t) = 0.5\nabla \times \boldsymbol{u}_0(\boldsymbol{x},t) + \nu \boldsymbol{p}_1 \times \mathbf{E}[\boldsymbol{u}_0](\boldsymbol{x},t) \cdot \boldsymbol{p}_1$, the corresponding characteristic flows $X(t,s,\boldsymbol{x})$ in Ω and $Y(t,s,\boldsymbol{x},\mathbf{R})$ on $\mathcal{SO}(3)$ as well as the combined flow $Z(t,s,(\boldsymbol{x},\mathbf{R}))$ are defined analogously to Remark 46. As we allowed $\boldsymbol{\omega}$ to depend on $\mathbf{R}$ in Remark 46, we immediately find that the push-forward measure of $\psi_t(.) = \psi_0 \circ Z(t,0,.)^{-1}$ is a weak solution to (3.55c) and indeed fulfills $\psi_t(\Omega \times \mathcal{SO}(3)) = 1$. Additionally, if ψ_t is absolutely continuous with respect to the product of Lebesgue and Haar measure, then its density ϱ solves (3.55c) in the strong sense and is given in terms of the initial condition, the characteristic flow Z and the determinants of the Jacobians of X and Y, J respectively K. Since $\nabla_{\boldsymbol{x}} \cdot \boldsymbol{u}_0 = 0$, $J \equiv 1$ but in contrast to the case of Remark 46 as $\boldsymbol{\omega}$ depends on $\boldsymbol{p}_1 = \mathbf{R} \cdot \boldsymbol{e}_1$*

$$
\begin{aligned}
\text{div}_{\mathcal{G}}(\mathcal{L}[B(\boldsymbol{\omega})]) &= -\sum_{ijm} \left(\frac{\partial}{\partial R_{j1}} \omega_i \right) \epsilon_{jim} R_{m1} \\
&= -\nu \sum_{ijm} \epsilon_{ij\ell}(\mathbf{E}[\boldsymbol{u}_0])_{\ell n} R_{n1} \epsilon_{jim} R_{m1} + \epsilon_{in\ell}(\mathbf{E}[\boldsymbol{u}_0])_{\ell j} R_{n1} \epsilon_{jim} R_{m1} \\
&= 3\nu \boldsymbol{p}_1 \cdot \mathbf{E}[\boldsymbol{u}_0] \cdot \boldsymbol{p}_1 \neq 0
\end{aligned}
$$

if the shear rate is not zero and thus, $K \neq 1$ in general.

In case of heavy particles the velocity $\boldsymbol{v}_1$ depends also on the rotation $\mathbf{R}$, implying that X and Y are mutually coupled. Hence, Z is still a one-to-one characteristic flow on $\Omega \times \mathcal{SO}(3)$, but in order to derive similar conditions to (3.80) for the preservation of Lebesgue measure, the approach of Remark 46 must be extended to contribute for the additional coupling, which we not pursue at this point.

3.6 Conclusion

Our aim was to derive an approximation of the full deterministic suspension system (3.1). The latter models N_ϵ small particles suspended in an incompressible Newtonian carrier fluid, which interact only through the fluid medium. The fluid itself is influenced by the particle presence as free fluid flow is only possible in the fluid domain Ω_ϵ, while the velocity in the particle domain, $\Omega \backslash \Omega_\epsilon$, is restricted by the condition of rigid body motion. The approximation presented, as summarized in Theorems 36, 38, 40 and Corollaries 42, 44, 48, consists of a momentum equation for the effective fluid in Ω which contains the particle effects as additional force terms and describes the particle motion by the corresponding continuity equation on the particle phase space $\Omega \times \mathcal{SO}(3)$. The model accounts not only for small particle inertia, that is modeled by an appropriate choosing of the density scaling function introduced in the one-particle model in Section 2.12, but also for particle interaction.

The foundation of the model is an extension of the asymptotic approach presented in [71], i.e., an expansion of the involved unknowns in the particle size ratio ϵ. In order to justify the expansion in case of the fluid quantities, we assume that the fluid flow is essentially undisturbed by the particles. Thus, we presume a global and a local contribution, the latter is generated by the particle presence and lies in $\mathcal{O}(\epsilon)$. Moreover, by assuming a dilute or semi-dilute suspension, a terminology that describes whether the hydrodynamic particle interaction is of order $\mathcal{O}(\epsilon)$ (dilute) or of $\mathcal{O}(1)$ (semi-dilute), complemented by a minimal distance assumption we are able to consider the local part as a superposition of each particle contribution. Using the resulting ansatz in the full problem (3.1), we find a suitable system of equations which describes the particle motion, given the global velocity is sufficiently smooth (Lemma 19, Remark 20). This immediately leads to the approximation of the full system if the global fluid flow is given by a smooth Navier-Stokes solution (Theorem 21). Both results hold for heavy particles under the condition that the particle number is chosen accordingly. In the heavy particles regime, this condition allows only a constant particle number as $\epsilon \to 0$. In order to circumvent this fact, we discuss the assumption of a chaotic particle distribution in space, which is characterized by presuming that the interaction terms are sufficiently smooth (Remark 24). At this point we have an approximation of the full problem which consists of the incompressible Navier-Stokes equations in space and a large system of equations which describe the motion of each particle and its local contribution to the overall fluid flow.

In order to get a model of the suspension as a homogeneous medium, we apply a mean field approach similar to [20, 53]. More precisely: by using the empirical measure for the particle positions and rotations, we identify the equations of motion of the particles as characteristics of a continuity equation for the empirical measure (Lemma 27) with advection operators of integro-differential kind that depend on the measure itself as well as on the global velocity and pressure. Similarly, we can also interpret the superposition of the local particle contributions to the overall velocity and pressure as an integral operator depending on the empirical measure as well as on the global quantities. Plugging the original expansion into the fluid momentum equation and expressing the resulting terms as the corresponding integral operators results in integro-differential operators in the momentum equation for the global fluid velocity. The transport operators in the continuity equation for the measure as well as the operators in the momentum equation for the global velocity can be extended onto a class of more regular Borel measures (Lemma 28, Lemma 31, Remark 29, Remark 30). Additionally, we approximate (Lemma 32, Remark 33, Remark 34) some of the operators in the $\mathcal{L}^2$ norm in order to get more regular force terms which still encompass the macroscopic effects of the suspension. This leads then to the complete macroscopic description in Theorem 36 which consists of a modified Navier-Stokes system for the fluid velocity and a continuity equation for the probability measure of the particle phase space, which consists of position in space and orientation in the special orthogonal group. The connection to the original problem is established by assuming that there exists an empirical measure such that its Wasserstein distance to the regular probability measure is small.

We showed that this approach leads to similar results as in our previous work [119], which heavily relies on the ergodicity of the suspension in space (Corollary 42, Remark 43), an assumption which is not needed in the presented approach here. This

also implies that the momentum equation for the fluid velocity in our model includes the well-known viscosity increase found by Einstein [42] as well as the particle extra stress tensor due to Bachelor [12]. This is illustrated by applying our model to rigid spheres (Corollary 44) and prolate ellipsoids (Corollary 48).

There are different limitations of the approach. The first being the chaos assumption which is necessary in case of heavy particles (Theorem 38) and in case of the $\mathcal{O}(\epsilon^2)$ approximation of the suspension of normal or light-weighted particles (Theorem 40). This assumption essentially ensures that the superposition of local particle velocities scaled by the large factor ϵ^{-1} is still bounded independent of ϵ. As discussed in Remark 24 and Remark 37 we can not mitigate this requirement as otherwise either the approximation property of the continuum model (Theorem 38, 40) or the well-definition of the particle equations (Lemma 19) is lost. It is hard to check, whether a given particle configuration fulfills (3.36), and, moreover, does it for all $t \in [0, T]$, especially considering that we allow for small particle inertia. The minimal distance assumption (Assumption 15, 3)) leads to a similar problem. As we assume that the particles are always sufficiently separated, we are able to use simple Stokes solutions in order to approximate the generated velocity fields. Both of these assumptions are due to the chosen ansatz for the local velocity induced by the particle presence. In order to circumvent them, one could study a partition of the domain, where in each subdomain a sufficiently small number of interacting particles is present, while the interaction of the subdomains is modeled by an effective law. The next limitation is the assumption on the Wasserstein distance between the regular Borel measure of the continuus model and a suitable empirical measure, which is needed in order to connect the continuum model (3.55) to the full model (3.1) and, thus, establish the approximation property. We note, that in this work we assume this distance being small for all $t \in [0, T]$. In similar problems it is possible to show that the distance for $t > 0$ is controllable by the initial distance. As a consequence, the empirical measure then converges in the weak topology of measures to the measure of the continuum model as $N_\epsilon \to \infty$, [53]. This then results in the easier problem of checking the assumption for the initial configuration. The extension of the corresponding results to the product space $\Omega \times \mathcal{SO}(3)$ would directly lead to an analogous result in our context. However, as the study of this non-trivial problem does not fit the context of the present thesis, we omit it to a possible later work.

Other limitations in the present work are less severe. We considered here only particles of the same shape. Each operator in the equations of the continuum model which depends on the particle shape is essentially defined as a sum over all particles in the domain. In case of particles of different kind, we can partition the summation into parts belonging to each species and hence write the corresponding operator as an integral with respect to the probability measure belonging to the corresponding particle type. This leads to a system of continuity equations coupled by interaction terms with each other and also with a Navier-Stokes like equation similar to the presented one in this work. Another limitation is that of deterministic forces. As mentioned in the introduction of this chapter, the motion of the particles might be perturbed by effects on much smaller scales which are modeled as stochastic forces. In our context this would imply that the particle equations of motion in Lemma 19 have noisy linear and angular velocities, i.e., the equations of motions become stochastic differential equations. As the equations of motion play the role of characteristics of the continuity

equation for the probability measure, we get in case of stochastic differential equations instead a Fokker-Planck equation for the description of the probability measure [26, 31]. Additionally, the noise also enters the momentum balance of the fluid.

The novelty of this work lies in the generalization of classical suspension descriptions to the case of a non-homogeneous, non-ergodic dilute suspension of orientable small tracer particles in a bounded domain. Unlike in classical approaches we persued the approximation of the deterministic multi particle system which is coupled to the Navier-Stokes equations and paid attention to the hydrodynamic particle interaction. We also discussed, how to classify different concentration regimes in the asymptotical deterministic context and explored, to what degree we can extend our results to the semi-dilute concentration regime. Additionally, we allowed the particle density to differ significantly from the fluid density in the asymptotical context and were therefore able to account for small effects of particle inertia. We point out, that in all of our considerations the particles still essentially follow the streamlines of the surrounding flow. Thus, their motion is completely determined by the velocity of the carrier fluid and so is their retroactive effect on the fluid. This implies that we do not have a Brinkman like force term in the momentum equation as, for example, in [20] or [49] which persue similar approaches, but where the particle motion can differ significantly from the fluid flow. Nonetheless, we find that the impact of the depicted small inertia and of interaction is at least of the same asymptotical order as the classical particle extra stress tensor found by Batchelor in [12]. Therefore, our model is only applicable to the case of nearly inertialess particles. If inertia plays a more important role, Brinkman like models as in [20, 49] are more suitable. In the latter case the momentum equation for the fluid has to be coupled to a homogenized momentum equation for the particle impulse, according to the actio-reactio principle of Newton, as, e.g., carried out in [28] for fibers. Then both equations must be coupled to a continuity equation for the particle phase space, consisting of the position, momentum and, possibly, rotation and angular momentum.

4 Numerics of stochastic fiber dynamics

4.1 Introduction

Non-woven fabric materials appear in many applications and products for personal, medical as well as industrial use. Examples are filters for respiration masks, wipes, absorbent hygiene products, surgical gowns or face masks, wound dressings, support and insulation layers in mattresses, insulation panels or fire-blockers, but also engine fuel filters or light-weight and durable interior parts of cars [25, 32]. The production methods of the corresponding materials depend on the particular application [100, 122], one of which being the air-lay process. In the latter, numerous short fibers are inserted into a turbulent air flow, which entangles them and transports them onto a perforated conveyor belt, where a random, three-dimensional web is formed. The resulting mat is then subjected to additional steps, such as thermobonding in order generate the final material [54]. The material properties of the resulting product depend strongly on the micro-structure generated during the fiber lay down. The ability to predict the material properties by a numerical simulation of such production processes [19, 54, 73, 92] enables the manufacturers to optimize their product in a very cost and time efficient way. Such simulations often demand fast and accurate numerical computations of a large number of fibers moving in a turbulent air flow, possibly interacting with each other and influencing the carrier fluid. It is therefore of great interest, how the necessary computational costs in the fiber simulation might be decreased.

The fiber in the sketched air-lay process typically has a length ℓ of a few centimeters, a diameter d at the scale of micrometers and is made of wool or polyester. Since it is also subjected to turbulence, its motion can be described by the dynamics of a stochastic fiber which is thin and elastic [54]. Due to the slenderness of the fiber ($\epsilon = d/\ell \ll 1$), it can be modeled as an inextensible, one-dimensionally parametrized elastic beam. Thus, the resulting momentum equation for the fiber is a stochastic partial differential algebraic equation (SPDAE) for the parametrized fiber position in the Euclidean space. It can be viewed as a reformulation of the Kirchhoff-Love equations [78] that describe the asymptotic limit model of an elastic Euler-Bernoulli rod as ϵ and the Mach number (ratio between fiber velocity and typical speed of sound) approach zero [14]. Rigorous derivations of such inextensible Kirchhoff beam models from three-dimensional hyper-elasticity can be found in [29, 95]. The solvability of extensible stochastic beam equations is studied in, e.g., [13, 23, 31]. Deterministic inextensible fiber models are investigated in [38, 56, 97, 102] analytically and numerically. Deterministic elastic flows of constrained curves in different model variants are also a topic of recent numerical investigations, see [7, 9, 10, 33]. An error analysis for a spatially semi-discrete scheme is performed for closed parametrized curves with preservation of the global length in [33]. A fully implicit finite element method with

equidistribution of vertices is explored in [7]. Curves with local length preservation are handled in [9, 10] by employing a temporal semi-discretization and studying the resulting sequence of partial differential equations in space. A rigorous convergence analysis for this setting can be found in [56]. A framework for the rigorous formulation and analysis of the spatially semi-discrete inextensible stochastic beam model accompanied by the proof of existence and uniqueness of a global strong solution is given in [84], where we contributed numerical studies to the analytical investigations.

We aim for the reduction of computational costs in the simulation of a stochastic inextensible fiber. In order to achieve this goal, we investigate three possible techniques. The first one is a predictor-corrector method, where the solution to the implicit Euler time integration step is predicted by a different, inexpensive scheme. This leads to a reduction of needed Newton iterations in each step and hence to a reduction of overall computational time. The second technique is the replacement of the underlying white noise by a correlated noise process. The correlation is carried out by different methods, which are characterized as a direct smoothing of the corresponding Wiener process. This leads to a more regular force term, slightly reducing the needed computational time, while still generating suitable approximations of the mean of the fiber position. Finally, we also apply the Wiener chaos expansion [44] to the constrained fiber model, which separates the stochastic and deterministic influences, allowing a nearly instant generation of stochastic realizations and directly generating the mean of the solution components. The novelty of the present work is the study of explicit estimators in the simulation of stochastic inextensible fiber models, the extension of the correlation methods for the white noise and the study of their impact on the solution of spatially semi-discretized SPDAE and the derivation of the Wiener chaos expansion for the constrained SPDE with an inextensibility constraint.

This chapter is mainly based on the preliminary works [120] and [84]. It is structured as follows: in the spirit of Section 2.2 and 3.2 we first derive the mathematical model for the deterministic fiber in Section 4.2.1 starting from a general system of equations which describe a special Cosserat rod following [90]. Here we also introduce the characteristic quantities of the resulting system and formulate the dimensionless partial differential equation. In Sec. 4.2.2, we introduce the model for the stochastic force, which is a simplified model motivated by [90]. In Sec. 4.2.3 we then present the used spatial semi-discretization, which is based on a finite volume discretization of the one-dimensionally parametrized fiber combined with finite differences on a staggered grid, which allows small discretization stencils. We also state the rigorous meaning of the semi-discretized stochastic system following [84] in terms of a manifold-valued Itô-type stochastic differential equation. Afterwards, in Sec. 4.2.4 we discuss the typical parameters of the air-lay process setting given in [54], which forms the basis for the parameter choice in the numerical experiments. In Sec. 4.3 we present the used time integration schemes for the semi-discretized system as well as the predictor methods for the implicit Euler method. The two presented methods are derived from the explicit Euler method on the one hand and from the Lobatto IIIA-IIIB pair on the other. Section 4.4 is dedicated to the introduction of the different smoothing techniques of the white noise (Sec. 4.4.1), which are partly discussed in [16], as well as for the Wiener chaos expansion (Sec. 4.4.2), which was studied for the stationary, extensible and inertialess fiber in [16]. The numerical investigations are collected in Sec. 4.5, where we first validate the convergence behavior of the different integration schemes
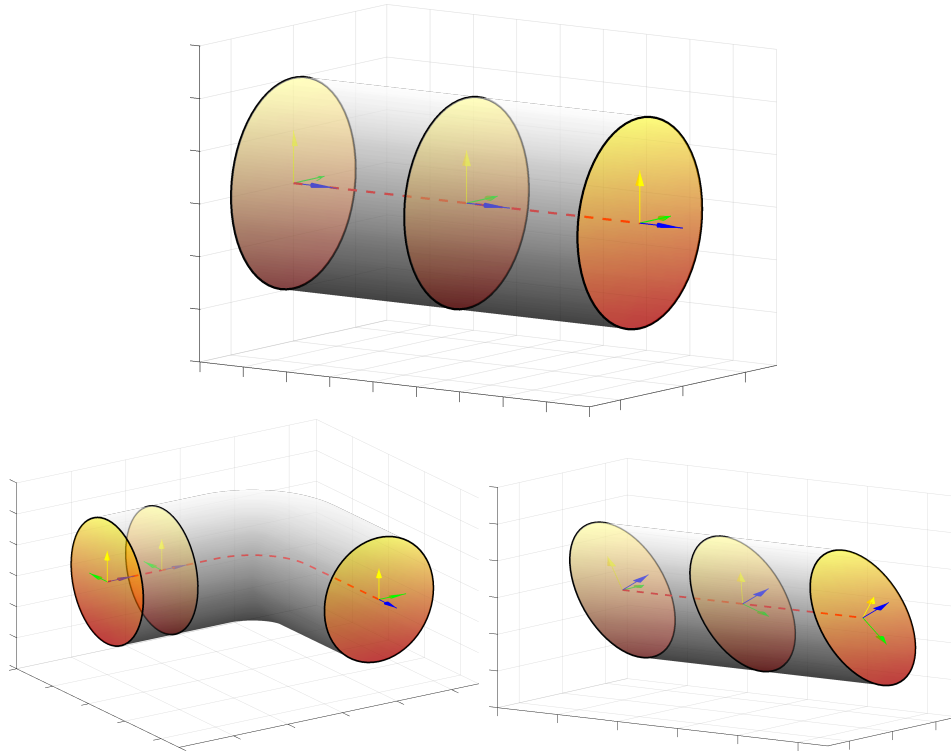
Figure 4.1.: A special Cosserat rod in reference state (top), subject to dilatation and flexure (bottom left) and subject to shear and torsion (bottom right). The rod is parametrized by the centerline $\boldsymbol{r}$ (red, dashed) and its cross sections (here at $s = 0, s = \ell/2, s = \ell$), which are characterized by the family of director triads $\boldsymbol{d}_1, \boldsymbol{d}_2, \boldsymbol{d}_3$ (green, yellow and blue arrows respectively).

and discuss the solution behavior under the chosen benchmark scenarios (Sec. 4.5.1 and Sec. 4.5.2). The validation of the integration schemes in the stochastic case is carried out in Sec. 4.5.3. Thereafter, in Sec. 4.5.4 we study the different predictors to the implicit Euler scheme, in Sec. 4.5.5 the smoothing techniques and in Sec. 4.5.6 the results of the Wiener chaos, which we apply to a model with a simplified, Stokes-like air-drag model. Finally, in Sec. 4.6 we discuss the results of our simulation results.

4.2 Elastic fiber

In this section we first present the model of the deterministic elastic fiber following [90]. Then we modify the fiber dynamics by adding noise in Sec. 4.2.2 and, after the presentation of the spatial semi-discretization in Sec. 4.2.3, discuss the typical parameter setting in case of an air-lay process in Sec. 4.2.4.

4.2.1 Deterministic model

The dynamics of an elastic fiber can be described using the Kirchhoff-Love theory for Cosserat rods [78, 90], which allows flexure, torsion and shear of the body. This model uses a one dimensional parametrization of the rod by a time-dependent centerline $\boldsymbol{r}(s,t) \in \mathbb{R}^3$, $(s,t) \in [0,\ell] \times [0,T]$, and by a description of each (rigid) cross section in terms of a family of local orthonormal directors $[\boldsymbol{d}_1, \boldsymbol{d}_2, \boldsymbol{d}_1 \times \boldsymbol{d}_2](s,t) = \mathbf{R}(s,t) \in \mathcal{SO}(3)$.

Thus, in case of circular cross sections of constant diameter d, each point of the body is given as $\boldsymbol{z}(\boldsymbol{y}, s, t) = \boldsymbol{r}(s, t) + \mathsf{R}(s, t) \cdot \boldsymbol{y}$ for $\boldsymbol{y} \in \$_{d/2}^1$, see Fig. 4.1. The dynamics of the rod of constant density ρ, given by the linear and angular momentum balance, then simplify to a second order partial differential system of equations for $\boldsymbol{r}$ and R

$$\rho A \partial_{tt} \boldsymbol{r} = \partial_s \boldsymbol{q} + \boldsymbol{f} \,, \quad \rho I \sum_{i=1}^{2} (\partial_{tt} \boldsymbol{d}_i \times \boldsymbol{d}_i) = \partial_s \boldsymbol{m} + \partial_s \boldsymbol{r} \times \boldsymbol{q} + \boldsymbol{\ell}$$

with an outer line force $\boldsymbol{f}$ and an outer line torque* $\boldsymbol{\ell}$. The system is closed by constitutive laws for the inner forces $\boldsymbol{q}$ and moments $\boldsymbol{m}$. The term A denotes the cross-sectional area, $A = \pi d^2/4$ and $I = \pi d^4/64$ the moment of inertia. In case of a long, slender fiber, i.e., $\epsilon = d/\ell \ll 1$, elongation or compression as well as shear are negligible compared to flexure effects. This is modeled by the algebraic constraint $\|\partial_s \boldsymbol{r}(s, t)\|_2 = 1$ for all s, t, which also enforces global length conservation, as well as $\boldsymbol{d}_1 \times \boldsymbol{d}_2 = \partial_s \boldsymbol{r}$. For further simplifications, the following assumptions are met and the characteristic system quantities are chosen accordingly:

- The characteristic time scale $\bar{t}$ allows motion on the complete length scale of the fiber, $\bar{u} = \ell/\bar{t}$.

- The characteristic force $\overline{F}$ induces acceleration of the complete fiber within the characteristic time scale, $\overline{F} = \rho A \ell \bar{u}/\bar{t}$.

- Due to inextensibility, the characteristic fiber length is the same as the characteristic parametrization length $\bar{s}$, and is set to the total fiber length $\bar{s} = \ell$.

The characteristic inner moment, inner force, outer torque density and outer force density are denoted by $\overline{m}, \overline{q}, \overline{l}, \overline{f}$, respectively. The non-dimensionalization of the system† has the consequence that the angular momentum balance reads as

$$\frac{1}{16} \epsilon^2 \sum_{i=1}^{2} (\partial_{tt} \boldsymbol{d}_i \times \boldsymbol{d}_i) = \frac{\overline{m}}{\overline{F} \ell} \partial_s \boldsymbol{m} + \frac{\overline{q}}{\overline{F}} \partial_s \boldsymbol{r} \times \boldsymbol{q} + \frac{\overline{l}}{\overline{F}} \boldsymbol{\ell} \,. \tag{4.1}$$

Since the inner force $\boldsymbol{q}$ must contain a force contribution which enforces the inextensibility constraint, it must be of the same magnitude as the characteristic force independent of the slenderness parameter, $\overline{q}/\overline{F} \gg \epsilon$. Neglecting the $\mathcal{O}(\epsilon^2)$ term in (4.1) leads to a stationary system for the inner forces balancing the torques and inner moments. This system can be further simplified by using the linear Bernoulli-Euler beam theory for the inner moments, $\boldsymbol{m}(\mathsf{R}, \boldsymbol{\kappa}) = (\overline{m} \ell)^{-1} \mathsf{R} \cdot \operatorname{diag}(EI, EI, GJ) \cdot \boldsymbol{\kappa}$ with E, G, J denoting respectively the Young's and shear moduli as well as the moment of inertia, the latter fulfilling $J = 2I$. The vector family $\boldsymbol{\kappa} = (\kappa_1, \kappa_2, \tau)(s, t)$ contains the dimension-free flexures κ_1, κ_2 and torsion τ, i.e.,

$$\partial_s \mathsf{R} = B(\mathsf{R} \cdot \boldsymbol{\kappa}) \cdot \mathsf{R} \,.$$

---

*The force and torque are given here as line densities, i.e., $[\boldsymbol{f}]_{SI} = \mathrm{N/m}$, $[\boldsymbol{\ell}]_{SI} = \mathrm{N}$.
†Similarly to Section 2.2.5 we do not distinguish between the physical quantities equipped with units and non-dimensionalized functions which will be used from here on.

By plugging the expression for $\boldsymbol{m}$ into (4.1) neglecting the $\mathcal{O}(\epsilon^2)$ term, setting the outer torques $\boldsymbol{\ell} = \boldsymbol{0}$ and using the inextensibility constraint, the inner force $\boldsymbol{q}$ follows as

$$\boldsymbol{q} = \lambda \partial_s \boldsymbol{r} - \frac{EI}{\overline{q}\ell^2}\partial_{sss}\boldsymbol{r} + \frac{GJ}{\overline{q}\ell^2}\tau_0 \partial_s \boldsymbol{r} \times \partial_{ss}\boldsymbol{r} \tag{4.2}$$

with τ_0 being a constant torsion applied throughout the fiber. The scalar-valued function $\lambda = \lambda(s,t)$ denotes the intensity and direction of an inner force solely acting tangential to the fiber curve. Due to the inextensibility constraint, any force acting on the fiber at $\boldsymbol{r}(s,t)$ parallel to $\partial_s \boldsymbol{r}(s,t)$ must be canceled out, hence, λ can be read as the Lagrangian multiplier to the inextensibility constraint. Setting the constant torsion $\tau_0 = 0$ and using the expression for the inner force in (4.2), we then arrive at the following description of a long, slender, elastic and inextensible fiber [90]:

$$\partial_{tt}\boldsymbol{r} = \partial_s(\lambda \partial_s \boldsymbol{r}) - \frac{EI}{\overline{F}\ell^2}\partial_{ssss}\boldsymbol{r} + \frac{\ell \overline{f}}{\overline{F}}\boldsymbol{f}\,, \qquad \|\partial_s \boldsymbol{r}\|_2^2 = 1\,, \tag{4.3}$$

where we rescaled the Lagrangian multiplier λ by the factor $\overline{q}/\overline{F}$. In our context, the fiber is moving in an air flow. Thus, the force density $\boldsymbol{f}$ consists of gravity and aerodynamic forces, $\overline{f}\boldsymbol{f} = \rho A g \boldsymbol{e}_g + \overline{f}_a \boldsymbol{f}_a$ with $g, \boldsymbol{e}_g$ the gravitational acceleration and direction and the aerodynamic force density $\boldsymbol{f}_a = \boldsymbol{f}_a(\boldsymbol{r}(s,t), \partial_t \boldsymbol{r}(s,t), \partial_s \boldsymbol{r}(s,t), t)$, [90, 92]. In order to characterize the system, we use the following dimensionless quantities: the Froude number $\mathrm{Fr} = \overline{u}/\sqrt{\ell g}$ (ratio of inertial and gravitational forces, analogously to Section 2.2.5), the bending number $\alpha = \ell \overline{u}\sqrt{\rho A/(EI)}$ (ratio of inertia and bending) and the drag number $\mathrm{Dr} = \overline{u}\sqrt{\rho A/(\ell \overline{f}_a)}$ (ratio of inertial and aerodynamic forces), [84]. Finally, we denote the terms in the right-hand side of the momentum equation in (4.3) as

$$\boldsymbol{f}_o(s,t) = \frac{\ell}{\overline{F}}\left(\rho A g \boldsymbol{e}_g + \overline{f}_a \boldsymbol{f}_a(\boldsymbol{r}(s,t), \partial_t \boldsymbol{r}(s,t), \partial_s \boldsymbol{r}(s,t), t)\right)$$
$$= \mathrm{Fr}^{-2}\boldsymbol{e}_g + \mathrm{Dr}^{-2}\boldsymbol{f}_a(\boldsymbol{r}(s,t), \partial_t \boldsymbol{r}(s,t), \partial_s \boldsymbol{r}(s,t), t)\,, \tag{4.4a}$$
$$\boldsymbol{\phi}(s,t) = \lambda(s,t)\partial_s \boldsymbol{r}(s,t) - \frac{EI}{\overline{F}\ell^2}\partial_{sss}\boldsymbol{r}(s,t)$$
$$= \lambda(s,t)\partial_s \boldsymbol{r}(s,t) - \alpha^{-2}\partial_{sss}\boldsymbol{r}(s,t)\,. \tag{4.4b}$$

Hence, the problem we consider in this chapter is given as

$$\partial_{tt}\boldsymbol{r}(s,t) = \partial_s \boldsymbol{\phi}(s,t) + \boldsymbol{f}_o(s,t)\,, \tag{4.5a}$$
$$\|\partial_s \boldsymbol{r}\|_2^2 = 1\,, \tag{4.5b}$$

for $(s,t) \in [0, L] \times [0, T]$ with $L, T \in \mathbb{R}^+$. Due to our choice of the relation between the total fiber length and the characteristic length, the dimensionless total length fulfills $L = 1$. Nonetheless, we keep L as a parameter in the remainder of this chapter in order to keep the considerations as general as possible[‡]. Initial conditions

---

[‡]Another possibility to allow different dimensionless fiber lengths is to set $\ell = \overline{s}L$. In this case we would also introduce additional freedom in the choice of appropriate time and force scales, which we do not pursue here.

$\boldsymbol{r}(.,0), \partial_t \boldsymbol{r}(.,0), \lambda(.,0)$ and boundary conditions at $s \in \{0, L\}$ complete the system. We particularly use

$$
\begin{aligned}
\boldsymbol{r}(0,t) = \hat{\boldsymbol{r}}, \quad \partial_s \boldsymbol{r}(0,t) = \hat{\boldsymbol{\tau}}, \quad \|\hat{\boldsymbol{\tau}}\| = 1, \\
\lambda(L,t) = 0, \quad \partial_{ss}\boldsymbol{r}(L,t) = \boldsymbol{0}, \quad \partial_{sss}\boldsymbol{r}(L,t) = \boldsymbol{0}
\end{aligned} \tag{4.6a}
$$

in case of a fiber clamped at one end $(s = 0)$ and stress-free at the other end $(s = L)$ as well as

$$
\lambda(s,t) = 0, \quad \partial_{ss}\boldsymbol{r}(s,t) = \boldsymbol{0}, \quad \partial_{sss}\boldsymbol{r}(s,t) = \boldsymbol{0}, \quad s \in \{0, L\} \tag{4.6b}
$$

in case of a free moving fiber.

Remark 50 (2d-Setting). *We sketched the derivation for a three-dimensional rod. Nonetheless, the model (4.5) is also valid in case of a two-dimensional setting. Assume, for example, $\boldsymbol{r}(.,t) \cdot \boldsymbol{e}_3 \equiv 0$ for some $t \in [0,T]$, then the kth partial derivative, $\partial_s^k \boldsymbol{r}$, fulfills $\partial_s^k \boldsymbol{r}(.,t) \cdot \boldsymbol{e}_3 \equiv 0$ for any k implying $\partial_s \boldsymbol{\phi}(.,t) \cdot \boldsymbol{e}_3 \equiv 0$. Hence, if additionally $\boldsymbol{f}_o(.,t) \cdot \boldsymbol{e}_3 \equiv 0$ holds, there is no acceleration in direction of $\boldsymbol{e}_3$ at this point in time. If, moreover, $\partial_t \boldsymbol{r}(.,t) \cdot \boldsymbol{e}_3 \equiv 0$, there is also no inertial drift in this direction. Thus, $\boldsymbol{r}(.,\tau) \cdot \boldsymbol{e}_3 \equiv 0$ must hold for some neighborhood of t. Therefore, demanding $\boldsymbol{r}(.,0) \cdot \boldsymbol{e}_3 \equiv 0, \partial_t \boldsymbol{r}(.,0) \cdot \boldsymbol{e}_3 \equiv 0$ and $\boldsymbol{f}_o(.,t) \cdot \boldsymbol{e}_3 \equiv 0$ for all $t \in [0,T]$ yields a completely two-dimensional setting. Thus, $\boldsymbol{r} \in \mathbb{R}^d$, $d \in \{2,3\}$ is assumed in the following sections.*

Remark 51 (Stress free boundary condition). *Due to the algebraic constraint (4.5b) it holds $\partial_s \boldsymbol{r} \cdot \partial_{ss}\boldsymbol{r} = 0$ and therefore*

$$
\|\partial_{ss}\boldsymbol{r}\|^2 = -\partial_s \boldsymbol{r} \cdot \partial_{sss}\boldsymbol{r}.
$$

The expression for the inner forces (4.2) then implies for $\tau_0 = 0$

$$
\begin{aligned}
\boldsymbol{q} \cdot \partial_s \boldsymbol{r} &= \lambda - c\partial_{sss}\boldsymbol{r} \cdot \partial_s \boldsymbol{r} = \lambda + c\|\partial_{ss}\boldsymbol{r}\|_2^2, \\
\boldsymbol{q} \cdot \partial_s \boldsymbol{r}^\perp &= -c\partial_{sss}\boldsymbol{r} \cdot \partial_s \boldsymbol{r}^\perp
\end{aligned}
$$

with some constant c and where $\partial_s \boldsymbol{r}^\perp$ is any orthogonal vector to $\partial_s \boldsymbol{r}$. Hence, the boundary conditions $\lambda = 0, \partial_{sss}\boldsymbol{r} = \boldsymbol{0}$ imply no stress at the boundary, $\boldsymbol{q} = \boldsymbol{0}$ with $\partial_{ss}\boldsymbol{r} = \boldsymbol{0}$ being a compatibility condition.

Remark 52 (Energy formulation). *In case of a purely conservative outer force, i.e., $\boldsymbol{f}_a = \boldsymbol{0}$ in our setting, the system (4.5) is conservative. In this case, the kinetic and potential energy of the fiber are given as*

$$
\begin{aligned}
E_{kin}(s,t) &= 0.5\|\partial_t \boldsymbol{r}(s,t)\|^2, \quad E_{pot}(s,t) = E_{pot,g}(s,t) + E_{pot,b}(s,t), \\
E_{pot,g}(s,t) &= -\mathrm{Fr}^{-2}\boldsymbol{e}_g \cdot \boldsymbol{r}(s,t), \quad E_{pot,b}(s,t) = \alpha^{-2}0.5\|\partial_{ss}\boldsymbol{r}(s,t)\|^2.
\end{aligned}
$$

The Lagrangian function reads as

$$
M(\boldsymbol{r}, \boldsymbol{\tau}, \boldsymbol{v}, \boldsymbol{w}) = 0.5\|\boldsymbol{w}\|^2 + \mathrm{Fr}^{-2}\boldsymbol{e}_g \cdot \boldsymbol{r} - \alpha^{-2}0.5\|\boldsymbol{v}\|^2 - 0.5\lambda(\|\boldsymbol{\tau}\|^2 - 1),
$$

with the Lagrangian functional

$$
\mathcal{L}(\boldsymbol{r}) = \int_0^T \int_0^L M(\boldsymbol{r}(s,t), \partial_s \boldsymbol{r}(s,t), \partial_{ss}\boldsymbol{r}(s,t), \partial_t \boldsymbol{r}(s,t))\,\mathrm{d}s\mathrm{d}t.
$$

For any smooth function with compact support, $\boldsymbol{\rho} \in \mathcal{C}_c^\infty([0,L]\times[0,T];\mathbb{R}^d)$, the variation of the Lagrangian then follows as

$$D\mathcal{L}(\boldsymbol{r}+h\boldsymbol{\rho})_{|h=0} = \int_0^T \int_0^L \partial_{\boldsymbol{r}} M \cdot \boldsymbol{\rho} + \partial_{\boldsymbol{\tau}} M \cdot \partial_s \boldsymbol{\rho} + \partial_{\boldsymbol{v}} M \cdot \partial_{ss}\boldsymbol{\rho} + \partial_{\boldsymbol{w}} M \cdot \partial_t \boldsymbol{\rho}\,\mathrm{d}s\mathrm{d}t\,.$$

In the case of a clamped fiber at $s = 0$, $\boldsymbol{\rho}(0,t) = \mathbf{0} = \partial_s\boldsymbol{\rho}(0,t)$. Since an initial condition is given, it also holds $\boldsymbol{\rho}(s,0) = \mathbf{0} = \partial_t\boldsymbol{\rho}(s,0)$. Partial integration yields

$$\begin{aligned}
D\mathcal{L}(\boldsymbol{r}+h\boldsymbol{\rho})_{|h=0} &= \int_0^T \int_0^L \left(\partial_{\boldsymbol{r}} M - \partial_s\left(\partial_{\boldsymbol{\tau}} M\right) + \partial_{ss}\left(\partial_{\boldsymbol{v}} M\right) - \partial_t\left(\partial_{\boldsymbol{w}} M\right)\right)\cdot\boldsymbol{\rho}\,\mathrm{d}s\mathrm{d}t \\
&+ \int_0^T \left(\partial_{\boldsymbol{\tau}} M \cdot \boldsymbol{\rho} + \partial_{\boldsymbol{v}} M \cdot \partial_s\boldsymbol{\rho} - \partial_s\left(\partial_{\boldsymbol{v}} M\right)\cdot\boldsymbol{\rho}\right)|_{s=0}^{s=L}\,\mathrm{d}t \\
&+ \int_0^L \partial_{\boldsymbol{w}} M \cdot \boldsymbol{\rho}|_{t=0}^{t=T}\,\mathrm{d}s\,.
\end{aligned}$$

The boundary conditions and the properties of the test function reveal

$$D\mathcal{L}(\boldsymbol{r}+h\boldsymbol{\rho})_{|h=0} = \int_0^T \int_0^L \left(\partial_{\boldsymbol{r}} M - \partial_s\left(\partial_{\boldsymbol{\tau}} M\right) + \partial_{ss}\left(\partial_{\boldsymbol{v}} M\right) - \partial_t\left(\partial_{\boldsymbol{w}} M\right)\right)\cdot\boldsymbol{\rho}\,\mathrm{d}s\mathrm{d}t$$

and the fundamental lemma of calculus of variations [105] leads to the Lagrange's equations

$$\partial_t\left(\partial_{\boldsymbol{w}} M\right) = \partial_{\boldsymbol{r}} M - \partial_s\left(\partial_{\boldsymbol{\tau}} M\right) + \partial_{ss}\left(\partial_{\boldsymbol{v}} M\right)$$

subject to the inextensibility constraint $0.5\lambda(\|\partial_s\boldsymbol{r}\|^2 - 1) = 0$, which is identical to (4.5). On the other hand, multiplying (4.5) with $\partial_t\boldsymbol{r}$ and integrating over space and time, we find

$$\begin{aligned}
&\int_0^T \int_0^L \partial_t\left(0.5\|\partial_t\boldsymbol{r}\|^2\right)\,\mathrm{d}s\mathrm{d}t \\
&= \int_0^T \int_0^L \partial_t\left(\mathrm{Fr}^{-2}\boldsymbol{e}_g\cdot\boldsymbol{r} - \alpha^{-2}0.5\|\partial_{ss}\boldsymbol{r}\|^2 - 0.5\lambda(\|\partial_s\boldsymbol{r}\|^2 - 1)\right)\,\mathrm{d}s\mathrm{d}t \\
&+ \alpha^{-2}\int_0^T \left(\partial_{ss}\boldsymbol{r}\cdot\partial_{st}\boldsymbol{r} - \partial_{sss}\boldsymbol{r}\cdot\partial_t\boldsymbol{r}\right)|_{s=0}^{s=L}\,\mathrm{d}t \\
&+ \int_0^T \int_0^L 0.5\partial_t\lambda(\|\partial_s\boldsymbol{r}\|^2 - 1)\,\mathrm{d}s\mathrm{d}t + \int_0^T (\lambda\partial_s\boldsymbol{r}\cdot\partial_t\boldsymbol{r})|_{s=0}^{s=L}\,\mathrm{d}t\,.
\end{aligned}$$

Applying the boundary conditions, the identity $\partial_t\boldsymbol{r}(0,t) = \partial_{st}\boldsymbol{r}(0,t) = \mathbf{0}$, since $\boldsymbol{r}(0,t)$ is assumed fixed, $\partial_s\boldsymbol{r}(0,t) \equiv \hat{\boldsymbol{\tau}}$ and the constraint, we find

$$\int_0^L E_{kin}(s,T) + E_{pot}(s,T)\,\mathrm{d}s = \int_0^L E_{kin}(s,0) + E_{pot}(s,0)\,\mathrm{d}s\,.$$

Thus, the equations (4.5) preserves energy.

4.2.2 Stochastic model

In the scenario of a turbulent air flow, the aerodynamic drag can be modeled as the superposition of a deterministic drag originating from the mean velocity of the fluid and an additional stochastic drag due to turbulence [90, 92]. In particular, given a probability space $(\Omega, \mathcal{A}, \varsigma)$, the aerodynamic drag is given for any $\omega \in \Omega$ as

$$\boldsymbol{f}_a = \boldsymbol{f}_{ad}(\boldsymbol{r}(s,t), \partial_t \boldsymbol{r}(s,t), \partial_s \boldsymbol{r}(s,t), t) + \beta \mathbf{A}(\boldsymbol{r}(s,t), \partial_t \boldsymbol{r}(s,t), \partial_s \boldsymbol{r}(s,t), t) \cdot \boldsymbol{\xi}(s,t,\omega) \,.$$

The term $\boldsymbol{\xi}$ denotes a multiplicative vector-valued space-time Gaussian white noise with a flow-dependent amplitude $\mathbf{A}$, characterized by the dimensionless number β, the turbulent fluctuation number [84]. In this case, the fiber curve becomes a random field $\boldsymbol{r} : [0, L] \times [0, T] \times \Omega \to \mathbb{R}^d$, $d \in \{2, 3\}$ whose dynamics are described by the stochastic partial differential algebraic equation formally given as (4.5). In the following we will suppress the dependence of the involved functions on ω. In order to differentiate between the deterministic drag and stochastic forces, we split the two contributions by modifying (4.4a) in the following way

$$\boldsymbol{f}_o(s,t) = \boldsymbol{f}_{od}(s,t) + \mathbf{D}(s,t) \cdot \boldsymbol{\xi}(s,t) \,, \tag{4.8a}$$

$$\boldsymbol{f}_{od}(s,t) = \mathrm{Fr}^{-2} \boldsymbol{e}_g + \mathrm{Dr}^{-2} \boldsymbol{f}_{ad}(\boldsymbol{r}(s,t), \partial_t \boldsymbol{r}(s,t), \partial_s \boldsymbol{r}(s,t), t) \,, \tag{4.8b}$$

$$\mathbf{D}(s,t) = \beta \mathrm{Dr}^{-2} \mathbf{A}(\boldsymbol{r}(s,t), \partial_t \boldsymbol{r}(s,t), \partial_s \boldsymbol{r}(s,t), t) \,. \tag{4.8c}$$

We also define the planar Wiener process as following, [84, 125].

Definition 53 (Gaussian white noise, planar Wiener process). *Consider $\mathcal{L}^2(\Omega, \mathcal{A}, \varsigma; \mathbb{R}^d)$ to be the space of $\mathbb{R}^d$-valued random variables with finite second moments on a sufficiently rich probability space $(\Omega, \mathcal{A}, \varsigma)$, and let $\mathcal{B}([0, L] \times [0, T])$ be the family of Borel sets on $[0, L] \times [0, T]$. Then a mapping $\boldsymbol{\xi} : \mathcal{B}([0, L] \times [0, T]) \to \mathcal{L}^2(\Omega, \mathcal{A}, \varsigma; \mathbb{R}^d)$ is called Gaussian white noise, if it fulfills:*

1. *For any set $B \in \mathcal{B}$, $\boldsymbol{\xi}(B)$ is a $\mathcal{N}(\mathbf{0}, |B|\mathbf{I})$ distributed random variable.*

2. *For any disjoint sets $B, C \in \mathcal{B}$, $\boldsymbol{\xi}(B)$ and $\boldsymbol{\xi}(C)$ are independent and $\boldsymbol{\xi}(B \cup C) = \boldsymbol{\xi}(B) + \boldsymbol{\xi}(C)$ holds.*

Furthermore, $\boldsymbol{w} : [0, L] \times [0, T] \to \mathcal{L}^2(\Omega, \mathcal{A}, \varsigma; \mathbb{R}^d)$ given by $\boldsymbol{w}(s,t) = \boldsymbol{\xi}((0, s] \times (0, t])$ is called a planar Wiener process. The associated filtration is denoted by $\mathcal{F}_{s,t}$ for $0 \le s \le L$ and $0 \le t \le T$.

Since $\boldsymbol{\xi}$ is a random measure, $\boldsymbol{\xi}(s,t)$ is not naturally defined, instead the equations (4.5) must be read as an Itô-type stochastic partial differential equation (for the construction of a multi-parameter Itô integral see, e.g., [69, 125]). Moreover, as the driving force of the fiber is irregular in space and time, so is the Lagrangian multiplier, hence $\partial_s \lambda$ is not well-defined. Therefore, by speaking of a solution of (4.5) with $\boldsymbol{f}_o$ given in (4.8a), we presume, that the solutions of the semi-discrete system presented in Sec. 4.2.3 converge to $\mathcal{F}_{s,t}$-measurable random fields $\boldsymbol{r}(s,t) \in \mathcal{L}^2(\Omega, \mathcal{F}_{L,T}, \varsigma; \mathbb{R}^d)$ and $\lambda(s,t) \in \mathcal{L}^2(\Omega, \mathcal{F}_{L,T}, \varsigma; \mathbb{R})$ as $\Delta s \to 0$ with sufficient regularity in space, as in [56] for the deterministic case.

4.2.3 Semidiscretized system

The fiber model (4.5) is a wave-like system with elliptic regularization. For the spatial discretization of the deterministic version different approaches can be found in literature, such as, e.g., geometric Lagrangian methods [79], finite element schemes [7, 10, 56] or finite volume approaches [122]. We apply a finite volume method in combination with a finite difference approximation for the constraint [84]. The usage of a staggered grid allows particularly for small discretization stencils. In the deterministic case, it is a conservative first-order scheme. A rigorous interpretation of the stochastic semi-discrete system is given in [84].

For the following, we denote the fiber velocity as $\partial_t \boldsymbol{r} = \boldsymbol{v}$, this implies $\partial_{tt}\boldsymbol{r} = \partial_t \boldsymbol{v}$. We consider a finite volume discretization that is based on a conforming partition of $[0, L]$ into subintervals (control cells) I_i of length Δs. The partition is identified with the sequence of nodes $\{s_i\}_i$. The idea is to formally integrate the evolution equations in (4.5) over the control cells $I_i = [s_{i-1/2}, s_{i+1/2}]$, $s_{i\pm1/2} = s_i \pm \Delta s/2$ for $i = 1, ..., N$, and to set up a stochastic differential system in time for the cell averages $\boldsymbol{\varphi}_i(t) = \int_{I_i} \boldsymbol{\varphi}(s, t)\mathrm{d}s/\Delta s$ of the unknowns $\boldsymbol{\varphi} \in \{\boldsymbol{r}, \boldsymbol{v}\}$. In this way the fiber position and velocity are assigned to the cell nodes, $\boldsymbol{r}_i(t)$, $\boldsymbol{v}_i(t)$, whereas we assign the inner traction, and consequently also the constraint, to the cell edges, $\lambda_{i\pm1/2}(t) = \lambda(s_{i\pm1/2}, t)$. The integral equations yield

$$\frac{\mathrm{d}}{\mathrm{d}t}\boldsymbol{r}_i(t) = \boldsymbol{v}_i(t)\,, \tag{4.9}$$

$$\frac{\mathrm{d}}{\mathrm{d}t}\boldsymbol{v}_i(t) = \frac{1}{\Delta s}\left(\boldsymbol{\phi}(s_{i+1/2}, t) - \boldsymbol{\phi}(s_{i-1/2}, t) + \int_{I_i} \boldsymbol{f}_{od}(s, t)\,\mathrm{d}s + \int_{I_i} \mathbf{D}(s, t)\cdot\boldsymbol{\xi}(s, t)\,\mathrm{d}s\right)\,,$$

$$\|\partial_s\boldsymbol{r}(s_{i-1/2}, t)\| = 1\,.$$

We evaluate the remaining integrals by means of trapezoidal quadrature rules,

$$\int_{I_i} \boldsymbol{f}_{od}(s, t)\,\mathrm{d}s \approx \frac{1}{2}(\boldsymbol{f}_{od}(s_{i+1/2}, t) + \boldsymbol{f}_{od}(s_{i-1/2}, t))\Delta s\,, \tag{4.10a}$$

$$\int_{I_i} \mathbf{D}(s, t)\boldsymbol{\xi}(s, t)\,\mathrm{d}s \approx \frac{1}{2}(\mathbf{D}(s_{i+1/2}, t) + \mathbf{D}(s_{i-1/2}, t))\cdot\int_{I_i} \boldsymbol{\xi}(s, t)\,\mathrm{d}s\,. \tag{4.10b}$$

Moreover, we approximate all function values of $\boldsymbol{r}$, $\boldsymbol{v}$ as well as $\partial_s\boldsymbol{r}$, $\partial_{ss}\boldsymbol{r}$, $\partial_{sss}\boldsymbol{r}$ occurring at the cell edges $s_{i\pm1/2}$ by a linear interpolation over the neighboring cells and first order finite differences, respectively, i.e.,

$$\boldsymbol{\varphi}(s_{i-1/2}, t) \approx (\boldsymbol{\varphi}_i(t) + \boldsymbol{\varphi}_{i-1}(t))/2, \qquad \boldsymbol{\varphi} \in \{\boldsymbol{r}, \boldsymbol{v}\},$$

$$\partial_s\boldsymbol{r}(s_{i-1/2}, t) \approx (\boldsymbol{r}_i(t) - \boldsymbol{r}_{i-1}(t))(\Delta s)^{-1},$$

$$\partial_{ss}\boldsymbol{r}(s_{i-1/2}, t) \approx (\boldsymbol{r}_{i+1}(t) - \boldsymbol{r}_i(t) - \boldsymbol{r}_{i-1}(t) + \boldsymbol{r}_{i-2}(t))(\Delta s)^{-2}/2,$$

$$\partial_{sss}\boldsymbol{r}(s_{i-1/2}, t) \approx (\boldsymbol{r}_{i+1}(t) - 3\boldsymbol{r}_i(t) + 3\boldsymbol{r}_{i-1}(t) - \boldsymbol{r}_{i-2}(t))(\Delta s)^{-3}.$$

Consequently, plugging the discretization stencils into the integral equations yields a semi-discrete system for $\boldsymbol{r}_i$, $\boldsymbol{v}_i$ and $\lambda_{i-1/2}$. The traction $\lambda_{i-1/2}(t)$ appearing in the flux term acts particularly as Lagrange multiplier to the discretized inextensibility constraint

$$\|\boldsymbol{r}_i(t) - \boldsymbol{r}_{i-1}(t)\| = \Delta s.$$

Due to the constraint, the spatially discrete fiber becomes a polygon line with a fixed geometrical spacing for the fiber points. In the sequel we denote the used approximations of the function values at the cell edges by the index $_{i\pm1/2}$, e.g., $\mathbf{D}_{i\pm1/2}(t) \approx \mathbf{D}(s_{i\pm1/2}, t)$.

To incorporate the boundary conditions (4.6) into the scheme, we introduce ghost points, i.e., artificial points which are not governed by the dynamical system (4.5). This way we do not have to adapt the discretization stencils. The spatial grid for a one-sided clamped fiber (4.6a) is visualized in Fig. 4.2. We realize the clamped boundary condition of a fixed position $\hat{r}$ and tangent $\hat{\tau}$ at $s = 0$ by setting the node $s_1 = 1.5\Delta s$, where $\Delta s = L/(N + 1)$, and introducing the additional nodes $s_{-1} = -0.5\Delta s$ and $s_0 = 0.5\Delta s$. The associated fiber points r_i, $i = -1, 0$ are then given algebraically at every time $t \geq 0$, they are coupled with the dynamical system via the constraint for the unknown traction $\lambda_{1/2}$,

$$r_{-1} + r_0 = 2\hat{r}\,, \qquad r_0 - r_{-1} = \Delta s\hat{\tau}\,, \qquad \|r_1 - r_0\| = \Delta s\,. \qquad (4.11)$$

In particular, $r_0 = \hat{r} + \Delta s\hat{\tau}/2$ is constant and hence considered as a ghost point although $s_0 \in [0, L]$. The associated velocity of the ghost points at s_{-1}, s_0 is prescribed as $v_{-1} = v_0 = 0$, as $\hat{\tau}$ and $\hat{r}$ are assumed constant in time. For the realization of a stress-free boundary at $s = L$, we set $s_N = L - 0.5\Delta s$ and add $s_{N+i} = L + (i - 0.5)\Delta s$, $i = 1, 2$. According to the discretization stencils the corresponding fiber points and traction fulfill

$$r_{N+2} - 3r_{N+1} + 3r_N - r_{N-1} = 0\,, \quad r_{N+2} - r_{N+1} - r_N + r_{N-1} = 0\,, \quad \lambda_{N+1/2} = 0\,. \tag{4.12}$$

The equations for the velocities at the ghost points s_{N+1}, s_{N+2} are chosen accordingly. Note that this approach also ensures that the additional points fulfill the length constraint. In case of a free moving fiber (4.6b) the handling of the stress-free boundary conditions for both ends is straightforward.
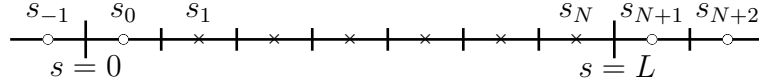
Figure 4.2.: Spatial grid for semi-discretization of one-sided clamped fiber. Crosses mark the dynamical grid points, whereas circles label the ghost points due to the realization of the boundary conditions (4.6a).

In what follows we will focus on the analysis of the one-sided clamped fiber as this case covers the difficulties of both types of boundary conditions.

We denote the polygon line as $r = (r_i)_{i=1,\dots,N}$ and its velocity by $v = (v_i)_{i=1,\dots,N}$. The vector of the discrete Lagrangian multipliers is given by $\lambda = (\lambda_{i-1/2})_{i=1,\dots,N}$ and the holonomic constraint by the function $g : \mathbb{R}^{dN} \to \mathbb{R}^N$, $g(r) = (g_{i-1/2}(r))_{i=1,\dots,N}$ with

$$g_{1/2}(x) = 0.5 \left(1 - \frac{\|r_0 - x_1\|_2^2}{\Delta s^2}\right)\,, \qquad g_{i-1/2}(x) = 0.5 \left(1 - \frac{\|x_{i-1} - x_i\|_2^2}{\Delta s^2}\right)$$

for $i = 2, \dots, N$ and any $x = (x_1, \dots, x_N) \in \mathbb{R}^{dN}$. Then we have in the deterministic case for (4.5) the resulting high dimensional differential algebraic equation (DAE)

$$\frac{\mathrm{d}}{\mathrm{d}t}r = v\,, \tag{4.13a}$$

$$\frac{\mathrm{d}}{\mathrm{d}t}v = a + \nabla g(r) \cdot \lambda, \tag{4.13b}$$

$$g(r) = 0 \tag{4.13c}$$

for all $t \in (0, T)$ where the driving force $a = a(r, v, t) = (\boldsymbol{a}_i(r, v, t))_{i=1,\dots,N}$ is given in terms of

$$\boldsymbol{a}_i(r, v, t) = -\frac{\boldsymbol{r}_{i+2} - 4\boldsymbol{r}_{i+1} + 6\boldsymbol{r}_i - 4\boldsymbol{r}_{i-1} + \boldsymbol{r}_{i-2}}{\alpha^2 \Delta s^4} + \frac{\boldsymbol{f}_{od}(s_{i+1/2}, t) + \boldsymbol{f}_{od}(s_{i-1/2}, t)}{2},$$

$$\boldsymbol{f}_{od}(s_{i-1/2,t}) = \mathrm{Fr}^{-2}\boldsymbol{e}_g + \mathrm{Dr}^{-2}\boldsymbol{f}_{ad}\left(\frac{\boldsymbol{r}_{i-1} + \boldsymbol{r}_i}{2}, \frac{\boldsymbol{v}_{i-1} + \boldsymbol{v}_i}{2}, \frac{\boldsymbol{r}_i - \boldsymbol{r}_{i-1}}{\Delta s}, t\right).$$

In [84] it is shown that in case of $\boldsymbol{f}_o$ given by (4.8a), the semi-discrete system belonging to (4.5) can be interpreted as an Itô-type stochastic differential equation. To be precise, the formal expression

$$\frac{1}{2\Delta s} \int_0^\tau \left(\mathbf{D}(s_{i+1/2}, t) + \mathbf{D}(s_{i-1/2}, t)\right) \cdot \int_{I_i} \boldsymbol{\xi}(s, t)\,\mathrm{d}s\,\mathrm{d}t \tag{4.14}$$

from (4.10b) is read as an integral with respect to the measure $\boldsymbol{\xi}$, formally $\boldsymbol{\xi}(s, t)\mathrm{d}s\mathrm{d}t = \mathrm{d}\boldsymbol{\xi}$ presuming continuity and $\mathcal{F}_{s,t}$-adaptness of $\mathbf{D}_{i-1/2}(t)$. Using Def. 53, we have

$$\boldsymbol{\xi}((s_{i-1/2}, s_{i+1/2}] \times (0, t]) = \boldsymbol{\xi}((0, s_{i+1/2}] \times (0, t]) - \boldsymbol{\xi}((0, s_{i-1/2}] \times (0, t])$$
$$= \boldsymbol{w}(s_{i+1/2}, t) - \boldsymbol{w}(s_{i-1/2}, t)$$

and as $\boldsymbol{\xi}((s_{i-1/2}, s_{i+1/2}] \times (0, t]) \sim \mathcal{N}(\mathbf{0}, t\Delta s\mathbf{I})$, we set the standard $\mathbb{R}^d$-valued Wiener process in time as $\boldsymbol{w}_i(t) = (\boldsymbol{w}(s_{i+1/2}, t) - \boldsymbol{w}(s_{i-1/2}, t))/\sqrt{\Delta s}$. Then, due to our approximation (4.10b) of the amplitude $\mathbf{D}$ in space, the stated interpretation of (4.14) (and therefore of (4.8a)) is given by

$$\int_{I_i \times [0,\tau]} \frac{\mathbf{D}(s_{i+1/2}, t) + \mathbf{D}(s_{i-1/2}, t)}{2\Delta s} \cdot \mathrm{d}\boldsymbol{\xi} = \int_0^\tau \frac{\mathbf{D}(s_{i+1/2}, t) + \mathbf{D}(s_{i-1/2}, t)}{2\sqrt{\Delta s}} \cdot \mathrm{d}\boldsymbol{w}_i(t), \tag{4.15}$$

i.e., by an Itô integral with respect to a standard one-parameter, $\mathbb{R}^d$-valued Wiener process. Similarly, as stated before (see Section 4.2.2), the Lagrangian multiplier is not a regular random field in the stochastic setting. Thus, the time integral over the corresponding term in the semi-discretization of the flux $\boldsymbol{\phi}$, see (4.9), namely

$$\frac{1}{\Delta s} \int_0^\tau \lambda_{i+1/2}\frac{\boldsymbol{r}_{i+1} - \boldsymbol{r}_i}{\Delta s} - \lambda_{i-1/2}\frac{\boldsymbol{r}_i - \boldsymbol{r}_{i-1}}{\Delta s}\,\mathrm{d}t \tag{4.16}$$

is also interpreted as a stochastic integral. Formally, $\lambda_{i-1/2}(t)\mathrm{d}t = \mathrm{d}\mu_{i-1/2}(t)$, where $(\mu_{i-1/2}(t))_{t\geq 0} \subset \mathbb{R}$ is a family of continuous and $\mathcal{F}_{L,t}$-adapted semi-martingales. Then, the integral in (4.16) is given by

$$\int_0^\tau \frac{\boldsymbol{r}_{i+1} - \boldsymbol{r}_i}{\Delta s^2}\,\mathrm{d}\mu_{i+1/2} - \int_0^\tau \frac{\boldsymbol{r}_i - \boldsymbol{r}_{i-1}}{\Delta s^2}\,\mathrm{d}\mu_{i-1/2} \tag{4.17}$$

which is well-defined, given $(\boldsymbol{r}_i(t))_{t\geq 0}$ is continuous and $\mathcal{F}_{L,t}$-adapted, [84]. Using the abbreviation $\mu = (\mu_{i-1/2})_{i=1,\dots,N}$ and $w = (\boldsymbol{w}_i)_{i=1,\dots,N}$, we finally state the semi-discretized system as the Itô-type stochastic DAE

$$\mathrm{d}r = v\,\mathrm{d}t, \tag{4.18a}$$

$$\mathrm{d}v = a\,\mathrm{d}t + B \cdot \mathrm{d}w + \nabla g(r) \cdot \mathrm{d}\mu \,, \tag{4.18b}$$

$$g(r) = 0 \,, \tag{4.18c}$$

with the stochastic amplitude $B = B(r, v, t) = (\mathbf{B}_{ij}(r, v, t))_{i,j=1,\dots,N}$ given in terms of

$$\mathbf{B}_{ij}(r, v, t) = \frac{1}{2\sqrt{\Delta s}} \left(\mathbf{D}_{i+1/2}(t) + \mathbf{D}_{i-1/2}(t) \right) \delta_{ij} \,,$$

$$\mathbf{D}_{i-1/2}(t) = \beta \mathrm{Dr}^{-2} \mathbf{A} \left(\frac{\boldsymbol{r}_{i-1} + \boldsymbol{r}_i}{2}, \frac{\boldsymbol{v}_{i-1} + \boldsymbol{v}_i}{2}, \frac{\boldsymbol{r}_i - \boldsymbol{r}_{i-1}}{\Delta s}, t \right) \,.$$

Both systems, (4.13) and (4.18) are completed with consistent initial conditions for $r(0), v(0)$, and $\lambda(0)$ or $\mu(0)$, respectively. Considering the solvability of (4.13), we refer to [56], in case of the system (4.18), we cite the main result of [84]:

Proposition 54 (Existence and uniqueness of a global solution to (4.18)). *For any $T, R > 0$, let a, B be Lipschitz-continuous in r, v and possess at most linear growth, i.e. there exist $c_1 = c_1(T, R) \geq 1$ and $c_2 = c_2(T) \geq 1$, such that*

$$\|a(r_1, v_1, t) - a(r_2, v_2, t)\| + \|B(r_1, v_1, t) - B(r_2, v_2, t)\| \leq c_1 \|(r_1, v_1) - (r_2, v_2)\| \,,$$

$$\|a(t, r, v)\| + \|B(t, r, v)\| \leq c_2 (1 + \|(r, v)\|) \,.$$

for all $\|(r_i, v_i)\| \leq R$, $i = 1, 2$, all $(r, v) \in \mathbb{R}^{2dN}$ and any $t \in [0, T]$. Let the initial condition $r_0 \in \mathbb{R}^{dN}$ be given, such that $g(r_0) = 0$ with an admissible initial velocity $v_0 \in \mathbb{R}^{dN}$. Then, there exists a unique global solution (r, v, μ) to (4.18) with $r(0) = r_0, v(0) = v_0$. Additionally, the following equality holds ς-almost surely for all $t \in [0, T]$ with ς denoting the measure on the probability space of Def. 53:

$$\mu(t) = -\int_0^t G^{-1}(r(\tau)) \cdot \left([a(r(\tau), v(\tau), \tau) \cdot \nabla]g(r(\tau)) + [v(\tau) \cdot \nabla]^2 g(r(\tau)) \right) \mathrm{d}\tau$$

$$- \int_0^t G^{-1}(r(\tau)) \cdot \nabla g(r(\tau))^T \cdot B(r(\tau), v(\tau), \tau) \cdot \mathrm{d}w(\tau)$$

with the $N \times N$ Gram matrix $G(r) = (\nabla g^T \cdot \nabla g)(r)$. Finally, there exists a $c > 0$ independent of T, such that

$$\mathbb{E}[\sup_{t \in [0,T]} \|(r(t), v(t))\|^4] \leq c(\|(r_0, v_0)\|^4 + c_2^2 T^3) \exp(cc_2^2 T^3) \,,$$

for all $T \geq 1$.

Remark 55 (Energy preservation of the discrete system). *As stated in the beginning of this section, the deterministic discrete system (4.13) is conservative. Thus, if $\boldsymbol{f}_o$ is conservative ($\boldsymbol{f}_a \equiv \boldsymbol{0}$), the energies in the system are given as (see also Remark 52)*

$$E_{kin}(t) = 0.5\|v(t)\|^2 \,, \qquad\qquad E_{pot}(t) = E_{pot,g}(t) + E_{pot,b}(t) \,, \tag{4.19a}$$

$$E_{pot,g}(t) = -\mathrm{Fr}^{-2} E_g \cdot r(t) \,, \qquad E_{pot,b}(t) = \alpha^{-2} 0.5\|X \cdot r(t) + b\|^2 \,, \tag{4.19b}$$

where $E_g = (\boldsymbol{e}_g, \boldsymbol{e}_g, \dots, \boldsymbol{e}_g) \in \mathbb{R}^{dN}$, and $b = (\boldsymbol{r}_0/\Delta s^2, \boldsymbol{0}, \dots, \boldsymbol{0}) \in \mathbb{R}^{dN}$ as well as $X \in \mathbb{R}^{dN \times dN}$ belong to the following discretization of $\partial_{ss} \boldsymbol{r}(s_i, t)$:

$$(X \cdot r + b)_i = \frac{\boldsymbol{r}_{i-1} - 2\boldsymbol{r}_i + \boldsymbol{r}_{i+1}}{\Delta s^2} \,, \quad for \quad i = 1, \dots, N-1$$

and $(X \cdot r + b)_N = \mathbf{0}$. Hence, X is given by

$$
X = \frac{1}{\Delta s^2}
\begin{bmatrix}
-2\mathbf{I} & \mathbf{I} & & & & & \\
\mathbf{I} & -2\mathbf{I} & \mathbf{I} & & & & \\
& \mathbf{I} & -2\mathbf{I} & \mathbf{I} & & & \\
& & \ddots & \ddots & \ddots & & \\
& & & \mathbf{I} & -2\mathbf{I} & \mathbf{I} & \\
& & & & \mathbf{I} & -2\mathbf{I} & \mathbf{I} \\
& & & & & \mathbf{0} & \mathbf{0}
\end{bmatrix}
$$

with $\mathbf{0}, \mathbf{I} = (\delta_{ij})_{ij} \in \mathbb{R}^{d \times d}$. Note that the boundary condition (4.6a) states $\partial_{ss} r(s, t) = \mathbf{0}$ for $s = s_{N+1/2}$, instead for $s = s_N$. But it holds

$$
\partial_{ss} \boldsymbol{r}(s_N, t) = \partial_{ss} \boldsymbol{r}(s_{N+1/2}, t) - \frac{\Delta s}{2} \partial_{sss} \boldsymbol{r}(s_{N+1/2}, t) + \mathcal{O}(\Delta s^2) = \mathcal{O}(\Delta s^2)
$$

due to the boundary conditions on the free end, which is consistent with the accuracy of the central difference for $\partial_{ss} \boldsymbol{r}(s_i, t)$ chosen here. Similarly, we express the vectors $\partial_s \boldsymbol{r}(s_{i-1/2}, t)$, as

$$
(Z \cdot r - b\Delta s)_i = \frac{\boldsymbol{r}_i - \boldsymbol{r}_{i-1}}{\Delta s} \, .
$$

Therefore, the $\mathbb{R}^{dN \times dN}$-matrix Z is given by

$$
Z = \frac{1}{\Delta s}
\begin{bmatrix}
\mathbf{I} & & & & \\
-\mathbf{I} & \mathbf{I} & & & \\
& -\mathbf{I} & \mathbf{I} & & \\
& & \ddots & \ddots & \\
& & & -\mathbf{I} & \mathbf{I}
\end{bmatrix}
\in \mathbb{R}^{dN \times dN} \, .
$$

This way, the constraint force can be expressed as

$$
\frac{1}{\Delta s} \left(\frac{\boldsymbol{r}_{i+1} - \boldsymbol{r}_i}{\Delta s} \lambda_{i+1/2} - \frac{\boldsymbol{r}_i - \boldsymbol{r}_{i-1}}{\Delta s} \lambda_{i-1/2} \right) = \left(-Z^T \cdot \Lambda \cdot (Z \cdot r - b\Delta s) \right)_i \, ,
$$

with $\Lambda = \mathrm{diag}(\lambda_{1/2}\mathbf{I}, \ldots, \lambda_{N-1/2}\mathbf{I})$. Considering the bending force, it holds

$$
(X^T \cdot (X \cdot r + b))_1 = \frac{\boldsymbol{r}_{-1} - 4\boldsymbol{r}_0 + 6\boldsymbol{r}_1 - 4\boldsymbol{r}_2 + \boldsymbol{r}_3}{\Delta s^4} - \frac{\boldsymbol{r}_{-1} - 2\boldsymbol{r}_0 + \boldsymbol{r}_1}{\Delta s^4} \, ,
$$

$$
(X^T \cdot (X \cdot r + b))_i = \frac{\boldsymbol{r}_{i+2} - 4\boldsymbol{r}_{i+1} + 6\boldsymbol{r}_i - 4\boldsymbol{r}_{i-1} + \boldsymbol{r}_{i-2}}{\Delta s^4} \, , \quad i = 2, N - 2 \, ,
$$

$$
(X^T \cdot (X \cdot r + b))_{N-1} = \frac{\boldsymbol{r}_{N-3} - 4\boldsymbol{r}_{N-2} + 6\boldsymbol{r}_{N-1} - 4\boldsymbol{r}_N + \boldsymbol{r}_{N+1}}{\Delta s^4}
$$
$$
- \frac{\boldsymbol{r}_{N-1} - 2\boldsymbol{r}_N + \boldsymbol{r}_{N+1}}{\Delta s^4} \, ,
$$

$$
(X^T \cdot (X \cdot r + b))_N = \frac{\boldsymbol{r}_{N-2} - 4\boldsymbol{r}_{N-1} + 6\boldsymbol{r}_N - 4\boldsymbol{r}_{N+1} + \boldsymbol{r}_{N+2}}{\Delta s^4}
$$
$$
- \frac{-2\boldsymbol{r}_{N-1} + 5\boldsymbol{r}_N - 4\boldsymbol{r}_{N+1} + \boldsymbol{r}_{N+2}}{\Delta s^4}
$$

and we find from (4.12)

$$\boldsymbol{r}_{N-1} - 2\boldsymbol{r}_N + \boldsymbol{r}_{N+1} = \boldsymbol{0}\,, \quad -2\boldsymbol{r}_{N-1} + 5\boldsymbol{r}_N - 4\boldsymbol{r}_{N+1} + \boldsymbol{r}_{N+2} = \boldsymbol{0}\,.$$

Considering $i = 1$, we have by definition of $\boldsymbol{r}_1$ as cell average and due to (4.11):

$$\boldsymbol{r}_{-1} - 2\boldsymbol{r}_0 + \boldsymbol{r}_1 = -\hat{\boldsymbol{r}} - \frac{3}{2}\Delta s \hat{\boldsymbol{\tau}} + \frac{1}{\Delta s}\int_{\Delta s}^{2\Delta s} \boldsymbol{r}(s,t)\,\mathrm{d}s$$

$$= -\hat{\boldsymbol{r}} - \frac{3}{2}\Delta s \hat{\boldsymbol{\tau}} + \frac{1}{\Delta s}\int_{\Delta s}^{2\Delta s} \hat{\boldsymbol{r}} + \hat{\boldsymbol{\tau}}s + \sum_{k=2}^{4} \frac{1}{k!}\partial_s^k \boldsymbol{r}(0,t)s^k\,\mathrm{d}s + \mathcal{O}(\Delta s^5)\,.$$

Hence, if the continuous solution is sufficiently regular, i.e., $\partial_s^k \boldsymbol{r}(0,t)$ vanish for $k \in \{2,3,4\}$, we find[§] $\boldsymbol{r}_{-1} - 2\boldsymbol{r}_0 + \boldsymbol{r}_1 = \mathcal{O}(\Delta s^5)$. In total, if $\boldsymbol{f}_a \equiv \boldsymbol{0}$, the system (4.13) is equivalent to

$$\frac{\mathrm{d}^2}{\mathrm{d}t^2}r = -\alpha^{-2}X^T \cdot (X \cdot r + b) - Z^T \cdot \Lambda \cdot (Z \cdot r - b\Delta s) + \mathrm{Fr}^{-2}\,E_g\,. \tag{4.20}$$

Multiplying (4.20) with the velocity and integrating over t yields the conservation of energy:

$$\begin{aligned}
E_{kin}(t) - E_{kin}(0) &= \int_0^t \frac{\mathrm{d}}{\mathrm{d}t}\frac{1}{2}\left\|\frac{\mathrm{d}}{\mathrm{d}t}r\right\|^2 \mathrm{d}t \\
&= \int_0^t \frac{\mathrm{d}}{\mathrm{d}t}\left(-\frac{\alpha^{-2}}{2}\|X \cdot r + b\|^2 + \mathrm{Fr}^{-2}\,E_g \cdot r\right)\mathrm{d}t \\
&\quad - \sum_{i=1}^{N}\int_0^t \frac{\lambda_{i-1/2}}{2}\frac{\mathrm{d}}{\mathrm{d}t}\|(Z \cdot r - b\Delta s)_i\|^2\,\mathrm{d}t \\
&= -E_{pot}(t) + E_{pot}(0)\,,
\end{aligned}$$

since due to the constraint $\|(Z \cdot r - b\Delta s)_i\|^2 \equiv 1$.

4.2.4 Typical setting

In what follows, we examine different numerical schemes in order to approximate and solve (4.13) and (4.18). In order to formulate a benchmark setting for the numerical experiments, we choose the model parameters typical for the application in an air-lay process. In particular, we use a setting similar to the one presented in [54], where short, slender synthetic polyester fibers (PES/PET) are put into a turbulent air flow. The characteristic quantities in this case are listed in Tab. 4.1. As the air drag model, we take the regularized universal drag model proposed in [92]. For small turbulent kinetic energy, the deterministic air drag on a fiber can be modeled as

$$\overline{f}_a\boldsymbol{f}_{ad} = \frac{\rho_{air}\nu_{air}^2}{d}\boldsymbol{g}\left(\partial_s\boldsymbol{r}, \frac{\overline{u}d}{\nu_{air}}(\boldsymbol{u}(\boldsymbol{r},t) - \partial_t\boldsymbol{r})\right)\,, \quad \text{with} \tag{4.21}$$

[§]Note that $\partial_s^k \boldsymbol{r}(0,t)$ for $k \in \{2,3,4\}$ is not part of the model. Nonetheless, this assumption is reasonable as a smooth clamped fiber with finite bending stiffness leaves the mounting point as a straight line.

$$\boldsymbol{g}(\boldsymbol{\tau}, \boldsymbol{w}) = r_n(w_n)\Big(\mathbf{I} - \boldsymbol{\tau} \otimes \boldsymbol{\tau}\Big) \cdot \boldsymbol{w} + r_\tau(w_n)\boldsymbol{\tau} \otimes \boldsymbol{\tau} \cdot \boldsymbol{w}\,,$$

$$w_n = w_n(\boldsymbol{\tau}, \boldsymbol{w}) = \sqrt{\|\boldsymbol{w}\|^2 - (\boldsymbol{w} \cdot \boldsymbol{\tau})^2}$$

and drag related resistance coefficients r_n, r_τ whose behavior is seen in Fig. 4.3. The latter depend on the normal velocity component and on the nonlinear drag coefficients c_n, c_τ and are given as

$$r_n(w_n) = \begin{cases} \sum_{j=0}^{3} s_{n,j} w_n^j\,, & w_n < w_0 \\ w_n c_n(w_n)\,, & w_n \geq w_0 \end{cases}, \quad r_\tau(w_n) = \begin{cases} \sum_{j=0}^{3} s_{\tau,j} w_n^j\,, & w_n < w_0 \\ w_n c_\tau(w_n)\,, & w_n \geq w_0 \end{cases}$$

where w_0 is a transition velocity given in (4.22) and $s_{n,j}, s_{\tau,j}$ are the following constants

$$s_{n,0} = r_{n,s}\,, \quad s_{n,1} = 0\,,$$
$$s_{n,2} = \frac{2w_0 c_n(w_0) - w_0^2 c_n'(w_0) - 3r_{n,s}}{w_0^2}\,,$$
$$s_{n,3} = \frac{-w_0 c_n(w_0) + w_0^2 c_n'(w_0) + 2r_{n,s}}{w_0^3}\,,$$
$$r_{n,s} = \pi \frac{4 - (\ln(4\epsilon^{-1}))^{-1}}{\ln(4\epsilon^{-1})}\,,$$

$$s_{\tau,0} = r_{\tau,s}\,, \quad s_{\tau,1} = 0\,,$$
$$s_{\tau,2} = \frac{2w_0 c_\tau(w_0) - w_0^2 c_\tau'(w_0) - 3r_{\tau,s}}{w_0^2}\,,$$
$$s_{\tau,3} = \frac{-w_0 c_\tau(w_0) + w_0^2 c_\tau'(w_0) + 2r_{\tau,s}}{w_0^3}\,,$$
$$r_{\tau,s} = 2\pi \frac{1 + (4\ln(4\epsilon^{-1}))^{-1}}{\ln(4\epsilon^{-1})}\,,$$

with the slenderness parameter $\epsilon = d/\ell$. The drag coefficients c_n, c_τ are given as

$$c_n(w_n) = \begin{cases} \frac{4\pi}{S(w_n)w_n}\left(1 - \frac{S(w_n)^2 - S(w_n)/2 + 5/16}{32S(w_n)}w_n^2\right)\,, & w_n < w_1 \\ \exp(\sum_{j=0}^{3} p_{n,j} \ln^j(w_n))\,, & w_n \in [w_1, w_2] \\ \frac{2}{\sqrt{w_n}} + \frac{1}{2}\,, & w_n > w_2 \end{cases}$$

$$c_\tau(w_n) = \begin{cases} \frac{4\pi}{w_n(2S(w_n)-1)}\left(1 - \frac{2S(w_n)^2 - 2S(w_n)+1}{16(2S(w_n)-1)}w_n^2\right)\,, & w_n < w_1 \\ \exp(\sum_{j=0}^{3} p_{\tau,j} \ln^j(w_n))\,, & w_n \in [w_1, w_2] \\ \frac{2}{\sqrt{w_n}}\,, & w_n > w_2 \end{cases}$$

with $S(w_n) = 2.0022 - \ln(w_n)$ and the constants

$$p_{n,0} = 1.6911\,, \quad p_{n,1} = -6.7222 \cdot 10^{-1}\,, \quad p_{n,2} = 3.3287 \cdot 10^{-2}\,, \quad p_{n,3} = 3.5015 \cdot 10^{-3}\,,$$
$$p_{\tau,0} = 1.1552\,, \quad p_{\tau,1} = -6.8479 \cdot 10^{-1}\,, \quad p_{\tau,2} = 1.4884 \cdot 10^{-2}\,, \quad p_{\tau,3} = 7.4966 \cdot 10^{-4}\,.$$

The transition velocities are given as

$$w_0 = 2\exp(2.0022 - 4\pi r_{n,s}^{-1})\,, \quad w_1 = 0.1\,, \quad w_2 = 100\,. \tag{4.22}$$

In the particular application of an air-lay process, the air flow possess approximately room temperature, hence its kinematic viscosity is assumed constant. Additionally, also the air density in the application is approximately constant. Both quantities are given in Tab. 4.1. The typical relative velocity is then characterized by the dimensionless number

$$\gamma = \frac{\bar{u}d}{\nu_{air}} = 4.6 \cdot 10\,.$$
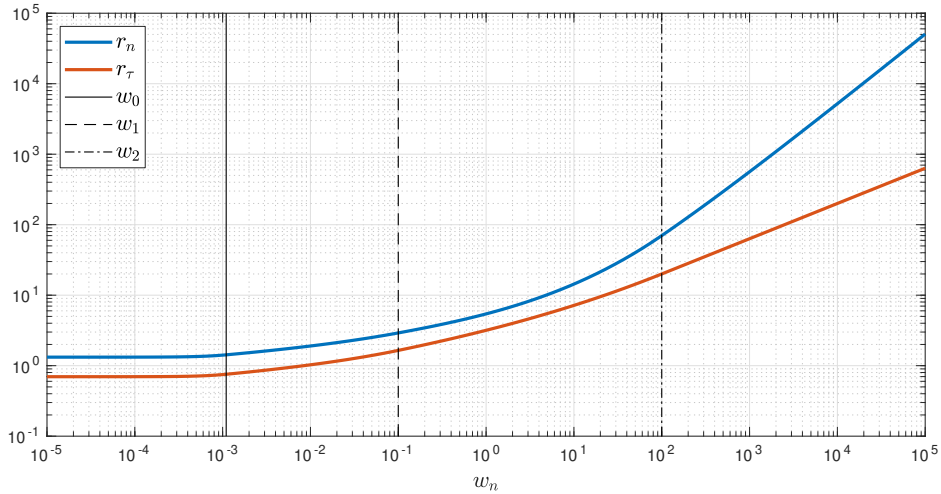
Figure 4.3.: Behavior of the resistance coefficients r_n, r_τ with the transition velocities w_1 (solid line), w_2 (dashed line), w_3 (dashed and dotted line).

The typical aerodynamic force $\overline{f}_a$ can now be defined in terms of the air density, viscosity and fiber diameter according to (4.21). However, since the typical aerodynamic force depends on the relative velocity, we consider instead the scaled quantity

$$\gamma \overline{f}_a = \gamma \frac{\rho_{air} \nu_{air}^2}{d} = 5.4 \cdot 10^{-4} \frac{\text{kg}}{\text{s}^2} \, .$$

This defines the scaled drag number $\hat{\text{Dr}} = \text{Dr}/\sqrt{\gamma}$ given in Tab. 4.1. The resulting model for $\boldsymbol{f}_{ad}$ is then given by

$$\boldsymbol{f}_{ad} = \boldsymbol{g}(\partial_s \boldsymbol{r}, \gamma(\boldsymbol{u}(\boldsymbol{r}, t) - \partial_t \boldsymbol{r})) \, .$$

Since our test scenarios will not use actual simulation data and instead apply academic examples as the outer air flow $\boldsymbol{u}$, we use a simplified, linear model for the stochastic amplitude. In particular, we set

$$\beta \text{Dr}^{-2} \mathbf{A} = \beta \text{Dr}^{-2} \gamma \mathbf{C}(\partial_s \boldsymbol{r}) \tag{4.23}$$

with $\mathbf{C}$ and β chosen artificially in order to scale the deterministic and stochastic influences.

As can be seen from Tab. 4.1 and (4.8a), the typical situation in an air-lay process is that of a fiber driven mostly by air drag with a small force due to bending, $\gamma \text{Dr}^{-2} \gg \text{Fr}^{-2} \gg \alpha^{-2}$.

Remark 56 (Self-penetration of the fiber). *We point out, that the system* (4.5a) *with the discussed force terms does not possess any possibility to prevent the fiber curve from overlapping, see Fig. 4.19 which is of course not meaningful for a physical object. This could be corrected by detecting overlapping of the curve and applying opposing constraint forces at the neighboring fiber points at an earlier time step. However, since such situations are not very likely in a full 3d simulation with real flow data and due to the significant additional computational cost the mentioned solution possibility is not pursued here.*

Name	Symbol	Value	SI unit
Fiber Length	ℓ	$6.0 \cdot 10^{-2}$	m
Fiber Diameter	d	$2.3 \cdot 10^{-5}$	m
Fiber Density	ρ	$1.3 \cdot 10^{3}$	$\mathrm{kg/m^3}$
Young's modulus	E	$3.0 \cdot 10^{9}$	$\mathrm{N/m^2}$
Mean velocity	$\overline{u}$	$3.0 \cdot 10$	m/s
Gravitational acceleration	g	9.8	$\mathrm{m/s^2}$
Air density	ρ_{air}	1.2	$\mathrm{kg/m^3}$
Air kinematic viscosity	ν_{air}	$1.5 \cdot 10^{-5}$	m^2/s
Typical air drag	$\gamma \overline{f}_a$	$5.4 \cdot 10^{-4}$	$\mathrm{kg/s^2}$
Froude number	Fr	$3.9 \cdot 10$	
Bending number	α	$2.1 \cdot 10^{2}$	
Relative velocity	γ	$4.6 \cdot 10$	
Scaled Drag number	$\mathrm{Dr}/\sqrt{\gamma}$	3.9	

Table 4.1.: Characteristic quantities typical for an air-lay process, [54, 91] and resulting model parameters.

4.3 Time integration schemes

Here, we present the time integration techniques which are used in the numerical investigations. For the time discretization, we partition the finite time interval $[0, T]$ into subintervals $[t^n, t^{n+1}]$, $n = 0, ..., M - 1$, of fixed length $\Delta t = T/M$. The numerical approximation to the solution at a time level t^n is indicated by the respective index ^{n}, e.g., $r^n \approx r(t^n)$.

4.3.1 Implicit Euler, Euler-Maruyama

The system of equations (4.13) is a differential-algebraic equation of differentiation index 3, which generally have worse convergence behavior than systems of index 2, cf. [59]. Hence, we use the Gear-Gupta-Leimkuhler (GGL) formulation [48] of (4.13). The latter enforces the so-called hidden constraint which arises analytically as

$$0 = \frac{\mathrm{d}}{\mathrm{d}t} g(r(t)) = \partial_x g(r(t)) \cdot v(t) \,. \tag{4.24}$$

In order to account for this additional constraint an additional Lagrangian multiplier is added and the following index 2 system is used in the deterministic case

$$\frac{\mathrm{d}}{\mathrm{d}t} r = v + \nabla g(r) \cdot \kappa \,, \tag{4.25a}$$

$$\frac{\mathrm{d}}{\mathrm{d}t} v = a + \nabla g(r) \cdot \lambda \,, \tag{4.25b}$$

$$g(r) = 0\,, \tag{4.25c}$$

$$v \cdot \nabla g(r) = 0\,. \tag{4.25d}$$

Due to (4.25d) and the regularity of $G(r) = \partial_x g(r) \cdot \nabla g(r)$, $\kappa = 0$ for the exact solution. A first order discretization of (4.25) by the implicit Euler method is given by

$$r^{n+1} = r^n + \Delta t v^{n+1} + \Delta t \nabla g(r^{n+1}) \cdot \kappa^{n+1}\,, \tag{4.26a}$$

$$v^{n+1} = v^n + \Delta t a^{n+1} + \Delta t \nabla g(r^{n+1}) \cdot \lambda^{n+1}\,, \tag{4.26b}$$

$$g(r^{n+1}) = 0\,, \quad v^{n+1} \cdot \nabla g(r^{n+1}) = 0\,. \tag{4.26c}$$

It is a one stage Radau IIA method, with convergence rate $p = 1$ for both, the dynamic variables r, v and the algebraic ones, κ, λ [61]. In case of the stochastic system, we apply the analogous Euler-Maruyama scheme [75], still treating $\lambda^{n+1} = (\mu^{n+1} - \mu^n)/\Delta t$ as the Lagrangian multiplier to $g(r^{n+1}) = 0$. The amplitude of the white noise is evaluated explicitly in this case. In total, we have

$$r^{n+1} = r^n + \Delta t v^{n+1} + \Delta t \nabla g(r^{n+1}) \cdot \kappa^{n+1}\,, \tag{4.27a}$$

$$v^{n+1} = v^n + \Delta t a^{n+1} + \Delta t \nabla g(r^{n+1}) \cdot \lambda^{n+1} + B^n \cdot (w^{n+1} - w^n)\,, \tag{4.27b}$$

$$g(r^{n+1}) = 0\,, \quad v^{n+1} \cdot \nabla g(r^{n+1}) = 0\,. \tag{4.27c}$$

In the numerical investigations, we call solutions generated by (4.26) and (4.27) implicit Euler-Gear-Gupta-Leimkuhler (IEGGL).

4.3.2 Energy preserving midpoint rule

As stated earlier (see Rem. 52, Rem. 55), the fiber system is energy preserving under conservative forces. The time integration scheme (4.26) does not preserve this property. Hence, we also consider an energy preserving modification of the classical midpoint rule, [83] given as

$$\frac{r^{n+1} - r^n}{\Delta t} = \frac{1}{2}(v^{n+1} + v^n) + \frac{1}{2}\left(\nabla g(r^{n+1}) + \nabla g(r^n)\right) \cdot \kappa^{n+1}\,, \tag{4.28a}$$

$$\frac{v^{n+1} - v^n}{\Delta t} = \frac{1}{2}(a^{n+1} + a^n) + \frac{1}{2}\left(\nabla g(r^{n+1}) + \nabla g(r^n)\right) \cdot \lambda^{n+1}$$

$$- \frac{1}{2}\left(\nabla g(v^{n+1}) + \nabla g(v^n)\right) \cdot \kappa^{n+1} \tag{4.28b}$$

$$g(r^{n+1}) = 0\,, \quad v^{n+1} \cdot \nabla g(r^{n+1}) = 0\,. \tag{4.28c}$$

Multiplying (4.28b) by the displacement $r^{n+1} - r^n$ yields the energy conservation, i.e., $E(t) = E(0)$ with $E(t) = E_{kin}(t) + E_{pot}(t)$ given in (4.19). We call results of (4.28) "conservative midpoint GGL" (cMPGGL).

4.3.3 Semi-explicit projection based schemes and estimators

Deterministic case Differential algebraic equations with the present holonomic constraint are often dealt with in the field of Molecular Dynamics [93]. Here, the dynamics is given by a constrained Hamiltonian system, such that the driving force solely depends on the position and not on velocity. The SHAKE algorithm of [108] is based

on the Störmer (Verlet, leapfrog) time integration combined with a simplified Newton method for the realization of the constraint. If the Newton iteration matrix is not approximated, this procedure is called M-SHAKE [77]. The RATTLE-algorithm [4] is a modification of SHAKE combined with a projection of the velocity in order to fulfill the hidden constraint. In particular, it can be seen as the special case of the symplectic partitioned Runge-Kutta method given by the two stage Lobatto IIIA-IIIB pair [61]. The latter is given for (4.13)¶ by

$$v^{n+1/2} = v^n + \frac{\Delta t}{2}(a(r^n, v^{n+1/2}, t_{n+1/2}) + \nabla g(r^n) \cdot \kappa^{n+1}), \tag{4.29a}$$

$$r^{n+1} = r^n + \Delta t v^{n+1/2}, \tag{4.29b}$$

$$g(r^{n+1}) = 0, \tag{4.29c}$$

$$v^{n+1} = v^{n+1/2} + \frac{\Delta t}{2}(a(r^{n+1}, v^{n+1/2}, t_{n+1}) + \nabla g(r^{n+1}) \cdot \lambda^{n+1}), \tag{4.29d}$$

$$v^{n+1} \cdot \nabla g(r^{n+1}) = 0. \tag{4.29e}$$

The scheme (4.29) is convergent with order $p = 2$ for the dynamic variables, [60]. In the conservative case, a depends only on r, which implies that (4.29) then consists of two nonlinear equations for each time step. First, the position is integrated explicitly, then a projection onto the solution manifold is carried out by using Newton's method whereupon the new velocity is calculated by an explicit integration and subsequent projection.

All stated methods from Molecular Dynamics rely on the following approximation in order to calculate r^{n+1} in the conservative case

$$g(r^{n+1}) = g(\widetilde{r}^{n+1} + 0.5\Delta t^2 \nabla g(r^n) \cdot \kappa^{n+1})$$
$$= g(\widetilde{r}^{n+1}) + \frac{1}{2}\Delta t^2 \partial_x g(\widetilde{r}^{n+1}) \cdot \nabla g(r^n) \cdot \kappa^{n+1} + \mathcal{O}(\Delta t^4) \tag{4.30}$$

which follows from (4.29a)-(4.29c), where $\widetilde{r}^{n+1}$ depends on the particular scheme. Neglecting the error term in (4.30) then leads to a Newton iteration method in order to determine r^{n+1} fulfilling $g(r^{n+1}) = 0$. Since in general $\ker(\partial_x g(\widetilde{r}^{n+1}))^\perp \neq \mathrm{im}(\partial_x g(r^n)^T)$, Δt must be chosen sufficiently small in order to find r^{n+1} by (4.30) in our setting which contradicts the desire for simulations with large step sizes Δt and sufficiently small Δs. Additionally, in the non-conservative case (4.29a)-(4.29c) is already a non-linear system of the same dimension as the systems IEGGL and cMPGGL, and another non-linear system given by (4.29d)-(4.29e) must be solved. Hence, the scheme (4.29) is much more costly without providing any benefits in the non-conservative case. Therefore, we explore a modification of (4.29) by evaluating ∇g in (4.29a) at r^{n+1} and the acceleration a fully explicit in (4.29a) and implicit in (4.29d):

$$v^{n+1/2} = v^n + \frac{\Delta t}{2}(a(r^n, v^n, t_n) + \nabla g(r^{n+1}) \cdot \kappa^{n+1}), \tag{4.31a}$$

$$r^{n+1} = r^n + \Delta t v^{n+1/2}, \tag{4.31b}$$

¶Note that (4.29) is indeed a Lobatto IIIA-IIIB formulation of the original index 3-system, instead of its GGL-stabilized version (4.25), since the partitioned Runge-Kutta methods for constrained systems as defined by [61] automatically introduce additional Lagrangian multipliers in order to enforce algebraic constraints for the interim integration steps.

$$g(r^{n+1}) = 0 \,, \tag{4.31c}$$

$$v^{n+1} = v^{n+1/2} + \frac{\Delta t}{2}\left(a(r^{n+1}, v^{n+1}, t_{n+1}) + \nabla g(r^{n+1}) \cdot \lambda^{n+1}\right), \tag{4.31d}$$

$$v^{n+1} \cdot \nabla g(r^{n+1}) = 0 \,. \tag{4.31e}$$

We address the original system (4.29) by "velocity Strömer-Verlet" (VSV) and the modification (4.31) by "VSVm". We emphasize that the Lagrangian multipliers in (4.29a) and (4.31a) are not the same as in (4.25a), (4.25b). Unlike cMPGGL, the non-linear system associated with VSVm is decoupled and might provide a reduction in computational cost also in case of stochastic simulations. In order to adapt (4.31) for the stochastic case, we add $0.5B^n \cdot (w^{n+1} - w^n)$ to both velocity equations (4.31a) and to (4.31d). Thus, the noise is kept constant during the full step from t_n to t_{n+1}.

Next, we also consider a fully explicit scheme combined with projections onto the solution manifold after each iteration. Differentiating the hidden constraint (4.24) yields the relation $\partial_x g \cdot \frac{\mathrm{d}}{\mathrm{d}t} v = -[v \cdot \nabla]^2 g$ implying an expression for the Lagrangian multiplier in (4.13b)

$$\lambda = -G^{-1} \cdot \left(\partial_x g \cdot a + [v \cdot \nabla]^2 g\right), \tag{4.32}$$

with $G = \nabla g \cdot \partial_x g$. Setting the projector $P = I - \nabla g \cdot G^{-1} \cdot \partial_x g$ we thus find for the deterministic system (4.13) the index 1 formulation

$$\frac{\mathrm{d}}{\mathrm{d}t} r = v \,, \quad \frac{\mathrm{d}}{\mathrm{d}t} v = P \cdot a - \nabla g \cdot G^{-1} \cdot [v \cdot \nabla]^2 g \,. \tag{4.33}$$

The system (4.33) can now be integrated explicitly, i.e.,

$$\widetilde{r}^{n+1} = r^n + \Delta t v^n \,, \tag{4.34a}$$

$$\widetilde{v}^{n+1} = v^n + \Delta t\left(P(r^n) \cdot a^n - \nabla g(r^n) \cdot G^{-1}(r^n) \cdot [v^n \cdot \nabla]^2 g(r^n)\right). \tag{4.34b}$$

Using (4.34) directly in order to solve (4.13) leads to drift-off effects in both constraints. Hence, in order to find the corresponding r^{n+1} which fulfills the constraint, we solve

$$\min_{g(r^{n+1})=0} \frac{1}{2}\|r^{n+1} - \widetilde{r}^{n+1}\|_2^2 \tag{4.35}$$

by using the Karush-Kuhn-Tucker conditions of (4.35). In order to reduce the computational costs even more, instead of applying Newton's method to the $N(d+1)$-dimensional non-linear system $r^{n+1} = \widetilde{r}^{n+1} + \nabla g(r^{n+1}) \cdot \mathfrak{k}$, with $g(r^{n+1}) = 0$ and the corresponding Lagrangian multiplier $\mathfrak{k} \in \mathbb{R}^N$, we adopt the ideas of the before mentioned algorithms from Molecular Dynamics and assume that $r^{n+1} - \widetilde{r}^{n+1}$ is small. Then, for $h \in \ker(\partial_x g(\widetilde{r}^{n+1}))^\perp$, i.e. $h = \nabla g(\widetilde{r}^{n+1}) \cdot \mathfrak{k}$, with $\|\mathfrak{k}\| \ll 1$ it holds

$$g(\widetilde{r}^{n+1} + h) \approx g(\widetilde{r}^{n+1}) + G(\widetilde{r}^{n+1}) \cdot \mathfrak{k} \,,$$

which we apply iteratively to find $r^{n+1} = \widetilde{r}^{n+1} + \nabla g(\widetilde{r}^{n+1}) \cdot \mathfrak{k}$ fulfilling the constraint. Afterwards we project $\widetilde{v}^{n+1}$ orthogonally onto the tangent space of the manifold at r^{n+1}, i.e. $v^{n+1} = P(r^{n+1}) \cdot \widetilde{v}^{n+1}$. We address this method in the following as "explicit Euler, projection based" (EEP). We note that the Lagrangian multiplier $\mathfrak{k}$ is not related to λ of (4.13), the latter being determined by (4.32).

Stochastic case In the stochastic case, the Lagrangian multiplier is given in Proposition 54 explicitly as

$$\mathrm{d}\mu = -G^{-1} \cdot \left(\partial_x g \cdot (a\,\mathrm{d}t + B \cdot \mathrm{d}w) + [v \cdot \nabla]^2 g\,\mathrm{d}t \right) \tag{4.36}$$

and similarly to (4.33), the stochastic algebraic equation (4.18) equivalently reads as

$$\mathrm{d}r = v\,\mathrm{d}t\,, \quad \mathrm{d}v = P \cdot (a\,\mathrm{d}t + B \cdot dw) - \nabla g \cdot G^{-1} \cdot [v \cdot \nabla]^2 g\,\mathrm{d}t\,.$$

This results in the analogue to the first explicit scheme (4.34)

$$\widetilde{r}^{n+1} = r^n + \Delta t v^n\,, \tag{4.37a}$$

$$\widetilde{v}^{n+1} = v^n + \Delta t \left(P(r^n) \cdot \left(a^n + B^n \cdot \frac{w^{n+1} - w^n}{\Delta t} \right) \right.$$
$$\left. - \nabla g(r^n) \cdot G^{-1}(r^n) \cdot [v^n \cdot \nabla]^2 g(r^n) \right)\,, \tag{4.37b}$$

with subsequent determination of r^{n+1} and v^{n+1}.

Predictor-corrector schemes Implicit schemes are generally much more stable than explicit ones and allow larger step sizes. However, the increase in step size is paid by also increasing the computational time in each time step due to a higher amount of Newton iterations for the solution of the non-linear systems. Thus, we also compare different estimators for IEGGL in the stochastic case. In particular, we study the effect of predicting the new solution by an explicit step by EEP without projecting $\widetilde{r}^{n+1}$ to the solution manifold, i.e.,

$$r_{est}^{n+1} = \widetilde{r}^{n+1}\,, \quad v_{est}^{n+1} = P(r_{est}^{n+1}) \cdot \widetilde{v}^{n+1}$$

with $(\widetilde{r}^{n+1}, \widetilde{v}^{n+1})$ given by (4.37), which we address as "EEP predictor". Another possibility is motivated by VSV(m) and the modification of RATTLE, called WIGGLE [82] where the forces in (4.31a) and (4.31d) are first projected onto the tangent space of the solution manifold. In particular, we use

$$v^{n+1/2} = v^n + \frac{\Delta t}{2} \left(P(r^n) \cdot \left(a^n + B^n \cdot \frac{w^{n+1} - w^n}{\Delta t} \right) \right.$$
$$\left. - \nabla g(r^n) \cdot G^{-1}(r^n) \cdot [v^n \cdot \nabla]^2 g(r^n) \right)\,,$$
$$\widetilde{r}^{n+1} = r^n + \Delta t v^{n+1/2}\,,$$
$$\widetilde{v}^{n+1} = v^{n+1/2} + \frac{\Delta t}{2} P(\widetilde{r}^{n+1}) \cdot \left(a(\widetilde{r}^{n+1}, v^{n+1/2}, t_{n+1}) + B^n \cdot \frac{w^{n+1} - w^n}{\Delta t} \right)\,,$$
$$r_{est}^{n+1} = \widetilde{r}^{n+1}\,, \quad v_{est}^{n+1} = P(r_{est}^{n+1}) \cdot \widetilde{v}^{n+1}\,.$$

In the expression for $\widetilde{v}^{n+1}$ we omitted the term associated with $[v^{n+1/2} \cdot \nabla]^2 g(\widetilde{r}^{n+1})$, since it lies in the image of $\nabla g(\widetilde{r}^{n+1})$ and $P(r_{est}^{n+1}) \cdot \nabla g(\widetilde{r}^{n+1}) = 0$. We call this estimator "VSV predictor". In both cases the Lagrangian multipliers are estimated as follows: The multiplier in the momentum equation, formally given as $\lambda^{n+1} = (\mu^{n+1} - \mu^n)/\Delta t$ can be estimated by (4.36) as

$$\lambda_{est}^{n+1} = -G^{-1}(r_{est}^{n+1}) \cdot \partial_x g(r_{est}^{n+1}) \cdot \left(a(r_{est}^{n+1}, v_{est}^{n+1}, t_{n+1}) + B^n \cdot \frac{w^{n+1} - w^n}{\Delta t} \right)$$
$$- G^{-1}(r_{est}^{n+1}) \cdot [\widetilde{v}^{n+1} \cdot \nabla]^2 g(r_{est}^{n+1}) \,.$$

The multiplier in the equation for the position can be estimated by multiplying (4.27a) with $\partial_x g$, which yields

$$\kappa_{est}^{n+1} = \frac{1}{\Delta t} G^{-1}(r_{est}^{n+1}) \cdot \partial_x g(r_{est}^{n+1}) \cdot (r_{est}^{n+1} - r^n - \Delta t v_{est}^{n+1}) \,.$$

Both estimation schemes involve no Newton iterations, but a number of $N \times N$ linear equations associated with the Gram-matrix G. In total, both predictors have to solve 4 linear systems: EEP needs two for v and one for each Lagrangian multiplier, while the VSV predictor needs one for r, one for v and one for each Lagrangian multiplier. The VSV predictor is still more expensive, since it evaluates the driving force a three times instead of two as in case of EEP.

4.4 Approximation of white noise

4.4.1 Smoothing techniques

As we will see in the numerical simulations, adding noise to the force not only decreases the order of convergence, it makes it also more difficult to carry out each integration step since Newton's method needs much more iterations to find a suitable solution. One should note, however, that due to the inextensibility constraint, the finite bending stiffness and the fiber inertia, the acceleration of neighboring fiber points is highly correlated in space and time. Due to Newton's laws of motion this implies that the superposition of the constraint and turbulent forces also constitute a correlated force in space and time. We can incorporate this fact by replacing the white noise by a correlated random force field. Hence, we investigate different smoothing methods for the white noise and study the effect of its approximation. There are several methods we propose here, which we first introduce for an ordinary, one-parameter scalar-valued Wiener process w. In the following we search for a suitable approximation $\sigma_{\Delta t}(t_i)$ for the random measure $\xi_i = \xi((t_{i-1}, t_i]) \sim \mathcal{N}(0, \Delta t)$ for a given equidistant discretization of $[0, T]$. Afterwards, we generalize these methods to the case of a $\mathbb{R}$-valued planar Wiener process, the extension to $\mathbb{R}^d$-valued processes is then given by the applying the techniques to each component.

Forward-backward averaging The first smoothing method is based on the average force in a time interval. Thus, instead of using the random measure of the time interval,

$$\int_{t_{i-1}}^{t_i} \mathrm{d}w = w(t_i) - w(t_{i-1}) = \xi_i \,,$$

as stochastic force we use the arithmetic mean over $2N_t + 1$ intervals, with N_t denoting the smoothing length, i.e.

$$\sigma_{\Delta t}^{\mathrm{fba}}(t_i) = \frac{1}{2N_t + 1} \left(\xi_i + \sum_{k=1}^{N_t} \xi_{i+k} + \xi_{i-k} \right) = \frac{1}{2N_t + 1} \int_{t_{i-1-N_t}}^{t_{i+N_t}} \mathrm{d}w \,. \tag{4.38}$$
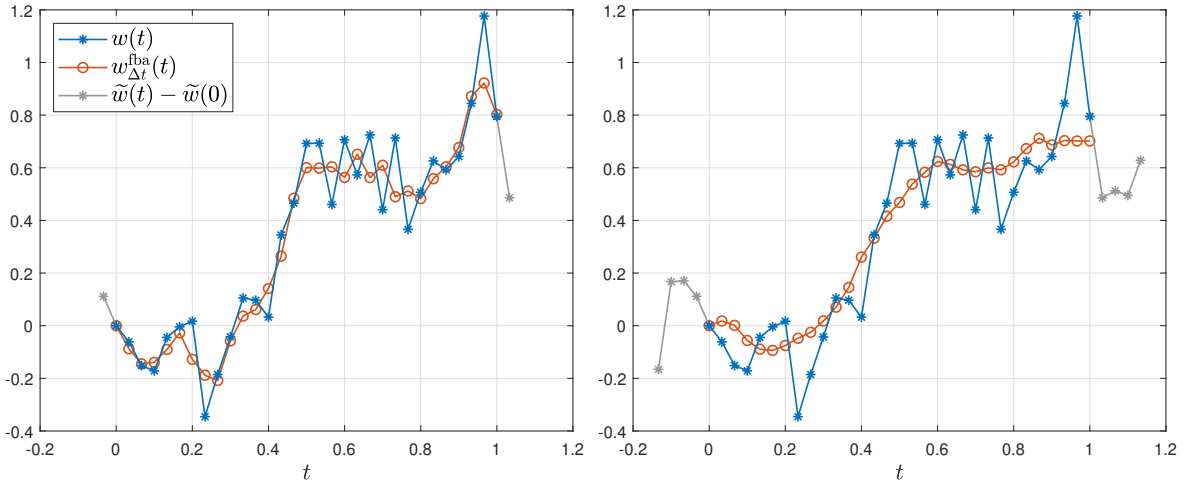
Figure 4.4.: Forward-backward averging for w generated with 30 random variables. Left: $N_t = 1$, right: $N_t = 4$.

This can be viewed as the approximation

$$\xi((t_{i-1}, t_i]) \approx \frac{\xi((t_{i-1-N_t}, t_{i+N_t}])}{2N_t + 1}, \qquad (4.39)$$

which is exactly true for the Lebesgue measure, while yielding a correlated force in case of the random measure. Using this averaging method, we need N_t additional random variables at each boundary of the time interval, which is equivalent to assuming that w is a normalized cut-out of a Wiener process $\widetilde{w}$ on the larger time-interval $[-N_t \Delta t, T + N_t \Delta t]$. Then, w is given as $w(t) = \widetilde{w}(t) - \widetilde{w}(0)$ for $t \in [-N_t \Delta t, T + N_t \Delta t]$. Given the $M + 2N_t$ increments $\xi_i \sim \mathcal{N}(0, \Delta t)$, $i = 1 - N_t, \ldots, M + N_t$, the Wiener process fulfills $w(t_i) = \sum_{k=1}^{i} \xi_k$, for $i = 1, \ldots, M$. Due to the averaging of the increments (4.38), we also get a smoothed discrete version of the Wiener process, given as

$$w_{\Delta t}^{\text{fba}}(t_i) = \sum_{k=1}^{i} \sigma_{\Delta t}^{\text{fba}}(t_k) = \frac{1}{2N_t + 1}\left(w(t_i) + \sum_{\ell=1}^{N_t} w(t_{i+\ell}) - w(t_\ell) + w(t_{i-\ell}) - w(t_{-\ell})\right)$$

$$= \frac{1}{2N_t + 1}\sum_{\ell=-N_t}^{N_t} w(t_{i+\ell}) - \frac{1}{2N_t + 1}\sum_{\ell=-N_t}^{N_t} w(t_\ell).$$

The effect of the smoothing technique for $N_t \in \{1, 4\}$ is shown in Fig. 4.4 for a discrete approximation of a Wiener process generated by 30 random variables.

Coarser resolution of Wiener Process The next possibility is to consider a coarser resolution of the Wiener Process and assign the average force to all time intervals within the averaging interval. Assume $(0, T] = \cup_{i=0}^{M-1}(t_i, t_{i+1}] = \cup_{j=1}^{M_t} \cup_{i=0}^{N_t-1} (t_{(j-1)N_t+i}, t_{(j-1)N_t+i+1}]$, where $M = M_t N_t$. Then we set for any $i \in \{0, \ldots, N_t - 1\}$ and $j \in \{1, \ldots, M_t\}$

$$\xi((t_{(j-1)N_t+i}, t_{(j-1)N_t+i+1}]) \approx \frac{\xi((t_{(j-1)N_t}, t_{jN_t}])}{N_t} \qquad (4.40)$$

116
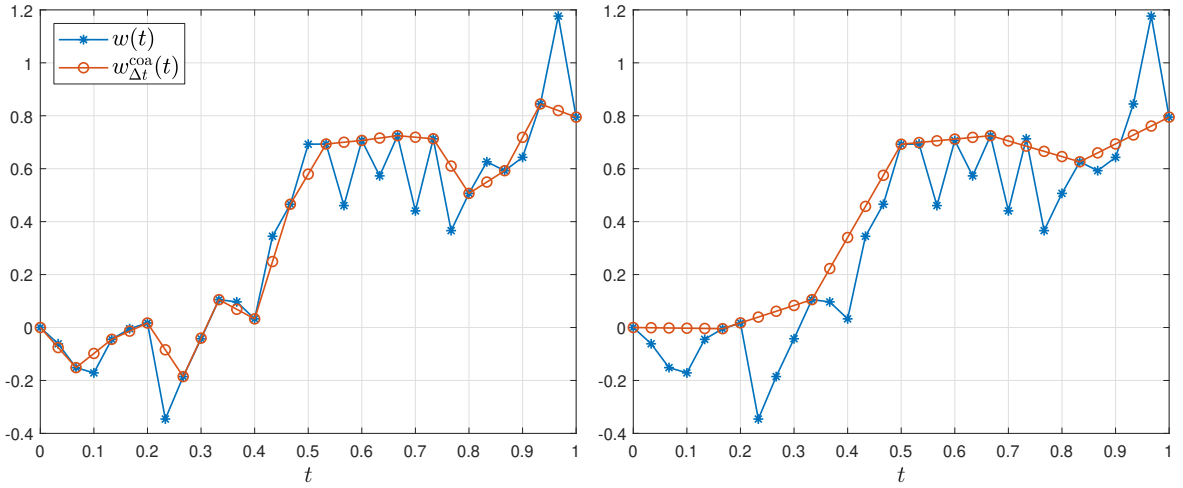
Figure 4.5.: Coarser resolution for w generated with 30 random variables. Left: $M_t = 15, N_t = 2$, right: $M_t = 6, N_t = 5$.

which is again exactly true for the Lebesgue measure. This results in the approximation

$$\sigma^{\text{coa}}_{\Delta t}(t_{(j-1)N_t+i+1}) = \frac{1}{N_t} \sum_{k=0}^{N_t-1} \xi_{(j-1)N_t+k+1} = \frac{w(t_{jN_t}) - w(t_{(j-1)N_t})}{N_t}$$

for all $i = 0, \ldots, N_t - 1$. The resulting approximation of the Wiener process is given as

$$
\begin{aligned}
w^{\text{coa}}_{\Delta t}(t_{(j-1)N_t+i}) &= \sum_{k=1}^{j-1} \sum_{\ell=0}^{N_t-1} \sigma^{\text{coa}}_{\Delta t}(t_{(k-1)N_t+\ell+1}) + \sum_{\ell=0}^{i-1} \sigma^{\text{coa}}_{\Delta t}(t_{(j-1)N_t+\ell+1}) \\
&= \sum_{k=1}^{j-1} \sum_{\ell=0}^{N_t-1} \frac{w(t_{kN_t}) - w(t_{(k-1)N_t})}{N_t} + \sum_{\ell=0}^{i-1} \frac{w(t_{jN_t}) - w(t_{(j-1)N_t})}{N_t} \\
&= w(t_{(j-1)N_t}) + \frac{w(t_{jN_t}) - w(t_{(j-1)N_t})}{N_t} i
\end{aligned}
$$

since $w(t_0) = w(0) = 0$. Hence, $w^{\text{coa}}_{\Delta t}$ is a discretized linear interpolation spline of w on the scale of the averaging discretization. Two realizations of $w^{\text{coa}}_{\Delta t}$ can be seen in Fig. 4.5.

Convolution of the Wiener Process Finally, we also consider the smoothing of the Wiener process directly by the convolution of w with a smoothing kernel which was studied in [16]. For two functions $\phi, f \in \mathcal{L}^2(\mathbb{R})$, the convolution is denoted as

$$(\varphi \star f)(\tau) = \int_{\mathbb{R}} \varphi(\tau - t) f(t) \mathrm{d}t \,.$$

As smoothing kernels we choose different probability densities over $\mathbb{R}$ with compact support. Additionally, for a given smoothing kernel φ with $\text{supp}(\varphi) = \mathcal{S} \subset \mathbb{R}$ and a scaling factor $\delta > 0$, we set the scaled kernel $\varphi_\delta(t) = \delta^{-1}\varphi(t\delta^{-1})$. The latter is a probability density and fulfills $\text{supp}(\varphi_\delta) = \delta\mathcal{S}$. As scaling factor we use $\delta = N_t\Delta t$ for $N_t \geq 1$. The discrete smoothed approximation of the Wiener process is then given as $w^\star(t_i) = (\varphi_\delta \star w)(t_i)$ and the force approximation as $\sigma^\star(t_i) = w^\star(t_i) - w^\star(t_{i-1})$. Since w is known only on the grid points t_i, we use the trapezoidal rule for the quadrature of the convolution integral, which results in approximations for $w^\star$ and $\sigma^\star$.
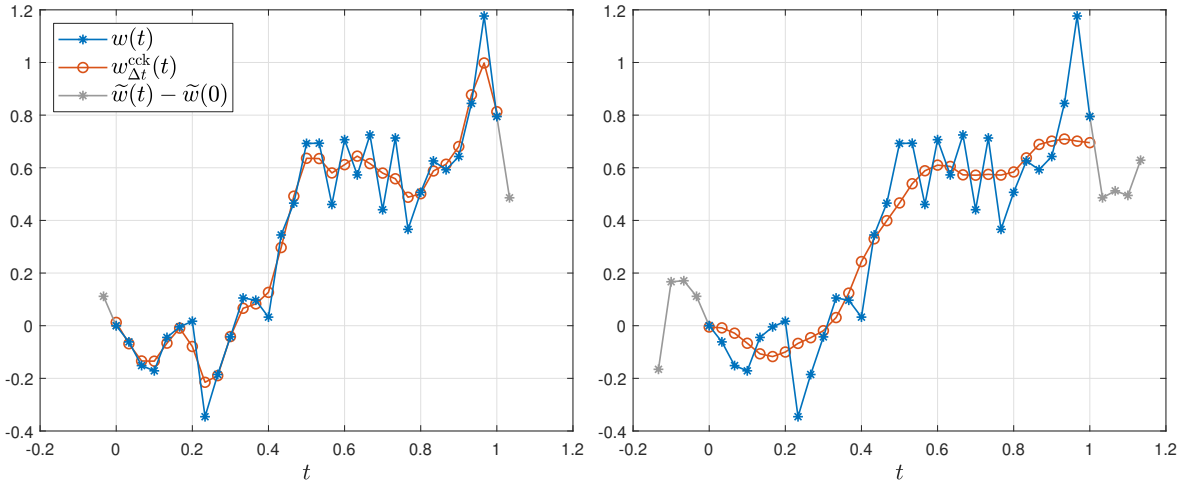
Figure 4.6.: Convolution with central constant kernel for w generated with 30 random variables. Left: $N_t = 1$, right: $N_t = 4$.

Convolution with central constant kernel Setting $\varphi(t) = 0.5\chi_{[-1,1]}(t)$, i.e., a central constant kernel yields

$$(\varphi_{N_t\Delta t} \star w)(t_i) = \frac{1}{2N_t\Delta t} \int_{t_i-N_t\Delta t}^{t_i+N_t\Delta t} w(t)\,\mathrm{d}t = \frac{1}{2N_t\Delta t} \sum_{k=1}^{N_t} \left(\int_{t_{i-k}}^{t_{i-k+1}} w(t)\,\mathrm{d}t + \int_{t_{i+k-1}}^{t_{i+k}} w(t)\,\mathrm{d}t \right).$$

Using the trapezoidal rule for the quadrature, we get

$$(\varphi_{N_t\Delta t} \star w)(t_i) \approx \frac{1}{4N_t} \sum_{k=1}^{N_t} (w(t_{i-k+1}) + w(t_{i-k}) + w(t_{i+k}) + w(t_{i+k-1}))$$

$$= \frac{1}{2N_t} \sum_{\ell=-N_t}^{N_t} w(t_{i+\ell}) - \frac{w(t_{i+N_t}) + w(t_{i-N_t})}{4N_t} = w_{\Delta t}^{\mathrm{cck}}(t_i)$$

which yields the approximation $\sigma_{\Delta t}^{cck}$. Similarly to the case of forward-backward averaging, here we also need to interpret w as a cut-out of a Wiener process $\widetilde{w}$ on the time interval $[-N_t\Delta t, T + N_t\Delta t]$. Two realizations of this technique are seen in Fig. 4.6.

Convolution with forward constant kernel In case of $\varphi(t) = \chi_{[-1,0]}(t)$, which we denote as a forward constant kernel, we get

$$(\varphi_{N_t\Delta t} \star w)(t_i) = \frac{1}{N_t\Delta t} \int_{t_i}^{t_i+N_t} w(t)\mathrm{d}t \approx \frac{1}{2N_t} \sum_{j=1}^{N_s} (w(t_{i+j-1}) + w(t_{i+j}))$$

$$= \frac{1}{N_t} \sum_{\ell=0}^{N_t} w(t_{i+\ell}) - \frac{w(t_{i+N_t}) + w(t_i)}{2N_t} = w_{\Delta t}^{\mathrm{fck}}(t_i).$$

The behavior of the convolution with the constant forward kernel is seen in Fig. 4.7.
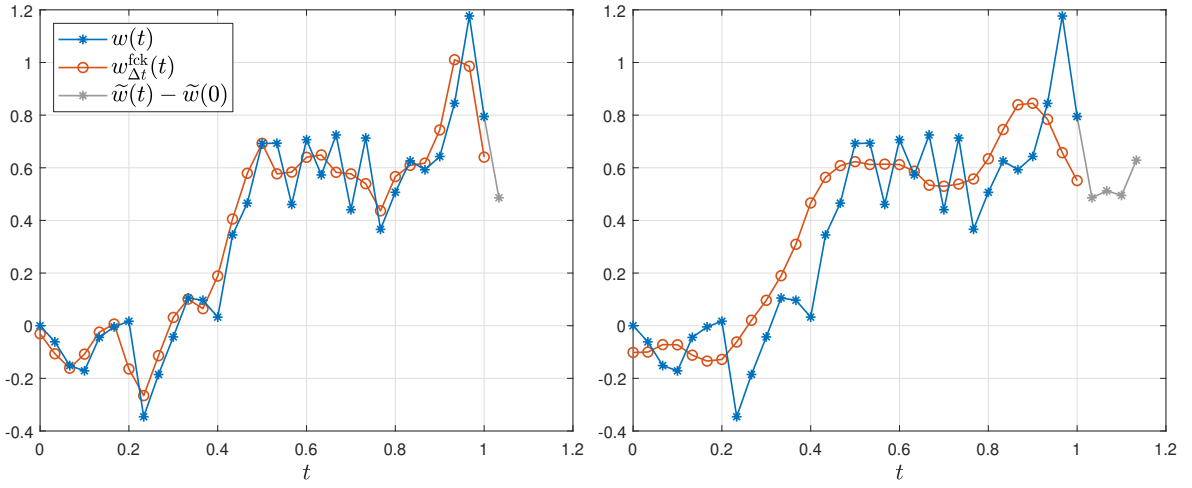
Figure 4.7.: Convolution with constant forward kernel for w generated with 30 random variables. Left: $N_t = 1$, right: $N_t = 4$.
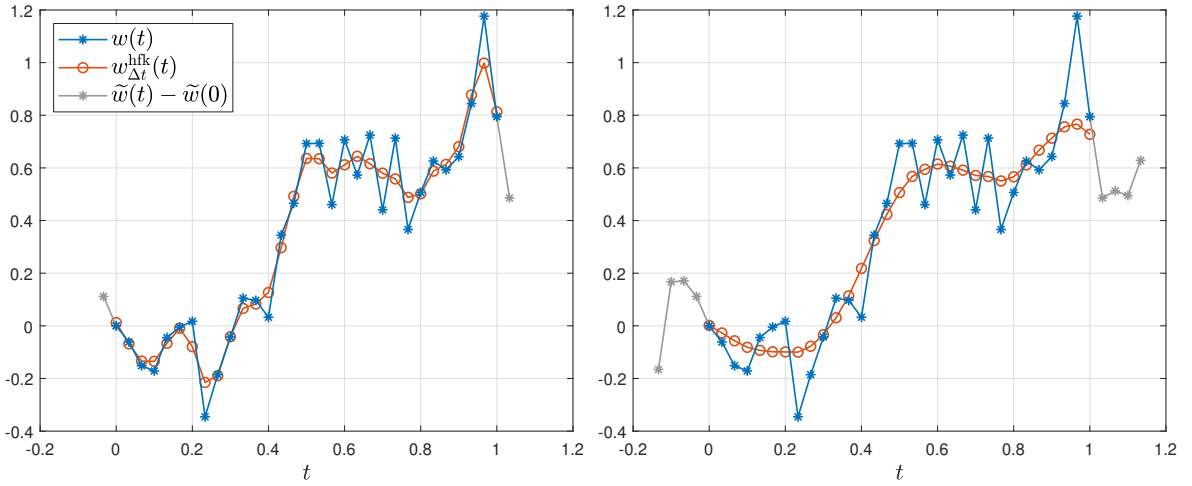
Figure 4.8.: Convolution with hat function kernel for w generated with 30 random variables. Left: $N_t = 2$, right: $N_t = 5$.

Convolution with hat functions   Taking the hat functions as the integration kernel, $\varphi(t) = (1 - |t|)\chi_{[-1,1]}$, results in

$$
\begin{aligned}
(\varphi_{N_t \Delta t} \star w)(t_i) &= \frac{1}{N_t \Delta t} \int_{t_{i-N_t}}^{t_{i+N_t}} \left(1 - \frac{|t_i - t|}{N_t \Delta t}\right) w(t)\, \mathrm{d}t \\
&\approx \frac{1}{N_t}\left(w(t_i) + \sum_{k=1}^{N_t-1} \frac{N_t - k}{N_t}\big(w(t_{i-k}) + w(t_{i+k})\big)\right) \\
&= \frac{1}{N_t}\sum_{\ell=-N_t+1}^{N_t-1} \frac{N_t - |\ell|}{N_t} w(t_{i+\ell}) = w_{\Delta t}^{\mathrm{hfk}}(t_i)\,.
\end{aligned}
$$

The behavior can be seen in Fig. 4.8.
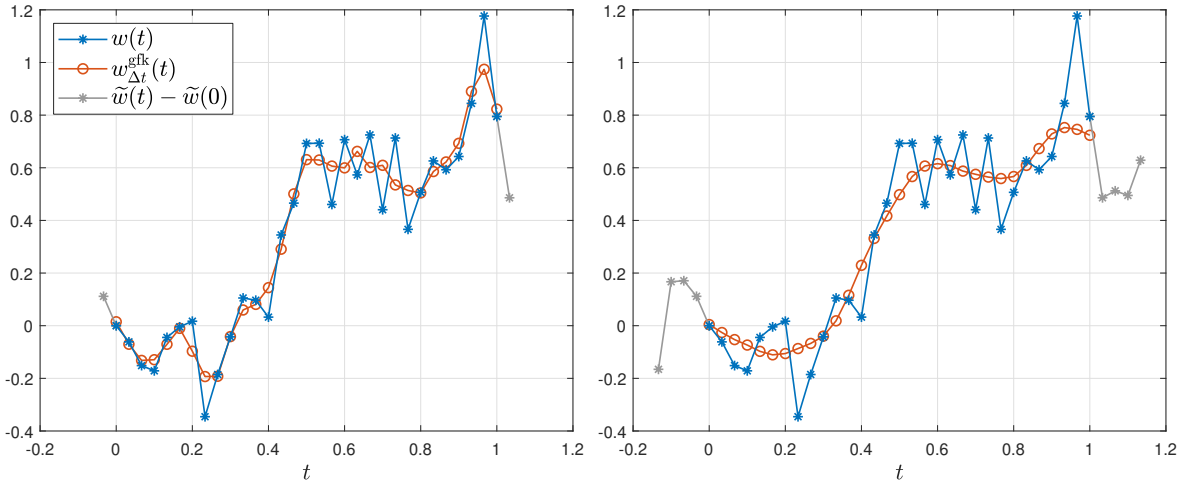
Figure 4.9.: Convolution with Gaussian kernel for w generated with 30 random variables. Left: $N_t = 2$, right: $N_t = 5$.

Convolution with Gaussian kernel Taking the Gaussian kernel, $\varphi(t) = C \exp((t^2 - 1)^{-1})\chi_{(-1,1)}$ with C being the normalizing constant, gives

$$
(\varphi_{N_t \Delta t} \star w)(t_i) = \frac{1}{N_t \Delta t} \int_{t_{i-N_t}}^{t_{i+N_t}} \varphi\left(\frac{t_i - t}{N_t \Delta t}\right) w(t)\, \mathrm{d}t
$$

$$
\approx \frac{1}{N_t}\left(\varphi(0)w(t_i) + \sum_{k=1}^{N_t-1} \varphi\left(\frac{k}{N_t}\right)(w(t_{i-k}) + w(t_{i+k}))\right)
$$

$$
= \frac{1}{N_t} \sum_{\ell=-N_t+1}^{N_t-1} \phi\left(\frac{\ell}{N_t}\right) w(t_{i+\ell}) = w_{\Delta t}^{\mathrm{gfk}}(t_i)
$$

due to symmetry and $\lim_{t \to \pm 1} \phi(t) = 0$. The behavior can be seen in Fig. 4.9.

Extension of smoothing techniques to a planar Wiener process The extension of the forward-backward averaging technique to the 2d case follows by applying (4.39) to a planar random measure. In this case the rectangle $(s_{i-1-N_s}, s_{i+N_s}] \times (t_{j-1-N_t}, t_{j+N_t}]$ with $N_s, N_t \geq 1$ consists of $(2N_s + 1)(2N_t + 1)$ rectangles of Lebesgue measure $\Delta s \Delta t$, hence we use the approximation

$$
\xi((s_{i-1}, s_i] \times (t_{j-1}, t_j]) \approx \frac{\xi((s_{i-1-N_s}, s_{i+N_s}] \times (t_{j-1-N_t}, t_{j+N_t}])}{(2N_t + 1)(2N_s + 1)}.
$$

Setting $\xi_{i,j} = \xi((s_{i-1}, s_i] \times (t_{j-1}, t_j])$, this results in the approximation of the force and of the Wiener process given as

$$
\sigma_{\Delta s, \Delta t}^{\mathrm{fba}}(s_i, t_j) = \sum_{k=1}^{N_s} \sum_{\ell=1}^{N_t} \frac{\xi_{i+k,j+\ell} + \xi_{i+k,j-\ell+1} + \xi_{i-k+1,j+\ell} + \xi_{i-k+1,j-\ell+1}}{(2N_t + 1)(2N_s + 1)}
$$

$$
+ \sum_{k=1}^{N_s} \frac{\xi_{i+k,j-N_t} + \xi_{i-k+1,j-N_t}}{(2N_t + 1)(2N_s + 1)} + \sum_{\ell=1}^{N_t} \frac{\xi_{i-N_s,j+\ell} + \xi_{i-N_s,j-\ell+1}}{(2N_t + 1)(2N_s + 1)} + \frac{\xi_{i-N_s,j-N_t}}{(2N_t + 1)(2N_s + 1)},
$$

120

$$w^{\text{fba}}_{\Delta s,\Delta t}(s_i,t_j) = \sum_{k=-N_s}^{N_s}\sum_{\ell=-N_t}^{N_t}\frac{w(s_{i+k},t_{j+\ell}) + w(s_k,t_\ell) - w(s_k,t_{j+\ell}) - w(s_{i+k},t_\ell)}{(2N_t+1)(2N_s+1)}\,.$$

In order to define values of $w(s,t)$ for $s<0,t<0$, we consider $w(s,t)$ on $[0,L]\times[0,T]$ as a normalized cut-out of a Wiener process $\widetilde{w}$ on $[-N_s\Delta s, L+N_s\Delta s]\times[-N_t\Delta t, T+N_t\Delta t]$ given as $w(s,t) = \widetilde{w}(s,t) - \widetilde{w}(0,t) - \widetilde{w}(s,0) + \widetilde{w}(0,0)$, analogously to the 1d case.

Similarly, the coarser resolution follows by first considering the partition of $(0,L]\times(0,T]$ given as

$$(0,L]\times(0,T] = \cup_{i=0}^{N-1}\cup_{j=0}^{M-1}(s_i,s_{i+1}]\times(t_j,t_{j+1}]$$
$$= \cup_{i=1}^{M_s}\cup_{k=0}^{N_s-1}\cup_{j=1}^{M_t}\cup_{\ell=0}^{N_t-1}(s_{(i-1)N_s+k},s_{(i-1)N_s+k+1}]\times(t_{(j-1)N_t+\ell},t_{(j-1)N_t+\ell+1}],$$

with $N = M_sN_s, M = M_tN_t$. Analogously to (4.40) we then use the approximation

$$\xi\big((s_{(i-1)N_s+k},s_{(i-1)N_s+k+1}]\times(t_{(j-1)N_t+\ell},t_{(j-1)N_t+\ell+1}]\big)$$
$$\approx \frac{\xi\big((s_{(i-1)N_s},s_{iN_s}]\times(t_{(j-1)N_t},t_{jN_t}]\big)}{N_tN_s}$$

for all i,j,k,ℓ. This results in the approximation for the force given as

$$\sigma^{\text{coa}}_{\Delta s,\Delta t}(s_{(i-1)N_s+k+1},t_{(j-1)N_t+\ell+1}) = \frac{1}{N_sN_t}\sum_{m=0}^{N_s-1}\sum_{n=0}^{N_t-1}\xi_{(i-1)N_s+m+1,(j-1)N_t+n+1}$$
$$= \frac{w(s_{iN_s},t_{jN_t}) + w(s_{(i-1)N_s},t_{(j-1)N_t}) - w(s_{(i-1)N_s},t_{jN_t}) - w(s_{iN_s},t_{(j-1)N_t})}{N_sN_t}$$

for all i,j,k,ℓ. The smooth approximation of the Wiener process then follows as the local bilinear approximation

$$w^{\text{coa}}_{\Delta s,\Delta t}\big(s_{(i-1)N_s+k},t_{(j-1)N_t+\ell}\big)$$
$$= \frac{1}{N_tN_s}\Big(w(s_{(i-1)N_s},t_{(j-1)N_t})(N_s-k)(N_t-\ell) + w(s_{iN_s},t_{(j-1)N_t})k(N_t-\ell)$$
$$+ w(s_{(i-1)N_s},t_{jN_t})(N_s-k)\ell + w(s_{iN_s},t_{jN_t})k\ell\Big).$$

Considering the convolution based techniques, we use the product of two smoothing kernels ϕ,ψ on $\mathbb{R}$ as a kernel on $\mathbb{R}^2$ given as $\varphi(s,t) = \phi(s)\psi(t)$. In fact, if ϕ,ψ are compactly supported in $\mathbb{R}$, the support of φ is compact in $\mathbb{R}^2$ and if ϕ,ψ are probability densities on $\mathbb{R}$, so is φ on $\mathbb{R}^2$. Given two scaling factors $\delta_1,\delta_2 > 0$, we set $\varphi_{\delta_1,\delta_2}(s,t) = (\delta_1\delta_2)^{-1}\phi(s/\delta_1)\psi(t/\delta_2)$. We explore here only products of the same kind of kernels. In this case, the usage of the central constant kernel in combination with the trapezoidal rule in each dimension leads to

$$(\varphi_{N_s\Delta s,N_t\Delta t}\star w)(s_i,t_j) \approx \frac{1}{16N_sN_t}\sum_{k=-N_s}^{N_s-1}\sum_{\ell=-N_t}^{N_t-1}\Big(w(s_{i+k+1},t_{j+\ell+1}) + w(s_{i+k},t_{j+\ell})$$
$$+ w(s_{i+k+1},t_{j+\ell}) + w(s_{i+k},t_{j+\ell+1})\Big) = w^{\text{cck}}_{\Delta s,\Delta t}\,.$$

	coa	fba	cck	fck	hfk	gfk
1d	$p \approx 0.52$	$p \approx 0.49$	$p \approx 0.51$	$p \approx 0.50$	$p \approx 0.53$	$p \approx 0.44$
2d	$p \approx 0.54$	$p \approx 0.46$	$p \approx 0.50$	$p \approx 0.50$	$p \approx 0.57$	$p \approx 0.53$

Table 4.2.: Measured exponent of the relative error $e_{1,\delta}^{\mathrm{method}} = cN_t^p$.

In case of the forward constant kernel the approximation follows as

$$
(\varphi_{N_s\Delta s,N_t\Delta t} \star w)(s_i,t_j) \approx \frac{1}{4N_sN_t} \sum_{k=1}^{N_s} \sum_{\ell=1}^{N_t} \Big(w(s_{i+k},t_{j+\ell}) + w(s_{i+k-1},t_{j+\ell-1})
$$
$$
+ w(s_{i+k},t_{j+\ell-1}) + w(s_{i+k-1},t_{j+\ell}) \Big) = w_{\Delta s,\Delta t}^{\mathrm{fck}} .
$$

Similarly, since the hat function and Gauss kernels are symmetric and both fulfill $\phi(1) = 0$, we have

$$
(\varphi_{N_s\Delta s,N_t\Delta t} \star w)(s_i,t_j) \approx \sum_{k=-N_s+1}^{N_s-1} \sum_{\ell=-N_t+1}^{N_t-1} \frac{w(s_{i+k},t_{j+\ell})}{N_sN_t} \phi\left(\frac{k}{N_s}\right) \phi\left(\frac{\ell}{N_t}\right) = w_{\Delta s,\Delta t}^{\mathrm{hfk/gfk}} .
$$

Summary of smoothing techniques   The behavior of the relative error with respect to the Wiener process,

$$
e_{1,\delta}^{\mathrm{method}} = \frac{\|w - w_\delta^{\mathrm{method}}\|}{\|w\|} ,
$$

with $\|w\|^2 = \sum_{i=0}^{M} w(t_i)^2 \Delta t$ in the 1d case and $\|w\|^2 = \sum_{i=0}^{N} \sum_{j=0}^{M} w(s_i,t_j)^2 \Delta s \Delta t$ in the 2d case, is seen in Fig. 4.11 for the different smoothing techniques. The error behaves for all methods as $\sqrt{N_t}$ in 1d and $\sqrt{N_s} + \sqrt{N_t}$ in the planar case, the measured least squares exponents are listed in Tab. 4.2. Additionally, the error has approximately the same amplitude for all methods. The approximation by the hat function kernel is closest to the original process, while generating very smooth fields as seen in Fig. 4.8 and Fig. 4.10. Since we replace the Wiener process by a more regular field in order to improve the computation cost and increase the regularity of the resulting fiber curve, a relatively large error e_δ is expected. Since it is not practicable to draw the complete Wiener process on a fine scale, apply the smoothing technique and afterwards adapt the approximation to the desired, coarse spatial and time discretization, the smoothing technique is applied to the coarsely discretized Wiener process directly. Hence, it is of interest, whether the smooth approximation $w_\delta^{\mathrm{method}}$ with a fixed correlation length N_s, N_t converges as $\delta \to 0$. In order to examine this behavior, we generate a reference field $w_{\delta_{\mathrm{fine}}}^{\mathrm{method}}$ and consider the error with respect to this reference field,

$$
e_{2,\delta}^{\mathrm{method}} = \frac{\|w_{\delta_{\mathrm{fine}}}^{\mathrm{method}} - w_\delta^{\mathrm{method}}\|}{\|w_{\delta_{\mathrm{fine}}}^{\mathrm{method}}\|}
$$

for $\delta > \delta_{\mathrm{fine}}$. As seen in Fig. 4.12, $e_{2,\Delta t}^{\mathrm{method}} \in \mathcal{O}(\sqrt{\Delta t})$ as $\Delta t \to \Delta t_{\mathrm{fine}}$ in the 1d case and similarly $e_{2,\Delta s\Delta t}^{\mathrm{method}} \in \mathcal{O}(\sqrt{\Delta s} + \sqrt{\Delta t})$ as $\Delta s \to \Delta s_{\mathrm{fine}}, \Delta t \to \Delta t_{\mathrm{fine}}$ for all considered smoothing methods.
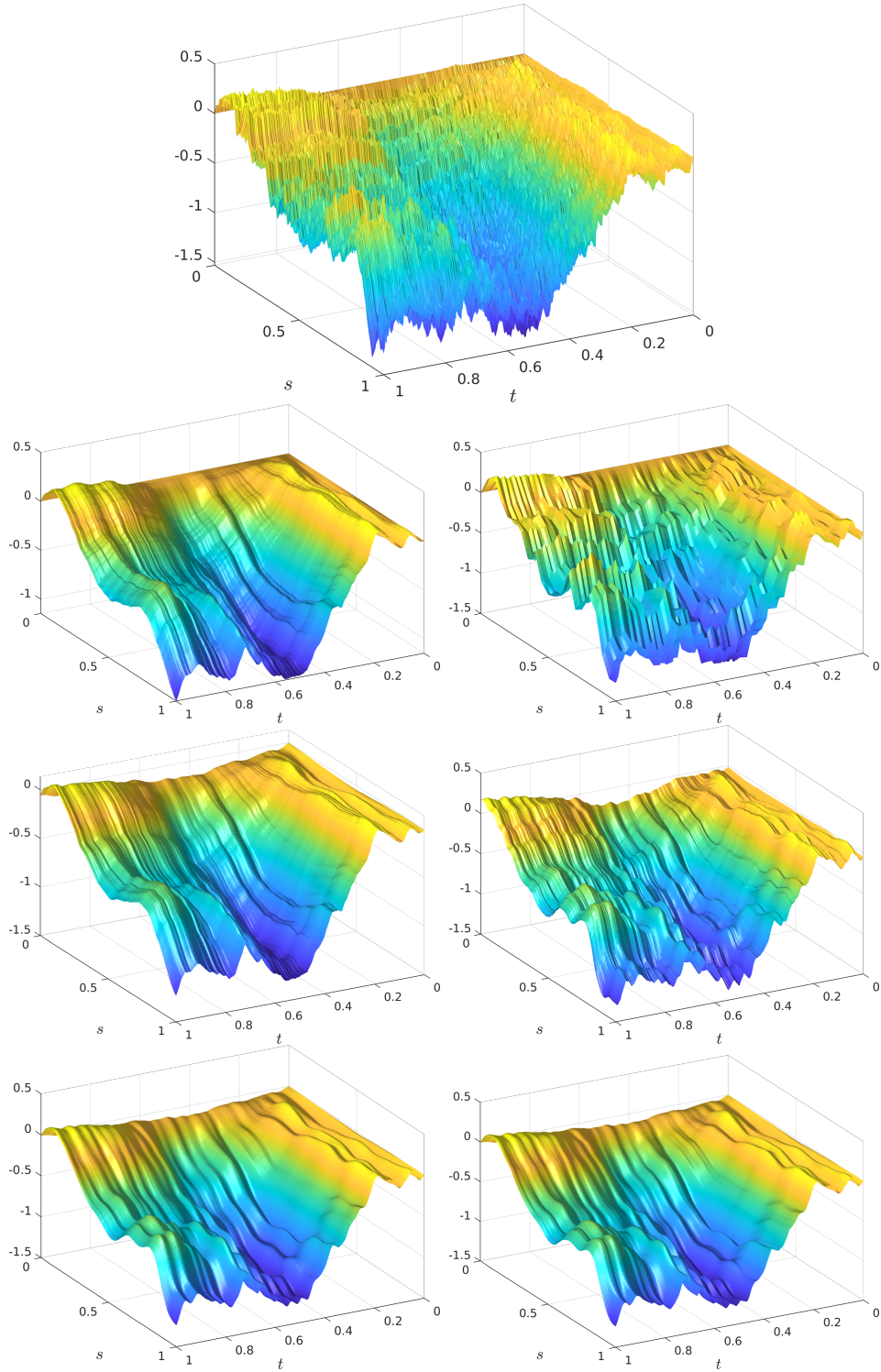
Figure 4.10.: Different smoothing techniques applied to a planar Wiener process. Top original process generated with $\Delta s = 10^{-2}, \Delta t = 10^{-3}$ with $T = 1 = L$. From top to bottom, from left to right: Forward-backward averaging, with $N_s = 10, N_t = 20$; coarser resolution with $N_s = 5, N_t = 10$; convolution with central constant kernel, forward constant kernel, hat function kernel and Gaussian kernel with $N_s = 10, N_t = 20$.

123

	coa	fba	cck	fck	hfk	gfk
1d, $N_t = 2$	$p \approx 0.49$	$p \approx 0.57$	$p \approx 0.58$	$p \approx 0.57$	$p \approx 0.55$	$p \approx 0.55$
2d, $N_t = 2$	$p \approx 0.49$	$p \approx 0.64$	$p \approx 0.65$	$p \approx 0.65$	$p \approx 0.59$	$p \approx 0.59$
1d, $N_t = 4$	$p \approx 0.52$	$p \approx 0.58$	$p \approx 0.59$	$p \approx 0.58$	$p \approx 0.59$	$p \approx 0.59$
2d, $N_t = 4$	$p \approx 0.54$	$p \approx 0.64$	$p \approx 0.66$	$p \approx 0.67$	$p \approx 0.66$	$p \approx 0.66$
1d, $N_t = 8$	$p \approx 0.53$	$p \approx 0.59$	$p \approx 0.58$	$p \approx 0.58$	$p \approx 0.60$	$p \approx 0.59$
2d, $N_t = 8$	$p \approx 0.57$	$p \approx 0.65$	$p \approx 0.66$	$p \approx 0.66$	$p \approx 0.69$	$p \approx 0.68$

Table 4.3.: Measured exponent of the relative error $e_{2,\delta}^{\mathrm{method}} = c\delta^p$.
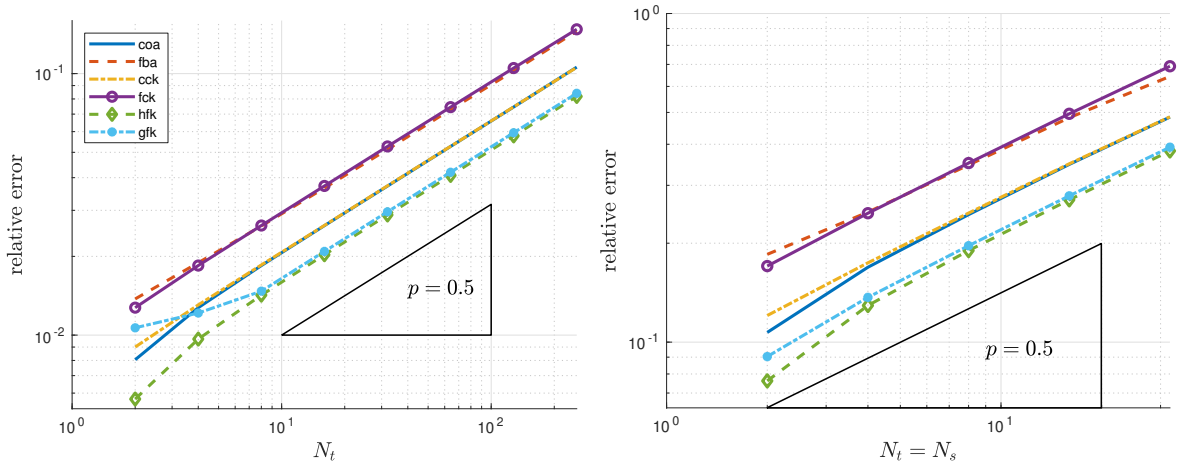
Figure 4.11.: Error behavior of the Wiener Process: Error with respect to w. Approximation by coarser resolution ("coa"), forward-backward averaging ("fba") and convolution by central constant ("cck"), forward constant ("fck"), hat function ("hfk") and Gaussian ("gfk") kernels. Left: 1d case, $T = 1, \Delta t = 2^{-14}$. Right: 2d case, $T = L = 1, \Delta t = \Delta s = 2^{-7}$.
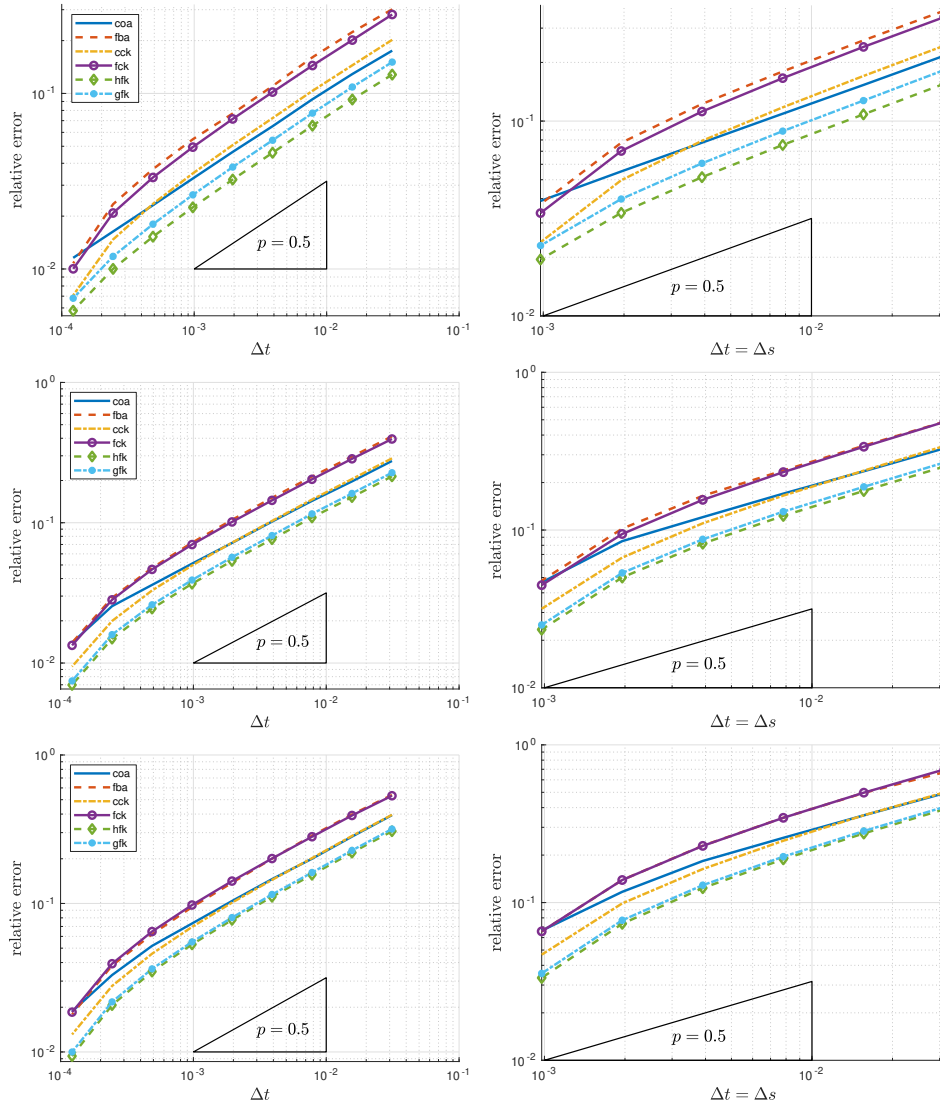
Figure 4.12.: Error behavior of the Wiener Process: Error with respect to w^s. Approximation by coarser resolution ("coa"), forward-backward averaging ("fba") and convolution by central constant ("cck"), forward constant ("fck"), hat function ("hfk") and Gaussian ("gfk") kernels. Left: 1d case, $T = 1$, reference generated with $\Delta t = 2^{-14}$. Right: 2d case, $T = L = 1$, $N_t = N_s$, reference generated with $\Delta t = \Delta s = 2^{-11}$. Top: $N_t = 2$; center: $N_t = 4$; bottom: $N_t = 8$.

4.4.2 Wiener chaos expansion

The so-called Wiener chaos expansion (WCE) for stochastic differential equations yields an effective splitting between deterministic and stochastic effects, allowing an efficient computation of the mean behavior of the system under consideration. It is based on a Fourier expansion of the underlying white noise with respect to a deterministic basis, giving stochastic coefficients. Expanding the unknowns in polynomials of these white noise coefficients leads then to a deterministic system of differential equations which inherits the complete information of the stochastic system [44, 66, 89]. In order to explore the feasibility of a WCE-based numerical method for the Kirchhoff beam model (4.5) under the influence of a planar white noise, we consider a simplified, linear aerodynamic drag by using

$$f_{ad}(r, \partial_t r, \partial_s r, t) = \gamma(u(r, t) - \partial_t r)$$

in (4.8b) instead of the universal drag model. As outer flow field we use a time-independent linear flow, $u(r, t) \equiv u(r) = A \cdot r$. Additionally, we consider only additive white noise by setting $C \equiv I$ for the stochastic amplitude (4.23). Since we introduced the scaled drag number $\hat{Dr}$ which fulfills $Dr = \hat{Dr}\sqrt{\gamma}$ (see Section 4.2.4), γ cancels out in the resulting momentum equation, and we arrive at the resulting system

$$\partial_{tt} r = \partial_s(\lambda \partial_s r) - \alpha^{-2}\partial_{ssss} r + \hat{Dr}^{-2}(A \cdot r - \partial_t r) + \beta \hat{Dr}^{-2}\xi, \quad \|\partial_s r\|^2 = 1 \quad (4.41)$$

with boundary and initial conditions (4.6). As stated before (see Section 4.2.2), we assume that the solution components (r, λ) of (4.41) are $\mathcal{F}_{s,t}$-measurable random fields with $r_i(s, t), \lambda(s, t) \in \mathcal{L}^2(\Omega, \mathcal{F}_{L,T}, \mu; \mathbb{R})$, $i \in \{1, \dots, d\}$.

The Wiener chaos expansion is based on an orthogonal decomposition of the underlying space $\mathcal{L}^2(\Omega, \mathcal{A}, \mu; \mathbb{R})$. Following [44] we denote by $\mathcal{H}$ a Gaussian Hilbert space, i.e., a complete linear subspace of $\mathcal{L}^2(\Omega, \mathcal{A}, \mu; \mathbb{R})$ containing centered Gaussian random variables. Then the set $P_n(\mathcal{H})$ of M-variate polynomials $p(\kappa_1, \dots, \kappa_M)$ for $M \in \mathbb{N}$ of degree $\deg(p) \leq n$ with $\kappa_i \in \mathcal{H}$ is a linear subspace of $\mathcal{L}^2$. This holds also for its closure $\overline{P}_n(\mathcal{H})$. Setting $H_0 = \overline{P}_0(\mathcal{H})$ and $H_n = \overline{P}_n(\mathcal{H}) \cap P_{n-1}^\perp$ for $n \geq 1$, with orthogonal complement $\perp$, we arrive at a pairwise orthogonal decomposition of $\mathcal{L}^2(\Omega, \sigma(\mathcal{H}), \mu; \mathbb{R})$ with σ-algebra $\sigma(\mathcal{H})$ generated by $\mathcal{H}$. For $\sigma(\mathcal{H}) = \mathcal{A}$, the Cameron-Martin theorem [24] holds, stating $\mathcal{L}^2(\Omega, \mathcal{A}, \mu; \mathbb{R}) = \cup_n H_n$. This statement can be extended to $\mathcal{L}^2(\Omega, \mathcal{A}, \mu; \mathbb{R}^d)$, since every component of a d-dimensional random variable has a finite second moment on the corresponding one-dimensional space. To derive an appropriate set $\mathcal{H}$, we follow [66] and introduce the Fourier expansion of the planar white noise.

Definition 57 (Fourier expansion of planar white noise). *Let $\{b_{ij}\}_{i,j \in \mathbb{N}}$ be an orthonormal basis of $\mathcal{L}^2([0, L] \times [0, T]; \mathbb{R})$ with $b_{ij}(s, t) = \phi_i(s)\psi_j(t)$, where $\{\phi_i\}_{i \in \mathbb{N}}$ and $\{\psi_i\}_{i \in \mathbb{N}}$ form orthonormal bases of $\mathcal{L}^2([0, L]; \mathbb{R})$ and $\mathcal{L}^2([0, T]; \mathbb{R})$ respectively. The Fourier expansion of the white noise components $(w)_i = w_i$, $1 \leq i \leq d$ is given in terms of stochastic coefficients $\kappa_{ik\ell}$ that are determined by an Itô integral,*

$$w_i(s, t, \omega) = \sum_{k\ell} \kappa_{ik\ell}(\omega, L, T) \int_0^s \int_0^t \phi_k(\sigma)\psi_\ell(\tau) \, d\sigma d\tau, \quad \kappa_{ik\ell} = \int_0^L \int_0^T \phi_k\psi_\ell \, d\xi_i.$$

Remark 58 (Properties of the Fourier expansion)**.**

1. *The stochastic coefficients of the white noise are independent identically distributed $\mathcal{N}(0,1)$ random variables as can be shown using the Itô-isometry [125].*

2. *For the trigonometric basis $\phi_1(s) \equiv L^{-1/2}$, $\phi_i(s) = (2/L)^{1/2} \cos((i-1)\pi s/L)$, $i \geq 2$, analogously for ψ_i, the mean square error of the truncated expansion w_i^a of the white noise behaves as $\mathbb{E}[w_i - w_i^a]^2 = \mathcal{O}(LT(N_L^{-1} + N_T^{-1}))$, where N_L and N_T denote the number of basis functions ϕ_i and ψ_i, respectively.*

For the construction of the orthogonal polynomial basis, we choose the Gaussian Hilbert space as $\mathcal{H} = \overline{\mathrm{span}\{\kappa_{ik\ell}\}}$ and introduce a bijective mapping $\eta : \{1,\dots,d\} \times \mathbb{N} \times \mathbb{N} \to \mathbb{N}$ to enumerate each component. In this case $\mathcal{F}_{L,T} = \sigma(\mathcal{H})$ holds [69] and the system of orthonormal polynomials on $\mathcal{L}^2(\Omega, \mathcal{F}_{L,T}, \mu; \mathbb{R}^d)$ is given by products of Hermite polynomials [44]. We denote by $h_n : \mathbb{R} \to \mathbb{R}$ the nth order Hermite polynomial which is normalized with respect to the Gaussian measure [114], i.e., $\{h_n\}$ fulfill

$$\int_{\mathbb{R}} h_n(x) h_m(x) (2\pi)^{-1/2} e^{-x^2/2} \, \mathrm{d}x = \delta_{nm} \;,$$

with Kronecker delta δ_{nm}. Furthermore, we consider a set of multi-indices $J \subset \mathbb{N}_0^{\mathbb{N}}$ by $J = \{\iota = (\iota_i)_{i \geq 1} | \iota_i \in \mathbb{N}_0, |\iota| < \infty\}$ with $0_J = (0,0,\dots) \in J$, $|\iota| = \sum_i \iota_i$ and introduce the so-called Wick polynomial $p_\iota(\kappa) = \Pi_{i=1}^\infty h_{\iota_i}(\kappa_{\eta^{-1}(i)})$ indicated by $\iota \in J$ for a multi-variable $\kappa \in \mathbb{R}^d \times \mathbb{R}^{\mathbb{N}} \times \mathbb{R}^{\mathbb{N}}$. This way we can conclude the following statement from the Cameron-Martin-Theorem.

Lemma 59. *For $(s,t) \in [0,L] \times [0,T]$ let $r_i(s,t), \lambda(s,t) \in \mathcal{L}^2(\Omega, \mathcal{F}_{L,T}, \mu; \mathbb{R})$, $i = 1,\dots,d$ be $\mathcal{F}_{s,t}$ adapted solutions of (4.41). Then $\boldsymbol{r}$ and λ are given as*

$$\boldsymbol{r}(s,t,\omega) = \sum_{\iota \in J} \boldsymbol{r}_\iota(s,t) p_\iota(\kappa(\omega)) \;, \quad \lambda(s,t,\omega) = \sum_{\iota \in J} \lambda_\iota(s,t) p_\iota(\kappa(\omega)) \;, \qquad (4.42)$$

with the deterministic coefficients $\boldsymbol{r}_\iota = \mathbb{E}[\boldsymbol{r}p_\iota]$, $\lambda_\iota = \mathbb{E}[\lambda p_\iota]$ and κ as in Def. 57.

We aim a system of equations that describes the behavior of the deterministic coefficients of the expansion (4.42). Therefore, we formally rewrite the momentum equation in (4.41) into a system of first order partial differential equations in space or time, integrate over suitable time and space intervals accounting for the initial and boundary conditions, multiply each equation with the polynomial p_ι and take the expectation. The algebraic constraint in (4.41) is handled by inserting the Fourier-Hermite expansion, multiplying with p_ι and taking the expectation. To obtain the final system of equations, we apply the following properties of Wick polynomials [89].

Lemma 60. *The product of two random variables a, b which are expressed in terms of their Fourier-Hermite expansion fulfills*

$$ab = \sum_\iota \left(\sum_\mu \sum_{0_J \leq \nu \leq \iota} C(\iota, \mu, \nu) a_{\iota - \nu + \mu} b_{\nu + \mu} \right) p_\iota \;,$$

$$C(\iota, \mu, \nu) = \left[\binom{\iota}{\nu} \binom{\mu + \nu}{\mu} \binom{\iota + \mu - \nu}{\mu} \right]^{1/2} \;,$$

where the operators $+, -, \leq$ are defined component-wise and $\iota! = \iota_1!\iota_2!\cdots$. The expectations of the product of two Wick polynomials and of the product of the Wiener process and a Wick polynomial satisfy

$$\mathbb{E}[p_\iota(\kappa)p_\mu(\kappa)] = \delta_{\iota,\mu} , \qquad\qquad\qquad with\ \delta_{\iota,\mu} = \Pi_i \delta_{\iota_i,\mu_i} ,$$

$$\mathbb{E}[p_\iota w_i(s,t)] = \sum_{k\ell} \delta_{\iota,\nu} \int_0^s \int_0^t \phi_k \psi_\ell \, d\sigma d\tau , \qquad with\ \nu = (\delta_{\eta(i,k,\ell),j})_{j\in\mathbb{N}} .$$

Consequently, the deterministic coefficients associated to the Kirchhoff beam model are described by

$$\partial_{tt}\boldsymbol{r}_\iota = \sum_\mu \sum_{0_J \leq \nu \leq \iota} C(\iota,\mu,\nu)\partial_s(\lambda_{\iota-\nu+\mu}\partial_s\boldsymbol{r}_{\nu+\mu}) - \alpha^{-2}\partial_{ssss}\boldsymbol{r}_\iota + \delta_{\iota,0_J}\mathrm{Fr}^{-2}\boldsymbol{e}_g \qquad (4.43a)$$

$$+ \mathrm{Dr}^{-2}(\mathbf{A}\cdot\boldsymbol{r}_\iota - \partial_t\boldsymbol{r}_\iota) + \beta\mathrm{Dr}^{-2}\sum_{k\ell}\sum_{i=1}^d \boldsymbol{e}_i\delta_{\iota,(\delta_{\eta(i,k,\ell),j})_{j\in\mathbb{N}}}\phi_k\psi_\ell ,$$

$$\sum_\mu \sum_{0_J \leq \nu \leq \iota} C(\iota,\mu,\nu)\partial_s\boldsymbol{r}_{\iota-\nu+\mu} \cdot \partial_s\boldsymbol{r}_{\nu+\mu} = 0 . \qquad\qquad (4.43b)$$

System (4.43) is completed by the boundary and initial conditions (4.6) for $\boldsymbol{r}_{0_J}$ and λ_{0_J} and vanishing boundary and initial conditions for $\iota \neq 0_J$.

We use the same spatial and temporal discretization for both, the WCE system (4.43) and the original constrained stochastic system (4.41). In time we take an implicit Euler scheme. We choose a truncation of the expansion (4.42). For that purpose, we fix $N_s, N_t \in \mathbb{N}$ and consider a subset of the basis on $\mathcal{L}^2([0,L]\times[0,T])$ given by $\{\phi_i\psi_j\}$ for $i \leq N_s$, $j \leq N_t$. In addition, we restrict the degree of the Wick polynomials by setting $|\iota| \leq n \in \mathbb{N}$, which results in the truncated multi-index set $J_{N_sN_t,n}$.

4.5 Numerical simulations

All numerical simulations in this section were carried out on a PC equipped with an Intel® Core™ i7-8700 CPU and 32 GiB RAM. We used Matlab® R2019a for the calculations. In particular, the linear systems appearing in all numerical schemes except for the Wiener chaos expansion in Sec. 4.5.6 were solved using the band solver implemented in Matlab's backslash-operator. Due to the coupling of the WCE-system in Sec. 4.5.6 we used the LU-decomposition instead. The absolute tolerance of Newton's method, which was the stopping criterion, was set for all simulations to 10^{-10}.

The structure of this section takes an increasing degree of model difficulty into account: We start with the conservative case in Sec. 4.5.1, verifying the principal numerical schemes which are used in this section as well as the model properties itself. We then add aerodynamic drag into the system in Sec. 4.5.2 and afterwards also stochastic forces in Sec. 4.5.3. This gradually increases the complexity of the problem and leads to an increase of computational time of the numerical simulations. The following Sections 4.5.4-4.5.6 are then dedicated to the numerical studies of possible reduction techniques for the computational costs as discussed in Sec. 4.3.3, Sec. 4.4.1 and Sec. 4.4.2.
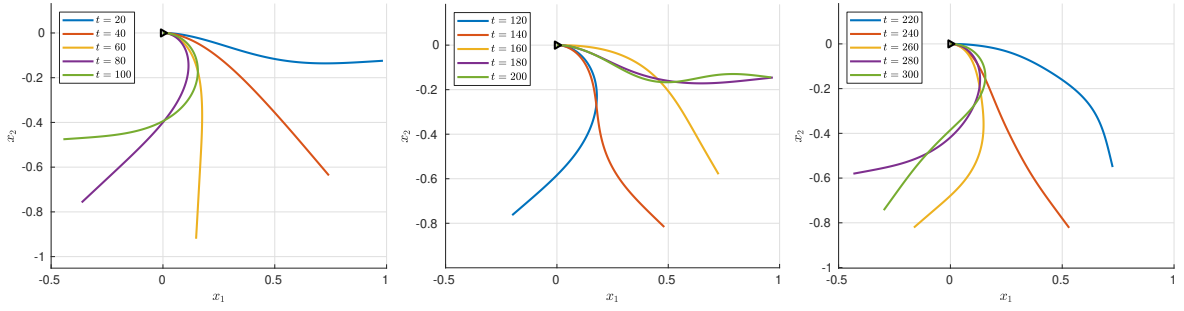
Figure 4.13.: Fiber behavior in the conservative scenario.

4.5.1 Conservative model

At first, we verify the numerical schemes cMPGGL (4.28), IEGGL (4.26), VSV (4.29), VSVm (4.31) and EEP (4.34). In order to do so, we apply them to the conservative case. We set the aerodynamic forces to zero and use the following model parameters in order to define a benchmark scenario: $L = 1, \mathrm{Fr} = 40, \alpha = 200, T = 300$. We consider a 2d setting and assume that the direction of gravity is $\boldsymbol{e}_g = -\boldsymbol{e}_2$. The fiber is fixed at the origin, $\hat{\boldsymbol{r}} = \boldsymbol{0}$, and its direction of the nozzle is $\hat{\boldsymbol{\tau}} = \boldsymbol{e}_1$. The initial condition is that of a stress free fiber at rest, given by $\boldsymbol{r}(s,0) = s\boldsymbol{e}_1, s \in [0,1]$ and $\partial_t \boldsymbol{r}(s,0) = \boldsymbol{0}$.

The dynamic behavior of the fiber is seen in Figure 4.13, where the simulation was carried out with $\Delta s = 10^{-2} = \Delta t$ by the energy-preserving time integration scheme cMPGGL, (4.28). In Fig. 4.14 we see a direct comparison between the solutions of the different numerical schemes at $T = 300$ for different space discretizations Δs calculated with $\Delta t = 10^{-2}$. We see that the projection based explicit scheme EEP stays stable for $\Delta s = 10^{-1}$. For finer space discretizations, simulations with EEP demand much smaller time step sizes $\Delta t \ll \Delta s^2$ in order to be feasible. On the other hand, the methods VSV and VSVm, which are both similar to EEP in the conservative case, as the acceleration does not depend on the velocity, are much more stable and lead to similar results compared to the implicit methods cMPGGL and IEGGL. However, as the equation for the position (4.29a) of VSV evaluates ∇g at r^n instead of r^{n+1}, Newton's method is unable to find sufficiently small solutions for $\Delta s = 10^{-2}$ if $\Delta t = 10^{-2}$. The fully implicit scheme deviates slightly in the velocity from cMPGGL and VSVm (as well as VSV) as seen in the velocity magnitude, nonetheless, this deviation is much smaller than that of EEP. Considering the energy conservation, we see in Fig. 4.15 similar behavior to the case of ordinary differential equations, namely the explicit Euler increases the total energy, the fully implicit scheme IEGGL shows numerical dissipation, while cMPGGL and VSV preserve it. The modified VSV scheme, VSVm acts also slightly dissipative.

In order to examine the numerical convergence, we use the discrete $\mathcal{L}^2([0, L])$-norm

$$\|z\|_{\mathcal{L}^2}^2 = \sum_{i=1}^{N} \|z_i\|^2 \Delta s\,, \tag{4.44}$$

where $z_i \in \mathbb{R}^d$ for $z \in \{r, v\}$ and $z_i \in \mathbb{R}$ for $z \in \{\lambda, \kappa\}$. We consider the relative $\mathcal{L}^2$ errors for the dynamic components and the absolute $\mathcal{L}^2$ errors for the Lagrangian multipliers at $t = T$ with respect to a reference solution. Thus, for a given solution generated with Δt, $z_{\Delta t}(t) \in \mathbb{R}^{nN}$ and a reference solution $z_{ref}(t) \in \mathbb{R}^{nN}$, the relative
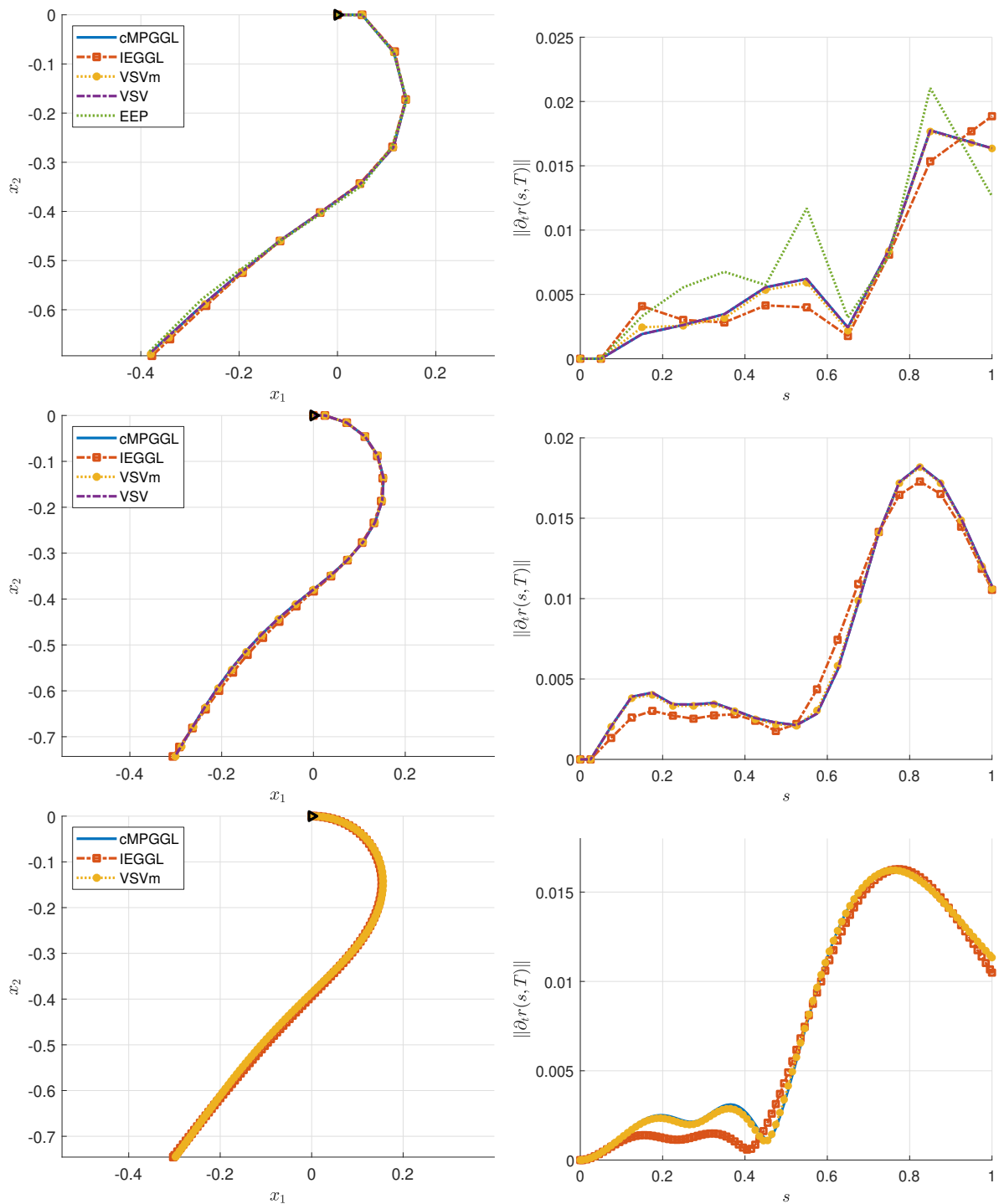
Figure 4.14.: Solutions of the conservative scenario at $t = T$ generated by different time integration schemes with $\Delta t = 10^{-2}$. Left: fiber, Right: velocity magnitude. Top: $\Delta s = 10^{-1}$, center: $\Delta s = 0.5 \cdot 10^{-1}$, bottom $\Delta s = 10^{-2}$.
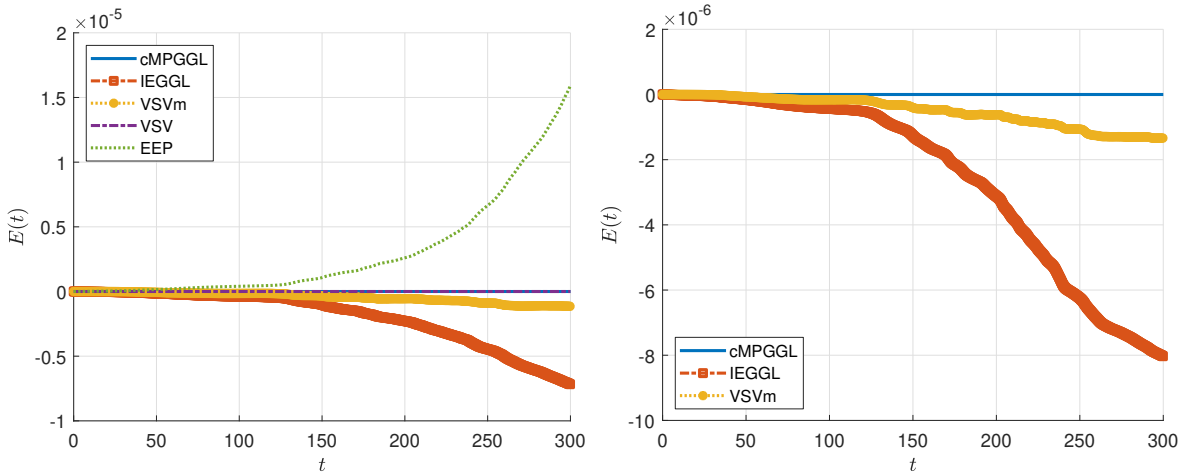
Figure 4.15.: Total energy of the conservative scenario, generated by different time integration schemes with $\Delta t = 10^{-2}$. Left: $\Delta s = 10^{-1}$, Right: $\Delta s = 10^{-2}$.

and absolute errors are given as

$$
e_{rel}(\Delta t) = \frac{\|z_{\Delta t}(T) - z_{ref}(T)\|_{\mathcal{L}^2}}{\|z_{ref}(T)\|_{\mathcal{L}^2}} , \quad e_{abs}(\Delta t) = \|z_{\Delta t}(T) - z_{ref}(T)\|_{\mathcal{L}^2} ,
$$

where $n = d$, if $z \in \{r, v\}$ and $n = 1$, if $z \in \{\lambda, \kappa\}$. As reference we use a numerical solution generated with a finer time discretization. Both, $z_{\Delta t}$ and z_{ref} are generated by the same integration scheme.

The convergence behavior of the different schemes is seen in Fig. 4.16 and Fig. 4.17, the least squares fit of the measured convergence orders is given in Tab. 4.4 and Tab. 4.5. The reference solutions are generated with $\Delta t = 2^{-15}$. We observe that the convergence order of the dynamical variables r, v is $p = 2$ for VSV as well as $p = 1$ for IEGGL in accordance with the expected values. The schemes EEP and VSVm are of first order. The conservative cMPGGL scheme converges with $p = 2$, although for $\Delta s = 1/100$ this rate is achieved for the velocity only for $\Delta t \lesssim 10^{-4}$. Considering the algebraic variables, we observe that λ converges linearly for all schemes. The second Lagrangian multiplier, κ, converges with $p = 2$ in case of cMPGGL and $p = 1$ for the other schemes. We emphasize that in case of VSV and VSVm, κ and λ together have the role of the constraint force in (4.13b) at different points in time, which explains, why there is a huge difference in κ compared to the one generated by cMPGGL as seen in Figure 4.17. In fact, this is the reason, why we omitted the projection vector $\mathfrak{k}$ of EEP, since it is a purely artificial quantity with the amplitude of the constraint force being given by (4.32) which converges with $p = 1$ since r and v do.

Finally, we compare the computational cost of the different schemes. The number of equations, i.e., the dimension of the corresponding Jacobian as well as the number of non-zero entries in the Jacobian for each scheme is given in Tab. 4.6. The average number of Newton-iterations and the average time per integration step needed to generate the solutions shown in Fig. 4.14 are given in Tab. 4.7. The conservative midpoint rule has the same dimension of the Jacobian as IEGGL but 20% more entries for large N, which is also seen in the corresponding increase of computational time of around 20%.
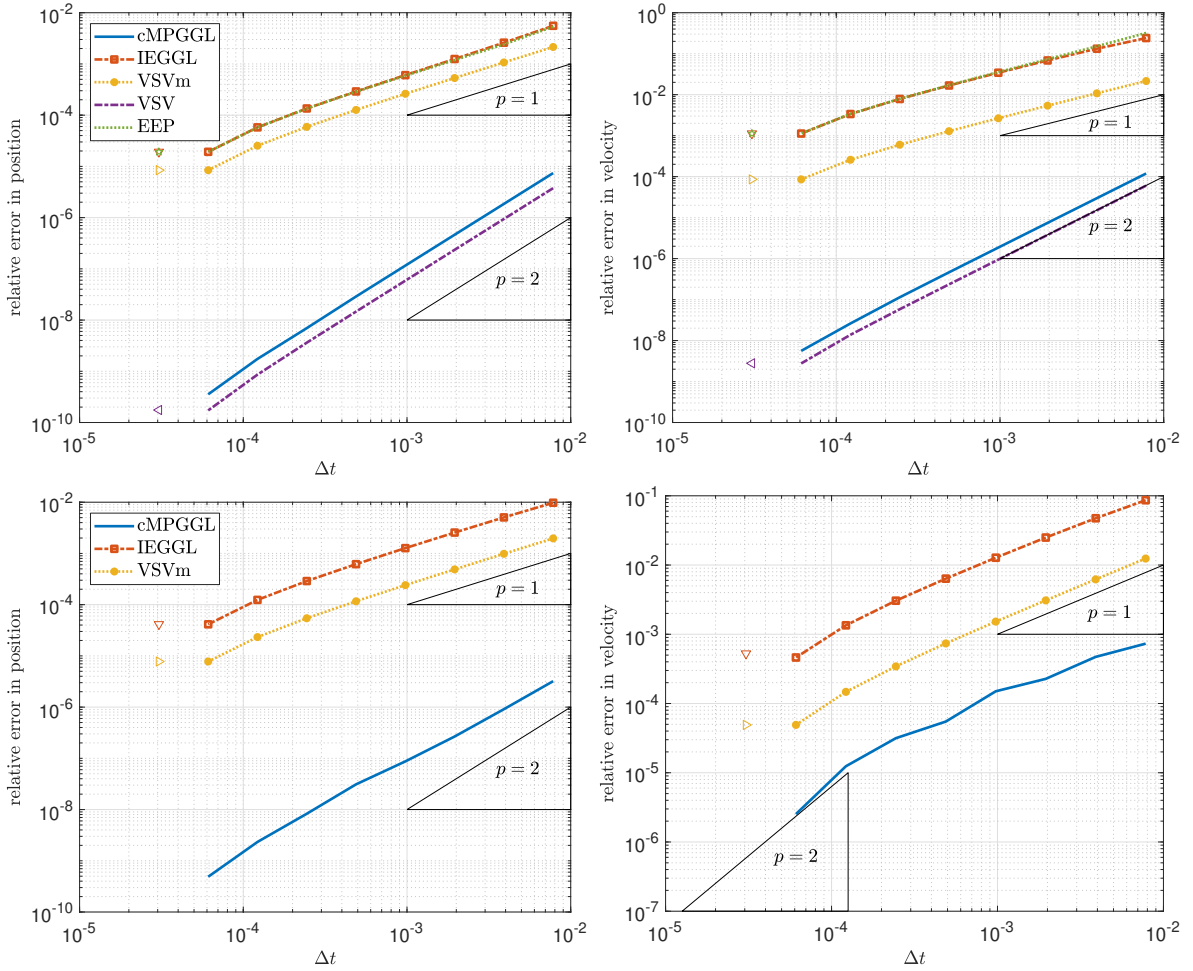
Figure 4.16.: Numerical convergence of dynamical variables for different time integration schemes. Top: $\Delta s = 10^{-1}$, bottom: $\Delta s = 10^{-2}$. Triangles denote relative error with respect to cMPGGL.

	$\Delta s = 10^{-1}$	$\Delta s = 10^{-2}$
cMPGGL	$p_r \approx 2.03, p_v \approx 2.04$	$p_r \approx 1.77, p_v \approx 1.11$
IEGGL	$p_r \approx 1.14, p_v \approx 1.08$	$p_r \approx 1.10, p_v \approx 1.05$
VSVm	$p_r \approx 1.11, p_v \approx 1.11$	$p_r \approx 1.11, p_v \approx 1.11$
VSV	$p_r \approx 2.04, p_v \approx 2.04$	-
EEP	$p_r \approx 1.12, p_v \approx 1.13$	-

Table 4.4.: Measured convergence orders of the different integration schemes for the dynamic components.
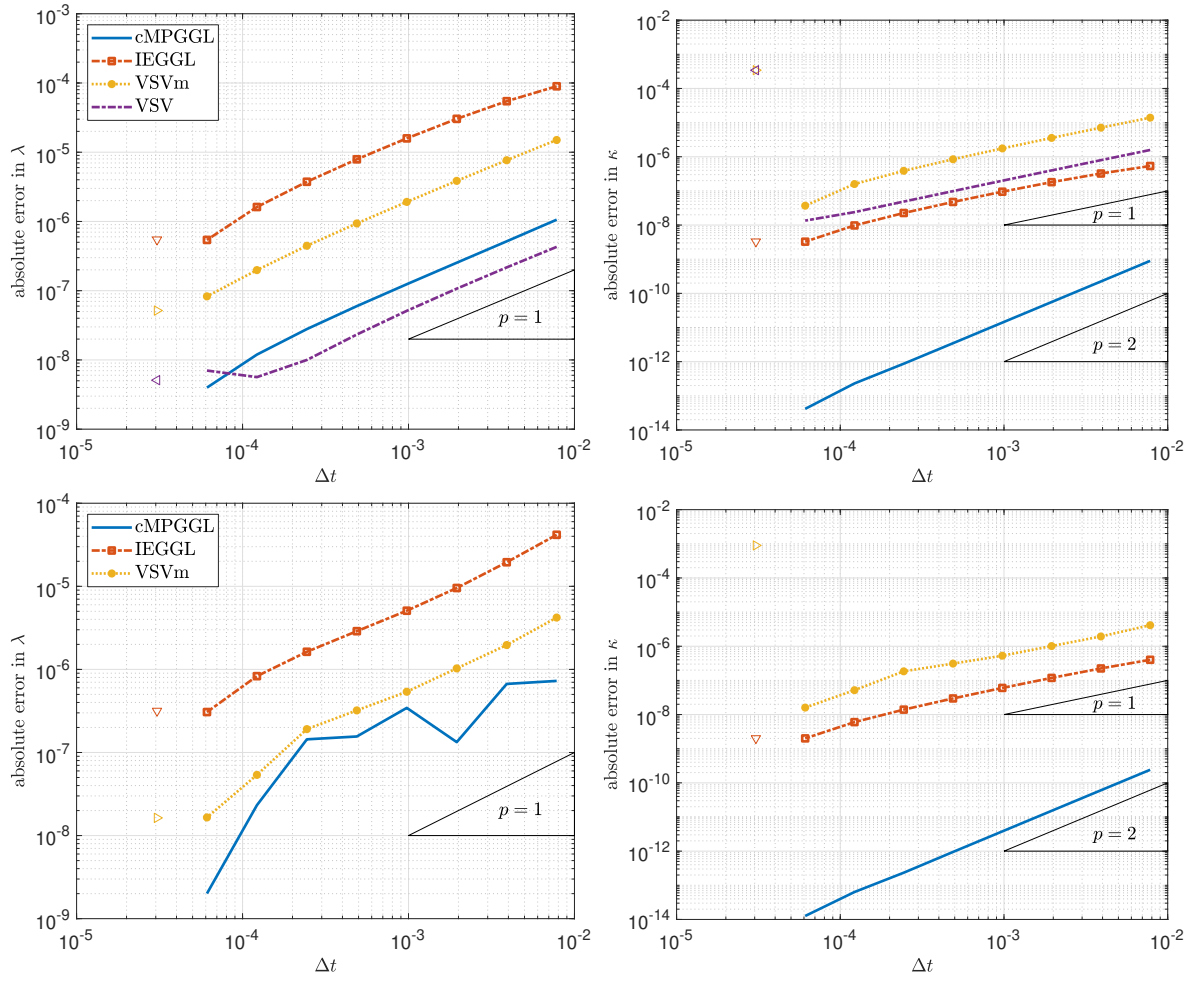
Figure 4.17.: Behavior of the Lagrangian multipliers λ (left) and κ (right), absolute error. Top: $\Delta s = 10^{-1}$, bottom: $\Delta s = 10^{-2}$. Triangles denote the error with respect to cMPGGL.

	$\Delta s = 10^{-1}$	$\Delta s = 10^{-2}$
cMPGGL	$p_\lambda \approx 1.12, p_\kappa \approx 2.03$	$p_\lambda \approx 1.01, p_\kappa \approx 2.01$
IEGGL	$p_\lambda \approx 1.04, p_\kappa \approx 1.03$	$p_\lambda \approx 0.96, p_\kappa \approx 1.07$
VSVm	$p_\lambda \approx 1.06, p_\kappa \approx 1.17$	$p_\lambda \approx 1.07, p_\kappa \approx 1.08$
VSV	$p_\lambda \approx 0.94, p_\kappa \approx 0.99$	-

Table 4.5.: Measured convergence orders of the different integration schemes for the Lagrangian multipliers.

Scheme	Number of equations	Non-zero entries of Jacobian
cMPGGL	$2(d+1)(N+4)$	$8d(3N+2)+8$
IEGGL	$2(d+1)(N+4)$	$4d(5N+4)+8$
VSVm	$(d+1)(N+4)$	$d(7N+8)+4$
VSV	N	$d(3N-2)$
EEP	N	$d(3N-2)$

Table 4.6.: Dimension and number of non-zero entries of the Jacobian for different time integration schemes in the conservative scenario.

Scheme	$\Delta s = 10^{-1}$	$\Delta s = 0.5 \cdot 10^{-1}$	$\Delta s = 10^{-2}$
cMPGGL	2.00, 0.63 ms	2.00, 0.73 ms	2.56, 1.93 ms
IEGGL	2.00, 0.53 ms	2.00, 0.58 ms	2.53, 1.61 ms
VSVm	2.00, 0.40 ms	2.00, 0.42 ms	2.04, 0.66 ms
VSV	1.00, 0.22 ms	1.32, 0.26 ms	-
EEP	1.00, 0.14 ms	-	-

Table 4.7.: Average number of Newton-iterations and average time per integration step in the conservative scenario.

The semi-explicit schemes, EEP and VSV demand the solution of a non-linear system with only N equations but like VSVm they also imply a projection step for the calculation of v^{n+1}, which is equivalent to solving one $N \times N$ linear equation, which is also carried out in every Newton iteration step. Nonetheless, due to much smaller dimension, the needed computational time is less than one half of IEGGL for both, EEP and VSV. The modified scheme VSVm has only one half of the equations of IEGGL, since the velocity is evaluated explicitly in the conservative case, which provides a significant decrease in computational time.

4.5.2 Deterministic air drag

In order to examine the deterministic, non-conservative case we use the aerodynamic drag model presented in Sec. 4.2.4. We choose the model parameters as $L = 1, \text{Fr} = 40, \alpha = 200, \gamma = 45, \text{Dr}/\sqrt{\gamma} = 4$. We use a 2d setting with direction of gravity $\boldsymbol{e}_g = -\boldsymbol{e}_2$. The fiber orientation is given by $\hat{\boldsymbol{r}} = \boldsymbol{0}, \hat{\boldsymbol{\tau}} = -\boldsymbol{e}_2$ with the initial condition $\boldsymbol{r}(s,0) = -s\boldsymbol{e}_2$ for $s \in [0, L]$. The fiber is initially at rest and stress free. The dynamic behavior of the fiber depends in this case strongly on the prescribed outer flow $\boldsymbol{u}$. We use here only stationary and linear flows, which may result in a stationary solution as seen in Fig 4.18 for $\boldsymbol{u}_i(\boldsymbol{x}) = \mathbf{A}_i \cdot \boldsymbol{x} + \boldsymbol{c}_i, i \in \{1, 2\}$ with

$$\mathbf{A}_1 = \frac{1}{10}(\boldsymbol{e}_1 \otimes \boldsymbol{e}_2 - \boldsymbol{e}_2 \otimes \boldsymbol{e}_1), \qquad \boldsymbol{c}_1 = -\frac{1}{20}\boldsymbol{e}_1,$$
$$\mathbf{A}_2 = \frac{1}{10}\boldsymbol{e}_1 \otimes \boldsymbol{e}_2, \qquad \boldsymbol{c}_2 = \frac{1}{20}\boldsymbol{e}_1.$$
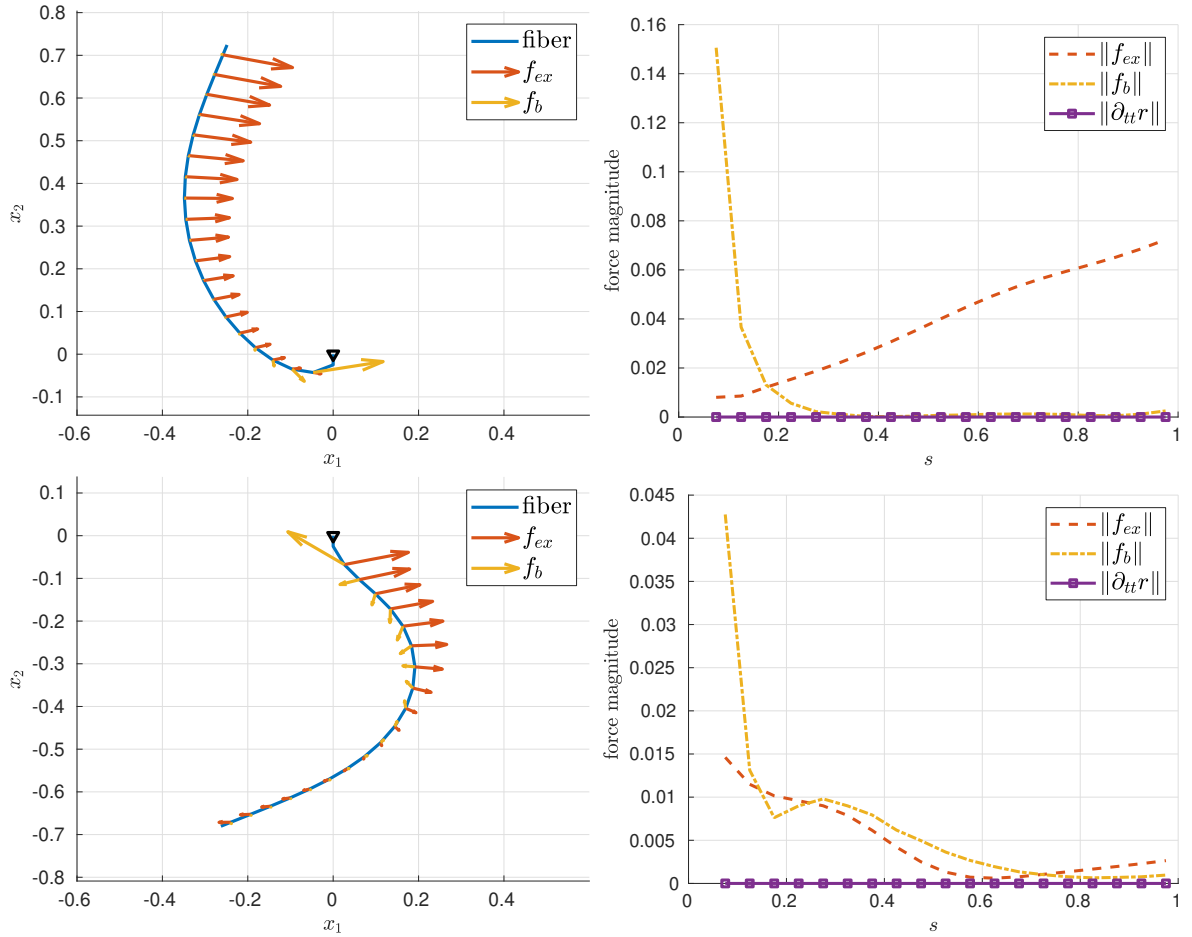
Figure 4.18.: Fiber position and behavior of external forces $\boldsymbol{f}_{ex}$ (gravity and aerodynamic drag), bending forces $\boldsymbol{f}_b$ as well as of the acceleration at $t = T$ for outer flow $\boldsymbol{u}_1$ (top) and $\boldsymbol{u}_2$ (bottom). Simulation generated by cMPGGL with $T = 200, \Delta t = 10^{-2}, \Delta s = 0.5 \cdot 10^{-2}$.

Thus, $\boldsymbol{u}_1$ is a rotational flow with $\boldsymbol{u}_1 = \boldsymbol{0}$ for $\boldsymbol{x} = (0, 1/2)$ and $\boldsymbol{u}_2$ is a shear flow with $\boldsymbol{u}_2 = \boldsymbol{0}$ for all $\boldsymbol{x} \in \mathbb{R}^d$ with $\boldsymbol{x} \cdot \boldsymbol{e}_2 = -1/2$. In order to avoid the stationary solution in the convergence tests, we choose T sufficiently small ($T = 50$) and also consider the following (non-physical) scenario, which admits no stationary solution. Under the rotational flow $\boldsymbol{u}_3$ given in terms of

$$\mathbf{A}_3 = \frac{1}{5}(\boldsymbol{e}_1 \otimes \boldsymbol{e}_2 - \boldsymbol{e}_2 \otimes \boldsymbol{e}_1), \quad \boldsymbol{c}_3 = \boldsymbol{0}$$

the fiber overlaps itself and generates loops, while following the fluid flow continuously as seen in Fig. 4.19 (generated by cMPGGL with $\Delta s = 10^{-2} = \Delta t$).

In Fig. 4.20 and Fig. 4.21 we see the convergence behavior of the different integration schemes for the outer flow fields $\boldsymbol{u}_1$ and $\boldsymbol{u}_3$. We observe similar results to the conservative case: cMPGGL shows second order convergence in the dynamic variables (for $\Delta t \lessapprox 2 \cdot 10^{-4}$ for $\Delta s = 1/100$), while IEGGL, VSVm and EEP are of first order. The Lagrangian multipliers converge with $p = 1$ in all schemes except cMPGGL, where κ shows second order convergence for sufficiently small Δt. The measured least squares fits in Tab. 4.8 and Tab. 4.9 show smaller convergence orders in case of cMPGGL and
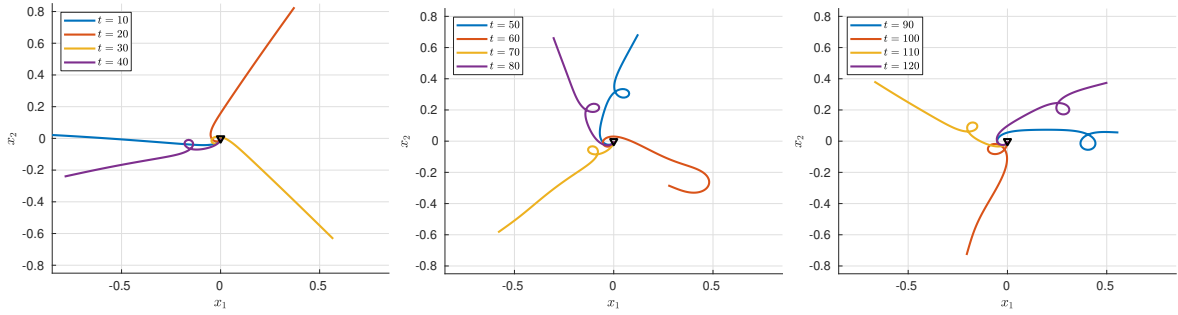
Figure 4.19.: Fiber behavior in the non-conservative scenario with outer flow $\boldsymbol{u}_3$.

	$\Delta s = 10^{-1}, \boldsymbol{u}_1$	$\Delta s = 10^{-2}, \boldsymbol{u}_1$	$\Delta s = 10^{-2}, \boldsymbol{u}_3$
cMPGGL	$p_r \approx 2.04, p_v \approx 2.08$	$p_r \approx 0.77, p_v \approx 0.46$	$p_r \approx 1.65, p_v \approx 1.58$
IEGGL	$p_r \approx 1.02, p_v \approx 1.04$	$p_r \approx 1.11, p_v \approx 1.11$	$p_r \approx 1.07, p_v \approx 1.07$
VSVm	$p_r \approx 1.10, p_v \approx 1.10$	$p_r \approx 1.11, p_v \approx 0.85$	$p_r \approx 1.08, p_v \approx 1.06$
EEP	$p_r \approx 1.24, p_v \approx 1.19$	-	-

Table 4.8.: Measured convergence orders of the different integration schemes for the dynamic components.

VSVm, since they account for all discretizations depicted in Fig. 4.20 and Fig. 4.21. The reference solutions for the convergence studies were generated by $\Delta t = 2^{-15}$ for the $\boldsymbol{u}_1$ cases and by $\Delta t = 2^{-18}$ in the $\boldsymbol{u}_3$ case.

Considering the numerical costs, the number of equations is the same as in the conservative case for cMPGGL, IEGGL and EEP. In case of VSVm, we now evaluate the velocity implicitly, thus introducing a second non-linear equation of dimension $(d+1)(N+4)$ which is independent of the projection step. The number of non-zero entries now increased for the implicit schemes due to the derivative of the aerodynamic drag as shown in Tab. 4.10.

	$\Delta s = 10^{-1}, \boldsymbol{u}_1$	$\Delta s = 10^{-2}, \boldsymbol{u}_1$	$\Delta s = 10^{-2}, \boldsymbol{u}_3$
cMPGGL	$p_\lambda \approx 1.16, p_\kappa \approx 1.46$	$p_\lambda \approx 0.38, p_\kappa \approx 1.16$	$p_\lambda \approx 1.07, p_\kappa \approx 1.35$
IEGGL	$p_\lambda \approx 1.04, p_\kappa \approx 0.97$	$p_\lambda \approx 1.30, p_\kappa \approx 1.11$	$p_\lambda \approx 1.07, p_\kappa \approx 1.07$
VSVm	$p_\lambda \approx 1.08, p_\kappa \approx 1.08$	$p_\lambda \approx 0.67, p_\kappa \approx 0.57$	$p_\lambda \approx 1.04, p_\kappa \approx 1.04$

Table 4.9.: Measured convergence orders of the different integration schemes for the Lagrangian multipliers.
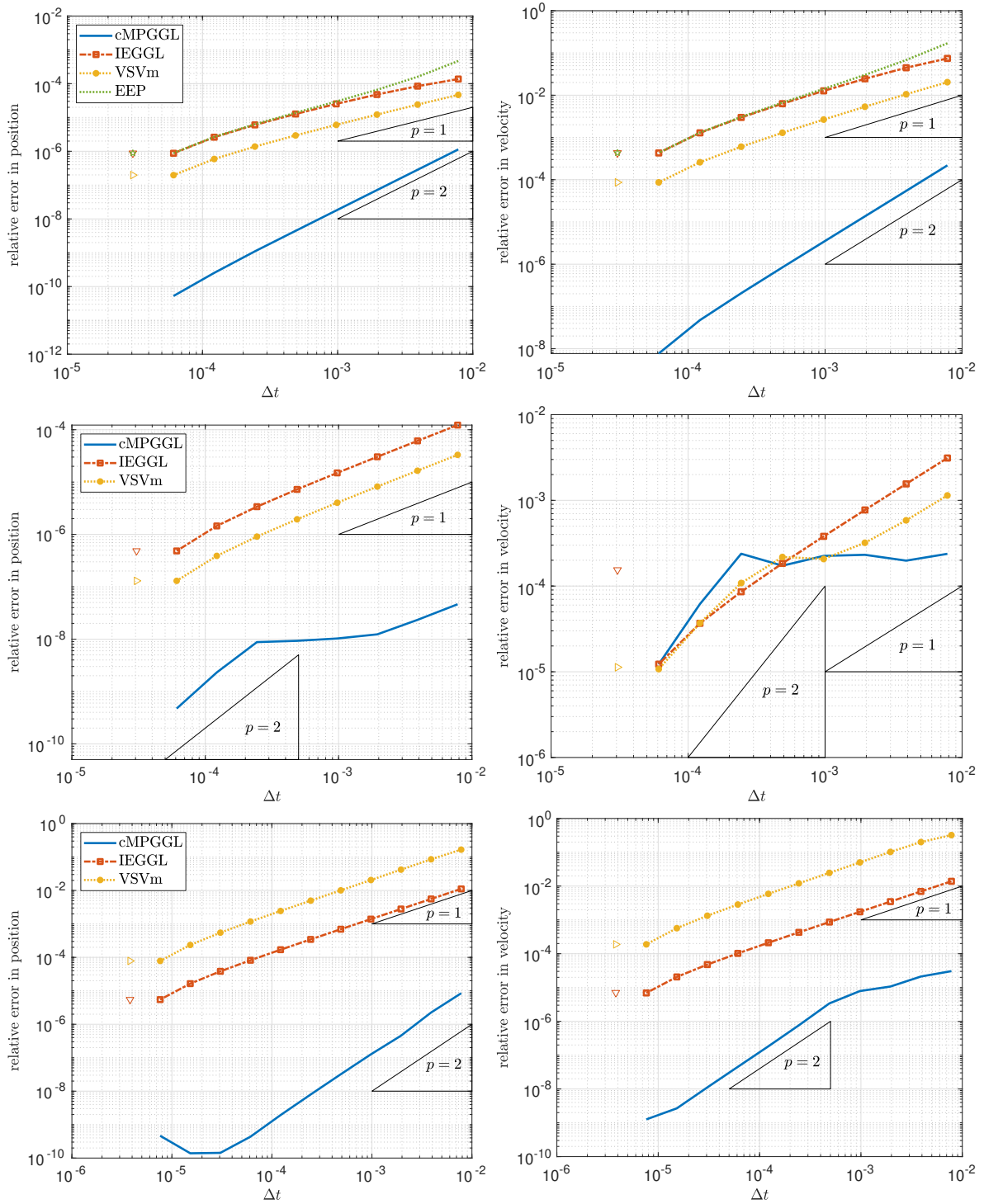
Figure 4.20.: Numerical convergence of dynamical variables for different time integration schemes. Top: $\Delta s = 10^{-1}$, $\boldsymbol{u}_1$; center: $\Delta s = 10^{-2}$, $\boldsymbol{u}_1$; bottom: $\Delta s = 10^{-2}$, $\boldsymbol{u}_3$. Triangles denote relative error with respect to cMPGGL.
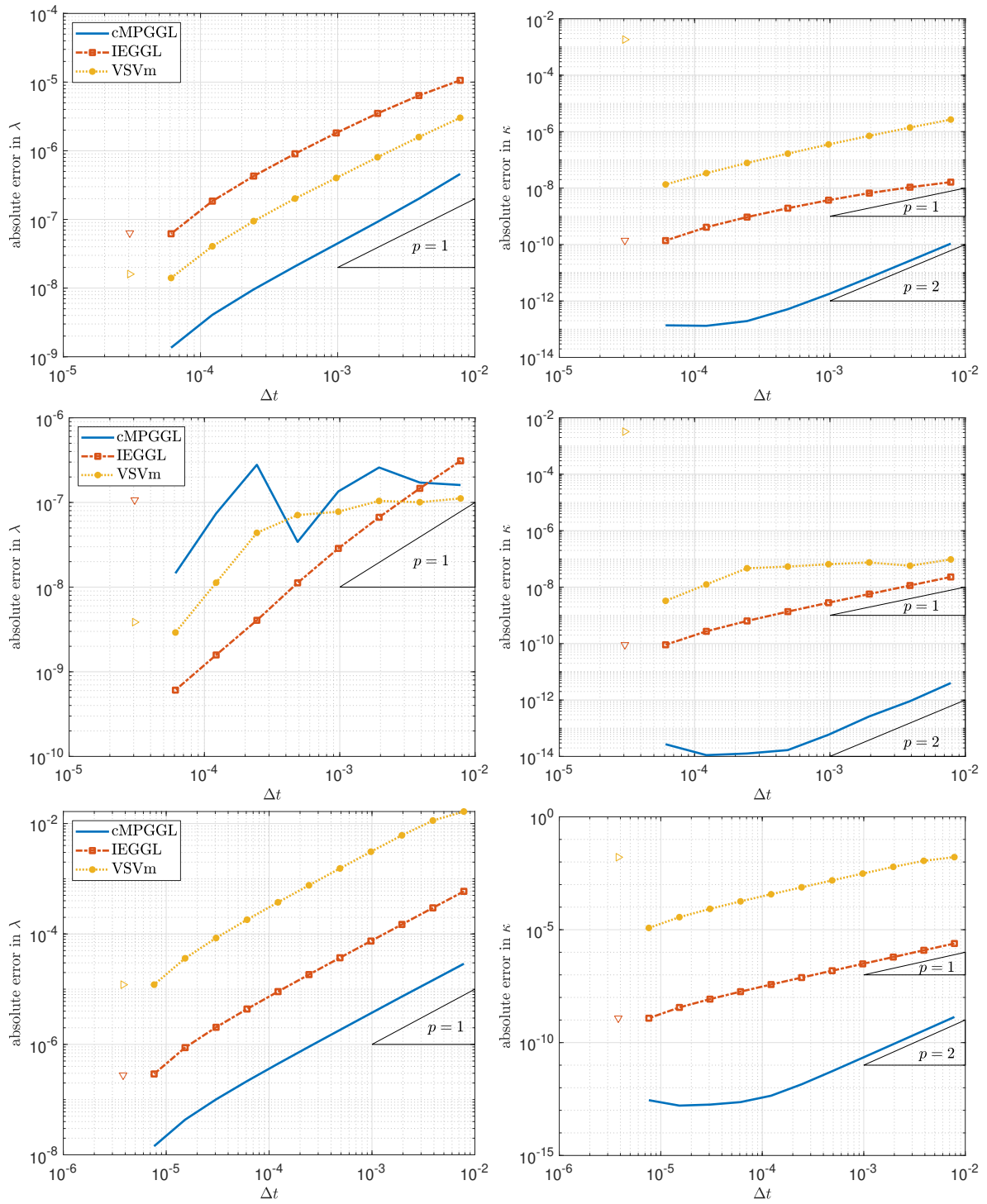
Figure 4.21.: Behavior of the Lagrangian multipliers λ (left) and κ (right), absolute error. Top: $\Delta s = 10^{-1}$, $\boldsymbol{u}_1$; center: $\Delta s = 10^{-2}$, $\boldsymbol{u}_1$; bottom: $\Delta s = 10^{-2}$, $\boldsymbol{u}_3$. Triangles denote the error with respect to cMPGGL.

Scheme	Number of equations	Non-zero entries of Jacobian
cMPGGL	$2(d+1)(N+4)$	$6d^2N + 2d(9N+8) + 8$
IEGGL	$2(d+1)(N+4)$	$6d^2N + 16d(N+1) + 8$
VSVm, r-eq.	$(d+1)(N+4)$	$d(7N+8) + 4$
VSVm, v-eq.	$(d+1)(N+4)$	$3d^2N + 4d(N+2) + 4$
EEP	N	$d(3N-2)$

Table 4.10.: Dimension and number of non-zero entries of the Jacobian for different time integration schemes in the non-conservative scenario.

Scheme	$\Delta s = 10^{-1}$, $\boldsymbol{u}_1$	$\Delta s = 10^{-2}$, $\boldsymbol{u}_1$	$\Delta s = 10^{-2}$, $\boldsymbol{u}_3$
cMPGGL	2, 2.53 ms	2.45, 4.84 ms	2.99, 5.56 ms
IEGGL	2, 2.12 ms	2.45, 3.89 ms	2.99, 4.48 ms
VSVm	1.59, 2, 2.28 ms	1.97, 2.31, 3.39 ms	2, 2.99, 3.54 ms
EEP	1, 0.48 ms	-	-

Table 4.11.: Average number of Newton-iterations and average time per integration step in the non-conservative scenario. VSVm has two Newton-iteration entries, since it consists of two non-linear systems in the non-conservative case.

4.5.3 Stochastic air drag, direct simulations

In order to verify the numerical schemes in the stochastic case, we use a similar setup to the one used in Sec. 4.5.2. As the outer flow, we consider only shear flow, $\boldsymbol{u}_2$ and as the stochastic amplitude, we explore two simplified models:

$$\mathsf{C}_1(\boldsymbol{\tau}) \equiv \mathsf{I}, \quad \mathsf{C}_2(\boldsymbol{\tau}) = r_n(0)(\mathsf{I} - \boldsymbol{\tau} \otimes \boldsymbol{\tau}) + r_\tau(0)\boldsymbol{\tau} \otimes \boldsymbol{\tau},$$

with r_n, r_τ denoting the non-linear resistance coefficients of the universal drag model given in Sec. 4.2.4. In Fig. 4.22 we see the behavior of two stochastic realizations for $\beta \in \{0.2, 0.6\}$. In this section we choose the turbulent fluctuation number as $\beta = 0.2$ and the final time as $T = 1$. In Fig. 4.23 and Tab. 4.12 we see that the dynamic variables converge with approximately $p = 1$, while λ behaves irregular as seen in Fig. 4.24. This is also to be expected, as formally $\lambda = -G^{-1} \cdot \partial_x g \cdot (a - \mathrm{d}w/\mathrm{d}t)$, i.e., λ behaves as a vector of independent random variables. The second Lagrangian multiplier still converges for cMPGGL and IEGGL, since it approaches zero as $\Delta t \to 0$ due to its role in the GGL formulation. The reference solution was generated here with $\Delta t = 2^{-19}$ and the study consisted of 20 Monte-Carlo simulations.

Considering the numerical costs, neither the dimensions of the non-linear equations nor the non-zero entries of the Jacobians changed compared to the non-conservative case considered in Sec. 4.5.2. But due to the irregularity of the force, the Newton method needs much more iterations in order to find a solution. In fact, also the Armijo line search triggers in nearly every step if $\Delta t = 10^{-3}$ with every integration scheme which increases the computation time significantly as seen in Tab. 4.13.
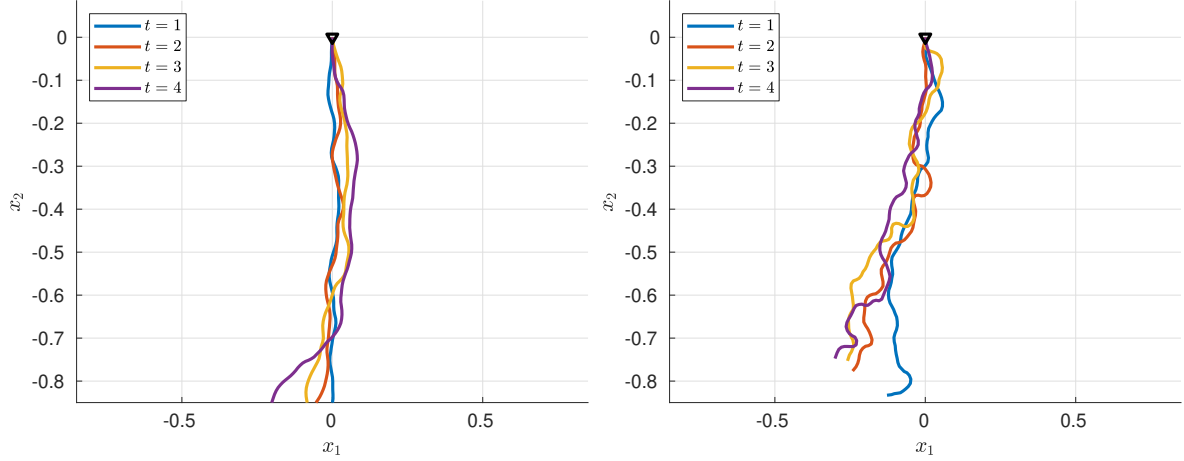
Figure 4.22.: Fiber behavior in the stochastic scenario with stochastic amplitude $\mathbf{C}_2$ and $\beta = 0.2$ (left), $\beta = 0.6$ (right).

	$\Delta s = 10^{-1}$, $\mathbf{C}_1$	$\Delta s = 10^{-2}$, $\mathbf{C}_1$	$\Delta s = 10^{-1}$, $\mathbf{C}_2$	$\Delta s = 10^{-2}$, $\mathbf{C}_2$
cMPGGL	$p_r \approx 1.05$	$p_r \approx 0.90$	$p_r \approx 1.04$	$p_r \approx 0.81$
	$p_v \approx 0.99$	$p_v \approx 0.86$	$p_v \approx 0.99$	$p_v \approx 0.76$
IEGGL	$p_r \approx 1.07$	$p_r \approx 0.53$	$p_r \approx 1.07$	$p_r \approx 0.45$
	$p_v \approx 1.07$	$p_v \approx 0.32$	$p_v \approx 1.07$	$p_v \approx 0.23$
VSVm	$p_r \approx 1.06$	$p_r \approx 0.83$	$p_r \approx 1.07$	$p_r \approx 0.77$
	$p_v \approx 1.03$	$p_v \approx 0.71$	$p_v \approx 1.04$	$p_v \approx 0.64$
EEP	$p_r \approx 1.08$	-	$p_r \approx 1.08$	-
	$p_v \approx 1.07$	-	$p_v \approx 1.07$	-

Table 4.12.: Measured convergence orders of the different integration schemes for the dynamic components.

	$\Delta s = 10^{-1}$, $\mathbf{C}_1$	$\Delta s = 10^{-2}$, $\mathbf{C}_1$	$\Delta s = 10^{-1}$, $\mathbf{C}_2$	$\Delta s = 10^{-2}$, $\mathbf{C}_2$
cMPGGL	2.09, 2.49 ms	5.50, 10.71 ms	2.17, 3.00 ms	5.76, 12.92 ms
IEGGL	2.06, 1.94 ms	3.03, 4.47 ms	2.18, 2.53 ms	3.12, 5.25 ms
VSVm	2, 2, 2.36 ms	2, 3.62, 3.58 ms	2, 2, 2.61 ms	2, 3.91, 3.86 ms
EEP	1.00, 0.41 ms	-	1.00, 0.60 ms	-

Table 4.13.: Average number of Newton-iterations and average time per integration step in the stochastic scenario. VSVm has two Newton-iteration entries, since it consists of two non-linear systems in the non-conservative case.
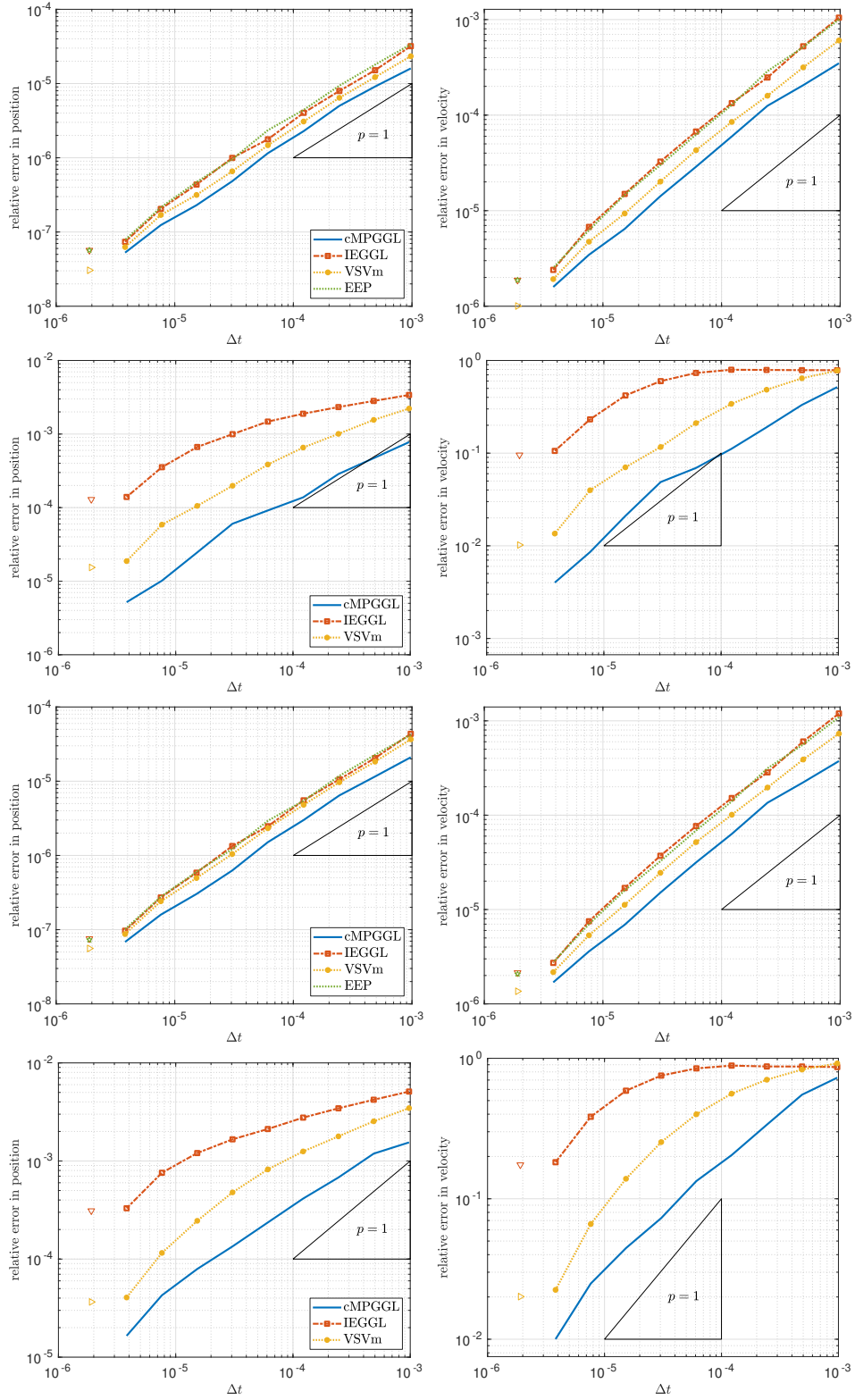
Figure 4.23.: Numerical convergence of dynamical variables for different time integration schemes, stochastic case. From top to bottom: $\Delta s = 10^{-1}, \mathbf{C}_1$, $\Delta s = 10^{-2}, \mathbf{C}_1$, $\Delta s = 10^{-1}, \mathbf{C}_2$, $\Delta s = 10^{-2}, \mathbf{C}_2$. Triangles denote relative error with respect to cMPGGL.
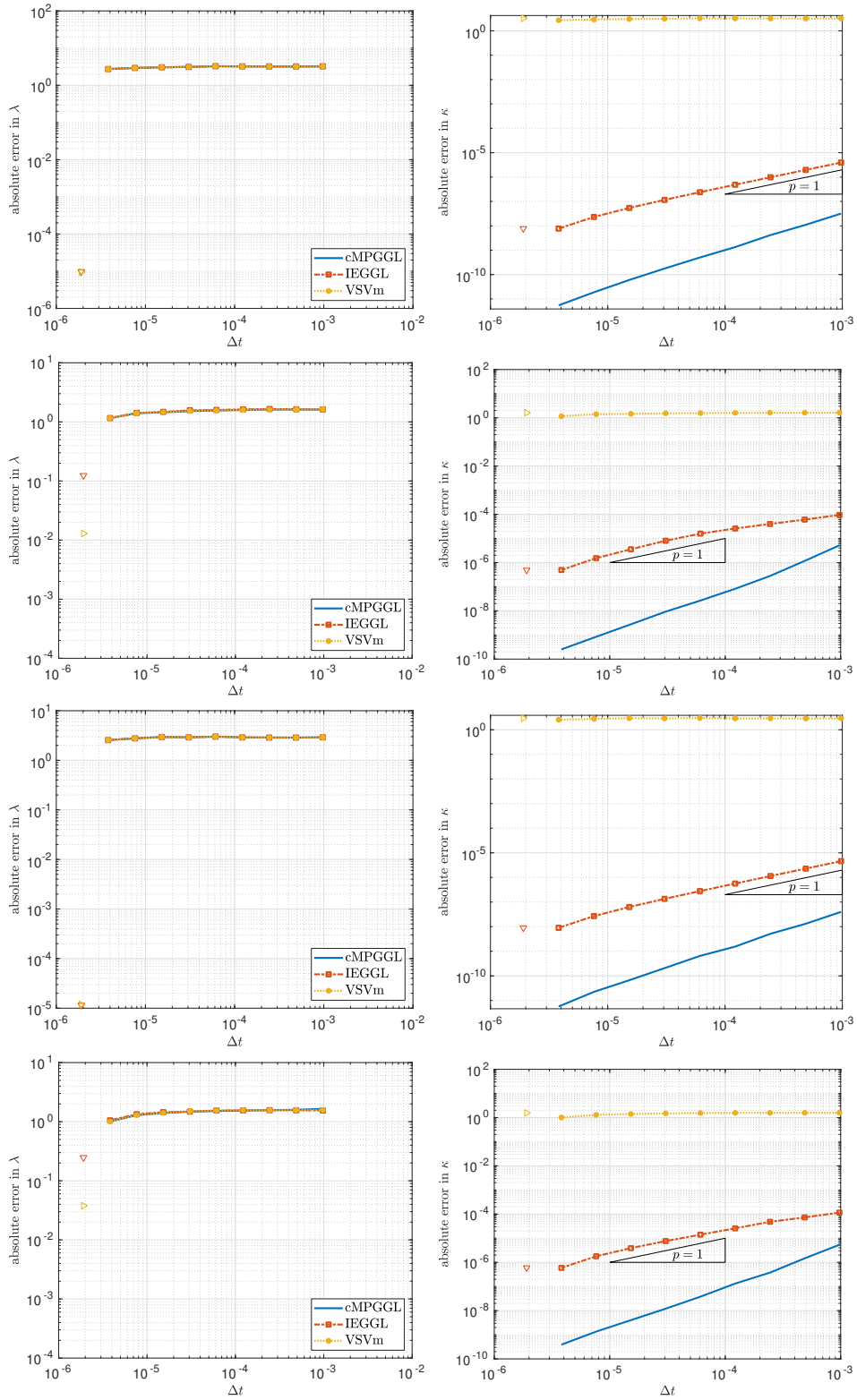
Figure 4.24.: Behavior of the Lagrangian multipliers λ (left) and κ (right) in the stochastic case, absolute error. From top to bottom: $\Delta s = 10^{-1}, \mathbf{C}_1$, $\Delta s = 10^{-2}, \mathbf{C}_1$, $\Delta s = 10^{-1}, \mathbf{C}_2$, $\Delta s = 10^{-2}, \mathbf{C}_2$. Triangles denote the error with respect to cMPGGL.

4.5.4 Stochastic air drag, predictor-corrector schemes

The simulations used for the generation of the measurements of Tab. 4.13 were carried out using the values of r and v from the previous time step as estimator for the Newton method, while λ and κ were estimated by zero. As stated in Section 4.3.3, one possibility to decrease the computational costs is to use one explicit time integration step as an estimator for the actual integration by an implicit method. We explore here the impact of different estimators combined with IEGGL. In order to do so, we once again use a similar scenario to the one used in Section 4.5.2 with the shear flow $\boldsymbol{u}_2$ as air velocity and with the orientation dependent stochastic amplitude $\mathbf{C}_2$ given in Sec. 4.5.3. We choose $T = 50$ as final time for the simulation and $\Delta t = 10^{-2}$ as time resolution. In Fig. 4.25 we see the average number of iterations and average computational time needed for one time integration step by IEGGL with different estimators and for different stochastic turbulence numbers β. The estimators are labeled as "type" followed by the variables which are determined by the predictor "type", the remaining variables are estimated by zero. The possible predictor types are given as "old", denoting estimation by the solution of the previous time step, "VSV" for the VSV predictor and "EEP" for the EEP predictor presented in Section 4.3.3. Figure 4.26 and Fig. C.1,C.2 in the appendix show the average $\mathcal{L}^2$-distances between the estimator $y_{est}(t_n)$ for the component $y \in \{r_i, v_i, \lambda, \kappa\}, i = 1, 2$ and the actual solution $y(t_n)$ at the corresponding time step t_n, i.e. $\|y_{est}(t_n) - y(t_n)\|_{\mathcal{L}^2}$ with the discrete $\mathcal{L}^2$-norm given in (4.44). We generated the data by 20 Monte-Carlo simulations for each predictor type and used the same stochastic noise for all predictor types given a fixed space resolution N. Hence, if a data point is missing in the corresponding plot, it indicates that at least one simulation failed under the given β, N and estimator type.

The $\mathcal{L}^2$ distances show that the VSV predictor yields the best position approximation for all considered values of β and N, while the estimate by the preceding time step leads to poor estimations in comparison. A similar statement for velocity estimation is no more valid for $N = 150$, here the old time step is much closer to the real solution than both estimator types. This is also true for the estimation of λ, here however the estimation by zero is, in fact, even closer to the final solution than any other estimation. In case of the second Lagrangian multiplier, κ, VSV gives the best results in case $N \in \{10, 50\}$ while for $N \in \{100, 150\}$, the old value is much closer to the final solution. Thus, we expect that VSV leads to the least amount of Newton iterations in case of $N \in \{10, 50\}$, while the estimation by the old time step gives best results for $N = 150$. This is confirmed in Fig. 4.25: For $N = 10$, VSV reduces the number of Newton iterations by one and for $N = 50$ by approximately 2 compared to the usual estimation by the old time step. For $N = 150$, the VSV and EEP estimators increase the number of Newton iterations, nearly doubling the computational cost in case of VSV. For $N = 100$ however, VSV is still decreasing the needed number of iterations by 1-2. The reason for this behavior is that the explicit schemes fail to be stable for large N and not sufficiently small Δt, which leads to poor estimations especially of the velocity as well as of the Lagrangian multipliers, which are given by algebraic expressions depending on the velocity estimation.
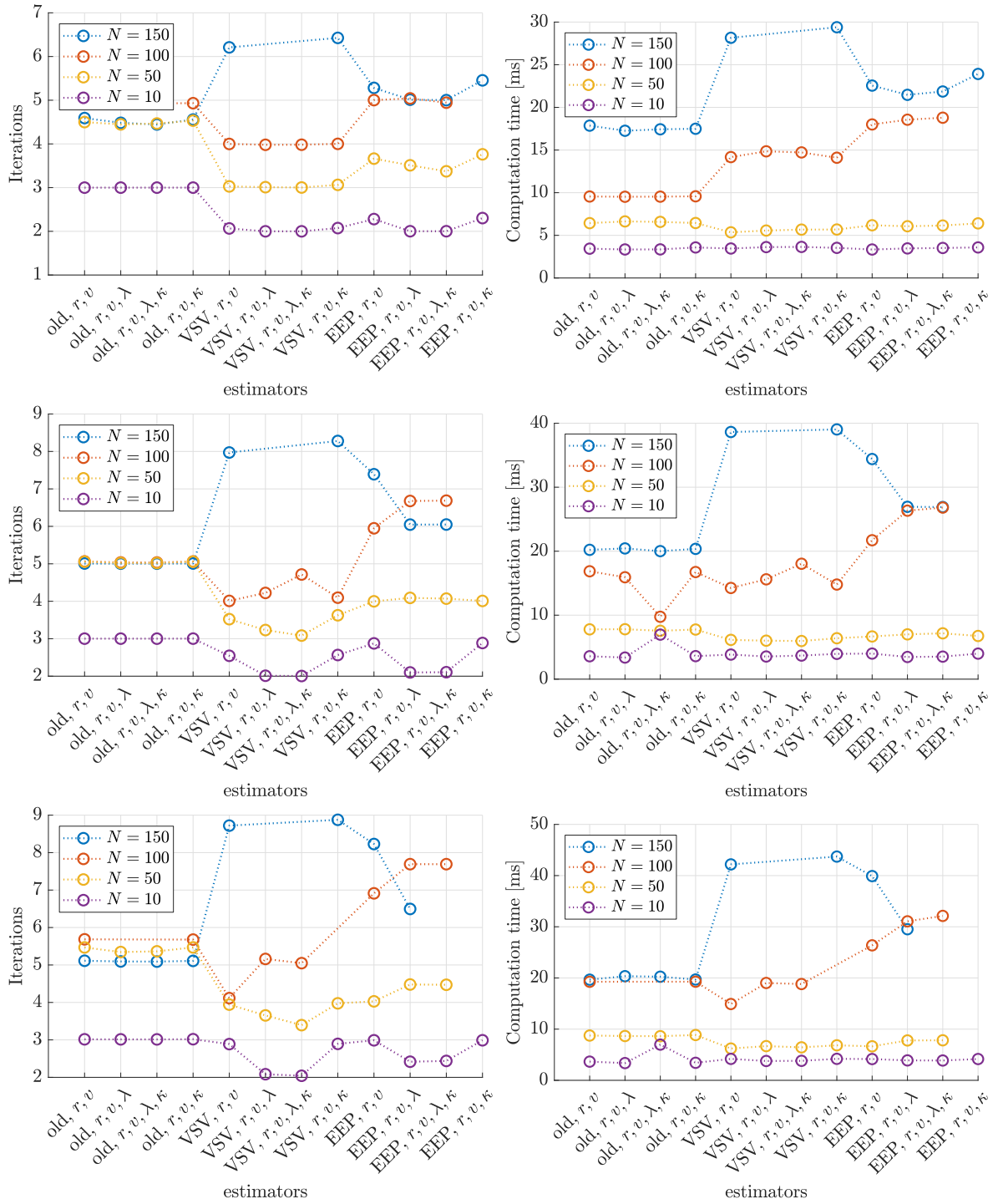
Figure 4.25.: Iterations and computation time for one integration step. Top: $\beta = 0.2$, center: $\beta = 0.4$, bottom: $\beta = 0.6$.
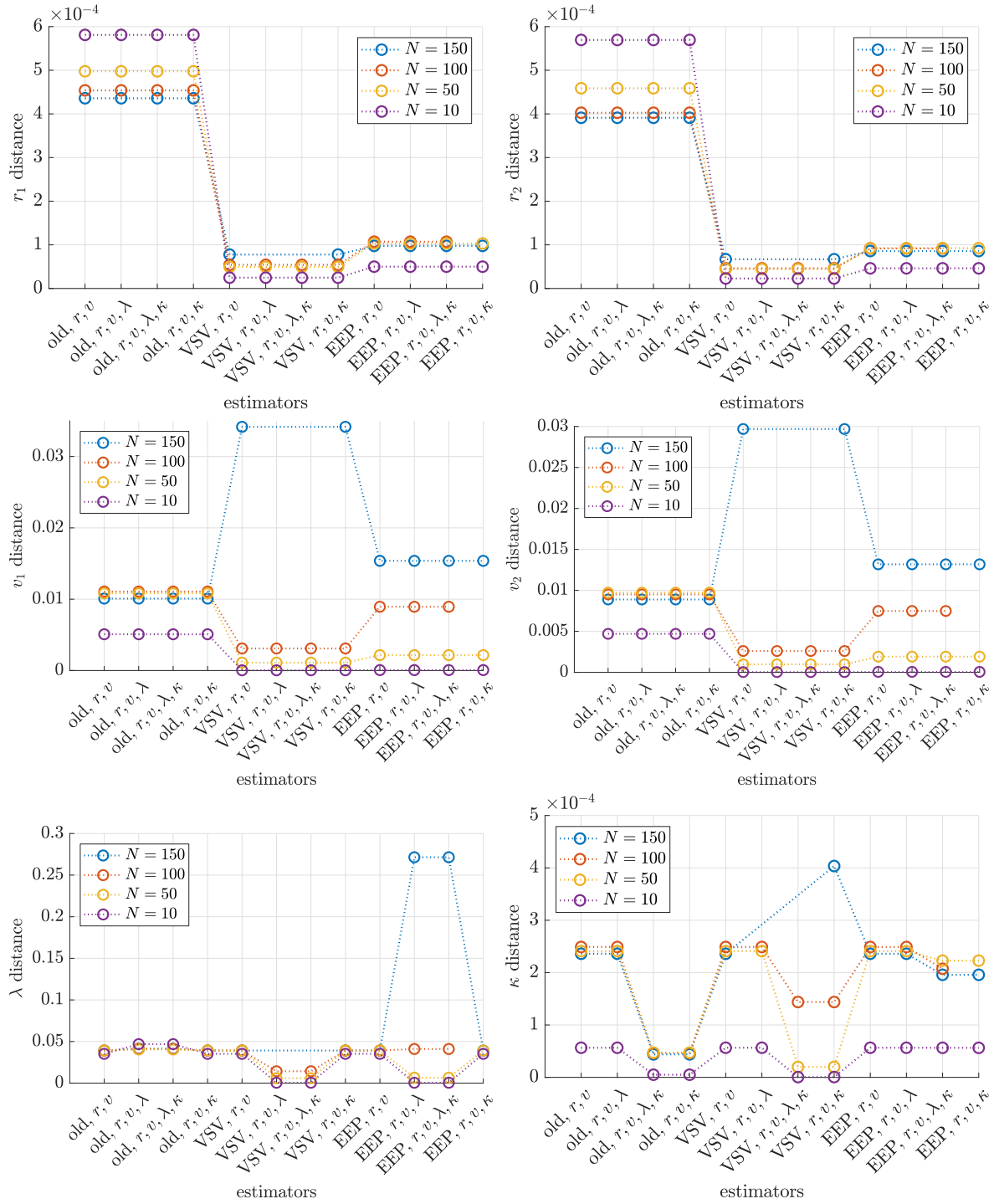
Figure 4.26.: Average $\mathcal{L}^2([0, L])$ distance between y and y_{est} for $y \in \{r_1, r_2, v_1, v_2, \lambda, \kappa\}$, $\beta = 0.2$.

4.5.5 Stochastic air drag, smoothing techniques

In order to examine the smoothing techniques presented in Sec. 4.4.1, we use the IEGGL scheme and first verify the convergence of the resulting model. For this we employ the stochastic scenario used in Sec. 4.5.3 with the stochastic amplitude given by $\mathbf{C}_2$. Since all smoothing techniques behave very similarly in the approximation of the Wiener process, we use only the methods which differ by the underlying approximation idea, i.e., the coarse resolution, the forward-backward averaging and the convolution. For the latter, we choose the hat function kernel, since it provides the closest approximation to the discretized white noise as found in Sec. 4.4.1. We study both, the case of smoothing in space only ($1d$ case), and the application of the smoothing techniques in space and time ($2d$ case). We use 20 Monte-Carlo simulations for this study. Figures 4.27, and C.3 show the convergence behavior of the dynamic variables for $N \in \{32, 128\}$, with Tab. 4.14 showing the measured least squares fit of the convergence order. The scheme converges for all considered smoothing lengths and techniques with convergence rate $p \approx 0.5$ for position and velocity. The Lagrangian multiplier κ converges linearly as seen in Fig. C.4 and C.5, while λ still behaves as $\mathcal{O}(1)$ similarly to the white noise case.

By replacing the white noise with a correlated force term, we can not expect to get a close pathwise approximation of the original solution. In fact, Fig. 4.28 and C.6 in the appendix show that the solutions generated with correlated noise do not converge to the stochastic solution, regardless of the smoothing techniques. Especially the velocity and λ (see Fig. C.7, C.8) differ significantly from the stochastic solution. Since the Lagrangian multiplier κ converges to zero as $\Delta t \to 0$, for any force term, it shows convergent behavior.

As we see from the pathwise behavior, the relative error of the solutions in position is less than 10% and up to 100% in the velocity for $\beta = 0.2$ and $N \in \{32, 128\}$, $T = 1$. In technical applications the statistical properties of the solution are of more interest than the pathwise behavior of the fiber. Hence, we increase the time interval to $T = 5$ and consider a coarse time discretization for the simulation chosen as $\Delta t = 10^{-2}$. For the tests, we use $\beta \in \{0.2, 0.4, 0.6\}$, $N \in \{10, 50, 100, 150\}$ and consider convolution with hat functions with $N_s = 2$ ($N_t = 2$ in the $2d$ smoothing case) as smoothing technique. Tab. 4.15, C.1 and C.2 show that the mean value of the position is well approximated by the smoothed solutions with $\mathcal{L}^2$ distances of a few percent, given that N is sufficiently large. In case of a coarse spatial discretization ($N = 10$), the impact of the additional stochastic increments leads to the significant change of the mean behavior of the fiber position. The mean value of the velocity, however, differs significantly from the stochastic solution. At the same time, the considered correlation techniques have only a small impact on the number of Newton iterations for $N = 10$ and $N = 150$ with even an increase of the average iteration number by 0.02 in the $1d$ smoothing case for $N = 150$, $\beta = 0.2$. For $N \in \{50, 100\}$, the correlated noise reduces the iteration number by up to 0.84 iterations.
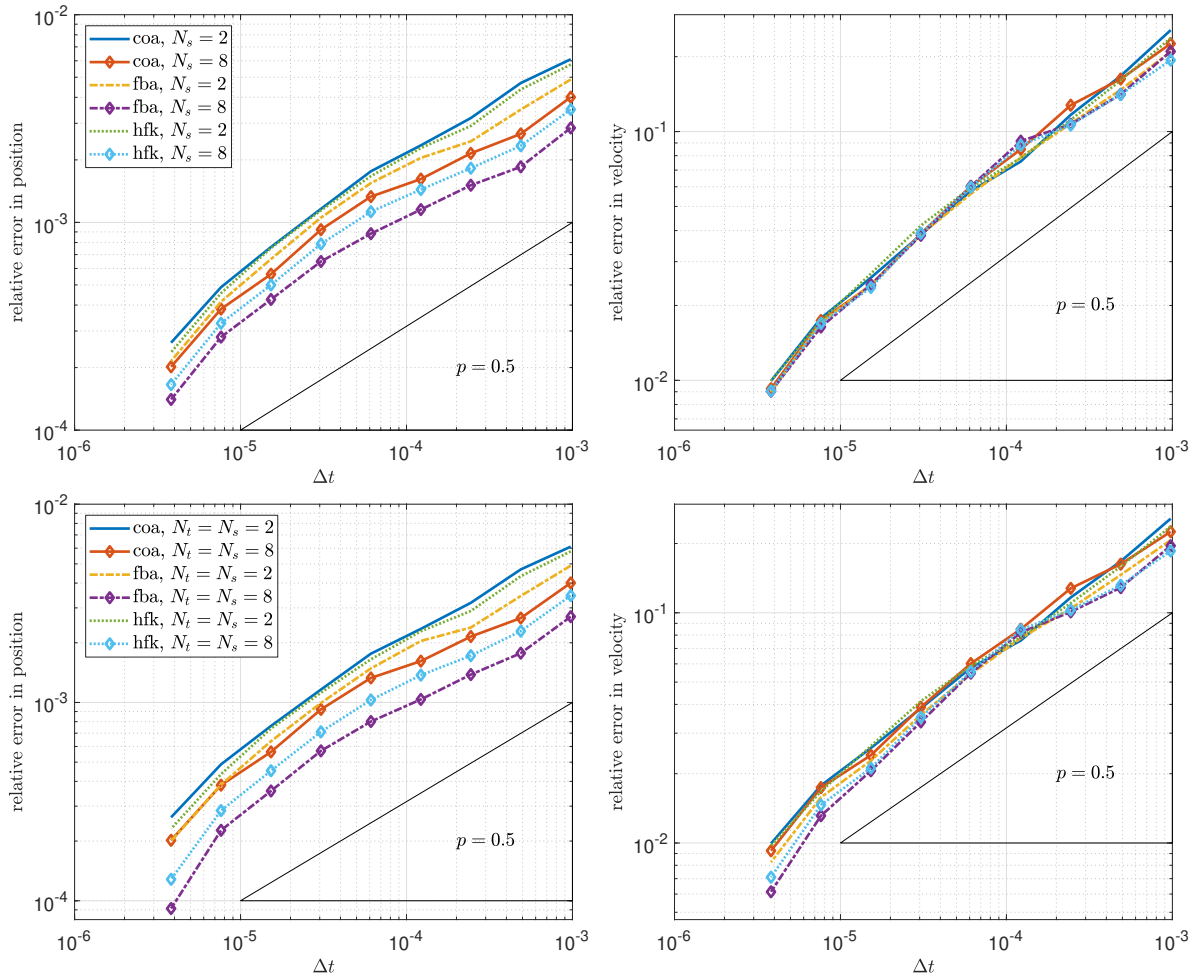
Figure 4.27.: Relative error of the dynamic variables for $N = 32$. Left: r, right: v. Top: Smoothing in space, bottom smoothing in space and time.

| | 1d-smoothing | | | | | |
| | $N_s = 2$ | | | $N_s = 8$ | | |
	coa	fba	hfk	coa	fba	hfk
$N = 32,\ p_r$	0.55	0.53	0.55	0.51	0.50	0.51
$N = 32,\ p_v$	0.56	0.55	0.55	0.57	0.55	0.54
$N = 128,\ p_r$	0.52	0.53	0.54	0.53	0.52	0.52
$N = 128,\ p_v$	0.38	0.54	0.56	0.57	0.59	0.58
	2d-smoothing					
	$N_s = 2 = N_t$			$N_s = 8 = N_t$		
	coa	fba	hfk	coa	fba	hfk
$N = 32,\ p_r$	0.55	0.55	0.56	0.51	0.55	0.55
$N = 32,\ p_v$	0.56	0.56	0.55	0.57	0.60	0.57
$N = 128,\ p_r$	0.52	0.53	0.54	0.53	0.54	0.53
$N = 128,\ p_v$	0.38	0.54	0.56	0.57	0.61	0.60

Table 4.14.: Convergence rates of the dynamic variables for different smoothing techniques.

	Smoothing dim.	r	v	λ	κ	Newton-it.
$N = 10$	$1d$	12.39%	33.64%	37.42%	41.17%	2.98
$N = 10$	$2d$	12.39%	33.57%	49.68%	41.39%	2.96
$N = 50$	$1d$	1.33%	4.78%	28.18%	40.54%	3.88
$N = 50$	$2d$	1.35%	4.92%	36.61%	41.77%	3.79
$N = 100$	$1d$	0.49%	3.20%	21.07%	23.07%	4.34
$N = 100$	$2d$	0.57%	3.63%	36.21%	28.23%	4.20
$N = 150$	$1d$	0.19%	2.05%	9.35%	12.61%	4.62
$N = 150$	$2d$	0.28%	2.57%	31.70%	21.79%	4.30

Table 4.15.: Relative $\mathcal{L}^2$-distance of solution components and average Newton-iterations for smoothing by convolution with hat functions for different space resolutions and smoothing dimensions. Simulation with $\beta = 0.2$, $T = 5$, $\Delta t = 10^{-2}$, $N_s = 2$ and $N_t = 2$ in the $2d$-case. Average Newton iterations without smoothing: 2.99, 4.62, 4.96, 4.60 for $N = 10$, $N = 50$, $N = 100$, $N = 150$ respectively.
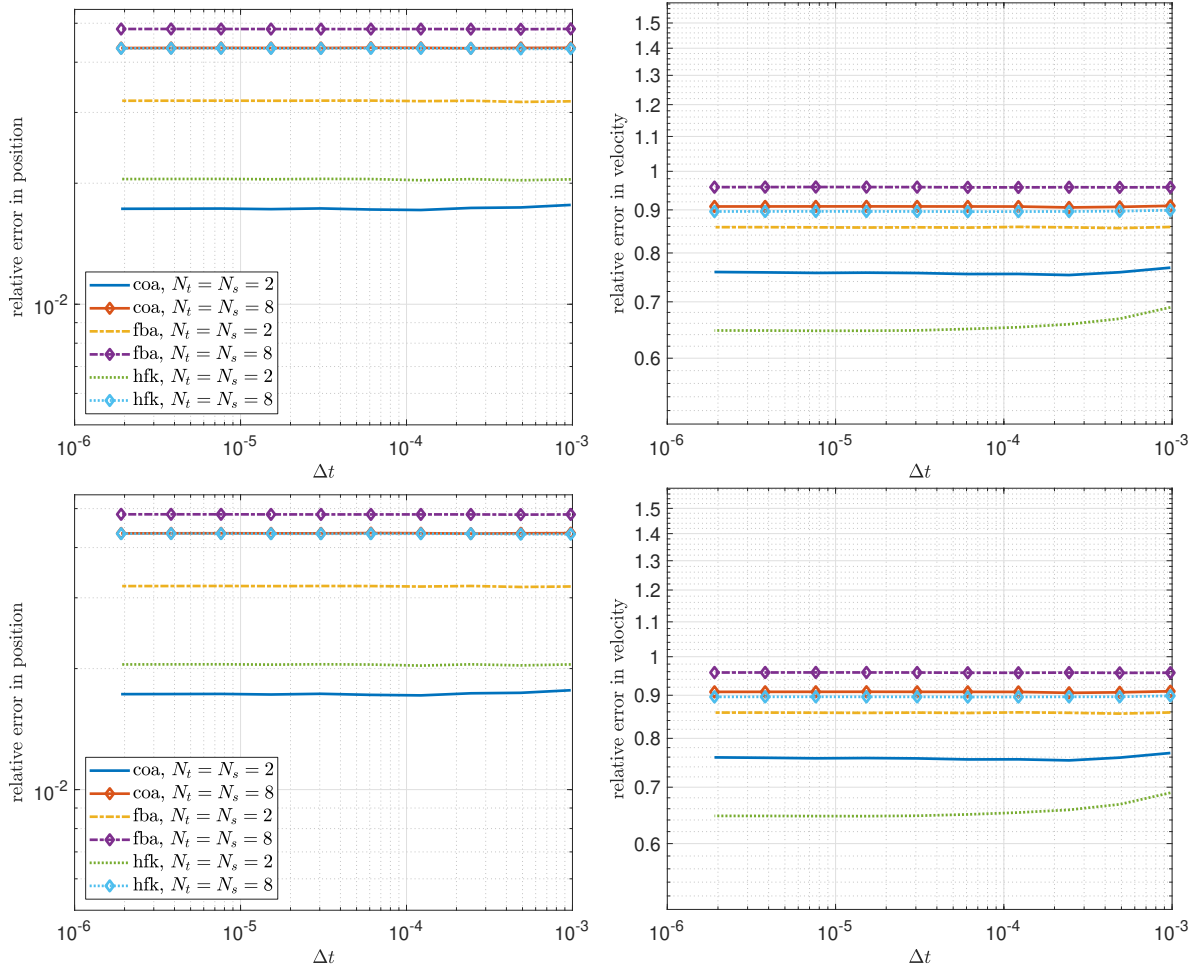
Figure 4.28.: Relative error of the dynamic variables with respect to the stochastic solution for $N = 32$. Left: r, right: v. Top: Smoothing in space, bottom smoothing in space and time.

4.5.6 Stochastic air drag, Wiener chaos expansion

In order to test the Wiener chaos expansion presented in Sec. 4.4.2 we use the model parameters $\alpha, \hat{\mathrm{Dr}}, \mathrm{Fr}$ as well as the boundary and initial conditions used in Sec. 4.5.2. As outer flow we take the rotational flow $\mathbf{A} = 10 \cdot (\boldsymbol{e}_1 \otimes \boldsymbol{e}_2 - \boldsymbol{e}_2 \otimes \boldsymbol{e}_1)$, the gravitational direction is kept as $\boldsymbol{e}_g = -\boldsymbol{e}_2$. The turbulent fluctuation number is chosen as $\beta = 1$, the final time as $T = 1$ and the spatial and temporal grid size as $\Delta s = 10^{-2}$ and $\Delta t = 5 \cdot 10^{-3}$, respectively. For the Fourier expansion of the Wiener process we choose the trigonometric basis, see Rem. 58.

Solving the WCE system (4.43) once allows the creation of an arbitrary number of stochastic realizations of (4.41) by generating the corresponding Wiener processes, calculating their Fourier stochastic coefficients and applying Lem. 59. Additionally, the expressions (4.42) and Lem. 60 yield algebraic formulas for the calculation of the first and second moments of $\boldsymbol{r}$ and λ in terms of polynomials of their deterministic coefficients. Thus, the WCE approach is in principle efficiently superior to classical Monte-Carlo simulations (MCS). To study the feasibility of WCE for the constrained stochastic beam model in industrial applications we investigate the performance of the approach (accuracy, computational costs) in comparison to MCS. The results from 1000 MCS turn out to be suitable as reference. In Fig. 4.29 we see that WCE with first order Wick polynomials yields solutions which catch the overall behavior of the fiber curve $\boldsymbol{r}$. In fact, first and second moments (Fig. 4.30) show a deviation of up to 10% in the mean and up to 20% in the variance of the position for $n = 1$ and $N_s = N_t = 10$ which is a comparably coarse resolution. On the other hand, the increase of polynomial degree without a refinement of the Fourier basis seems not to increase the approximation quality. However, first order Wick polynomials with larger N_s and N_t are not able to improve the approximation quality of the constraint, instead we observe a deterioration. This is also seen in the behavior of the Lagrangian multiplier λ, Fig. 4.31.

The results indicate that the WCE approach (4.43) yields only reasonable approximations of the constrained system (4.41), given higher order polynomials (and N_s, N_t sufficiently large) are used. This poses a severe numerical challenge, since the number of coefficient systems grows as $(n + z)!/(n!z!)$ with $z = dN_sN_t$, $d \in \{2, 3\}$. Thus, in cases where the number of degrees of freedom is large due to the required spatial resolution, the WCE approach becomes impracticable in contrast to MCS. Additionally, the variables are strongly coupled as seen in the structure of the Jacobian of the non-linear system in Fig. 4.32. Another restriction on the applicability of WCE in industrial problems is given by the evaluation of the mixed moment of the force term and a Wick polynomial $\mathbb{E}[\boldsymbol{f}p_\iota]$ (and the treatment of the stochastic amplitude). The drag forces depend in general on fluid flow simulations in complicated geometries. Hence, an approximation of such forces is required to formulate a closed WCE system analogously to (4.43). Consequently, WCE is not suited as a direct numerical technique for accurate stochastic fiber simulations but instead it could be applied for moment approximation or for variance reduction in a hybrid WCE-MCS approach as proposed in [89].
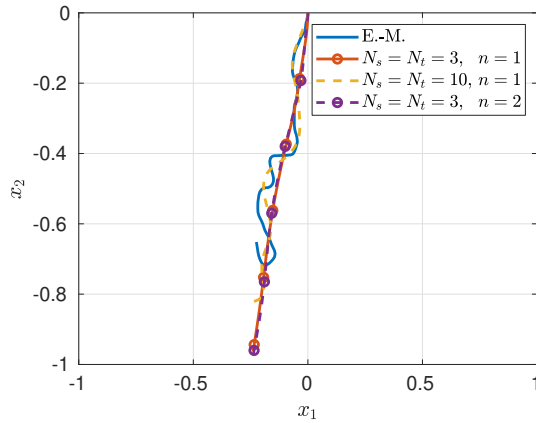
Figure 4.29.: Fiber curve $\boldsymbol{r}(.,T,\omega)$. Solution of original system (4.41) (Euler-Maruyama method, E.-M.) and WCE system (4.43) for different N_s, N_t and n.
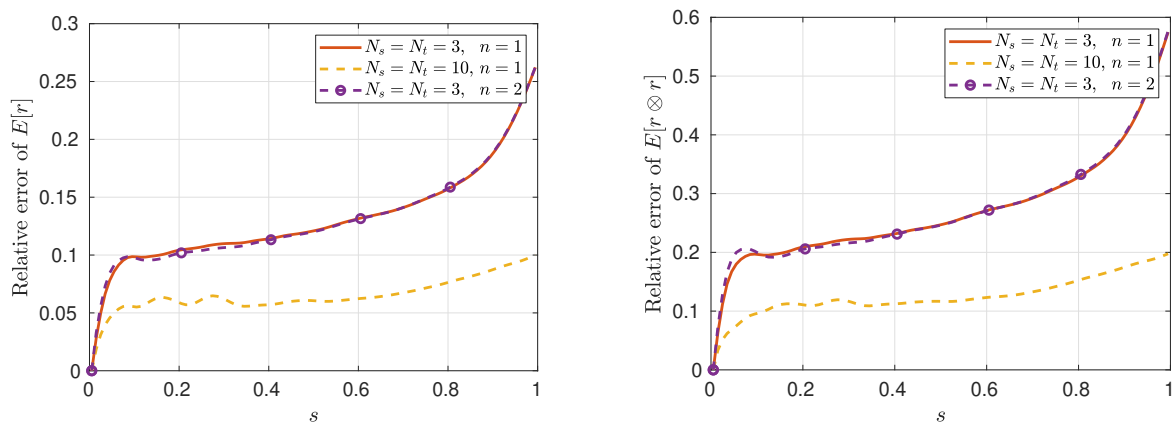

Figure 4.30.: Relative error for expectation $\mathbb{E}[\boldsymbol{r}(.,T)]$ (left) and second moment $\mathbb{E}[(\boldsymbol{r} \otimes \boldsymbol{r})(.,T)]$ (right) between WCE-approximations and (reference) results from 1000 MCS.

4.6 Conclusion

Our aim was to explore different methods for the reduction of computational cost in the simulation of the stochastic partial differential algebraic equation (4.5) with the stochastic force (4.8). The system under consideration describes the dynamics of a slender, inextensible fiber subjected to a turbulent air flow with boundary and initial conditions (4.6) realizing a fixed or freely moving fiber. The fiber is $1d$-parametrized and thus characterized by its position $\boldsymbol{r} : [0, L] \times [0, T] \times \Omega \to \mathbb{R}^d$ with $d \in \{2, 3\}$ and $(\Omega, \mathcal{A}, \varsigma)$ denoting the probability space. After a semi-discretization in space by finite volumes, the resulting system is given by a $(2d+1)N$-dimensional stochastic differential algebraic equation, with N denoting the number of cells in the discretization. We stated two predictor methods for the implicit Euler-Maruyama integration scheme in Sec. 4.3.3 which are able to reduce the computational cost of the fiber simulation as seen in Sec. 4.5.4. The usage of a correlated noise, which is generated by various methods given in Sec. 4.4.1 leads to a much smaller effect on the computational cost, nonetheless it shows to be a viable technique as seen in Sec. 4.5.5. The Wiener chaos
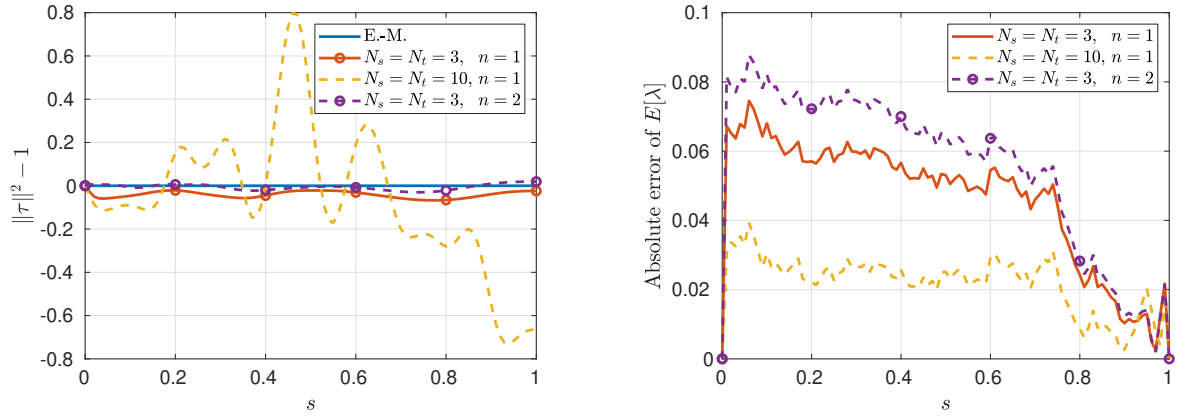
Figure 4.31.: Left: Error in the algebraic constraint of the solution to (4.41) (E.-M.) and the WCE-approximations at $t = T$. Right: Absolute error for expectation $\mathbb{E}[\lambda(.,T)]$ between WCE-approximations and (reference) result from 1000 MCS.
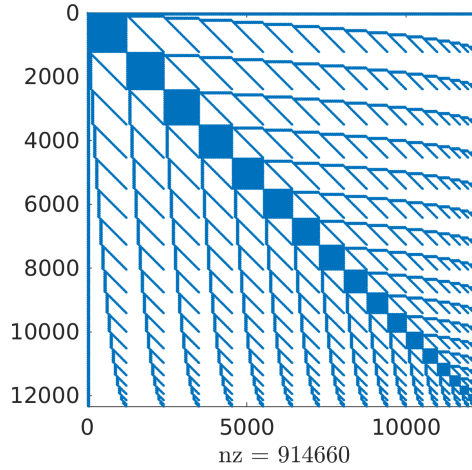

Figure 4.32.: Structure of non-zero entries of Jacobian for $N_s = N_t = 3$, $n = 2$ and $N = 10$. Total number of variables: 12350.

expansion presented in Sec. 4.4.2 leads naturally to the most cost-efficient results. Its applicability, however, is limited to only a special class of problems.

The used fiber model is characterized by three dimensionless quantities: the drag number Dr (ratio of fiber inertia and aerodynamic forces), the bending number α (ratio of inertia and bending) and the Froude number Fr (ratio of inertia and gravity). Its behavior ranges from a nearly stationary and stiff $1d$-rod with little to no effect of outer forces (Dr $\gg 1$ or Fr $\gg 1$, $\alpha \ll 1$) to a nearly inertialess chain of mass points following the outer forces instantly similar to a polymer chain (Dr $\ll 1$ or Fr $\ll 1$, $\alpha \gg 1$) as explored in [16]. Hence, the computational costs differ heavily, depending on the choice of the model parameters which also affects the usefulness of the corresponding cost reduction technique. Therefore, we discussed the typical setting of an air-lay process in Sec. 4.2.4 also defining the aerodynamic drag model used in all numerical investigations except for the Wiener chaos expansion. All subsequent numerical simulations were carried out with parameters chosen in range of this typical setting. In Sec. 4.3 we first presented the Gear-Gupta-Leimkuhler formulation of the

original semi-discretized fiber problem, which leads to better convergence behavior of integration schemes due to the reduction of the differentiation index [60]. Additionally, it also allows a fair comparison of the solutions generated by implicit schemes, such as the implicit Euler method given in Sec. 4.3.1, with projection based methods, where the velocity is projected onto the tangential space of the solution manifold (see Sec. 4.3.3). We then presented the mainly used integration scheme for the fiber equation given as the implicit Euler(-Maruyama) method as well as a modification which ensures energy preservation in case of a deterministic and conservative problem. The implicit Euler-Maruyama method is well suited for the integration of the stochastic fiber model as it is much more stable than any explicit method, while still being the cheapest of the implicit methods. The non-linear system equations associated with the Euler scheme is solved by applying the Newton method. As the latter is only locally convergent, a well-chosen initial guess for the solution is highly important in the computation. The default choice for the initial guess is the solution of the previous time step for the dynamic variables. Due to the stochastic nature of the Lagrangian multipliers, we estimate them with zero in the default case. In order to derive better suited predictors, we also present the explicit Euler method, based on the expression for the Lagrangian multiplier given in [84], as well as the Lobatto IIIA-IIIB pair, whose variants are often used in the field of Molecular Dynamics, in Sec. 4.3.3 amending a modification better suited for efficient fiber simulations. We verified the presented schemes in Sec. 4.5.1 for the deterministic conservative case, in Sec. 4.5.2 for the deterministic case with air drag and in Sec. 4.5.3 for the stochastic case by checking the numerical convergence behavior of the semi-discrete system as $\Delta t \to 0$. We also briefly discussed the dynamical behavior of the fiber as well as the computational costs needed by each integration scheme.

The first predictor method (EEP) investigated in this work is based on the explicit Euler integration scheme (4.37), the second technique (VSV) has its foundation in the Lobatto IIIA-IIIB pair (4.29). Since the latter is an implicit method in case of forces which depend on the velocity, we modified the expression for the estimator in a way which avoids implicit velocity evaluations and projects the force onto the tangent space of the solution manifold. The final estimation is given as one explicit step by the respective method, which in both methods amounts to up to 4 solutions of linear equations of dimension $N \times N$. We compared the estimation quality for each component with the default guess by the solution of the previous time step in Sec. 4.5.4. We observed that the estimation by VSV leads to the best estimation in the position for a wide range of spatial discretizations. Similarly, also the velocity is estimated best by VSV as long as the spatial discretization is coarse enough. If the time discretization fulfills $\Delta t \gg 1/N$, the underlying explicit scheme becomes sufficiently unstable, such that even one step leads to disastrous estimations. In this case the previous time step leads to the best estimation. The estimations by EEP are for all considered cases in between the performance of VSV and the default estimation. Considering the Lagrangian multipliers, again, the estimation by VSV leads to the best estimations as long as N is small enough. For $N = 150$, which was the maximal spatial discretization tested here, the activation of the λ estimation by VSV even led to the breakdown of the Newton method. In this case, the estimation by zero for both Lagrangian multipliers yielded the best results. In the best cases, VSV reduced the average needed number of iterations from 5 to 3, while EEP reduced them only by 1 iteration. This can lead to a significant decrease of computational time, here up

to $\approx 26\%$ less than in the default case. However, as it strongly depends on whether the chosen discretization is appropriate for VSV, using it as a default estimator would not result in a robust integration scheme. This recovers our findings presented in [84], where we only explored the EEP predictor and observed a similar behavior under a simplified scenario. In order to use the VSV predictor in a robust way, it can be used in an adaptive strategy, which checks whether the full VSV estimation is feasible and beneficial, if not, it might be still viable to use the VSV estimation for the position (this requires only one solution of the $N \times N$ linear system), the previous value of the velocity and zero for the Lagrangian multipliers. If this hybrid prediction is also not usable or leads to more Newton iterations than the default estimator, then the latter is used. Performing this check at the beginning of the simulation would retain the robustness of the implicit scheme and benefit from possible speedup by the proposed VSV predictor.

The idea for the correlation of the white noise by the methods presented in Sec. 4.4.1 stems from the fact that due to the inextensibility constraint and the bending stiffness, the acceleration of the fiber is strongly correlated for neighboring points, i.e., on the length scale of a few $\Delta s = 1/N$. Due to Newton's laws of motion, the combination of the constraint force and the white noise acting on the fiber is therefore also a correlated force on this length scale. Since the exact reconstruction of the constraint force, which is a virtual quantity, is not relevant for any industrial or physical application, we can therefore exchange the white noise by a more suitable, correlated stochastic field. The investigated correlation methods presented in Sec. 4.4.1 consist of the averaging of the noise increments, of the usage of a coarser resolution of the Wiener Process and of convolution of the Wiener Process with chosen integration kernels. All of these methods can be read as a smoothing technique for the Wiener Process and although they lead to different regularized stochastic fields, the qualitative behavior is the same for all investigated methods. The error between the regularized field and the original Wiener Process behaves as $\mathcal{O}(\sqrt{N_s})$, where $N_s \Delta s$ is the corresponding correlation length. If the regularization is applied at each time level, the resulting regularized fields converge as $\mathcal{O}(\sqrt{\Delta s})$ for $\Delta s \to 0$. As studied in Sec. 4.5.5, the discretized fiber model with the regularized random force field also converges as $\Delta t \to 0$. However, the convergence order is decreased (given as $\mathcal{O}(\sqrt{\Delta t})$) compared to the original stochastic system which converges linearly in the dynamic variables. Moreover, the pathwise solutions do not converge to the original stochastic solutions. However, the mean behavior is well approximated by the regularized model and even for small correlation lengths of $3\Delta s$ a reduction in the Newton iterations of up to 1 iteration can be observed. These observations are consistent with the experiments performed in [16], where the smoothing by convolution was examined for the fiber model in a different setting. The major problem of the smoothing approach is that the choice of the particular method and of the length scale are arbitrary combined with the fact that even small correlation lengths lead to significant deviations from the original Wiener Process. This way it is hard to argue, whether a particular choice still leads to solutions which catch all necessary physical properties of the fiber dynamics. Hence, in order to retain the notion of a well-defined solution, the correlation method and length should be considered as part of the fiber model instead of an algorithmic tool. The choice of the particular technique should then account for the physical quantities such as the bending stiffness, fiber inertia and characteristic length scale.

The Wiener chaos expansion presented in Sec. 4.4.2 takes advantage of the Fourier expansion of the Wiener Process and of a finite dimensional polynomial approximation of the solution domain of the SPDAE. By expressing the fiber position and the Lagrangian multiplier in the original SPDAE as a series of products of deterministic coefficient functions with Wick polynomials which depend only on the Fourier coefficients of the Wiener Process, the stochastic and deterministic influence is separated. Since the Wick polynomials form an orthonormal basis of the solution space, the description of the dynamics of the deterministic coefficients follows by testing the original SPDAE with these random polynomials and taking the expectation. This last step implies that the method is only applicable, if the expectation of the outer force multiplied with a Wick polynomial can be calculated efficiently. Already in case of the universal drag model given in Sec. 4.2.4 combined with the used stationary flow fields, the analytical computation of such mean values is a highly complicated task, which is the reason why we used a linear, Stokes-like air drag model for the investigation of the applicability of WCE, which is given in (4.41). This simplification avoids a non-linear, analytic force term but still preserves the quadratic constraint. The resulting system of equations then consists of a coupled system of deterministic partial differential algebraic equations (PDAE) for the coefficient functions. In order to arrive at a finite dimensional system, first the expansion of the Wiener Process is truncated which restricts the solution space to polynomials of arbitrary degree but with finite number of arguments. Hence, additionally the degree of the Wick polynomials is restricted. The final finite dimensional system then follows by a spatial semi-discretization. In Sec. 4.5.6 we observed that the WCE approach leads to reasonable approximations of the first and second moments of fiber position already for coarse discretizations of the solution space. However, the pathwise approximations do not fulfill the inextensibility constraint unless the degree of the Wick polynomials is sufficiently large. This observations are consistent to the findings in [120], where we investigated the WCE method in a similar scenario. The advantage of the WCE method is that once the solution of the deterministic coefficient system is solved, an arbitrary number of stochastic realizations can be generated nearly instantly just by generating the Fourier coefficients of the Wiener Process and evaluating the truncated superposition of products of the coefficients with the Wick polynomials. There are, however, two major problems of this approach. The first one being that the number of coefficient systems grows as $(n + z)!/(n!z!)$ with $z = dN_sN_t$ with N_s, N_t denoting the number of basis functions in space and time of the Fourier expansion and n the degree of the Wick polynomials. This implies that even for a two-dimensional setting with $n = 4$, and 5 basis functions in space and time, there are over $3 \cdot 10^5$ coupled coefficient systems. A spatial semi-discretization with only $N = 10$ then results in $\approx 1.6 \cdot 10^7$ variables. Hence, the direct application of the WCE method is only viable, if a small degree of Wick polynomials is sufficient for the approximation. The second problem is given by the fact that the mean value of the outer forces multiplied with the Wick polynomials is needed in order to state the coefficient system. In real applications this is not possible analytically, since the fluid flow is given in terms of simulation data. This expectation can then be computed only by Monte-Carlo simulations, which contradicts the idea of replacing the Monte-Carlo simulations by the WCE method.

The novelty of the presented work consists of the study of suitable estimators for the simulation of inextensible elastic Kirchoff fibers tailored to increase the efficiency of the

computations. The basis of the presented prediction techniques are novel analytical insights into the solution theory of stochastic differential equations subject to holonomic constraints [84] as well as classical numerical methods especially in the field of Molecular Dynamics [4]. The investigation of additional correlation techniques not based on convolution and the investigation of their influence on the dynamic behavior in the context of an air-lay process poses a natural extension of the studies in [16]. Finally, the extension of the WCE approach, which was successfully applied to a stationary fourth order elliptic partial differential equation by [16], to SPDAEs driven by a planar Wiener Process is a novel approach to the simulation of elastic inextensible Kirchhoff fibers.

A Matrix spaces

In this part we collect some essential statements concerning symmetric and skew-symmetric matrices and the special orthogonal group. The latter is a matrix Lie group and therefore a manifold, which is the reason why we also recap some basic definitions and statements regarding manifolds and matrix Lie groups in Sec. A.1.

A.1 Manifolds and Matrix Lie groups

In this section we first briefly recap the basic definitions needed to justify probability measures and transport on the $\mathcal{SO}(3)$ group.

Basics on manifolds

To introduce the corresponding concepts regarding manifolds, we follow [121].

Definition A.1 (Coordinate map, coordinate system)**.** *Let $(\mathcal{M}, \mathcal{O})$ be a second countable Hausdorff topological space. A k-dimensional coordinate map (chart) ϕ on $\mathcal{M}$ is a homeomorphism $\phi : \mathcal{U} \to \mathcal{V}$, where $\mathcal{U} \subset \mathcal{M}, \mathcal{V} \subset \mathbb{R}^k$ for $k \geq 1$ are open sets and $\mathbb{R}^k$ is equipped with the Euclidean topology. The pair $(\mathcal{U}, \phi)$ is called a coordinate system.*

Definition A.2 (Differentiable structure, atlas)**.** *A differentiable structure $\mathcal{A}$ of class $\mathcal{C}^\ell$ (a maximal $\mathcal{C}^\ell$-atlas), $\ell \geq 1$ is a collection of coordinate systems, $\{(\mathcal{U}_\alpha, \phi_\alpha) | \alpha \in \mathcal{I}\}$ for some index set $\mathcal{I}$, with the properties*

  (i) the coordinate systems cover $\mathcal{M}$: $\cup_{\alpha \in \mathcal{I}} \mathcal{U}_\alpha = \mathcal{M}$,

  (ii) the transition map $\phi_\alpha \circ \phi_\beta^{-1} : \phi_\beta(\mathcal{U}_\alpha \cap \mathcal{U}_\beta) \to \phi_\alpha(\mathcal{U}_\alpha \cap \mathcal{U}_\beta)$ is $\mathcal{C}^\ell$ for all $\alpha, \beta \in \mathcal{I}$,

  (iii) the collection is maximal, i.e., if a coordinate system $(\mathcal{U}, \phi)$ fulfills that both, $\phi \circ \phi_\alpha^{-1}$, and $\phi_\alpha \circ \phi^{-1}$ are $\mathcal{C}^\ell$, then it belongs to $\mathcal{A}$.

Definition A.3 (k-dimensional smooth manifold)**.** *We call a topological space $(\mathcal{M}, \mathcal{O})$ as in Definition A.1 equipped with a differentiable structure $\mathcal{A}$, built of k-dimensional coordinate maps, a k-dimensional differentiable manifold of class $\mathcal{C}^\ell$.*

Proposition A.4 (Product of manifolds)**.** *Let $\mathcal{M}_i$ equipped with smooth structures $\mathcal{A}_i$, $i = 1, 2$, be smooth d_i-dimensional manifolds. Then $\mathcal{M} = \mathcal{M}_1 \times \mathcal{M}_2$ equipped with the product topology and smooth structure made of local coordinate systems $(\mathcal{U}, \phi)$ of the form $\mathcal{U} = \mathcal{U}_1 \times \mathcal{U}_2$, $\phi(p, q) = (\phi_1(p), \phi_2(q))$, $(\mathcal{U}_i, \phi_i) \in \mathcal{A}_i$, is a smooth $(d_1 + d_2)$-dimensional manifold.*

Remark A.5 (Short notation, smooth manifold).

1) *Since we discuss neither the underlying topology on $\mathcal{M}$, nor the corresponding smooth structure, we shorten the notation calling the set $\mathcal{M}$ a k-dimensional manifold of class $\mathcal{C}^\ell$ with the topology and smooth structure understood.*

2) *In case $\ell = \infty$, we call the manifold smooth.*

Definition A.6 (Differentiable function on manifold). *Consider two manifolds $\mathcal{M}_1, \mathcal{M}_2$ of dimension d_1, d_2 and of class $\mathcal{C}^\ell$ as well as a mapping $f : \mathcal{M}_1 \to \mathcal{M}_2$. We call f m-times continuously differentiable or $f \in \mathcal{C}^m(\mathcal{M}_1; \mathcal{M}_2)$, $m \leq \ell$, if $\phi_2 \circ f \circ \phi_1^{-1} \in \mathcal{C}^m(\mathbb{R}^{d_1}; \mathbb{R}^{d_2})$ for all coordinate maps ϕ_1 on $\mathcal{M}_1$ and ϕ_2 on $\mathcal{M}_2$. In case $\mathcal{M}_2 = \mathbb{R}$, we write briefly $f \in \mathcal{C}^m(\mathcal{M}_1)$ and call f an m-times differentiable function or $\mathcal{C}^m$-function on $\mathcal{M}_1$.*

Remark A.7. *The following definitions, which depend on the regularity of the underlying manifolds, are introduced for the smooth case. It is, however, also possible to introduce the corresponding objects with respect to less regular structures, by carrying the class of the manifold in the definitions.*

Definition A.8 (Germ). *Let $\mathcal{M}$ be a smooth manifold, $p \in \mathcal{M}$. For two $\mathcal{C}^1$-functions f, g defined on a neighborhood $\mathcal{V}$ of p, we define the equivalence relation $f \sim_p g$ if there exists a neighborhood $\mathcal{U} \subset \mathcal{V}$ of p, such that $f = g$ on $\mathcal{U}$. We call the equivalence classes, $[f]_p$, germs and the set of germs at p is denoted by $\mathcal{F}_p$.*

Proposition A.9. *The quotient set $\mathcal{F}_p$ forms an algebra over $\mathbb{R}$.*

Definition A.10 (Tangent vector, tangent space). *Given a smooth manifold $\mathcal{M}$, a tangent vector v at $p \in \mathcal{M}$ is a linear, real valued map, $v \in \mathrm{Lin}(\mathcal{F}_p; \mathbb{R})$ fulfilling the product rule*

$$v([f]_p[g]_p) = v([f]_p)[g]_p(p) + [f]_p(p)v([g]_p).$$

The set of tangent vectors at p is called tangent space (to $\mathcal{M}$ at p) and is denoted by $\mathcal{T}_p\mathcal{M}$.

Proposition A.11 (Properties of tangent space). *The tangent space $\mathcal{T}_p\mathcal{M}$ to a k-dimensional smooth manifold $\mathcal{M}$ is a real vector space of dimension k.*

Remark A.12 (Application of tangent vectors to functions). *In order to keep a simple notation, we apply tangent vectors to representatives of germs throughout this work. Thus, we set*

$$V(f) = v([f]_p)$$

for any $\mathcal{C}^1$, real valued function on a neighborhood of $p \in \mathcal{M}$. The notation of the tangent space is kept, i.e., $V \in \mathcal{T}_p\mathcal{M}$.

Remark A.13 (Notation for special tangent vectors). *Given a k-dimensional smooth manifold $\mathcal{M}$, a coordinate system $(\mathcal{U}, \phi)$ and $p \in \mathcal{U}$, we set for any $i = 1, \ldots, k$ the tangent vectors*

$$\left. \frac{\partial}{\partial_{\phi_i}} \right|_p \in \mathcal{T}_p\mathcal{M} \quad as \quad \left. \frac{\partial}{\partial_{\phi_i}} \right|_p (f) = \left. \frac{\partial}{\partial_{x_i}} (f \circ \phi^{-1}) \right|_{\phi(p)}$$

for any $\mathcal{C}^1$-function f on a neighborhood of p. The tangent vectors $\partial/\partial_{\phi_i}|_p$ form a basis of $\mathcal{T}_p\mathcal{M}$.

Definition A.14 (Differential at a point). *Consider a C^1-function between two smooth manifolds of dimension d_1, d_2, $f : \mathcal{M}_1 \to \mathcal{M}_2$. For $p \in \mathcal{M}_1$ we call the linear map $\mathrm{d}f_p \in \mathrm{Lin}(\mathcal{T}_p\mathcal{M}_1; \mathcal{T}_{f(p)}\mathcal{M}_2)$ differential of f at p, defined as*

$$\mathrm{d}f_p(V)(g) = V(g \circ f)$$

for all tangent vectors $V \in \mathcal{T}_p\mathcal{M}_1$ and all real valued functions $g : \mathcal{M}_2 \to \mathbb{R}$ which are C^1 on a neighborhood of $f(p)$.

Remark A.15 (Properties of the differential).

P1) Let $f_1 : \mathcal{M}_1 \to \mathcal{M}_2$ and $f_2 : \mathcal{M}_2 \to \mathcal{M}_3$ be C^1-functions between smooth manifolds $\mathcal{M}_i$. Then

$$\mathrm{d}(f_2 \circ f_1)|_p = \mathrm{d}f_2|_{f_1(p)} \circ \mathrm{d}f_1|_p \in \mathrm{Lin}(\mathcal{T}_p\mathcal{M}_1; \mathcal{T}_{f_2 \circ f_1(p)}\mathcal{M}_3) \,,$$

which is the chain rule on manifolds.

P2) For a C^1-curve, i.e., a C^1-mapping $\gamma : (a,b) \to \mathcal{M}$, the differential at point t, $\mathrm{d}\gamma_t(\mathrm{d}/\mathrm{d}t|_t) \in \mathcal{T}_{\gamma(t)}\mathcal{M}$, reads for any $t \in (a,b)$, as

$$\mathrm{d}\gamma_t \left(\frac{\mathrm{d}}{\mathrm{d}t}\bigg|_t \right)(f) = \frac{\mathrm{d}}{\mathrm{d}t}(f \circ \gamma)\bigg|_t \,.$$

Proposition A.16 (Tangent bundles). *Let $\mathcal{M}$ be a smooth k-dimensional manifold, set*

$$\mathcal{T}\mathcal{M} = \cup_{p \in \mathcal{M}} \mathcal{T}_p\mathcal{M} \,.$$

Then there exists a topology $\mathcal{O}$ and a smooth differentiable structure $\mathcal{G}$ on $\mathcal{T}\mathcal{M}$, such that $\mathcal{T}\mathcal{M}$ is a smooth $2k$-dimensional manifold.

Definition A.17 (Vector field). *Let $\pi : \mathcal{T}\mathcal{M} \to \mathcal{M}$ be the projection given as $\pi(W) = p$ for all $W \in \mathcal{T}_p\mathcal{M}$. A map $V : \mathcal{U} \to \mathcal{T}\mathcal{M}$ for an open set $\mathcal{U} \subset \mathcal{M}$ which fulfills*

$$\pi \circ V(p) = p$$

for all $p \in \mathcal{U}$ is called a vector field.

Basics on Lie groups

Following [62], we briefly discuss the properties of matrix Lie groups.

Definition A.18 (General linear group). *The general linear group, $\mathcal{GL}(n; \mathbb{R})$ is the set of all regular matrices in $\mathbb{R}^{n \times n}$.*

Definition A.19 (Matrix Lie group). *Let $\mathcal{G} \subset \mathcal{GL}(n; \mathbb{R})$ be a subgroup. We call $\mathcal{G}$ a matrix Lie group, if the limes of any convergent sequence $\{A_m\}_m \subset \mathcal{G}$, i.e., $\lim_{m \to \infty}(A_m)_{ij} = (A)_{ij}$ for $i, j = 1, \ldots, n$, is either in $\mathcal{G}$ or not regular.*

Proposition A.20 (Matrix exponential, [62, 63]). *Let M be any $n \times n$ real matrix, then the matrix exponential,*

$$\exp(M) = \sum_{k=0}^{\infty} \frac{1}{k!} M^k$$

is a smooth function $\exp : \mathbb{R}^{n \times n} \to \mathbb{R}^{n \times n}$. It fulfills

$$\exp(G \cdot M \cdot G^{-1}) = G \cdot \exp(M) \cdot G^{-1}$$

for any invertible matrix $G \in \mathbb{R}^{n \times n}$. Furthermore, $t \mapsto \exp(tM)$ is a smooth curve in the set of $n \times n$ matrices with real entries and

$$\frac{\mathrm{d}}{\mathrm{d}t} \exp(tM) = M \cdot \exp(tM) = \exp(tM) \cdot M \,.$$

Definition A.21 (Lie algebra of matrix Lie group). *Let $\mathcal{G}$ be a matrix Lie group. The set of all matrices M such that $\exp(tM) \in \mathcal{G}$ for all $t \in \mathbb{R}$ is called Lie algebra of $\mathcal{G}$, denoted by $\mathfrak{g}$.*

Proposition A.22 (Exponential parametrization). *Let $G \subset \mathcal{GL}(n, \mathbb{R})$ be a matrix Lie group with Lie algebra $\mathfrak{g}$. Set $\mathcal{U}_\epsilon = \{M \in \mathbb{R}^{n \times n} \mid \|M\| < \epsilon\}$, with $\|.\|$ denoting the Frobenius norm and the corresponding neighborhood of I, $V_\epsilon = \exp(\mathcal{U}_\epsilon \cap \mathfrak{g}) \subset \mathcal{G}$. Then there exists $\epsilon \in (0, \ln 2)$, such that $\exp : \mathcal{U}_\epsilon \cap \mathfrak{g} \to V_\epsilon$ is a $\mathcal{C}^\infty$-diffeomorphism.*

Proposition A.23 (Dimension of Lie group). *Every matrix Lie group $\mathcal{G} \subset \mathcal{GL}(n, \mathbb{R})$ is a smooth k-dimensional manifold with $k \leq n^2$.*

Proposition A.24 (Dimension of Lie algebra). *If $\mathcal{G}$ is a k-dimensional manifold, the matrix Lie algebra $\mathfrak{g}$ is a linear vector space of dimension k. Furthermore, $\mathfrak{g} = \mathcal{T}_I \mathcal{G}$.*

Definition A.25 (Compact Lie group). *A matrix Lie group $\mathcal{G}$ is called compact, if it is closed and bounded in any matrix norm.*

Lie derivatives

In order to define the notion of Lie derivatives and integration on Lie groups, we follow [27].

Definition A.26 (Lie derivative). *For a matrix $M \in \mathfrak{g}$ the left and right Lie derivatives $\mathcal{L}[M]|_G$, resp. $\mathcal{R}[M]|_G$ are given by*

$$\mathcal{L}[M]|_G (f) = \left. \frac{\mathrm{d}}{\mathrm{d}\tau} f(\exp(-\tau M) \cdot G) \right|_{\tau=0},$$

$$\mathcal{R}[M]|_G (f) = \left. \frac{\mathrm{d}}{\mathrm{d}\tau} f(G \cdot \exp(\tau M)) \right|_{\tau=0}$$

for all $f \in \mathcal{C}^1(\mathcal{G}; \mathbb{R})$.

Lemma A.27 (Properties of Lie derivative). *The left and right Lie derivatives are tangent vectors and span $\mathcal{T}_G \mathcal{G}$.*

Proof. Let $\mathcal{U} \subset \mathcal{G}$ be a neighborhood of $G \in \mathcal{G}$ and $f, g \in \mathcal{C}^1(\mathcal{U}; \mathbb{R})$. Due to Prop. A.20 $\tau \mapsto f(G \cdot \exp(\tau M)) \in \mathcal{C}^1(\mathbb{R}; \mathbb{R})$ (analogously for g). Then for any $a, b \in \mathbb{R}$ it holds

$$
\begin{aligned}
\mathcal{R}[M]|_G (af + bg) &= \frac{\mathrm{d}}{\mathrm{d}\tau}(af + bg)(G \cdot \exp(\tau M))\bigg|_{\tau=0} \\
&= a\,\frac{\mathrm{d}}{\mathrm{d}\tau}f(G \cdot \exp(\tau M))\bigg|_{\tau=0} + b\,\frac{\mathrm{d}}{\mathrm{d}\tau}g(G \cdot \exp(\tau M))\bigg|_{\tau=0}\,,\\
\mathcal{R}[M]|_G (fg) &= \frac{\mathrm{d}}{\mathrm{d}\tau}(fg)(G \cdot \exp(\tau M))\bigg|_{\tau=0} \\
&= g(G)\,\frac{\mathrm{d}}{\mathrm{d}\tau}f(G \cdot \exp(\tau M))\bigg|_{\tau=0} + f(G)\,\frac{\mathrm{d}}{\mathrm{d}\tau}g(G \cdot \exp(\tau M))\bigg|_{\tau=0}
\end{aligned}
$$

which follows from the linearity and the product rule for derivatives of functions $\widetilde{f}$: $\mathcal{C}^1(\mathbb{R}; \mathbb{R})$. Thus, according to Def. A.10 and Rem. A.12, $\mathcal{R}[M]|_G \in \mathcal{T}_G\mathcal{G}$ (analogously for $\mathcal{L}[M]|_G$).

Let $\mathcal{G} \subset \mathcal{GL}(n; \mathbb{R})$ be a k-dimensional manifold, by Prop. A.11, the linear vector space $\mathcal{T}_G\mathcal{G}$ is also k-dimensional as is $\mathfrak{g}$ by Prop. A.24. Hence, let $\{E_i\}_{i=1,\ldots,k}$ be an orthonormal basis of $\mathfrak{g}$ with respect to the Frobenius scalar product over $\mathbb{R}^{n\times n}$, i.e., $(E_i : E_j) = \sum_{k,\ell=1}^{n}(E_i)_{k\ell}(E_j)_{k\ell} = \delta_{ij}$, we show that $\mathcal{B}^{\mathcal{R}} = \{\mathcal{R}[E_i]|_G\}_i$ is a basis of $\mathcal{T}_G\mathcal{G}$. Let $\lambda_1, \ldots, \lambda_k \in \mathbb{R}$ be arbitrary and assume that $\sum_i \lambda_i\,\mathcal{R}[E_i]|_G = 0$. By definition, for any $f \in \mathcal{C}^1(\mathcal{G}; \mathbb{R})$ it holds

$$
0 = \sum_{i=1}^{k} \lambda_i\,\mathcal{R}[E_i]|_G (f) = \sum_{i=1}^{k} \lambda_i\,\frac{\mathrm{d}}{\mathrm{d}\tau}f(G \cdot \exp(\tau E_i))\bigg|_{\tau=0}.
$$

Since $\mathcal{C}^1(\mathbb{R}^{n\times n}; \mathbb{R}) \subset \mathcal{C}^1(\mathcal{G}; \mathbb{R})$, the above relation holds for f chosen as

$$
f(Z) = \sum_{i=1}^{k} \lambda_i (G^{-T} \cdot E_i) : Z
$$

on a neighborhood $\mathcal{U}$ of G, $\mathcal{U} \subset \mathbb{R}^{n\times n}$. Then,

$$
\begin{aligned}
0 &= \sum_{i=1}^{k} \lambda_i \sum_{j\ell} \partial_{Z_{j\ell}} f\big|_{Z=G} (G \cdot E_i)_{j\ell} = \sum_{i=1}^{k} \lambda_i \sum_{j\ell} \sum_{m=1}^{k} \lambda_m (G^{-T} \cdot E_m)_{j\ell}(G \cdot E_i)_{j\ell} \\
&= \sum_{i,m=1}^{k} \lambda_i\lambda_m \sum_{j\ell op} (G^{-T})_{jo}(E_m)_{o\ell}(G)_{jp}(E_i)_{p\ell} = \sum_{i,m=1}^{k} \lambda_i\lambda_m (E_m : E_i) = \|\lambda\|^2
\end{aligned}
$$

by Prop. A.20 and due to $G^{-1} \cdot G = I$. Thus, $\mathcal{B}^{\mathcal{R}}$ is a basis of $\mathcal{T}_G\mathcal{G}$. An analogous calculation shows that the left Lie derivatives also form a basis of $\mathcal{T}_G\mathcal{G}$ for each $G \in \mathcal{G}$. $\qquad\square$

Lemma A.28 (Expression of Lie derivatives). *Let $M \in \mathfrak{g}$, $M = \sum_{i=1}^{k} x_i E_i$ with a given basis $\{E_1, \ldots, E_k\}$ of $\mathfrak{g}$, then the left and right Lie derivatives can be expressed as*

$$
\mathcal{L}[M]|_G = \sum_{i=1}^{k} x_i\,\mathcal{L}[E_i]|_G\,,
$$

$$\mathcal{R}[M]|_G = \sum_{i=1}^{k} x_i \, \mathcal{R}[E_i]|_G \, .$$

Proof. By Lemma A.27, $\mathcal{R}[M]|_G \in \mathcal{T}_G\mathcal{G}$ and $\mathrm{span}\{\mathcal{R}[E_i]|_G\}_i = \mathcal{T}_G\mathcal{G}$. Thus, there is a $\mu \in \mathbb{R}^k$, such that

$$\sum_i \mu_i \, \mathcal{R}[E_i]|_G \, (f) - \mathcal{R}[M]|_G \, (f) = 0$$

for all $f \in \mathcal{C}^1(\mathcal{G}; \mathbb{R})$. In particular, this is true for any $f \in \mathcal{C}^1(\mathbb{R}^{n \times n}; \mathbb{R})$ and hence

$$0 = \sum_{ij} \left(\partial_{G_{ij}} f(G)(G \cdot M)_{ij} - \sum_{\ell=1}^{k} \mu_\ell \partial_{G_{ij}} f(G)(G \cdot E_\ell)_{ij} \right)$$

$$= \sum_{\ell=1}^{k} (x_\ell - \mu_\ell) \sum_{ij} \partial_{G_{ij}} f(G)(G \cdot E_\ell)_{ij} \, .$$

Taking $f(Z) = \sum_{i=1}^{k}(x_i - \mu_i)(G^{-T} \cdot E_i) : Z$ for all Z in a neighborhood $\mathcal{U} \subset \mathbb{R}^{n \times n}$ with $G \in \mathcal{U}$ analogously to the proof of Lemma A.27, it follows $x = \mu$. An analogous calculation shows the claim for $\mathcal{L}[M]|_G$. $\qquad \square$

Lemma A.29 (Transformation of Lie derivatives)**.** *Let G be an element of the matrix Lie group $\mathcal{G} \subset \mathbb{R}^{n \times n}$ and $\mathfrak{g} = \mathrm{span}(\{E_1, \dots, E_k\})$ with orthonormal basis elements E_i, then*

$$\mathcal{R}[E_i]|_G = - \sum_{j=1}^{k} \left((G \cdot E_i \cdot G^{-1}) : E_j \right) \mathcal{L}[E_j]|_G$$

for any $i \in \{1, \dots, k\}$.

Proof. By Lemma A.27 there exists a $\lambda \in \mathbb{R}^k$ such that for all $f \in \mathcal{C}^1(\mathbb{R}^{n \times n})$

$$0 = \mathcal{R}[E_i]|_G \, (f) - \sum_{j=1}^{k} \lambda_j \, \mathcal{L}[E_j]|_G \, (f) = \sum_{k\ell} \partial_{G_{k\ell}} f(G) \left(G \cdot E_i + \sum_{j=1}^{k} \lambda_j E_j \cdot G \right)_{k\ell} \, .$$

Since f can be chosen arbitrary and E_j form an orthonormal basis it holds

$$-(G \cdot E_i \cdot G^{-1}) : E_\ell = \lambda_\ell$$

for any $\ell \in \{1, \dots, k\}$ which implies the claim. $\qquad \square$

Lemma A.30 (Smooth curves in $\mathcal{G}$)**.** *Let $\mathcal{G}$ be a matrix Lie group with a k-dimensional Lie algebra $\mathfrak{g}$. Assume that $G \in \mathcal{C}^1(\mathbb{R}; \mathcal{G})$ is a curve in $\mathcal{G}$. Then it holds*

$$G(t)^{-1} \cdot \frac{\mathrm{d}}{\mathrm{d}t} G(t) \in \mathfrak{g}, \quad \frac{\mathrm{d}}{\mathrm{d}t} G(t) \cdot G(t)^{-1} \in \mathfrak{g} \, .$$

Proof. Let $\epsilon > 0$ be chosen such that Prop. A.22 holds, i.e., the matrix exponential maps $\mathcal{U}_\epsilon \cap \mathfrak{g}$ diffeomorphicly onto $\mathcal{V}_\epsilon = \exp(\mathcal{U}_\epsilon \cap \mathfrak{g})$. Since $G(.)$ and the matrix multiplication are continuous and $I \in \mathcal{V}_\epsilon$, for any $t_0 \in \mathbb{R}$ there exists a $\tau > 0$, with

$G(t_0)^{-1} \cdot G(t) \in \mathcal{V}_\epsilon$ for all $t \in (t_0 - \tau, t_0 + \tau)$. Due to Prop. A.22, there is a unique $M = M(t_0, t) \in \mathfrak{g} \cap \mathcal{U}_\epsilon$ with

$$G(t_0)^{-1} \cdot G(t) = \exp(M(t_0, t))$$

which is a continuously differentiable curve for $t \in (t_0 - \tau, t_0 + \tau)$. Since $I = \exp(0)$, $M(t_0, t_0) = 0$ and due to the regularity of the mapping $t \mapsto M(t_0, t)$, the Taylor expansion of M around t_0 gives $M(t_0, t_0 + \delta) = \delta M_1(t_0) + R(t_0, \delta)$ with $R \in o(\delta)$ as $\delta \to 0$ and $M_1(t_0) \in \mathfrak{g}$ since $\mathfrak{g}$ is a linear vector space. Since the matrix exponential is smooth, also

$$\exp(M(t_0, t_0 + \delta)) = \exp(\delta M_1(t_0)) + o(\delta)$$

holds and therefore

$$\frac{\mathrm{d}}{\mathrm{d}t} \exp(M(t_0, t)) \bigg|_{t=t_0} = \lim_{\delta \to 0} \frac{\exp(M(t_0, t_0 + \delta)) - I}{\delta} = \lim_{\delta \to 0} \frac{\exp(\delta M_1(t_0)) - I}{\delta}$$

$$= \frac{\mathrm{d}}{\mathrm{d}t} \exp(t M_1(t_0)) \bigg|_{t=0} = M_1(t_0) \in \mathfrak{g} \,.$$

We therefore conclude that

$$\frac{\mathrm{d}}{\mathrm{d}t} \left(G(t_0)^{-1} \cdot G(t) \right) \bigg|_{t=t_0} = G(t_0)^{-1} \cdot \frac{\mathrm{d}}{\mathrm{d}t} G(t) \bigg|_{t=t_0} \in \mathfrak{g} \,.$$

As t_0 was arbitrary, the claim follows. For $\mathrm{d}G(t)/\mathrm{d}t \cdot G(t)^{-1} \in \mathfrak{g}$ an analogous calculation can be carried out as also $G(t) \cdot G(t_0)^{-1} \in \mathcal{V}_\epsilon$. □

Lemma A.31 (Smooth curves and Lie derivatives). *Let $\mathcal{G} \subset \mathcal{GL}(n, \mathbb{R})$ be a matrix Lie group and $(\mathcal{U}, \phi)$ a local coordinate system with $\phi \in \mathcal{C}^1(\mathcal{U}; \mathcal{V})$, $\mathcal{V} \subset \mathbb{R}^k$ and corresponding inverse $G : \mathcal{V} \to \mathcal{U}$. Then there exist $\omega^i \in \mathcal{C}^0(\mathbb{R}^k; \mathbb{R}^k)$, $i = 1, \ldots, k$ such that*

$$G(q)^{-1} \cdot \frac{\partial}{\partial q_i} G(q) = \sum_{\ell=1}^{k} \omega_\ell^i(q) E_\ell$$

where $\{E_\ell\}_\ell$ is an orthonormal basis with respect to the Frobenius scalar product of $\mathfrak{g}$. Additionally, the differential fulfills

$$\mathrm{d}G_q \left(\frac{\partial}{\partial q_i} \bigg|_q \right) = \mathcal{R} \left[\sum_{\ell=1}^{k} \omega_\ell^i(q) E_\ell \right] \bigg|_{G(q)} \,.$$

Proof. For the first part, we fix q_j, $j \neq i$, then $q_i \mapsto G(q_1, \ldots, q_{i-1}, q_i, q_{i+1}, \ldots, q_k)$ is a $\mathcal{C}^1(\mathcal{V}_i; \mathcal{U})$ curve with $\mathcal{V}_i \subset \mathcal{V}$. Therefore, Lemma A.30 holds and

$$\omega^i(q) = \sum_{\ell=1}^{k} \left(\left(G(q)^{-1} \cdot \frac{\partial}{\partial q_i} G(q) \right) : E_\ell \right) e_\ell$$

with a continuous right-hand side in q. For the second part, we note that $dG_q \in \mathrm{Lin}(\mathcal{T}_q \mathbb{R}^k; \mathcal{T}_{G(q)}\mathcal{G})$. Hence, for any $\partial/\partial q_i|_q \in \mathcal{T}_q \mathbb{R}^k$,

$$
\mathrm{d}G_q \left(\left. \frac{\partial}{\partial q_i} \right|_q \right) \in \mathcal{T}_{G(q)}\mathcal{G} \, .
$$

Using Prop. A.27, there exists a $\varpi^i \in \mathbb{R}^k$ with

$$
\mathrm{d}G_q \left(\left. \frac{\partial}{\partial q_i} \right|_q \right) = \sum_{\ell=1}^{k} \varpi_\ell^i \, \mathcal{R} \left[E_\ell \right]|_{G(q)} \, .
$$

Thus, for all $f \in \mathcal{C}^1(\mathcal{G}; \mathbb{R})$ it holds

$$
0 = \mathrm{d}G_q \left(\left. \frac{\partial}{\partial q_i} \right|_q \right)(f) - \sum_{\ell=1}^{k} \varpi_\ell^i \, \mathcal{R} \left[E_\ell \right]|_{G(q)} (f) = \left. \frac{\partial}{\partial q_i} \left(f \circ G \right) \right|_q - \sum_{\ell=1}^{k} \varpi_\ell^i \, \mathcal{R} \left[E_\ell \right]|_{G(q)} (f) \, .
$$

In particular, we find for $f \in \mathcal{C}^1(\mathbb{R}^{n \times n}; \mathbb{R})$

$$
\left. \frac{\partial}{\partial q_i} (f \circ G) \right|_q = \sum_{jk} \partial_{G_{jk}} f(G)(G \cdot G^{-1} \cdot \partial_{q_i} G)_{jk} = \sum_{m=1}^{k} \omega_m^i \sum_{jk\ell} \partial_{G_{jk}} f(G) G_{j\ell} (E_m)_{\ell k}
$$

$$
= \sum_{m=1}^{k} \omega_m^i \left. \frac{\mathrm{d}}{\mathrm{d}\tau} f(G \cdot \exp(\tau E_m)) \right|_{\tau=0} = \sum_{m=1}^{k} \omega_m^i \, \mathcal{R}[E_m]|_{G(q)} (f) \, .
$$

By choosing $f \in \mathcal{C}^1(\mathbb{R}^{n \times n}; \mathbb{R})$ similarly to the proof of Prop. A.28 immediately shows $\varpi^i = \omega^i$. $\qquad \square$

Remark A.32 (Lie derivative, vector field, divergence). *We note, that in the definition of the Lie derivative the parameter τ plays the role of the infinitesimal step size in the direction of M in the tangent space to $\mathcal{G}$. Hence, we can consider $\mathcal{G} \times \mathbb{R}^+$-dependent coordinate functions x_i with the corresponding function $M : \mathcal{G} \times \mathbb{R}^+ \to \mathfrak{g}$ given by $M(G, t) = \sum_i x_i(G, t) E_i$ and define a time-dependent vector field $\mathcal{L} \in \mathcal{T}\mathcal{G}$ given as $\mathcal{L}[M](G, t) = \mathcal{L}[M(G, t)]|_G$. Then it still holds*

$$
\mathcal{L}[M](G, t) = \sum_{i=1}^{k} x_i(G, t) \, \mathcal{L}[E_i]|_G \, .
$$

Next, if $x_i(., t) \in \mathcal{C}^1(\mathcal{G}; \mathbb{R})$ for all t, we can define the following divergence operator associated with $\mathcal{L}$

$$
\mathrm{div}_{\mathcal{G}}(\mathcal{L}[M])(G, t) = \sum_{i=1}^{k} \mathcal{L}[E_i]|_G \, (x_i(., t)) \, .
$$

Proposition A.33 (Haar measure). *On any compact Lie group, there exists a unique left- and right-invariant Borel probability measure h, called Haar measure, i.e., $h(GA) = h(AG)$ for all Borel sets A and any fixed $G \in \mathcal{G}$.*

Proposition A.34 (Partial integration on Lie group). *Let $f_1, f_2 \in \mathcal{C}^1(\mathcal{G}; \mathbb{R})$ and denote by h the Haar measure on the compact Lie group $\mathcal{G}$, then*

$$\int_{\mathcal{G}} \mathcal{L}[E_i]|_G (f_1) f_2(G) \, \mathrm{d}h(G) = - \int_{\mathcal{G}} \mathcal{L}[E_i]|_G (f_2) f_1(G) \, \mathrm{d}h(G) \,.$$

From Proposition A.34 and Remark A.32 we then immediately find

Corollary A.35. *Let $M(G) = \sum_i x_i(G) E_i \in \mathfrak{g}$ with $x_i \in \mathcal{C}^1(\mathcal{G}; \mathbb{R})$, and $f_1, f_2 \in \mathcal{C}^1(\mathcal{G}; \mathbb{R})$, then*

$$\int_{\mathcal{G}} \mathcal{L}[M](f_1) f_2 \, \mathrm{d}h = - \int_{\mathcal{G}} \mathcal{L}[M](f_2) f_1 + \mathrm{div}_{\mathcal{G}}(\mathcal{L}[M]) f_1 f_2 \, \mathrm{d}h \,.$$

Remark A.36 (Ordinary differential equations on Lie group and Lie derivatives). *We often apply a differentiable function to a smooth curve in a matrix Lie group and calculate the derivative with respect to the parameter of the curve. Hence, for $f \in \mathcal{C}^1(\mathcal{G}; \mathbb{R})$ and $G \in \mathcal{C}^1(\mathbb{R}; \mathcal{G})$, we consider $\mathrm{d}f(G(t))/\mathrm{d}t$. Using the definition of the differential, Def. A.14 and Lemma A.31 we find*

$$\frac{\mathrm{d}}{\mathrm{d}t} f \circ G(t) = \frac{\mathrm{d}}{\mathrm{d}t}(f \circ G)\Big|_t = \mathrm{d}G_t \left(\frac{\mathrm{d}}{\mathrm{d}t}\Big|_t \right) (f) = \mathcal{R}[M(t)]|_{G(t)} (f)$$

where the matrix-valued function $M(t) = \sum_i \omega_i(t) E_i \in \mathfrak{g}$ is defined by the evolution equation

$$\frac{\mathrm{d}}{\mathrm{d}t} G(t) = G(t) \cdot M(t) \,.$$

An analogous result follows for the left Lie derivative and the function $N : \mathbb{R} \to \mathfrak{g}$ governing the equation

$$\frac{\mathrm{d}}{\mathrm{d}t} G(t) = N(t) \cdot G(t) \,.$$

In this case we find

$$\frac{\mathrm{d}}{\mathrm{d}t} f \circ G(t) = - \mathcal{L}[N(t)]|_{G(t)} (f) \,.$$

Remark A.37 (The product space $\mathbb{R}^\ell \times \mathcal{G}$). *By Prop. A.4, the product space $\mathbb{R}^\ell \times \mathcal{G}$, where $\mathcal{G}$ is a matrix Lie group and the vector space $\mathbb{R}^\ell$ is equipped with the euclidean topology, is an $\ell + k$-dimensional smooth manifold (with k being the dimension of $\mathfrak{g}$). For $(x, G) \in \mathbb{R}^\ell \times \mathcal{G}$ set the tangent vectors $\partial/\partial x_i|_{(x,G)}$, $\mathcal{L}[E_j]|_{(x,G)} \in \mathcal{T}_{(x,G)} \mathbb{R}^\ell \times \mathcal{G}$, $i = 1, \ldots, \ell$, $j = 1, \ldots, k$ as*

$$\frac{\partial}{\partial x_i}\Big|_{(x,G)} (f) = \frac{\partial}{\partial x_i} f(x, G) \,, \quad \mathcal{L}[E_j]|_{(x,G)} (f) = \mathcal{L}[E_j]|_G (f(x, .))$$

for any $f \in \mathcal{C}^1(\mathbb{R}^\ell \times \mathcal{G})$ and consider the set $\mathcal{B}^{\mathcal{L}} = \{ \partial/\partial x_i|_x \,, \mathcal{L}[E_j]|_G \}_{ij}$. By Prop. A.11, $\dim(\mathcal{T}_{(x,G)} \mathbb{R}^\ell \times \mathcal{G}) = \ell + k$, and by choosing test functions similar to the ones in proof of Lemma A.27, one can immediately show the linear independence of the vectors in $\mathcal{B}^{\mathcal{L}}$. Thus, $\mathcal{B}^{\mathcal{L}}$ is a basis of $\mathcal{T}_{(x,G)} \mathbb{R}^\ell \times \mathcal{G}$. This implies that we can relate ordinary

differential equations on $\mathbb{R}^\ell \times \mathcal{G}$ to directional derivatives similarly to Rem. A.37 in the following way: Let $N \in \mathcal{C}^0(\mathbb{R}; \mathfrak{g})$, $v \in \mathcal{C}^0(\mathbb{R}; \mathbb{R}^\ell)$ and the differentiable curve $z = (c, G) \in \mathcal{C}^1(\mathbb{R}; \mathbb{R}^\ell \times \mathcal{G})$ fulfilling

$$\frac{\mathrm{d}}{\mathrm{d}t}c(t) = v(t), \quad \frac{\mathrm{d}}{\mathrm{d}t}G(t) = N(t) \cdot G(t),$$

then for any $f \in \mathcal{C}^1(\mathbb{R}^\ell \times \mathcal{G})$ it holds

$$\frac{\mathrm{d}}{\mathrm{d}t}f \circ z(t) = \mathrm{d}z_t\left(\left.\frac{\mathrm{d}}{\mathrm{d}t}\right|_t\right)(f) = \sum_{i=1}^{\ell} v_i \left.\frac{\partial}{\partial x_i}\right|_{(x,G)}(f) - \sum_{j=1}^{k}(N : E_j)\left.\mathcal{L}[E_j]\right|_{(x,G)}(f)$$
$$= [v \cdot \nabla_x]f(x, G) - \left.\mathcal{L}[N]\right|_G(f(x, .)).$$

Remark A.38 (Transport equations on Lie group, weak forms). *Having the notion of directional derivatives, of an invariant measure and partial integration, we next consider transport equations on a compact Lie group. Therefore, let $M \in \mathcal{C}^1(\mathcal{G} \times \mathbb{R}^+; \mathfrak{g})$ and the initial data $\psi_0 \in \mathcal{C}^1(\mathcal{G}; \mathbb{R})$. Then we assume that $\psi \in \mathcal{C}^1(\mathcal{G} \times \mathbb{R}^+; \mathbb{R})$ is a solution to*

$$\partial_t \psi + \mathcal{L}[M](\psi) = 0, \quad in \ \mathcal{G} \times \mathbb{R}^+ \tag{A.1}$$

and $\psi(., 0) = \psi_0$. By multiplying (A.1) with an arbitrary $f \in \mathcal{C}^1(\mathcal{G}; \mathbb{R})$ and applying the partial integration from Corollary A.35, as well as denoting by $(f_1, f_2) = \int_{\mathcal{G}} f_1 f_2 \,\mathrm{d}h$ the scalar product on $\mathcal{G}$ with respect to the Haar measure, we get the weak form of the transport equation (A.1) as

$$\frac{\mathrm{d}}{\mathrm{d}t}(\psi, f) = (\psi, \mathcal{L}[M](f)) + (\psi, \mathrm{div}_{\mathcal{G}}(\mathcal{L}[M])f). \tag{A.2}$$

Similarly, the weak form of

$$\partial_t \psi + \mathcal{L}[M](\psi) + \mathrm{div}_{\mathcal{G}}(\mathcal{L}[M])\psi = 0 \tag{A.3}$$

is given by

$$\frac{\mathrm{d}}{\mathrm{d}t}(\psi, f) = (\psi, \mathcal{L}[M](f)). \tag{A.4}$$

In the more general case, where ψ is a time-dependent Borel probability measure on $\mathcal{G}$, i.e., $\psi = \psi_t(A)$ for all $A \in \mathcal{B}(\mathcal{G})$ and $t \in \mathbb{R}^+$, the weak forms of (A.1) and (A.3) in the sense of distributions are respectively given as

$$\frac{\mathrm{d}}{\mathrm{d}t}\int_{\mathcal{G}} f(G) \,\mathrm{d}\psi_t(G) = \int_{\mathcal{G}} \left.\mathcal{L}[M(G, t)]\right|_G(f) + f(G)\mathrm{div}_{\mathcal{G}}(\mathcal{L}[M])(G, t) \,\mathrm{d}\psi_t(G), \tag{A.5}$$

$$\frac{\mathrm{d}}{\mathrm{d}t}\int_{\mathcal{G}} f(G) \,\mathrm{d}\psi_t(G) = \int_{\mathcal{G}} \left.\mathcal{L}[M(G, t)]\right|_G(f) \,\mathrm{d}\psi_t(G). \tag{A.6}$$

We note that if ψ_t possess a Radon derivative with respect to the Haar measure with density $\phi : \mathcal{G} \times \mathbb{R}_0^+ \to \mathbb{R}_0^+$ integrable in the first argument and continuously differentiable in the second, the relations (A.5) and (A.2) are equivalent as are (A.6) and (A.4).

Expression of Haar measure with respect to Lebesgue measure, Change of variables formula

The change of variables formula for Lebesgue integrable functions on $\mathbb{R}^n$ is an important tool in analysis. In order to derive a similar result for the Haar measure on compact Lie groups, we need an explicit expression of the Radon derivative of the Haar measure with respect to the Lebesgue measure. The corresponding statements demand the definition of additional objects stated similarly to [26] in this section.

Definition A.39 (Permutations). *We denote a permutation of n elements as a bijective map $\pi : \{1, \ldots, n\} \to \{1, \ldots, n\}$. The set of all such permutations is denoted as Π_n.*

Proposition A.40 (Symmetric group). *The set of permutations together with the operation of the composition, $(\Pi_n, \circ)$, where*

$$(\pi \circ \varpi)(k) = \pi(\varpi(k))$$

for any $\pi, \varpi \in \Pi_n$ and $k \in \{1, \ldots, n\}$, is a group called the symmetric group. The neutral element, π_0, is given as the identity mapping $\pi_0(i) = i$, for $i \in \{1, \ldots, n\}$.

Definition A.41 (Transposition). *A permutation $\pi \in \Pi_n$ which swaps exactly two elements is called a transposition.*

Proposition A.42 (Signature of permutation). *Let $\pi \in \Pi_n$, then there exist transpositions $\varpi_1, \ldots, \varpi_k \in \Pi_n$ such that*

$$\pi = \varpi_1 \circ \varpi_2 \circ \ldots \circ \varpi_k \circ \pi_0$$

and the number $\operatorname{sign}(\pi) = (-1)^k$ is well-defined.

Definition A.43 (Exterior product). *Let V be an n-dimensional vector space and $v_1, \ldots, v_k \in V$ with $k \leq n$. Then*

$$v_1 \wedge v_2 \wedge \ldots \wedge v_k = \frac{1}{k!} \sum_{\pi \in \Pi_k} \operatorname{sign}(\pi) v_{\pi(1)} \otimes v_{\pi(2)} \otimes \ldots \otimes v_{\pi(k)}$$

is called a k-vector. The vector space of all k-vectors over V, the kth exterior power of V, is denoted as $\Lambda^k(V)$.

Proposition A.44 (Dimension of exterior power over V). *Let V be an n-dimensional vector space and $k \leq n$, then*

$$\dim(\Lambda^k(V)) = \left(\begin{array}{c} n \\ k \end{array} \right).$$

Proposition A.45 (Determinant and exterior product). *Let $A \in \mathbb{R}^{n \times n}$ and the vectors $v_1, \ldots, v_n \in \mathbb{R}^n$, then it holds*

$$(A \cdot v_1) \wedge (A \cdot v_2) \wedge \ldots \wedge (A \cdot v_n) = \det(A)(v_1 \wedge v_2 \wedge \ldots \wedge v_n).$$

Next, we follow [27] and introduce the abbreviation for the identification of a k-dimensional Lie algebra $\mathfrak{g}$ and $\mathbb{R}^k$.

Notation A.46 (The "vee" operator)**.** *Let $\mathfrak{g}$ be a k-dimensional Lie algebra, $M \in \mathfrak{g} \subset \mathbb{R}^{n\times n}$, $\{E_i\}_i$ an orthonormal basis of $\mathfrak{g}$ with respect to the Frobenius scalar product on $\mathbb{R}^{n\times n}$. Then we set*

$$(M)^\vee = \sum_{i=1}^k (M : E_i) e_i \,,$$

where $e_i \in \mathbb{R}^k$ are the Cartesian unit vectors.

Remark A.47. *The following statements are carried out assuming one global parametrization of the group $\mathcal{G}$. In case of the $\mathcal{SO}(3)$ group, which is most relevant in this work, the exponential map yields a global smooth parametrization up to a set of measure zero [27]. In general, a partition of unity of $\mathcal{G}$ subordinate to a locally finite open cover by coordinate systems $(\mathcal{U}_\alpha, \phi_\alpha)_{\alpha \in \mathcal{I}}$ is used to define the integral over the manifold [63]. In this case the following considerations can be carried out analogously using the local charts on each $\mathcal{U}_\alpha$.*

Proposition A.48 (Radon derivative of Haar measure on compact matrix Lie groups)**.** *Let $\mathcal{G}$ be a compact matrix Lie group with a global parametrization $G \in \mathcal{C}^\infty(\mathbb{R}^k; \mathcal{G})$ with chart $\phi \in \mathcal{C}^\infty(\mathcal{G}; \mathbb{R}^k)$, i.e., $G(\phi(R)) = R \in \mathcal{G}$ and $\phi(G(q)) = q \in \mathbb{R}^k$. Then the Haar measure on $\mathcal{G}$ is given in terms of the Lebesgue measure as*

$$h(A) = \int_{\phi(A)} \left(G^{-1}(q) \cdot \partial_{q_1} G(q) \right)^\vee \wedge \left(G^{-1}(q) \cdot \partial_{q_2} G(q) \right)^\vee \wedge \ldots \wedge \left(G^{-1}(q) \cdot \partial_{q_k} G(q) \right)^\vee \, \mathrm{d}q$$

for all Borel sets $A \in \mathcal{B}(\mathcal{G})$ and where G^{-1} denotes the inverse of the group element G.

Remark A.49 (Volume form of Haar measure)**.** *We note that the expression for h in Prop. A.48 involves a k-vector, which is given in terms of*

$$v^i(q) = \left(G^{-1}(q) \cdot \partial_{q_i} G(q) \right)^\vee = \sum_{\ell=1}^k e_\ell (E_\ell : \left(G^{-1}(q) \cdot \partial_{q_i} G(q) \right)) = \omega^i(q) \in \mathbb{R}^k \,,$$

where we used Notation A.46 and Lemma A.31. As stated in Prop. A.44, the vector space of this k-vectors is one-dimensional, i.e., $v^1(q) \wedge \ldots \wedge v^k(q)$ can be identified with a scalar-valued function $w : \mathbb{R}^k \to \mathbb{R}$.

Theorem A.50 (Change of variables formula)**.** *For a compact matrix Lie group $\mathcal{G}$ with a k-dimensional Lie algebra $\mathfrak{g} = \mathrm{span}\{E_1, \ldots, E_k\}$, with $(E_i : E_j) = \delta_{ij}$, let $\Phi : \mathcal{G} \to \mathcal{G}$ be a $\mathcal{C}^1$-diffeomorphism. Set the matrix valued mapping $C[\Phi] : \mathcal{G} \to \mathbb{R}^{k\times k}$ as*

$$(C[\Phi])_{pm}(R) = \sum_{j\ell r} (E_p)_{r\ell} \left(\Phi(R)^{-1} \right)_{rj} \mathcal{R} \left[E_m \right]\big|_R (\Phi_{j\ell}) \,.$$

Then it holds for all integrable functions $f : \mathcal{G} \to \mathbb{R}$

$$\int_{R \in \Phi(A)} f(R) \, \mathrm{d}h(R) = \int_{H \in A} f(\Phi(H)) \det(C[\Phi](\Phi(H))) \, \mathrm{d}h(H) \,.$$

Proof. Let $f : \mathcal{G} \to \mathbb{R}$ be a Haar-integrable function and $A \in \mathcal{B}(\mathcal{G})$. In order to distinguish between the group inverse and the inverse of the diffeomorphism, we denote the former by Φ^{-1} and the latter by Ψ, i.e., $\Phi^{-1} \cdot \Phi = I$ and $\Psi \circ \Phi(R) = R$. Analogously, the chart ϕ is the inverse to the parametrization G, while $G^{-1} \cdot G = I$. Since Φ is continuous, $\Phi(A) \in \mathcal{B}$ and

$$\int_{R \in \Phi(A)} f(R) \, dh(R) = \int_{H \in A} f(\Phi(H)) \, dh \circ \Phi(H)$$

where $H = \Psi(R)$. Since $\widetilde{G} = \Phi \circ G : \mathbb{R}^k \to \mathcal{G}$ is a new parametrization of class $\mathcal{C}^1$ with chart $\widetilde{\phi} = \phi \circ \Psi$, the expression in Prop. A.48 is still well-defined and for $B = \Phi(A)$ it holds

$$h(B) = \int_{q \in \widetilde{\phi}(B)} w(\widetilde{G}(q)) \, dq \, .$$

The function w is given as the k-vector (see Rem. A.49) in terms of the vectors $v^i = v^i(q) \in \mathbb{R}^k$,

$$v^i(q) = \sum_{p=1}^{k} \left(\left(\widetilde{G}(q)^{-1} \cdot \frac{\partial}{\partial q_i} \widetilde{G}(q) \right) : E_p \right) e_p \, .$$

Since $\widetilde{G}_{j\ell} \in \mathcal{C}^1(\mathbb{R}^3; \mathbb{R})$ and $\Phi_{j\ell} \in \mathcal{C}^1(\mathcal{G}; \mathbb{R})$, it holds by Def. A.13 and Def. A.14

$$\frac{\partial}{\partial q_i} \widetilde{G}_{j\ell}(q) = \left. \frac{\partial}{\partial q_i} \widetilde{G}_{j\ell} \right|_q = \left. \frac{\partial}{\partial q_i} \right|_q (\Phi_{j\ell} \circ G) = dG_q \left(\left. \frac{\partial}{\partial q_i} \right|_q \right) (\Phi_{j\ell}) \, .$$

Lemma A.31 in combination with Lem. A.28 then reveal

$$\frac{\partial}{\partial q_i} \widetilde{G}_{j\ell}(q) = \sum_{m=1}^{k} \omega_m^i(q) \, \mathcal{R} \left[E_m \right]|_{G(q)} (\Phi_{j\ell}) \, .$$

Thus, the elements of the k-vector are given as

$$v^i(q) = \sum_{m=1}^{k} \omega_m^i(q) \sum_{p=1}^{k} \sum_{j\ell r} \left((E_p)_{r\ell} \left(\Phi(G(q))^{-1} \right)_{rj} \mathcal{R} \left[E_m \right]|_{G(q)} (\Phi_{j\ell}) \right) e_p \, .$$

Setting $C[\Phi](G(q)) \in \mathbb{R}^{k \times k}$ as $(C[\Phi])_{pm} = \sum_{j\ell r} (E_p)_{r\ell} \left(\Phi(G(q))^{-1} \right)_{rj} \mathcal{R} \left[E_m \right]|_{G(q)} (\Phi_{j\ell})$, it holds $v^i(q) = C[\Phi](G(q)) \cdot \omega^i(q)$. Applying Prop. A.45 then yields

$$v^1(q) \wedge v^2(q) \wedge \ldots \wedge v^k(q) = \det(C[\Phi](G(q))) \omega^1(q) \wedge \omega^2(q) \ldots \wedge \omega^k(q)$$
$$= \det(C[\Phi](G(q))) w(G(q))$$

and therefore

$$h \circ \Phi(A) = \int_{q \in \phi(A)} \det(C[\Phi](G(q))) w(G(q)) \, dq \, .$$

Which also implies due to $\Phi(H) = R = G(q)$

$$\int_{R \in \Phi(A)} f(R) \, dh(R) = \int_{H \in A} f(\Phi(H)) \det(C[\Phi](\Phi(H))) \, dh(H) \, .$$

$\square$

In order to derive the connection between the Jacobi determinant of a time-dependent diffeomorphism and the divergence of its driving velocity in Sec. 3.5, we need an additional statement regarding the chain rule stated in the following lemma.

Lemma A.51. *Let Φ be a $\mathcal{C}^1$-diffeomorphism on a Lie group $\mathcal{G}$, $f \in \mathcal{C}^1(\mathcal{G})$ and $\{E_1, \ldots, E_k\}$ an orthonormal basis of $\mathfrak{g}$. Then it holds for all $m = 1, \ldots, k$ and $G \in \mathcal{G}$*

$$\frac{\mathrm{d}}{\mathrm{d}t} f(\Phi(G \cdot \exp(tE_m)))\Big|_{t=0} = \sum_{\ell=1}^{k} (C[\Phi])_{\ell m}(G) \, \mathcal{R}[E_\ell]|_{\Phi(G)} (f)$$

with $C[\Phi] : \mathcal{G} \to \mathbb{R}^{k \times k}$ given in Theorem A.50. Additionally, if $N \in \mathfrak{g}$ with $N = \sum_{m=1}^{k} x_m E_m$, then

$$\frac{\mathrm{d}}{\mathrm{d}t} f(\Phi(G \cdot \exp(tN)))\Big|_{t=0} = \sum_{\ell=1}^{k} (C[\Phi](G) \cdot x)_\ell \, \mathcal{R}[E_\ell]|_{\Phi(G)} (f) .$$

Proof. Fix $G \in \mathcal{G}$, $N \in \mathfrak{g}$ and set $\Phi^N(t) = \Phi(G \cdot \exp(tN))$. Then $\Phi^N \in \mathcal{C}^1(\mathbb{R}; \mathcal{G})$ and $\mathrm{d}\Phi_t^N \in \mathrm{Lin}(\mathcal{T}_t\mathbb{R}; \mathcal{T}_{\Phi^N(t)}\mathcal{G})$, thus due to Rem. A.36 there exists an $M = M(t) \in \mathfrak{g}$ such that

$$\mathrm{d}\Phi_t^N \left(\frac{\partial}{\partial t}\Big|_t \right) = \mathcal{R}[M(t)]|_{\Phi^N(t)} .$$

Thus, for any $g \in \mathcal{C}^1(\mathbb{R}^{n \times n}) \subset \mathcal{C}^1(\mathcal{G})$ it holds

$$0 = \mathrm{d}\Phi_t^N \left(\frac{\partial}{\partial t}\Big|_t \right)(g) - \mathcal{R}[M(t)]|_{\Phi^N(t)}(g) = \frac{\mathrm{d}}{\mathrm{d}t} g(\Phi^N(t)) - \frac{\mathrm{d}}{\mathrm{d}\tau} g(\Phi^N(t) \cdot \exp(\tau M(t)))\Big|_{\tau=0}$$

$$= \sum_{ij} \partial_{G_{ij}} g(\Phi^N(t)) \left(\frac{\mathrm{d}}{\mathrm{d}t} \Phi^N(t) - \Phi^N(t) \cdot M(t) \right)_{ij} .$$

Using $g(G) = e_i \otimes e_j : G$ for fixed i, j as test functions, with $\{e_i\}_i$ being the Cartesian basis of $\mathbb{R}^n$, implies that

$$M(t) = (\Phi^N(t))^{-1} \cdot \frac{\mathrm{d}}{\mathrm{d}t} \Phi^N(t) .$$

This results in particular in

$$M_{ij}(0) = \sum_{p} \left((\Phi^N(0))^{-1} \right)_{ip} \frac{\mathrm{d}}{\mathrm{d}t} \Phi_{pj}^N(t)\Big|_{t=0} = \sum_{p} \left(\Phi(G)^{-1} \right)_{ip} \frac{\mathrm{d}}{\mathrm{d}t} \Phi_{pj}(G \cdot \exp(tN))\Big|_{t=0}$$

$$= \sum_{p} \left(\Phi(G)^{-1} \right)_{ip} \mathcal{R}[N]|_G (\Phi_{pj}) .$$

Since $M(0) \in \mathfrak{g}$ and $\{E_\ell\}_\ell$ is an orthonormal basis, it also holds $M(0) = \sum_{\ell=1}^{k} (M(0) : E_\ell) E_\ell$ and thus by Lemma A.28

$$M(0) = \sum_{\ell=1}^{k} \left(\sum_{ijp} \left(\Phi(G)^{-1} \right)_{ip} \mathcal{R}[N]|_G (\Phi_{pj})(E_\ell)_{ij} \right) E_\ell$$

170

$$= \sum_{m=1}^{k} x_m \sum_{\ell=1}^{k} \left(\sum_{ijp} \left(\Phi(G)^{-1} \right)_{ip} \mathcal{R}[E_m]|_G \, (\Phi_{pj})(E_\ell)_{ij} \right) E_\ell$$

$$= \sum_{\ell=1}^{k} (C[\Phi](G) \cdot x)_\ell E_\ell$$

which implies the claims. $\qquad\square$

A.2 Symmetric, skew-symmetric and trace-free matrices

The following set of matrices forms an orthonormal basis of the matrix space $\mathbb{R}^{3\times3}$ under the Frobenius scalar product given as $\mathbf{A} : \mathbf{B} = \sum_{ij} A_{ij} B_{ij}$

$$(\mathbf{B}_i)_{k\ell} = \frac{1}{\sqrt{2}} \epsilon_{i\ell k}, \quad i = 1, 2, 3, \qquad (\mathbf{B}_i)_{k\ell} = \frac{1}{\sqrt{2}} \epsilon^2_{(i-3)\ell k}, \quad i = 4, 5, 6, \tag{A.7a}$$

$$(\mathbf{B}_7)_{k\ell} = \frac{1}{\sqrt{2}} (\delta_{1k}\delta_{1\ell} - \delta_{2k}\delta_{2\ell}), \qquad (\mathbf{B}_8)_{k\ell} = \frac{1}{\sqrt{6}} (\delta_{1k}\delta_{1\ell} + \delta_{2k}\delta_{2\ell} - 2\delta_{3k}\delta_{3\ell}), \tag{A.7b}$$

$$(\mathbf{B}_9)_{k\ell} = \frac{1}{\sqrt{3}} \delta_{k\ell}. \tag{A.7c}$$

In particular, we may specify the real vector spaces of trace-free, skew-symmetric and symmetric matrices as

$$\text{span}(\mathbf{B}_1, \ldots, \mathbf{B}_8) = \{\mathbf{M} \in \mathbb{R}^{3\times3} \mid \text{tr}(\mathbf{M}) = 0\} \qquad = \mathcal{M}_{tr}, \tag{A.8a}$$

$$\text{span}(\mathbf{B}_1, \mathbf{B}_2, \mathbf{B}_3) = \{\mathbf{M} \in \mathbb{R}^{3\times3} \mid \mathbf{M}^T = -\mathbf{M}\} \qquad = \mathcal{M}_{skew}, \tag{A.8b}$$

$$\text{span}(\mathbf{B}_4, \ldots, \mathbf{B}_9) = \{\mathbf{M} \in \mathbb{R}^{3\times3} \mid \mathbf{M}^T = \mathbf{M}\} \qquad = \mathcal{M}_{sym}, \tag{A.8c}$$

$$\text{span}(\mathbf{B}_4, \ldots, \mathbf{B}_8) = \{\mathbf{M} \in \mathbb{R}^{3\times3} \mid \mathbf{M}^T = \mathbf{M}, \text{tr}(\mathbf{M}) = 0\} = \mathcal{M}_{sym,tr}. \tag{A.8d}$$

By means of (A.8b) we can identify the cross-product in $\mathbb{R}^3$ as

$$\boldsymbol{e}_i \times \boldsymbol{v} = \sqrt{2} \mathbf{B}_i \cdot \boldsymbol{v}, \quad i = 1, 2, 3$$

for any $\boldsymbol{v} \in \mathbb{R}^3$. This way, we define the linear map between $\mathcal{M}_{skew}$ and $\mathbb{R}^3$ which characterizes the cross-product as

$$B : \mathbb{R}^3 \to \mathcal{M}_{skew}, \quad \boldsymbol{v} \mapsto \sqrt{2} \sum_{i=1}^{3} (\boldsymbol{v} \cdot \boldsymbol{e}_i) \mathbf{B}_i, \tag{A.9a}$$

$$B^{-1} : \mathcal{M}_{skew} \to \mathbb{R}^3, \quad \mathbf{M} \mapsto \frac{1}{\sqrt{2}} \sum_{i=1}^{3} (\mathbf{M} : \mathbf{B}_i) \boldsymbol{e}_i. \tag{A.9b}$$

Proposition A.52 (Properties of the skew-symmetric mapping)**.** *The skew-symmetric linear mapping $B(.)$ given in (A.9a) has the following properties for any $\boldsymbol{v}, \boldsymbol{w} \in \mathbb{R}^3$ and any orthogonal matrix $\mathbf{R} \in \mathcal{SO}(3)$*

$$B(\boldsymbol{v}) \cdot \boldsymbol{w} = \boldsymbol{v} \times \boldsymbol{w}, \tag{A.10a}$$

$$B(\mathbf{R} \cdot \boldsymbol{v}) = \mathbf{R} \cdot B(\boldsymbol{v}) \cdot \mathbf{R}^T, \tag{A.10b}$$

$$B(\mathbf{R}^T \cdot \boldsymbol{v}) = \mathbf{R}^T \cdot B(\boldsymbol{v}) \cdot \mathbf{R} \,, \tag{A.10c}$$

$$B(\boldsymbol{v}) \cdot B(\boldsymbol{w}) = \boldsymbol{w} \otimes \boldsymbol{v} - (\boldsymbol{v} \cdot \boldsymbol{w})\mathbf{I} \,, \tag{A.10d}$$

Additionally, $B(.)$ is an orthogonal map between $(\mathbb{R}^3, \cdot)$ and $(\mathcal{M}_{skew}, :^\star)$, with the scaled Frobenius scalar product given as $(\mathbf{A} :^\star \mathbf{B}) = 0.5(\mathbf{A} : \mathbf{B})$.

Proof. The first property (A.10a) follows directly from (A.9a). To show the transformation under rotations (A.10b), we denote the columns of an arbitrary orthogonal matrix $\mathbf{R} \in \mathcal{SO}(3)$ by $\boldsymbol{r}_i$, $i = 1, 2, 3$. By definition they form a right-handed orthonormal basis of $\mathbb{R}^3$, thus

$$\begin{aligned}
(B(\mathbf{R} \cdot \boldsymbol{e}_i))_{jk} = (B(\boldsymbol{r}_i))_{jk} &= \sqrt{2} \sum_\ell (\boldsymbol{r}_i \cdot \boldsymbol{e}_\ell)(\mathbf{B}_\ell)_{jk} = \sum_\ell (\boldsymbol{r}_i \cdot \boldsymbol{e}_\ell)\epsilon_{\ell kj} \\
&= \sum_\ell (\boldsymbol{r}_i \cdot \boldsymbol{e}_\ell)\boldsymbol{e}_\ell \cdot (\boldsymbol{e}_k \times \boldsymbol{e}_j) = \sum_{n,m}(\boldsymbol{e}_k \cdot \boldsymbol{r}_m)(\boldsymbol{e}_j \cdot \boldsymbol{r}_n)\boldsymbol{r}_i \cdot (\boldsymbol{r}_m \times \boldsymbol{r}_n) \\
&= \sum_{n,m}(\boldsymbol{e}_k \cdot \boldsymbol{r}_m)(\boldsymbol{e}_j \cdot \boldsymbol{r}_n)\epsilon_{imn} = \sqrt{2} \sum_{\ell,m,n}(\boldsymbol{e}_k \cdot \boldsymbol{r}_m)(\boldsymbol{e}_j \cdot \boldsymbol{r}_n)(\boldsymbol{e}_i \cdot \boldsymbol{e}_\ell)(\mathbf{B}_\ell)_{nm} \\
&= (\mathbf{R} \cdot B(\boldsymbol{e}_i) \cdot \mathbf{R}^T)_{jk} \,.
\end{aligned}$$

By linearity of $B(.)$ the claim holds for any $\boldsymbol{v} \in \mathbb{R}^3$. The transformation under the inverse rotation (A.10c) follows immediately by applying (A.10b) to $\boldsymbol{w} = \mathbf{R}^T \cdot \boldsymbol{v}$. The relation (A.10d) is the Grassmann identity (see e.g. [98]), i.e., for any $\boldsymbol{u}, \boldsymbol{v}, \boldsymbol{w} \in \mathbb{R}^3$ it holds

$$B(\boldsymbol{v}) \cdot B(\boldsymbol{w}) \cdot \boldsymbol{u} = \boldsymbol{v} \times (\boldsymbol{w} \times \boldsymbol{u}) = (\boldsymbol{v} \cdot \boldsymbol{u})\boldsymbol{w} - (\boldsymbol{v} \cdot \boldsymbol{w})\boldsymbol{u} = (\boldsymbol{w} \otimes \boldsymbol{v} - (\boldsymbol{v} \cdot \boldsymbol{w})\mathbf{I}) \cdot \boldsymbol{u}$$

which proofs the claim. The last claim follows by direct computation and (A.9a). $\quad\square$

Remark A.53 (Inverse of skew-symmetric mapping). *Since $\mathcal{M}_{skew}$ is three-dimensional and $B(.)$ an orthogonal mapping, it is also bijective and therefore its inverse (A.9b) is well-defined. In particular, for any skew-symmetric matrix $\mathbf{M} \in \mathcal{M}_{skew}$ there exists a unique $\boldsymbol{v} \in \mathbb{R}^3$ with $\mathbf{M} = B(\boldsymbol{v})$.*

Next, we set the linear mapping between $\mathbb{R}^8$ and $\mathcal{M}_{tr}$ as

$$M : \mathbb{R}^8 \to \mathcal{M}_{tr} \,, \quad v \mapsto \sum_{i=1}^8 (v \cdot e_i)\mathbf{B}_i \,, \tag{A.11a}$$

$$M^{-1} : \mathcal{M}_{tr} \to \mathbb{R}^8 \,, \quad \mathbf{M} \mapsto \sum_{i=1}^8 (\mathbf{M} : \mathbf{B}_i)e_i \,, \tag{A.11b}$$

where e_i denotes the ith Cartesian unit vector in $\mathbb{R}^8$.

Remark A.54. *The mapping $M(.)$ is an orthogonal mapping between the Euclidean space $(\mathbb{R}^8, \cdot)$ and $(\mathcal{M}_{tr}, :)$ as direct computation and (A.8a) show, thus (A.11b) is well-defined. Extending the domain of M^{-1} to the whole $\mathbb{R}^{3\times3}$, the linear map given by $M \circ M^{-1}$ forms an orthogonal projection onto $\mathcal{M}_{tr}$ and it follows for arbitrary $\mathbf{M}_1 \in \mathbb{R}^{3\times3}, \mathbf{M}_2 \in \mathcal{M}_{tr}$*

$$\mathbf{M}_1 : \mathbf{M}_2 = M \circ M^{-1}(\mathbf{M}_1) : \mathbf{M}_2 = M^{-1}(\mathbf{M}_1) \cdot M^{-1}(\mathbf{M}_2) \,.$$

A.3 Special orthogonal group

Here, we briefly discuss the properties of the special orthogonal group $\mathcal{SO}(3)$ needed in this work.

Lemma A.55 (Angular velocity). *Let $\mathbf{R} : \mathbb{R}_0^+ \to \mathcal{SO}(3)$ be a continuously differentiable mapping and denote the columns of the rotation by $\boldsymbol{r}_i$, $i = 1, 2, 3$, then there exists a uniquely defined continuous function $\boldsymbol{\omega} : \mathbb{R}_0^+ \to \mathbb{R}^3$, such that*

$$\frac{\mathrm{d}}{\mathrm{d}t}\boldsymbol{r}_i = \boldsymbol{\omega} \times \boldsymbol{r}_i \tag{A.12}$$

for all $i = 1, 2, 3$.

Proof. Since $\mathbf{R}(t) \in \mathcal{SO}(3)$ for all $t \geq 0$, it holds

$$\mathbf{0} = \frac{\mathrm{d}}{\mathrm{d}t}\left(\mathbf{R}(t) \cdot \mathbf{R}^T(t)\right) = \left(\frac{\mathrm{d}}{\mathrm{d}t}\mathbf{R}(t)\right) \cdot \mathbf{R}^T(t) + \left(\left(\frac{\mathrm{d}}{\mathrm{d}t}\mathbf{R}(t)\right) \cdot \mathbf{R}^T(t)\right)^T .$$

Thus, the matrix $\mathrm{d}\mathbf{R}/\mathrm{d}t \cdot \mathbf{R}^T$ is skew-symmetric and by Remark A.53, there exists a unique $\boldsymbol{\omega}(t) \in \mathbb{R}^3$, such that

$$B(\boldsymbol{\omega}(t)) = \left(\frac{\mathrm{d}}{\mathrm{d}t}\mathbf{R}(t)\right) \cdot \mathbf{R}^T(t) \tag{A.13}$$

for all $t \geq 0$. Since the right-hand side of (A.13) is continuous in time and $B^{-1}(.)$ is a linear mapping, $t \mapsto \boldsymbol{\omega}(t)$ is continuous. $\qquad\square$

Proposition A.56 (Properties of $\mathcal{SO}(3)$).

1) *The $\mathcal{SO}(3)$ group is a path-connected, compact Lie group.*

2) *The three-dimensional skew-symmetric matrices, $\mathcal{M}_{skew}$, form the Lie algebra of $\mathcal{SO}(3)$.*

Proposition A.57 (Eulerian angles). *Given a fixed Cartesian coordinate system $\boldsymbol{e}_1$, $\boldsymbol{e}_2$, $\boldsymbol{e}_3$, we set the three elemental rotations around the three axis $\mathbf{R}_1(\phi_1), \mathbf{R}_2(\phi_2), \mathbf{R}_3(\phi_3)$ by three independent angles $\phi_1, \phi_2, \phi_3 \in \mathbb{R}$ as*

$$\mathbf{R}_1(\phi_1) = \begin{bmatrix} 1 & 0 & 0 \\ 0 & \cos(\phi_1) & -\sin(\phi_1) \\ 0 & \sin(\phi_1) & \cos(\phi_1) \end{bmatrix}, \quad \mathbf{R}_2(\phi_2) = \begin{bmatrix} \cos(\phi_2) & 0 & -\sin(\phi_2) \\ 0 & 1 & 0 \\ \sin(\phi_2) & 0 & \cos(\phi_2) \end{bmatrix},$$

$$\mathbf{R}_3(\phi_3) = \begin{bmatrix} \cos(\phi_3) & -\sin(\phi_3) & 0 \\ \sin(\phi_3) & \cos(\phi_3) & 0 \\ 0 & 0 & 1 \end{bmatrix}.$$

Then, the mapping $\mathbf{R} : \mathbb{R}^3 \to \mathcal{SO}(3)$, $\mathbf{R}(\boldsymbol{\phi}) = \mathbf{R}_1(\phi_1) \cdot \mathbf{R}_2(\phi_2) \cdot \mathbf{R}_3(\phi_3)$ is surjective.

B Properties of stationary Stokes systems

In this appendix, we collect statements related to the stationary Stokes problem which are needed in Sec. 2 and Sec. 3.

B.1 General properties of Stokes systems

First we state some important results which hold for stationary Stokes systems on general domains. One such property is a Green identity summarized in the following lemma.

Lemma B.1 (Green formula for the Stokes-system [47, 115]). *Let Ω be an open bounded or exterior domain with boundary $\partial\Omega$ of class $\mathcal{C}^1$ and $\boldsymbol{u}_i, p_i$, $i = 1, 2$ sufficiently smooth solenoidal velocity fields and scalar fields. If Ω is an exterior domain, $\boldsymbol{u}_i, p_i$ are assumed to fulfill the decay properties*

$$\nabla^k \boldsymbol{u}_i \in \mathcal{O}(\|\boldsymbol{x}\|^{-(1+k)}), \quad \nabla p_i \in \mathcal{O}(\|\boldsymbol{x}\|^{-2})$$

for $k = 1, 2$ and $\|\boldsymbol{x}\| \to \infty$. Then setting $\Delta\boldsymbol{u}_i - \nabla p_i = \boldsymbol{f}_i$ in Ω it holds

$$
\begin{aligned}
&\int_{\partial\Omega} \boldsymbol{u}_2 \cdot (\partial_{\boldsymbol{n}}\boldsymbol{u}_1 - p_1\boldsymbol{n})\,\mathrm{d}s - \int_\Omega \boldsymbol{u}_2 \cdot \boldsymbol{f}_1\,\mathrm{d}\boldsymbol{x} \\
&= \int_{\partial\Omega} \boldsymbol{u}_1 \cdot (\partial_{\boldsymbol{n}}\boldsymbol{u}_2 - p_2\boldsymbol{n})\,\mathrm{d}s - \int_\Omega \boldsymbol{u}_1 \cdot \boldsymbol{f}_2\,\mathrm{d}\boldsymbol{x} \\
&= \int_\Omega \nabla\boldsymbol{u}_1 : \nabla\boldsymbol{u}_2\,\mathrm{d}\boldsymbol{x}\,,
\end{aligned}
\tag{B.1a}
$$

and similarly for the Newtonian stress tensor $\mathsf{S}[\boldsymbol{u}_i] = 2\mathsf{E}[\boldsymbol{u}_i] - p_i\mathsf{I}$ with the symmetric deformation gradient $\mathsf{E}[\boldsymbol{u}_i] = 0.5(\nabla\boldsymbol{u}_i + \nabla\boldsymbol{u}_i^T)$

$$
\begin{aligned}
&\int_{\partial\Omega} \boldsymbol{u}_2 \cdot \mathsf{S}[\boldsymbol{u}_1] \cdot \boldsymbol{n}\,\mathrm{d}s - \int_\Omega \boldsymbol{u}_2 \cdot \boldsymbol{f}_1\,\mathrm{d}\boldsymbol{x} \\
&= \int_{\partial\Omega} \boldsymbol{u}_1 \cdot \mathsf{S}[\boldsymbol{u}_2] \cdot \boldsymbol{n}\,\mathrm{d}s - \int_\Omega \boldsymbol{u}_1 \cdot \boldsymbol{f}_2\,\mathrm{d}\boldsymbol{x} \\
&= 2\int_\Omega \mathsf{E}[\boldsymbol{u}_1] : \mathsf{E}[\boldsymbol{u}_2]\,\mathrm{d}\boldsymbol{x}\,.
\end{aligned}
\tag{B.1b}
$$

In order to establish direct expressions for the Stokes solutions we follow [72, 115] and first introduce the Stokes fundamental tensor (Oseen tensor), as well as the corresponding pressure field tensor as

$$\mathsf{G}(\boldsymbol{x}) = \frac{1}{8\pi}\left(\|\boldsymbol{x}\|^{-3}\boldsymbol{x} \otimes \boldsymbol{x} + \|\boldsymbol{x}\|^{-1}\mathsf{I}\right), \quad \boldsymbol{p}(\boldsymbol{x}) = \frac{1}{4\pi}\|\boldsymbol{x}\|^{-3}\boldsymbol{x}\,. \tag{B.2}$$

In this case we find for $\boldsymbol{x} \neq \boldsymbol{0}$

$$\partial_{x_k} G_{ij}(\boldsymbol{x}) = \frac{1}{8\pi}\left(-3\|\boldsymbol{x}\|^{-5}x_i x_j x_k + \|\boldsymbol{x}\|^{-3}(\delta_{ik}x_j + \delta_{jk}x_i - \delta_{ij}x_k)\right)$$

$$\sum_i \partial_{x_i} G_{ij}(\boldsymbol{x}) = 0$$

$$\Delta G_{ij}(\boldsymbol{x}) = \frac{1}{4\pi}\left(-3\|\boldsymbol{x}\|^{-5}x_i x_j + \|\boldsymbol{x}\|^{-3}\delta_{ij}\right) = \partial_{x_i}p_j(\boldsymbol{x})$$

$$\nabla \cdot \boldsymbol{p} = \boldsymbol{0}, \quad \Delta \boldsymbol{p} = \boldsymbol{0}.$$

This implies, that the velocity fields $\boldsymbol{u}_j = (G_{ij})_i$ are solenoidal as well as $\Delta \boldsymbol{u}_j - \nabla q_j = \boldsymbol{0}$ for $\boldsymbol{x} \neq \boldsymbol{0}$. Next we consider a smooth vector field $\boldsymbol{v}$ and scalar field q which solve

$$\Delta \boldsymbol{v} = \nabla q, \quad \nabla \cdot \boldsymbol{v} = 0, \quad \boldsymbol{y} \in \Omega$$

for an open bounded or exterior domain $\Omega \subset \mathbb{R}^3$. For a fixed $\boldsymbol{x} \in \mathbb{R}^3$ and $j = 1, 2, 3$, we set $\boldsymbol{v}_j(\boldsymbol{y}) = \boldsymbol{u}_j(\boldsymbol{x} - \boldsymbol{y})$, $q_j(\boldsymbol{y}) = -p_j(\boldsymbol{x} - \boldsymbol{y})$ as well as $\boldsymbol{v}_4(\boldsymbol{y}) = \boldsymbol{p}(\boldsymbol{x} - \boldsymbol{y})$, $q_4 = 0$. Then each $\boldsymbol{v}_j$ is a solenoidal field and

$$\Delta_{\boldsymbol{y}} \boldsymbol{v}_j - \nabla_{\boldsymbol{y}} q_j = \boldsymbol{0}$$

for all $\boldsymbol{y} \neq \boldsymbol{x}$. If $\boldsymbol{x} \notin \overline{\Omega}$ we then can apply (B.1b) and we find

$$\int_{\partial\Omega} \boldsymbol{v} \cdot \mathbf{S}_{\boldsymbol{y}}[\boldsymbol{v}_j] \cdot \boldsymbol{n} \, \mathrm{d}s_y = \int_{\partial\Omega} \boldsymbol{v}_j \cdot \mathbf{S}_{\boldsymbol{y}}[\boldsymbol{v}] \cdot \boldsymbol{n} \, \mathrm{d}s_y$$

On the other hand, if $\boldsymbol{x} \in \Omega$, then there exists an $r > 0$, such that $\overline{\mathcal{B}}_r(\boldsymbol{x}) \subset \Omega$ and (B.1b) is applicable on $\Omega \setminus \overline{\mathcal{B}}_\rho(\boldsymbol{x})$ for all $\rho \in (0, r)$ yielding

$$0 = \int_{\partial(\Omega\setminus\overline{\mathcal{B}}_\rho)} \boldsymbol{v} \cdot \mathbf{S}_{\boldsymbol{y}}[\boldsymbol{v}_j] \cdot \boldsymbol{n} \, \mathrm{d}s_y - \int_{\partial(\Omega\setminus\overline{\mathcal{B}}_\rho)} \boldsymbol{v}_j \cdot \mathbf{S}_{\boldsymbol{y}}[\boldsymbol{v}] \cdot \boldsymbol{n} \, \mathrm{d}s_y$$

$$= \int_{\partial\Omega} \boldsymbol{v} \cdot \mathbf{S}_{\boldsymbol{y}}[\boldsymbol{v}_j] \cdot \boldsymbol{n} \, \mathrm{d}s_y - \int_{\partial\Omega} \boldsymbol{v}_j \cdot \mathbf{S}_{\boldsymbol{y}}[\boldsymbol{v}] \cdot \boldsymbol{n} \, \mathrm{d}s_y$$

$$- \int_{\partial\mathcal{B}_\rho} \boldsymbol{v} \cdot \mathbf{S}_{\boldsymbol{y}}[\boldsymbol{v}_j] \cdot \boldsymbol{n} \, \mathrm{d}s_y + \int_{\partial\mathcal{B}_\rho} \boldsymbol{v}_j \cdot \mathbf{S}_{\boldsymbol{y}}[\boldsymbol{v}] \cdot \boldsymbol{n} \, \mathrm{d}s_y \, .$$

For the last two integrals we note that $\boldsymbol{n} = (\boldsymbol{y} - \boldsymbol{x})/\rho$ and it holds for $j \leq 3$

$$\int_{\partial\mathcal{B}_\rho} \boldsymbol{v} \cdot \mathbf{S}_{\boldsymbol{y}}[\boldsymbol{v}_j] \cdot \boldsymbol{n} \, \mathrm{d}s_y = -\sum_{ik} \int_{\partial\mathcal{B}_\rho} v_i(\partial_{x_k}G_{ij} + \partial_{x_i}G_{kj} - \delta_{ik}p_j)n_k \, \mathrm{d}s_y$$

$$= -\frac{3}{4\pi\rho^4}\sum_i \int_{\partial\mathcal{B}_\rho} v_i(\boldsymbol{y})(\boldsymbol{x}-\boldsymbol{y})_i(\boldsymbol{x}-\boldsymbol{y})_j \, \mathrm{d}s_y$$

$$= -\frac{3}{4\pi\rho^4}\sum_i \int_{\partial\mathcal{B}_\rho(\boldsymbol{0})} v_i(\boldsymbol{x}-\boldsymbol{z})z_i z_j \, \mathrm{d}s_z$$

$$= -\frac{3}{4\pi\rho^3}\sum_i \int_{\mathcal{B}_\rho(\boldsymbol{0})} \partial_{z_i}(v_i(\boldsymbol{x}-\boldsymbol{z})z_j) \, \mathrm{d}\boldsymbol{z}$$

$$= -\frac{3}{4\pi\rho^3} \int_{\mathcal{B}_\rho(\boldsymbol{0})} v_j(\boldsymbol{x}-\boldsymbol{z}) \, \mathrm{d}\boldsymbol{z} = -v_j(\boldsymbol{x}) + \mathcal{O}(\rho^2)$$

since $\boldsymbol{v} \in \mathcal{C}^2(\Omega)$ and $\mathcal{B}_\rho \subset \Omega$. The second integral then similarly yields

$$
\begin{aligned}
\int_{\partial \mathcal{B}_\rho} \boldsymbol{v}_j \cdot \mathbf{S}_{\boldsymbol{y}}[\boldsymbol{v}] \cdot \boldsymbol{n} \, \mathrm{d}s_y &= \frac{1}{8\pi\rho} \sum_{ik} \int_{\partial \mathcal{B}_\rho} \left(\rho^{-2}(\boldsymbol{x} - \boldsymbol{y})_i (\boldsymbol{x} - \boldsymbol{y})_j + \delta_{ij} \right) (\mathbf{S}_{\boldsymbol{y}}[\boldsymbol{v}])_{ik} n_k \, \mathrm{d}s_y \\
&= \frac{1}{8\pi\rho^3} \sum_{ik} \int_{\mathcal{B}_\rho} \partial_{y_k} \left((\boldsymbol{x} - \boldsymbol{y})_i (\boldsymbol{x} - \boldsymbol{y})_j (\mathbf{S}_{\boldsymbol{y}}[\boldsymbol{v}])_{ik} \right) \, \mathrm{d}\boldsymbol{y} \\
&\quad + \frac{1}{8\pi\rho} \int_{\mathcal{B}_\rho} \nabla_{\boldsymbol{y}} \cdot \mathbf{S}_{\boldsymbol{y}}[\boldsymbol{v}] \, \mathrm{d}\boldsymbol{y} \cdot \boldsymbol{e}_j \\
&= \frac{1}{8\pi\rho^3} \int_{\mathcal{B}_\rho} \operatorname{tr}(\mathbf{S}_{\boldsymbol{y}}[\boldsymbol{v}])(\boldsymbol{x} - \boldsymbol{y})_j \, \mathrm{d}\boldsymbol{y} \\
&\quad + \frac{1}{8\pi\rho^3} \int_{\mathcal{B}_\rho} (\boldsymbol{x} - \boldsymbol{y}) \cdot \mathbf{S}_{\boldsymbol{y}}[\boldsymbol{v}] \, \mathrm{d}\boldsymbol{y} \cdot \boldsymbol{e}_j \\
&\quad + \frac{1}{8\pi\rho^3} \int_{\mathcal{B}_\rho} (\boldsymbol{x} - \boldsymbol{y})_j (\boldsymbol{x} - \boldsymbol{y}) \cdot (\nabla_{\boldsymbol{y}} \cdot \mathbf{S}_{\boldsymbol{y}}[\boldsymbol{v}]) \, \mathrm{d}\boldsymbol{y} \\
&= -\frac{3\rho}{8\pi} \int_{\mathcal{B}_1(\boldsymbol{0})} q(\boldsymbol{x} - \rho \boldsymbol{z}) z_j \, \mathrm{d}\boldsymbol{z} \\
&\quad + \frac{\rho}{8\pi} \int_{\mathcal{B}_1(\boldsymbol{0})} \boldsymbol{z} \cdot \mathbf{S}_{\boldsymbol{y}}[\boldsymbol{v}](\boldsymbol{x} - \rho \boldsymbol{z}) \, \mathrm{d}\boldsymbol{z} \cdot \boldsymbol{e}_j \\
&= \mathcal{O}(\rho) \,.
\end{aligned}
$$

In case $j = 4$, we find

$$
\begin{aligned}
\int_{\partial \mathcal{B}_\rho} \boldsymbol{v} \cdot \mathbf{S}_{\boldsymbol{y}}[\boldsymbol{v}_j] \cdot \boldsymbol{n} \, \mathrm{d}s_y &= -\frac{1}{2\pi\rho^3} \int_{\partial \mathcal{B}_\rho} \boldsymbol{v} \cdot (-3\boldsymbol{n} \otimes \boldsymbol{n} + \mathbf{I}) \cdot \boldsymbol{n} \, \mathrm{d}s_y \\
&= \frac{1}{\pi\rho^3} \int_{\partial \mathcal{B}_\rho} \boldsymbol{v} \cdot \boldsymbol{n} \, \mathrm{d}s_y = 0 \\
\int_{\partial \mathcal{B}_\rho} \boldsymbol{v}_j \cdot \mathbf{S}_{\boldsymbol{y}}[\boldsymbol{v}] \cdot \boldsymbol{n} \, \mathrm{d}s_y &= \frac{1}{4\pi\rho^3} \int_{\partial \mathcal{B}_\rho} (\boldsymbol{x} - \boldsymbol{y}) \cdot \mathbf{S}_{\boldsymbol{y}}[\boldsymbol{v}] \cdot \boldsymbol{n} \, \mathrm{d}s_y \\
&= \frac{1}{4\pi\rho^3} \int_{\mathcal{B}_\rho} -\operatorname{tr}(\mathbf{S}_{\boldsymbol{y}}[\boldsymbol{v}]) + (\boldsymbol{x} - \boldsymbol{y}) \cdot \nabla_{\boldsymbol{y}} \cdot \mathbf{S}_{\boldsymbol{y}}[\boldsymbol{v}] \, \mathrm{d}\boldsymbol{y} \\
&= \frac{3}{4\pi\rho^3} \int_{\mathcal{B}_\rho(\boldsymbol{0})} q(\boldsymbol{x} - \boldsymbol{z}) \, \mathrm{d}\boldsymbol{z} = q(\boldsymbol{x}) + \mathcal{O}(\rho) \,.
\end{aligned}
$$

Taking the limit $\rho \to 0$, we therefore get

$$
\int_{\partial \Omega} \boldsymbol{v} \cdot \mathbf{S}_{\boldsymbol{y}}[\boldsymbol{v}_j] \cdot \boldsymbol{n} \, \mathrm{d}s_y - \int_{\partial \Omega} \boldsymbol{v}_j \cdot \mathbf{S}_{\boldsymbol{y}}[\boldsymbol{v}] \cdot \boldsymbol{n} \, \mathrm{d}s_y = \begin{cases} -(\boldsymbol{v}(\boldsymbol{x}), q(\boldsymbol{x}))_j & \boldsymbol{x} \in \Omega \\ 0 & \boldsymbol{x} \notin \overline{\Omega} \end{cases} \,.
$$

If we set $\mathbf{D}(\boldsymbol{x}, \boldsymbol{y}) = (\mathbf{S}_{\boldsymbol{y}}[\boldsymbol{v}_j](\boldsymbol{x}, \boldsymbol{y}) \cdot \boldsymbol{n}(\boldsymbol{y}))_j \in \mathbb{R}^{4 \times 3}$, we can express $\mathbf{D}$ as

$$
D_{ij}(\boldsymbol{x}, \boldsymbol{y}) = \frac{3}{4\pi} \|\boldsymbol{x} - \boldsymbol{y}\|^{-5} (\boldsymbol{x} - \boldsymbol{y})_i (\boldsymbol{x} - \boldsymbol{y})_j (\boldsymbol{x} - \boldsymbol{y}) \cdot \boldsymbol{n}(\boldsymbol{y}), \quad i = 1, 2, 3
$$

$$
D_{4j}(\boldsymbol{x}, \boldsymbol{y}) = \frac{1}{2\pi} \left(3\|\boldsymbol{x} - \boldsymbol{y}\|^{-5} (\boldsymbol{x} - \boldsymbol{y})_j (\boldsymbol{x} - \boldsymbol{y}) \cdot \boldsymbol{n}(\boldsymbol{y}) - \|\boldsymbol{x} - \boldsymbol{y}\|^{-3} n_j(\boldsymbol{y}) \right) \,.
$$

Additionally, we set $\mathbf{E}(\boldsymbol{x}, \boldsymbol{y}) \in \mathbb{R}^{4 \times 3}$ as $E_{ij}(\boldsymbol{x}, \boldsymbol{y}) = G_{ij}(\boldsymbol{x} - \boldsymbol{y})$ for $i = 1, 2, 3$ and $E_{4j}(\boldsymbol{x}, \boldsymbol{y}) = p_j(\boldsymbol{x} - \boldsymbol{y})$, then

$$\int_{\partial\Omega} \mathbf{D} \cdot \boldsymbol{v}\, \mathrm{d}s_y - \int_{\partial\Omega} \mathbf{E} \cdot \mathbf{S}_{\boldsymbol{y}}[\boldsymbol{v}] \cdot \boldsymbol{n}\, \mathrm{d}s_y = \begin{cases} -(\boldsymbol{v}(\boldsymbol{x}), q(\boldsymbol{x})) & \boldsymbol{x} \in \Omega \\ 0 & \boldsymbol{x} \notin \overline{\Omega} \end{cases}.$$

This way we may express the values of the velocity and pressure in Ω by their boundary values and boundary stresses. In case of an exterior domain, this expression also allows to calculate the stresses on the boundary by knowing only the boundary condition $\boldsymbol{v} \in \partial\Omega$ and having the decay properties at infinity. This then allows expressing $(\boldsymbol{v}, q)$ as a functional of $\boldsymbol{v}_{|\partial\Omega}$ solely. This fact is summarized in the following Section, Lemma B.3.

B.2 Single particle in unbounded domain

Here, we collect some important results considering the solutions of stationary Stokes systems in the exterior of a bounded domain. The following statements will often use the notation of Appendix A, in particular, the basis $\mathbf{B}_i$ of the space of trace-free matrices $\mathcal{M}_{\mathrm{tr}}$ and the orthogonal mapping $M : \mathcal{M}_{\mathrm{tr}} \to \mathbb{R}^8$ as well as its inverse (A.11).

First we state a solution theorem for a Fredholm equation on the particle boundary followed by an existence theorem for the Stokes problem on exterior domains and a corresponding expression for the solution, see [115].

Lemma B.2 (Surface density equation). *Let $\mathcal{E} \subset \mathbb{R}^3$ be an open and bounded domain of class $\mathcal{C}^2$ and $\boldsymbol{u}_\Gamma \in \mathcal{C}(\partial\mathcal{E})$ a given function. Then for any $\eta > 0$ there exists a unique solution $\boldsymbol{\psi} \in \mathcal{C}(\partial\mathcal{E})$ to*

$$\boldsymbol{u}_\Gamma = K\boldsymbol{\psi}$$

with $K \in \mathrm{Lin}(\mathcal{C}(\partial\mathcal{E}); \mathcal{C}(\partial\mathcal{E}))$ being an integral operator given as

$$K\boldsymbol{\psi} = -\frac{1}{2}\boldsymbol{\psi} - \int_{\partial\mathcal{E}} \begin{bmatrix} \mathrm{diag}(1,1,1) & \mathbf{0} \end{bmatrix} \cdot (\mathbf{D}(\boldsymbol{x}, \boldsymbol{y}) + \eta\mathbf{E}(\boldsymbol{x}, \boldsymbol{y})) \cdot \boldsymbol{\psi}(\boldsymbol{y})\, \mathrm{d}s_y\,.$$

Lemma B.3 (Classical solution of stationary Stokes equations on exterior domains). *Let $\Omega = \mathbb{R}^3 \setminus \overline{\mathcal{E}}$ with $\mathcal{E}$ being an open and bounded domain of class $\mathcal{C}^2$. Then for any $\boldsymbol{u}_\Gamma \in \mathcal{C}(\partial\mathcal{E})$, the homogeneous stationary Stokes problem*

$$\Delta\boldsymbol{u} - \nabla p = \mathbf{0}, \quad \nabla \cdot \boldsymbol{u} = 0, \quad \boldsymbol{x} \in \Omega$$
$$\boldsymbol{u} = \boldsymbol{u}_\Gamma, \quad \boldsymbol{x} \in \partial\mathcal{E},$$
$$\nabla^k\boldsymbol{u} \in \mathcal{O}(\|\boldsymbol{x}\|^{-(1+k)}), \quad k = 0, 1, \quad p \in \mathcal{O}(\|\boldsymbol{x}\|^{-2})$$

possesses a unique solution $\boldsymbol{u} \in \mathcal{C}^\infty(\Omega) \cap \mathcal{C}(\overline{\Omega})$, $p \in \mathcal{C}^\infty(\Omega)$. The solution can be expressed by means of a hydrodynamical surface potential as

$$(\boldsymbol{u}, p)(\boldsymbol{x}) = S[\boldsymbol{u}_\Gamma](\boldsymbol{x}) = -\int_{\partial\Omega} (\mathbf{D}(\boldsymbol{x}, \boldsymbol{y}) + \eta\mathbf{E}(\boldsymbol{x}, \boldsymbol{y})) \cdot \boldsymbol{\psi}[\boldsymbol{u}_\Gamma](\boldsymbol{y})\, \mathrm{d}s_y$$

for $\boldsymbol{x} \in \Omega$, where $\mathbf{D}, \mathbf{E}$ are given in Section B.1, $\eta > 0$ is a constant and $\boldsymbol{\psi}[\boldsymbol{u}_\Gamma] \in \mathcal{C}(\partial\mathcal{E}; \mathbb{R}^3)$ is the uniquely determined source density of Lemma B.2 satisfying

$$\|\boldsymbol{\psi}[\boldsymbol{u}_\Gamma]\|_{p,\partial\Omega} \leq c(p, \mathcal{E})\|\boldsymbol{u}_\Gamma\|_{p,\partial\Omega}, \quad p \in [1, \infty)\,.$$

Due to Lemma B.3, we find for all $\boldsymbol{x} \in \mathbb{R}^3$ with $\|\boldsymbol{x}\| > 2R > \max(1, \operatorname{diam}(\mathcal{E}))$, where $\mathcal{E} \subset \mathcal{B}_R(\boldsymbol{0})$

$$\|\boldsymbol{u}(\boldsymbol{x})\| \leq c(\eta) \int_{\partial\mathcal{E}} \left(\|\boldsymbol{x} - \boldsymbol{y}\|^{-1} + \|\boldsymbol{x} - \boldsymbol{y}\|^{-2} \right) \|\boldsymbol{\psi}[\boldsymbol{u}_\Gamma](\boldsymbol{y})\| \, \mathrm{d}s_y$$
$$\leq c(\eta)\|\boldsymbol{x}\|^{-1} \int_{\partial\mathcal{E}} \|\boldsymbol{\psi}[\boldsymbol{u}_\Gamma](\boldsymbol{y})\| \, \mathrm{d}s_y \leq c(\mathcal{E}, \eta)\|\boldsymbol{u}_\Gamma\|_{1, \partial\mathcal{E}} \|\boldsymbol{x}\|^{-1} .$$

Analogously we find similar estimations for $\nabla^k \boldsymbol{u}$ and $\nabla^k p$ which we summarize in the following corollary.

Corollary B.4 (Decay properties of classical solutions of the stationary Stokes problem). *Let Lemma B.3 be fulfilled and take $R > 1/2$ such that $\mathcal{E} \subset \mathcal{B}_R(\boldsymbol{0})$. Then for any $0 \leq k < \infty$ it holds for all $\boldsymbol{x} \in \mathbb{R}^3$ with $\|\boldsymbol{x}\| > 2R$*

$$\|\nabla^k \boldsymbol{u}(\boldsymbol{x})\| \leq c(\mathcal{E}, \eta, k)\|\boldsymbol{u}_\Gamma\|_{1, \partial\mathcal{E}} \|\boldsymbol{x}\|^{-(1+k)} ,$$
$$\|\nabla^k p(\boldsymbol{x})\| \leq c(\mathcal{E}, \eta, k)\|\boldsymbol{u}_\Gamma\|_{1, \partial\mathcal{E}} \|\boldsymbol{x}\|^{-(2+k)} .$$

Furthermore, if

$$\int_{\partial\Omega} \mathsf{E} \cdot \boldsymbol{\psi} \, \mathrm{d}s_y = \boldsymbol{0} \tag{B.3}$$

for all $\boldsymbol{x} \in \Omega$, then

$$\|\nabla^k \boldsymbol{u}(\boldsymbol{x})\| \leq c(\mathcal{E}, \eta, k)\|\boldsymbol{u}_\Gamma\|_{1, \partial\mathcal{E}} \|\boldsymbol{x}\|^{-(2+k)} ,$$
$$\|\nabla^k p(\boldsymbol{x})\| \leq c(\mathcal{E}, \eta, k)\|\boldsymbol{u}_\Gamma\|_{1, \partial\mathcal{E}} \|\boldsymbol{x}\|^{-(3+k)}$$

for all $\|\boldsymbol{x}\| > 2R$.

Lemma B.5 (Properties of the 1-particle Compatibility matrix). *Let $\mathcal{E} \subset \mathbb{R}^3$ be an open domain with a smooth boundary $\partial\mathcal{E}$. Consider $\boldsymbol{w}_i, p_i$ as the 11 solutions of the systems*

$$\triangle \boldsymbol{w}_i - \nabla p_i = \boldsymbol{0} , \quad \nabla \cdot \boldsymbol{w}_i = 0 , \quad \boldsymbol{x} \in \mathbb{R}^3 \setminus \overline{\mathcal{E}} ,$$
$$\boldsymbol{w}_i = \hat{\boldsymbol{w}}_i , \quad \boldsymbol{x} \in \partial\mathcal{E} , \quad \|\boldsymbol{w}_i\| \to 0 , \quad \|\boldsymbol{x}\| \to \infty$$

with $\hat{\boldsymbol{w}}_i = \boldsymbol{e}_i$ for $i = 1, 2, 3$ and $\hat{\boldsymbol{w}}_{i+3} = \mathsf{B}_i \cdot \boldsymbol{x}$ for $i = 1, \ldots, 8$. Then the matrix $\mathsf{A} \in \mathbb{R}^{11 \times 11}$ given by

$$A_{ij} = \int_{\partial\mathcal{E}} \partial_{\boldsymbol{n}} \boldsymbol{w}_i - p_i \boldsymbol{n} \, \mathrm{d}s \cdot \boldsymbol{e}_j , \quad j = 1, 2, 3 ,$$
$$A_{i,j+3} = \int_{\partial\mathcal{E}} (\partial_{\boldsymbol{n}} \boldsymbol{w}_i - p_i \boldsymbol{n}) \otimes \boldsymbol{x} \, \mathrm{d}s : \mathsf{B}_j , \quad j = 1, \ldots, 8$$

is negative definite.

Proof. Take an arbitrary $\boldsymbol{z} \in \mathbb{R}^{11}$ and set $\boldsymbol{v} = \sum_{i=1}^3 \boldsymbol{e}_i z_i$ as well as $\mathsf{C} = \sum_{i=1}^8 \mathsf{B}_i z_{i+3}$, then

$$\boldsymbol{z} \cdot \mathsf{A} \cdot \boldsymbol{z} = \sum_i z_i \left(\int_{\partial\mathcal{E}} (\partial_{\boldsymbol{n}} \boldsymbol{w}_i - p_i \boldsymbol{n}) \cdot \boldsymbol{v} \, \mathrm{d}s + \int_{\partial\mathcal{E}} (\partial_{\boldsymbol{n}} \boldsymbol{w}_i - p_i \boldsymbol{n}) \cdot \mathsf{C} \cdot \boldsymbol{x} \, \mathrm{d}s \right)$$

$$= \int_{\partial \mathcal{E}} (\partial_{\boldsymbol{n}} \boldsymbol{w} + p\boldsymbol{n}) \cdot \boldsymbol{w} \,\mathrm{d}s$$

with $\boldsymbol{w}, p$ denoting the single particle Stokes solution with boundary condition $\boldsymbol{w} = \boldsymbol{v} + \mathbf{C} \cdot \boldsymbol{x}$ at $\partial \mathcal{E}$. Noting that $\boldsymbol{n}$ points into the fluid domain, we find from (B.1a)

$$\boldsymbol{z} \cdot \mathbf{A} \cdot \boldsymbol{z} = -\|\nabla \boldsymbol{w}\|^2_{2, \mathbb{R}^3 \setminus \mathcal{E}} \leq 0 \,.$$

Since $\|\nabla \boldsymbol{w}\|_{2, \mathbb{R}^3 \setminus \mathcal{E}} = 0$ if and only if $\boldsymbol{w} = const$ a.e. we conclude by the boundary condition $\boldsymbol{z} \cdot \mathbf{A} \cdot \boldsymbol{z} < 0$ for $\boldsymbol{z} \neq \boldsymbol{0}$. $\qquad \square$

Remark B.6. *If we consider the Newtonian stress tensor in the direction of the outer normal instead of the force term in the integrals of the compatibility matrix in Lemma B.5, i.e.,*

$$\widetilde{A}_{ij} = \int_{\partial \mathcal{E}} \mathbf{S}[\boldsymbol{w}_i] \cdot \boldsymbol{n} \,\mathrm{d}s \cdot \boldsymbol{e}_j \,, \quad j = 1, 2, 3 \,, \tag{B.4a}$$

$$\widetilde{A}_{i,j+3} = \int_{\partial \mathcal{E}} (\mathbf{S}[\boldsymbol{w}_i] \cdot \boldsymbol{n}) \otimes \boldsymbol{x} \,\mathrm{d}s : \mathbf{B}_j \,, \quad j = 1, \ldots, 8 \tag{B.4b}$$

then we may apply (B.1b), showing $\boldsymbol{z} \cdot \widetilde{\mathbf{A}} \cdot \boldsymbol{z} < 0$ since $\mathbf{E}[\boldsymbol{w}] = \boldsymbol{0}$ if and only if $\boldsymbol{w}$ is a rigid body motion a.e. contradicting the boundary condition at infinity.

Lemma B.7 (Compatibility conditions of a single particle)**.** *Let Lemma B.5 hold and $\boldsymbol{u}, p$ shall solve*

$$\triangle \boldsymbol{u} - \nabla p = \boldsymbol{0} \,, \quad \nabla \cdot \boldsymbol{u} = 0 \,, \quad \boldsymbol{x} \in \mathbb{R}^3 \setminus \overline{\mathcal{E}} \,,$$
$$\boldsymbol{u} = \boldsymbol{v} + \mathbf{C} \cdot \boldsymbol{x} \,, \quad \boldsymbol{x} \in \partial \mathcal{E} \,, \quad \|\boldsymbol{u}\| \to 0 \,, \quad \|\boldsymbol{x}\| \to \infty \,,$$

with $\boldsymbol{v} \in \mathbb{R}^3, \mathbf{C} \in \mathcal{M}_{\mathrm{tr}}$. Then it holds $(\boldsymbol{f}, M^{-1}(\mathbf{F})) = \mathbf{A} \cdot (\boldsymbol{v}, M^{-1}(\mathbf{C}))$ for the two force moments

$$\boldsymbol{f} = \int_{\partial \mathcal{E}} \partial_{\boldsymbol{n}} \boldsymbol{u} - p\boldsymbol{n} \,\mathrm{d}s \,, \quad \mathbf{F} = \int_{\partial \mathcal{E}} (\partial_{\boldsymbol{n}} \boldsymbol{u} - p\boldsymbol{n}) \otimes \boldsymbol{x} \,\mathrm{d}s$$

and the matrix $\mathbf{A}$ given in Lemma B.5.

Proof. For $i = 1, 2, 3$ it holds by applying (B.1a)

$$\boldsymbol{e}_i \cdot \boldsymbol{f} = \int_{\partial \mathcal{E}} (\partial_{\boldsymbol{n}} \boldsymbol{u} - p\boldsymbol{n}) \cdot \boldsymbol{w}_i \,\mathrm{d}s = \int_{\partial \mathcal{E}} \partial_{\boldsymbol{n}} \boldsymbol{w}_i - p_i \boldsymbol{n} \,\mathrm{d}s \cdot \boldsymbol{v} + \int_{\partial \mathcal{E}} (\partial_{\boldsymbol{n}} \boldsymbol{w}_i - p_i \boldsymbol{n}) \otimes \boldsymbol{x} \,\mathrm{d}s : \mathbf{C}$$

$$= \sum_{j=1}^{3} \int_{\partial \mathcal{E}} \partial_{\boldsymbol{n}} \boldsymbol{w}_i - p_i \boldsymbol{n} \,\mathrm{d}s \cdot \boldsymbol{e}_j v_j + \sum_{j=1}^{8} \int_{\partial \mathcal{E}} (\partial_{\boldsymbol{n}} \boldsymbol{w}_i - p_i \boldsymbol{n}) \otimes \boldsymbol{x} \,\mathrm{d}s : \mathbf{B}_j M_j^{-1}(\mathbf{C}) \,.$$

Similarly, for $i = 1, \ldots, 8$

$$\boldsymbol{e}_i \cdot M^{-1}(\mathbf{F}) = \mathbf{F} : \mathbf{B}_i = \int_{\partial \mathcal{E}} (\partial_{\boldsymbol{n}} \boldsymbol{u} - p\boldsymbol{n}) \cdot \boldsymbol{w}_{i+3} \,\mathrm{d}s$$

$$= \sum_{j=1}^{3} \int_{\partial \mathcal{E}} \partial_{\boldsymbol{n}} \boldsymbol{w}_{i+3} - p_{i+3} \boldsymbol{n} \,\mathrm{d}s \cdot \boldsymbol{e}_j v_j$$

$$+ \sum_{j=1}^{8} \int_{\partial \mathcal{E}} (\partial_{\boldsymbol{n}} \boldsymbol{w}_{i+3} - p_{i+3} \boldsymbol{n}) \otimes \boldsymbol{x} \,\mathrm{d}s : \mathbf{B}_j M^{-1}(\mathbf{C}) \cdot \boldsymbol{e}_j \,.$$

$\qquad \square$

Corollary B.8 (Compatibility conditions in the case of rigid body motion). *Let Lemma B.7 hold, if $\mathbf{C} \in \mathcal{M}_{skew}$, then the forces and torques*

$$\boldsymbol{f} = \int_{\partial \mathcal{E}} \partial_{\boldsymbol{n}} \boldsymbol{u} - p\boldsymbol{n} \, \mathrm{d}s \,, \quad \boldsymbol{t} = \int_{\partial \mathcal{E}} \boldsymbol{x} \times (\partial_{\boldsymbol{n}} \boldsymbol{u} - p\boldsymbol{n}) \, \mathrm{d}s$$

fulfill $(\boldsymbol{f}, \boldsymbol{t}/\sqrt{2}) = \hat{\mathbf{A}} \cdot (\boldsymbol{v}, \sqrt{2}\boldsymbol{\omega})$ with $\boldsymbol{\omega} = B^{-1}(\mathbf{C})$ and the regular matrix $\hat{\mathbf{A}} \in \mathbb{R}^{6 \times 6}$ given as $\hat{A}_{ij} = A_{ij}$ for $i, j = 1, \ldots, 6$.

Proof. Noting that since $\boldsymbol{z} \cdot \mathbf{A} \cdot \boldsymbol{z} < 0$ for any $\boldsymbol{z} \neq \boldsymbol{0}$, this holds especially for all $\boldsymbol{z}$ with $z_i = 0$ for $i = 7, \ldots, 11$, thus $\hat{\mathbf{A}}$ is negative definite and the definition of the skew-symmetric mapping B with respect to the basis of $\mathcal{M}_{\mathrm{tr}}$, (A.9) completes the proof. $\qquad \square$

Remark B.9. *Following Remark B.6, we may use the Newtonian stress tensor in Lemma B.7 and get an analogous result with matrix $\widetilde{\mathbf{A}}$ defined in Remark B.6, i.e., it holds $(\widetilde{\boldsymbol{f}}, M^{-1}(\widetilde{\mathbf{F}})) = \widetilde{\mathbf{A}} \cdot (\boldsymbol{v}, M^{-1}(\mathbf{C}))$ with*

$$\int_{\partial \mathcal{E}} \mathbf{S}[\boldsymbol{u}] \cdot \boldsymbol{n} \, \mathrm{d}s = \widetilde{\boldsymbol{f}} \,,$$

$$\int_{\partial \mathcal{E}} \mathbf{S}[\boldsymbol{u}] \cdot \boldsymbol{n} \otimes \boldsymbol{x} \, \mathrm{d}s = \widetilde{\mathbf{F}} \,.$$

Analogously, Corollary B.8 implies $(\widetilde{\boldsymbol{f}}, \widetilde{\boldsymbol{t}}/\sqrt{2}) = \hat{\widetilde{\mathbf{A}}} \cdot (\boldsymbol{v}, \sqrt{2}\boldsymbol{\omega})$ with the negative definite matrix $\hat{\widetilde{A}}_{ij} = \widetilde{A}_{ij}$ for $i, j = 1, \ldots, 6$ and

$$\int_{\partial \mathcal{E}} \boldsymbol{x} \times \mathbf{S}[\boldsymbol{u}] \cdot \boldsymbol{n} \, \mathrm{d}s = \widetilde{\boldsymbol{t}} \,.$$

B.3 Details on ellipsoidal geometry and related problems

Here we summarize some fundamental results of different works for ellipsoidal particles, the individual results are from Oberbeck [96], Edwardes [40], Jeffery [70] and Junk & Illner [71]. First we introduce all relevant functions needed to formulate the solutions of Oberbeck and Jeffery in Lemma B.11, also analyzing the decay properties of the involved quantities in Lemma B.10. Next, we briefly present the necessary steps for the analytical computation of the surface moments arising in the solvability conditions of Lemma 5 by using Lemma B.11.

Oberbeck and Jeffery solutions

As stated in Section 2.4, an ellipsoid is a set $\mathcal{E} = \mathbf{D}\mathcal{B}_1$ with $\mathbf{D} = \mathrm{diag}(d_1, d_2, d_3)$, $d_i > 0$ and unit ball $\mathcal{B}_1$ in $\mathbb{R}^3$. This implies $\mathcal{E} = \{\boldsymbol{y} \in \mathbb{R}^3 \mid \|\mathbf{D}^{-1}\boldsymbol{y}\|^2 < 1\}$. Consider the function $\lambda : \mathbb{R}^3 \setminus \mathcal{E} \to \mathbb{R}_0^+$ defined as

$$\frac{y_1^2}{d_1^2 + \lambda(\boldsymbol{y})} + \frac{y_2^2}{d_2^2 + \lambda(\boldsymbol{y})} + \frac{y_3^2}{d_3^2 + \lambda(\boldsymbol{y})} = 1 \tag{B.5a}$$

whose existence and regularity are guaranteed by the implicit function theorem. The formulation of solutions for the Stokes problems in $\mathbb{R}^3 \setminus \mathcal{E}$ are based on the following geometry associated functions

$$\delta(\lambda) = \det(\mathbf{D}_\lambda)^{1/2}, \quad \chi(\lambda) = \int_\lambda^\infty \delta(s)^{-1}\,\mathrm{d}s, \quad \alpha_j(\lambda) = \int_\lambda^\infty (d_j^2 + s)^{-1}\delta(s)^{-1}\,\mathrm{d}s,$$

$$\beta_j(\lambda) = \int_\lambda^\infty (d_j^2 + s)\delta(s)^{-3}\,\mathrm{d}s, \quad \gamma_j(\lambda) = \int_\lambda^\infty (d_j^2 + s)s\delta(s)^{-3}\,\mathrm{d}s \tag{B.5b}$$

for $j = 1, 2, 3$, with $\mathbf{D}_\lambda = \mathbf{D}_\lambda(\lambda) = \mathrm{diag}(d_i^2 + \lambda, i = 1, 2, 3)$. When $\alpha_j, \beta_j, \gamma_j$ and χ are evaluated at zero, we abbreviate the function value with the index ^{o}, e.g. $\chi^o = \int_0^\infty \delta(s)^{-1}\,\mathrm{d}s$. Additionally, we introduce $\psi_j(\boldsymbol{y}) = \beta_j(\lambda(\boldsymbol{y}))y_k y_\ell$, where (j, k, ℓ) is a permutation of $(1, 2, 3)$, and $\omega(\boldsymbol{y}) = \int_{\lambda(\boldsymbol{y})}^\infty \delta(s)^{-1}f_{el}(\boldsymbol{y}, s)\,\mathrm{d}s$, where $f_{el}(\boldsymbol{y}, \lambda) = \boldsymbol{y} \cdot \mathbf{D}_\lambda^{-1} \cdot \boldsymbol{y} - 1$. In the following some derivatives of the above functions are needed. We set $\mu(\boldsymbol{y}, \lambda) = (\boldsymbol{y} \cdot \mathbf{D}_\lambda^{-2} \cdot \boldsymbol{y})^{-1}$, in other words $\partial_\lambda f_{el} = -\mu^{-1}$. It follows for $\boldsymbol{y} \in \mathbb{R}^3 \setminus \mathcal{E}$

$$\partial_{\boldsymbol{y}}\chi(\lambda(\boldsymbol{y})) = -2\frac{\mu}{\delta}\boldsymbol{y} \cdot \mathbf{D}_\lambda^{-1}, \qquad\qquad \partial_{\boldsymbol{y}}\omega = 2\boldsymbol{y} \cdot \mathrm{diag}(\alpha_1, \alpha_2, \alpha_3), \tag{B.6a}$$

$$\partial_{\boldsymbol{y}\boldsymbol{y}}\chi(\lambda(\boldsymbol{y})) = -2\frac{\mu}{\delta}\left(\mathbf{D}_\lambda^{-1} - 2\mu\left(\mathbf{D}_\lambda^{-2} \cdot \boldsymbol{y} \otimes \mathbf{D}_\lambda^{-1} \cdot \boldsymbol{y} + \mathbf{D}_\lambda^{-1} \cdot \boldsymbol{y} \otimes \mathbf{D}_\lambda^{-2} \cdot \boldsymbol{y}\right)\right) \tag{B.6b}$$

$$-2\frac{\mu^2}{\delta}\left(-\mathrm{tr}(\mathbf{D}_\lambda^{-1}) + 4\mu\boldsymbol{y} \cdot \mathbf{D}_\lambda^{-3} \cdot \boldsymbol{y})\mathbf{D}_\lambda^{-1} \cdot \boldsymbol{y} \otimes \mathbf{D}_\lambda^{-1} \cdot \boldsymbol{y}\right),$$

$$\partial_{\boldsymbol{y}\boldsymbol{y}}\omega = 2\,\mathrm{diag}(\alpha_1, \alpha_2, \alpha_3) - 4\frac{\mu}{\delta}\left(\mathbf{D}_\lambda^{-1} \cdot \boldsymbol{y} \otimes \mathbf{D}_\lambda^{-1} \cdot \boldsymbol{y}\right), \tag{B.6c}$$

$$\partial_{y_i y_j y_k}\omega = -4\frac{\mu}{\delta}\left(\frac{\delta_{jk}y_i}{(d_i^2 + \lambda)(d_j^2 + \lambda)} + \frac{\delta_{ij}y_k + \delta_{ik}y_j}{(d_j^2 + \lambda)(d_k^2 + \lambda)}\right) \tag{B.6d}$$

$$+8\frac{\mu^2}{\delta}\frac{y_i y_j y_k\left(\sum_{\ell \in \{i,j,k\}}(d_\ell^2 + \lambda)^{-1} + 0.5\,\mathrm{tr}(\mathbf{D}_\lambda^{-1}) - 2\mu\boldsymbol{y} \cdot \mathbf{D}_\lambda^{-3} \cdot \boldsymbol{y}\right)}{(d_i^2 + \lambda)(d_j^2 + \lambda)(d_k^2 + \lambda)}.$$

Let (i, j, k) be an even permutation of $(1, 2, 3)$, the derivatives of ψ_i read as:

$$\partial_{y_\ell}\psi_i = -2\frac{\mu}{\delta^3}(\mathbf{D}_\lambda)_{ii}(\mathbf{D}_\lambda^{-1} \cdot \boldsymbol{y})_\ell y_j y_k + \beta_i(\delta_{\ell j}y_k + \delta_{\ell k}y_j), \tag{B.6e}$$

$$\partial_{y_m y_\ell}\psi_i = \beta_i(\delta_{\ell j}\delta_{km} + \delta_{\ell k}\delta_{jm}) \tag{B.6f}$$

$$-2y_j y_k\frac{\mu}{\delta^3}\left(2\mu(\mathbf{D}_\lambda^{-1} \cdot \boldsymbol{y})_m(\mathbf{D}_\lambda^{-1} \cdot \boldsymbol{y})_\ell + (\mathbf{D}_\lambda)_{ii}(\mathbf{D}_\lambda^{-1})_{\ell m}\right)$$

$$-2\frac{\mu}{\delta^3}(\mathbf{D}_\lambda)_{ii}\left((\mathbf{D}_\lambda^{-1} \cdot \boldsymbol{y})_m(\delta_{\ell j}y_k + \delta_{\ell k}y_j) + (\mathbf{D}_\lambda^{-1} \cdot \boldsymbol{y})_\ell(\delta_{jm}y_k + \delta_{km}y_j)\right)$$

$$+4y_j y_k\frac{\mu^2}{\delta^3}(\mathbf{D}_\lambda)_{ii}\left((\mathbf{D}_\lambda^{-2} \cdot \boldsymbol{y})_\ell(\mathbf{D}_\lambda^{-1} \cdot \boldsymbol{y})_m + (\mathbf{D}_\lambda^{-2} \cdot \boldsymbol{y})_m(\mathbf{D}_\lambda^{-1} \cdot \boldsymbol{y})_\ell\right)$$

$$-2y_j y_k\frac{\mu^2}{\delta^3}(\mathbf{D}_\lambda)_{ii}(4\mu\boldsymbol{y} \cdot \mathbf{D}_\lambda^{-3} \cdot \boldsymbol{y} - 3\,\mathrm{tr}(\mathbf{D}_\lambda^{-1}))(\mathbf{D}_\lambda^{-1} \cdot \boldsymbol{y})_\ell(\mathbf{D}_\lambda^{-1} \cdot \boldsymbol{y})_m.$$

From (B.6b), (B.6c) and (B.6f) it follows

$$\Delta_{\boldsymbol{y}}\chi = -2\frac{\mu}{\delta}(\mathrm{tr}(\mathbf{D}_\lambda^{-1}) - 4\mu\boldsymbol{y} \cdot \mathbf{D}_\lambda^{-3} \cdot \boldsymbol{y} + (-\mathrm{tr}(\mathbf{D}_\lambda^{-1}) + 4\mu\boldsymbol{y} \cdot \mathbf{D}_\lambda^{-3} \cdot \boldsymbol{y})) = 0, \tag{B.7a}$$

$$\Delta_{\boldsymbol{y}}\psi_i = -4\frac{\mu}{\delta^3}(\mathbf{D}_\lambda)_{ii}y_jy_k(\operatorname{tr}(\mathbf{D}_\lambda^{-1}) - (\mathbf{D}_\lambda^{-1})_{ii}) - 2\frac{\mu}{\delta^3}y_jy_k(2 + (\mathbf{D}_\lambda)_{ii}\operatorname{tr}(\mathbf{D}_\lambda^{-1}))$$

$$+ 8\frac{\mu^2}{\delta^3}(\mathbf{D}_\lambda)_{ii}y_jy_k\boldsymbol{y}\cdot\mathbf{D}_\lambda^{-3}\cdot\boldsymbol{y} - 2\frac{\mu}{\delta^3}(\mathbf{D}_\lambda)_{ii}y_jy_k(4\mu\boldsymbol{y}\cdot\mathbf{D}_\lambda^{-3}\cdot\boldsymbol{y} - 3\operatorname{tr}(\mathbf{D}_\lambda^{-1}))$$

$$= 0, \tag{B.7b}$$

$$\Delta_{\boldsymbol{y}}\omega = -4\left(-\frac{1}{2}\int_{\lambda(\boldsymbol{y})}^\infty \frac{\operatorname{tr}(\mathbf{D}_s^{-1})}{\delta}\,\mathrm{d}s + \frac{1}{\delta}\right) = -4\left(\int_{\lambda(\boldsymbol{y})}^\infty \partial_s\frac{1}{\delta}\,\mathrm{d}s + \frac{1}{\delta}\right) = 0, \tag{B.7c}$$

since $\partial_\lambda\delta^{-1} = -0.5\delta^{-1}\operatorname{tr}(\mathbf{D}_\lambda^{-1})$ and $\lim_{s\to\infty}\delta^{-1} = 0$. This is an important feature of the functions, which will be used in Lemma B.11. Next, we present some asymptotic properties of these functions for $\|\boldsymbol{y}\| \to \infty$.

Lemma B.10 (Asymptotical properties). *The geometry associated functions defined in* (B.5) *fulfill the following properties for $r = \|\boldsymbol{y}\|$, $r \to \infty$:*

$$\lambda \sim r^2, \quad \alpha_i \sim \frac{2}{3}r^{-3}, \quad \beta_i \sim \frac{2}{5}r^{-5}, \quad \gamma_i \sim \frac{2}{3}r^{-3}, \quad \chi \sim 2r^{-1}, \quad \delta \sim r^3, \quad \mu \sim r^2,$$

where the notation $f \sim \phi$ stands for $f = \phi + o(\phi)$.

Proof. From the definition of $\lambda(\boldsymbol{y})$, it holds

$$1 = \boldsymbol{y}\cdot\mathbf{D}_\lambda^{-1}\cdot\boldsymbol{y} \begin{cases} \leq (\min_i d_i^2 + \lambda)^{-1}r^2 \\ \geq (\max_i d_i^2 + \lambda)^{-1}r^2 \end{cases},$$

and thus $0 \leq \min_i d_i^2 \leq r^2 - \lambda \leq \max_i d_i^2$, which implies

$$\lim_{r\to\infty}\frac{r^2 - \lambda}{r^2} = 0.$$

Set $\hat{d} = \max_i d_i$, then the behavior of the algebraic functions δ and μ results as

$$\frac{\delta - r^3}{r^3} \leq r^{-3}\left((\hat{d}^2 + \lambda)^{3/2} - r^3\right) = \left(\frac{\hat{d}^2}{r^2} + \frac{\lambda}{r^2}\right)^{3/2} - 1 \to 0,$$

$$\frac{\mu - r^2}{r^2} \leq r^{-2}\left(\sum_i y_i^2/(\hat{d}^2 + \lambda)^2\right)^{-1} - 1 = r^{-4}(\hat{d}^2 + \lambda)^2 - 1 \to 0.$$

For the integral functions the following statement is used: Let $g : (0, \infty) \to \mathbb{R}^+$ be a continuous function with $\int_0^\infty g\,\mathrm{d}s < \infty$. Define $f(t, Q) = \int_t^Q g\,\mathrm{d}s$, then for any $Q \in \mathbb{R}^+$ it holds

$$f(\lambda(\boldsymbol{y}), Q) - f(r^2(\boldsymbol{y}), Q) = \int_{\lambda(\boldsymbol{y})}^{r^2(\boldsymbol{y})} g\,\mathrm{d}s \leq (r^2 - \lambda)\max_{s\in[\lambda, r^2]} g \leq \hat{d}^2\max_{s\in[\lambda, r^2]} g.$$

Since Q was arbitrary, this is still true for $Q \to \infty$. Another statement also needed is: Let $\alpha, a, s > 0$ then $1 - (a/s + 1)^{-\alpha} \leq \alpha a/s$. This can be directly concluded

from the fact that the function $f(s) = \alpha a/s + (a/s + 1)^{-\alpha}$ is strictly decreasing and $\lim_{s\to\infty} f = 1$. Consequently,

$$
\left| \frac{\chi - 2r^{-1}}{2r^{-1}} \right| \leq \frac{1}{2r^{-1}} \left| \int_{\lambda}^{r^2} \delta(s)^{-1} \, \mathrm{d}s \right| + \frac{1}{2r^{-1}} \left| \int_{r^2}^{\infty} \delta(s)^{-1} - s^{-3/2} \, \mathrm{d}s \right|
$$

$$
\leq \frac{\hat{d}^2}{2r^{-1}} \max_{s\in[\lambda,r^2]} \delta(s)^{-1} + \frac{1}{2r^{-1}} \int_{r^2}^{\infty} s^{-3/2} - \delta(s)^{-1} \, \mathrm{d}s
$$

$$
\leq \frac{\hat{d}^2 \lambda^{-3/2}}{2r^{-1}} + \frac{1}{2r^{-1}} \int_{r^2}^{\infty} s^{-3/2} \left(1 - \left(\hat{d}^2 s^{-1} + 1 \right)^{-3/2} \right) \, \mathrm{d}s
$$

$$
\leq \frac{\hat{d}^2}{2} r^{-2} \left(\frac{\lambda}{r^2} \right)^{-3/2} + \frac{1}{2r^{-1}} \int_{r^2}^{\infty} s^{-3/2} \frac{3}{2} \hat{d}^2 s^{-1} \, \mathrm{d}s
$$

$$
= \frac{\hat{d}^2}{2} \left(r^{-2} \left(\frac{\lambda}{r^2} \right)^{-3/2} + r^{-2} \right) \to 0.
$$

The same steps lead to

$$
\left| \frac{\alpha_i - 2/3r^{-3}}{2/3r^{-3}} \right| \leq \frac{\hat{d}^2}{2/3} r^{-2} \left(\left(\frac{\lambda}{r^2} \right)^{-5/2} + 1 \right) \to 0,
$$

$$
\left| \frac{\beta_i - 2/5r^{-5}}{2/5r^{-5}} \right| \leq \frac{\hat{d}^2}{2/5} r^{-2} \left(\left(\frac{\lambda}{r^2} \right)^{-7/2} + 1 \right) \to 0,
$$

$$
\left| \frac{\gamma_i - 2/3r^{-3}}{2/3r^{-3}} \right| \leq \frac{\hat{d}^2}{2/3} r^{-2} \left(\left(\frac{\lambda}{r^2} \right)^{-5/2} + \frac{7}{5} \right) \to 0.
$$

$\square$

We summarize some results of [40, 70, 96] for the disturbance flow of an ellipsoid in a Stokes flow in Lemma B.11.

Lemma B.11 (Oberbeck and Jeffery solutions)**.** *Consider an ellipsoid with its geometry associated functions. Let $\boldsymbol{v} \in \mathbb{R}^3, \mathbf{A} \in \mathbb{R}^{3\times 3}$ be a constant vector, respectively matrix, where $\mathrm{tr}(\mathbf{A}) = 0$. Define*

$$
\boldsymbol{u}_{Ob} = (\chi \mathbf{I} - \nabla_{\boldsymbol{y}}\chi \otimes \boldsymbol{y} + 0.5\partial_{\boldsymbol{yy}}\omega \cdot \mathbf{D}^2) \cdot \mathbf{O} \cdot \boldsymbol{v}, \tag{B.8}
$$

$$
\boldsymbol{u}_{Je} = \begin{bmatrix} \partial_{y_1}\psi_1 & \partial_{y_1}\psi_2 & \partial_{y_1}\psi_3 \\ \partial_{y_2}\psi_1 & \partial_{y_2}\psi_2 & \partial_{y_2}\psi_3 \\ \partial_{y_3}\psi_1 & \partial_{y_3}\psi_2 & \partial_{y_3}\psi_3 \end{bmatrix} \cdot \begin{pmatrix} R \\ S \\ T \end{pmatrix} + \nabla_{\boldsymbol{y}} \times \begin{pmatrix} U\psi_1 \\ V\psi_2 \\ W\psi_3 \end{pmatrix}
$$

$$
+ \partial_{\boldsymbol{yy}}\omega \cdot \mathbf{M}^T \cdot \boldsymbol{y} - \mathbf{M} \cdot \nabla_{\boldsymbol{y}}\omega, \tag{B.9}
$$

as well as $p_{Ob} = -2\nabla_{\boldsymbol{y}}\chi \cdot \mathbf{O} \cdot \boldsymbol{v}$ and $p_{Je} = 2\mathbf{M} : \partial_{\boldsymbol{yy}}\omega$ with the matrices

$$
\mathbf{O} = \mathrm{diag}(\chi^o + d_i^2 \alpha_i^o, i = 1, 2, 3)^{-1}, \qquad \mathbf{M} = \begin{bmatrix} A & H & G^\star \\ H^\star & B & F \\ G & F^\star & C \end{bmatrix}
$$

and the corresponding coefficients given by

$$
A = -\frac{2\gamma_1^o A_{11} - \gamma_2^o A_{22} - \gamma_3^o A_{33}}{6(\gamma_2^o \gamma_3^o + \gamma_1^o \gamma_3^o + \gamma_1^o \gamma_2^o)},
$$

183

$$B = -\frac{2\gamma_2^o A_{22} - \gamma_3^o A_{33} - \gamma_1^o A_{11}}{6(\gamma_2^o \gamma_3^o + \gamma_1^o \gamma_3^o + \gamma_1^o \gamma_2^o)},$$

$$C = -\frac{2\gamma_3^o A_{33} - \gamma_1^o A_{11} - \gamma_2^o A_{22}}{6(\gamma_2^o \gamma_3^o + \gamma_1^o \gamma_3^o + \gamma_1^o \gamma_2^o)},$$

$$F = -\frac{\alpha_2^o(A_{23} + A_{32})/2 - d_3^2 \beta_1^o(A_{32} - A_{23})/2}{2\beta_1^o(d_2^2 \alpha_2^o + d_3^2 \alpha_3^o)},$$

$$F^\star = -\frac{\alpha_3^o(A_{23} + A_{32})/2 + d_2^2 \beta_1^o(A_{32} - A_{23})/2}{2\beta_1^o(d_2^2 \alpha_2^o + d_3^2 \alpha_3^o)},$$

$$G = -\frac{\alpha_3^o(A_{13} + A_{31})/2 - d_1^2 \beta_2^o(A_{13} - A_{31})/2}{2\beta_2^o(d_3^2 \alpha_3^o + d_1^2 \alpha_1^o)},$$

$$G^\star = -\frac{\alpha_1^o(A_{13} + A_{31})/2 + d_3^2 \beta_2^o(A_{13} - A_{31})/2}{2\beta_2^o(d_3^2 \alpha_3^o + d_1^2 \alpha_1^o)},$$

$$H = -\frac{\alpha_1^o(A_{12} + A_{21})/2 - d_2^2 \beta_3^o(A_{21} - A_{12})/2}{2\beta_3^o(d_1^2 \alpha_1^o + d_2^2 \alpha_2^o)},$$

$$H^\star = -\frac{\alpha_2^o(A_{12} + A_{21})/2 + d_1^2 \beta_3^o(A_{21} - A_{12})/2}{2\beta_3^o(d_1^2 \alpha_1^o + d_2^2 \alpha_2^o)}$$

$$R = (A_{23} + A_{32})/(2\beta_1^o), \quad S = (A_{13} + A_{31})/(2\beta_2^o), \quad T = (A_{12} + A_{21})/(2\beta_3^o),$$
$$U = 2d_2^2 B - 2d_3^2 C, \quad V = 2d_3^2 C - 2d_1^2 A, \quad W = 2d_1^2 A - 2d_2^2 B.$$

Then $(\boldsymbol{u}, p) \in \{(\boldsymbol{u}_{Ob}, p_{Ob}), (\boldsymbol{u}_{Je}, p_{Je})\}$ *is a solution of*

$$\nabla_{\boldsymbol{y}} \cdot \mathbf{S}[\boldsymbol{u}]^T = \boldsymbol{0}, \qquad \nabla_{\boldsymbol{y}} \cdot \boldsymbol{u} = 0, \qquad \boldsymbol{y} \in \mathbb{R}^3 \setminus \mathcal{E},$$
$$\boldsymbol{u} = \boldsymbol{h}, \qquad \boldsymbol{y} \in \partial\mathcal{E},$$
$$\boldsymbol{u} \to \boldsymbol{0}, \qquad \|\boldsymbol{y}\| \to \infty,$$

with the decay properties $\|\boldsymbol{u}\| \leq c\|\boldsymbol{y}\|^{-1}$ *and* $\|\nabla_{\boldsymbol{y}} \boldsymbol{u}\|, |p| \leq \hat{c}\|\boldsymbol{y}\|^{-2}$, $c, \hat{c} \geq 0$. *The Dirichlet condition reads as* $\boldsymbol{h} = \boldsymbol{v}$ *for* $\boldsymbol{u} = \boldsymbol{u}_{Ob}$ *and* $\boldsymbol{h} = \mathbf{A} \cdot \boldsymbol{y}$ *for* $\boldsymbol{u} = \boldsymbol{u}_{Je}$.

Proof. The proof of this lemma can be found in [96] for the translational boundary condition and in [70] for the linear one. For the sake of completeness, we show the relevant steps here. First, using $0 = \Delta_{\boldsymbol{y}} \chi = \Delta_{\boldsymbol{y}} \omega = \Delta_{\boldsymbol{y}} \psi_j$ from (B.7) implies

$$\nabla_{\boldsymbol{y}} \cdot \boldsymbol{u}_{Ob} = \left(\nabla_{\boldsymbol{y}} \chi - \nabla_{\boldsymbol{y}} \chi - \boldsymbol{y} \Delta_{\boldsymbol{y}} \chi + 0.5\nabla_{\boldsymbol{y}} \Delta_{\boldsymbol{y}} \omega \cdot \mathbf{D}^2\right) \cdot \mathbf{O} \cdot \boldsymbol{v} = 0,$$
$$\nabla_{\boldsymbol{y}} \cdot \boldsymbol{u}_{Je} = \sum_j \Delta_{\boldsymbol{y}} \psi_j a_j^R + \nabla_{\boldsymbol{y}} \Delta_{\boldsymbol{y}} \omega \cdot \mathbf{M}^T \cdot \boldsymbol{y} + \mathbf{M} : \partial_{\boldsymbol{yy}} \omega - \mathbf{M} : \partial_{\boldsymbol{yy}} \omega = 0.$$

by means of the identity $\nabla \cdot \nabla \times \boldsymbol{w} = 0$ for any vector $\boldsymbol{w}$. Here, $\boldsymbol{a}^R = (R, S, T)^T$. Moreover,

$$\Delta_{\boldsymbol{y}} \boldsymbol{u}_{Ob} = \left(\Delta_{\boldsymbol{y}} \chi \mathbf{I} - \nabla_{\boldsymbol{y}} \Delta_{\boldsymbol{y}} \chi \otimes \boldsymbol{y} - 2\partial_{\boldsymbol{yy}} \chi + 0.5\partial_{\boldsymbol{yy}} \Delta_{\boldsymbol{y}} \omega \cdot \mathbf{D}^2\right) \cdot \mathbf{O} \cdot \boldsymbol{v}$$
$$= \nabla_{\boldsymbol{y}}(-2\nabla_{\boldsymbol{y}} \chi \cdot \mathbf{O} \cdot \boldsymbol{v}),$$
$$\Delta_{\boldsymbol{y}} \boldsymbol{u}_{Je} = \nabla_{\boldsymbol{y}} \sum_j \Delta_{\boldsymbol{y}} \psi_j a_j^R + \nabla_{\boldsymbol{y}} \times (U\Delta_{\boldsymbol{y}} \psi_1, V\Delta_{\boldsymbol{y}} \psi_2, W\Delta_{\boldsymbol{y}} \psi_3)^T + \partial_{\boldsymbol{yy}} \Delta_{\boldsymbol{y}} \omega \cdot \mathbf{M}^T \cdot \boldsymbol{y}$$
$$+ 2\nabla_{\boldsymbol{y}} \partial_{\boldsymbol{yy}} \omega : \mathbf{M}^T - \mathbf{M} \cdot \nabla_{\boldsymbol{y}} \Delta_{\boldsymbol{y}} \omega = \nabla_{\boldsymbol{y}}(2\partial_{\boldsymbol{yy}} \omega : \mathbf{M}).$$

The matrices $\mathbf{O}$, $\mathbf{A}$ and the coefficients $R, \ldots, W$ are chosen in a way such that the boundary conditions on $\partial\mathcal{E}$ hold:

$$\boldsymbol{u}_{Ob} = \left(\chi^o\mathbf{I} + 2\frac{(\boldsymbol{y} \cdot \mathbf{D}^{-4} \cdot \boldsymbol{y})^{-1}}{\det(\mathbf{D})}\mathbf{D}^{-2} \cdot \boldsymbol{y} \otimes \boldsymbol{y},\right.$$

$$+ 0.5\left(2\operatorname{diag}(\alpha_i^o, i = 1, 2, 3) - 4\frac{(\boldsymbol{y} \cdot \mathbf{D}^{-4} \cdot \boldsymbol{y})^{-1}}{\det(\mathbf{D})}\mathbf{D}^{-2} \cdot \boldsymbol{y} \otimes \mathbf{D}^{-2} \cdot \boldsymbol{y}\right)\mathbf{D}^2\right) \cdot \mathbf{O} \cdot \boldsymbol{v}$$

$$= \left(\chi^o\mathbf{I} + \operatorname{diag}(\alpha_i^o, i = 1, 2, 3) \cdot \mathbf{D}^2\right) \cdot \operatorname{diag}(\chi^o + d_i^2\alpha_i^o, i = 1, 2, 3)^{-1} \cdot \boldsymbol{v} = \boldsymbol{v},$$

analogously for $\boldsymbol{u}_{Je}$. Last, the decreasing properties for $r = \|\boldsymbol{y}\| \to \infty$ are shown. This follows from the definition of the velocities (B.8) and (B.9) as well as the corresponding pressures,

$$\|\boldsymbol{u}_{Ob}\| \le c(|\chi| + \|\partial_{\boldsymbol{y}}\chi\|r + \|\partial_{\boldsymbol{yy}}\omega\|), \qquad\qquad |p_{Ob}| \le c\|\partial_{\boldsymbol{y}}\chi\|,$$
$$\|\boldsymbol{u}_{Je}\| \le c(\max_k \|\partial_{\boldsymbol{y}}\psi_k\| + \|\partial_{\boldsymbol{yy}}\omega\|r + \|\partial_{\boldsymbol{y}}\omega\|), \qquad |p_{Je}| \le c\|\partial_{\boldsymbol{yy}}\omega\|,$$

$$\|\partial_{\boldsymbol{y}}\boldsymbol{u}_{Ob}\| \le c(\|\partial_{\boldsymbol{y}}\chi\| + \|\partial_{\boldsymbol{yy}}\chi\|r + \|\partial_{\boldsymbol{yyy}}\omega\|),$$
$$\|\partial_{\boldsymbol{y}}\boldsymbol{u}_{Je}\| \le c(\max_k \|\partial_{\boldsymbol{yy}}\psi_k\| + \|\partial_{\boldsymbol{yyy}}\omega\|r + \|\partial_{\boldsymbol{yy}}\omega\|),$$

with appropriate constants $c > 0$. For r sufficiently big, it is known from (B.6), Lemma B.10 that

$$|\chi| \le cr^{-1}, \qquad \|\partial_{\boldsymbol{y}}\chi\| \le cr^{-2}, \quad \|\partial_{\boldsymbol{yy}}\chi\| \le cr^{-3}, \qquad \|\partial_{\boldsymbol{y}}\omega\| \le cr^{-2}$$
$$\|\partial_{\boldsymbol{yy}}\omega\| \le cr^{-3}, \quad \|\partial_{\boldsymbol{yyy}}\omega\| \le cr^{-4}, \quad \|\partial_{\boldsymbol{y}}\psi_k\| \le cr^{-4}, \quad \|\partial_{\boldsymbol{yy}}\psi_k\| \le cr^{-5},$$

yielding the proposed decay properties:

$$\|\boldsymbol{u}_{Ob}\| \le cr^{-1}, \quad |p_{Ob}| \le cr^{-2}, \quad \|\partial_{\boldsymbol{y}}\boldsymbol{u}_{Ob}\| \le cr^{-2},$$
$$\|\boldsymbol{u}_{Je}\| \le cr^{-2}, \quad |p_{Je}| \le cr^{-3}, \quad \|\partial_{\boldsymbol{y}}\boldsymbol{u}_{Je}\| \le cr^{-3}.$$

$\qquad\qquad\qquad\qquad\qquad\qquad\qquad\qquad\qquad\qquad\qquad\qquad\qquad\qquad\qquad\qquad$ □

Determination of surface moments

For the solvability conditions (2.20) we provide the surface moments of an ellipsoid. Computing the Newtonian stresses of Oberbeck and Jeffery solutions for the Stokes problems (Lemma B.11) on $\partial\mathcal{E}$ yields

$$\mathbf{S}[\boldsymbol{u}_{Ob}](\boldsymbol{y}) = \frac{4\mu}{\delta}\left(-(\tilde{\boldsymbol{v}} \cdot \mathbf{D}^{-2} \cdot \boldsymbol{y})\mathbf{I} - \tilde{\boldsymbol{v}} \otimes \mathbf{D}^{-2} \cdot \boldsymbol{y} - \mathbf{D}^{-2} \cdot \boldsymbol{y} \otimes \tilde{\boldsymbol{v}}\right.$$

$$\left. + 2\mu(\tilde{\boldsymbol{v}} \cdot \mathbf{D}^{-2} \cdot \boldsymbol{y})\mathbf{D}^{-2} \cdot \boldsymbol{y} \otimes \mathbf{D}^{-2} \cdot \boldsymbol{y}\right),$$

$$\mathbf{S}[\boldsymbol{u}_{Je}](\boldsymbol{y}) = \mathbf{A} + \mathbf{A}^T - 16\frac{\mu^2}{\delta}(\boldsymbol{y} \cdot \mathbf{D}^{-2} \cdot \mathbf{M} \cdot \mathbf{D}^{-2} \cdot \boldsymbol{y})\mathbf{D}^{-2} \cdot \boldsymbol{y} \otimes \mathbf{D}^{-2} \cdot \boldsymbol{y}$$

$$+ \frac{8\mu}{\delta}\left(\mathbf{M} \cdot \mathbf{D}^{-2} \cdot \boldsymbol{y} \otimes \mathbf{D}^{-2} \cdot \boldsymbol{y} + \mathbf{D}^{-2} \cdot \boldsymbol{y} \otimes \mathbf{M} \cdot \mathbf{D}^{-2} \cdot \boldsymbol{y}\right)$$

$$- 4\mathbf{M} : (\operatorname{diag}(\alpha_1^o, \alpha_2^o, \alpha_3^o) - 2\frac{\mu}{\delta}\mathbf{D}^{-2} \cdot \boldsymbol{y} \otimes \mathbf{D}^{-2} \cdot \boldsymbol{y})\mathbf{I},$$

where $\mu = (\boldsymbol{y} \cdot \mathbf{D}^{-4} \cdot \boldsymbol{y})^{-1}$, $\delta = \det(\mathbf{D})$ and $\tilde{\boldsymbol{v}} = \mathbf{O} \cdot \boldsymbol{v}$. For $\boldsymbol{z} \in \mathbb{S}_1^2$ the following identities hold:

$$\mathbf{S}[\boldsymbol{u}_{Ob}](\mathbf{D} \cdot \boldsymbol{z}) \cdot \mathbf{D}^{-1} \cdot \boldsymbol{z} = -\frac{4}{\delta} \tilde{\boldsymbol{v}}, \tag{B.10a}$$

$$\mathbf{S}[\boldsymbol{u}_{Je}](\mathbf{D} \cdot \boldsymbol{z}) \cdot \mathbf{D}^{-1} \cdot \boldsymbol{z} = \left(\mathbf{A} + \mathbf{A}^T + \frac{8}{\delta} \mathbf{M} - 4(\mathbf{M} : \mathrm{diag}(\alpha_i^o, i = 1, 2, 3)) \mathbf{I} \right) \cdot \mathbf{D}^{-1} \cdot \boldsymbol{z}.$$

The last result simplifies further, if $\mathbf{A}$ is skew-symmetric, i.e., $\mathbf{A} = B(\boldsymbol{v})$ for some $\boldsymbol{v} \in \mathbb{R}^3$. Then,

$$\mathbf{S}[\boldsymbol{u}_{Je}](\mathbf{D} \cdot \boldsymbol{z}) \cdot \mathbf{D}^{-1} \cdot \boldsymbol{z} = -\frac{4}{\delta} B(\mathrm{diag}(c_i, i = 1, 2, 3) \cdot \boldsymbol{v}) \cdot \mathbf{D} \cdot \boldsymbol{z}, \tag{B.10b}$$

with the constants $c_i = (d_j^2 \alpha_j^o + d_k^2 \alpha_k^o)^{-1}$, where (i, j, k) is a permutation of $(1, 2, 3)$.

To evaluate the integrals over the surface of an ellipsoid we transform them to the unit sphere. According to [71] it holds:

$$\int_{\partial \mathcal{E}} \mathbf{F}(\boldsymbol{y}) \cdot \boldsymbol{n}(\boldsymbol{y}) \mathrm{d}s(\boldsymbol{y}) = \int_{\partial \mathcal{E}} \mathbf{F}(\boldsymbol{y}) \cdot \frac{\mathbf{D}^{-2} \cdot \boldsymbol{y}}{\|\mathbf{D}^{-2} \cdot \boldsymbol{y}\|} \mathrm{d}s(\boldsymbol{y})$$

$$= \int_{\mathbb{S}_1^2} \mathbf{F}(\mathbf{D} \cdot \boldsymbol{z}) \cdot \frac{\mathbf{D}^{-1} \cdot \boldsymbol{z}}{\|\mathbf{D}^{-1} \cdot \boldsymbol{z}\|} \det(\mathbf{D}) \|\mathbf{D}^{-1} \cdot \boldsymbol{z}\| \mathrm{d}s(\boldsymbol{z})$$

$$= \delta \int_{\mathbb{S}_1^2} \mathbf{F}(\mathbf{D} \cdot \boldsymbol{z}) \cdot \mathbf{D}^{-1} \cdot \boldsymbol{z} \mathrm{d}s(\boldsymbol{z}), \tag{B.11}$$

for an integrable function $\mathbf{F} : \mathbb{R}^3 \to \mathbb{R}^3 \times \mathbb{R}^3$.

Now consider the six Stokes problems in Lemma 5. According to Lemma B.11 the analytical solutions $(\boldsymbol{w}_q, p_q)$ are given by (B.8) with $\boldsymbol{v} = \boldsymbol{e}_q$ for $q = 1, 2, 3$ and by (B.9) with $\mathbf{A} = 1/\sqrt{2} B(\boldsymbol{e}_{q-3})$ for $q = 4, 5, 6$. To calculate the surface moments $\boldsymbol{s}_q, \boldsymbol{t}_q, \mathbf{V}_q$ and W_q, we first apply the transformation to the unit sphere (B.11) and afterwards use (B.10a) or (B.10b) for the corresponding moments:

$$\boldsymbol{s}_q = \int_{\partial \mathcal{E}} B(\boldsymbol{y}) \cdot \mathbf{S}[\boldsymbol{w}_q] \cdot \boldsymbol{n} \, \mathrm{d}s(\boldsymbol{y}) \quad = -4 \int_{\mathbb{S}_1^2} B(\mathbf{D} \cdot \boldsymbol{z}) \cdot \boldsymbol{v}_q(\boldsymbol{z}) \mathrm{d}s(\boldsymbol{z}),$$

$$\boldsymbol{t}_q = \int_{\partial \mathcal{E}} \mathbf{S}[\boldsymbol{w}_q] \cdot \boldsymbol{n} \, \mathrm{d}s(\boldsymbol{y}) \quad = -4 \int_{\mathbb{S}_1^2} \boldsymbol{v}_q(\boldsymbol{z}) \mathrm{d}s(\boldsymbol{z}),$$

$$(\mathbf{V}_q)_{ij} = \left(\int_{\partial \mathcal{E}} y_i \mathbf{S}[\boldsymbol{w}_q] \cdot \boldsymbol{n} \, \mathrm{d}s(\boldsymbol{y}) \right)_j \quad = -4 \left(\int_{\mathbb{S}_1^2} (\mathbf{D} \cdot \boldsymbol{z})_i \boldsymbol{v}_q(\boldsymbol{z}) \mathrm{d}s(\boldsymbol{z}) \right)_j,$$

$$(W_q)_{ijk} = \left(\int_{\partial \mathcal{E}} y_i y_j \mathbf{S}[\boldsymbol{w}_q] \cdot \boldsymbol{n} \, \mathrm{d}s(\boldsymbol{y}) \right)_k = -4 \left(\int_{\mathbb{S}_1^2} (\mathbf{D} \cdot \boldsymbol{z})_i (\mathbf{D} \cdot \boldsymbol{z})_j \cdot \boldsymbol{v}_q(\boldsymbol{z}) \mathrm{d}s(\boldsymbol{z}) \right)_k,$$

with $\boldsymbol{v}_q = \mathbf{O} \cdot \boldsymbol{e}_q$ and $\boldsymbol{v}_{q+3} = c_q/\sqrt{2} B(\boldsymbol{e}_q) \cdot \mathbf{D} \cdot \boldsymbol{z}$ for $q = 1, 2, 3$. Since the integral of a homogeneous polynomial $p(\boldsymbol{z})$ fulfills $\int_{\mathbb{S}_1^2} p(\boldsymbol{z}) \mathrm{d}s(\boldsymbol{z}) = 0$ if p has odd degree, it follows

$$\boldsymbol{s}_q = \mathbf{0}, \qquad \mathbf{V}_q = \mathbf{0}, \qquad \text{for } q = 1, 2, 3,$$
$$\boldsymbol{t}_q = \mathbf{0}, \qquad W_q = 0, \qquad \text{for } q = 4, 5, 6.$$

The other moments follow, considering $\int_{\mathbb{S}_1^2}(\mathbf{D}\cdot\boldsymbol{z})_i(\mathbf{D}\cdot\boldsymbol{z})_j\mathrm{d}s = (\mathbf{D}^2)_{ij}4\pi/3$ and $|\mathbb{S}_1^2| = 4\pi$,

$$
\begin{aligned}
(\boldsymbol{s}_{q+3})_k &= -\frac{16\pi}{3\sqrt{2}}\sum_{i,j,\ell,m}(c_q\boldsymbol{e}_q)_\ell\epsilon_{jki}\epsilon_{j\ell m}(\mathbf{D}^2)_{im}\\
&= -\frac{16\pi}{3\sqrt{2}}\sum_{i\ell m}(c_q\boldsymbol{e}_q)_\ell(\delta_{k\ell}\delta_{im} - \delta_{km}\delta_{i\ell})(\mathbf{D}^2)_{im}\\
&= c_q\frac{16\pi}{3\sqrt{2}}\left((\mathbf{D}^2 - \mathrm{tr}(\mathbf{D}^2)\mathbf{I})\cdot\boldsymbol{e}_q\right)_k\\
&= \zeta_{q+3}|\mathcal{E}|\left((\mathbf{D}^2 - \mathrm{tr}(\mathbf{D}^2)\mathbf{I})\cdot\boldsymbol{e}_q\right)_k,\\
(\mathbf{V}_{q+3})_{ij} &= -\frac{16\pi}{3\sqrt{2}}\sum_{k,\ell}(\mathbf{D}^2)_{i\ell}\epsilon_{k\ell j}(c_q\boldsymbol{e}_q)_k = c_q\frac{16\pi}{3\sqrt{2}}(\mathbf{D}^2\cdot B(\boldsymbol{e}_q))_{ij}\\
&= \zeta_{q+3}|\mathcal{E}|(\mathbf{D}^2\cdot B(\boldsymbol{e}_q))_{ij},\\
\boldsymbol{t}_q &= -16\pi\mathbf{O}\cdot\boldsymbol{e}_q = 3\zeta_q|\mathcal{E}|\boldsymbol{e}_q,\\
(W_q)_{ijk} &= -\frac{16\pi}{3}\mathbf{D}_{ij}^2(\mathbf{O}\cdot\boldsymbol{e}_q)_k = \zeta_q|\mathcal{E}|(\mathbf{D}^2\otimes\boldsymbol{e}_q)_{ijk},
\end{aligned}
$$

for $q = 1,2,3$, where $\zeta_q = -4\det(\mathbf{D})^{-1}O_{qq}$ and $\zeta_{q+3} = 4\det(\mathbf{D})^{-1}c_q/\sqrt{2}$, with $\mathbf{O}$ given in Lemma B.11 and the constants $c_i = (d_j^2\alpha_j^o + d_k^2\alpha_k^o)^{-1}$, here (i,j,k) is a permutation of $(1,2,3)$.

C Additional simulation data

C.1 Predictor-corrector schemes

In order to complement the numerical observations of Sec. 4.5.4 we provide additional simulation data to for the behavior of the estimators. In particular, Fig. C.1 and Fig. C.2 show the average $\mathcal{L}^2$ distances between the estimated component and the actual solution by the IEGGL scheme for the benchmark scenario of Sec. 4.5.4 in cases $\beta \in \{0.4, 0.6\}$.
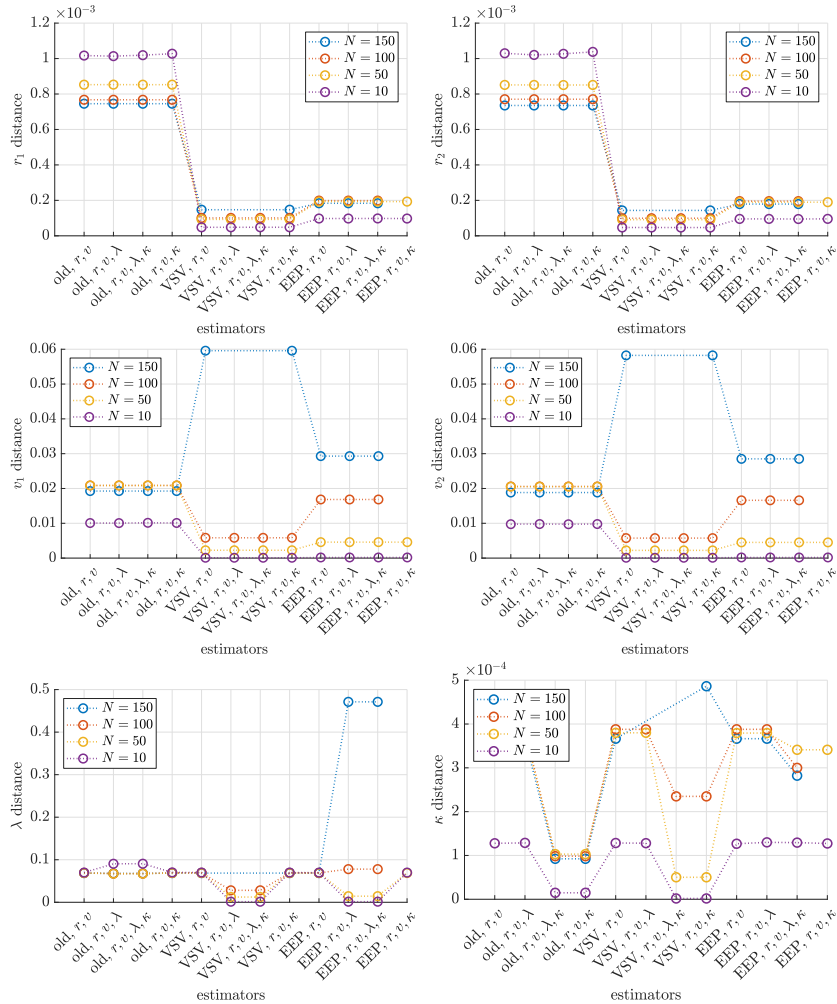

Figure C.1.: Average $\mathcal{L}^2([0, L])$ distance between y and y_{est} for $y \in \{r_1, r_2, v_1, v_2, \lambda, \kappa\}$, $\beta = 0.4$.
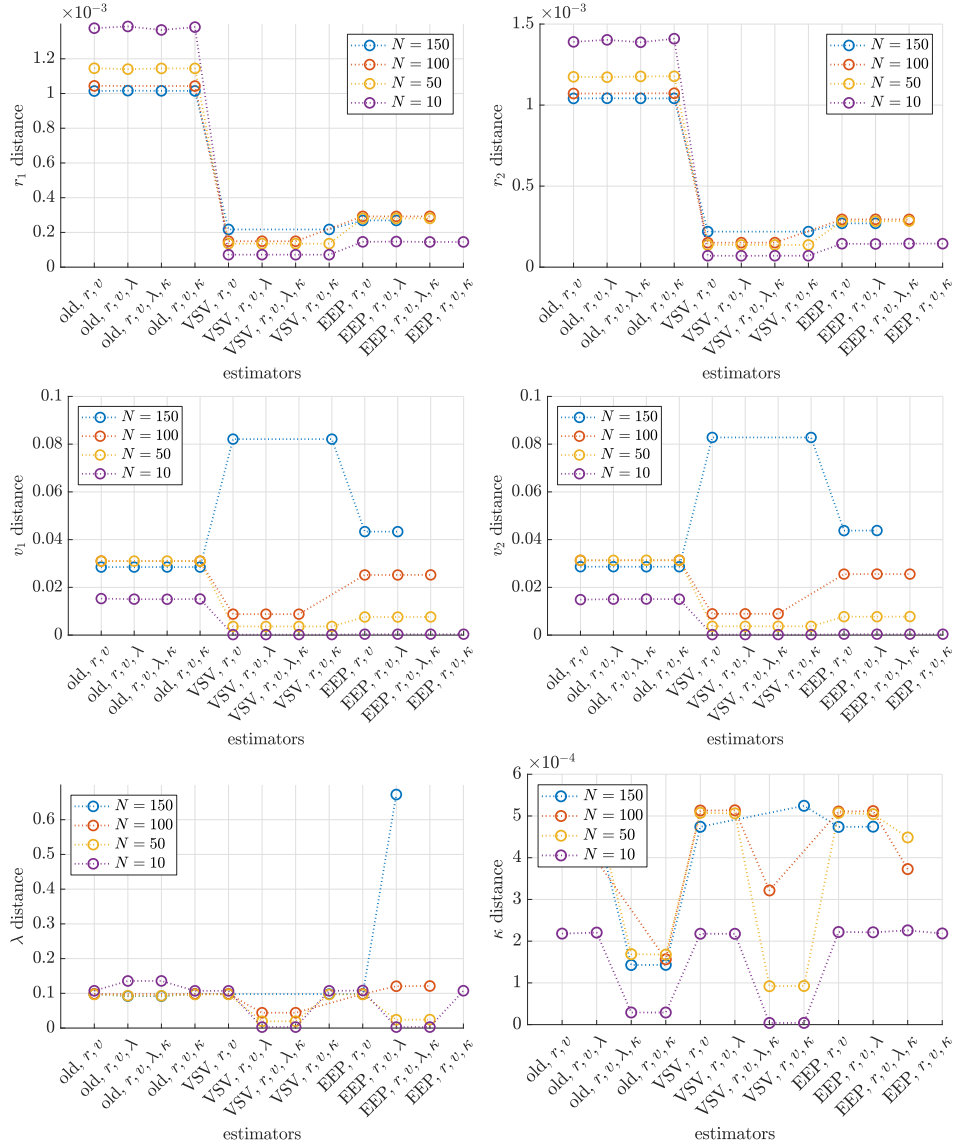
Figure C.2.: Average $([0, L])$ distance between y and y_{est} for $y \in \{r_1, r_2, v_1, v_2, \lambda, \kappa\}$, $\beta = 0.6$.

C.2 Smoothing techniques

In case of the study of smoothing techniques of Sec. 4.5.5, we provide an additional convergence study for $N = 128$ in Fig. C.3 as well as the behavior of the Lagrangian multipliers in Fig. C.4 and Fig. C.5 for $N = 32$ and $N = 128$, respectively. Furthermore, Fig. C.6 shows the relative distances of the dynamic components with respect to the stochastic solution for $N = 128$. The distances of the Lagrangian multipliers with respect to the stochastic solution are presented in Fig. C.7 and Fig. C.8 for $N = 32$ resp. $N = 128$.

The tables Tab. C.1 and Tab. C.2 show the relative distance between the expectation generated by the regularized stochastic field and the one generated by the white noise. Additionally, the average number of Newton iterations needed in the simulation is shown.
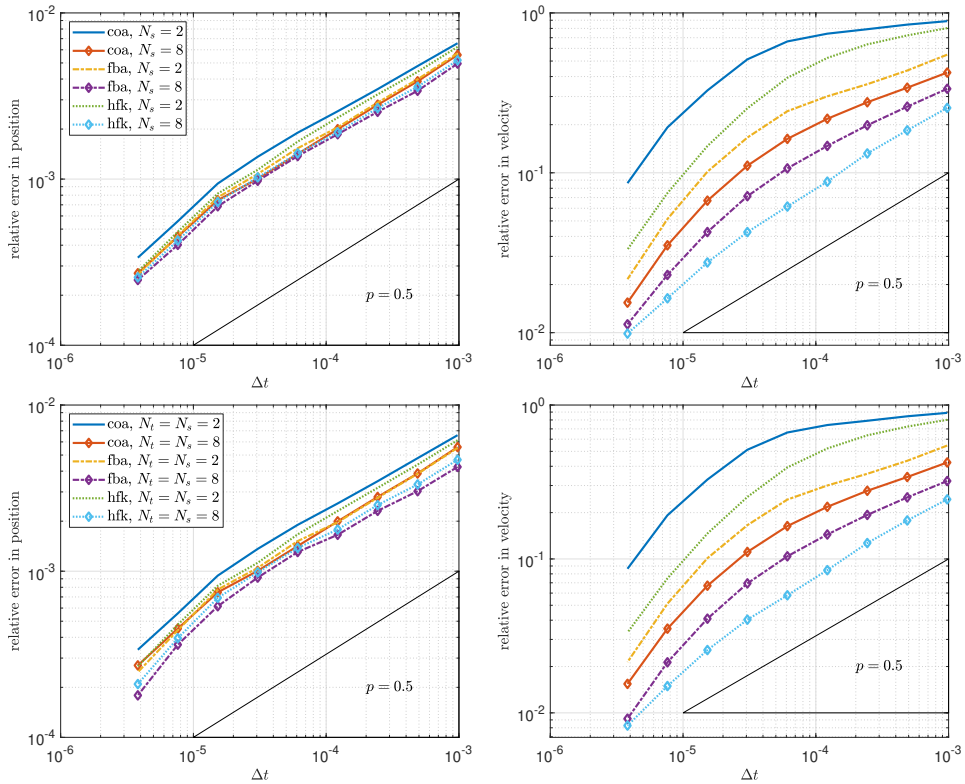

Figure C.3.: Relative error of the dynamic variables for $N = 128$. Left: r, right: v. Top: Smoothing in space, bottom smoothing in space and time.
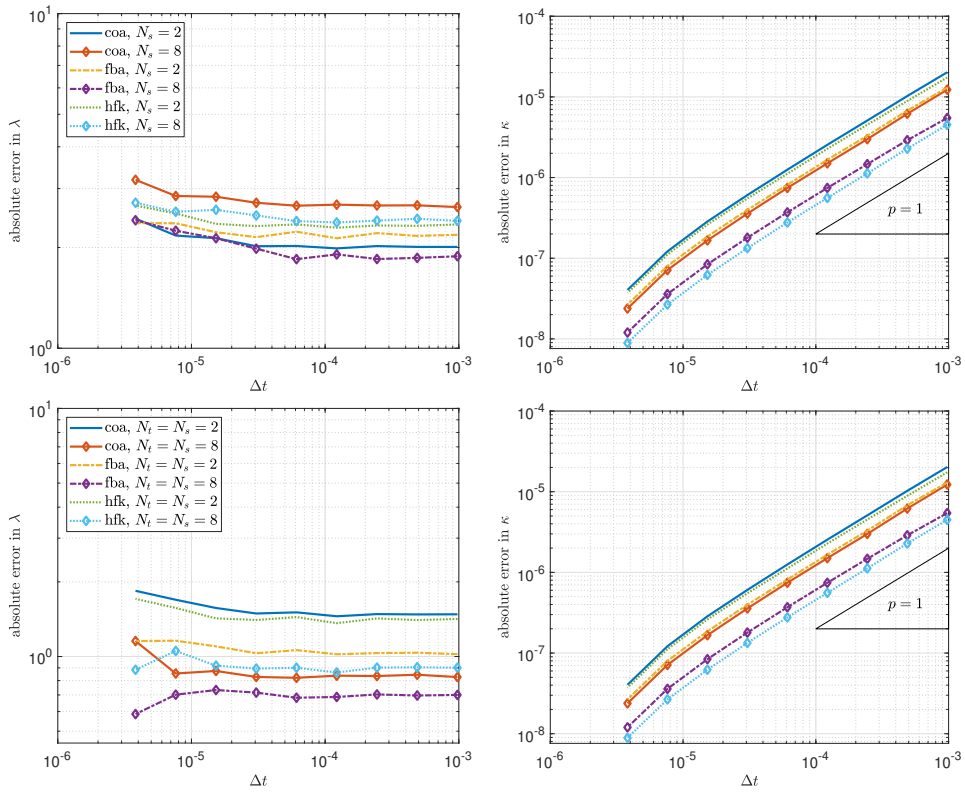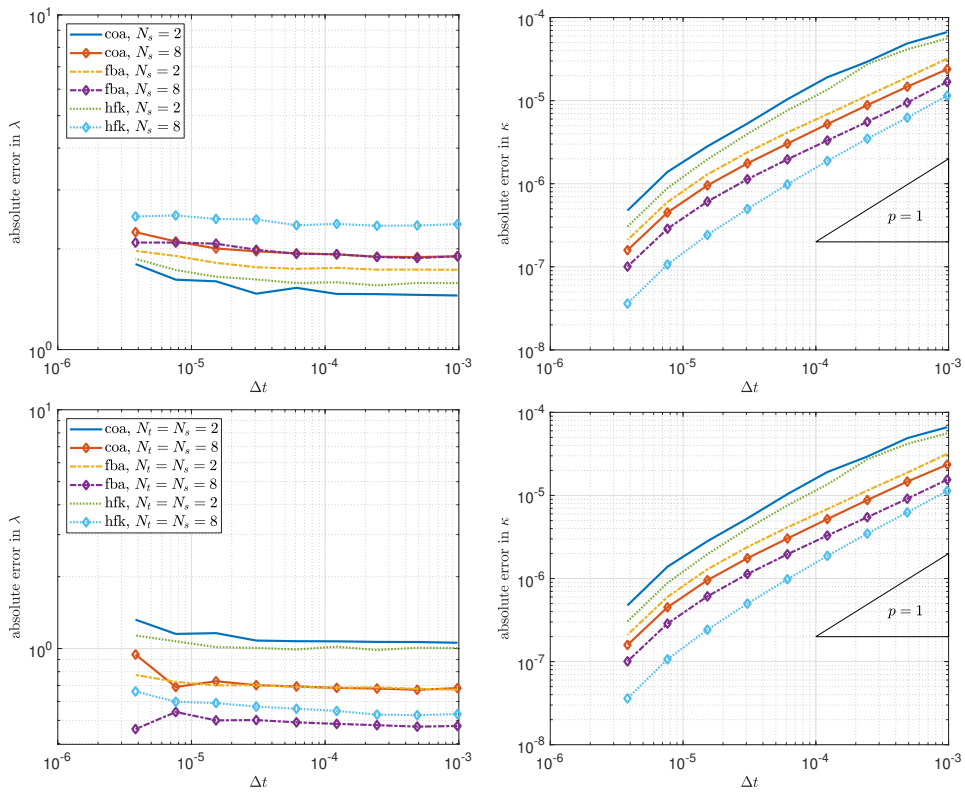
Figure C.4.: Absolute error of the algebraic variables for $N = 32$. Left: λ, right: κ. Top: Smoothing in space, bottom smoothing in space and time.

Figure C.5.: Absolute error of the algebraic variables for $N = 128$. Left: λ, right: κ. Top: Smoothing in space, bottom smoothing in space and time.
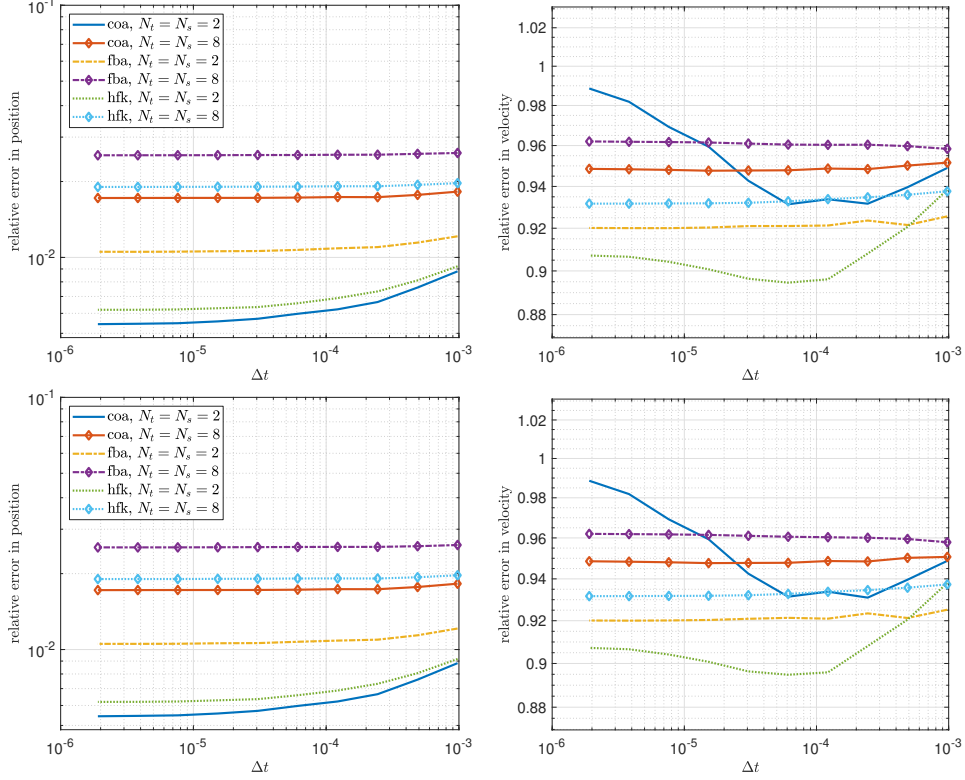
Figure C.6.: Relative error of the dynamic variables with respect to the stochastic solution for $N = 128$. Left: r, right: v. Top: Smoothing in space, bottom smoothing in space and time.

	Smoothing dim.	r	v	λ	κ	Newton-it.
$N = 10$	$1d$	29.79%	35.17%	49.20%	37.45%	2.99
$N = 10$	$2d$	29.79%	34.92%	50.68%	37.96%	2.99
$N = 50$	$1d$	4.09%	12.34%	57.77%	40.07%	4.22
$N = 50$	$2d$	4.16%	12.55%	68.79%	42.60%	4.24
$N = 100$	$1d$	1.55%	9.02%	42.20%	23.46%	4.98
$N = 100$	$2d$	1.79%	9.34%	43.10%	29.79%	4.89
$N = 150$	$1d$	0.48%	6.81%	34.64%	13.24%	5.01
$N = 150$	$2d$	0.80%	7.83%	38.12%	22.60%	4.95

Table C.1.: Relative $\mathcal{L}^2$-distance of solution components and average Newton-iterations for smoothing by convolution with hat functions for different space resolutions and smoothing dimensions. Simulation with $\beta = 0.4$, $T = 5$, $\Delta t = 10^{-2}$, $N_s = 2$ and $N_t = 2$ in the $2d$-case. Average Newton iterations without smoothing: 3.00, 5.06, 5.08, 5.01 for $N = 10$, $N = 50$, $N = 100$, $N = 150$ respectively.
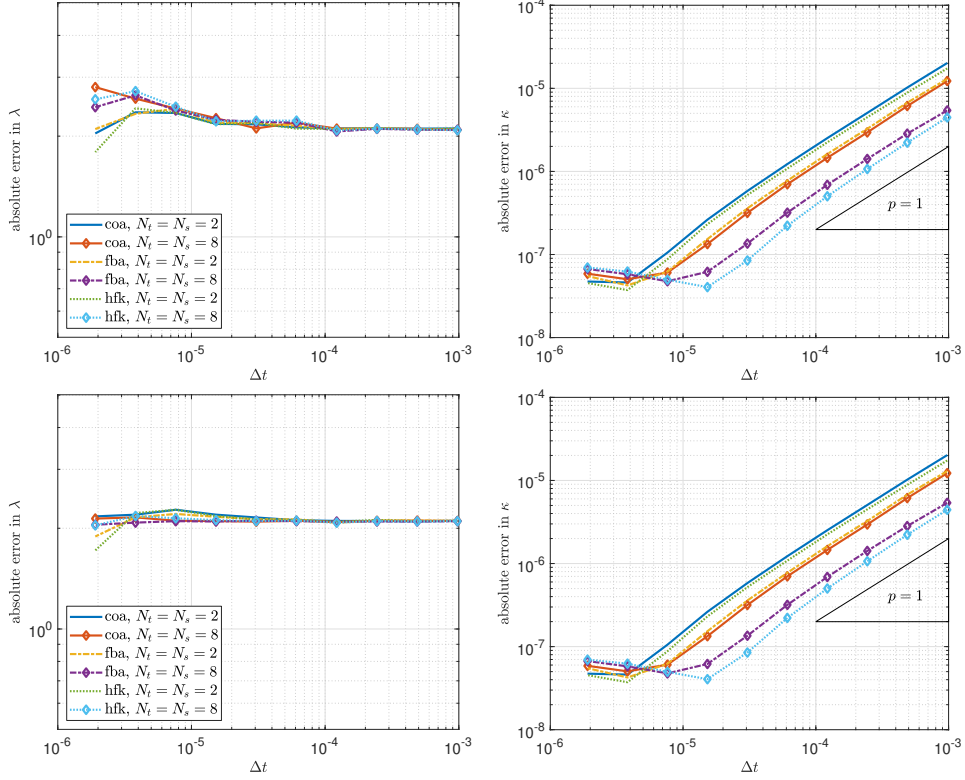
Figure C.7.: Absolute error of the algebraic variables with respect to the stochastic solution for $N = 32$. Left: λ, right: κ. Top: Smoothing in space, bottom smoothing in space and time.

	Smoothing dim.	r	v	λ	κ	Newton-it.
$N = 10$	$1d$	48.19%	26.59%	55.01%	36.94%	2.99
$N = 10$	$2d$	48.21%	26.52%	52.20%	37.78%	2.99
$N = 50$	$1d$	8.65%	13.20%	55.03%	37.06%	4.70
$N = 50$	$2d$	8.94%	12.82%	66.54%	37.39%	4.66
$N = 100$	$1d$	2.33%	13.40%	53.68%	24.89%	5.10
$N = 100$	$2d$	2.82%	12.98%	45.46%	31.70%	5.05
$N = 150$	$1d$	0.84%	10.93%	29.16%	13.95%	5.17
$N = 150$	$2d$	1.38%	9.99%	34.51%	24.40%	5.07

Table C.2.: Relative $\mathcal{L}^2$-distance of solution components and average Newton-iterations for smoothing by convolution with hat functions for different space resolutions and smoothing dimensions. Simulation with $\beta = 0.6$, $T = 5$, $\Delta t = 10^{-2}$, $N_s = 2$ and $N_t = 2$ in the $2d$-case. Average Newton iterations without smoothing: 3.00, 5.48, 5.83, 5.16 for $N = 10$, $N = 50$, $N = 100$, $N = 150$ respectively.
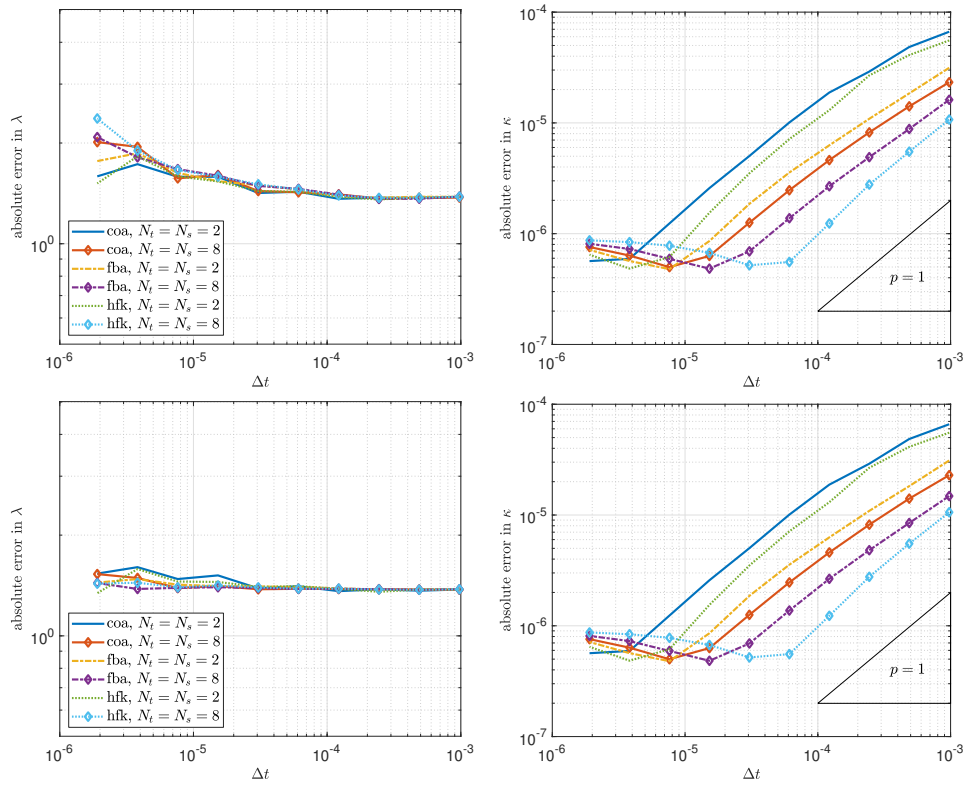
Figure C.8.: Absolute error of the algebraic variables with respect to the stochastic solution for $N = 128$. Left: λ, right: κ. Top: Smoothing in space, bottom smoothing in space and time.

Notation

The following notation was used throughout this work:

Sets, scalars, vectors, matrices and higher order tensors

$\mathbb{N}$ ($\mathbb{N}_0$)	Natural numbers, $\mathbb{N} = \{1, 2, \ldots\}$ (with zero)
$\mathbb{Z}$	Integer numbers, $\mathbb{Z} = \{\ldots, -2, -1, 0, 1, 2, \ldots\}$
$\mathbb{R}$ ($\mathbb{R}_0^+$)	Real numbers (positive real numbers with zero)
$\mathbb{R}^n$	n-dimensional real vector space
$\mathbb{R}^{n \times m}$	nm-dimensional real vector space of matrices with n rows and m columns
$\mathcal{E}$	Set, Class
$\partial \mathcal{E}$	Boundary of set $\mathcal{E}$
$\overline{\mathcal{E}}$	Closure of set $\mathcal{E}$
$\mathcal{B}(r, x), \mathcal{B}_r(x)$	Ball of radius r around point x
$\mathcal{B}_r, \mathcal{B}(r, 0)$	Ball of radius r around origin
$\mathbb{S}^k, \partial \mathcal{B}_1$	k-dimensional unit sphere
$\mathbb{S}_r^k$	k-dimensional sphere of radius r around origin
$x, \overline{x}, \hat{x}$	Scalar quantity, element of a set
$\boldsymbol{x}$	Element of $\mathbb{R}^3$
$\mathbf{X}$	Matrix in $\mathbb{R}^{3 \times 3}$
X	Higher order tensor

Indices, subscripts, superscripts

a_i	$a \in \mathbb{R}^n$	ith entry of vector a
$(\boldsymbol{a})_i = a_i$	$\boldsymbol{a} \in \mathbb{R}^3$	ith entry of $\boldsymbol{a} \in \mathbb{R}^3$
$M_{i,j} = M_{ij}$	$M \in \mathbb{R}^{n \times m}$	Element in ith row and jth column of matrix M
$(\mathbf{M})_{ij} = M_{ij}$	$\mathbf{M} \in \mathbb{R}^{3 \times 3}$	Element in ith row and jth column of matrix $\mathbf{M}$
$(a_i)_j$	$a_i \in \mathbb{R}^n$	jth entry of vector a_i
$(\boldsymbol{a}_i)_j$	$\boldsymbol{a}_i \in \mathbb{R}^3$	jth entry of vector a_i
$(\boldsymbol{a}_i^j)_k$	$\boldsymbol{a}_i^j \in \mathbb{R}^3$	kth entry of vector $\boldsymbol{a}_i^j$
$(E_i)_{jk}$	$E_i \in \mathbb{R}^{n \times m}$	Element in jth row and kth column of matrix E_i
$(\mathbf{E}_i)_{jk}$	$\mathbf{E}_i \in \mathbb{R}^{3 \times 3}$	Element in jth row and kth column of matrix $\mathbf{E}_i$

Declaration of vectors, matrices and vector/matrix families

$(a_1, \ldots, a_n)$	$a_i \in \mathbb{R}$	Declaration of vector $a \in \mathbb{R}^n$
$(a_i)_{i=1,\ldots,n}$	$a_i \in \mathbb{R}$	Declaration of vector $a \in \mathbb{R}^n$
$(a_i)_i$	$a_i \in \mathbb{R}$	Short notation for $(a_i)_{i=1,\ldots,n}$ if dimension is obvious from context
$(M_{ij})_{\substack{i=1,\ldots,n \\ j=1,\ldots,m}}$	$M_{ij} \in \mathbb{R}$	Declaration of matrix $M \in \mathbb{R}^{n \times m}$
$(M_{ij})_{ij}$	$M_{ij} \in \mathbb{R}$	Short version of $(M_{ij})_{\substack{i=1,\ldots,n \\ j=1,\ldots,m}}$ if dimensions are obvious from context
$\{v_1, \ldots, v_k\}$	$v_i \in \mathbb{R}^n$	Declaration of a subset of $\mathbb{R}^n$
$\{v_i\}_{i=1,\ldots,k}$	$v_i \in \mathbb{R}^n$	Alternative notation for $\{v_1, \ldots, v_k\}$
$\{v_i\}_i$	$v_i \in \mathbb{R}^n$	Short notation for $\{v_1, \ldots, v_k\}$ if number of elements is obvious from context

Operators

δ_{ij}	$i, j \in \mathbb{N}$	Kronecker delta, $\delta_{ij} = 1$ if and only if $i = j$
ϵ_{ijk}	$i, j, k \in \mathbb{N}$	Levi-Civita symbol:
		$\epsilon_{ijk} = 1$ if $(i, j, k) \in \{(1, 2, 3)\ ,\ (2, 3, 1)\ ,\ (3, 1, 2)\}$;
		$\epsilon_{ijk} = -1$ if $(i, j, k) \in \{(1, 3, 2)\ ,\ (2, 1, 3)\ ,\ (3, 2, 1)\}$;
		$\epsilon_{ijk} = 0$ if $i = j$, or $i = k$, or $j = k$
$a \cdot b$	$a, b \in \mathbb{R}^n$	Scalar product: $a \cdot b = \sum_{j=1}^{n} a_i b_i$
$a \otimes b$	$a, b \in \mathbb{R}^n$	Dyadic product: $(a \otimes b) \cdot c = (b \cdot c)a$ for any $c \in \mathbb{R}^n$
$\boldsymbol{a} \times \boldsymbol{b}$		
$A : B$	$A, B \in \mathbb{R}^{n \times m}$	Frobenius scalar product $A : B = \sum_{i=1}^{n} \sum_{j=1}^{m} A_{ij} B_{ij}$
$\mathcal{X}_1 \times \mathcal{X}_2$	$\mathcal{X}_1, \mathcal{X}_2$ sets	Cartesian product of two sets
$\prod_{i=1}^{n} \mathcal{X}_i$	$\mathcal{X}_i,\ i = 1, \ldots, n$ sets	Cartesian product of n sets
$A \cdot b$	$A \in \prod_{i=1}^{k} \mathbb{R}^{n_i}$, $b \in \mathbb{R}^{n_k}$	Application of linear mapping $A \cdot b \in \prod_{i=1}^{k-1} \mathbb{R}^{n_i}$
$b \cdot A$	$A \in \prod_{i=1}^{k} \mathbb{R}^{n_i}$, $b \in \mathbb{R}^{n_1}$	Application of linear mapping $b \cdot A \in \prod_{i=2}^{k} \mathbb{R}^{n_i}$
A^T	$A \in \mathbb{R}^{n \times m}$	Transpose of matrix A
$\mathrm{tr}(A)$	$A \in \mathbb{R}^{n \times n}$	Trace of matrix A
$\mathrm{adj}(A)$	$A \in \mathbb{R}^{n \times n}$	Transpose of cofactor matrix of matrix A
$\mathrm{diag}(v)$	$v \in \mathbb{R}^n$	Diagonal matrix with $(\mathrm{diag}(v))_{ij} = v_i$
$B(\boldsymbol{x})$	$\boldsymbol{x} \in \mathbb{R}^3$	Skew-symmetric matrix in $\mathbb{R}^{3 \times 3}$ fulfilling $B(\boldsymbol{x}) \cdot \boldsymbol{y} = \boldsymbol{x} \times \boldsymbol{y}$ for all $\boldsymbol{x}, \boldsymbol{y} \in \mathbb{R}^3$
$\mathrm{diam}(\mathcal{A})$	$\mathcal{A}$ domain	Diameter of $\mathcal{A}$
$f \in \mathcal{O}(g)$	$f, g : \mathbb{R}^n \to \mathbb{R}$	Landau notation for asymptotic behavior of functions as $x \to x_0$; there exist $C > 0, R > 0$, such that $\|f\| \leq C\|g\|$ for all $x \in \mathcal{B}_R(x_0)$
$f \in o(g)$	$f, g : \mathbb{R}^n \to \mathbb{R}$	Landau notation for asymptotic behavior of functions as $x \to x_0$; for any $C > 0$, there exists an $R > 0$, such that $\|f\| < C\|g\|$ for all $x \in \mathcal{B}_R(x_0)$

Differential operators

$\partial_{x_k} f$	$f : \mathbb{R}^n \to \mathbb{R}^m$	partial derivative with respect to x_k, $k \in \{1, \dots, n\}$
$\partial_x f$	$f : \mathbb{R}^n \to \mathbb{R}^m$	Jacobian of f, $\partial_x f \in \mathbb{R}^{m \times n}$
∇f	$f : \mathbb{R}^n \to \mathbb{R}^m$	Gradient of f, $\nabla f = \partial_x f^T \in \mathbb{R}^{n \times m}$; if $m = 1$, then $\nabla f = \partial_x f$
$\nabla_x f$	$f : \mathbb{R}^n \to \mathbb{R}^m$	Gradient of f with respect to variable x, used in order to emphasize the difference between local and global coordinates
$[a \cdot \nabla] f$	$f : \mathbb{R}^n \to \mathbb{R}^m$	Directional derivative of f in direction $a \in \mathbb{R}^n$, $[a \cdot \nabla] f = \partial_x f \cdot a$
$\partial_x^k f$	$f : \mathbb{R}^n \to \mathbb{R}$	kth order derivative of f with respect to x, $\partial_x^k f \in \prod_{i=1}^k \mathbb{R}^n$
$\underbrace{\partial_{x, \dots, x}}_{k \text{ times}} f$	$f : \mathbb{R}^n \to \mathbb{R}$	kth order derivative of f; used if k is small
$[A : \nabla^2] f$	$f : \mathbb{R}^n \to \mathbb{R}^m$, $A \in \mathbb{R}^{n \times n}$	$[A : \nabla^2] f = \sum_{i=1}^n \sum_{j=1}^n A_{ij} \partial_{x_i x_j} f$
$\nabla \cdot u$	$u : \mathbb{R}^n \to \mathbb{R}^n$	Divergence of vector field u, $\nabla \cdot u = \sum_i \partial_{x_i} u_i$
$\mathbf{S}[\boldsymbol{u}]$	$\boldsymbol{u} : \mathbb{R}^3 \to \mathbb{R}^3$	Newtonian stress tensor of solenoidal velocity field $\boldsymbol{u}$ and associated pressure p
$\mathbf{E}[\boldsymbol{u}]$	$\boldsymbol{u} : \mathbb{R}^3 \to \mathbb{R}^3$	Symmetric deformation gradient of $\boldsymbol{u}$, $\mathbf{E}[\boldsymbol{u}] = 0.5(\nabla \boldsymbol{u} + \nabla \boldsymbol{u}^T)$
$\mathrm{D}_t f$	$f : \mathbb{R}^{n+1} \to \mathbb{R}^n$	Material derivative of f, $\mathrm{D}_t f = \partial_t f + [f \cdot \nabla] f$
Δf	$f : \mathbb{R}^n \to \mathbb{R}^n$	Laplacian of f, $\Delta f = \sum_i \partial_{x_i x_i} f$
$\mathcal{L}[M]_G(f)$	$M \in \mathfrak{g}$, $G \in \mathcal{G}$, $f : \mathcal{G} \to \mathbb{R}$	Left Lie derivative for differentiable function f over Lie group $\mathcal{G}$ with Lie algebra $\mathfrak{g}$ at point $G \in \mathcal{G}$
$\mathcal{R}[M]_G(f)$	$M \in \mathfrak{g}$, $G \in \mathcal{G}$, $f : \mathcal{G} \to \mathbb{R}$	Right Lie derivative for differentiable function f over Lie group $\mathcal{G}$ with Lie algebra $\mathfrak{g}$ at point $G \in \mathcal{G}$
$\mathrm{div}_{\mathcal{G}}(\mathcal{L}[M])(G)$	$M : \mathcal{G} \to \mathfrak{g}$, $G \in \mathcal{G}$	Divergence of vector field given by the left Lie derivative operator determined by a differentiable function M with values in the Lie algebra $\mathfrak{g}$ of Lie group $\mathcal{G}$, evaluated at $G \in \mathcal{G}$

Special mappings, norms

$\lvert x \rvert$	$x \in \mathbb{R}$	Absolute value
$\lvert \mathcal{E} \rvert$	$\mathcal{E} \subset \mathbb{R}^n$	Lebesgue measure of $\mathcal{E}$
$\lVert x \rVert$	$x \in \mathbb{R}^n$	Euclidean norm of x
$\lVert x \rVert_p$	$x \in \mathbb{R}^n$	finite dimensional p-norm of x: $\lVert x \rVert_p^p = \sum_i x_i^p$ for $p \in [1, \infty)$ $\lVert x \rVert_\infty = \max_i \lvert x_i \rvert$
$\lVert M \rVert$	$M \in \mathbb{R}^{n \times n}$	Frobenius norm of M
$\lVert f \rVert_{\mathcal{C}^k, \Omega}$	$f : \Omega \to \mathbb{R}^m$	Norm of k times continuously differentiable function f over $\Omega \subset \mathbb{R}^n$, $k \in \mathbb{N}_0$: $\lVert f \rVert_{\mathcal{C}^k, \Omega} = \max_{0 \leq \lVert \alpha \rVert_1 \leq k} \max_{x \in \Omega} \lVert \partial_x^\alpha f \rVert$ with multi-index $\alpha = (\alpha_1, \ldots, \alpha_n)$ and $\partial_x^\alpha f = \partial_{x_1}^{\alpha_1} \partial_{x_2}^{\alpha_2} \ldots \partial_{x_n}^{\alpha_n} f$
$\lVert f \rVert_{\mathcal{C}^k}$	$f : \Omega \to \mathbb{R}^m$	Short notation for $\lVert f \rVert_{\mathcal{C}^k, \Omega}$, if domain is obvious from context
$\lVert f \rVert_{p, \Omega}$	$f : \Omega \to \mathbb{R}^m$	$\mathcal{L}^p$-norm for Lebesgue measurable function f: $\lVert f \rVert_{p, \Omega}^p = \int_\Omega \lVert f \rVert^p \, \mathrm{d}x$ for $p \in [1, \infty)$; $\lVert f \rVert_{\infty, \Omega} = \inf\{ C \geq 0 \mid \lambda(\{ x \in \Omega \mid \lVert f(x) \rVert > C \}) = 0 \}$ with λ denoting the Lebesgue measure over Ω
$\lVert f \rVert_p$	$f : \Omega \to \mathbb{R}^m$	Short notation of $\lVert f \rVert_{p, \Omega}$, if domain of integration is obvious from context
$\mathbb{1}_{\mathcal{E}}(\boldsymbol{x})$	$\mathcal{E}$ a set, $\boldsymbol{x}$ a point	Indicator function of $\mathcal{E}$

Function spaces

$\mathcal{C}^k(\Omega; \mathbb{R}^m)$	$\Omega \subset \mathbb{R}^n$	Space of k times continuously differentiable functions over Ω, $k \in \mathbb{N}_0$ i.e., $\|f\|_{\mathcal{C}^k, \Omega} < \infty$ for all $f \in \mathcal{C}^k(\Omega; \mathbb{R}^m)$
$\mathcal{C}^\infty(\Omega; \mathbb{R}^m)$	$\Omega \subset \mathbb{R}^n$	Space of smooth functions over Ω, i.e., $\|f\|_{\mathcal{C}^k, \Omega} < \infty$ for all $k \in \mathbb{N}_0$ for all $f \in \mathcal{C}^\infty(\Omega; \mathbb{R}^m)$
$\mathcal{C}^k(\Omega)$	$\Omega \subset \mathbb{R}^n$	Short notation for $\mathcal{C}^k(\Omega; \mathbb{R}^m)$, if image is obvious from context
$\mathcal{C}^k$		Short notation for $\mathcal{C}^k(\Omega; \mathbb{R}^m)$, if domain and image are obvious from context
$\mathcal{C}$		Short notation for continuous functions, $\mathcal{C}^0$
$\mathcal{C}^k_N$		
$\mathcal{L}^p(\Omega; \mathbb{R}^m)$	$\Omega \subset \mathbb{R}^n$	Space of Lebesgue measurable functions with $\|f\|_{p, \Omega} < \infty$ for all $f \in \mathcal{L}^p(\Omega; \mathbb{R}^m)$
$\mathcal{L}^p(\Omega), \mathcal{L}^p$		Short notations for $\mathcal{L}^p(\Omega; \mathbb{R}^m)$ if the corresponding sets are obvious from context
$\mathcal{W}^{p,q}(\Omega; \mathbb{R}^m)$	$\Omega \subset \mathbb{R}^n$	Sobolev space of Lebesgue measurable functions over Ω whose weak derivatives up to pth order are Lebesgue measurable and have finite $\mathcal{L}^q$-norm
$\mathcal{W}^{p,q}_{\mathrm{loc}}(\Omega; \mathbb{R}^m)$	$\Omega \subset \mathbb{R}^n$	Sobolev space of Lebesgue measurable functions over Ω whose weak derivatives up to pth order are Lebesgue measurable and have finite $\mathcal{L}^q$-norm on any compact set $A \subset \Omega$

Bibliography

[1] N. Aboobaker, D. Blackmore, and J. Meegoda. "Mathematical modeling of the movement of suspended particles subjected to acoustic and flow fields". In: *Applied Mathematical Modelling* 29(6) (2005), pp. 515–532. DOI: 10.1016/j.apm.2004.09.013.

[2] M. Abramowitz and I. A. Stegun, eds. *Handbook of mathematical functions*. U.S. Dept. of Commerce, National Bureau of Standards, Washington, D.C, 1972.

[3] M. Ahlers. "Carbon Core – die neue BMW 7er Karosserie". In: *Karosseriebautage Hamburg 2016*. Ed. by G. Tecklenburg. Springer Vieweg, Wiesbaden, 2016, pp. 125–135. DOI: 10.1007/978-3-658-14144-8_9.

[4] H. C. Andersen. "Rattle: A "velocity" version of the shake algorithm for molecular dynamics calculations". In: *Journal of Computational Physics* 52(1) (1983), pp. 24–34. DOI: 10.1016/0021-9991(83)90014-1.

[5] W. Arne et al. "Finite volume approach for the instationary Cosserat rod model describing the spinning of viscous jets". In: *Journal of Computational Physics* 294 (2015), pp. 20–37. DOI: 10.1016/j.jcp.2015.03.042.

[6] M. Ashby. "Designing architectured materials". In: *Scripta Materialia* 68(1) (2013), pp. 4–7. DOI: 10.1016/j.scriptamat.2012.04.033.

[7] J. W. Barrett, H. Garcke, and R. Nürnberg. "The approximation of planar curve evolutions by stable fully implicit finite element schemes that equidistribute". In: *Numerical Methods for Partial Differential Equations* 27(1) (2011), pp. 1–30. DOI: 10.1002/num.20637.

[8] J. W. Barrett, D. J. Knezevic, and E. Süli. *Kinetic models of dilute polymers: Analysis, approximation and computation*. Nečas Center for Mathematical Modeling: 11th School on Mathematical Theory in Fluid Mechanics. 2009.

[9] S. Bartels. "A simple scheme for the approximation of elastic vibrations of inextensible curves". In: *IMA Journal of Numerical Analysis* 36(3) (2016), pp. 1051–1071. DOI: 10.1093/imanum/drv054.

[10] S. Bartels. "A simple scheme for the approximation of the elastic flow of inextensible curves". In: *IMA Journal of Numerical Analysis* 33(4) (2013), pp. 1115–1125. DOI: 10.1093/imanum/drs041.

[11] G. K. Batchelor. "The stress generated in a non-dilute suspension of elongated particles by pure straining motion". In: *Journal of Fluid Mechanics* 46(4) (1971), pp. 813–829. DOI: 10.1017/S0022112071000879.

[12] G. K. BATCHELOR. "The stress system in a suspension of force-free particles". In: *Journal of Fluid Mechanics* 41(3) (1970), pp. 545–570. DOI: 10.1017/S0022112070000745.

[13] B. BAUR, M. GROTHAUS, and T. T. MAI. "Analytically weak solutions to linear SPDEs with unbounded time-dependent differential operators and an application". In: *Communications on Stochastic Analysis* 7(4) (2013), pp. 551–571. DOI: 10.31390/cosa.7.4.05.

[14] F. BAUS et al. "Low-Mach-number and slenderness limit for elastic Cosserat rods and its numerical investigation". In: *Asymptotic Analysis* 120(1–2) (2020), pp. 103–121. DOI: 10.3233/ASY-191581.

[15] M. BEREZHNYI and E. KHRUSLOV. "Asymptotic behavior of a suspension of oriented particles in a viscous incompressible fluid". In: *Asymptotic Analysis* 83(4) (2013), pp. 331–353. DOI: 10.3233/ASY-131162.

[16] M. BERGER. "Stochastische Balkendynamik. Rauschmodellierung und -diskretisierung". MA thesis. Friedrich-Alexander Universität Erlangen-Nürnberg, 2016.

[17] L. BERLYAND and E. KHRUSLOV. "Homogenized non-Newtonian viscoelastic rheology of a suspension of interacting particles in a viscous Newtonian fluid". In: *SIAM Journal on Applied Mathematics* 64(3) (2004), pp. 1002–1034. DOI: 10.1137/S0036139902403913.

[18] R. B. BIRD, R. C. ARMSTRONG, and O. HASSAGER. *Dynamics of polymeric liquids*. Vol. 1. John Wiley & Sons, Inc., 1987.

[19] L. L. BONILLA et al. "Hydrodynamic limit of a Fokker-Planck equation describing fiber lay-down processes". In: *SIAM Journal on Applied Mathematics* 68(3) (2007), pp. 648–665. URL: http://www.jstor.org/stable/40233739.

[20] F. BOUCHUT, F. GOLSE, and M. PULVIRENTI. *Kinetic equations and asymptotic theory*. Ed. by B. PERTHAME and L. DESVILLETTES. Series in Applied Mathematics. Elsevier, 2000. URL: https://hal.archives-ouvertes.fr/hal-00538692.

[21] L. BREIMAN. *Probability*. SIAM, Philadelphia, PA, 1992. DOI: 10.1137/1.9781611971286.

[22] U. P. BREUER. *Commercial aircraft composite technology*. Springer International Publishing, 2016. DOI: 10.1007/978-3-319-31918-6.

[23] Z. BRZEŹNIAK, B. MASLOWSKI, and J. SEIDLER. "Stochastic nonlinear beam equations". In: *Probability Theory and Related Fields* 132(1) (2005), pp. 119–149. DOI: 10.1007/s00440-004-0392-5.

[24] R. H. CAMERON and W. T. MARTIN. "The orthogonal development of nonlinear functionals in series of Fourier-Hermite functionals". In: *Annals of Mathematics* 48(2) (1947), pp. 385–392. DOI: 10.2307/1969178.

[25] R. A. CHAPMAN, ed. *Applications of nonwovens in technical textiles*. Woodhead Publishing, 2010.

[26] G. S. CHIRIKJIAN. *Stochastic models, information theory, and Lie groups, volume 1*. Birkhäuser, 2009. DOI: 10.1007/978-0-8176-4803-9.

[27] G. S. Chirikjian. *Stochastic models, information theory, and Lie groups, volume 2.* Birkhäuser, 2012. DOI: `10.1007/978-0-8176-4944-9`.

[28] T. M. Cibis. "Homogenisierungsstrategien für Filament-Strömungs-Wechselwirkungen". PhD thesis. Friedrich-Alexander Universität Erlangen-Nürnberg, 2015.

[29] B. D. Coleman et al. "On the dynamics of rods in the theory of Kirchhoff and Clebsch". In: *Archive for Rational Mechanics and Analysis* 121(4) (1993), pp. 339–359. DOI: `10.1007/BF00375625`.

[30] D. Crowdy. "Flipping and scooping of curved 2D rigid fibers in simple shear: The Jeffery equations". In: *Physics of Fluids* 28(5) (2016), p. 053105. DOI: `10.1063/1.4948776`.

[31] G. Da Prato and J. Zabczyk. *Stochastic equations in infinite dimensions.* 2nd ed. Encyclopedia of Mathematics and its Applications. Cambridge University Press, 2014. DOI: `10.1017/CBO9781107295513`.

[32] D. Das and B. Pourdeyhimi, eds. *Composite nonwoven materials.* Woodhead Publishing, 2014.

[33] K. Deckelnick and G. Dziuk. "Error analysis for the elastic flow of parametrized curves". In: *Mathematics of Computation* 78(266) (2009), pp. 645–671. DOI: `10.1090/S0025-5718-08-02176-5`.

[34] L. Desvillettes, F. Golse, and V. Ricci. "The mean-field limit for solid particles in a Navier-Stokes flow". In: *Journal of Statistical Physics* 131(5) (2008), pp. 941–967. DOI: `10.1007/s10955-008-9521-3`.

[35] S. M. Dinh. "On the rheology of concentrated fiber suspensions". PhD thesis. Massachusetts Institute of Technology, 1981. eprint: `http://hdl.handle.net/1721.1/17163`.

[36] M. Doi and S. F. Edwards. "Dynamics of rod-like macromolecules in concentrated solution. Part 1". In: *Journal of the Chemical Society, Faraday Transactions 2* 74(0) (1978), pp. 560–570. DOI: `10.1039/F29787400560`.

[37] J. Dupire, M. Socol, and A. Viallat. "Full dynamics of a red blood cell in shear flow". In: *Proceedings of the National Academy of Sciences of the United States of America* 109(51) (2012), pp. 20808–20813. DOI: `10.1073/pnas.1210236109`.

[38] G. Dziuk, E. Kuwert, and R. Schätzle. "Evolution of elastic curves in $\mathbb{R}^n$: Existence and computation". In: *SIAM Journal on Mathematical Analysis* 33(5) (2002), pp. 1228–1245. DOI: `10.1137/S0036141001383709`.

[39] C. Eck, H. Garcke, and P. Knabner. *Mathematische Modellierung.* Springer Berlin, Heidelberg, 2008. DOI: `10.1007/978-3-540-74968-4`.

[40] D. Edwardes. "Steady motion of a viscous liquid in which an ellipsoid is constrained to rotate about a principal axis". In: *The quarterly journal of pure and applied mathematics* 26 (1893), pp. 70–78.

[41] J. Einarsson, J. R. Angilella, and B. Mehlig. "Orientational dynamics of weakly inertial axisymmetric particles in steady viscous flows". In: *Physica D: Nonlinear Phenomena* 278-279 (2014), pp. 79–85. DOI: `10.1016/j.physd.2014.04.002`.

[42] A. EINSTEIN. "Eine neue Bestimmung der Moleküldimensionen". In: *Annalen der Physik* 324(2) (1906), pp. 289–306. DOI: 10.1002/andp.19063240204.

[43] J. EITNER and E. WIEST, eds. *Smart solutions to join carbon fiber reinforced plastics and metal.* Report. 2019. URL: https://www.fraunhofer.de/en/press/research-news/2019/march/smart-solutions-to-join-carbon-fiber-reinforced-plastics-and-metal.html.

[44] O. G. ERNST et al. "On the convergence of generalized polynomial chaos expansions". In: *ESAIM: Mathematical Modelling and Numerical Analysis* 46(2) (2012), pp. 317–339. DOI: 10.1051/m2an/2011045.

[45] L. C. EVANS. *Partial differential equations.* 2nd ed. Graduate studies in mathematics, volume 19. American Mathematical Society, Providence, Rhode Island, 2015.

[46] F. FOLGAR and C. L. TUCKER. "Orientation behavior of fibers in concentrated suspensions". In: *Journal of Reinforced Plastics and Composites* 3(2) (1984), pp. 98–119. DOI: 10.1177/073168448400300201.

[47] G. P. GALDI. *An introduction to the mathematical theory of the Navier-Stokes equations.* Springer, 2011. DOI: 10.1007/978-0-387-09620-9.

[48] C. W. GEAR, B. LEIMKUHLER, and G. K. GUPTA. "Automatic integration of Euler-Lagrange equations with constraints". In: *Journal of Computational and Applied Mathematics* 12–13 (1985), pp. 77–90. DOI: 10.1016/0377-0427(85)90008-1.

[49] D. GÉRARD-VARET and M. HILLAIRET. "Analysis of the viscosity of dilute suspensions beyond Einstein's formula". In: *Archive for Rational Mechanics and Analysis* 238 (2020), pp. 1349–1411. DOI: 10.1007/s00205-020-01567-7.

[50] H. GIESEKUS. "Elasto-viskose Flüssigkeiten, für die in stationären Schichtströmungen sämtliche Normalspannungskomponenten verschieden groß sind". In: *Rheologica Acta* 2(1) (1962), pp. 50–62. DOI: 10.1007/BF01972555.

[51] H. GOLDSTEIN, C. P. POOLE, and J. L. SAFKO. *Klassische Mechanik.* 3rd ed. Wiley-VCH, Weinheim, 2006.

[52] F. GOLSE, C. MOUHOT, and V. RICCI. "Empirical measures and Vlasov hierarchies". In: *Kinetic and Related Models* 6(4) (2013), pp. 919–943. DOI: 10.3934/krm.2013.6.919.

[53] F. GOLSE. "On the dynamics of large particle systems in the mean field limit". In: *Macroscopic and Large Scale Phenomena: Coarse Graining, Mean Field Limits and Ergodicity.* Ed. by A. MUNTEAN, J. RADEMACHER, and A. ZAGARIS. Springer, Cham, 2016, pp. 1–144. DOI: 10.1007/978-3-319-26883-5_1.

[54] S. GRAMSCH et al. "Aerodynamic web forming: process simulation and material properties". In: *Journal of Mathematics in Industry* 6(13) (2016). DOI: 10.1186/s13362-016-0034-4.

[55] D. GROSS et al. *Technische Mechanik 1.* 11th ed. Springer Berlin, Heidelberg, 2011. DOI: 10.1007/978-3-642-13806-5.

[56] M. Grothaus and N. Marheineke. "On a nonlinear partial differential algebraic system arising in the technical textile industry: analysis and numerics". In: *IMA Journal of Numerical Analysis* 36(4) (2015), pp. 1783–1803. DOI: `10.1093/imanum/drv056`.

[57] J. S. Guasto, R. Rusconi, and R. Stocker. "Fluid mechanics of planktonic microorganisms". In: *Annual Review of Fluid Mechanics* 44(1) (2012), pp. 373–400. DOI: `10.1146/annurev-fluid-120710-101156`.

[58] B. M. Haines and A. L. Mazzucato. "A proof of Einstein's effective viscosity for a dilute suspension of spheres". In: *SIAM Journal on Mathematical Analysis* 44(3) (2012), pp. 2120–2145. DOI: `10.1137/100810319`.

[59] E. Hairer, C. Lubich, and M. Roche. *The numerical solution of differential-algebraic systems by Runge-Kutta methods.* Lecture Notes in Mathematics. Springer, Berlin Heidelberg, 1989. DOI: `10.1007/BFb0093947`.

[60] E. Hairer, C. Lubich, and G. Wanner. *Geometric numerical integration.* Springer Series in Computational Mathematics. Springer, Berlin Heidelberg, 2006. DOI: `10.1007/3-540-30666-8`.

[61] E. Hairer and G. Wanner. *Solving ordinary differential equations II.* Springer Series in Computational Mathematics. Springer, Berlin Heidelberg, 1996. DOI: `10.1007/978-3-642-05221-7`.

[62] B. C. Hall. *Lie groups, Lie algebras, and representations. An elementary introduction.* Springer, New York, NY, 2003. DOI: `10.1007/978-0-387-21554-9`.

[63] J. Hilgert and K.-H. Neeb. *Structure and geometry of Lie groups.* Springer, New York, NY, 2012. DOI: `10.1007/978-0-387-84794-8`.

[64] M. Hillairet. "On the homogenization of the Stokes problem in a perforated domain". In: *Archive for Rational Mechanics and Analysis* 230 (2018), pp. 1179–1228. DOI: `10.1007/s00205-018-1268-7`.

[65] M. H. Holmes. *Introduction to perturbation methods.* Springer, New York, 1998. DOI: `10.1007/978-1-4612-5347-1`.

[66] T. Y. Hou et al. "Wiener chaos expansions and numerical solutions of randomly forced equations of fluid mechanics". In: *Journal of Computational Physics* 216(2) (2006), pp. 687–706. DOI: `10.1016/j.jcp.2006.01.008`.

[67] F. Hübsch et al. "Random field sampling for a simplified model of melt-blowing considering turbulent velocity fluctuations". In: *Journal of Statistical Physics* 150(6) (2013), pp. 1115–1137. DOI: `10.1007/s10955-013-0715-y`.

[68] P.-E. Jabin and F. Otto. "Identification of the dilute regime in particle sedimentation". In: *Communications in Mathematical Physics* 250(2) (2004), pp. 415–432. DOI: `10.1007/s00220-004-1126-3`.

[69] S. Janson. *Gaussian Hilbert spaces.* Cambridge Tracts in Mathematics. Cambridge University Press, Cambridge, 1997. DOI: `10.1017/CBO9780511526169`.

[70] G. B. Jeffery. "The motion of ellipsoidal particles immersed in a viscous fluid". In: *Proceedings of the Royal Society A: Mathematical, Physical and Engineering Sciences* 102(715) (1922), pp. 161–179. DOI: `10.1098/rspa.1922.0078`.

[71]   M. JUNK and R. ILLNER. "A new derivation of Jeffery's equation". In: *Journal of Mathematical Fluid Mechanics* 9(4) (2007), pp. 455–488. DOI: `10.1007/s00021-005-0208-0`.

[72]   S. KIM and S. J. KARRILA. *Microhydrodynamics.* Dover Publications, Inc., Mineola, New York, 2005.

[73]   A. KLAR, N. MARHEINEKE, and R. WEGENER. "Hierarchy of mathematical models for production processes of technical textiles". In: *ZAMM - Journal of Applied Mathematics and Mechanics* 89(12) (2009), pp. 941–961. DOI: `10.1002/zamm.200900282`.

[74]   D. KLEIN, W. MALEZKI, and S. WARTZACK. "Introduction of a computational approach for the design of composite structures at the early embodiment design stage". In: *Proceedings of the 20th International Conference on Engineering Design (ICED 15) Vol 4.* Ed. by C. WEBER et al. The Design Society, Glasgow, Scotland, UK, 2015.

[75]   P. E. KLOEDEN and E. PLATEN. *Numerical solution of stochastic differential equations.* Stochastic Modelling and Applied Probability. Springer, Berlin Heidelberg, 1992. DOI: `10.1007/978-3-662-12616-5`.

[76]   D. M. KOCHMANN, J. B. HOPKINS, and L. VALDEVIT. "Multiscale modeling and optimization of the mechanics of hierarchical metamaterials". In: *MRS Bulletin* 44(10) (2019), pp. 773–781. DOI: `10.1557/mrs.2019.228`.

[77]   V. KRÄUTLER, W. F. van GUNSTEREN, and P. H. HÜNENBERGER. "A fast SHAKE algorithm to solve distance constraint equations for small molecules in molecular dynamics simulations". In: *Journal of Computational Chemistry* 22(5) (2001), pp. 501–508. DOI: `10.1002/1096-987X(20010415)22:5<501::AID-JCC1021>3.0.CO;2-V`.

[78]   L. D. LANDAU and E. M. LIFSHITZ. *Theory of elasticity.* Course of Theoretical Physics. Pergamon Press, 1970.

[79]   J. LANGER and D. A. SINGER. "Lagrangian aspects of the Kirchhoff elastic rod". In: *SIAM Review* 38(4) (1996), pp. 605–618. DOI: `10.1137/S0036144593253290`.

[80]   L. G. LEAL and E. J. HINCH. "The effect of weak Brownian rotations on particles in shear flow". In: *Journal of Fluid Mechanics* 46(4) (1971), pp. 685–703. DOI: `10.1017/S0022112071000788`.

[81]   L. G. LEAL and E. J. HINCH. "Theoretical studies of a suspension of rigid particles affected by Brownian couples". In: *Rheologica Acta* 12(2) (1973), pp. 127–132. DOI: `10.1007/BF01635092`.

[82]   S.-H. LEE, K. PALMO, and S. KRIMM. "WIGGLE: A new constrained molecular dynamics algorithm in Cartesian coordinates". In: *Journal of Computational Physics* 210(1) (2005), pp. 171–182. DOI: `10.1016/j.jcp.2005.04.006`.

[83]   E. V. LENS, A. CARDONA, and M. GÉRADIN. "Energy preserving time integration for constrained multibody systems". In: *Multibody System Dynamics* 11(1) (2004), pp. 41–61. DOI: `10.1023/B:MUBO.0000014901.06757.bb`.

[84] F. Lindner et al. "Stochastic dynamics for inextensible fibers in a spatially semi-discrete setting". In: *Stochastics and Dynamics* 17(2) (2017). doi: 10.1142/S0219493717500162.

[85] S. B. Lindström and T. Uesaka. "A numerical investigation of the rheology of sheared fiber suspensions". In: *Physics of Fluids* 21(8) (2009), p. 083301. doi: 10.1063/1.3195456.

[86] S. B. Lindström and T. Uesaka. "Simulation of semidilute suspensions of non-Brownian fibers in shear flow". In: *The Journal of Chemical Physics* 128(2) (2008), p. 024901. doi: 10.1063/1.2815766.

[87] M. Lorenz, N. Marheineke, and R. Wegener. "On simulations of spinning processes with a stationary one-dimensional upper convected Maxwell model". In: *Journal of Mathematics in Industry* 4(2) (2014). doi: 10.1186/2190-5983-4-2.

[88] F. Lundell, L. D. Söderberg, and P. H. Alfredsson. "Fluid mechanics of papermaking". In: *Annual Review of Fluid Mechanics* 43(1) (2011), pp. 195–217. doi: 10.1146/annurev-fluid-122109-160700.

[89] W. Luo. "Wiener chaos expansion and numerical solutions of stochastic partial differential equations". PhD thesis. California Institute of Technology, 2006. doi: 10.7907/RPKX-BN02.

[90] N. Marheineke and R. Wegener. "Fiber dynamics in turbulent flows: General modeling framework". In: *SIAM Journal on Applied Mathematics* 66(5) (2006), pp. 1703–1726. doi: 10.1137/050637182.

[91] N. Marheineke and R. Wegener. "Fiber dynamics in turbulent flows: Specific taylor drag". In: *SIAM Journal on Applied Mathematics* 68(1) (2007), pp. 1–23. doi: 10.1137/06065489X.

[92] N. Marheineke and R. Wegener. "Modeling and application of a stochastic drag for fibers in turbulent flows". In: *International Journal of Multiphase Flow* 37(2) (2011), pp. 136–148. doi: 10.1016/j.ijmultiphaseflow.2010.10.001.

[93] J. P. Mesirov, K. Schulten, and D. W. Sumners, eds. *Mathematical approaches to biomolecular structure and dynamics*. The IMA Volumes in Mathematics and its Applications. Springer, New York, 1996. doi: 10.1007/978-1-4612-4066-2.

[94] L. R. Meza et al. "Resilient 3D hierarchical architected metamaterials". In: *Proceedings of the National Academy of Sciences* 112(37) (2015), pp. 11502–11507. doi: 10.1073/pnas.1509120112.

[95] M. G. Mora and S. Müller. "Derivation of the nonlinear bending-torsion theory for inextensible rods by Γ-convergence". In: *Calculus of Variations and Partial Differential Equations* 18(3) (2003), pp. 287–305. doi: 10.1007/s00526-003-0204-2.

[96] A. Oberbeck. "Ueber stationäre Flüssigkeitsbewegungen mit Berücksichtigung der inneren Reibung". In: *Journal für die reine und angewandte Mathematik* 81 (1876), pp. 62–80.

[97] D. B. Öelz. "On the curve straightening flow of inextensible, open, planar curves". In: *SeMA Journal* 54(1) (2011), pp. 5–24. DOI: `10.1007/BF03322585`.

[98] M. Päsler. *Grundzüge der Vektor- und Tensorrechnung*. Walter de Gruyter Berlin, 1977.

[99] N. A. Patankar et al. "A new formulation of the distributed Lagrange multiplier/fictitious domain method for particulate flows". In: *International Journal of Multiphase Flow* 26(9) (2000), pp. 1509–1524. DOI: `10.1016/S0301-9322(99)00100-7`.

[100] J. R. A. Pearson. *Mechanics of polymer processing*. Elsevier, New York, 1985.

[101] N. Phan-Thien and A. L. Graham. "A new constitutive model for fibre suspensions: flow past a sphere". In: *Rheologica Acta* 30(1) (1991), pp. 44–57. DOI: `10.1007/BF00366793`.

[102] S. C. Preston. "The motion of whips and chains". In: *Journal of Differential Equations* 251(3) (2011), pp. 504–550. DOI: `10.1016/j.jde.2011.05.005`.

[103] A. Prosperetti. "The average stress in incompressible disperse flow". In: *International Journal of Multiphase Flow* 30(7) (2004), pp. 1011–1036. DOI: `10.1016/j.ijmultiphaseflow.2004.05.003`.

[104] A. Prosperetti, Q. Zhang, and K. Ichiki. "The stress system in a suspension of heavy particles: antisymmetric contribution". In: *Journal of Fluid Mechanics* 554 (2006), pp. 125–146. DOI: `10.1017/S0022112006009402`.

[105] F. Rindler. *Calculus of variations*. Springer, 2018. DOI: `10.1007/978-3-319-77637-8`.

[106] C. Rolf et al. "Lidar observation and model simulation of a volcanic-ash-induced cirrus cloud during the Eyjafjallajökull eruption". In: *Atmospheric Chemistry and Physics* 12(21) (2012), pp. 10281–10294. DOI: `10.5194/acp-12-10281-2012`.

[107] W. B. Russel, D. A. Saville, and W. R. Schowalter. *Colloidal dispersions*. Cambridge Univ. Press, Cambridge, 2001.

[108] J.-P. Ryckaert, G. Ciccotti, and H. J. C. Berendsen. "Numerical integration of the cartesian equations of motion of a system with constraints: molecular dynamics of *n*-alkanes". In: *Journal of Computational Physics* 23(3) (1977), pp. 327–341. DOI: `10.1016/0021-9991(77)90098-5`.

[109] S. Schiessl. "Jet and fiber dynamics with high elongations: Models, numerical strategies and applications". PhD thesis. Friedrich-Alexander-Universität Erlangen-Nürnberg, 2017.

[110] H. Schlichting and K. Gersten. *Grenzschicht-Theorie*. Springer, Berlin, Heidelberg, 2006. DOI: `10.1007/3-540-32985-4`.

[111] K. D. Schmidt. *Maß und Wahrscheinlichkeit*. Springer, Berlin, Heidelberg, 2011. DOI: `10.1007/978-3-642-21026-6`.

[112] G. G. Stokes. "On the effect of the internal friction of fluids on the motion of pendulums". In: *Transactions of the Cambridge Philosophical Society* 9(2) (1851), pp. 8–106.

[113] H. STROOT. "Strong approximation of stochastic mechanical systems with holonomic constraints". PhD thesis. Technische Universität Kaiserslautern, 2019.

[114] G. SZEGÖ. *Orthogonal polynomials*. American Math. Soc., Providence, RI, 1985.

[115] W. VARNHORN. *The Stokes equations*. Akademie Verlag, Berlin, 1994.

[116] A. VIBE. "Kinetische Modellierung ausgedehnter Partikel in Strömungen". MA thesis. Friedrich-Alexander Universität Erlangen-Nürnberg, 2014.

[117] A. VIBE and N. MARHEINEKE. "Impact of weak particle inertia on a dilute suspension of ellipsoids". In: *Journal of Computational and Theoretical Transport* 45(5) (2016), pp. 396–409. DOI: 10.1080/23324309.2016.1181090.

[118] A. VIBE and N. MARHEINEKE. "Mean field surrogate model of a dilute and chaotic particle suspension". In: *PAMM – Proceedings in Applied Mathematics and Mechanics*. Ed. by J. EBERHARDSTEINER and M. SCHÖBERL. Vol. 19. Wiley-VCH, 2019. DOI: 10.1002/pamm.201900360.

[119] A. VIBE and N. MARHEINEKE. "Modeling of macroscopic stresses in a dilute suspension of small weakly inertial particles". In: *Kinetic & Related Models* 11(6) (2018), pp. 1443–1474. DOI: 10.3934/krm.2018057.

[120] A. VIBE and N. MARHEINEKE. "Wiener chaos expansion for an inextensible Kirchhoff beam driven by stochastic forces". In: *Progress in Industrial Mathematics at ECMI 2016*. Ed. by P. QUINTELA et al. Springer, Cham, 2017, pp. 761–768. DOI: 10.1007/978-3-319-63082-3_112.

[121] F. W. WARNER. *Foundations of differentiable manifolds and Lie groups*. Graduate Texts in Mathematics. Springer, 1983. DOI: 10.1007/978-1-4757-1799-0.

[122] R. WEGENER, N. MARHEINEKE, and D. HIETEL. "Virtual production of filaments and fleeces". In: *Currents in Industrial Mathematics*. Ed. by H. NEUNZERT and D. PRÄTZEL-WOLTERS. Springer, Berlin Heidelberg, 2015, pp. 103–162. DOI: 10.1007/978-3-662-48258-2_6.

[123] M. WIEDEMANN et al., eds. *Innovationsbericht 2018*. Report. www.dlr.de/fa. 2018.

[124] M. WIELAND et al. "Melt-blowing of viscoelastic jets in turbulent airflows: Stochastic modeling and simulation". In: *Applied Mathematical Modelling* 76 (2019), pp. 558–577. DOI: 10.1016/j.apm.2019.06.023.

[125] E. WONG and M. ZAKAI. "Martingales and stochastic integrals for processes with a multi-dimensional parameter". In: *Zeitschrift für Wahrscheinlichkeitstheorie und Verwandte Gebiete* 29(2) (1974), pp. 109–122. DOI: 10.1007/BF00532559.

[126] Q. ZHANG and A. PROSPERETTI. "Physics-based analysis of the hydrodynamic stress in a fluid-particle system". In: *Physics of Fluids* 22(3) (2010), p. 033306. DOI: 10.1063/1.3365950.

Curriculum vitae

Personal Details

Name	Alexander Vibe
Born	14.12.1987, Temirtau, Kasachstan

Education

2008	Abitur, Otto-Hahn-Gymnasium Marktredwitz
2012	B.Sc. Technomathematics, Friedrich-Alexander-Universität Erlangen-Nürnberg (FAU)
	Bachelor-thesis "Asymptotik und Numerik für partielle differential-algebraische Systeme elastischer Stab- und Balkenmodelle"
2014	M.Sc. Mathematics, FAU Erlangen-Nürnberg
	Master-thesis "Kinetische Modellierung ausgedehnter Partikel in Strömungen"
2014 – 2020	PhD student in mathematics at FAU Erlangen-Nürnberg and University of Trier, doctoral advisor Prof. Dr. Nicole Marheineke